11th Australia and New Zealand Young Geotechnical Professionals Conference



Queenstown, New Zealand

25-28 October 2016

NEW ZEALAND GEOTECHNICAL SOCIETY INC

AUSTRALIAN GEOMECHANICS SOCIETY

11YGPC gratefully acknowledge the support of:

Platinum Sponsor

OPUS

Gold Sponsors

Tonkin+Taylor

MARCH

Dinner Sponsor

GEOTECHNICS

Field trip Sponsor

AECOM

Silver Sponsors

CLL SERVICE & SOLUTIONS

DCN Drilling Ltd

DRILLFORCE THE DRILLING SPECIALISTS

GEOTECHNICS

Bronze Sponsors

Southern Geophysical Ltd

COVER IMAGE COURTESY OF LUKE STORIE

A Joint initiative of the AUSTRALIAN GEOMECHANICS SOCIETY and

NEW ZEALAND GEOTECHNICAL SOCIETY

11th Australia and New Zealand Young Geotechnical Professionals Conference

11YGPC

Queenstown, New Zealand, October 2016

ORGANISING COMMITTEE:

Frances Neeson	Opus International Consultants	New Zealand
David Buxton	Hawthorn Geddes	New Zealand
David Lacey	Foundation Specialists Group	Australia
Luke Storie	Tonkin and Taylor	New Zealand

PUBLISHED BY:

The New Zealand Geotechnical Society

PO Box 12241, Wellington, NZ

Proceedings of the 11th Australia and New Zealand Geotechnical Symposium.
Eds. Neeson, F.C; Lacey, D.; Buxton, D.; Storie, L.; Queenstown (2016)
ISBN 978-0-473-37653-6

The 11YGPC Organising Committee would like to thank the following reviewers for the arduous task of undertaking reviews of papers presented in these Proceedings

TECHNICAL REVIEWERS

Gavin Alexander
Kevin Anderson
Hayden Bowen
Andrew Campbell
Guy Cassidy
C Y Chin
Stephen Crawford
Fernando Della Pasqua
Tony Fairclough
Debra Fellows
Eleni Gkeli
Sally Hargraves
Campbell Keepa
Andrew Langbein
Don McFarlane
Rebecca McMahon
Andy Mott
Charlie Price
Stuart Read
Ross Roberts
Nick Rogers
Greg Saul
Andrew Stiles
David Airey
Derek Arnott
Tom Bowling
Robert Day
Mahdi Disfani
Jim Hambleton
Jinsong Huang
Richard Kaser
Hadi Khabbaz
Burt Look
Peter Mitchell
Mark Orr
Derek Pennington
Rick Piovesan
Mizanur Rahman
Diacho Sheng
Ian Shipway
Adrian Smith
Mogana Sundaram
Abbas Taheri
Ramtin Tajeddin
Megan Walske
David Williams

The Graphic Design assistance provided by Karryn Muschamp is gratefully acknowledged.

FOREWORD

It is with great pleasure and excitement that the organising committee welcome you to the 11th Australia and New Zealand Young Geotechnical Professionals Conference which is being held at the Crowne Plaza Hotel, Queenstown from 25th to 28th October 2016.

Held every 2 years, the Young Geotechnical Professional Conference (YGPC) events are unique 3 day conferences facilitated by a joint initiative of Australian Geomechanics Society (AGS) and New Zealand Geotechnical Society.

The aim of the 11YGPC conference is to provide younger professionals both in industry and academia, experience in technical paper preparation and conference presentation. Presenting at this conference is the culmination of many months of paper preparation, peer review by senior professionals and uniquely conference attendance is limited to only presenting authors with what is likely to be their first technical paper to their peers and a panel of senior industry professionals. It is also important to note that for this YGPC there were a the record number of abstracts received, so unfortunately we were unable to accept all authors wanting to present and therefore attendance has been highly competitive.

We are delighted to have Nick Wharmby (March Construction), Darren Paul (Golder & AGS Immediate Past National Chair), and Charlie Price (MWH & NZGS Chair) as our senior industry mentoring panel. This panel not only has vast technical knowledge but also provides a direct link between the Young Professionals and both Trans-Tasman learned societies. We hope that delegates not only gain professional development but learn more about the AGS and NZGS and the work they do to promote and advocate for our industry. AGS have also illustrated their commitment to the industry in a wider capacity than Australasia and this is the first occasion where we are pleased to extend a warm welcome to a colleague from Africa who has been supported by AGS to attend.

YGPC events also include a field trip into the surrounding region, and we are thrilled to have the assistance of Don McFarlane (AECOM) and Greg Saul (Opus) to provide what will no doubt be an interesting, informative and entertaining commentary on the Cromwell Gorge Landslides and Clyde Dam. No conference is complete without a number of social events to encourage interaction between the delegates, and this conference is no exception. We look forward to showcasing Queenstown during these events.

We wish to acknowledge the financial support provided by the Sponsors of this conference. Without their support and assistance this event could not occur and we thank each and every one of these organisations. We also thank the peer reviewers who gave their time and technical expertise to provide thorough and supportive reviews of the papers.

Finally I wish to acknowledge the hard work and commitment of the organising committee and guidance of both AGS and NZGS national committees. Without their efforts and the support of their respective home organisations this conference would not be possible.

I hope the 11YGPC provides an enjoyable and informative event aimed at the development of future leaders in the geotechnical profession.



Frances Neeson
11YGPC Organising Committee Chair and NZGS Young Professionals Representative.

AUSTRALIAN GEOMECHANICS SOCIETY



WELCOME FROM THE AGS NATIONAL CHAIR

On behalf of the Australian Geomechanics Society (AGS) I extend a warm welcome to participants at the 11th Australia and New Zealand Young Geotechnical Professionals Conference (11YGPC). This series of conferences for young geotechnical professionals have been supported by AGS and the New Zealand Geotechnical Society (NZGS) since 1994 and occupy a high rank in the calendar of joint events from the two national groups of the Australasia region of the International Society for Soil Mechanics and Geotechnical Engineering (ISSMGE). Young geotechnical professionals represent the future of the geomechanics profession in the region and both AGS and NZGS are committed to continue supporting this conference and to provide many other continued professional development opportunities for young geotechnical professionals.

The event aims to bring together young researchers and practitioners with senior academics and professionals to report on and discuss the current state of geotechnical engineering in the region. It provides the opportunity to young professionals to deliver a paper presentation in a supportive environment, be mentored through the process, receive constructive feedback and build relationships. Participants will also have the opportunity to learn about the initiatives and activities of AGS and NZGS and to become more active in those learned societies.

This conference also aims to encourage young geotechnical practitioners to develop a broader scope in geotechnical engineering and be aware of the current challenges of the profession. On this occasion, the AGS is offering a young geotechnical professional from Africa the opportunity to attend 11YGPC. The nominee selection process was managed independently by the Vice-President for Africa of ISSMGE among the countries in that region. This initiative seeks to promote collaboration with developing countries in the African region.

11YGPC also provides the opportunity to make new contacts and friends that are at a similar stage of career development and that attendees may find again during their future professional development. I hope participants will make the most of all the technical and social opportunities that the 11YGPC provides to strengthen networking among young geotechnical professionals in the ANZ region.

On a related note, young professionals may know that the International Conference on Soil Mechanics and Geotechnical Engineering is held once every four years. The first one was held in Harvard University in Cambridge (USA) in 1936, that is, 80 years ago. The next one – number 19 in the series – will be held in 2017 in Seoul, Republic of Korea. In the long history of the event, it has not come to the Australasian region despite six previous bids from AGS. I hope participants of 11YGPC agree that is time to bring the event to the Australasian region and I would like to let you know that AGS is bidding again to host the event in Sydney in 2021. I invite 11YGPC delegates to support our regional bid and to promote it among their worldwide networks of young geotechnical professionals.

On behalf of AGS I would also like to thank the Conference Organising Committee, the reviewers of papers and all the sponsors who have played a vital part in making this event affordable. The names of those individuals and organisations are acknowledged elsewhere in the conference proceedings.

Finally, I trust attendees to 11YGPC will leave the event better informed and with new ideas to implement in their daily practice/research and that the overall experience will contribute highly to their future careers, full of challenges, achievements and service to the profession and our communities.

Dr Hugo Acosta-Martinez
National Chair, Australian Geomechanics Society

New Zealand Geotechnical Society

ISSMGE *Outstanding Member Society*



WELCOME FROM THE NZGS CHAIR

Welcome from the NZGS to this the 11th New Zealand and Australian Young Geotechnical Professionals Conference. I would like to offer a special welcome to our Australian colleagues and our delegate from Africa.

Over the next couple of days you will present, and listen to others presenting, technical papers on challenging, or interesting, topics that you have come across in your working lives. These technical challenges are what drive us all, they are what makes for such rewarding careers in geotechnical engineering, and they are what will keep each of you intrigued for your entire careers, indeed the rest of your lives. However, there are also other aims to this conference which are equally important to your career. These include fostering professional and collegial relationships within the geotechnical community and encouraging you to think carefully about continuing professional development in your individual careers. Interpersonal professional and collegial relationships are becoming more important as our world is becoming increasingly dominated by technology, isolating us as individuals behind our screens and devices. This conference and all its social events provide an opportunity to develop support and networks and we hope that you will carry these forward into your careers. Please take this opportunity to get to know your colleagues, and enjoy the conference.

As a mentor to the conference this year, I will take the opportunity of talking to you about the relationship between engineers and geologists in our profession. During the last year the NZGS has taken on the task of developing two distinct 'Bodies of Knowledge and Skills', one for Geotechnical Engineers and one for Engineering Geologists. These 'BoKS', as they are known, are aimed at defining the knowledge that a professional in each discipline would be expected to have at the point of Professional Registration. These BoKS are new to the profession, so new that what I show you at the conference will not yet have been seen outside of the group of people that are developing them, and not yet published. I recommend that you familiarise yourselves with these documents once they are published, and get a clear understanding as to where your own knowledge and career skills lie.

This conference is just one of many events that your home societies will organise for your benefit during your career. We hope that you will continue to support the societies, and to become involved with running such events, remembering that the societies are only as active and vibrant as the people that contribute to them.

Health and safety are buzzwords of the modern industry, and there have been significant changes in this aspect of our profession across the length of my career. One thing that I hope you, the delegates, will take away from this conference is this, that health and safety starts with self-protection and self-care, in the same way that charity begins at home, and the person best equipped to take care of this is yourself. By taking care of your own well-being, and treating your colleagues in the same light, you can make your and everyone else's lives safer and more enjoyable. So take care, enjoy the conference and make the best of your promising careers.

Charlie Price
Chair, New Zealand Geotechnical Society

PREVIOUS ANZ YOUNG GEOTECHNICAL PROFESSIONALS CONFERENCES

- 1st ANZ Young Geotechnical Professionals Conference, Sydney, Australia, 1994.
- 2nd ANZ Young Geotechnical Professionals Conference, Auckland, New Zealand, 1995.
- 3rd ANZ Young Geotechnical Professionals Conference, Melbourne, Australia, 1998
- 4th ANZ Young Geotechnical Professionals Conference, Perth, Australia, 2000
- 5th ANZ Young Geotechnical Professionals Conference, Rotorua, New Zealand, 2002.
- 6th ANZ Young Geotechnical Professionals Conference, Gold Coast, Australia, 2004.
- 7th ANZ Young Geotechnical Professionals Conference, Adelaide, Australia, 2006.
- 8th ANZ Young Geotechnical Professionals Conference, Wellington, New Zealand, 2008.
- 9th ANZ Young Geotechnical Professionals Conference, Melbourne, Australia, June 2012.
- 10th ANZ Young Geotechnical Professionals Conference, Noosa, Australia, September 2014.
- 11th ANZ Young Geotechnical Professionals Conference, Queenstown, New Zealand, 2016.

TABLE OF CONTENTS

Numerical modelling of toe buckling deformation in Haast Schist, Central Otago, New Zealand **1**
R. Ridl, M. Villeneuve and D. Bell

Design and construction of an egress tunnel beneath a working hospital **9**
M. L. Teoh, B. Shen and G. Mostyn

"Seeking Relief" Rising Pore Pressures in Earth Dams – A Case Study **15**
N. P. Burrows

Design, monitoring and back-analysis of highway embankments constructed over soft soil **21**
A. Podnar

Assessing the Strength of East Coast Bays Formation Soils using in-situ Testing Data **29**
S. Semmens and S. Anwar

Design of Mechanically Stabilised Earth Walls for Bridge Abutments on the Mackays to Peka Peka Expressway, New Zealand **35**
R. J. Everiss

Application of Artificial Intelligence Techniques for Rolling Dynamic Compaction **41**
R. A. T. M. Ranasinghe and M. B. Jaksa

Geotechnical Challenges of Brownfield Sites for use as Landfill **49**
N. Ruxton

Effect of Pre-Shearing during Cyclic Simple Shear Testing of Clean Sand for Liquefaction Analyses **57**
S. D. Rees

Design of Anchors in Weathered Greywacke - A Case Study in Wellington **63**
S. Cherfane and S. Moniz

Estimating pre-load induced settlement from laboratory test data and field monitoring records: A Case Study at Temple View Eastern Redevelopment Project, Hamilton **69**
D. P. Mills and D. J. Morton

Embankment Failures – Local Experiences **75**
E. G. Maynard

Liquefaction Resistance of Hamilton Pumiceous Sands **83**
E. E. Jacobs and D. L. Dennison

Seismically induced land damage on Whitewash Head, Christchurch, New Zealand **89**
C. C. Mangos

Liquefaction potential of the micaceous lake sediments in the Queenstown area **95**
A. S. Awad and J. Searle

A Comparison and Review of the Field Logging Standards and Guidelines in Australia and New Zealand **103**
K. Farry

Sydney Metro site investigation for the Sydney Harbour tunnel crossing **109**
N. J. C. Byrne and D. J. Och

Geotechnical design challenges associated with construction of the new AMCOR paper mill in Botany, NSW **115**
T. G. Cuniowski

Timber Piles for Ground Improvement in Fiji's Liquefiable Soil **123**
A. Pereira and I. McPherson

Capping of Tailings Deposits: Analysis, Design and Implementation **129**
W. M. Piper and D. R. Anderson

Interpreting geotechnical measurements and observations: Does one size fit all? **135**
R. E. Kristinof

Rockfall Protection Structures on a Critical Lifeline in Christchurch **141**
J. M. Engel

Soil-Pile-Structure Interaction at Lyttelton Oil Berth **147**
A. D. Wallace and H. J. Bowen

Managing Client Expectations for Central North Island Infrastructure Designs **153**
J. Kelly, B. A. Curley and B. Simms

The Value of Interpersonal Skills in Geotechnical Projects: a Millennial's Four Year Experience **159**
J. J. Lees

Back Analysis and Closure Considerations for the North-East Pit Wall at the Globe Progress Gold Mine, Reefton, New Zealand **165**
D. Meehan

Challenges and Experiences of Site Investigations Abroad **171**
H. L. McEwan and R. B. Graafhuis

Determination of Effective Stress Parameters for Clayey Silt using a Borehole Shear Test **177**
J. B. Fairhall

Deep Excavation Impact Assessment in Urban Environments: Predictions versus Reality **183**
G. Chan

The Use of Engineering Index Correlations with the Shrink-Swell Test **191**
J. Johnston and S. Fityus

Monitoring geohazards and trigger level response on Deans Head in the Port Hills, Christchurch **197**
Z. J. Pletz

The Undrained Cyclic Response of Monterey Sand in Direct Simple Shear **203**
C. Cappellaro and M. Cubrinovski

Modelling Behaviour of Soft Estuarine Clay in Newcastle using Soft Soil Creep Model **209**
R. C. Tanuwidjaja

Seismic Ground Response at a Deep Soft Soil Site: Comparing 1D Numerical Solutions with Observed Data from the Christchurch Earthquakes **215**
J. K. Lim

Topographic amplification on steep slopes during seismic events **223**
D. Gainsford and G. Salt

Estimating Geotechnical Parameters in Highly Heterogeneous Material Including Peat Deposits using Trial Embankment Data **231**
J. Leeves

Geotechnical challenges during design of Aokautere Reservoir – Palmerston North **237**
R. Sundar and M. Frampton

Static failure mechanisms in sensitive volcanic soils in the Tauranga Region, New Zealand **243**
P. R. Mills and V. G. Moon

Geotechnical investigations to address Earthquake Hazards for the Petone to Grenada Link Road, Wellington, New Zealand **249**
E. Boam and P. Brabhaharan

Counterfort Drain Performance in the Auckland Area **257**
S. M. Torvelainen

Geotechnical issues in seismic assessments: When do I need a geotechnical specialist? **263**
B. H. Rama and S. J. Palmer

Design and construction of a commercial building on a closed municipal solid waste landfill in Takapuna, Auckland **269**
N. Li

Adapting a Driven Pile Design to meet the Challenges encountered during Construction **275**
R. J. Reed R. E. Kristinof and A. T. Carter

Site characterization of the area surrounding a sinkhole, a case study **281**
M. P. Magagula and G. R. Wardle

Arching in geosynthetic reinforced column supported embankments – recent findings from a field case study **287**
D. King

An Assessment of Foundation Rocking Behaviour based on Field Observations **293**
S. J. Harris

Unmanned Aerial Vehicles: A new tool for landslide risk assessment **299**
I. C. Jaukovic and A. J. Hunter

Analysing Slope Change at Globe Progress Open Pit, Reefton **305**
T. Howard and A. Cantwell

SH20A to Airport: New Zealand's First Project adopting Screw Piles and Diaphragm Walls as a Trench Combination **311**
M. M. Yan

3D terrain and geological modelling for the design of a cut slope in Wellington **319**
M. K. H. Brown

AUTHOR INDEX **325**

Proceedings of the 11th ANZ Young Geotechnical Professionals Conference – 11YGPC
Queenstown, New Zealand
25 – 28 October 2016

Numerical modelling of toe buckling deformation in Haast Schist, Central Otago, New Zealand

R. Ridl[1], M. Villeneuve[1] and D. Bell[1].

[1]Department of Geological Sciences, University of Canterbury. P. O. Box 4800, Christchurch, 8140. Email: romyridl@gmail.com

ABSTRACT

Toe buckling deformation is an outward expression of strain which develops near the base of a slope in response to induced gravitational and tectonic stresses acting on a rock mass and can lead to kinematic slope instability. This deformation mechanism is considered responsible for anomalously oversteepened foliations identified underlying three deep-seated landslides within schist bedrock of Cromwell Gorge, Central Otago, New Zealand. Spatial and temporal complexities of schist behaviour in response to stress regimes were numerically modelled using Finite Element Methods based on site-specific field (slope and tunnel mapping, borehole logging) and laboratory (UCS, triaxial, indirect-tensile, point load, shear box) testing data. Sequential unloading was incorporated in the model to simulate the evolution of Cromwell Gorge from a low relief surface (Otago Peneplain) to present day topography (1400 m deep). Sensitivity analyses reveal that specific combinations of high locked-in tectonic stresses, foliation stiffness and orientation contributed to the development of flexural toe buckling at the base of Cromwell Gorge.

Keywords: Toe buckling, finite element method, numerical modelling, schist, Cromwell Gorge.

1 INTRODUCTION

Mountains are dynamic environments with shifting stress regimes associated with the formation of valleys due to uplift and erosion. The rock masses that form mountains develop a tectonic imprint of these ongoing stresses by constantly deforming to relieve stress in an attempt to reach equilibrium, often via creeping mass movements on a mountain range scale. As valleys deepen, orientation of principal stress axes progressively rotate, migrating toward the summit. Where these principal stresses coincide with anisotropic weaknesses within a rock mass, gravitational sagging may result in an outward expression of deformation concentrated at the toe of the slope, in the form of toe buckling. Variations of toe buckling deformation comprise curvilinear flexural buckling and three hinge buckling (see Cavers, 1981). This type of deformation is identified globally in a wide range of environments as a result of anthropogenic infrastructure such as road cuttings and open pit mines (Hu and Cruden 1993; Stead and Eberhardt 1997), natural large scale landslides associated with deep seated gravitational slope deformations (DSGSD) (Agliardi et al. 2001), as well as precursors to coseismic landslides such as the 1999 Chi Chi earthquake in Taiwan (Wang et al. 2003). It is therefore important to understand mechanisms governing toe buckling to assist with early hazard identification and comprehension of these large scale slides

Anomalously oversteepened foliations were identified beneath three large scale landslide complexes within Cromwell Gorge, Central Otago, in New Zealand's South Island. A pertinent research question arose, as to whether these deformations represented a form of toe buckling which developed in response to induced gravitational stresses associated with valley deepening, or whether these structural features were related to metamorphic processes predating the development of Cromwell Gorge. Numerical models simulating rock mass conditions can be utilised to answer this research question. This is possible due to recent advancements in computing technology, which permit realistic simulations of rock mass behaviour in response to induced stress through numerical modelling. Complex algorithms related to constitutive models constrain the behavioural response of the rock mass to various stress states. Both continuum and discontinuum numerical models have been successful in simulating deformations associated with DSGSD and toe buckling (Tommasi et al. 2009; Pereira and Lana 2013), and a continuum approach was selected for this research.

2 BACKGROUND

Extensive geotechnical investigations were carried out in several phases between 1975 and 1992, for the Clyde Power Station project in Central Otago. During this investigation seventeen major landslides within Lake Dunstan catchment were identified (Figure 1). Field mapping, borehole coring and excavation of exploration tunnels within this region indicated Cromwell Gorge generally comprises Rakaia Terrane Schists inclined at an average angle of 20° to 40° towards the southwest. However, anomalous oversteepened to overturned foliations were identified beneath the slide bases of three landslides, namely Nine Mile, No. 5 Creek and Dunlays Slides located on the Dunstan flank of the gorge (Beetham et al. 1991). Bedrock in this area is deformed with schistosity exhibiting flexural buckling steepening upwards toward the slide base at angles from 50° to 90° to completely overturned (Figure 2).

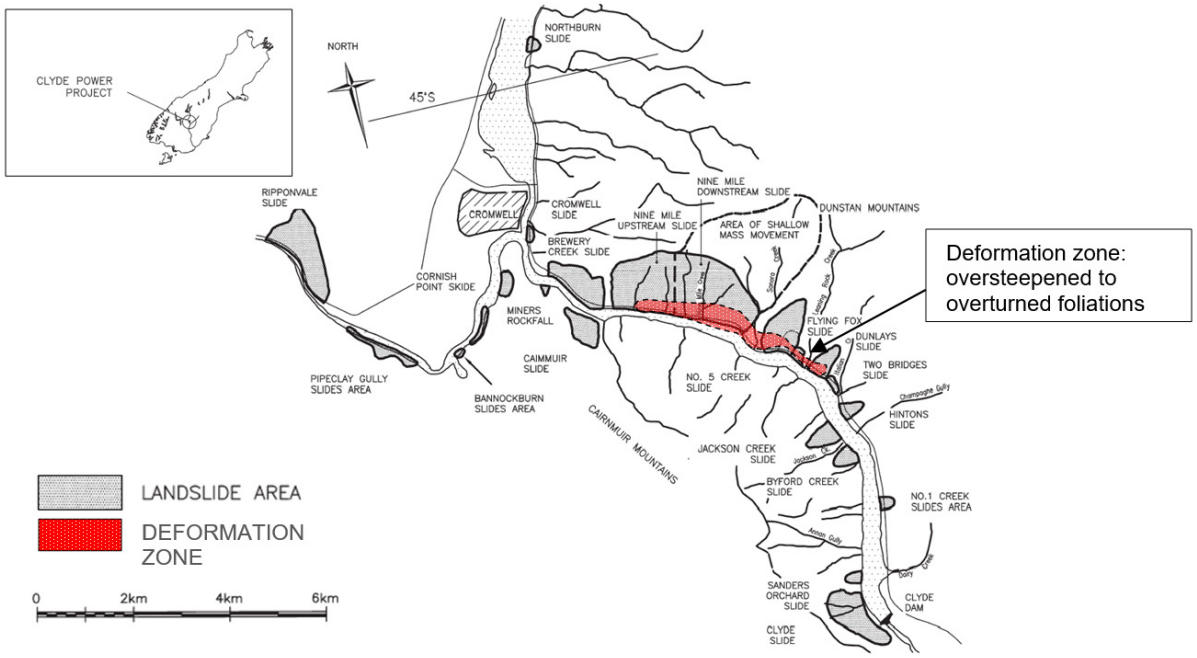


Figure 1. Locality map of Cromwell Gorge depicting approximate locations of major landslides within Lake Dunstan catchment (modifed from Macfarlane 2009).

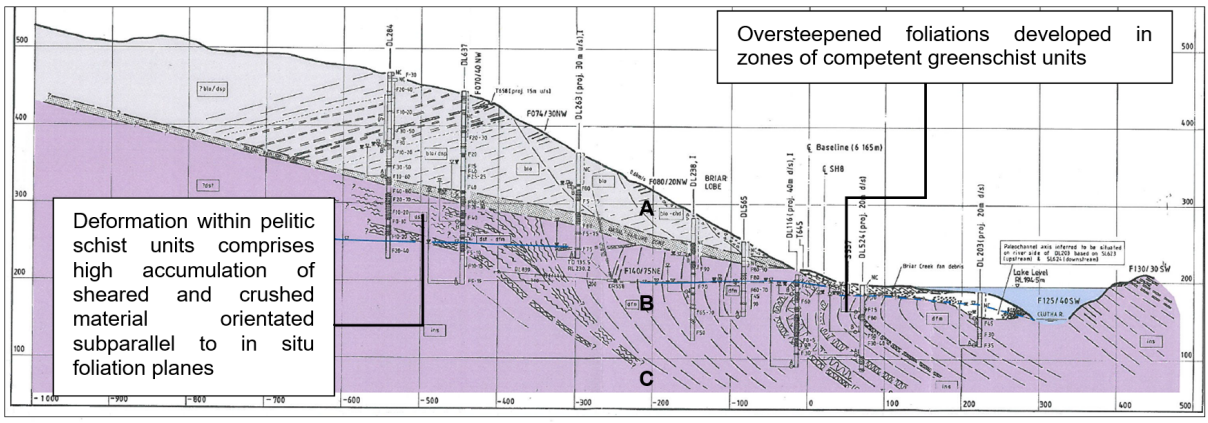


Figure 2. Inferred geological cross section of Nine Mile Slide illustrating three major lithological subdivisions, namely the upper landslide debris and associated basal shear zone (A) directly overlying a zone of deformation (B) which progressively grades into in situ bedrock (C) (from Macfarlane 2010).

3 GEOLOGY AND GEOMORPHOLOGY

The Dunstan flank of Cromwell Gorge is underlain by Rakaia Terrane Schist bedrock characterised by a pervasive schistosity orientated with a general dip of 20° to 40° towards Lake Dunstan. Lithological variations of schist comprise predominantly greyschist ranging from pelitic (micaceous-rich) to

psammitic (quartzofeldspathic-rich) end members with subordinate greenschist units. Central Otago is defined by a complex geological history comprising multiple deformation phases which imparted residual impacts on the rock mass of Cromwell Gorge, exhibited by compressional structures (mesoscopic folds) and extensional features (subparallel foliation shears) (Deckert et al. 2002). Preferential foliation planes impose an anisotropic behaviour of the rock mass in response to stress, defined by average anisotropic index ratios of 1.7 and 2.0 for greenschist and greyschist, respectively.

4 NUMERICAL MODELLING

4.1 Objectives

Deformation observed within Cromwell Gorge is considered to be the result of time-dependent rheological anamorphosis of the rock mass in response to accumulation of strain. Strain accumulated during the evolution of Cromwell Gorge, initiating from the Miocene low relief Waipounamu Erosion Surface (Otago peneplain) (Bishop 1994) progressively deepening through fluvial erosion and uplift (McSaveney et al. 1992). Increasing topographic relief is believed to have induced localised rotation of principal stress axes near the slope surface which coincided with the anisotropic rock mass plane of weakness (schistosity). Induced stresses were compounded by high horizontal far field tectonic stresses associated with the obliquely convergent stress regime of the ongoing Kaikoura Orogeny to produce the deformation observed at the toe of the Dunstan flank.

The primary objective of this study is to numerically simulate the rock mass response to induced stresses associated with progressive deepening of Cromwell Gorge commencing from a relatively low relief surface to present day topography (i.e. the 1400 m deep gorge). Results of the numerical simulation are compared to deformation observed beneath the slide bases of Nine Mile, No. 5 Creek and Dunlays Slides to gain an understanding of processes governing deformation mechanisms.

4.2 Methodology

Rocscience 2D Phase^2 program, a continuum, finite element method (FEM), was used to model the anisotropic nature of the schist rock mass by incorporating an elasto-plastic Mohr-Coulomb algorithm with an explicit joint network. The initiating model is based on the relatively level Otago Peneplain which is subjected to sequential unloading to simulate progressive valley deepening through fluvial erosion and uplift. Sensitivity analyses were undertaken to determine the major contributing parameters governing buckling deformation observed at the base of the Dunstan Mountain Range within Cromwell Gorge. Eighty three FEM models were processed by consecutively varying one parameter at time. Parameters varied in the models consists of rock mass properties, foliations orientations, number of stages taken to incise the valley to present day topography, topographic loading and relief, locked in tectonic stresses, seismic shaking as well as hydraulic conditions.

4.3 Boundary conditions and field stresses

Sequential unloading (Figure 3) commencing from the Otago Peneplain was developed by subdividing the geometric attributes of Cromwell Gorge evolution into four phases. Each phase pertained to a unique slope morphology based on assumptions regarding the catchment size of the gorge, associated channel width-to-depth relationships, and exhumation rates. Suggested exhumation rates of 0.28 mm/yr (Adams and Gabites 1985) becoming 0.6 mm/yr (Little et al. 1999) for last the 400 ka were applied by assuming congruent exhumation, whereby fluvial erosion (valley incision) was synchronous to uplift throughout Cromwell Gorge.

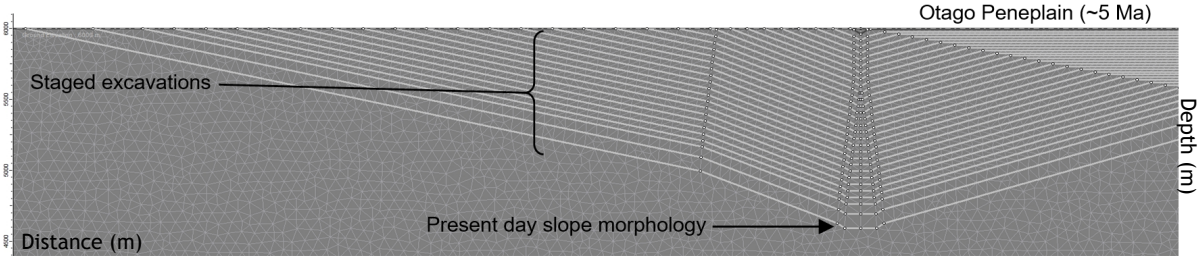


Figure 3. Sequential unloading (staged excavations) simulating valley evolution from Otago Peneplain to present day topography (1400 m deep).

In situ crustal stresses, including gravity and far field tectonic influences, were incorporated into sensitivity analyses using variable ratios (k) between horizontal (σ_h) and vertical (σ_v) stresses. Values for k ranged from 0.26 through to 5, representing purely gravitational stresses as a function of overburden weight and elastic deformation of the rock mass as well as topographical loading effects as suggested by Augustinus (1995) and Kinakin and Stead (2005).

Far field tectonic stresses associated with the obliquely convergent stress regime of the ongoing Kaikoura Orogeny were estimated from in situ field measurements carried out at Clyde Dam. In situ field stress measurements yielded maximum horizontal loads originating from the northwest (Table 1), coinciding with geodetic vectors associated with the Alpine Fault (Figure 4). FEM simulations of the topographic relief and rock mass properties at Clyde Dam produced induced gravitational stresses of similar magnitude to in situ minimum horizontal stresses. It was therefore deduced that the difference between the maximum and minimum in situ horizontal stresses corresponded to the far field tectonic stress regime, as indicated in Table 1. A locked in horizontal stress of 12.50-13.00 MPa were therefore incorporated into sensitivity analyses to represent active regional compressional tectonics.

Table 1. Locked in tectonic stresses derived from the difference between minimum and maximum in situ horizontal stresses (σ_h)

Analysis	In situ field stress results	FEM simulation results
Depth (m)	125.00	125.13
σ_v (MPa)	3.25	3.95
σ_h min. (MPa)	10.50	10.85
σ_h max. (MPa)	23.00	
σ_h max. (true bearing)	306^0 (similar direction as geodetic vectors indicated in Figure 4)	
Tectonic Stress (σ_h max. – σ_h min.)		12.50 – 13.00 MPa

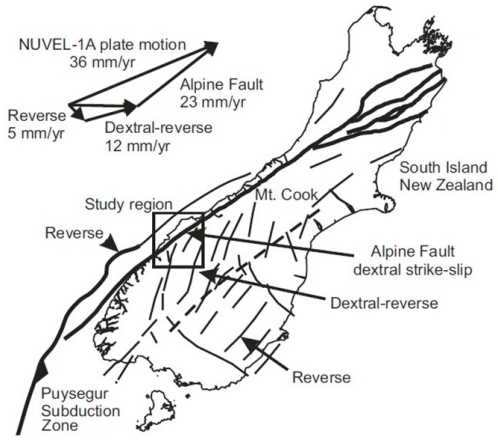


Figure 4. Geodetic measurement vectors for the NZ South Island, modified from Sutherland et. al. (2006) and DeMets et al. (1994).

4.4 Material properties

Mohr-Coulomb elasto-plastic rock strength parameters, derived during this study through a series of laboratory tests including Uniaxial Compression Strength (UCS), triaxial, indirect tensile, point load and direct shear box tests, were collated with existing literature pertaining to Otago schists. Selected parameters included in the FEM models are given in Table 2. Schistosity anisotropy was modelled by including an explicit joint network corresponding to foliation planes. Sensitivity variations included modelling the effects of i) anisotropy imposed by the intact filiations planes and ii) the effects of the lower shear strength subparallel foliation shear planes identified at an average spacing of 8 m throughout the Rakaia Terrane schist bedrock (related to extensional metamorphism). Geometric attributes (spacing and orientation) of foliation planes as well as Mohr-Coulomb properties were varied during sensitivity analyses. Foliation properties were modelled using both the intact rock strength and foliation shear planes, with a range of normal stiffness (k_n) between 438 to 5833 MPa/m, and shear stiffness (k_s) from 66 to 583 MPa/m.

Table 2. Peak and residual material properties derived for Cromwell Gorge Schists

	Poisson's ratio	Young's Modulus (MPa)		Tensile Strength (MPa)		Angle of friction (°)		Cohesion (MPa)	
		Peak	Res.	Peak	Res.	Peak	Res.	Peak	Res.
Greyschist	0.32[a]	3145[a]	2076[a]	0.005[a]	0	32[a]	28[a]	8.50[a]	0.12[a]
Greenschist	0.26[a]	6979[a]	4606[a]	0.005[a]	0	50[a]	27[b]	7.95[a]	0.26[b]
Foliation shears		-	-	0	0	27[a]	18.5[b]	0.12[a]	0.00[b]

[a] this study (2015-2016 data) [b] Smith and Salt (1991)

5 RESULTS

Sensitivity analyses reveal that specific combinations of high locked-in horizontal tectonic stresses, foliation stiffness and orientation contribute to the development of flexural toe buckling in the form of 'z-shaped' folds at the base of the Dunstan Mountain Range. Shear stress accumulates within a zone of abrupt maximum principal stress (σ_1) orientation change, which occurs between topographically induced gravitational stresses, where σ_1 is subparallel to the slope ('g' referenced stress trajectories in Figure 5), and far-field horizontal tectonic stresses, which dominate along the base of the slope ('t' referenced stress trajectories in Figure 5). Where moderately inclined foliations (30-40°) are orientated slightly steeper than the slope (23°), gravitationally induced σ_1 dominates the stress fields adjacent to the slope and acts subparallel to foliations, facilitating shearing along the preferential plane of weakness (foliations). Near the base of the slope, induced stress orientations are compounded by far field horizontal tectonic stresses, resulting in the abrupt rotation of σ_1 from subparallel to foliations to a sub horizontal orientation. This abrupt stress rotation reduces the magnitude of shear stress and subsequent displacement along foliation planes. High shear strains accumulate within this zone in the form of localised linear shear bands, which leads to the development of flexural 'z-shaped' folds resembling toe buckling (Figure 5). Deep-seated mass movements of the landslide complexes likely developed in response to toe breakout at the zone of maximum curvature along the 'z-shaped' flexural buckled folds and, were therefore influenced by the moderately inclined (30-40°) dip of the schist bedrock.

The anisotropic behaviour of schist is demonstrated using models with variable foliation orientations. Topographically induced gravitational stresses are obliquely oriented to sub horizontally to gently inclined (10-20°) and sub vertically (80°) inclined foliations. Maximum stress does not act directly parallel to the preferential plane of weakness represented by foliations, therefore, the magnitude of shear strain produced along foliation planes is reduced. Consequently, flexural 'z-shaped' folds do not develop, but deformation is expressed by flexural bending of the foliation planes as shown in Inserts A and B of Figure 5.

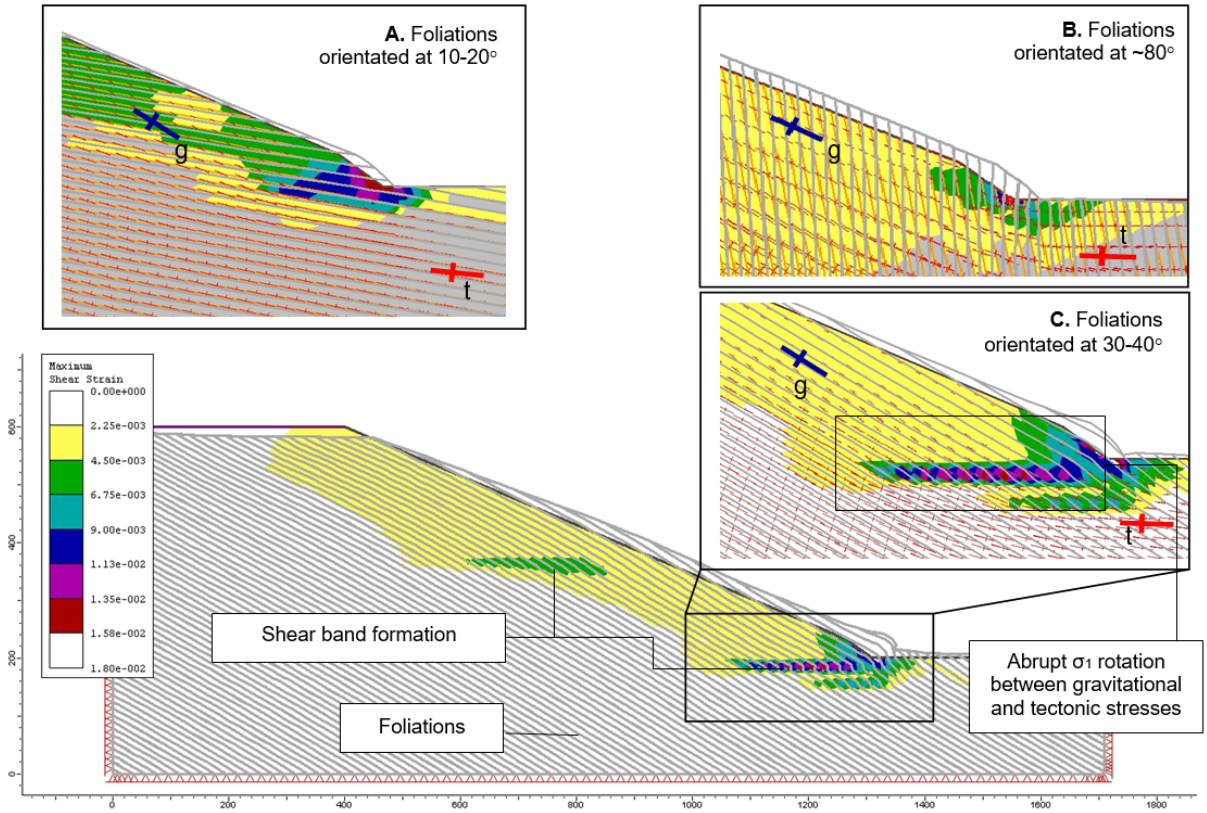


Figure 5. Foliations deform via flexural buckling developed along bands of maximum shear strain due to localised rotations of principal stress axes between induced gravitational (stress trajectories referenced g in insets) and far field tectonic principal stress (stress trajectories referenced t in insets) orientations. Note the height of the slope was scaled from 1400 m to 400 m for model simplification.

Development of flexural toe buckling is also influenced by stiffness of the material. A certain magnitude of competency is required to facilitate buckling. At low assigned shear and normal stiffness, the material yields along planar foliations because it has insufficient residual resistance and preferentially shears along existing planes of weakness (foliation shears). At higher stiffnesses, foliations facilitate plastic deformation withstanding complete dislocation, and deform in a curvilinear manner. The result of this behaviour is demonstrated beneath the slide base at Nine Mile Slide (Figure 2). Competency contrasts between stronger greenschist units deform through flexural buckling exhibiting oversteepened foliations, whereas the less competent pelitic greyschist completely shears without developing relative steepening along foliation planes.

6 CONCLUSION

Numerical FEM simulation of Cromwell Gorge's evolution from a relatively low relief surface corresponding to the Otago Peneplain to present day topography demonstrates that observed deformations at the base of the Dunstan flank of the gorge is a product of prolonged stresses acting on an anisotropic rock mass. Results indicate that a combination of induced gravitational stresses and high horizontal tectonic stresses coinciding with a lithologically variable rock mass are responsible for the anomalously oversteepened foliations beneath Nine Mile, No. 5 Creek and Dunlays Slides. Flexural toe buckling through shear and tensile dislocations of moderately inclined (30-40°) pervasively foliated schist bedrock develop in response to abrupt rotations of principal stress axes developed at the intersection of topographically induced slope parallel gravitational stresses and the far field horizontal tectonic stresses. Accumulation of strain in zones of localised rotation of principal stress axes initiate the development of flexural 'z-shaped' buckled folds at the toe of the slope. Progressive accumulation of strain along these buckled folds exceeded the low tensile and shear strength of the schist which led to toe break out and overall kinematic instability of the Dunstan flank of Cromwell Gorge.

7 ACKNOWLEDGEMENTS

This study would not have been possible without the permission of Contact Energy. For all the valuable input and reviews gratitude must be extended to D. Macfarlane, D. Beetham, D. Fergusson and R. Thomson. Two anonymous reviewers of this paper must also be thanked. Support and funding for this research was made possible by UC Master's Scholarship, Royal Commonwealth Society Canterbury Scholarship, Charles Cook, Warwick House Memorial Scholarship, Mason Trust Research Fund and Digitalglobe Foundation.

REFERENCES

Adams, C. and Gabites, J. (1985). "Age of metamorphism and uplift of Haast Schist Group at Haast Pass, Lake Wanaka and Lake Hawea, South Island, New Zealand", *New Zeal. J. Geol. Geophys*., 28, pp.85–96.

Agliardi, F., Crosta, G. and Zanchi, A. (2001). "Structural constraints on deep-seated slope deformation kinematics", *Eng. Geol*., 59, pp.83–102.

Augustinus, P. (1995). "Glacial valley cross-profile development: the influence of in situ rock stress and rock mass strength, with examples from the Southern Alps, New Zealand", *Geomorphology*, 14(95), pp.87–97.

Beetham, R., Moody, K., Fergusson, D., Jennings, D. and Waugh, P. (1991). "Landslide development in schist by toe buckling", in Bell, D. H. (ed.), *Proc. 6th Int. Symp. Landslides*, Christchurch, New Zealand, A.A Balkema, pp. 17–23.

Bishop, D.G. (1994). *Extent and regional deformation of the Otago peneplain,* Dunedin, Institute of Geological & Nuclear Sciences Science Report 94/1.

Cavers, D. (1981). "Simple methods to analyze buckling of rock slopes", *Rock Mech*., 14, pp.87–104.

Deckert, H., Ring, U. and Mortimer, N. (2002). "Tectonic significance of Cretaceous bivergent extensional shear zones in the Torlesse accretionary wedge, central Otago Schist, New Zealand", *New Zeal. J. Geol. Geophys*., 45(4), pp.537–547.

DeMets, C., Gordon, R., Argus, D. and Stein, S. (1994). "Effect of recent revisions to the geomagnetic reversal time scale on estimates of current plate motions", *Geophysical Research Letters*, 21(20), pp.2191–2194.

Hu, X. and Cruden, D. (1993). "Buckling deformation in the Highwood Pass, Alberta, Canada", *Can. Geotech. J*., 30, pp.276–286.

Kinakin, D. and Stead, D. (2005). "Analysis of the distributions of stress in natural ridge forms: Implications for the deformation mechanisms of rock slopes and the formation of sacking", *Geomorphology*, 65, pp.85–100.

Little, T., Mortimer, N. and McWilliams, M. (1999). "An episodic Cretaceous cooling model for the Otago-Marlborough Schist, New Zealand, based on 40 Ar/ 39 Ar white mica ages", *New Zeal. J. Geol. Geophys*., 42(3), pp.305–325.

Macfarlane, D. (2010). *Nine Mile (Downstream) Slide Performance Review*, URS New Zealand Limited.

Macfarlane, D. (2009). "Observations and predictions of the behaviour of large, slow-moving landslides in schist, Clyde Dam reservoir, New Zealand", *Eng. Geol*., 109, pp.5–15.

McSaveney, M., Thomson, R. and Turnbull, I.M. (1992). "Timing of relief and landslides in Central Otago, New Zealand", in Bell, D. H. (ed.), *Proc. 6th Int. Symp. Landslides*, Christchurch, New Zealand, A. A. Balkema, pp. 1451–1456.

Pereira, L. and Lana, M. (2013). "Stress-Strain Analysis of Buckling Failure in Phyllite Slopes", *Geotech. Geol. Eng*., 31, pp.297–314.

Smith, A. and Salt, G. (1991). *Clyde Power Station Reservoir. General report on geotechnical materials involved in landsliding: mineralogical, shear strength and related properties.* New Zealand Geological Survey.

Stead, D. and Eberhardt, E. (1997). "Developments in the analysis of footwall slopes in surface coal mining", *Eng. Geol.*, 46, pp.41–61.

Sutherland, R., Berryman, K. and Norris, R. (2006). "Quaternary slip rate and geomorphology of the Alpine fault: Implications for kinematics and seismic hazard in southwest New Zealand", *Geol. Soc. Am. Bull.*, 118(3-4), pp.464–474.

Tommasi, P., Verrucci, P. Campedel, P., Pettinelli, E. and Ribacchi, R. (2009). "Buckling of high natural slopes: The case of Lavini di Marco (Trento-Italy)", *Eng. Geol.*, 109(1-2), pp.93–108.

Wang, W., Chigira, M. and Furuya, T. (2003). "Geological and geomorphological precursors of the Chiu-fen-erh-shan landslide triggered by the Chi-chi earthquake in Central Taiwan", *Eng. Geol.*, 69(1-2), pp.1–13.

This page intentionally left blank

Proceedings of the 11th ANZ Young Geotechnical Professionals Conference – 11YGPC
Queenstown, New Zealand
25 – 28 October 2016

Design and construction of an egress tunnel beneath a working hospital

Mei Ling Teoh[1], Bernard Shen[2] and Garry Mostyn[3]

[1]Pells Sullivan Meynink, G3, 56 Delhi Road, North Ryde, 2113 New South Wales; PH (02) 9812 5000; email: meiling.teoh@psm.com.au
[2]Pells Sullivan Meynink, G3, 56 Delhi Road, North Ryde, 2113 New South Wales; PH (02) 9812 5000

ABSTRACT

This paper discusses the construction and underpinning design of a 24 m long egress tunnel as part of the expansion of an existing hospital in western suburbs of Sydney. The first part of the paper presents the site geology, subsurface conditions and the pre-construction condition of the egress tunnel site. The next part of the paper presents the construction methodologies that were considered and explains the basis for selecting a two heading approach. The final part of the paper details the two designs that were adopted for the underpinning works. The paper demonstrates the value of close collaboration between the designers and constructors which enabled the tunnel to be constructed without disruption to the hospital's daily operation.

Keywords: underpinning, tunnel, pedestrian tunnel

1 INTRODUCTION

A recent project was completed to expand an existing hospital in the western suburbs of Sydney to meet the future healthcare needs of the growing community. The project included a new seven storey clinical services building adjoining the current main hospital building with a new comprehensive cancer care centre, a six storey above ground car park, extensive refurbishment to the existing main hospital building, and a new main corridor (egress tunnel) to connect the new and existing main hospital buildings.

The existing main hospital building is located at the northern end of the hospital site. The hospital site slopes gently down towards the north and northwest. As a result of the slope, access to the existing main hospital building at the northern end is from Level 1 and access to the southern end is from Level 3 as presented in Figure 2. The egress tunnel is located beneath the Level 3 slab of the southern end and links Level 1 and Level 2 of the northern end of the existing hospital to the new hospital building. The internal dimension of the egress tunnel is 24 m long, 4 m wide and 8.4 m high. The plan and long section of the egress tunnel is presented in Figure 1 and Figure 2.

This paper discusses the design of the egress tunnel which was required to be both innovative and practical to construct as well as enabling the tunnel to be constructed without disruption to the hospital's daily operation.

2 SITE GEOLOGY

2.1 Site geology

The Penrith 1:100,000 Geological Sheet as per Clark and Jones (1991) indicates that the site is underlain by Bringelly Shale of the Wianamatta Group comprising shale, carbonaceous claystone, claystone, laminate, fine to medium grained lithic sandstone, rare coal and tuff.

2.2 Encountered subsurface condition

The subsurface conditions encountered at the egress tunnel site consist of residual soil overlying Class IV or V Shale, overlying Class III or better Shale as per the Pells et. al.(1998) classification for Sydney Shales. Class III Shale is typically moderately weathered with joints spaced between 3 to 10 m and intact rock strength between 2 and 15 MPa. Class IV and Class V Shale is more weathered and jointed with weaker intact rock strength.

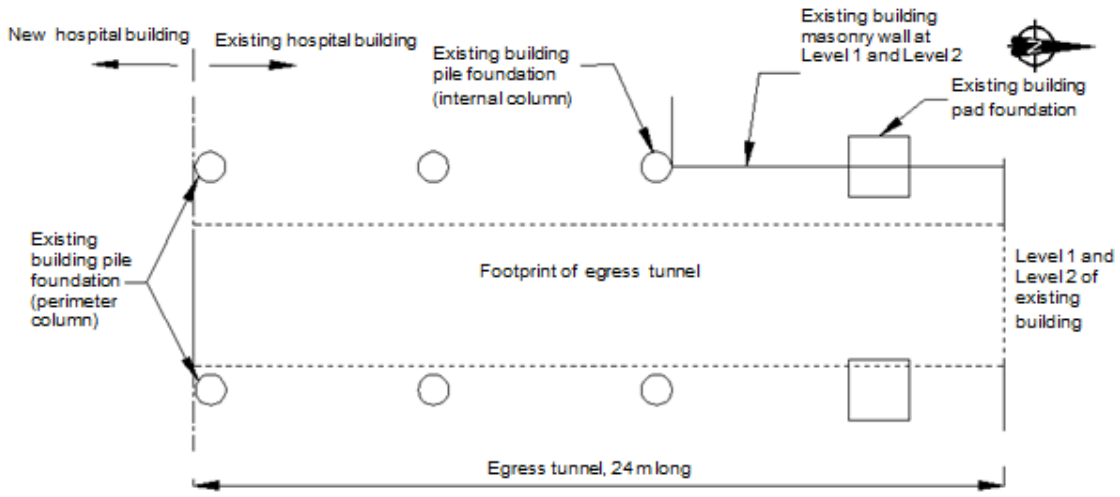


Figure 1. Plan of the egress tunnel site

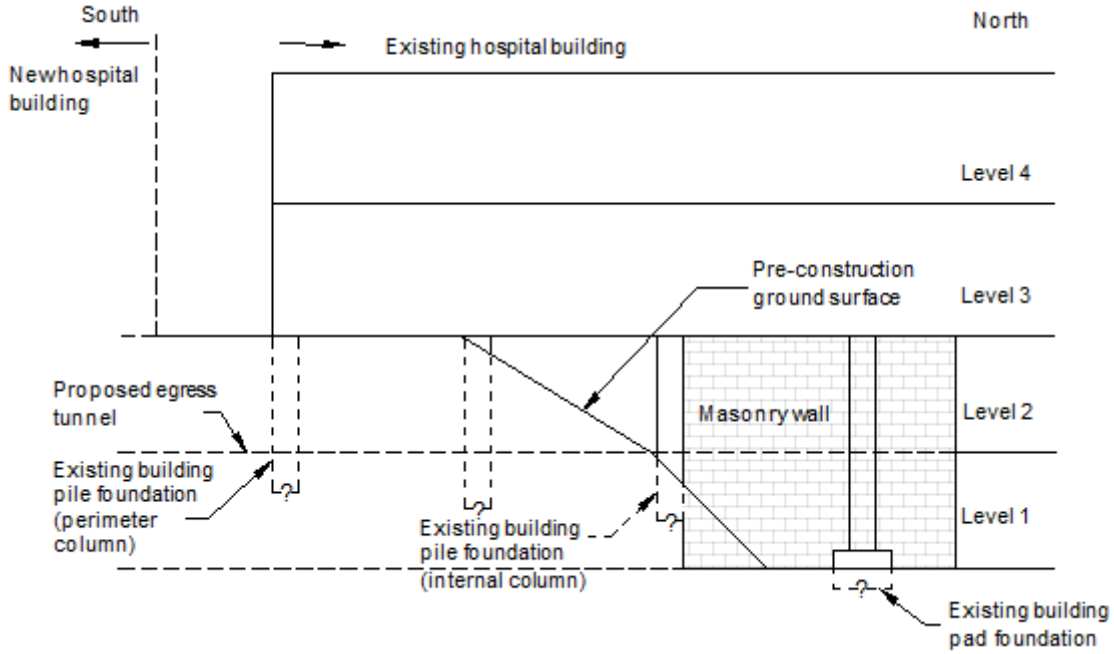


Figure 2. Long section of the egress tunnel prior to excavation and underpinning works

2.3 Existing site condition

A summary of the subsurface and existing site conditions at the egress tunnel site is presented in Figure 3.

Directly beneath the existing hospital Level 3 slab, there are existing live services hung from the slab. These services required to be serviceable during the construction of the egress tunnel to avoid disruption of the hospital daily operations.

There is also an existing masonry wall along the west end of the egress tunnel within the footprint of the egress tunnel. Next to the wall, there was a batter at an angle of approximately 30 degrees above horizontal, sloping upwards away from the wall. The batter was excavated during the construction of the existing hospital to allow for construction of this masonry wall and occupied space on the other side.

There were also existing building foundations immediately adjacent to the footprint of the egress tunnel supporting columns to the floors above. Design drawings of the existing hospital foundations showed that the foundations were unreinforced concrete piles socketed into the ground. The as built founding level of the piles was not provided.

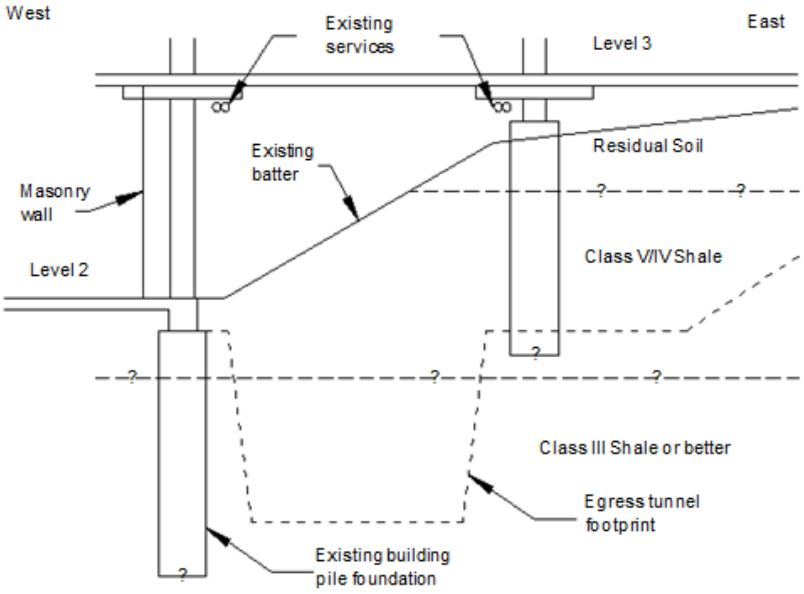


Figure 3. Cross section showing summary of encountered subsurface and existing conditions

3 CONSIDERED CONSTRUCTION AND UNDERPINNING METHODOLOGIES

3.1 Constraints

The design drawings of the existing hospital showed the existing building foundations along east side of the egress tunnel did not extend below the invert of the egress tunnel. The egress tunnel had to be constructed without affecting the columns supported by these. This may have required the columns to be underpinned to below the egress tunnel invert because:

- Rock was not strong enough to support the loads from the columns on a ledge.
- Unknown existing pile depth.
- Existing foundations are unreinforced and therefore could not handle the stress caused by the excavation of the egress tunnel.

Three different construction and underpinning methodologies were considered for the construction of the egress tunnel and are described briefly in the following section.

3.2 Temporary shoring option

The temporary shoring method involved transferring load from the existing column using a horizontal steel beam and vertical props. It was proposed that a steel beam would be placed below the drop-down of the column at the bottom of the Level 3 slab, extending from one column's drop-down to the next column's drop-down across the width of the egress tunnel. The shoring props would be located at each end of the beam as support to keep the beam in place. The construction of the underpinning would commence once the temporary shoring was in place. The temporary shoring would be removed after completion of the permanent underpinning works involving extension of the columns.

This option was eliminated due to the spatial constraints of the site. Approximately 6 m long beams would have been required to extend from one column to the other. The builder considered it would be a challenging task to place the beam at the intended locations due to the tight site access. This method was also excluded due to the availability of suitable shoring props in the market that were at least 4 m long and can withstand the high existing column loads.

3.3 Top down excavation option

The top down excavation method involved excavation of the egress tunnel without any underpinning works. The construction would have involved a 1.5 m deep and 2.2 m wide vertical excavation stage to allow for installation of the support which included anchors, strip drains and shotcrete prior to installation of the egress tunnel wall in front of the vertical face. The 1.5 m x 2.2 m excavation was

proposed due to uncertainty of the existing pile depth which might be affected due to the excavation of the egress tunnel and rock defects that might be encountered on the vertical face. Excavation for the next stage could only have proceeded once support installation for each stage was completed.

Whilst this method did not require underpinning as the existing piles would not have been exposed, it was deemed not to be feasible due to constructability of the excavation support. It would have required a repetitive process of excavation and installation of excavation support, increasing the construction time of the egress tunnel beyond that which was permitted in the tight programme.

3.4 Two heading excavation option

The two heading excavation approach involves excavation in two headings, a top heading and a lower heading. The top heading was excavated to the top of the Level 2 slab and the lower heading was excavated to the invert of the egress tunnel. The excavation of a top heading provided adequate access for underpinning works of the two internal columns and demolition of the two perimeter columns prior to excavation of the lower heading. At the same time the pile toes are kept below the base of the top heading. The lower heading excavation proceeded following the completion of the underpinning works.

This method was selected as it provides the best access beneath the existing hospital building and an efficient and practical design for the underpinning works. More importantly, the construction could be undertaken without compromising the integrity of the existing hospital building foundations and eliminated the potential risks caused by the site constraints.

4 TWO HEADING EXCAVATION METHOD

4.1 Construction sequence details

The construction sequence was carefully defined as it formed a critical part of the design. The egress tunnel was excavated from the southern end of existing hospital towards the Level 1 and Level 2 wall at the northern end. This sequence tied in well with the construction program which had allowed for excavation at the south of the existing hospital building for the new hospital building prior to excavation of the egress tunnel.

The construction sequence for the upper and lower headings is presented as a series of cross sections in Figure 4. The upper heading was excavated in 2.2 m advances to the Level 2 slab level. The 2.2 m advances allowed for careful excavation around the existing perimeter columns in order to inspect the location of the pile toes and allowed for an alternative design should the subsurface conditions differ and internal pile toe depths be higher than expected. The perimeter column pile toes were exposed within the upper heading excavation. The perimeter column loads were transferred temporarily to the adjacent shoring wall piles which were constructed for the new hospital building prior to further excavation of the upper heading. The load transfer was designed by the project's structural consultants. After the load transfer for each perimeter column was completed, the excavation progressed to complete the first 2.2 m advance. The east and west faces were excavated at 1.5H:1V batters. The underpinning works for the internal columns were then undertaken before commencement of the lower heading.

The lower heading was excavated to the invert of the egress tunnel. The excavation was undertaken in 6 m advances to allow for installation of face support prior to further excavation. The east and west faces of the excavation were excavated at 0.5H:1V batter permanently supported by anchors, strip drains, mesh and shotcrete prior to excavation of the next advance. The new perimeter columns were then constructed to complete the underpinning works. The loads which were temporarily transferred to the shoring wall piles were transferred into the new columns.

4.2 Underpinning design

4.2.1 Internal column underpinning

The construction sequence of the internal column underpinning is presented in Figure 4. The underpinning of each internal column involved construction of four new piles, two blade walls and a

rigid headstock. At each internal column, four new piles, two at each side of the column were drilled and poured from the completed upper heading excavation level to 0.5 m below the tunnel invert using a low head height piling rig. The piles were 0.5 m in diameter and 4.2 m long. Similar to the perimeter column design, the internal column piles were designed in accordance with AS3600. The two blade walls, one at each side of the column were constructed to the bottom of the headstock. The blade walls were 0.5 m long, 1.8 m wide and 3.2 m high. The headstock (2.9 m long x 1.8 m wide x 1.3m high) was then constructed to the existing column drop-down. Non-shrink grout was applied between the headstock and drop-down to provide uniform contact for load distribution from the column above to the headstock. The existing services within the headstock were protected with 50 mm compressible lagging. The exposed existing column face within the headstock was scabbled to ensure good surface contact between the existing concrete and new concrete.

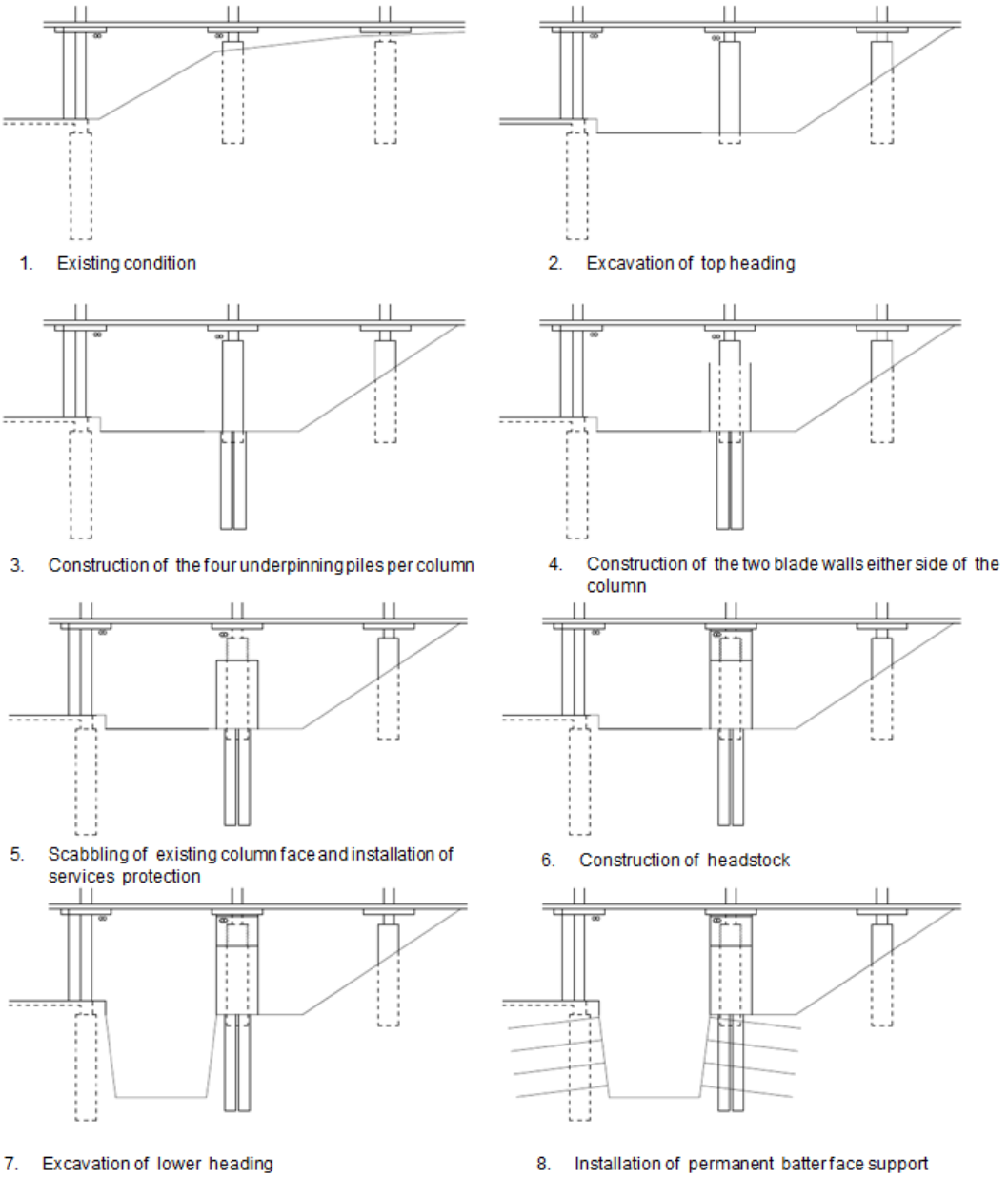


Figure 4. Lower heading, upper heading and internal columns construction sequence

4.2.2 Perimeter column underpinning

Figure 5 presents the construction sequence of the perimeter column underpinning. The perimeter column underpinning design involved demolition of existing columns and construction of new longer columns. The underpinning design adopted for the internal columns (as described in Section 4.2.2) could not be utilised for the perimeter columns due to its location which would have resulted in the

underpinning columns being within the tunnel envelope. Therefore, demolition and reconstruction of the existing perimeter columns was the approach adopted.

Each new perimeter column was constructed from base of the Level 3 existing edge beam to the invert of the egress tunnel. The columns were 0.75 m in diameter and 8.2 m long, socketed 0.5 m below the tunnel invert level. The columns were designed in accordance with Section 10 – Design of Columns for Strength and Serviceability of the AS3600-2009 Concrete Structures standard. Chemical anchors and non-shrink grout were used at the contact between the existing edge beam and the newly constructed column to provide a durable connection between the two structural elements. Once the new perimeter concrete gained adequate strength, the loads were removed from the shoring wall piles and introduced to the new columns.

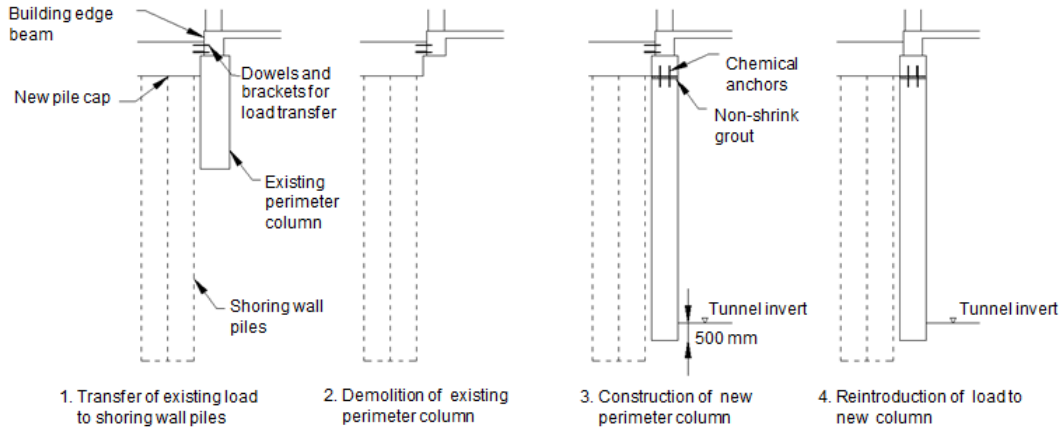


Figure 5. Northsouth cross section of perimeter columns construction sequence

5 CONCLUSION

The construction and underpinning design adopted for the egress tunnel demonstrate an innovative, practical and effective solution for a spatial constraint site. The construction of the egress tunnel was completed successfully without any impacts or disruption to the ongoing operation of the existing hospital.



(a) *(b)*

Figure 6. (a) The excavated egress tunnel looking north; and (b) a completed headstock and pair blade walls

REFERENCES

Clark, N. R. and Jones, D. C., (1991), "Penrith 1:100 000 Geological Sheet 9030, 1st edition". Geological Survey of New South Wales, Sydney.

Pells, P. J. N., Mostyn, G. and Walker, B, F., (1998), "Foundations on Sandstone and Shale in the Sydney Region". *Australian Geomechanics*, 33(3)

Bertuzzi, R. and Pells, P. J. N., (2002), "Geotechnical Parameters of Sydney Sandstone and Shale." *Australian Geomechanics*, 37(5)

AS3600 (2009), Concrete Structures

Proceedings of the 11th ANZ Young Geotechnical Professionals Conference – 11YGPC
Queenstown, New Zealand
25 – 28 October 2016

"Seeking Relief" Rising Pore Pressures in Earth Dams – A Case Study

N. P. Burrows[1], NZGS.

[1] Riley Consultants Ltd, P.O Box 100253 North Shore, Auckland 0745, PH (09) 489 7872; email:nburrows@riley.co.nz

ABSTRACT

Patea Dam is owned by Trustpower Ltd. (Trustpower) and is a zoned earth dam. On commissioning, lake pressures were observed to be transferring into the underlying geology. This created an increased artesian pressure within the footprint of the structure, reducing the dam's Factor of Safety (FoS) below what would be expected of a high Potential Impact Classification (PIC) dam. Remedial measures were investigated to correct long-term pressure trends at Patea Dam and ensure the long-term safety of the dam for its owner; the residents below the dam; and the recreational users of Lake Rotorangi. The approach of drilling relief wells into the underlying foundation is a method that had been historically used at Patea Dam, resulting in successful alleviation of excess artesian pressures. In April of 2015 a further two wells were commissioned to reduce the ongoing build-up of pore pressure. Numerous obstacles were overcome during the installation process, including challenging access and dangerous weather conditions to reach a satisfactory outcome for all parties involved. Initial results saw an approximate drop of 2m in the artesian pressures below the toe of the dam increasing the dams FoS and reducing artesian pressures to below identified alarm levels. This case study shows how relief wells can be successfully installed, even with numerous challenges, to safe-guard an important piece of New Zealand's infrastructure for the future.

1 INTRODUCTION AND PROJECT BACKGROUND

The Patea Hydro Electric Scheme owned by Trustpower and commissioned in 1984 consists of a zoned earth dam located 35km upstream from Patea Township in South Taranaki. The dam location was chosen due to a favourable diversion arrangement, simple geology, and the local availability of material suitable for dam construction. The dam has an overall crest length of 195m, with a maximum height of 78m and the upstream and downstream slopes of 1 in 2.5 and 1 in 2 respectively. Essentially the dam was constructed using the siltstone and sandstone material found in close proximity to the site. The dam was commissioned in 1984.

A series of monitoring piezometers were installed to monitor possible increases in artesian pressures within the toe of the dam. During the first month of filling it became apparent that lake pressures were being transmitted relatively rapidly into the sandstone layer below a limestone unit, creating artesian conditions that could lead to instability of the dam toe slope. As a remedial action, a series of 15 relief wells were installed in early 1984 to mitigate the rising artesian pressures. A second set of relief wells were installed in 1996 due to piezometric levels exceeding warning levels once again.

Following the 1996 relief well installation, a general rising trend in piezometric levels was observed with readings exceeding warning levels once more. As part of the 2010 Comprehensive Safety Review it was recommended that consideration be given to installing additional remedial measures (relief wells) to improve overall dam stability ensuring the future integrity of the dam.

2 REGIONAL GEOLOGY

The Institute of Geological Nuclear Sciences Ltd. (GNS) 1:250,000 geological map of the Taranaki area (GNS geological 2008 map 7) indicates the site is underlain by Matemateaonga Formation with Tangahoa Formation found above. The dam structure is founded within the Matemateaonga Formation. Matemateaonga Formation is predominately muddy sandstone with repeated shellbed limestone, siltstone, sandstone and minor conglomerate layers. These rocks are layered and dip gently towards the southwest at between 4° and 6° downstream.

2.1 Dam Site Geology

The geology encountered on-site during construction is shown schematically in Figure 1. The geological units were primary alternating limestone and sandstone/siltstone layers. The upper layer consisted of superficial protective tailrace backfill/riprap comprising large, irregular boulders from ground level to between 4m and 7m depth. A 1m thick, extremely strong limestone layer (Limestone 2) underlies the riprap layer. The base depth of Limestone 2 is deeper nearer to the powerhouse than by the right abutment. The boundary between the Limestone 2 and the underlying BS2 siltstone/ sandstone was observed as a sharp contact. BS2 siltstone/sandstone material comprised minor marine fossils found in the form of shell fragments. Another sharp contact was observed into an additional strong limestone layer (Limestone 1) with large shells, whole and fragmented. The final underlying layer is blue grey massive sandstone similar to BS2. An aquifer has been identified within this lower sandstone layer (BS2) and is capped in place by the Limestone 2 unit above.

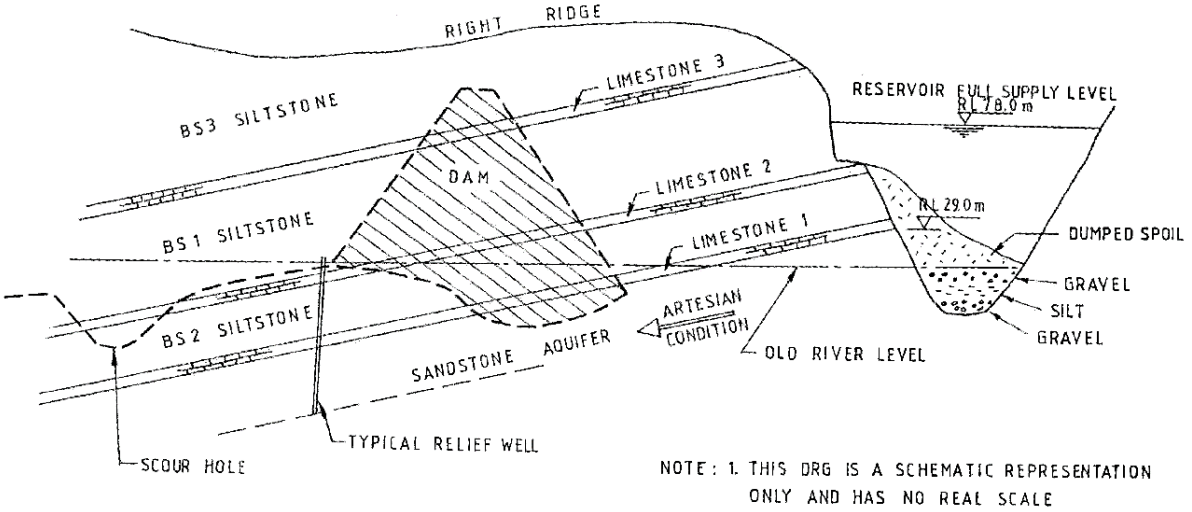


Figure 1. Schematic geological and artesian profile at Patea Dam

3 DAM STABILITY AND REMEDIAL MEASURES

The Patea Dam is considered a high Potential Impact Classification (PIC) dam which is a rating that represents the consequence of a dam failure. According to the guidelines (NZSOLD, 2015), high PIC dams are required to undergo a high level Comprehensive Safety Review (CSR) every five years. CSRs review the civil, geotechnical, mechanical and electrical safety aspects of a dam. The Commissioning Addendum report identified foundation piezometric levels, equating to a FoS against buoyant uplift of 1.5, for the purpose of determining appropriate alarm levels. These alarm levels were determined via stability analysis – for example a warning level of RL 26m was deduced. The 2010 CSR commented that W02 piezometric levels were close to the RL 26m and noted there would be a FoS reduction during a large seismic event (Grilli, 2010). The CSR reviewer recommended installing additional relief wells to reduce the increasing artesian pressures, or to place free draining rock-fill toe support. Trustpower indicated a preference for relief well installation.

4 RELIEF WELL DESIGN AND INSTALLATION

Two pressure relief wells (PR1 and PR2) were drilled to a depth of 38.5m and 40m respectively below the dam toe ground surface. Two open standpipe piezometers (PP1 and PP2) were drilled to a depth of 19m (1m into the aquifer) to replace existing damaged standpipe piezometers. The new pressure relief wells and piezometers were drilled at the dam toe marginally upslope of the original monitoring points. This allowed for monitoring of groundwater flows, groundwater depths, and to provide a safety buffer between the site crew and the variable tailwater levels for relief well installation. The locations of the above remedial measures are shown in Figure 2.

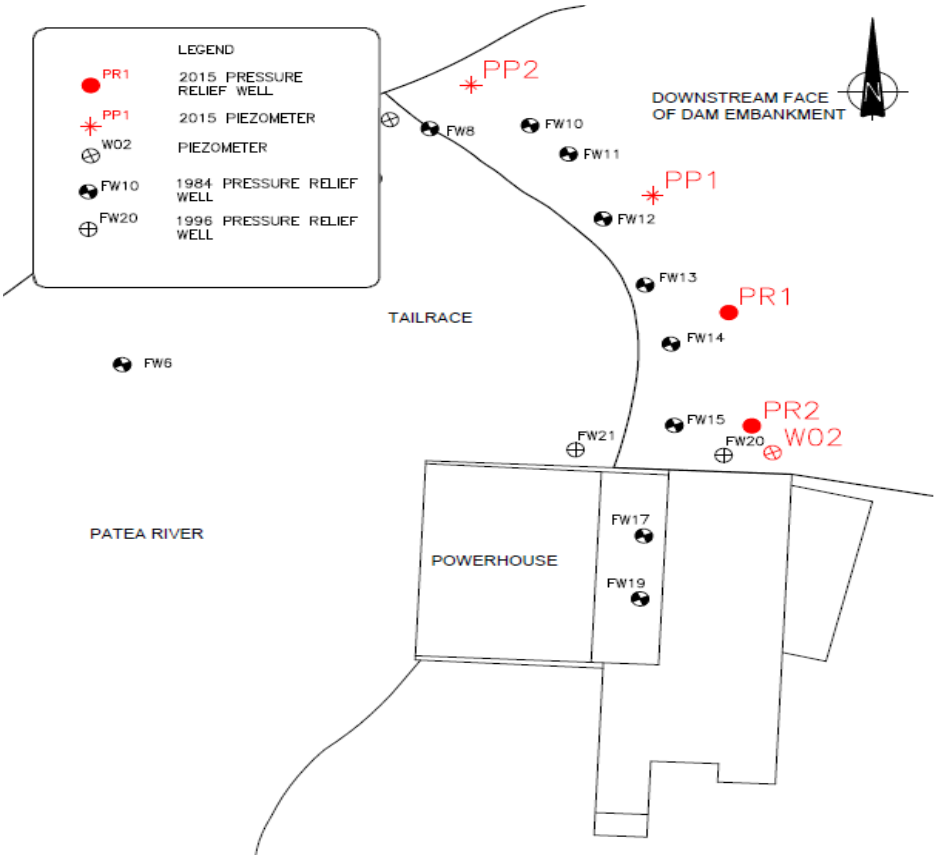


Figure 2. Patea dam remedial measures site plan

4.1 Relief Well Design

The 2015 relief well and piezometer configurations were retained from the original as-built design, with some exceptions. The elements retained from the original design included the casing material, grout backfill detail, non-return valves (to prevent high tailwater levels pressurising the foundation), and casing diameters. Target depths of 20m below the limestone were also retained in the final detail of the relief wells.

Some design modifications were required from the original relief well design to increase their longevity and usefulness. These are discussed below.

4.2 Design Modifications

4.2.1 Upstand Improvements

The original relief well design included cut gas slots around the full circumference of the well casing. This design was not conducive to flow monitoring, whereas the new relief well upstands have aligned spouts, which are more suitable for flow monitoring.

4.2.2 Relief Well and Piezometer Slotted Screen and Backfill Detail

Current practice for pressure relief well screens is for screen openings to be no greater than the D_{50} effective diameter of the backfill filter material, for example, gravelly sand (Fell 2014). D values are typically ascertained from particle size distribution curves. For uniformly graded filter material (as used in the 2015 installation) screen openings were no larger than the D_{15} value. This minimises excessive filter in-wash through slot openings and allows groundwater inflow. The 2015 relief well screen openings were 0.5mm, consistent with the original design.

A comparison of the 2015 relief well backfill with the equivalent used during construction/ commissioning was completed. The Commissioning Report (Beca, 1985) notes the backfill comprised filter sand and specifies the piezometer filter material as that used in Zone 4 of the embankment dam.

Zone 4 grading values, indicated a D_{15} value of 0.22mm. This value is noticeably lower than the 0.5mm slot openings and is low when compared with Fell's criterion for screens and filter material. Hence, it is suggested in-wash of fine filter material may have migrated into the older relief wells with time, reducing their effectiveness.

The backfill is also required to be sufficiently fine to act as a filter to the bedrock as seepage flows into the well. The D_{15} of 0.7mm meets the no erosion criteria for the siltstone/sandstone. It is noted that this is slightly coarser than the Zone 4 grading used in the 1984 and 1996 relief well installations.

4.3 Relief Well Drilling and Installation

Due to the remote nature of the site and difficult access (there is no road access to the dam toe), specialist equipment was required. This equipment comprised of the HPP150 (designed, built and customised by Webster Drilling Limited), heli-portable drill rig, steel drum mixers, tools and accessories.

Borehole pressure relief well 2 (PR2) was predominantly cored, with samples retrieved and classified according to the New Zealand Geomechanics Society (NZGS) Guidelines (NZGS, 2005). The remaining boreholes were classified from observations of drill rig vibrations, monitoring drilling water loss/gain, drill bit progression, observations of drill cuttings and return fluid.

The purpose of coring PR2 was to prove the underlying geological units. Remaining boreholes were drilled via augering and mud rotary drilling with direct circulation, whereby core sample was not retrieved. This method was used to speed up drilling times and to reduce the overall budget costs.

As expected, drilling progress through tailrace backfill (often comprising riprap boulder material) and limestone strata was slow and associated with moderate to heavy drill rig vibrations. Drilling in sandstone/siltstone was steady, with light drill rig vibrations.

An auger was used to drill through the tailrace/riprap layer, and the 200mm casing was inserted to varying depths. The casing was grouted in place and left overnight to set. Aside from PR2, drilling difficulties were encountered for all boreholes in the initial tailrace/riprap layer which meant the 200mm casing could not be inserted to 5m preferred depth. The site team reported that loose material, possibly due to elevated tailwater levels, collapsed back into the borehole, preventing full insertion of the 200mm casing.

Following installation of the 200mm casing, the team commenced a 100mm diameter drillhole through the grout backfill and into the limestone and BS2 layers. The 100mm diameter steel casing was then installed, with the base founded in Limestone 1, grouted and left overnight to set. The final stage of drilling was to reach target depths below Limestone 1. The 2015 drilling indicated that the geology was consistent with what we expected described in sections 2 and 2.1.

5 MONITORING RESPONSE AND OBSERVATIONS

Following the installation of the 2015 relief wells, foundation piezometer W02 responded with a noticeable decrease in piezometeric levels. Figure 3 highlights the W02 pressure trends and when relief wells were installed. Current W02 piezometric levels are the lowest since mid-2005 and are approximately 2m lower than the monitoring system warning level of RL 26m. This suggests an increased FoS above 1.5. Foundation piezometer W02 is a key piezometer as it has historically exhibited good response to relief well installations.

It was also noted that a gradual 1.2m decrease of piezometric levels occurred during drilling of PR1 to the newly installed Piezometer 1 (PP1), and Piezometer 2 (PP2) from 15 to 22 April 2015. Monitoring over this time also showed a piezometric level increase of 0.5m on 6 April 2015 followed by a 1m step decrease on 7 April 2015. It is unclear what caused W02 to increase and decrease from 6 to 7 April 2015, particularly as no drilling occurred during this period. Prior to Easter, PR2 drilling had only progressed into the (upper) Limestone 2 layer. One possibility may be a foundation response following a period of heavy rain and increased reservoir level. It is consider the W02 pressure decrease from 15 to 22 April 2015 was caused by the drilling and installation of PP1, PP2, PR1, and

PR2. The artesian pressure responses described during the duration of the 2015 relief well programme is shown in Figure 4.

Another observation noted from the completed relief wells was a sulphur-like smell of the discharged water. This was particularly noticeable following completion of PR2 and, to a lesser degree, PR1. It is assumed the groundwater odour may be due to water contact with limestone formations and/or organic content. This is not considered a dam safety issue.

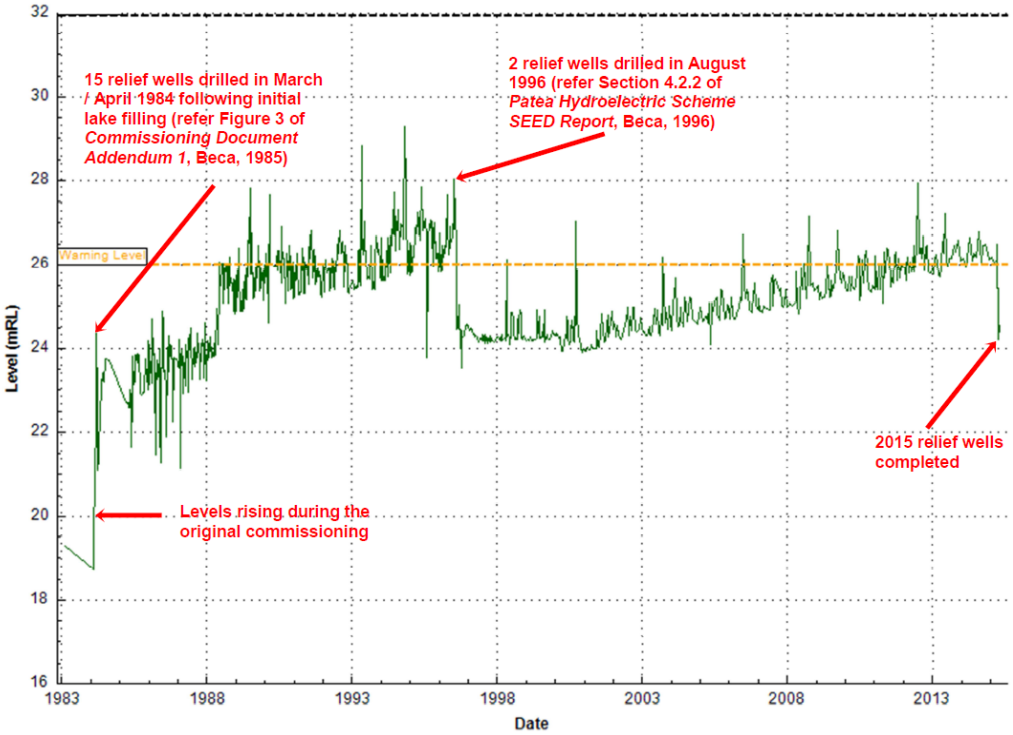


Figure 3. Annotated time series plot for foundation piezometer W02 (entire instrument history)

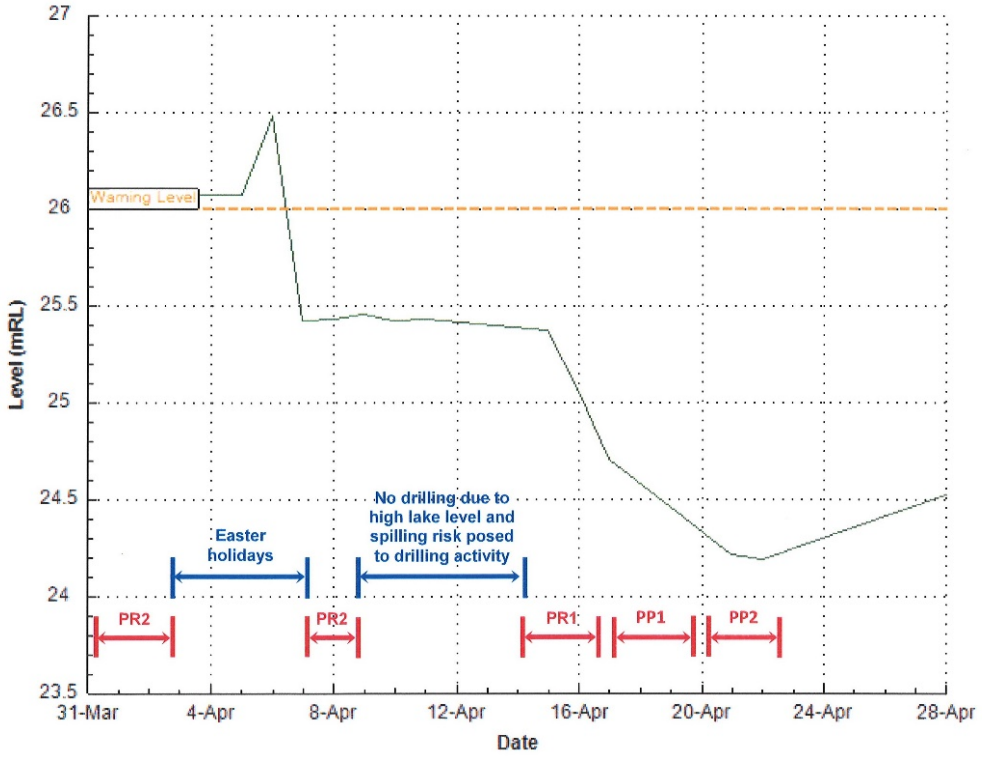


Figure 4. Annotated time series plot for foundation piezometer W02 during installation (four week period)

6 CONCLUSION

The purpose of the relief wells is to reduce gradually increasing artesian pressures that have developed under the dam since commissioning. Due to the high PIC rating of Patea Dam, implications of dam instability (potential or confirmed) should be investigated and remediated. The installation of relief wells into the aquifer below Limestone 1 was historically successful and was the preferred remediation to reduce artesian pressures in 2015. Installation of the 2015 wells was difficult due to access issues and geology that were successfully overcome. Relief wells installed had an immediate effect on artesian pressures below the dam with levels dropping during drilling. Currently piezometric levels are below warning levels indicating the relief wells installed in 2015 are performing satisfactorily.

REFERENCES

Beca Carter Hollings & Ferner Ltd. (1985). *Commissioning Document: Addendum 1 – for Egmont Electric Power Board*
Fell, R., MacGregor, P., Stapledon, D., Bell, G. and Foster, M. (2014). *Geotechnical Engineering of Dams (2nd Edition)*, Section 9.2.7.2
Grilli, J. and Pickford, T. (2010). *Patea Hydroelectric Scheme Dam Safety Review*
NZGS (2005). *Field Description of Soil and Rock* Guidelines
NZSOLD (2015). New Zealand Dam Safety Guidelines

Proceedings of the 11th ANZ Young Geotechnical Professionals Conference – 11YGPC
Queenstown, New Zealand
25 – 28 October 2016

Design, monitoring and back-analysis of highway embankments constructed over soft soil

A. Podnar[1]

[1]Douglas Partners Pty Ltd, 96 Hermitage Road, West Ryde, NSW, 2114, Australia, +61 9809 0666; email: adam.podnar@douglaspartners.com.au

ABSTRACT

The Pacific Highway is a highway between Sydney and Brisbane in Australia. It is currently being upgraded to a dual carriageway for its entire 1000 km length. The soft soil embankment design and transition zone design for one of the upgrade sections is presented herein. Due to the limited amount of reliable laboratory data and low embankment heights, the settlement was calculated using the coefficient of volume change, particularly from correlations from CPT results. A short construction programme necessitated the use of a combination of surcharge and wick drains. An in-house spreadsheet calculated the post construction settlement based on the ground conditions in each filled region based on applied ground treatments. Additionally, a unique transition zone solution was used for the bridges in this section of the highway which involved the use of driven piles at increasing spacings away from the bridge abutment. Construction survey data from both embankment settlement and transition zone settlement indicated that the design methods and ground treatments were effective provided a reasonable estimation of the actual ground behaviour.

Keywords: consolidation, wick drains, surcharge, transition zone, back-analysis, construction monitoring

1 INTRODUCTION

This paper presents a summary of the design, monitoring and back-analysis of highway embankments and bridge abutments on soft alluvial soils. The project is an upgrade of a 26 km long section of the Pacific Highway, between Frederickton and Eungai, in NSW, Australia which was designed and constructed by Thiess Contractors (later Leighton Contractors) for NSW Roads and Maritime Services (RMS). Douglas Partners (DP) provided geotechnical advice to Thiess during the tender period and were then appointed as geotechnical designers for the project. During construction DP provided geotechnical advice to the contractor and analysed the results of monitoring.

The RMS specification for the project included very tight criteria for settlement of embankments constructed on compressible soils, namely post construction settlements of less 15 mm and pavement changes in grade of less than 0.3%.

While the geotechnical investigations for the project included numerous boreholes, test pits and cone penetration tests (CPTs), the amount of laboratory testing which had been undertaken to measure the compressibility of the soft soils was very limited. Given that there was more than 5 km of the highway underlain by different sections of soft soils with varying depths and lateral extents, the limited laboratory testing was considered insufficient to adequately profile the soft soil layers. Further, environmental constraints prevented additional field testing and subsequent laboratory testing being completed in time for final design.

DP adopted a pragmatic approach to the problem by identifying that the CPTs provided the best available information on the soft soils and used correlations between the CPT data and soil properties to develop models for use in estimating settlements under the fill embankments. DP used these models to devise ground treatments to allow construction of the fills during the tight 2 year construction time frame and also designed transition zone treatments at bridge abutments to allow for a gradual increase in settlement away from the bridges.

During construction DP used the results of monitoring to refine the design models and material properties to allow prediction of post construction settlements.

2 EMBANKMENT SETTLEMENT DESIGN

2.1 Settlement Method and Parameters

The consolidation settlement under the fill embankments was calculated using the one-dimensional consolidation theory with the coefficient of volume change (m_v) method. The advantage of this method for this project was that correlations between m_v and CPT data could be used to allow values of m_v to be estimated at every CPT location and at 20 mm depth intervals. While m_v values for a particular soil change under different applied stresses, the correlations used were considered appropriate for the relatively small changes in stresses expected under the low fill embankments, which were mostly less than 4 m high.

The magnitude of the consolidation settlement was calculated from m_v values derived from correlations with CPT cone resistance (q_c) using a DP in-house method and a correlation proposed by Sangrelat 1972. The m_v values obtained from these correlations were compared to any oedometer results in the appropriate stress range and the limited dilatometer (DMT) test results. The settlement duration was calculated using $c_{v/h}$ obtained from a relationship between m_v and C_v using a data-matched hydraulic conductivity (from oedometer results), oedometer results and CPT dissipation tests. Creep settlement was calculated using C_α obtained from a correlation between m_v and C_α (Mesri 1994) and those oedometer test results that extended beyond the primary consolidation stage. An improvement in the creep coefficient as a result of surcharge was calculated using a method suggested by Conroy 2010, where the improved creep coefficient is given by:

$$C_\alpha' / C_\alpha = 1.823 - 1.094 \text{ Log } (\sigma_{vs}'-\sigma_{vf}')/ \sigma_{vf}') \quad (1)$$

Where: C_α'= 'improved' creep coefficient; C_a = creep coefficient; σ_{vs}' = surcharge stress; σ_{vf} = final stress.

The design process included generating geological long sections for each of the soft soil areas and identifying regions with similar geotechnical properties and embankment loadings. The CPT results for each of these regions were plotted and interpreted geotechnical parameters were derived for each layer. For design purposes both 'average' and 'conservative' (or sensitivity check) subsurface profiles were generated for each region. A typical graph of the interpreted parameters for each region is included in Figure 1.

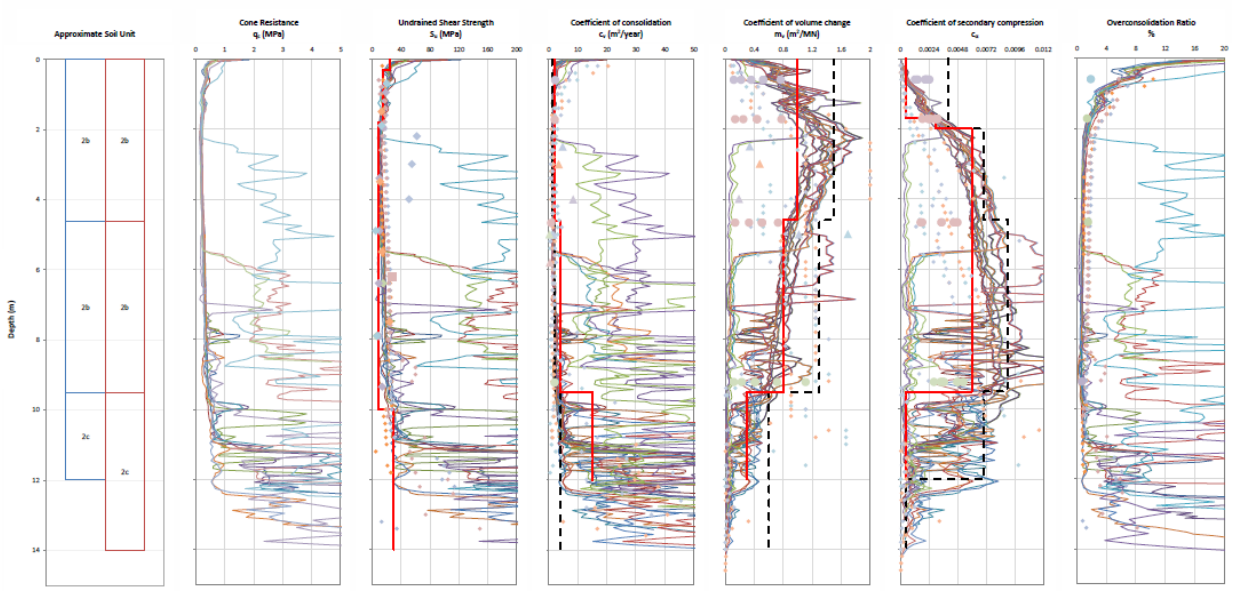


Figure 1. Graphed interpreted parameters for a typical soft soil region (red line = "average", black dotted line = "conservative")

In the design the ratio of the horizontal to vertical coefficients of consolidation (C_h / C_v) was conservatively taken as one. This was due to the lack of specific testing information for the project which meant that there was no evidence to justify a higher horizontal coefficient as commonly occurs

in alluvial deposits. The few test nearby dissipation tests and oedometer results suggested this was a appropriate assumption.

As there were many fill sections with individual subsurface profiles, the resulting parameters have not been reproduced here. There was a wide variability between even nearby alluvial deposits.

All the fill regions were analysed to estimate the post construction settlement assuming no ground treatment was applied. For those areas where the predicted post construction settlement was greater than 15 mm (defined as 'compressible' soil) ground treatment was required. The settlement calculations included an embankment creep value of 0.1% per log cycle, which accounted for about two-thirds of the allowable settlement for a 4 m high embankment over 40 years, which meant that the ground treatment had to virtually eliminate any post-construction consolidation settlement.

2.2 Ground Treatment Options

Given the extensive areas of fills underlain by soft soils (more than 5 km length) the project team decided to use a combination of wick drains and surcharge to accelerate the consolidation settlement. The tight two-year construction programme for the project meant that a maximum of 6 months was available for surcharging the fills.

DP analysed each of the soft soil sections to optimise the height and duration of the surcharge and spacing of wick drains required to ensure that the post construction settlement complied with the project specifications.

In the design of the wick drains the diameter of the wick drain smear zone was conservatively taken as $3d_w$ (d_w = wick drain diameter) and the ratio of undisturbed permeability versus smeared permeability (k_h / k_s) was taken as 2.

2.3 Calculation Method

For each of the soft soil sections the subsurface profile from CPT data, interpreted geotechnical parameters and ground treatment options were analysed using an in-house spreadsheet developed for and further refined throughout the project. The calculation time for full analysis of the 19 'compressible' fill regions was about 10 seconds. As additional field investigations were undertaken, the new geotechnical data was able to be included quickly and optimisation of the treatment options assessed. This resulted in subsequent savings in both construction programme and cost.

3 TRANSITION ZONE DESIGN

3.1 Problem Characterisation

A significant portion of the Pacific Highway in northern NSW is built over flood plains and is underlain by soft soils. Transitioning between relatively large settlements under fill embankments to negligible settlements at bridges founded on piles has historically presented both a comfort issue for motorists and ongoing maintenance issues at bridge approaches. For this project the, post construction change in grade was required to be limited to 0.3% with less than 50 mm post-construction settlement within 50 m of any bridge abutment.

3.2 Design Concept

The solution devised for this project to transition settlements beneath bridge abutments used driven piles founded in stiff to hard clays with increasing spacing moving away from the bridge abutment. In order to allow arching between the pile caps, a load transfer platform of rockfill and geogrids was used.

3.3 Detailed Design

The software package PLAXIS® was used to confirm the viability of and refine the transition zone design. A pile spacing was chosen to allow a gradual increase in the amount of load from the fill embankment which would be transferred to the soil between the piles and this, together with the load

transfer platform of rockfill and geogrids, was modelled for each transition zone for each bridge abutment. The proposed construction schedule was modelled, including application of surcharge and wick drains in the adjacent embankment.

For some bridge abutments the results of the analysis indicated that it would be better to decrease the length of piles which were further away from the bridge abutment. Additionally, localised ramped height surcharge was applied in order to smooth the post construction settlement change in grade.

A general arrangement of a transition zone model is presented in Figure 2.

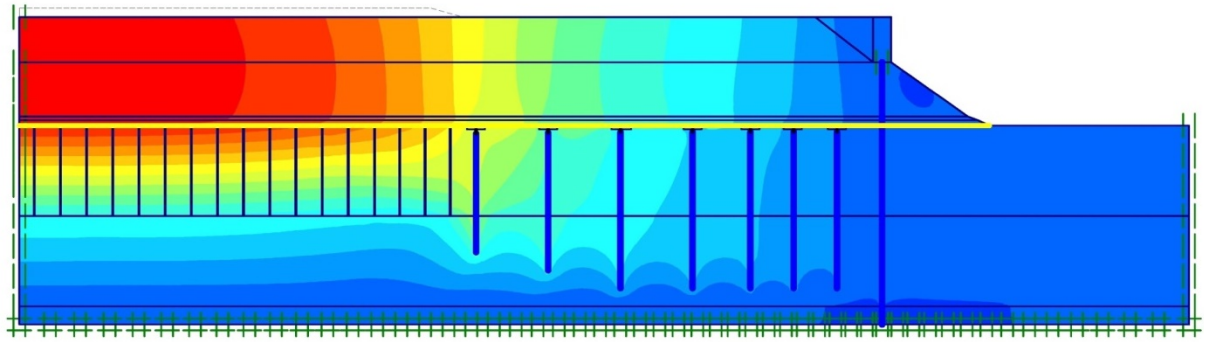


Figure 2. General arrangement of bridge transition zone

4 CONSTRUCTION PHASE SETTLEMENT

4.1 Survey Results

Under the contract instrument monitoring arrays were required to be installed every 100 m in areas underlain by 'compressible' soils. These arrays typically included settlement plates (x3), vibrating wire piezometers, horizontal profile gauges and inclinometers. These instruments were read at regular intervals before, during and after embankment construction. The monitoring results were made available to DP and the client through an online database.

Additionally, a graph of driving resistance over the depth of installation was supplied from the wick drain installation rig for each of the 70,000 wick drains installed on the project. Review of the information provided by the wick drain sub-contractor showed that the absolute magnitude of the driving resistance varied significantly and appeared to be uncontrolled, but there was a very apparent inflexion point in all the resistance data which showed the depths to the base of the soft soils. These depths were checked against the information from CPTs undertaken immediately adjacent to specific wicks. The interpreted depths to the base of the soft soils from each of the wick drains, together with the supplied co-ordinates, were used to map the depths of soft soils under the fills using GIS.

An example of the output from this information is presented in Figure 3. The figure shows that the soft soil profiles varied in thickness both along and across the fill areas. This data was compared to the interpreted profiles used in the design and, where necessary, the ground treatment was varied to suit the actual ground conditions.

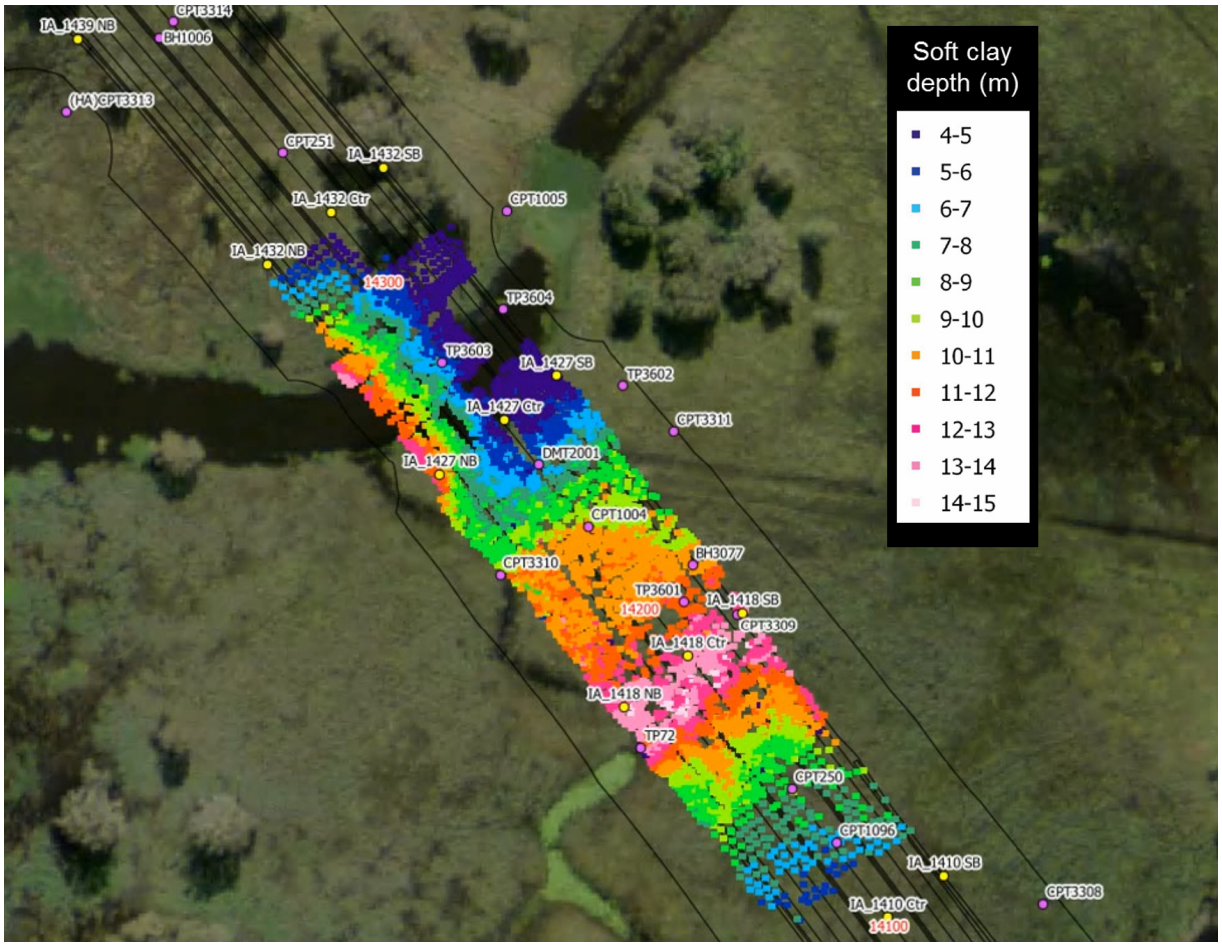


Figure 3. Soft clay depths based on wick rig installation logs

4.2 Back Analysis

An observational method was adopted for the project in which the actual settlements monitored during construction were progressively fed back into the design model to refine the predictions of post-construction settlement. This presented both an opportunity and a risk during construction that the durations of surcharge could be reduced or might be required to remain in place for a longer period.

With the additional information obtained from the wick drain installation, the settlement measured at each of the settlement plates were back-analysed to compare predictions and then to predict future performance. A further refinement to the analysis undertaken during construction was that the actual construction stages (fill heights and timing) were included in the analysis of the measured settlements.

Generally, the choice of relatively conservative parameters during design meant the settlement magnitudes were slightly overestimated (in the order of 10% - 20% in the regions with the most settlement). Similarly, the settlement durations were typically overestimated by about one order of magnitude for the same regions.

After slight modifications to layer thickness and interpreted soil properties all the measured settlements could be matched to settlement predictions for the interpreted soil profiles at each location. An example of one of the settlement predictions with the actual measured settlements results overlain is shown in Figure 4.

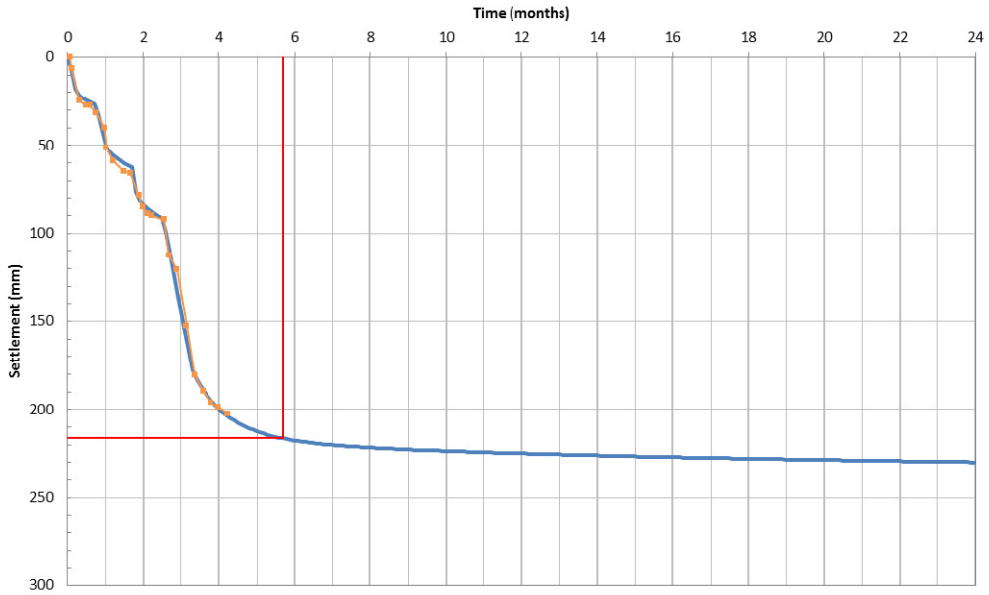


Figure 4. Example result of the settlement back-analysis (actual settlements shown in orange with predicted settlements shown in blue)

A report was prepared for each fill region using the results of the back analysis to recommend the length of time the surcharge should remain in place. Generally this surcharge period was either the same or slightly shorter than the surcharge period assumed during the detailed design. For one fill only the back-analysis indicated that the surcharge needed to remain in place for longer than the design assumed. The reports for each section were reviewed by both the client (RMS) and the project verifier prior to removal of the surcharge.

5 CONSTRUCTION PHASE TRANSITION ZONES

Instrument arrays were also installed within transition zones adjacent to bridge abutments. As expected, minimal pore pressure response was encountered in vibrating wire piezometers within the piled section of the transition zones which showed that the loads from the fill embankments were being effectively transferred to the piles. The settlement plate readings at the end of the surcharge period were compared to the analysis results from the same time period. An example of a well-matched prediction showing a gradual increase in settlement away from the bridge abutment is shown in Figure 5.

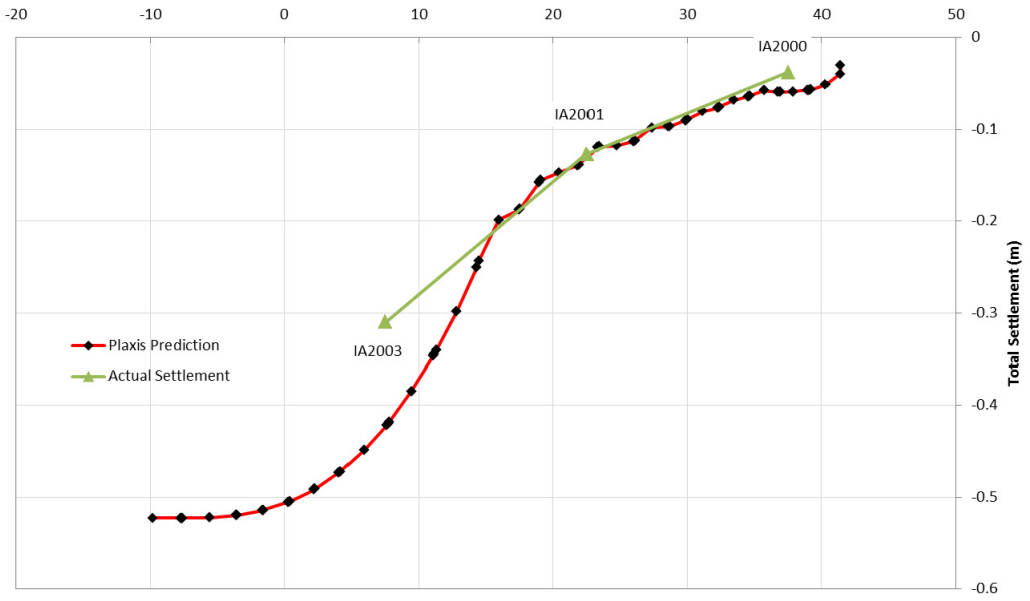


Figure 5. Comparison between predicted behaviour and surveyed results in transition zone

While not all predictions were as close to surveyed measurements, all surveyed results showed proportionally increasing settlement away from the bridge abutment, consistent with the design logic.

6 CONCLUSION

The availability of CPT test data and very limited laboratory test results for soft soils encouraged the use of correlations between CPT data and compressibility to be used on this project to predict settlements and allow design of ground treatments. While the adoption of slightly conservative parameters during design resulted in slightly conservative predictions of settlement, the monitoring of settlements during construction and back analysis of the actual settlements to refine the geotechnical models were successfully used to control the timing of surcharge removal and allow prediction of future settlements.

The results of monitoring during construction show that the design of the transition zones for the project using piles at increasing spacings, together with a load transfer platform of rockfill and geogrids, effectively managed the settlement such that it gradually increased away from the bridge abutments.

REFERENCES

Conroy, T., Fahey, D., Buggy, F. and Long, M. (2010). “Control of secondary creep in soft alluvium soil using surcharge loading” *Proceedings National Symposium on Bridge, Concrete and Infrastructure Research in Ireland* (BCR20), pp. 247-254

Mesri, G., LO, D.O.K. and Feng, T.W. (1994). “Settlement of embankment on soft clay”, *Proceedings of Settlement ‘94*, ASCE Geotchnical Special Publication No. 40(1), pp. 8-56.

Sangrelat, G. (1972). *The penetrometer and soil exploration*, Elsevier, Amsterdam

This page intentionally left blank

Proceedings of the 11th ANZ Young Geotechnical Professionals Conference – 11YGPC
Queenstown, New Zealand
25 – 28 October 2016

Assessing the Strength of East Coast Bays Formation Soils using in-situ Testing Data

S. Semmens[1] and S. Anwar[2]

[1]Senior Engineering Geologist, AECOM, 8 Mahuhu Crescent, Auckland, PH (+64) 9 967 9483; email: Stephen.Semmens@aecom.com
[2]Principal Geotechnical Engineer AECOM; 8 Mahuhu Crescent, Auckland, PH (+64) 9 967 9564; email: Sajjad.Anwar@aecom.com

ABSTRACT

AECOM undertook engineering geological mapping and geotechnical investigations to support resource consent for a proposed subdivision located west of Orewa. The development land consists of a central valley with gentle to moderate sloping upper sections, steep mid sections and moderate toe slopes. The site is underlain by a weathered East Coast Bays Formation (ECBF) sequence of the Waitemata Group, which comprises interbedded very weak sandstone and mudstone units that dip at a low angle northward. Past instability has affected the land and mapped features included head scarps, debris lobes and hummocky ground. Investigations included machine drillholes, machine excavated pits, hand augerholes, cone penetrometer (CPT) and dilatometer testing (DMT). Laboratory testing of select recovered materials was also undertaken, comprising Atterberg Limits, Standard Compaction, Moisture Content and Lime Reactivity tests. Ground conditions encountered in the geotechnical investigation comprise a mantle of weathered, reworked silt and clay to a depth of at least 3 m. Underlying this mantle is a weathered sequence of generally interbedded ECBF sandstone and siltstone. Alluvium/colluvium occurs in the valley floors, which in places are swampy. Geotechnical design parameters required for stability analysis were determined from both measured field vane shear strengths and those derived from CPT and DMT data. CPT empirically derived strengths were calibrated against in-situ vane shear strengths by adjusting the cone factor (N_{kt}) using Geologismiki software CPeTiT until a close fit between the field data was made. This paper presents a review of the investigation results, the geological model for the site and a comparison of measured and derived soil parameters.

Keywords: East Coast Bays Formation, CPT, CPeTiT, cone factor (N_{kt})

1 INTRODUCTION

AECOM was engaged by a developer to provide design services for a proposed residential subdivision located northeast of Orewa, New Zealand (refer Figure 1(a)). As part of the work undertaken AECOM provided a geotechnical assessment of the land to support an application for land use and earthworks consents for the subdivision.

The purpose of this paper is to highlight the risk of using CPT derived soil parameters in East Coast Bays Formation materials without calibration.

The authors note that specific details which could be used to identify the exact site and our client's details have been omitted from this paper at the client's request.

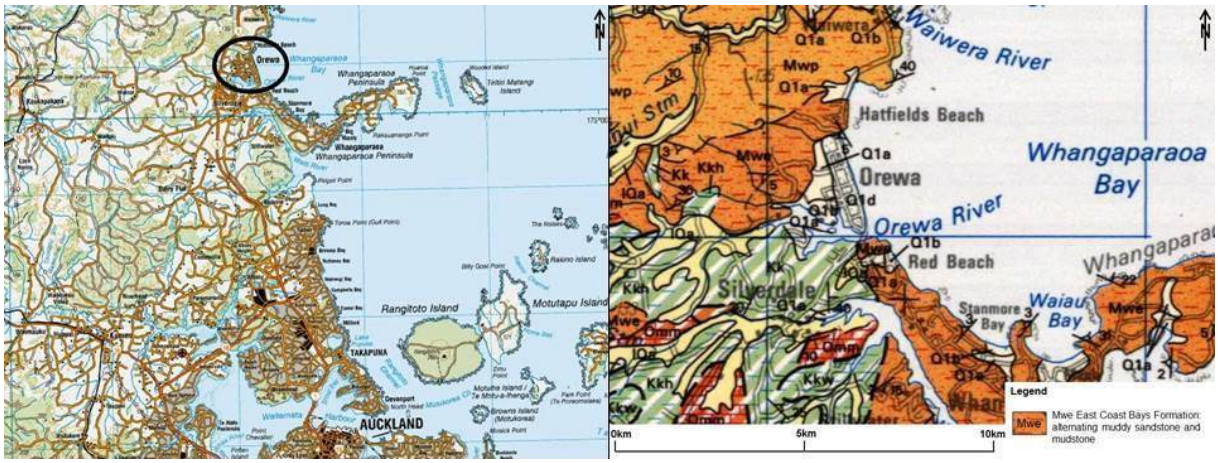
2 LAND DESCRIPTION AND ENGINEERING GEOLOGY

2.1 Description of the land

The development land has an area of approximately 375,000 m^2 and is currently used for pastoral farming. A Significant Ecological Area (SEA) borders the site to the north, with pastoral farming to the west, residential housing to the east and a new residential development to the south.

2.2 Geological setting

The published geological map of the area (Figure 1(b)) shows the site is underlain by East Coast Bays Formation (ECBF) of the Waitemata Group, which comprises very weak, interbedded sandstone and mudstone that dip at a low angle northward (Edbrooke 2001). These rocks are typically weathered to depths of about 5 m and commonly have a cover of 1 to 3 m of reworked weathered materials (slope debris), especially on the gentle ridge crests. Alluvium (including swamp deposits) occurs in the valley floors. No active faults are shown to occur in the area (GNS 2016).



(a) *(b)*

Figure 1. (a) Site location; and (b) Geological map extract (Edbrooke 2001)

2.3 Geomorphology

The dominant topography consists of a north trending horseshoe shaped valley in the centre of the site with gentle to moderate sloping upper sections, steep mid sections and moderate toe slopes (Figure 2). Small areas of flat to gently sloping land occur along the western portion of the site with small pockets around the central valley. The head of the valley is a broad, open basin with a radial pattern of shallowly incised ephemeral watercourses draining to an artificial pond in the valley floor. A central stream drains from the pond to the north. An SEA occupies the northern portion, steeper slopes and tributaries of the central valley.

Past instability has affected the land. Evidence of instability includes head scarps, debris lobes, mid-slope benches and hummocky ground. These instability features generally occur on the slopes between more stable ridgelines. Groundwater seepage and poor surface drainage is associated with some of the instability features. Mapped geomorphic features are shown on Figure 2.

3 GEOTECHNICAL INVESTIGATION

3.1 General

Engineering geological mapping and intrusive investigations were undertaken between August 2014 and October 2015. Investigations included machine drillholes, machine excavated pits, hand augerholes, cone penetrometer tests (CPTs) and dilatometer tests (DMTs).

Seventeen cored machine drillholes were drilled using HQ coring techniques to depths ranging from 15.5 to 24.45 m. Standard Penetration Tests (SPTs) were undertaken generally at 1.5 m centres as drilling progressed. Single standpipe piezometers were installed in all the drillholes and developed using an air compressor.

The first 1.5 m of each machine drillhole was advanced using a hand auger. A series of hand augerholes were also undertaken so that in-situ hand held vane shear strength tests could be undertaken.

Twenty five pits were excavated to depths between 1.5 and 4.2 m by a machine excavator to augment the machine drillholes and provide bulk samples for geotechnical and contamination laboratory testing.

Thirty four CPTs were undertaken using a tracked Pagani portable system to augment the drillhole and pit investigations and target areas requiring substantial engineering design. Two DMTs were undertaken to determine typical soil consolidation properties.

Materials encountered in the drillholes, augerholes and pits were logged on site according to the procedures in the New Zealand Geotechnical Society Field Description of Soil and Rock Guideline (New Zealand Geotechnical Society 2005). Hand held shear vane strength tests were performed where appropriate according to the New Zealand Geotechnical Society, 2001 guideline.

Geotechnical and contamination testing was carried out on a number of samples to determine material properties and potential re-use (such as engineering fill). Geotechnical laboratory testing included Consolidated Undrained Triaxial, Unconfined Compressive Strength, Atterberg Limits, Standard Compaction, Moisture Content and Lime Reactivity tests.

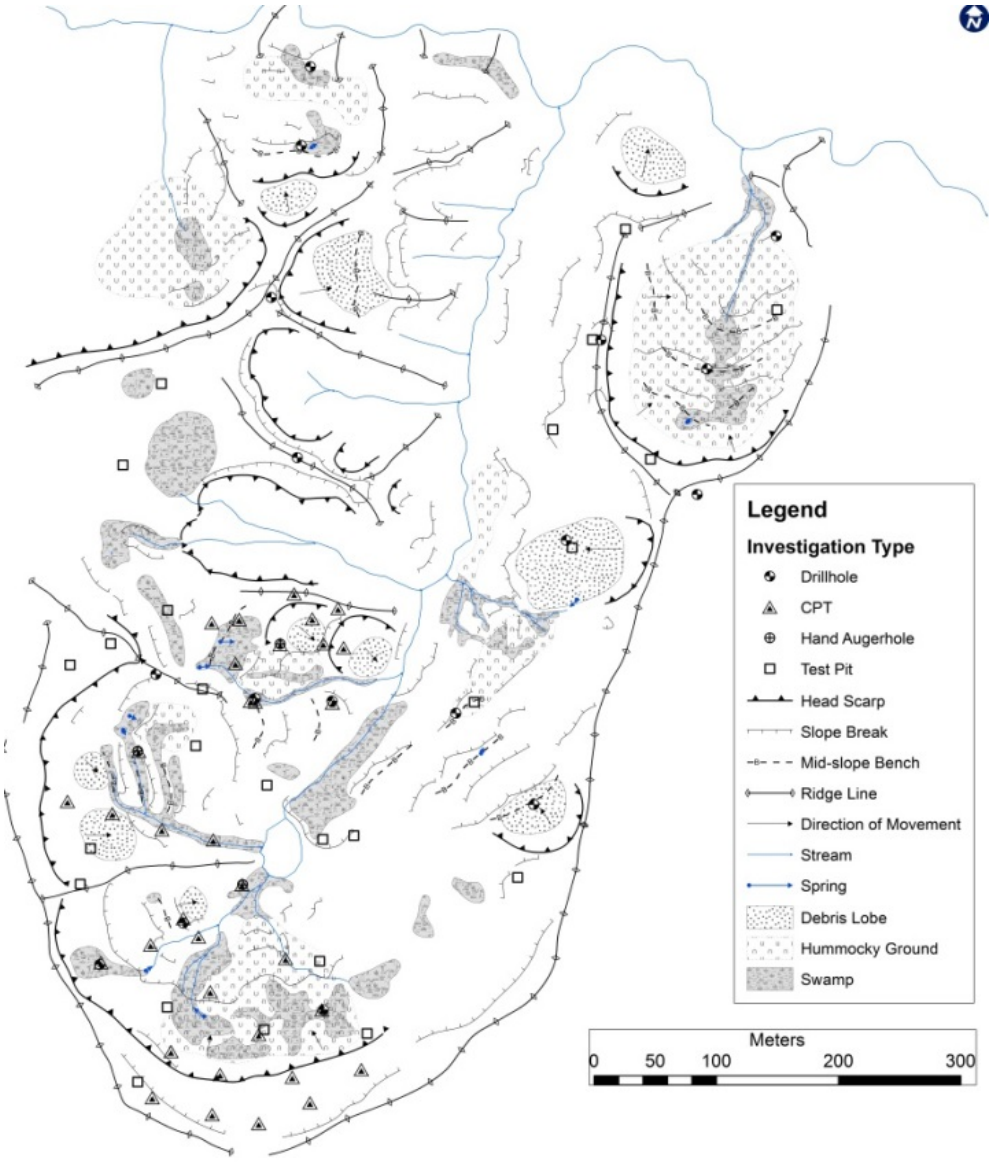


Figure 2. Site geomorphology

4 GEOTECHNICAL ASSESSMENT

4.1 Geological model

Geotechnical investigations and mapping confirmed ECBF underlies the site. Site ground conditions can be summarised as comprising thin topsoil layer (0.1 to 0.4 m) underlain by a mantle of weathered,

reworked silt and clay (slope debris) to a depth of up to 5 m. Underlying this mantle is a weathered sequence (completely to slightly weathered) of generally interbedded, sub-horizontal ECBF sandstone and siltstone.

Weathering grades were assigned based on field strength, visual inspection and colour. Reworked completely weathered (RCW) ECBF materials comprise firm to very stiff silt and clay derived from completely weathered siltstone and sandstone. The material has a disturbed homogenous appearance with variable organic content including broken decomposing rootlets. Completely weathered (CW) ECBF materials generally comprise firm to very stiff silt and clay derived from weathered siltstone and sandstone with some relict rock fabric (joints) remaining. Highly weathered (HW) ECBF materials generally comprise interbedded, very stiff silt and clay and loose to medium dense sand derived from weathered siltstone and sandstone with some relict rock fabric (joints) remaining. Moderately weathered (MW) ECBF generally comprises interbedded, very stiff to hard silt and clay and medium dense to dense sand with a rock strength ranging from extremely to very weak. Slightly weathered (SW) ECBF comprises very weak to weak, sub-horizontal, interbedded siltstone and sandstone. No defects with evidence of movement that may indicate deep seated instability was observed in the recovered core in slightly weathered ECBF.

Fill material associated with historic roads, a farm dam and landfill construction were identified to a maximum depth of 1 m in localised areas around the site. Fill generally comprised stiff to very stiff sandy and clayey silt and had a similar appearance to reworked ECBF materials.

Alluvium occurs in the valley floors (central valley) and generally comprises firm to stiff silt and clay with variable decomposing organic material and fibrous peat.

The geological units described above are presented in Table 1. Figure 3 presents a typical engineering geological cross section across one side of the central valley.

Table 1. Summary ground conditions and in-situ testing

Depth of Unit (m)	Geotechnical Unit						
	Alluvium	**Fill**	**RCW ECBF[a]**	**CW ECBF**	**HW ECBF**	**MW ECBF**	**SW ECBF**
Minimum	0.0	0.0	0.0	0.2	1.0	3.3	4.8
Maximum	1.5	0.0	5.0	10.5	18.4	20.1	24.5+
Corrected vane shear strengths Peak/remoulded (ave.)	83 / 37	105 / 46	113 / 57	131 / 68	140 / 55	N/A	N/A
SPT N Value Average (range)	N/A	N/A	2 (0-5)	4 (0-10)	12 (0-25)	30-50+	50+

[a] Topsoil included in the reworked ECBF unit
[b] Deepest investigation

Piezometers were installed in all of the drillholes. Measured water level depths range from 1.81 m for holes located at the base of the valley to 11.26 m for holes located on ridge tops.

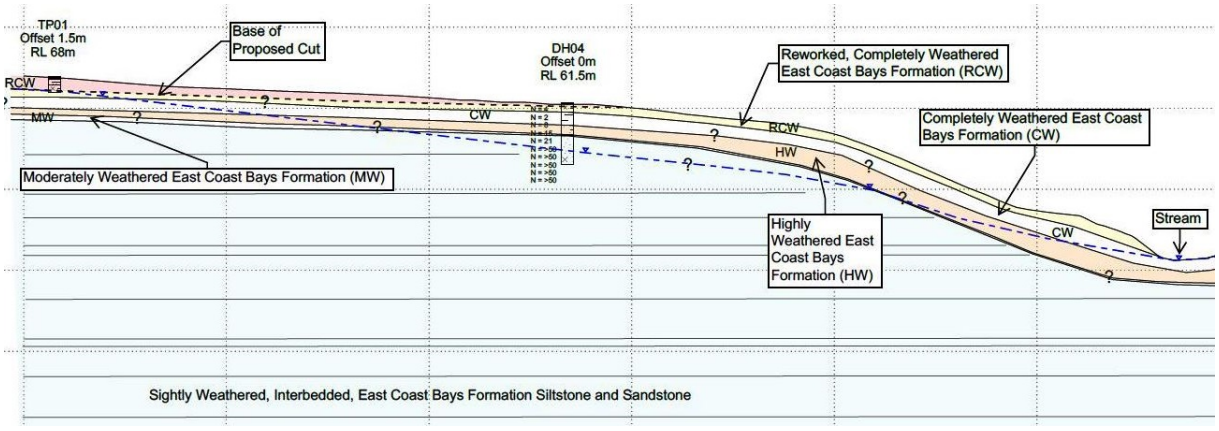


Figure 3. Typical engineering geological section across the site

4.2 Geotechnical Design Parameters

Geotechnical design parameters required for stability analysis and geotechnical design (subdivision infrastructure including retaining walls, roads, drainage etc.) were determined from measured in-situ strengths, strengths derived from CPT and DMT data, geotechnical laboratory testing and experience with similar materials in this area. Table 2 presents geotechnical design parameters used in stability analysis and design.

Table 2. Geotechnical design parameters

Geotechnical Unit	Unit Weight, γ (kN/m^3)	Total Stress	Effective Stress		Young's Modulus, E' (MPa)	Poisson's Ratio, ν
		Shear Strength S_u (kPa)	Cohesion c' (kPa)	Friction angle, ϕ (degrees)		
Alluvium	16	40	3	25	10	0.3
RCW & CW ECBF	17	30 to 60	5	28	10 to 20	0.3
HW ECBF	17.5	100	7	30	40	0.3
MW ECBF	18.5	150	10	32	70	0.2
SW ECBF	22	500	50	35	200	0.2

4.3 CPT undrained shear strength calibration

In order to utilise the extensive CPT data (34 CPTs and 2 DMTs), calibration with the undrained soil shear strengths (S_u) derived from the CPTs is required. The principal reason is that the CPT results were noticeably lower than hand held vane results from hand augerholes and would have led to overly conservative design. This calibration involved the adjustment of the CPT cone factor N_{kt} until the CPT derived shear strength values approximately matched corrected field hand held vane shear strength measurements.

CPT derived soil shear strength is controlled by various factors such as cone factor, soil plasticity, soil sensitivity and soil stress history. These factors are incorporated into empirical equations used to estimate shear strength for the respective test methods, e.g. cone factor N_{kt} is used for the CPT method.

For CPTs, N_{kt} typically ranges from 10 to 18, with an average of 14. N_{kt} tends to increase with increasing plasticity and decrease with increasing soil sensitivity (Robertson and Cabal 2015).

The following relationship is used for calculating shear strength from CPT data:

$$S_u = q_t – \sigma_v / N_{kt} \quad (1)$$

Where q_t is corrected cone resistance, σ_v is total overburden stress and N_{kt} is the cone factor.

Due to the broad spread of cone factor values i.e. 10 to 18, calibration of N_{kt} is undertaken. The calibration process is carried out using Geologismiki software CPeTiT. Equation (1) is built into the software program and automatically calculates soil shear strength using N_{kt} = 14 as a default value.

Shear strength values estimated by CPT and measured by hand held shear vane values are plotted side by side in CPeTiT. Based on plot results (Figure 4) it is observed that, for this site, the direct in-situ shear vane test measurements produce values of S_u higher than CPT derived values using the default N_{kt} = 14.

Calibration of N_{kt} is undertaken by trial and observation. The value of N_{kt} is adjusted until a best fit with the field shear vane results is achieved. It is reported that generally soil shear strength estimation based on field shear vanes and DMTs is more accurate and dependable for design (Marchetti et al. 2001) compared to other methods such as CPT, SPT.

From this assessment an N_{kt} value of 10 is found to have the best fit with measured field shear strengths (Figure 4). This is at the lower limit of the published range, i.e. 10 to 18.

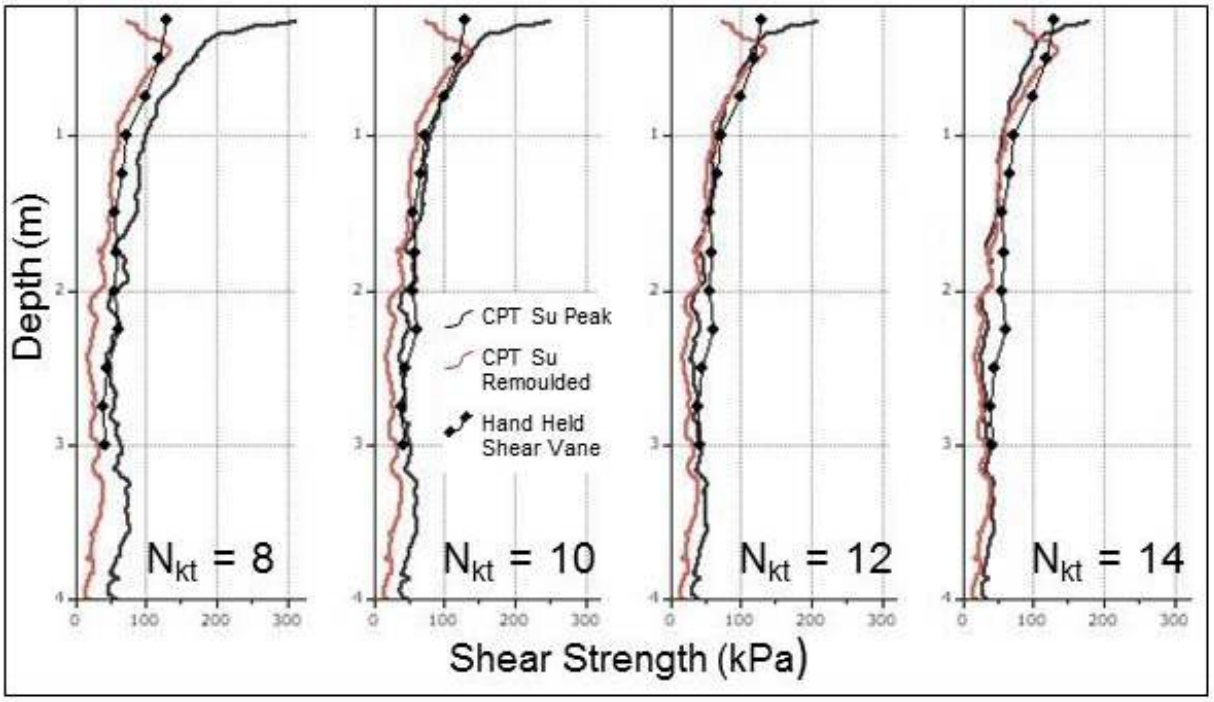


Figure 4. CPT cone factor, N_{kt} calibration with in-situ shear vane tests (N_{kt}=10 shows the best fit)

5 CONCLUSION

Ground conditions at the site comprise a mantle of reworked weathered material to at least 3 m depth. Underlying this mantle is a weathered sequence of interbedded East Coast Bays Formation sandstone and siltstone.

For this site it was found that direct in-situ shear vane measurements were higher than those predicted by CPT analysis using a default cone factor, N_{kt} of 14. Shear strength values derived from CPT were found to have a close fit with measured field vane values in weathered East Coast Bays Formation materials when using a cone factor, N_{kt} of 10.

Due to repeatability, relatively quick and portable testing, and low cost CPTs are deemed to be effective at determining shear strength over a large site provided calibration against in-situ testing is undertaken and appropriate cone factors are applied.

6 ACKNOWLEDGEMENTS

The authors would like to thank our client for allowing us to use and present the data in this paper.

REFERENCES

Edbrooke, S.W. (compiler) 2001: Geology of the Auckland area. Institute of Geological & Nuclear Sciences 1:250,000 geological map 3. 1 sheet + 74p. Lower Hutt, New Zealand. Institute of Geological and Nuclear Sciences Limited

GNS, 2016. The Institute of Geological and Nuclear Sciences Ltd. Active Fault Database. [Online] Available at: http://data.gns.cri.nz/af/index.html> (Oct. 1, 2014).

Marchetti S., Monaco P., Totani G. and Calabrese M. 2001. "The Flat Dilatometer Test (DMT) in Soil Investigations" A Report by the ISSMGE Committee TC16. *Proc. IN SITU 2001, Intnl. Conf. On In situ Measurement of Soil Properties*, Bali, Indonesia, May 2001, 41p.

New Zealand Geotechnical Society, 2001. *Guideline for hand held shear vane test*, New Zealand: NZ Geotechnical Society Inc. August 2001.

New Zealand Geotechnical Society, 2005. *Field Description of Soil and Rock – Guideline for the field classification and description of soil and rock for engineering purposes*, New Zealand: NZ Geotechnical Society Inc., December 2005.

Robertson, P.K. and Cabal, K.L., *Guide to Cone Penetration Testing for Geotechnical Engineering*, Prepared for Gregg Drilling & Testing Inc., 6th Edition, 2015, 143 p.

Proceedings of the 11th ANZ Young Geotechnical Professionals Conference – 11YGPC
Queenstown, New Zealand
25 – 28 October 2016

Design of Mechanically Stabilised Earth Walls for Bridge Abutments on the Mackays to Peka Peka Expressway, New Zealand

R. J. Everiss[1]

[1]Geotechnical Engineer, Beca Ltd, 21 Pitt Street, Auckland 1010; PH +64 9 300 9000; FAX +64 9 300 9300; email: ryan.everiss@beca.com

ABSTRACT

The new 18 km long, four lane MacKays to Peka Peka Expressway located in the Kāpiti Coast Region of New Zealand is currently under construction. On this project there are 18 bridges which incorporate Mechanically Stabilised Earth Walls (MSE walls) in some form within the bridge abutments. These walls are designed for the high seismicity of the Kāpiti Coast region with a design peak ground acceleration (PGA) of up to 0.98g under ultimate limit state design events. This exceeds typical design practice and presents a significant challenge to wall designers. Furthermore extensive sections of the route are prone to flooding, liquefaction and have complicated geometry (for example highly skewed bridges with piles going through the MSE wall reinforced block). This paper discusses the philosophy and approach adopted for the walls and how these design challenges were overcome.

Keywords: Retaining Walls, Seismic Design, Displacement, Liquefaction

1 INTRODUCTION

The Mackays to Peka Peka (M2PP) Expressway is an 18km four lane expressway. It is the first section of the Wellington Northern Corridor project under construction. The expressway passes through the Kapiti Coast region which is located 60km north of Wellington. Once complete it will separate local and highway traffic, resulting in safer and faster trips through the region. The project includes 18 bridges which utilise MSE walls for the bridge abutments as well as a number of other minor MSE structures including abutments for shared cycleway, walkway, bridleway and maintenance access bridges and freestanding MSE walls. This paper addresses the walls associated with the highway bridge structures.

A number of interesting design challenges were encountered by the team undertaking the MSE wall design on this project. The purpose of this paper is to describe these challenges and the innovative solutions that were adopted to overcome them. The challenges included:

1. The high design seismic loading. The Kapiti Coast area has one of the highest seismic loadings in New Zealand. This, in conjunction with the low annual probability of exceedance required for M2PP expressway, results in peak ground acceleration values approaching 1g.

2. The potential for flood events to cause inundation of the MSE walls. This presents a risk of wall undercutting or erosion of the dune sand used in wall construction. Such erosion could cause significant damage to, or even collapse of, the roadway.

3. The potential for liquefaction within sands underlying the wall. Liquefaction of underlying soils, particularly if occurring while strong shaking was ongoing, has the potential to result in large lateral displacements of bridge abutments.

4. The potential for differential settlement of compressible soils beneath the MSE walls. Differential settlement might result in poor driver comfort and damage to rigid elements such as precast wall panels and flood protection measures causing increased maintenance costs.

5. The bridge design requires foundation piles to pass through the reinforced block. This presents challenges in maintaining integrity of the reinforced block where the reinforcement is disrupted.

6. The adoption of highly skewed abutments for some bridges. A number of bridges along the alignment were skewed by up to 35 degrees. This results in geogrids clashing with other design elements making it difficult to achieve design embedment.

2 SEISMICITY OF THE AREA

The NZTA commissioned a site specific seismic hazard assessment (SSHA) for the expressway (M2PP Alliance 2014a). The SSHA determined design PGA levels, for the design of the main expressway bridges (1 in 2,500 year return period) of 0.98g for the southern part of the site (NZS1170.5 Site Subsoil Class C) and 0.74g for the central and northern sectors (NZS1170.5 Site Subsoil Class D).

3 GROUND CONDITIONS

The M2PP expressway is mostly underlain by dune sands and peats with alluvial sands and gravels at depth. Dune sands inter-finger with peat deposits in an unpredictable manner below the alignment. The water table is generally shallow, between 0 to 1m below ground, locally mounding where dunes rise up to 20m above surrounding ground. The high water table and seismicity make sand layers prone to liquefaction.

4 MSE WALL DESIGN

Uniaxial polyethylene geogrids were selected as MSE walls reinforcement for their historical good performance under seismic loads, ready availability, and familiarity of designers and constructors with product and commercial considerations. Dune sand was selected as the engineered fill due to its availability within the alignment, free draining characteristics and minimising truck movements along local roads. This was an important consideration due to the close proximity of residential zones.

MSE walls were designed in general accordance with AASHTO (2007, 2010) using the program MSEW 3.0 (Adama Engineering Ltd 2013) for external and internal stability. Figure 1 shows the six possible failure mechanisms analysed. Global stability was checked using Slope/W (Geo-Slope International Ltd 2014), a limit equilibrium program used for calculating circular slip surfaces. Seismic displacements were estimated using this program following (Jibson 2007). Plaxis 2D (Plaxis 2013) (a finite element analysis program) was used to provide a comparison against limit equilibrium methods and to assess the distribution of displacements within the walls.

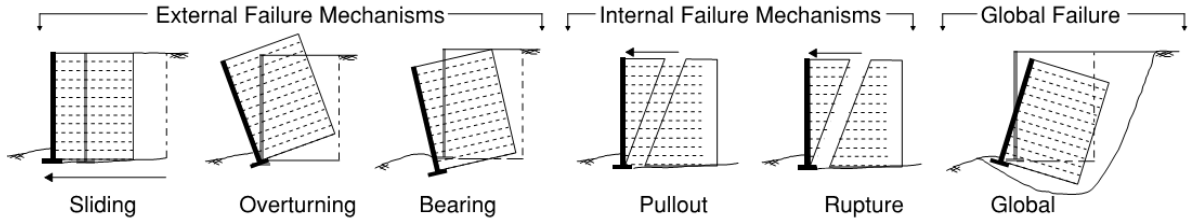


Figure 1. External, Internal and Global Failure Mechanism for MSE walls

5 GEOMETRY

In general, the abutment retaining walls comprise MSE blocks 5m to 9m high with the wall face sloping at angles to the horizontal between 70 and 90 degrees. Walls are reinforced in the longitudinal and transverse directions. In general terms there are two abutment types, a vertical abutment where the MSE is encapsulated within precast concrete panels or a spill through abutment where the grids are terminated within the embankment (refer to Figure 2 for typical wall geometry.)

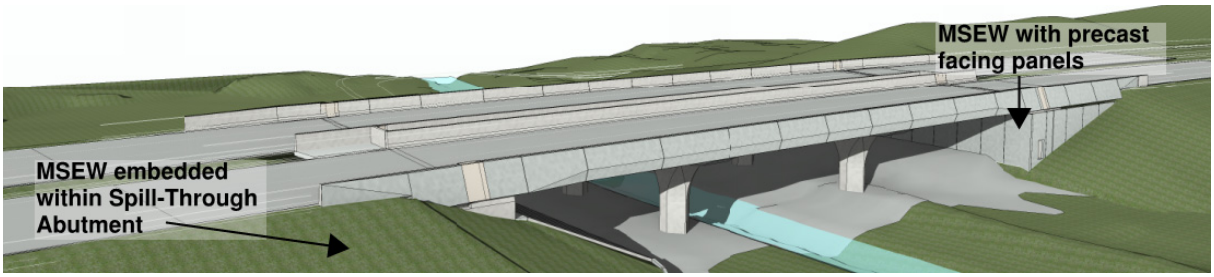


Figure 2. Typical MSE Wall Geometry (Wharemauku Stream Bridge)

6 FLOOD DESIGN

MSE walls adjacent to rivers are prone to inundation in flood events. Inundation of walls can cause a number of adverse effects, for example (1) Undercut of the wall, (2) erosion of wall fill and (3) rapid drawdown (additional hydrostatic load acting on walls). Figure 3 shows the design measures used to mitigate these effects. Specifically these measures included; (1) Rock riprap was placed upstream and downstream of each bridge with a minimum of least 600mm wall toe embedment below the underside of the riprap (frequently greater) to mitigate potential toe erosion, (2) A 1500mm wide cement stabilised backfill zone around the perimeter of the walls, (3) A geotextile to prevent horizontal migration of engineered fill, (4) A geotextile together with a 150mm thick filter layer to reduce vertical migration of engineered fill clogging up drainage layer, (5) A subsoil drainage pipe to lower flood levels as quickly as possible, (6) Slopes adjacent to walls were quickly vegetated to mitigate erosion from concentrated water flow. Areas that had not yet been vegetated suffered erosion during intense rainfall. Walls were also designed for rapid drawdown. External and internal failure mechanisms were checked with additional hydrostatic forces acting on wall.

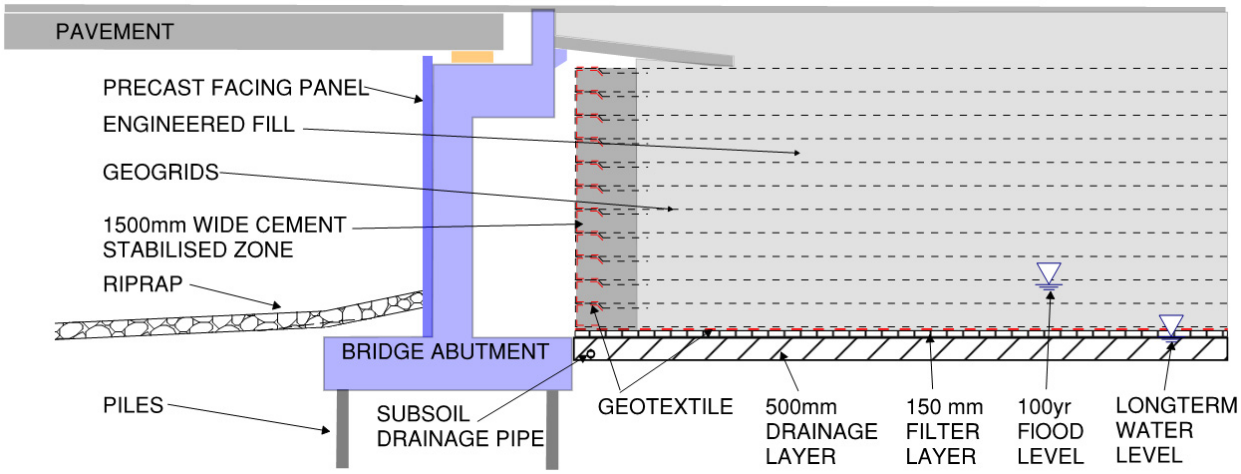


Figure 3. Flood Protection Design Elements

7 SEISMIC DESIGN

Seismic design was particularly difficult for this project due to high design accelerations and the potential for liquefaction and cyclic softening of foundation soils. It was not considered technically or economically feasible to prevent seismic induced displacements because of the site's high seismic acceleration and potential for strength loss in foundation soils. Displacement based design (allowing for movements of wall), with displacement limits in the region of 30 to 200mm effectively lowered the seismic forces considered in the wall design. Where displacement was excessive, ground improvement was specified. In this way ground improvement costs were optimised and a more efficient wall design achieved.

Seismic displacements were estimated using Slope/W following (Jibson 2007) method based on Newmark sliding block theory (Newmark 1965). The stability of the walls was checked in transverse and longitudinal directions and the distribution of displacements within the walls was assessed.

8 PILES THROUGH REINFORCED ZONE

8.1 Geogrid Layout

Some bridges required a secondary load path to provide vertical support to the superstructure to address the potential for loss of pile support following large abutment movements in a maximum considered earthquake (MCE) event. The secondary load path is provided by MSE walls extended beneath the bridge abutment and around the foundation piles. A consequence of this approach is that piles were required to extend through the reinforcement zone. The presence of piles reduces the coverage ratio locally at the wall face, furthermore because piles move laterally in a seismic event, an

additional reduction must be made in the coverage ratio. Designing walls for this reduced coverage ratio required careful detailing, use of stronger grids locally and cement stabilisation.

Details A and B of Figure 4 show the detailing around piles. Namely (1) longitudinal grids (tie strips) placed between piles connecting to wall constructed behind piles, (2) Geotextile placed horizontally through tie strips in front of piles to support soil between precast panels and piles, (3) Cement stabilisation of all reinforced fill below bridge abutment capping beam (4) widening of the abutment beam to spread the deck load through a wider block of MSE.

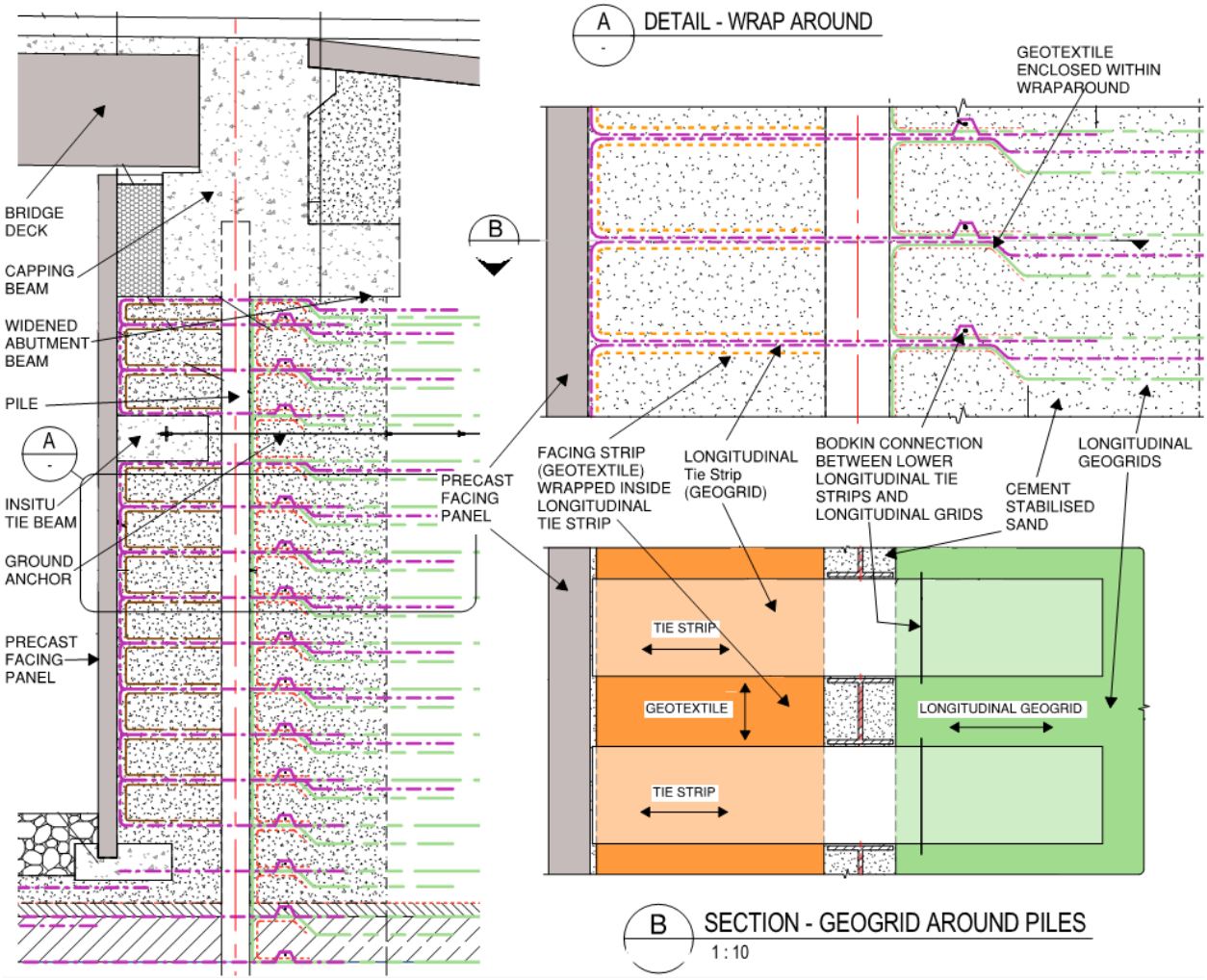


Figure 4. Section Piles through Reinforced Zone MSE Wall

9 GROUND IMPROVEMENT

Many bridges overlay soils that may liquefy during large earthquakes potentially resulting in large lateral displacement and bearing failure of walls. Furthermore settlement of compressible soft soils and liquefaction settlement could result in differential settlement resulting in poor driver comfort along the expressway and damage to rigid elements such as precast panels in front of walls and flood protection measures.

The extent of ground improvement was calculated from global stability analyses in Slope/W. The two main assumptions in this analysis were shear strength of bridge piles was ignored and improved ground was modelled using nominal soil parameters. It was assumed that ground improvement contributes only to the prevention of liquefaction, refer to Figure 5. To mitigate these adverse effects three ground improvement techniques were undertaken below MSE walls.

9.1 Densification of Soil

Liquefaction is more likely where loose to medium dense sands are present below the water table. To mitigate the effects of liquefaction the soil can be made denser by using rammed or vibro-compacted stone columns. This method is most effective for sandy soils with a relatively low silt content. It was the preferred ground improvement method on the M2PP project.

9.2 Shear Stiffening the Soil

Where sandy soils have a relatively high silt content densification methods have been found to be less effective. To mitigate liquefaction in these areas low strength concrete lattices on a regular grid were installed. This stiffens the soil in shear and reduces the risk of liquefaction.

9.3 Excavate and Replace

Where significant thicknesses of peat or fine grain deposits are present below bridge it was removed and replaced with engineered fill to reduce differential settlement effects on the walls. Excavation was carried out below the water table using GPS guided excavators and backfilled with cobble to boulder size material.

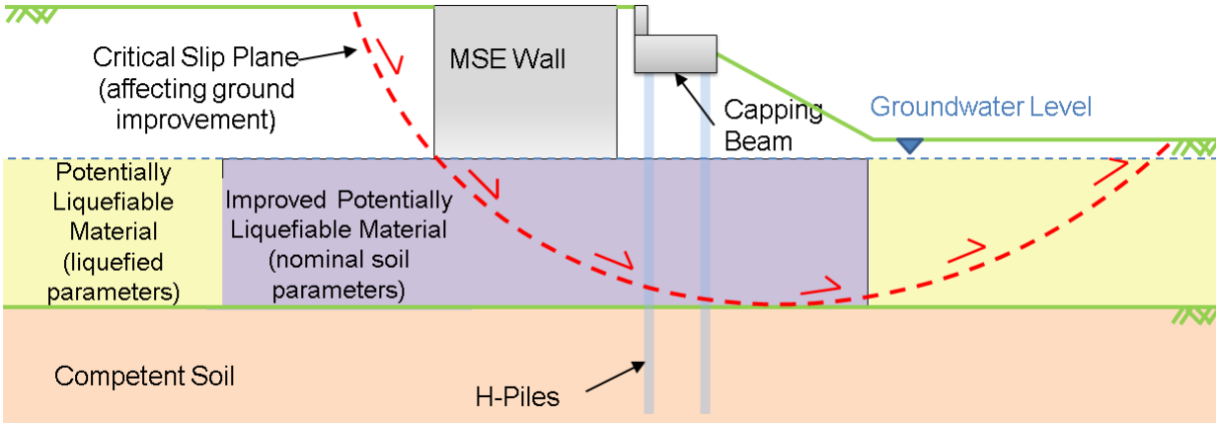


Figure 5. Ground Improvement of Liquefiable/ Compressible Materials

10 SKEWED BRIDGES

A number of bridges were highly skewed at up to 35 degrees because of the direction of existing rivers and local roads. This made it difficult to achieve the full design embedment in acute angle corners. Adequate embedment would not to be achieved if grids were placed perpendicular to the wall's face and so were skewed relative to precast side panel. Grids were locally offset where they overlapped existing grids to ensure frictional strength between grids and reinforced fill was achieved. Figure 6 shows the arrangement of grids in acute angle corners.

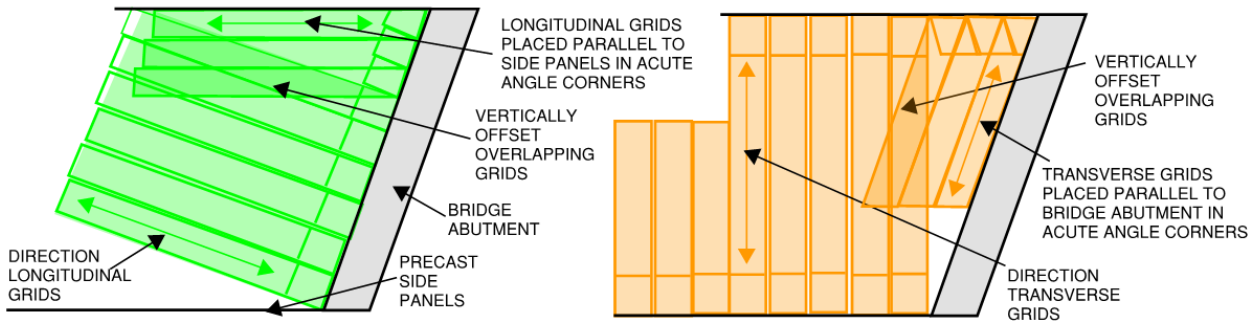


Figure 6. Arrangement of Longitudinal and Transverse Grid in Acute Angle Corners

11 CONCLUSIONS

The design of MSE walls on the M2PP expressway had six principle design challenges. The conclusions for overcoming these challenges are the following:

i. The project had high design peak ground accelerations up to 1g resulting in large seismic forces acting on walls. Displacement based design methods were used. This resulted in more economic MSE walls with less geogrids and ground improvement.

ii. The MSE walls are constructed from dune sand that is vulnerable to erosion during flood events. Therefore it was necessary to incorporate a number of design measures specifically to address the potential for erosion. These measures included the use of cement stabilised backfill immediately behind the wall face, carefully detailed drainage and comprehensive erosion protection.

iii. Many MSE walls overlay sandy soils that may liquefy and compressible soft soils. Ground improvement was adopted to control seismic lateral displacements and reduce differential settlement of walls.

iv. A secondary load path was required at some bridges if pile support could be lost because of large abutment movements during an MCE earthquake. This resulted in piles extending through the MSE reinforcement zone. Careful detailing of geogrids around piles and wall facing was required because of a reduction in reinforcement coverage ratio.

v. Some bridges were skewed because of the direction of existing rivers and local roads. This resulted in MSE walls with acute angle corners. Geogrids were skewed in these corners to achieve required pull out embedment and sliding resistance.

12 ACKNOWLEDGEMENTS

I would like to thank Mathava Dineshharan for his assistance in finite element analysis, Chris Grimes for his hard work in reviewing my design calculations and Phil Clayton and Gavin Alexander for their valuable technical input and verification of the overall design. Finally I would like to thank the M2PP Alliance for giving me to permission to publish this paper and the amount of technical knowledge I gained whilst working on this project.

REFERENCES

AASHTO (2007). *LRFD Bridge Design Specifications*, SI Units, 4th Edition, American Association of State Highway and Transportation Officials, Washington

AASHTO (2010). *LRFD Bridge Design Specifications*, SI Units, 5th Edition, American Association of State Highway and Transportation Officials, Washington

ADAMA Engineering Ltd (2013). MSEW 3.0 [Computer Software]

BBA (2013). *Tensar Geogrids: Tensar RE and RE500 Geogrids for Reinforced Soil Embankments*, HAPAS Certificate 13/H202.

BSI Standards Publication (2010). *Code of Practice for Strengthened/Reinforced Soils and Other Fill*, The British Standards Institution

FHWA (2009). *Geotechnical Engineering Circular No. 11 - Design and Construction of Mechanically Stabilized Earth Walls and Reinforced Soil Slopes*, Volume 1 (NHI-10-024), Federal Highways Authority, Washington D. C.

Geofabrics (2009). *Bidim Technical Data Sheet*. Geofabrics Australasia, Australia

Geo-Slope International Ltd (2014). Slope W [Computer Software]

Jibson R.W. (2007). "Regression models for estimating coseismic landslide displacement", *Engineering Geology*, 91(2), pp. 209-218

M2PP Alliance (2012). *M2PP Project Minimum Requirements (SMO31 App D5 Issue 6)*

M2PP Alliance (2013). *Geotechnical Interpretive Report (M2PP-25Y-D-RPT-0001)*

M2PP Alliance (2014a). *Design Philosophy Report – Geotechnical Seismic Design (M2PP-25Y-D-RPT-0003)*

M2PP Alliance (2014b). *Technical Specification for Excavation and Filling: Specification No C0203 (M2PP-220-D-SPC-81)*

Murashev, A. K. (2003). *Guidelines for design and construction of geosynthetic-reinforced soil structures in New Zealand,* Transfund New Zealand Research Report No. 239, Wellington, New Zealand.

Newmark, N. M. (1965). "Effects of earthquakes on dams and embankments", *Geotechnique*, 15(2), pp. 139-160

NZTA (2013). *Bridge manual (SP/M/022)*, Third edition, amendment 0

Plaxis (2013). Plaxis 2D [Computer Software]

TNZ (2005). *Bridge manual (SP/M/022)*, Second edition

TNZ F/1:1997. *Specification for Earthworks Construction.*

TNZ F/7:2003. *Specification for Geotextiles*.

Proceedings of the 11th ANZ Young Geotechnical Professionals Conference – 11YGPC
Queenstown, New Zealand
25 – 28 October 2016

Application of Artificial Intelligence Techniques for Rolling Dynamic Compaction

R. A. T. M. Ranasinghe[1] and M. B. Jaksa[2]

[1]School of Civil, Environmental and Mining Engineering, University of Adelaide, South Australia, 5005; email: tharanga.ranasinghe@adelaide.edu.au
[2]School of Civil, Environmental and Mining Engineering, University of Adelaide, South Australia, 5005; PH (+61) 8 8313 4314; FAX (+61) 8 8313 4359; email: mark.jaksa@adelaide.edu.au

ABSTRACT

Rolling dynamic compaction (RDC), involving non-circular modules towed behind a tractor, is now widespread and accepted among many other soil compaction methods. However, to date, there is no accurate method to reliably predict the increase in soil strength after the application of a given number of passes of RDC. This paper presents the application of artificial intelligence (AI) techniques in the form of artificial neural networks (ANNs) and genetic programming (GP) for a priori prediction of the density improvement by means of RDC in a range of ground conditions. These AI-based models are developed by using in situ soil test data, specifically cone penetration test (CPT) and dynamic cone penetration (DCP) test data obtained from several ground improvement projects that employed the 4-sided, 8-tonne 'impact roller'. The predictions of ANN- and GP-based models are compared with the corresponding actual values and they show strong correlations ($r > 0.8$). Additionally, the robustness of the optimal models is investigated in a parametric study and it is observed that the model predictions are in a good agreement with the expected behaviour of RDC.

Keywords: rolling dynamic compaction, artificial neural networks, genetic programming

1 INTRODUCTION

Impact rolling, generically known as rolling dynamic compaction (RDC), involves heavy (6–12 tonnes) non-circular modules (3-, 4- and 5-sided), which rotate about their corners and fall to the ground when drawn behind a tractor. The square (4-sided) impact rolling module, which is the focus of this study, is shown in Figure 1. RDC is now widespread globally in the construction industry, as this technique provides an alternative to the traditional approaches of ground improvement, with superior compaction capabilities. As such, RDC is effective in that it has a greater influence depth – more than 1 m beneath the ground surface and sometimes as deep as 3 m in some soils (Avalle and Carter, 2005) – compared to conventional static and vibratory compaction, where the influence depths are generally less than 0.5 m (Clifford, 1976). As a result, thicker lifts, in excess of 0.5 m, can be employed, as compared to traditional compaction lifts of approximately 0.3 m, which enhances RDC's cost effectiveness. Moreover, RDC traverses the ground at a speed of 9–12 km/h, which is far more efficient than traditional compaction using a vibratory roller, which travels at a speed of 4 km/h (Pinard, 1999). As a consequence of these improved capabilities, RDC is utilised in many applications worldwide, particularly, (i) in the civil construction industry for in situ densification and subgrade proof-rolling, (ii) in the agricultural sector mainly for the improvement of existing water storages, channels and embankments, (iii) in the mining industry for the construction of tailing dams, rock rubblisation in open cut mine waste tips and the compaction of capping over waste rocks.



Figure 1. The 4-sided 'impact roller' towed behind a tractor

However, to date, there is no reliable method available to predict the effectiveness of RDC in advance. As a result, RDC is often adopted based on experience from previous work undertaken in similar soils and site conditions. In addition, field trials are usually undertaken prior to site works to ascertain the operational parameters, especially the optimal number of roller passes required to achieve the desired percentage of maximum dry density. Therefore, this study aims to develop an accurate and robust tool for predicting the performance of RDC in a range of ground conditions. This research makes use of artificial intelligence (AI) in the form of artificial neural networks (ANNs) and genetic programming (GP), which have also been proven successful in the broader geotechnical engineering context [e.g. (Alavi et al., 2013; Shahin et al., 2005)]. The developed models are validated against a set of unseen data and, in addition, ANN-and GP-based models are compared with each other over a range of performance measures. Additionally, a parametric study is carried out to assess the robustness of the optimal models. It is important to note that these are the very first models that permit a priori prediction of ground improvement as a result of RDC.

2 DATABASE

The data used in this study have been obtained from the results of several field trials undertaken by Broons (SA) Hire, an Australian company operating a range of ground improvement technologies, including RDC. Attention is given to the 4-sided, 8 tonne 'impact roller' (BH-1300). The database is comprised of in situ strength data in the form of cone penetration test (CPT) and dynamic cone penetrometer (DCP) test results with respect to the number of roller passes. In total, the database contains 1,755 records from 91 CPT soundings and 2,048 DCP records from 12 field projects.

In this study, two sets of AI models (i.e. two ANNs and two GP models) have been developed incorporating each of the CPT and DCP datasets for model calibration and validation. The models are developed to predict the degree of density improvement of the ground with respect to the number of roller passes. Therefore, a single output variable of cone tip resistance after compaction, q_{cf} (MPa) is adopted for the CPT models, whilst the average DCP blow count per 300 mm is incorporated in the DCP models. However, it is important that the input variables of these models effectively address the significant factors that influence soil behaviour as a consequence of RDC. Hence, the input and output variables involved in the model development and their ranges are presented in Table 1.

Table 1. Input/output variable ranges used in model development

Data	Model variables		Range
CPT	Input	Depth of measurement, ***D*** (m)	0.2 – 4.0
		Cone tip resistance prior to compaction, q_{ci} (MPa)	0.19 – 50.65
		Sleeve friction prior to compaction, f_{si} (kPa)	1.67 – 473.86
		No. of Roller Passes, ***P***	5 – 40
	Output	Cone tip resistance after compaction, q_{cf} (MPa)	0.17 – 50.36
DCP	Input	Soil type	Sand–Clay, Clay–Silt, Sand–None, Sand–Gravel
		Average depth, ***D*** (m)	0.15 – 1.95
		Initial no. of roller passes, P_i	0 – 50
		Initial DCP count (blows/300 mm)	3 – 65
		Final no. of roller passes, P_f	2 – 60
	Output	Final DCP count (blows/300 mm)	2 – 84

3 ARTIFICIAL NEURAL NETWORKS (ANNS)

The ANN concept has emerged from knowledge of the functionality of the human brain and nervous system. ANNs are a data-driven approach and unlike the statistical modelling, they do not require prior knowledge of the underlying relationships among the variables. Besides, the functional relationships between inputs and outputs are learnt by the ANNs from a set of example data.

3.1 Development of ANN models

ANN modelling is carried out using the PC-based software, *Neuframe* version 4.0 (Neuframe, 2000). As described in §2, the model incorporating CPT data consists of 4 inputs along with a single output, whilst the model involving DCP data consists of 5 inputs and a single output. In this study, the cross-

validation technique (Stone, 1974) is used as the stopping criterion, which involves the division of the available dataset into three subsets: training, testing and validation. The training subset is used for model calibration, which involves optimisation of the connection weights in the network. With the testing set, model performance is periodically assessed during training, whereas the network is validated against the independent validation set once the model has been optimised. Data division is carried out in such a way that the training and validation sets contain 80% and 20% of the total data, respectively. The training set is further divided into two subsets; 80% for training and 20% for testing.

In this study, multi-layer perceptron (MLP) models are developed with the use of the back-propagation error method (Rumelhart et al., 1986). The selected MLP architecture is comprised of 3 layers: the input layer, one hidden layer and the output layer. The number of nodes in the input and output layers represent the number of model inputs and outputs and thus, the CPT- and DCP-based models consist of 4 and 5 nodes, respectively in the input layer, whilst both models contain a single node in the output layer. However, the optimisation of the nodes in the hidden layer is crucial so that the structure is neither too complex nor too simple, but appropriate enough to capture accurately the non-linearity of the relationships between the input and output parameters. Therefore, a stepwise, trial-and-error approach is adopted to achieve the optimal network architecture, where a number of ANN models are trained, beginning from the simplest form with a single hidden layer node model and successively increasing the number of nodes. As suggested by Caudill (1988), $2n + 1$ is the upper limit of hidden nodes for a network to map any continuous function, with n being the number of input nodes. Accordingly, the CPT- and DCP-based models are tested to a maximum number of hidden nodes of 9 and 11, respectively. The ANNs, with each trial number of hidden nodes, are initially trained having assigned the default software values to the internal parameters (i.e. learning rate = 0.2, momentum term = 0.8) and the sigmoidal transfer function is used for both the hidden and output layers. However, after determining the best topology, the network with the optimal number of hidden nodes is retrained with different combinations of internal parameters, specifically with different learning rates and momentum terms. After model training, model performance is assessed in terms of the coefficient of correlation (*R*), root mean square error (*RMSE*) and mean absolute error (*MAE*).

4 GENETIC PROGRAMMING (GP)

Genetic programming (GP) is an evolutionary computational approach inspired from biological evolution based on Darwinian Theory. The technique was first introduced by Koza (1992) as an extension to the genetic algorithm (GA). In GP, the computer programs are called individuals, which have been made up of a set of functions, variables and constants. In accordance with a GP algorithm, these individuals are automatically evolved into a solution for a given particular problem. In this study, a particular, robust variant of GP, namely linear genetic programming (LGP), is used. In contrast to the conventional tree-based GP approach, the data flow of evolved programs in LGP has a more general, register-based graph representation at the functional level. Additionally, the programs in LGP evolve either in an imperative programming language (e.g. C, C++) (Brameier and Banzhaf, 2007) or directly in machine language (Nordin, 1994). In brief, the LGP algorithm (Brameier and Banzhaf, 2007) involves:

i. *Initialising a population of randomly generated programs and evaluation of their fitness value;*
ii. *Running a tournament and selection of the winning programs;*
iii. In this step, 4 randomly selected programs are subjected to tournament selection, where two programs are selected as the winners based on their fitness.
iv. *Transforming the winner programs*;
v. The two selected winner programs are copied and transformed probabilistically into offsprings subjected to genetic operations; i.e. crossover and mutation.
vi. *Replacing the tournament losing programs with the offspring programs; and*
vii. *Repeating Steps 2 to 4 until the termination or convergence criteria are satisfied.*

4.1 Development of LGP models

LGP modelling utilises the same subsets of CPT and DCP data that are employed in the ANN model development, with the intention of conducting a fair comparison between the model performances. The commercially available software *Discipulus* version 5.2 (Francone, 2010) is used for the necessary computations. The selection of control parameters is considered to be vital in LGP modelling, since it has a direct impact on the model's generalisation capacity. In this modelling, the

control parameters are defined in accordance with the recommended values by previous similar LGP applications and also depending on the observations from preliminary runs. As presented in Table 2, several different parameter combinations, in terms of population size, number of demes and crossover rate, are investigated, whilst most of the other minor parameters are set to the software default values.

Table 2. Parameter settings used for the LGP model development

Parameter	Settings
Function set	+, –, ×, /, Absolute, Square Root, Trigonometric (*sin, cos*), Exponential
Population size	500, 1,000, 2,000, 5,000, 7,500, 10,000
Number of demes	10, 20
Program size	Initial = 80 bytes, Maximum = 512 bytes
Mutation frequency	95%
Crossover frequency	50%, 90%

A relatively large number of LGP projects are carried out, where all of the above listed combinations of parameters are tested and replicated 5 times for each setting, in order to address different random initial conditions. Each LGP project is made up of a series of runs, which begins in short and successively progresses in length during the course of a project. Within a run, large numbers of genetic programs are evolved and they are monitored for minimum error, as this study uses the mean square error (*MSE*) as the fitness function. A LGP run is terminated after a reasonable number of generations have evolved without improvement in terms of *MSE*. Finally, a LGP project is terminated given a reasonable time to evolve into an accurate model and when no further improvement in model performance is likely to occur.

5 RESULTS AND DISCUSSION

The following sections summarise the results of the optimal models, along with details of parametric study.

5.1 Performance analysis

The developed ANN- and LGP-based models are evaluated and compared using the performance measures as discussed above; i.e. *R*, *RMSE* and *MAE* with respect to each of the 3 data subsets. In regards to the ANN modelling, with respect to both the CPT and DCP datasets, the models with 4 nodes in the hidden layer were found to be the optimal. The results of these optimal models, along with the optimal LGP results, are presented in Table 3.

Table 3. Comparison of the performance statistics of the optimal ANN- and LGP-based models

Data	Model	*R*			*RMSE*+			*MAE*+		
		T	S	V	T	S	V	T	S	V
CPT	ANN	0.87	0.87	0.86	4.19	4.33	4.16	2.89	3.03	2.93
	LGP	0.87	0.88	0.87	4.05	4.08	4.03	2.72	2.73	2.71
DCP	ANN	0.85	0.83	0.79	6.45	6.52	7.54	4.88	4.74	5.59
	LGP	0.84	0.87	0.81	6.22	5.35	6.80	4.18	3.70	4.74

T: Training, S: Testing, V: Validation
+ For CPT models units is MPa and for DCP models units is blows/300 mm

As can be observed, the performances of the obtained optimal models, based on the CPT and DCP datasets, are very good given the strong correlation coefficient [i.e. $R > 0.8$ (Smith, 1993)] and relatively low error values (i.e. *RMSE* and *MAE*). Therefore, it can be concluded that both the ANN and LGP models developed in this study have the capability of predicting the effectiveness of RDC to a high degree of accuracy. Although both the ANN and LGP models exhibit similar performance, it is also apparent that the LGP approach slightly outperforms the ANN technique.

5.2 Parametric study

In order to further explore the accuracy and the validity of the selected optimal models, a parametric study is carried out. The model's generalisation capability is examined so that the model behaviour conforms to the known physical behaviour of the system. This involves investigating the model response to a new set of unseen synthetic input data, where only a single input parameter is varied at

a time, while the others are kept constant at a pre-defined value. It is essential that the input variables are varied between the lower and upper bounds of the training dataset, since the ANN- and LGP-based models perform best when interpolating rather than extrapolating.

For the ANN and LGP models incorporating CPT data, the output variable, q_{cf}, is examined, while the input variables of q_{ci}, f_{si}, P and D are varied. For instance, as illustrated in Figures 2 and 3, the predicted value of q_{cf} is studied for both the ANN and LGP models, respectively, by varying the input variables, q_{ci} = 2, 5 MPa, f_{si} = 50, 100 kPa and P = 10, 20, 30, 40. As can be seen, q_{cf} consistently improves as the number of passes, P, increases from 10 to 40, while q_{ci} and f_{si} remain constant at 2 or 5 MPa and 50 or 100 kPa, respectively. This indicates that the soil strength at a particular location is improved beyond the initial strength with successive roller passes. However, when comparing Figure 2(a) and (b) or Figure 3(a) and (b), it is observed that q_{cf} improves only marginally as f_{si} increases from 50 to 100 kPa, while q_{ci} remains constant either at 2 or 5 MPa. Hence, this suggests that f_{si} is less influential on q_{cf}. Nevertheless, it is evident from the parametric study that the distinct non-linear relationship between q_{cf} and P has been appropriately captured by these models.

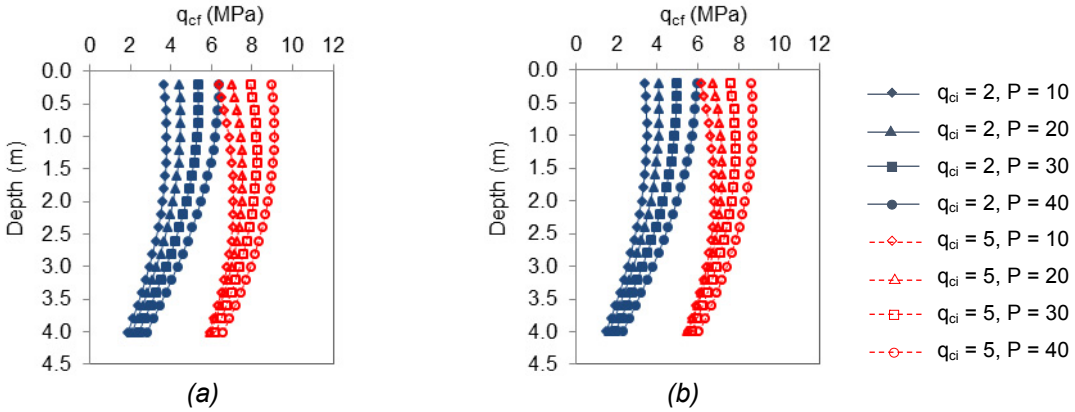


Figure 2. ANN model prediction of q_{cf} for varying q_{ci} (MPa) and number of roller passes, P when: (a) f_{si} = 50 kPa; and (b) f_{si} = 100 kPa

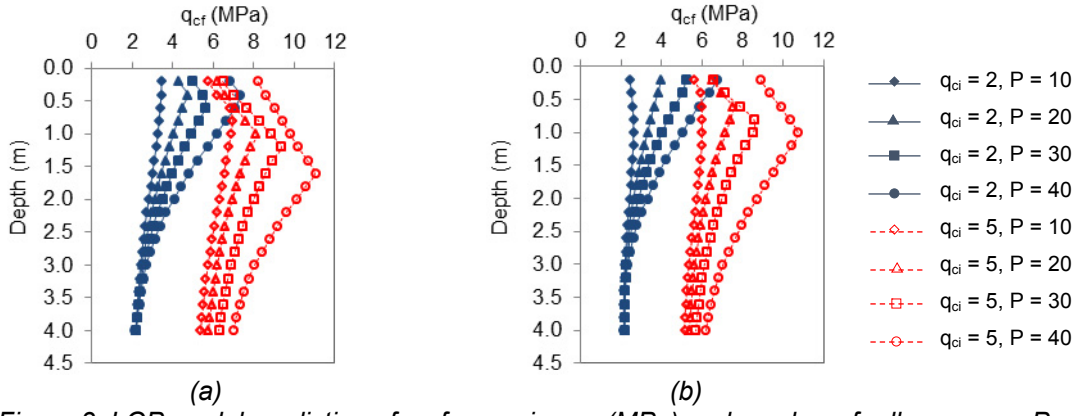


Figure 3. LGP model prediction of q_{cf} for varying q_{ci} (MPa) and number of roller passes, P when: (a) f_{si} = 50 kPa; and (b) f_{si} = 100 kPa

In a similar manner, the optimal ANN- and LGP-based models for DCP data are also investigated in a parametric study. Here, the post-compaction condition of the ground, represented by the final DCP blow count, is predicted from the optimal ANN and LGP models for a given initial DCP blow count (i.e. 5 and 15 blows/300 mm), in each of the different soil types (i.e. Sand–Clay, Clay–Silt, Sand–None and Sand–Gravel) and different numbers of roller passes (i.e. 5, 10, 15, 20, 30, 40). The resulting ANN and LGP model predictions are presented in Figures 4 and 5, respectively. It is observed that the final DCP blow count increases with increasing number of roller passes for a given initial DCP blow count in each of the soil types. It is evident from these results that the ground is significantly improved as a consequence of RDC. Moreover, this confirms the model predictions from the parametric study are in good agreement with the expected behaviour of RDC compaction. Therefore, it can be concluded that the optimal ANN and LGP models are robust when predicting the effectiveness of RDC and thus, they can be used with confidence.

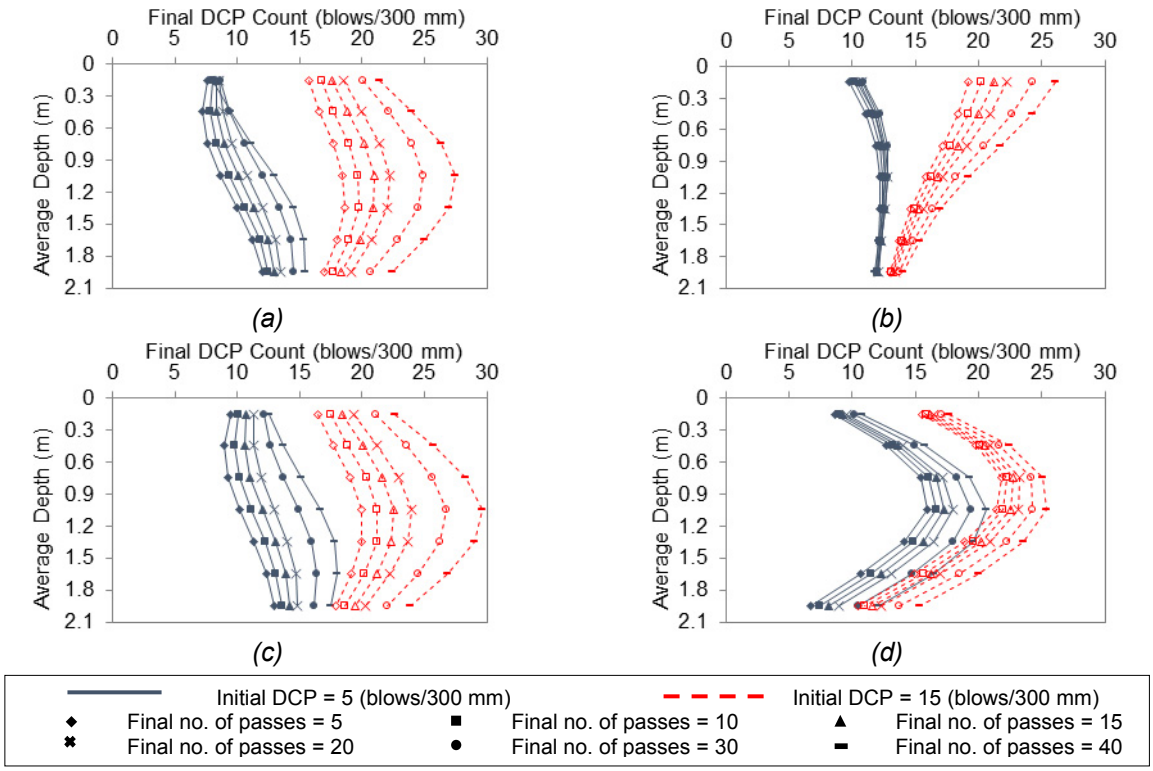


Figure 4. ANN model predictions of final DCP with respect to initial DCP and final number of roller passes in (a) Sand–Clay (b) Clay–Silt (c) Sand–None (d) Sand–Gravel

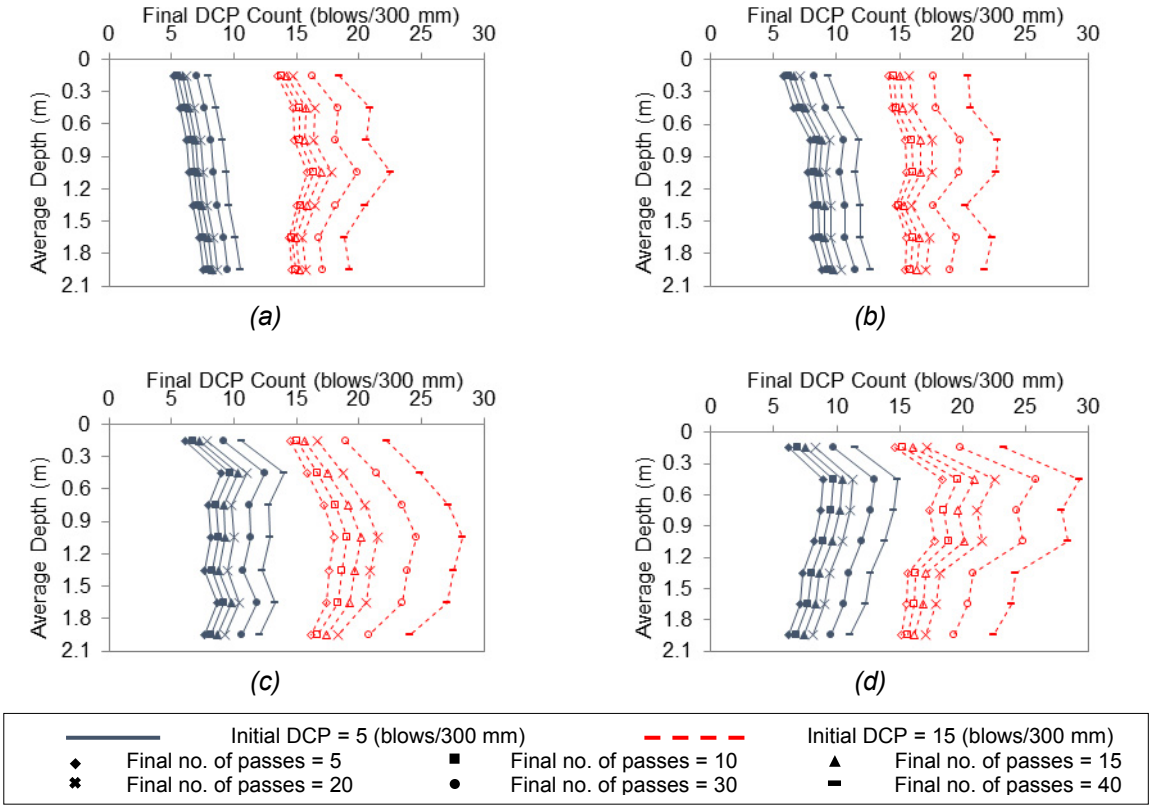


Figure 5. LGP model predictions of final DCP with respect to initial DCP and final number of roller passes in (a) Sand–Clay (b) Clay–Silt (c) Sand–None (d) Sand–Gravel

6 CONCLUSION

This paper investigates the effectiveness of rolling dynamic compaction (RDC) on different soil types and presents novel and unique predictive models based on artificial intelligence (AI) techniques in the form of artificial neural networks (ANNs) and linear genetic programming (LGP). These models incorporate an extensive database of ground density data in terms of cone penetration test (CPT) and dynamic cone penetrometer (DCP) test results associated with the Broons 4-sided, 8 tonne 'impact roller'. A total of 4 models have been developed: two involving ANNs – one for the CPT and the other for the DCP; and two LGP models – again, one for the CPT and the other for the DCP. The resulting optimal ANN- and LGP-based models yield high accuracy of model predictions, with a high coefficient of correlation (R > 0.8) and with lower error values, i.e. root mean square error (*RMSE*) and mean absolute error (*MAE*) when validated against a set of unseen data. The results indicate that the LGP-based models slightly outperform their ANN counterparts and overall produce slightly more accurate predictions. In addition, a parametric study has been carried out to assess the generalisation ability and robustness of these optimal models. The results of the parametric study demonstrate that the response of the models agrees well with the expected physical relationships among the input and output parameters. Therefore, it can be concluded that the developed models are both robust and reliable when forecasting the performance of RDC in various ground conditions. The models developed in this study are intended to provide initial predictions for planning purposes and may replace, or at the very least augment, the necessity for field trials prior to full-scale construction, which in turn contributes to significant cost savings.

7 ACKNOWLEDGEMENTS

This research was supported under Australian Research Council's Discovery Projects funding scheme (project number DP120101761). The authors wish to acknowledge Mr. Stuart Bowes at Broons Hire (SA) Pty Ltd for his kind assistance and continuing support, especially in providing access to the in situ test results upon which the numerical models are based. The authors are also grateful to colleagues Drs. Yin Lik Kuo and Fereydoon Pooya Nejad and Mr. Brendan Scott for their contribution to this work.

REFERENCES

Alavi, A. H., Gandomi, A. H., Mollahasani, A., Bazaz, J. B. and Talatahari, S. (2013). Linear and tree-based genetic programming for solving geotechnical engineering problems. *Metaheuristics in Water, Geotechnical and Transport Engineering*, 289-310.

Avalle, D. L. and Carter, J. P. (2005). *Evaluating the improvement from impact rolling on sand.* Paper presented at the 6th International Conference on Ground Improvement Techniques, Coimbra, Portugal; .

Brameier, M. F. and Banzhaf, W. (2007). *Linear genetic programming*: Springer Science & Business Media.

Caudill, M. (1988). Neural networks primer, part III. *AI Expert, 3*(6), 53-59.

Clifford, J. M. (1976). *Impact rolling and construction techniques*. Paper presented at the Australian Road Research Board (ARRB) Conference, Perth, Australia; .

Francone, F. (2010). Discipulus TM with Notitia and solution analytics owner's manual. Register Machine Learning Technologies Inc., Littleton, CO, USA.

Koza, J. R. (1992). *Genetic programming: on the programming of computers by means of natural selection* (Vol. 1): MIT press.

Neuframe. (2000). Neusciences. Neuframe Version 4.0. . Southampton, Hampshire: Neusciences Corp.

Nordin, P. (1994). A compiling genetic programming system that directly manipulates the machine code *Advances in genetic programming* (Vol. 1 pp. 311-331). MIT press, USA: Kenneth E. and Jr. Kinnear Editors.

Pinard, M. I. (1999). *Innovative developments in compaction technology using high energy impact compactors.* Paper presented at the 8th Australia New Zealand Conference on Geomechanics: Consolidating Knowledge, Hobart, Australia.

Rumelhart, D. E., Hinton, G. E. and Williams, R. J. (1986). Learning representations by backpropagating errors. *Nature, 323*(1), 533-536.

Shahin, M. A., Jaksa, M. B. and Maier, H. R. (2005). Neural network based stochastic design charts for settlement prediction. *Canadian Geotechnical Journal, 42*(1), 110-120.

Smith, M. (1993). *Neural networks for statistical modeling*. New York: Thomson Learning.

Stone, M. (1974). *Cross-Validatory Choice and Assessment of Statistical Predictions*. 36(2), 111-147.

This page intentionally left blank

Proceedings of the 11th ANZ Young Geotechnical Professionals Conference – 11YGPC
Queenstown, New Zealand
25 – 28 October 2016

Geotechnical Challenges of Brownfield Sites for Use as Landfill

Nigel Ruxton[1], BA BAI MA RPEQ CPEng MIEAust

[1]Golder Associates, 147 Coronation Drive, Milton BC, Queensland 4064; PH (61) 7 3721 5488; FAX (61) 7 3721 5401; email: nruxton@golder.com.au

ABSTRACT

This paper looks at the geotechnical challenges associated with siting a landfill at a brownfield site in south east Queensland. In particular, the geotechnical issues encountered at former quarry and mine voids and underground coal workings, when endeavouring to ascertain the maximum airspace at a proposed landfill site, will be considered. Geotechnical features will include highwall stability, managing the risk of subsidence of underground mine workings, dealing with residual waste materials such as carbonaceous material, tailings, spoil etc. and the management of spontaneous combustion of former coal workings and coal rejects. 3D conceptual models of underground workings and photogrammetry surveys of highwalls used to assist in the assessment of geotechnical risks are presented. Key emphasis will be given to the assessment of the stability of selected landfill lining systems for both basal lining and final closure, as innovation in this area can be key to maximising airspace and enhancing asset value. Critical factors affecting the performance of landfill lining/capping systems will also be discussed.

Keywords: landfill, geosynthetic lining systems, mine working, design, airspace, geotechnical

1 INTRODUCTION

This paper presents the geotechnical challenges associated with the use of brownfield sites as landfill in south east Queensland. Owing to the mining history of this region the brownfield sites utilised for landfill are typically existing voids formed as part of the extractive industry process, generally coal mining or rock quarrying. Legacy geotechnically significant features arising from these industries can include former underground tunnels and adits, remnant highwalls, stockpiles of coal rejects and other challenging materials. The geotechnical challenges associated with managing such features is heightened by uncertainty surrounding the accuracy of site development records, the variability of '*in situ*' material and often the presence of large volumes of water in the former open pits. This paper presents some approaches to these geotechnical challenges as well as the geotechnical challenges encountered when designing landfill lining systems for such conditions in a cost effective manner. This paper is not intended to provide an exhaustive overview of all geotechnical assessments or investigations required for the development of a landfill site in such environments. It is acknowledged that site history or geological and hydrogeological settings should also be considered, among other considerations.

2 BACKGROUND AND CONTEXT

The volumetric capacity of a landfill to accept waste, known as its airspace, together with the cost of developing this airspace, is a key indicator of the value of a landfill site to a waste management company. Maximising the airspace at a site requires an appreciation of the geotechnical constraints, which will invariably differ from site to site, and the ability to develop innovative and safe designs. The geotechnical analysis presented in this paper centres on former coal mines and quarries where consideration of highwalls and the optimisation of airspace is required.

The Queensland landfill guidelines require landfill designs to be based on a geotechnically stable subgrade. The guidelines do not provide prescriptive standards and require a risk based approach for the development and operation of landfill sites. This requires innovation on the part of the landfill designer to develop a cost effective liner system which maximises airspace by taking advantage of the geotechnical constraints. The maintenance of a risk register during the development of the design is an appropriate and necessary measure to ensure that risks are safely mitigated to the extent practical, and that the operator is informed of any residual risks once the design is completed.

3 GEOTECHNICAL CONSIDERATIONS

3.1 Former underground workings

Coal mines contain a complex history of underground and open cut mining activities, and often subsequent partial backfilling of the open cut voids with a wide range of material types, including overburden spoil, coal rejects and wet coal fines (tailings). It is necessary to review and interpret as-constructed plans of the former workings to develop an understanding of their potential impact on the proposed landfill. Typical plans of former mine workings are shown in Figure 1.

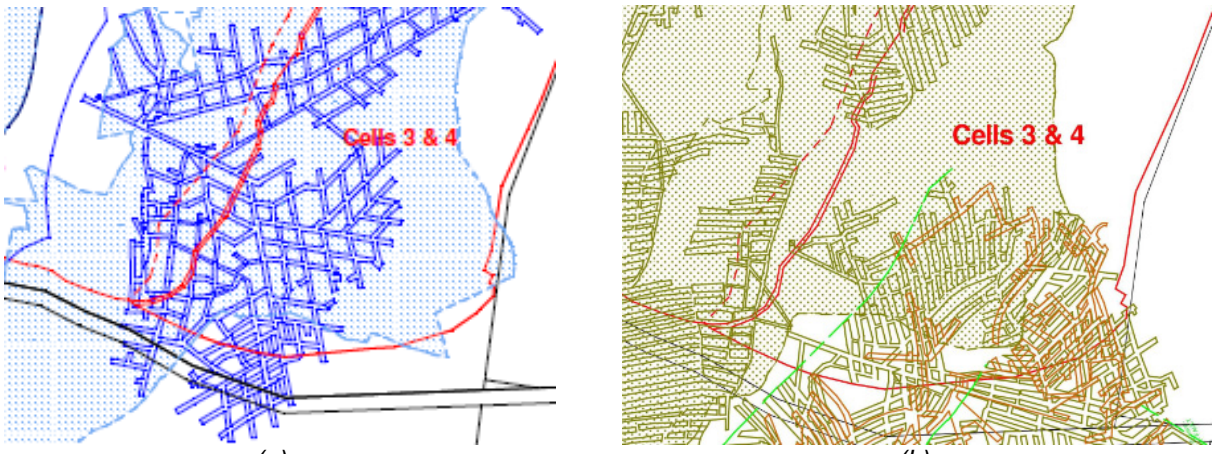


Figure 1. Mine Workings Plan (a) Seam 1; and (b) Seam 2

Review of historical plans for this site indicated that underground mining was undertaken in six coal seams underlying the site. The mining method utilised was board and pillar, a method that typically removes around 50% of the coal seam. Many of these workings were later removed by open cut mining, but some workings still remained at depth under the footprint of the proposed landfill. Following the open cut mining, there was a complex history of backfilling of the pit voids with material from a range of sources and with differing geotechnical characteristics. The variability of this backfill and the uncontrolled compaction required conservative assumptions for the material properties in the analyses undertaken at the site. Backfilled material also included carbonaceous materials and consideration of the risks of spontaneous combustion of these materials was required, including the development of a spontaneous combustion management plan.

The coal seams exploited by past mining operations at the site ranged in thickness between 1.5 and 4 metres. A 3D model of the site was prepared to allow for a better understanding of the former mining works. A screenshot of the model is provided in Figure 2, with the proposed landfill cell shown at the top of the figure, and the various seams (5) shown beneath the cell.

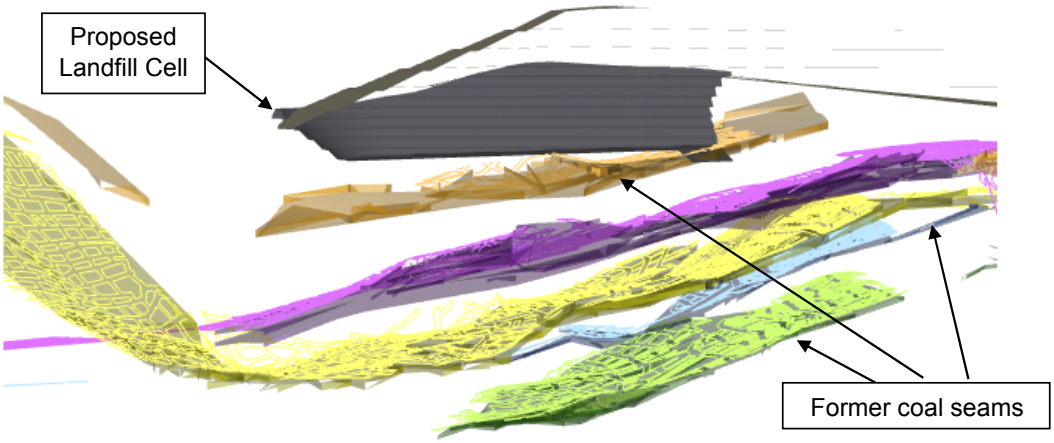


Figure 2. Cross-section of concept design and final profile (looking west) with underlying coal seams / workings

The development of the 3D model enabled the preparation of critical cross-sections of the site showing the relationship between the underground workings and the proposed landfill. Figure 3 shows an example cross section through the 3D model.

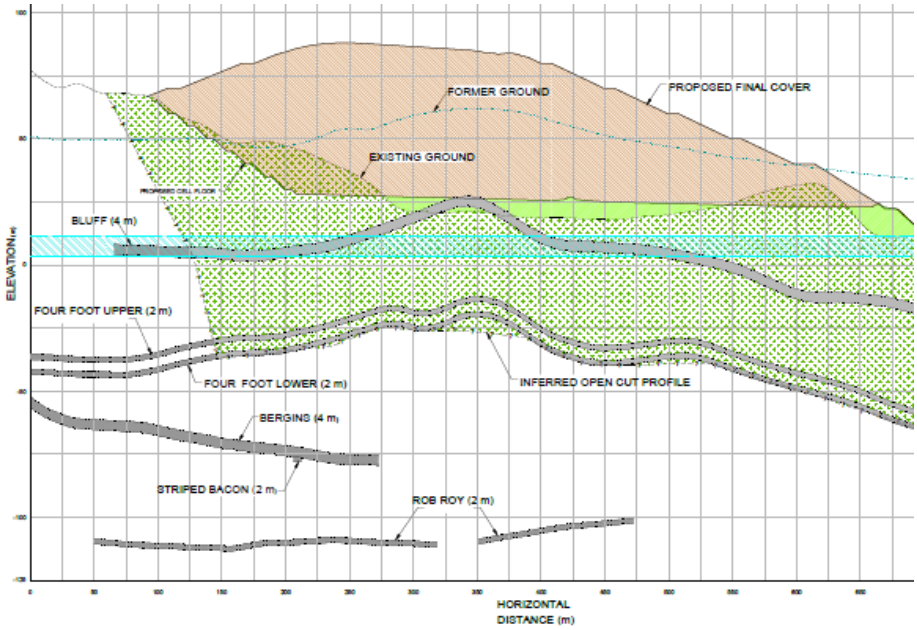


Figure 3. Cross section (looking north) of concept landfill design and underground workings

The 3D model was used to estimate the cut and fill requirements to develop the site, and to consider the potential for differential settlement. Figure 3 also includes the existing ground surface profile, pre-mining ground profile, approximate extent of open cut mining and the groundwater table.

3.2 Subsidence Potential due to Collapse of Underground Workings

The potential for subsidence of the proposed cell floors associated with pillar crushing or collapse of relict underground workings was considered, with reference to rock mechanics expertise and literature, for example, the National Coal Board (NCB) of the United Kingdom empirical method for prediction of surface subsidence. Analysis indicated a very low risk of subsidence associated with the upper seam, as it had been larger removed by open cut mining. Assessment of the subsidence associated with collapse of the seam closest to the bottom of the landfill, which was separated from the cell floor by between 65 m and 100 m, indicated that the worst case amount of subsidence at the landfill floor was limited to between 100 mm and 300 mm. If the underground workings were to collapse, the volume of the collapsed material would increase due to bulking and the upward propagation of the collapse would be arrested (or 'choked') when the void space has been completely filled by the bulked material. A number of areas were selected as worst case scenarios where total void volume as a proportion of the total seam volume was at its greatest. Based on the selected analytical method for prediction of surface subsidence, and assuming total catastrophic collapse of all of the coal pillars in the second deepest workings directly below the edge of proposed cell, the maximum predicted surface subsidence was calculated to be in the order of 300 mm. However, given width to height ratios of the pillars, such a catastrophic collapse was considered to be highly unlikely. If collapse of a small number of pillars were to occur, it was considered more likely that the load would be redistributed to the surrounding pillars and the remainder of the workings would remain stable. In this scenario, the maximum surface subsidence resulting from the localised pillar collapse was estimated to be in the order of 100 mm. The workings in these lower seams, based on analysis, were not considered to pose a subsidence risk to the proposed cell floor.

3.3 Settlement Modelling

Landfills require a firm subgrade to reduce the risk of subsidence limiting the effectiveness of the liner system. Based on the available information, the landfill cell floor was to be formed by cut and fill of the existing irregular ground surface. The assessment of subsidence was therefore necessary to ensure that the liner system was not subject to excessive strain. The cell was also partly underlain by mine

spoil that was placed in the old open cut void more than 20 years ago. The spoil comprises a mixture of 'overburden waste rock' and 'coal mine spoil' from the open cut mining operation. It was considered that the overburden waste rock would originally have consisted mainly of slightly weathered to fresh sedimentary rocks, including sandstone and shale of medium to high strength. Some degradation would have occurred in this material over time so the materials were likely to include extremely to distinctly weathered sandstone, shale, claystone and basalt in the mix. The coal mine spoil was carbonaceous shale, tailings and reject coal, which was also likely to have degraded over time.

A numerical model (PLAXIS) was used to assess the settlements using appropriate parameters, including site specific stiffness parameters. Figure 4 presents a representative analysis undertaken along a cross section of the site, showing the calculated settlements distribution.

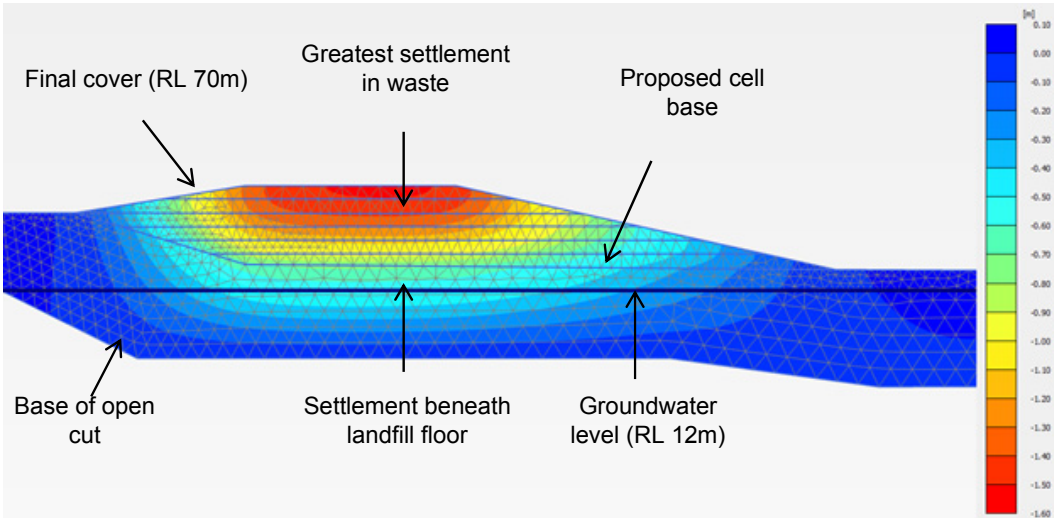


Figure 4. Graphic representation of the calculated settlements along site cross section

Based on the results of the analyses, the settlement (immediate, consolidation and long term creep) along the base of the cells was estimated to be vary between 300 mm and 900 mm, with the peak settlement located under the greatest height of landfill waste and thickest underlying mine waste spoil depth.

4 LANDFILL LINING SYSTEM DESIGN CONSIDERATIONS

4.1 Risk assessments

Assessing geotechnical risks should be undertaken in a phased manner to ensure that risks are documented and addressed appropriately. The first stage of such an assessment may involve a desktop study to identify potential risks and their relevance to the project. The second stage may involve intrusive or non-intrusive investigation of issues to further improve understanding of the risks. Further stages involve the development of a preliminary approach to mitigate the risk of geotechnical failure and optimise the airspace at the site. The risks should consider mitigation measures for both the design and operational stages, with the client being advised of how risks have been mitigated and whether residual risks exist.

4.2 Interaction between subgrade and lining system

Based on the geotechnical conditions a lining system needs to be developed that does not undergo excessive and unacceptable strain. In the case of former coal mines, such strain may be induced or enhanced by subsidence arising from poorly backfilled materials or the failure of underground workings. In the case of a former quarry or highwall with a near vertical lining system, the strain may be induced by settlement of the waste mass against a steep wall lining system, or by differential settlement of the subgrade adjacent to the highwall or steep wall lining system. A number of key considerations and approaches are presented by Jones and Dixon (2003) and these form a good basis for understanding risks and taking them into account in the design. It is not appropriate to undertake stability analysis of the subgrade and lining system in isolation, as the interaction between them can be interdependent. Geotechnical modelling of the subgrade in conjunction with the liner

system and waste loads may be necessary on a site by site basis to decide whether reinforcement of the lining system or subgrade is required.

4.3 Lining System Materials

Effective landfill lining systems typically consist of a combination of natural (clay, gravel etc.) and geosynthetic (geomembrane, geosynthetic clay liner (GCL), geotextiles, geocomposites, geogrids etc.) materials. Composite lining systems are more and more common and generally comprise a geomembrane with an underlying low permeability material such as compacted clay or a GCL. The non-prescriptive risk based approach required by the Queensland Landfill Guidelines allows for the certifying engineer to use discretion in selecting the most appropriate lining system, which must provide long term performance of the barrier and drainage elements of the lining system. Selecting the appropriate lining system, often balancing risk (environmental and geotechnical) against airspace, requires an appreciation of how individual components interact with the subgrade, each other and the overlying waste material.

4.4 Seepage and the influence of groundwater

Landfill lining systems are not impermeable and designers need to estimate the potential seepage through the lining system to assess the risk to the surrounding environment. Rowe et al (2004) presents a number of methods of estimating the seepage including factors for singular or composite lining systems. Further work by Chappel et al (2012) and Giroud and Wallace (2016) go on to consider the effect of wrinkles on seepage through the composite lining systems. Poor design, construction and quality control of the lining system could have direct implications on construction and operational costs if the groundwater levels are not well understood. In the case of the example presented long term groundwater monitoring of the area post mining gave confidence to the positioning of the cell floor around 5 metres above the recovered groundwater level. Dewatering of the former mine and quarry pits during the operational stage may result in depression of groundwater table, which may rebound post closure. Recharge of the groundwater table over time, or the impact of seasonal changes in the groundwater table due to regional factors, could lead to heaving of the lining system in the early stage of construction and initial waste placement. Such elevated groundwater levels may result in construction delays, reconstruction the lining system, or the need for long term dewatering beneath the lining system. Where dewatering is not undertaken, there is a risk of excess leachate generation due to inward seepage of the rebounding groundwater. This would lead to additional leachate management costs. The value of airspace below the long term predicted groundwater table therefore requires careful consideration.

4.5 Stability of highwalls

In former mines and quarries, the stability of highwalls and the landfill lining systems need careful consideration. A need to balance a stable and effective lining system against a desire to maximise airspace can lead to oversights by an inexperienced designer. Safety in design requires careful consideration of the health and safety risks introduced by steep wall lining systems during construction and operations, particularly next to a highwall. Figure 5 shows how photogrammetry helps the designer to develop a digital terrain model (DTM) and identify and measure key geotechnical features such as faults, toppling and rock wedges.

4.6 Steep wall lining systems

Identification of geotechnical features is necessary to ensure that they can be considered when designing the lining system, as the quality of the quarry face or highwall will affect the constructability and integrity of the lining system. Stabilisation of the rock face will often be required and the overall stability of any steep wall lining system needs to be considered. Dixon and Jones (2003) provide examples of some steep slope lining systems for use for steep slope batters. Most steep wall lining systems are constructed in lifts, due to the need to provide a stabilising buttress against the liner to ensure stability of the lining system. The buttress can be a waste material in a ‘Christmas tree’ lining system where clay is used without geomembrane, however the low stiffness of municipal solid waste can present issues in this regard and an additional layer may need to be introduced between the lining system and waste material. Geosynthetic barrier systems introduce a whole raft of other complications such as constructability, safety and long term performance issues for a steep lining system.

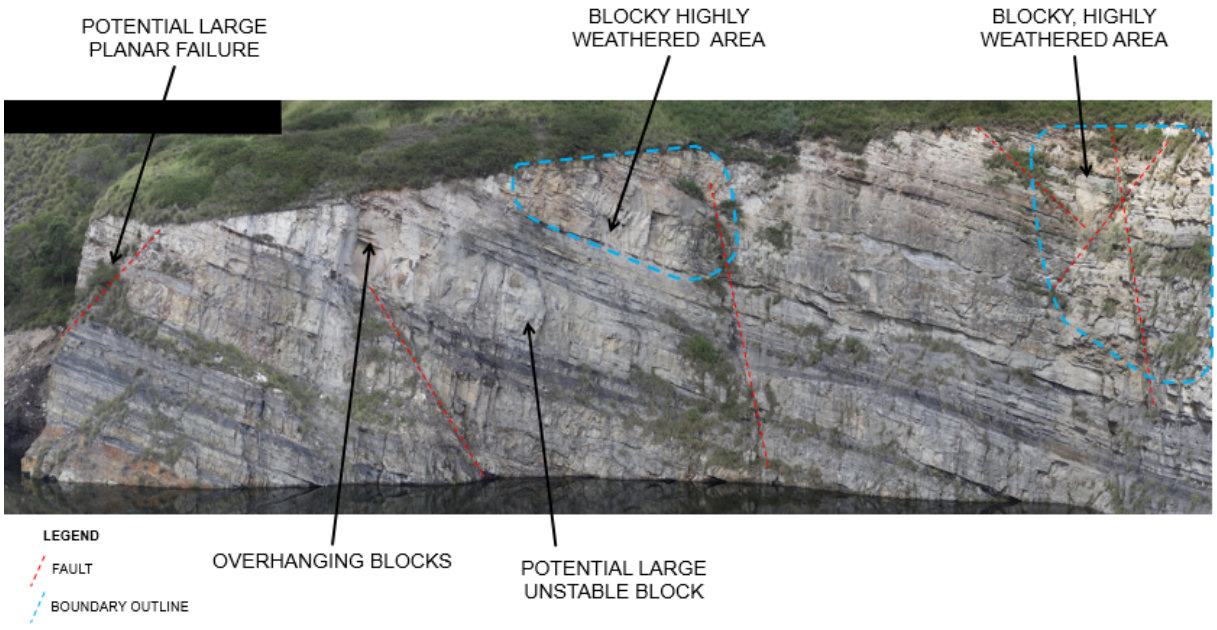


Figure 5. Photogrammetry of highwall showing some potential failure mechanisms

4.7 Effect of waste settlement on lining system

Settlement of waste has the potential to induce large strains on lining systems, in particular side wall or sloped liners. The strain can be managed through the introduction of an intermediary material between the waste and the barrier system. In the case of steep wall lining systems, the intermediary material could be a preferential sliding layer or a material of high stiffness, with the selection of the material depending on a range of factors.

4.8 Capping Interface Stability Analysis

A desire to maximise airspace can lead to over steepened external waste batters. When developing the capping system design, the risk of veneer failure of the capping system requires careful consideration by a landfill designer. Jones and Dixon (2003) presents an overview of the risks associated with poorly designed capping systems and an approach to assessing interface stability of the various lining systems. This approach has been developed by others including Koerner and Soong (2005) to include temporary loads and forces, including construction effects. The selection of interface strength values is a critical component during the design stage of the capping system. While consultants can benefit from an internal database of interface strength values, these values should be verified during construction. It is essential to assess the actual interface values based on the proposed capping materials. Additional consideration must be given to site specific factors such as settlement of waste, gas collection systems and stormwater management. The effect of seepage in a capping system needs to be carefully considered in conjunction with the cap stormwater management system, as the two are inter-related. The need for veneer reinforcement in the capping system should be considered by the designer on a site specific basis for the long term stability of the lining system and post closure maintenance requirements.

5 CONCLUSION

The appreciation of geotechnical risks is a fundamental part of landfill design. The variability of sites requires an understanding of a range of issues that may affect failures or present opportunities to increase airspace. The range of geotechnical challenges presented in this paper require the input of a range of specialists to provide the best outcome. The process of copying and pasting the previous design is not acceptable, nor is it in the best interest of the site owner.

6 ACKNOWLEDGEMENTS

The author wishes to acknowledge the input of Rob Morphet and Fred Gassner in the review of this paper. Golder reports prepared by Rob Morphet, Ken Karably, Fred Gassner and Peter Booth have also been used in the preparation of this paper.

REFERENCES

Department of Environment and Heritage Protection (2013). *Guideline-Landfill siting, design, operation and rehabilitation*, Version 2

Jones, D. R. V. and Dixon, N. (2003). *Stability of Landfill Lining Systems: Report 1 Literature Review*, Environment Agency

Jones, D. R. V. and Dixon, N. (2003). *Stability of Landfill Lining Systems: Report 2 Guidance*, Environment Agency

Rowe, R. K., Quigley, R. M., Brachman, R. W., Booker, J.R and Brachman, R. (2004). *Barrier Systems for Waste Disposal Systems*, Spon Press, pp. 190-197

Chappel, M. J., Brachman, R. W, I., Take, W. A. and Rowe, R. K. (2012). "Large-Scale Quantification of Wrinkles in Smooth Black HDPE Geomembrane", *Journal of Geotechnical and Geoenvironmental Engineering*,138(6), pp. 671-679.

Giroud, J. P. and Wallace, R. B. (2016). "Quantified Impact of Geomembrane Wrinkles on Leakage through Composite Liners", *Proceedings of GeoAmericas 2016 3rd Pan-American Conference on Geosynthetics*, 10–13th April, Miami Beach, USA

This page intentionally left blank

Proceedings of the 11th ANZ Young Geotechnical Professionals Conference – 11YGPC
Queenstown, New Zealand
25 – 28 October 2016

Effect of Pre-Shearing during Cyclic Simple Shear Testing of Clean Sand for Liquefaction Analyses

S. D. Rees[1], GIPENZ

[1]Geotechnical Engineer, Tonkin & Taylor Ltd, P.O. Box 13 055, Christchurch 8141; PH +64-3-363-2450;
email: srees@tonkintaylor.co.nz

ABSTRACT

The undrained cyclic direct simple shear test (CSS) is an advanced laboratory method well-suited to characterising the in-situ liquefaction resistance of clean and silty sands. This is due to it approximating the one-dimensional consolidation that occurs beneath level ground, and the shear deformations that develop in a soil mass during earthquake shaking. Currently however there is no recognised international standard for this test, which can lead to significant cyclic resistance ratio (CRR) errors being observed when factors such as the sand-apparatus interface and induced stress concentrations are not properly considered. Thus, while CSS testing may be employed as a critical component of detailed liquefaction analyses for important geotechnical projects, the testing itself must be executed with care and guidance. To further clarify CSS testing methodology, this paper systematically examines the effect drained cyclic pre-shearing has on the undrained cyclic resistance of Toyoura sand. The results from this study suggest pre-shearing clean sand CSS specimens under drained cyclic loading conditions, before carrying out undrained cyclic testing, produces CRR values that may be considered reasonably representative of in-situ cyclic response. Conversely, a lack of pre-shearing is shown to produce CRRs approximately 20 % lower in value, which would lead to unnecessary conservativism in design when undertaking detailed liquefaction assessments.

Keywords: liquefaction, undrained cyclic simple shear, drained cyclic pre-shearing, Toyoura sand

1 INTRODUCTION

Advanced laboratory testing of soils can form a critical component of detailed liquefaction analyses for important and/or unique geotechnical projects. The undrained cyclic direct simple shear test (CSS) is one laboratory method well-suited to characterising the in-situ liquefaction resistance of sandy soils. This is due to it approximating the one-dimensional consolidation that occurs beneath level ground, as well as the shear deformations that develop in a soil mass during earthquake shaking (Idriss and Boulanger 2008). When undisturbed samples from the field are tested in an NGI-type CSS apparatus (Bjerrum and Landva 1966), practical advantages over the often-used undrained cyclic triaxial test include the use of shorter specimens (typically 20 mm in height), which enables a greater number of tests to be performed per in-situ sample, and the ability to test specimens in a non-saturated state via the 'constant volume' condition (Dyvik et al. 1987), avoiding the need for time-consuming saturation.

The CSS test does however come with limitations. While issues such as stress and strain non-uniformities have been summarised in the literature (Boulanger et al. 1993), a noticeable practical problem for laboratories is the lack of an internationally-recognised test standard for performing CSS tests on sandy soils. Although ASTM D-6528–07 (ASTM International 2007) is widely referred to when performing direct simple shear tests, this standard was published to guide monotonic testing of cohesive soils only, and hence excludes important considerations for the cyclic testing of sandy soils that are otherwise discussed in the geotechnical literature. This means laboratories may conduct CSS tests without sufficient care and guidance, and subsequently estimate cyclic resistance ratios (CRR) that exhibit significant error. Note CRR is defined in this paper as the cyclic stress ratio (CSR) required for a double amplitude shear strain, γ_{DA}, of 15 % to be reached in 10 load cycles.

1.1 Drained cyclic pre-shearing during CSS tests on sandy soils

One CSS test consideration not included in any widely-available test standard, but discussed in literature relating to the laboratory testing of soils for offshore geotechnical engineering projects, is the effect a drained cyclic pre-shearing test stage can have on the CRR of sand when performed prior to undrained cyclic loading. Such a drained pre-shearing stage has typically consisted of 400 load cycles

being applied at a stress ratio of $\tau_{cyc}/\sigma'_{vc} \approx 0.04$ to 0.05, while the effective vertical consolidation stress, σ'_{vc}, is maintained constant (Finnie et al. 1999, Andersen 2009). It has been suggested by Andersen (2009) that the ultimate effect of this drained pre-shearing is an increase in the measured CRR of approximately 5 % to 25 %, with improved seating at the sand-apparatus interface, levelling out of stress concentrations induced during initial consolidation, increase in the horizontal stress, and changing of soil fabric providing mechanisms for the CRR increase. Randolph et al. (2005) have made similar comments, with drained pre-shearing procedures being developed in Australian laboratories to minimise specimen reconstitution and bedding effects. To date however there has been no systematic study detailing the effect drained pre-shearing has on the CRR of sands.

Given the suitability of CSS testing for use in liquefaction analyses, this paper systematically examines the effect drained cyclic pre-shearing has on the CSS response of Toyoura sand reconstituted to medium density. Toyoura sand was chosen given its long history of testing in Japanese laboratories as part of liquefaction studies, and cyclic data obtained from this study is subsequently compared with that from high-quality undrained cyclic simple shear tests previously performed on Toyoura sand in the hollow cylinder (HC) apparatus. The high-quality HC data is henceforth assumed to be a reliable benchmark when assessing how representative the data obtained from the CSS apparatus may be of in-situ response. It is however important to note that potential effects of differing soil fabric between in-situ and reconstituted states on the CRR are not specifically addressed in this paper.

2 LABORATORY TESTING

A total of ten undrained CSS tests were performed on reconstituted Toyoura sand specimens as part of this study. Details regarding the laboratory tests are given in the following sections.

2.1 Cyclic direct simple shear test apparatus

All tests were performed within a commercially-available NGI-type CSS apparatus. Full apparatus details can be found in the manufacturer's documentation (GDS Instruments 2015), however important aspects of the apparatus relevant to this study include: (i) Lateral specimen restraint was provided by a stack of Teflon-coated rings; (ii) Sintered-steel porous discs provided the sand-apparatus interface, and contained triangular-shaped ridges (1 mm in height) oriented perpendicular to the shearing direction; (iii) A 5 mm range LVDT was mounted directly between top and base specimen platens to accurately measure small-strain horizontal deformations; and (iv) Specimen height was actively maintained constant during undrained cyclic loading via feedback from a 5 mm range LVDT measuring vertical deformations.

2.2 Specimen preparation

The test specimens, nominally 70.4 mm in diameter and 18.3 mm in height, were reconstituted to approximately 50 % relative density, D_r, using a moist-tamping technique similar to that described in the literature (Ladd 1978). The moist sand was placed and tamped directly into a mould set up on the specimen base platen, which consisted of a latex membrane, the Teflon-coated ring stack, and an aluminium split mould. A small vacuum was applied through the split mould to pull the membrane against the ring stack, enabling the sand to be tamped across the full specimen diameter. The specific gravity, and maximum and minimum void ratios, e_{max} and e_{min}, of the Toyoura sand tested in this study were taken to be 2.65, 0.988 and 0.616 respectively (Zlatović 1994).

2.3 Test procedure

After securing the test specimen in the CSS apparatus, a vertical effective stress $\sigma'_v \approx 20$ kPa was applied while 150 mL of de-aired water was percolated through the sand. This was carried out to ensure no suction-related stresses were present. The specimen was then consolidated at $\sigma'_{vc} \approx 100$ kPa for at least one hour, before drained cyclic pre-shearing was performed. Here a stress ratio of $\tau_{cyc}/\sigma'_{vc} \approx 0.045$ was applied for a number of load cycles, $N_{c,ps}$, ranging from zero (i.e., no pre-shearing) to 1600. After pre-shearing, the specimen was left to consolidate at $\sigma'_{vc} \approx 100$ kPa for at least one hour, before undrained cyclic loading at a specified cyclic stress ratio (CSR) was executed at a loading frequency of 0.1 Hz. The number of load cycles required to reach failure, N_f, was defined as those taken to first reach a double amplitude shear strain, γ_{DA}, of 15 %. The CSR was defined as being equal to τ_{cyc}/p'_c, where τ_{cyc} = single amplitude horizontal shear stress and p'_c = mean effective stress.

2.4 Test results

Table 1 summarises the CSS tests performed on the reconstituted Toyoura sand specimens. Note the horizontal effective stress following consolidation and pre-shearing, σ'_{hc}, was estimated from $\sigma'_{hc} = K_0.\sigma'_{vc}$, assuming $K_0 = 1 - \sin\varphi'$, and $\varphi' \approx 34$ ° for Toyuora sand prepared to $D_r \approx 50$ % (Yoshimi et al. 1978). The mean effective stress, p'_c, was estimated from $p'_c = (\sigma'_{vc} + 2.\sigma'_{hc})/3$. $D_{r,vc}$ represents the specimen relative density following initial consolidation, while e_{vcps} and $D_{r,vcps}$ respectively denote the specimen void ratio and relative density following pre-shearing. Typical CSS response of the Toyoura sand is shown in Figure 1(a) – (d), obtained from Test 7. Note the circle in each plot highlights the point at which N_f was reached.

Table 1. Summary of undrained cyclic simple shear tests on Toyoura sand specimens

Test	σ'_{vc} (kPa)	σ'_{hc} (kPa)	p'_c (kPa)	$D_{r,vc}$ (%)	e_{vcps}	$D_{r,vcps}$ (%)	$N_{c,ps}$	CSR	N_f
1	99	46	62	45	0.821	45	0	0.197	4.2
2	99	44	62	47	0.813	47	0	0.142	11.6
3	99	44	62	44	0.824	44	10	0.142	12.8
4	99	44	62	47	0.813	47	100	0.142	26.2
5	105	44	66	47	0.809	48	400	0.251	3.6
6	99	44	62	45	0.817	46	400	0.197	7.7
7	99	44	62	50	0.798	51	400	0.164	16.2
8	99	44	62	46	0.817	46	400	0.142	32.7
9	99	44	62	44	0.817	46	800	0.142	32.2
10	99	44	62	45	0.817	46	1600	0.142	32.2

3 DISCUSSION

3.1 Effect of number of pre-shearing load cycles on relative density

The effect of drained cyclic pre-shearing on the Toyoura sand specimens was firstly investigated by checking the variation in relative density before and after the pre-shearing stage. From observing the difference in $D_{r,vc}$ and $D_{r,vcps}$ values in Table 1, it is noted D_r increased by 0 % to 2 % between the beginning and end of pre-shearing. This increase is relatively insignificant when compared with the 6 % variation in $D_{r,vc}$ observed across the 10 test specimens, suggesting specimen reconstitution has a more pronounced effect on the post-consolidation D_r than pre-shearing. This finding is consistent with the literature, where volume reduction during pre-shearing is described as generally being small (Andersen 2009).

The single amplitude shear strain recorded during each pre-shearing load cycle, γ_{cyc}, was also investigated. Here each specimen underwent an approximately consistent $\gamma_{cyc} \approx \pm 0.02$ % during each cycle, which is of the order of the elastic threshold for soils (Ishihara 1996). This suggests the sand experienced only limited plastic deformation, which is consistent with the limited change in D_r.

3.2 Effect of number of pre-shearing load cycles on cyclic resistance

The effect of pre-shearing was secondly investigated by comparing the number of undrained cyclic load cycles required to reach failure, N_f, with the number of applied pre-shearing cycles, $N_{c,ps}$. This comparison in displayed in Figure 2, with a CSR = 0.142 applied to all specimens. It is firstly noted from Figure 2 that N_f increased from 11.6 to 32.7 as $N_{c,ps}$ increased from 0 to 400. This clearly demonstrates an increased resistance to undrained cyclic loading provided by pre-shearing, consistent with the ultimate effect of pre-shearing described in the literature (Andersen 2009). This is further quantified in Section 3.3, in which CRR values are directly compared.

A second trend observed from Figure 2 is that N_f does not increase as $N_{c,ps}$ is raised further from 400 to 1600. Instead, the value of N_f remains approximately constant, varying by only 0.5. While there is limited data available in the literature for comparison, this result is broadly consistent with Andersen (2009), in which 'Soil 26', also prepared to 50 % D_r, shows a limited increase in cyclic strength for N_f = 10 when $N_{c,ps}$ is increased by an order of magnitude (from 400 to 4000). Overall this finding is considered physically reasonable, given prolonged cyclic loading at a shear strain amplitude near the elastic threshold is unlikely to continue resulting in significant plastic straining.

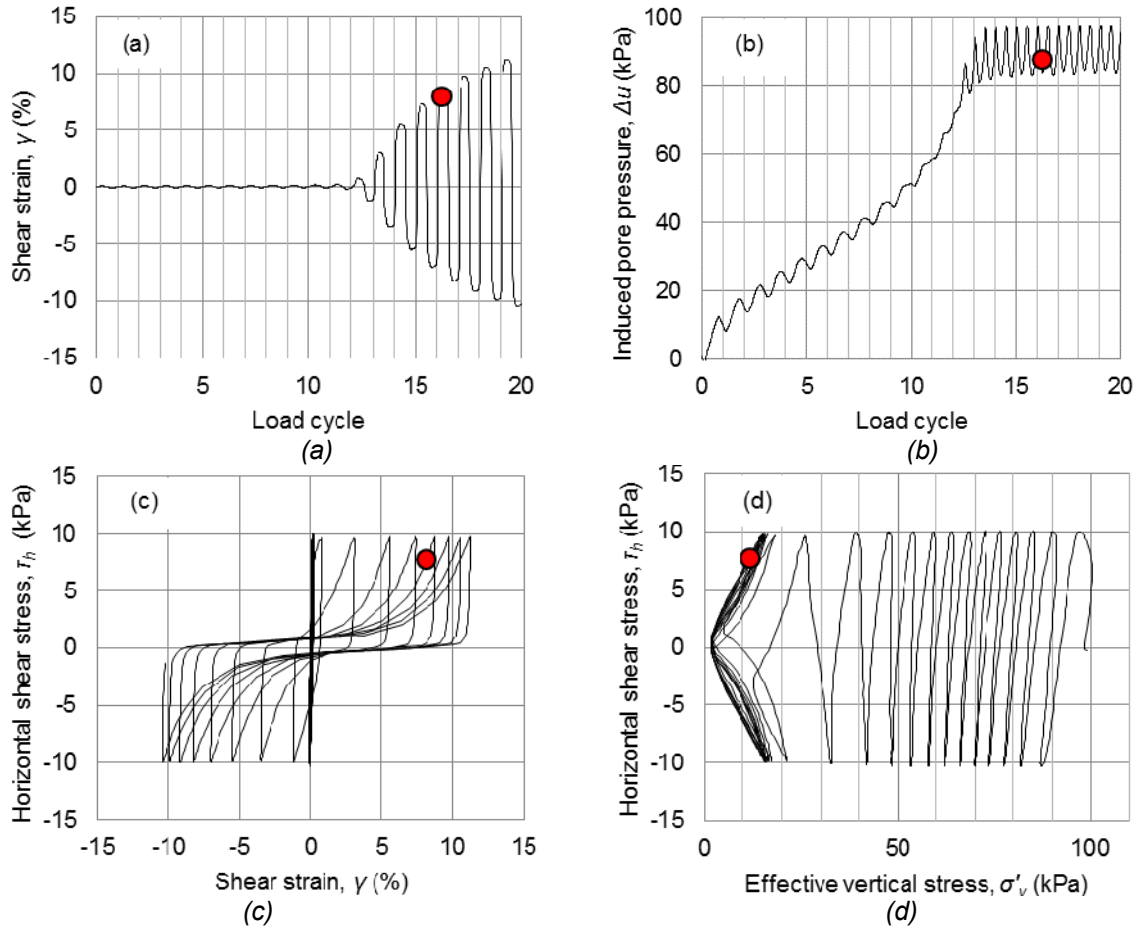


Figure 1. (a) – (d). Typical undrained cyclic simple shear response of the Toyoura sand.

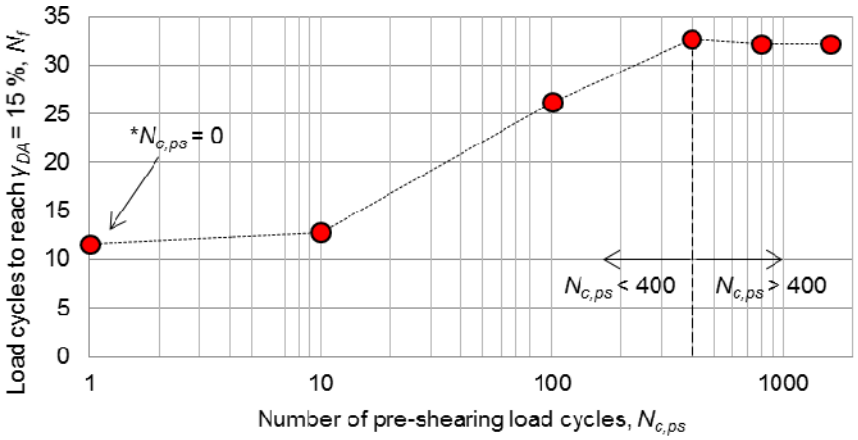


Figure 2. Effect of drained cyclic pre-shearing on the cyclic resistance of Toyoura sand.

3.3 Comparisons with data obtained from hollow cylinder testing

The effect of pre-shearing was lastly investigated by comparing the cyclic resistance data obtained from this study with that from five previous studies which employed the hollow cylinder apparatus (HC) to perform high-quality undrained cyclic simple shear tests on saturated Toyoura sand specimens prepared to $D_r \approx 50$ % (Tatsuoka et al. 1982, Tatsuoka et al. 1986, Koseki et al. 2005, Kiyota et al. 2008, Chiaro et al. 2012). A summary of this HC testing is provided in Table 2, while Figure 3 compares the cyclic resistance data from six of the Toyoura sand specimens tested in this study ($N_{c,ps}$ = 0 or 400) with that from the HC testing. In this figure three clear trends are observed. Firstly, the CRR of the Toyoura sand specimens tested in this study significantly decreases when no pre-shearing is applied. Here the CRR = 0.184 for $N_{c,ps}$ = 400, while the CRR = 0.147 for no pre-shearing. This corresponds to a 20 % decrease in CRR when pre-shearing is not employed, which is consistent with the effect of pre-shearing on cyclic resistance as reported by Andersen (2009).

Table 2. Undrained cyclic simple shear tests previously performed in the HC apparatus

Reference	Reconstitution	Failure definition	$\sigma'_{hc}/\sigma'_{vc}$ [b]	p'_c (kPa)	D_r (%)
Tatsuoka et al. 1982	Air-pluviation	γ_{DA} = 15 %	1.0	98	50
Tatsuoka et al. 1986	Moist-tamping	γ_{DA} = 15 %	$0.52e_i$ [a]	98	50
Koseki et al. 2005	Air-pluviation	γ_{DA} = 7.5 %	0.5	65	52 - 56
Kiyota et al. 2008	Air-pluviation	γ_{DA} = 10 %	1.0	100	40 - 50
Chiaro et al. 2012	Air-pluviation	γ_{SA} = 7.5 % (≈ γ_{DA}/2)	1.0	100	44 - 45

[a] e_i = initial specimen void ratio, [b] $\sigma'_{hc}/\sigma'_{vc}$ = 1.0 for test performed at a CSR = 0.147.

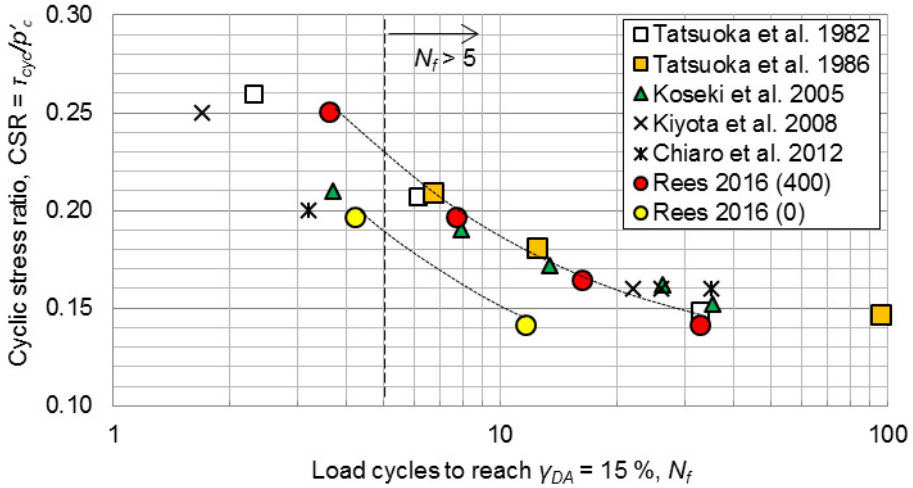


Figure 3. Cyclic data for Toyoura sand specimens tested in cyclic simple shear conditions.

Secondly, the cyclic resistance data for the Toyoura sand specimens with $N_{c,ps}$ = 400 compare well with the HC test data when N_f > 5. More specifically, the curve fitted to this study's data (for $N_{c,ps}$ = 400) locates to within 4 % of the Tatsuoka et al. 1986 data points, which is the most similar data set to this study (anisotropic consolidation, moist-tamping reconstitution). This observation suggests that, for Toyoura sand prepared to medium density, 400 cycles of pre-shearing will subsequently produce undrained cyclic simple shear response essentially equivalent to that obtained in the HC apparatus.

Finally, a significant amount of variation in the cyclic resistance data is observed when N_f < 5. It is however noted that all HC data in this region was obtained from air-pluviated specimens, and that a divergence in cyclic resistance has previously been reported between moist-tamped and air-pluviated specimens when N_f < 5 and D_r ≈ 50 % (Tatsuoka et al. 1982). In this previous study the moist-tamped specimens were shown to have larger cyclic resistances than air-pluviated specimens when N_f < 5, which is consistent with the trend observed in Figure 3.

3.4 Practical recommendations suggested from this study

The most encouraging observation discussed in this study is that application of drained cyclic pre-shearing using a relatively small stress ratio produces CRR values for Toyoura sand in an NGI-type CSS apparatus essentially equivalent to those derived from high-quality HC testing during previous liquefaction studies. This equivalence with the benchmark HC test data strongly suggests the primary effect of pre-shearing is to shift the overall test condition in the CSS apparatus closer to the idealised test model (through improved specimen-apparatus interfacing, minimisation of reconstitution effects, levelling out of stress concentrations etc.), as opposed to increasing the sand's inherent resistance to cyclic loading. Given this outcome, it is suggested the following steps are employed by laboratories when CSS tests are performed in an NGI-type apparatus on medium-dense (or looser) clean sands as part of detailed liquefaction assessments:

- At least 400 load cycles of drained cyclic pre-shearing should be applied to reconstituted specimens before undrained cyclic loading takes place; and,
- The drained pre-shearing stress ratio should be of the order of τcyc/σ'vc ≈ 0.04 to 0.05, with the shear strain approximately limited to the elastic threshold of the material.

Note it is currently unclear what effect pre-shearing has on the CRR of intact and/or high-quality undisturbed specimens. Given that pre-shearing appears to improve the overall CSS test condition, it is suggested pre-shearing be used. A future study investigating the effect of pre-shearing on the CRR of undisturbed specimens would however prove practically useful for test laboratories. It is also noted the observed improvement in CRR values presented in this study is limited to clean sand prepared to 50 % D_r and pre-sheared using a stress ratio of $\tau_{cyc}/\sigma'_{vc} \approx 0.045$. It is currently unclear what improvement in CRR values may be obtained when soil density and/or pre-shear stress ratio is varied.

4 CONCLUSIONS

Ten undrained cyclic direct simple shear (CSS) tests were performed on reconstituted medium density Toyoura sand specimens in an NGI-type apparatus to assess the effect of drained cyclic pre-shearing on the undrained cyclic resistance of clean sand. Pre-shearing was performed at a cyclic stress ratio of $\tau_{cyc}/\sigma'_{vc} \approx 0.045$ while the effective vertical consolidation stress was held constant.

It was observed that application of 400 pre-shearing load cycles produced cyclic resistances in the CSS apparatus essentially equivalent to those of Toyoura specimens tested in the hollow cylinder apparatus. When pre-shearing was not employed, the cyclic resistance was found to be approximately 20 % lower. Additionally, it was observed that pre-shearing does not significantly change relative density, and that pre-shearing beyond 400 load cycles does not further increase the cyclic resistance by a significant amount. It is therefore recommended that drained cyclic pre-shearing be employed when testing clean sand specimens in a CSS apparatus for use in liquefaction analyses. Exclusion of this component in a CSS test may result in CRR estimates significantly lower than what would be considered representative of in-situ behaviour, potentially leading to unnecessary conservatism in engineering design when working with liquefiable soil deposits.

5 ACKNOWLEDGEMENTS

The author wishes to thank L'École des Ponts ParisTech for kindly providing the Toyoura sand used in the laboratory study, the management team at GDS Instruments for providing the time and resources to complete the laboratory study, and all at Tonkin + Taylor Ltd for their support in writing this paper.

REFERENCES

Andersen, K. H. (2009). "Bearing capacity under cyclic loading – offshore, along the coast, and on load. The 21st Bjerrum Lecture presented in Oslo, 23 November 2007", *Canadian Geotechnical Journal*, 46(5), pp. 513-535.

ASTM International. (2007). *D 6528 – 07 Standard test method for consolidated undrained direct simple shear testing of cohesive soils*, ASTM International, West Conshohocken, 9 p.

Bjerrum, L., and Landva, A. (1966). "Direct simple-shear tests on a Norwegian quick clay", *Géotechnique*, 16(1), pp. 1-20.

Boulanger, R. W., Chan, C. K., Seed, H. B., Seed, R. B., and Sousa, J. B. (1993). "A low-compliance bi-directional cyclic simple shear apparatus", *Geotechnical Testing Journal*, 16(1), pp. 36-45.

Chiaro, G., Koseki, J., and Sato, T. (2012). "Effects of initial static shear on liquefaction and large deformation properties of loose saturated Toyoura sand in undrained cyclic torsional shear tests", *Soils and Foundations*, 52(3), pp. 498-510.

Dyvik, R., Berre, T., Lacasse, S., and Raadim, B. (1987). "Comparison of truly undrained and constant volume direct simple shear tests", *Géotechnique*, 37(1), pp. 3-10.

Finnie, I. M. S., Hospers, B., Nowacki, F., Andersen, K. H., and Kalnes, B. (1999). "Cyclic simple shear behaviour of a carbonate sand", in Al-Shafei, K. A. (eds.), *Proc. 2nd Int. Conf. on Eng. for Calcareous Sediments*, Vol. 1, A. A. Balkema, Rotterdam, pp. 87-100.

GDS Instruments. (2015). *The GDS electro-mechanical dynamic cyclic simple shear system hardware handbook,* GDS Instruments, Hook, 27 p.

Idriss, I. M., and Boulanger, R. W. (2008). *Soil liquefaction during earthquakes,* Earthquake Engineering Research Institute, MNO-12, Oakland, 243 p.

Ishihara, K. (1996). *Soil behaviour in earthquake geotechnics,* Oxford University Press, New York, 350 p.

Kiyota, T., Sato, T., Koseki, J., and Abadimarand, M. (2008). "Behavior of liquefied sands under extremely large strain levels in cyclic torsional shear tests", *Soils and Foundations*, 48(5), pp. 727-739.

Koseki, J., Yoshida, T., and Sato, T. (2005). "Liquefaction properties of Toyoura sand in cyclic tortional shear tests under low confining stress", *Soils and Foundations*, 45(5), pp. 103-113.

Ladd, R. S. (1978). "Preparing test specimens using undercompaction", *Geotechnical Testing Journal*, 1(1), pp. 16-23.

Randolph, M., Cassidy, M., Gourvenec, S., and Erbrich, C. (2005). "Challenges of offshore geotechnical engineering." *Proc. 16th Int. Conf. on Soil Mech. and Geotechnical Eng.*, Vol. 1, A. A. Balkema, Rotterdam, pp. 123-176.

Tatsuoka, F., Muramatsu, M., and Sasaki, T. (1982). "Cyclic undrained stress-strain behaviour of dense sands by torsional simple shear test." *Soils and Foundations*, 22(2), pp. 55-70.

Tatsuoka, F., Ochi, K., Fujii, S., and Okamoto, M. (1986). "Cyclic undrained triaxial and torsional shear strength of sands for different sample preparation methods." *Soils and Foundations*, 26 (3), 23-41.

Yoshimi, Y., Hatanaka, M., and Oh-oka, H. (1978). "Undisturbed sampling of saturated sands by freezing." *Soils and Foundations*, 18 (3), 59-73.

Zlatović, S. (1994). *Residual strength of silty soils*. PhD thesis, University of Tokyo.

Proceedings of the 11th ANZ Young Geotechnical Professionals Conference – 11YGPC
Queenstown, New Zealand
25 – 28 October 2016

Design of Anchors in Weathered Greywacke - A Case Study in Wellington

S. Cherfane[1] and S. Moniz[1]

[1]Level 18, Grand Plimmer Tower, 2-6 Gilmer Terrace, Wellington 6011, PO Box 25-047, Wellington 6146, emails: SCherfane@engeo.co.nz, SMoniz@engeo.co.nz

ABSTRACT

The variability in weathering conditions of Wellington greywacke whether among different sites or within the same site makes anchor design challenging for geotechnical engineers. Sacrificial ground anchors tests were analysed from 16 different projects located within the Wellington region. A correlation between the rock weathering grades and the bond capacities inferred from the anchors tests, and comparison with relative published data /research are presented in this paper. This correlation could be used as preliminary presumptive value to design the anchors. Quality logging of the target founding strata at the appropriate depth and understanding of the geological model is required to be able to utilise the correlation. Sacrificial anchor testing is recommended as the design progresses. A case study is also included to demonstrate a possible approach in designing anchors in such variable conditions. .

1 INTRODUCTION

Greywacke rock is the most abundant rock type in Wellington. The variability in weathering conditions of greywacke whether among different sites or even within the same site makes anchor design challenging. To account for this variability the anchor design must be a dynamic process which starts with an assumption about the design strength and evolves through the project after sacrificial and production anchor testing.

This paper explores the variability of greywacke through the review of ground anchor tests carried out at 16 locations in the Wellington region. It summarises the ranges of grout to ground capacities by each weathering grade. These ranges could be used by engineers to aid the selection of the initial design strength of anchors founded in greywacke. A case study is also included to demonstrate a possible approach in designing anchors in such variable conditions.

2 GREYWACKE WEATHERING

The bedrock which forms the foundation of the landscape in Wellington consist predominantly of sandstone and argillite - sand, silt and mud that have been buried and hardened. These rocks are often called “basement rocks” or “Wellington Greywacke”. All the basement rocks of wellington area are part of the Torlesse Complex. The layers of Torlesse sandstone (greywacke) are grey in colour, while the layers of mudstone (argillite) are dark grey to black (Begg, J. G. and Mazengarb, C. (1996)).

A brief description of the weathering classification of Greywacke is presented below (NZGS 2005):

- Grade 1, Unweathered (Fresh) Rock (UW): Rock mass shows no loss of strength, discoloration or other effects due to weathering. There may be slight discoloration on major rock mass defect surfaces or on clasts.
- Grade 2, Slightly Weathered (SW): The rock mass is not significantly weaker than when unweathered. Rock may be discoloured along defects, some of which may have been opened slightly.
- Grade 3, Moderately Weathered (MW): The rock mass is significantly weaker than the fresh rock and part of the rock mass may have been changed to a soil. Rock material may be discoloured, and defect and clast surfaces will have a greater discolouration, which also penetrates slightly into the rock material. Increase in density of defects due to physical disintegration process such as slaking, stress relief, thermal expansion/ contraction and freeze/thaw.

- Grade 4, Highly Weathered (HW): Most of the original rock mass strength is lost. Material is discoloured and more than half the mass is changed to a soil by chemical decomposition or disintegration (increase in density of defects/fractures). Decomposition adjacent to defects and at the surface of clasts penetrates deeply into the rock material. Lithorelicts or corestones of unweathered or slightly weathered rock may be present.
- Grade 5, Completely Weathered (CW): Original rock strength is lost and the rock mass changed to a soil either by chemical decomposition (with some rock fabric preserved) or by physical disintegration.
- Grade 6, Residual Soil (RS): Rock is completely changed to a soil with the original fabric estroyed.

3 GROUT TO GROUND CAPACITY DATA

A summary of the grout to ground capacity (minimum bond capacity) of greywacke material, obtained from sacrificial anchor test results carried out within Wellington, is presented in Figure 1. The data is collected from 16 projects within the greater Wellington region; indicative locations of anchors are presented in Figure 2. The anchors tested were embedded into greywacke material with the weathering grade varying between completely, highly and moderately weathered. The majority of the holes were logged in accordance with NZGS 2005. The grout diameter ranged between 100mm and 200mm and the bonded length between 1m and 8m.

Ground anchor testing in Wellington soils and weathered greywacke was also described in Christie et al (2015), in which the maximum bond capacity range obtained for completely weathered Greywacke was between 172kPa and 283kPa. These results can be considered consistent with the data summarised in Figure 1.

Bradshaw and Clayton (2013) discussed ground anchor testing for two projects in Karori, Wellington. Both project sites were noted to lack the typical greywacke weathering profile, instead moving quickly into slightly-weathered rock near surface. While largely unweathered, the rock was noted to be significantly weaker than might ordinarily be anticipated and the typical properties for a slightly weathered state were considered inappropriate. The maximum bond capacity range was between 200kPa and 300kPa. The ultimate bond capacities, from Bradshaw and Clayton (2013), for SW rock are not consistent with the results in Figure 1.

The weathering grades are listed below:

- Grade 2: Slightly Weathered;
- Grade 3: Moderately Weathered;
- Grade 3.5: Moderately to Highly weathered;
- Grade 4: Highly Weathered;
- Grade 4.5: Highly to completely weathered;
- Grade 5: Completely Weathered.

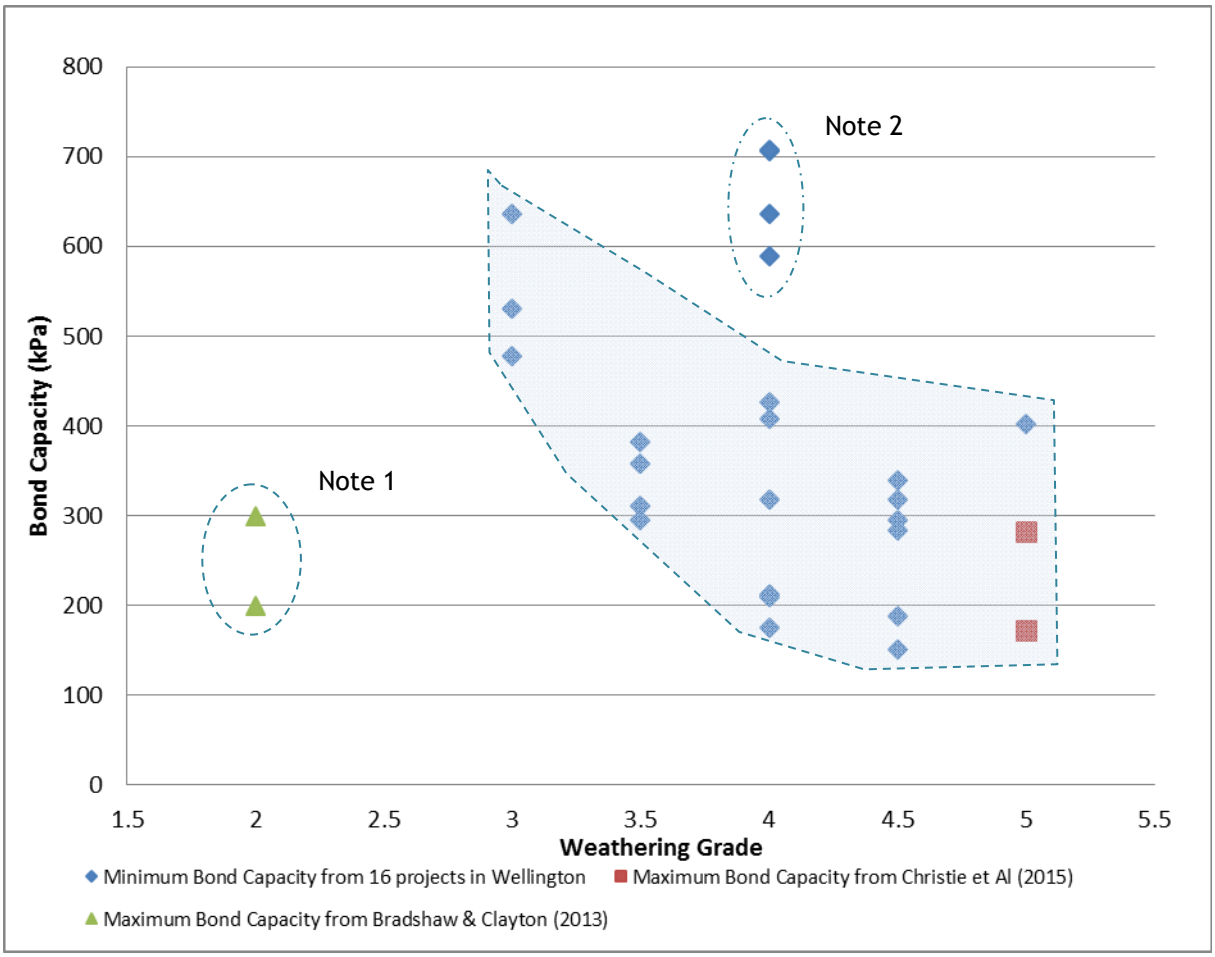


Figure 1. Anchor Bond Capacity

Note 1. Bradshaw and Clayton (2013) discussed ground anchor testing for two projects in Karori, Wellington. Both project sites were noted to lack the typical greywacke weathering profile, instead moving quickly into slightly-weathered rock near surface. While largely unweathered, the rock was noted to be significantly weaker than might ordinarily be anticipated and the typical properties for a slightly weathered state were considered inappropriate. The maximum bond capacity range was between 200kPa and 300kPa. The ultimate bond capacities, from Bradshaw and Clayton (2013), for SW rock are not consistent with the results in Figure 1.

Note 2. We believe that these higher bond capacities are outliers to this data set due to the use of high tensile capacity bars in this project. An increased data set size may confirm if this is indeed an outlier or not.

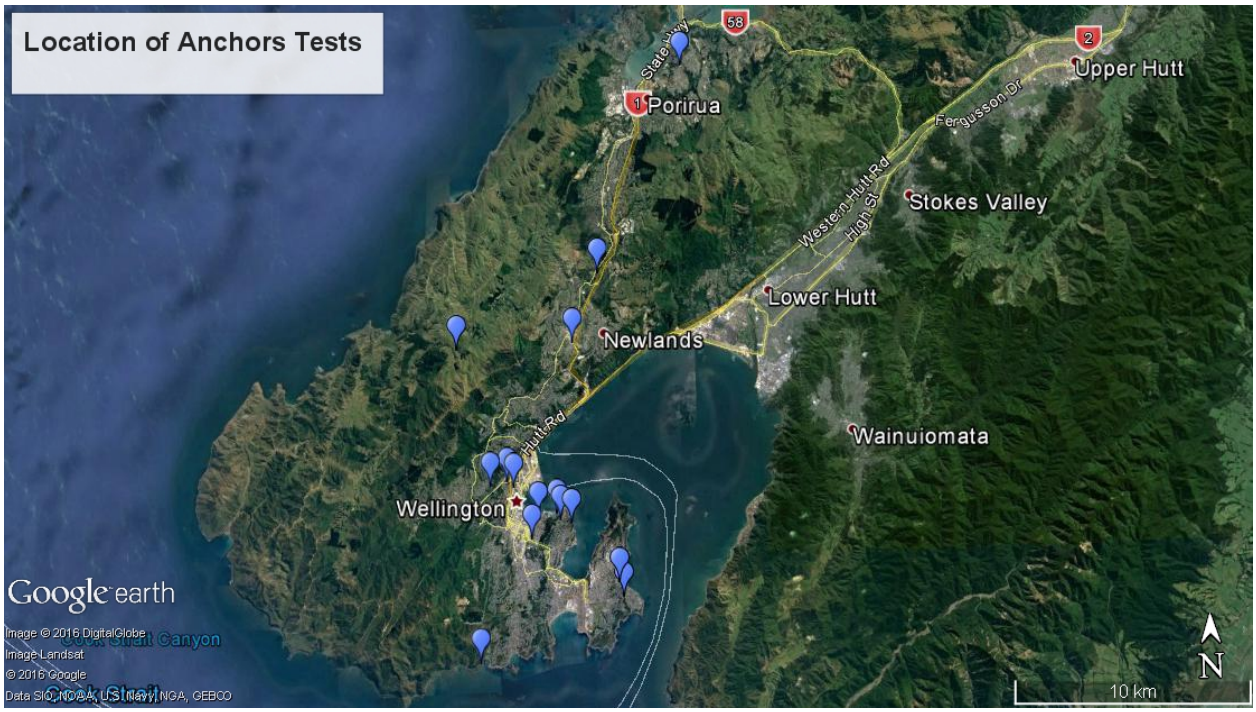


Figure 2. Indicative locations of sacrificial anchors tests

The variability of bond capacity depends on several factors including the degree of weathering in rock, methodology of testing, anchoring system, workmanship/experience of the contractor and disturbance to the anchor prior to testing.

The range of bond capacities inferred from the testing data is between 450kPa and 650kPa for MW rock, between 300kPa and 400kPa for MW to HW rock, between 200kPa and 700kPa for HW rock, between 150kPa to 350kPa for CW to HW rock and between 170kPa to 400kPa for CW.

The current scatter presented in Figure 1 suggests that there is a negative correlation between the weathering grade and bond capacity. However to reliably mathematically define this correlation more data is needed.

4 CASE STUDY

The following is a case study of a new commercial development in Porirua, Wellington. The development of the proposed building required a (maximum) 9m high cut in completely to highly weathered greywacke material. In plan the cut would be an 'L shape' running along the northern and western boundaries of the site. Due to the boundary constraints an anchored shotcrete retaining wall was designed for the 9m cut along the northern boundary of the site and cantilever steel post wall for the adjacent 6m cut along the western boundary.

During the design stage, and based on previous data for rock with similar weathering, the assumed bond capacity was taken as 300kPa. Prior to drilling of production anchors, four sacrificial anchor tests were carried out at different locations and heights, to confirm the assumed bond capacity of rock. The results of bond capacities deduced from tests varied between 150kPa and 340kPa.

Changing the design for all anchors using the minimum bond capacity obtained from test results increased the anchors' lengths and total cost. Therefore the anchors' design in our model was optimised using the specific bond capacity inferred from test results for each row of anchors.

With variable rock strengths and weathering the designer may select optimal rather than conservative design parameters; in this case the probability (and risk) of anchor failure dramatically increases. On this project an optimal design was adopted and the risk was efficiently managed by allowing for verification testing of anchors and then optimization of design using those test results.

Communication with relevant stakeholders at the design stage is necessary to impart understanding that deriving the right bond capacity for design is an iterative process.

5 CONCLUSION

The grout to ground capacity of Greywacke rock is variable across Wellington and depends on the grade of weathering in addition to other factors such as grout diameter and bonded length. We have plotted the relationships between (1) the grout diameter and bond capacity (2) bonded length and bond capacity, as well as (3) weathering of Greywacke and bond capacity. There was no discernable trend in the relationships between grout diameter and bond capacity as well as bonded length and bond capacity. From the data studied and presented above, it appears that there is a correlation between weathering and anchor bond stress. We propose that this can be used to develop presumptive bond strength in the absence of other data. The author acknowledges that with more data, the trend may change. Quality logging of the target founding strata at the appropriate depth and understanding of the geological model is required to be able to utilise the correlation. Other factors, such as drilling method, also need to be taken into account.

Because anchor load testing is relatively cheap (compared to, say, pile load testing), it is regularly used, which allows slightly more optimistic assumptions to be made at the design stage. FHWA GEC 007 (2015) recommends two verification tests (often called “sacrificial” tests) within each soil strata and production tests on 5% of production anchors. Depending on the size of the project and complexity of ground the number of sacrificial tests may vary, however the values obtained from different tests will help the designer in understanding the strength of ground and optimising the design.

6 ACKNOWLEDGEMENTS

The authors wish to thank ENGEO for providing the data and supporting this research work; special thanks to Guy Cassidy and Alan Wightman.

REFERENCES

Begg, J. G. and Mazengarb, C. (1996). “Geology of the Wellington Area”, scale 1:50 000, Geological Map 22, 1 sheet + 128 p. Lower Hutt, New Zealand: Institute of Geological and Nuclear Sciences Limited.

Bradshaw, J.D. and Clayton, P.J. (2013). “Ground conditions and implications for construction in close proximity to a major faultline”, in Chin, C.Y. (ed.), *Proc. 19th NZGS Geotechnical Symposium*, Queenstown

Christie et al. (2015). *Ground anchor testing in Wellington soils and weathered Greywacke*.

FHWA CEC 007 (2015). *Soil Nail Walls Reference Manual*. Publication No. FHWA-NHI-14-007, February 2015.

NZGS (2005). *Guidelines for the Classification and Field Description of Soils and Rocks in Engineering*. NZ Geotechnical Society Inc, Wellington, New Zealand.

This page intentionally left blank

Proceedings of the 11th ANZ Young Geotechnical Professionals Conference – 11YGPC
Queenstown, New Zealand
25 – 28 October 2016

Estimating pre-load induced settlement from laboratory test data and field monitoring records: A Case Study at Temple View Eastern Redevelopment Project, Hamilton

D. P. Mills[1], GIPENZ, D. J. Morton[2], MIPENZ, CPEng

[1]CMW Geosciences (NZ) Limited, Suite 2, 5 Hill Street, Hamilton P.O. Box 3204, PH +64 (07) 2820039; email: danm@cmwgeosciences.com
[2]CMW Geosciences Limited, Unit 19/127 Herdsman Parade, Wembley Green Offices, Wembley, WA 6014; PH +61 (08) 6555 4920; email: davem@cmwgeosciences.com

ABSTRACT

Predicting consolidation settlements in soft soils based on laboratory test data is commonly undertaken by geotechnical engineers, whereas the use of full scale trial embankments to compare these predictions is not always possible at the design phase. At Temple View both laboratory and trial embankment settlement data was used to predict fill induced consolidation settlements and to design surcharge embankments over compressible peat deposits to mitigate post construction creep settlements. Laboratory data used for the settlement analysis comprised oedometer tests that were undertaken on representative peat samples from across the site. The laboratory data was used to compute primary and secondary settlements under various surcharge heights. In comparison, settlement monitoring data from the trial embankment was used to back calculate both time rate (C_v) and settlement magnitude (C_c) parameters using the Asaoka graphical method. The parameters back calculated from the trial embankment data resulted in surcharge embankment design heights of between 0.5m and 1.5m lower than those designed from the laboratory parameters. The comparison has shown that laboratory values can be far higher than what full scale field data suggests and that reliance on 1D laboratory consolidation testing alone may be over conservative.

Keywords: consolidation settlement, creep settlement, Asaoka method, surcharge embankment, settlement monitoring, oedometer testing

1 INTRODUCTION

The proposed development site comprises a large block of land located on the eastern side of Tuhikaramea Road in Temple View, situated approximately 6km south-west of the Hamilton CBD. The western portion of the site, adjacent to Tuhikaramea Road, comprises elevated rolling hill topography that slopes down on to a low-lying alluvial floodplain encompassing the central and eastern areas of the site.

It was proposed to undertake bulk earthworks to raise the level of the low-lying floodplain, suitable for residential building construction, with the majority of the fill material sourced from excavation of adjacent rolling hills. The proposed earthworks will support the construction of single and two storey residential buildings plus a retirement village complex together with other ancillary buildings, associated roading and infrastructure.

Published geological information, and the geotechnical investigation results split the site into three main landforms. Landform Zone 1 comprises the elevated western portion of the site, Landform Zone 2 comprises the low-lying floodplain across the eastern part of the site and Landform Zone 3 is situated between Zones 1 and 2 and has been subject to more significant modification as part of historical site development. For the purposes of this paper only Landform Zone 2 was considered, as this area comprised the most geologically recent peat swamps, which are susceptible to significant primary and secondary settlement.

The primary purpose of the settlement analyses across the lower-lying areas was to assess a suitable surcharge design height that would limit future creep settlements beneath the proposed residential building platforms to a nominal value of 50mm (total) over a 50 year design life of the dwellings with differential settlements of no more than 25mm. It was a requirement that a minimum of 1.0m of structural filling was to be placed over the peat prior to the placement of any surcharge.

2 GROUND CONDITIONS - PEAT DEPOSITS

Peat is a characteristic soil deposit of the Waikato Basin comprising a network of open hollow cellular fibres (high void ratio), has a high water content, and has a high permeability, which makes it susceptible to significant settlement when subject to loading or drainage (i.e. change in effective stress). The general thickness of the peat across the lower-lying regions of the site was between 2.0m and 6.0m observed in trial pits, boreholes and interpreted from Cone Penetration Test (CPT) plots. The peat thickened towards the north and east of the site within the lowest lying areas and thinned out in the west where it sharply transitioned at depth (refer to Figure 1 below) into older elevated volcanic air-fall deposits.

The peat was typically amorphous, but had fibrous zones that contained large branches and tree trunks (up to 1.0m long and approx. 500m wide) and frequent roots. The tree fragments were fresh to moderately decomposed. The larger branches and roots were observed to provide pathways for water to seep into the trial pits during the investigation. Vane shear strengths (S_u) within the peat ranged from 20kPa to 100kPa, but were typically between 25kPa and 60kPa. As zones of peat were relatively fibrous, these larger, less decomposed fragments may have provided higher shear vane readings in places. CPT traces within the peats typically recorded cone resistance (q_c) values from 0.1 MPa to 1 MPa, with friction ratio values frequently alternating between approximately 1% and 7%.

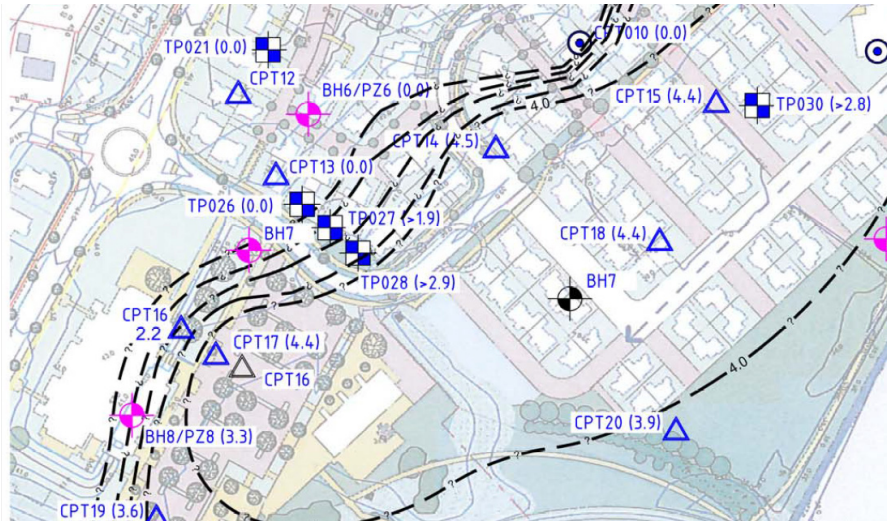


Figure 1. Depth Contours of Compressible Soils

Across the lower-lying portions of the site a non-saturated peat / fill crust (approx. 0.5m thick) was generally present above the peat. Ground-water was consistently observed at the base of this crust.

3 SOIL SAMPLING

Obtaining 'undisturbed' samples from peat soils can be challenging due to the common fibrous inclusions and as there is a high risk of soil degradation, loss of structure and moisture content during sampling and transportation of the sample from site to the laboratory. This can significantly affect the results of consolidation testing and therefore the sampling method was carefully considered. For this reason a series of push tubes (50mm in diameter) were used to recover the soil samples using an attachment on a rotary core drilling rig. The samplers were pushed into the ground without the use of drilling fluid and the retrieved core was then sealed at each end using melted wax. The samples were then sent to the laboratory at the earliest opportunity (within 2 to 3 days) to reduce the risk of further degradation within the sample. This sampling technique was favoured due to its cost-effectiveness and simplicity to carry-out and is generally undertaken as standard practice for retrieving one dimensional consolidation samples.

The locations of the tests targeted the thicker peat soils where the deposits were generally in excess of 4m thick. The spread of test locations aimed to pick up the variability in the peat soils across the site. The depths of the soil samples were also varied to account for the range of in-situ vertical stresses that the soils were currently subject to. The sample depth range for the peat soil was from approximately 1.5m to 5.0m below ground level.

4 GEOTECHNICAL PARAMETERS

4.1 Laboratory Testing

One-dimensional consolidation tests were undertaken on the peat samples received from the field to obtain the necessary soil parameters for estimating primary consolidation and secondary creep settlements. The oedometer testing was undertaken in accordance with the New Zealand Standard, NZS 4402:1986: Methods for testing soils for civil engineering purposes, Test 7.1. The average for the laboratory testing results used for corresponding settlement parameters were, initial moisture content 471.7%, Bulk Density 11.1 kN/m^3, initial void ratio (eo) 11.4, Compression Index (C_c) 4.84, Coefficient of consolidation (C_v) 5.5 m^2/yr. C_v and C_c values are reported for pressure increments, which represent an increase in additional design load with respect to the original pre-consolidation pressure, typically between 25 kPa to 50kPa.

The C_c values were estimated from the virgin compression slope of the e vs log σ'v plots and the C_v values were calculated using both the square root and logarithm of time fitting methods.

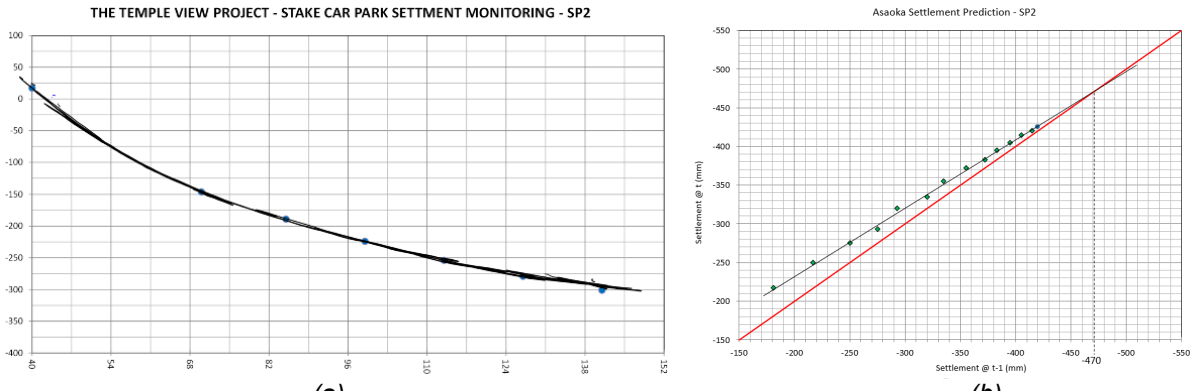
In general the laboratory results provide extremely high moisture contents and very low bulk densities, typical of juvenile peat deposits. The initial void ratio results are considered extremely high on some of the samples, but this is considered to fall within the typical range of values for peat soils.

4.2 Settlement Monitoring

A fill embankment was constructed across the low-lying peat-land immediately to the south of the current study area as part of the preparatory works for a previous stage of the development. A series of settlement monitoring pins were installed beneath the embankment to monitor the settlement. The observed settlement monitoring data therefore provided the opportunity to compare and contrast the laboratory derived settlement parameters. The trial fill embankment was approximately 1.8m high and comprised site-won fill with a bulk unit weight of approximately 16 kN/m^3. The ground beneath the preload consisted of a 0.5m over-consolidated crust underlain by 4.0m of peat. Groundwater was encountered at the base of the over-consolidated crust.

4.2.1 Predicting Total Settlements

In order to predict total primary consolidation settlements an analysis of four relevant settlement monitoring pins was undertaken by applying the Asaoka graphical Method (Asaoka, 1978). A time rate of settlement plot was developed for each monitoring point and a trend-line was drawn from when the full surcharge placement had begun. The settlement at a series of chosen t (mm) and t-1 (mm) values were then selected from the established trend-line and plotted against a 45^o regression line on a separate chart. Where the two lines converged a reading of total predicted settlements was taken. The Asaoka plots predicted total settlements to be between 470mm and 650mm with primary consolidation reaching between 84% (T_{84}) and 92% (T_{92}) for the four reviewed settlement monitoring pins. An example of the evaluated settlement monitoring data for one of the pins has been summarised in Figure 2(a) and Figure 2(b) below.



(a) *(b)*

Figure 2. (a) Time (Days) vs Settlement (mm) trendline; and (b) Asaoka Plot

4.2.2 Back-calculating Parameters

The following well known Terzaghi One Dimensional relationship was re-arranged to back-calculate representative C_c values based on the total primary consolidation settlements predicted from the Asaoka plots.

$$Sp = \frac{Cc}{1+e_0} H \log \frac{\sigma_v' + \Delta\sigma_v'}{\sigma_v'} \quad (1)$$

Where: Sp = primary consolidation settlement; C_c = compression index; e_0 = initial void ratio (from laboratory data); H = depth of compressible soil; σ_v' = initial vertical effective stress; $\Delta\sigma_v$' = change in vertical effective stress.

The back-calculated C_c values ranged from 3.25 to 3.78 with an average value of 3.53. These values were approximately 32% smaller than those derived from the laboratory test results.

4.2.3 Back-calculating Coefficient of Consolidation (C_v) Values

The following Terzaghi rate of settlement equation was then re-arranged and used to estimate the C_v values from the settlement monitoring data:

$$Tv = \frac{Cv\ t}{H^2 dr} \quad (2)$$

Where: Tv = Time Factor; C_v = Coefficient of Consolidation (m^2/yr); t = time (mins); H_{dr} = Height of drainage path (m).

C_v values were between 32.8 m^2/yr and 40.5 m^2/yr with an average value of 36.5 m^2/yr. Corroboration of the C_v values was undertaken by assessing the coefficient of horizontal consolidation (C_h) derived from a series of dissipation tests undertaken within the peat. The ratio of C_h to C_v values averaged between 2.4 and 4.0 based on T (theoretical time factor) values equal to 3 and 5, where:

$$C_h = \frac{R^2\ T}{t} \quad (3)$$

Where: C_h = coefficient of horizontal consolidation, R = average radius of CPT cone filter sensing pore pressures, T = theoretical time factor for given tip geometry and porous element location, t = time to reach given value of $\Delta u(t) / \Delta u$ where Δu is change in pore pressure.

The estimated C_h / C_v values were considered to fall within the expected range for peat soils and provided verification that the back-calculated C_v values from the settlement monitoring data were reasonable.

4.3 Comparison of Laboratory and Settlement Monitoring Parameters

A summary of the back-calculated C_c and C_v values using the different methods is provided in Table 1.

Table 1. Comparison of Derived Settlement Parameters

	Laboratory C_c	**Settlement Monitoring C_c**	**Laboratory C_v (m^2/yr)**	**Settlement Monitoring C_v (m^2/yr)**
	9.01	3.65	0.89	33.5
	5.2	3.45	0.53	39.3
	9.5	3.78	3	40.5
	4.46	3.25	26	32.8
	7.28	-	0.55	-
	1.19	-	1.9	-
	0.82	-	-	-
	1.25	-	-	-
Average	**4.84**	**3.53**	**5.48**	**36.53**
Range	**8.68**	**0.53**	**25.47**	**7.70**

Table 1 highlights the variability in both C_c and C_v values estimated from the laboratory results. The variability in the C_c values along with the high moisture contents and initial void ratios observed within the peat materials indicated that the laboratory results may provide too large a range to adequately predict total settlement within the peats, with average C_c values considered to be very high. The available settlement monitoring derived results then provided validation of the laboratory data, which was undertaken as a comparison prior to the design of surcharge heights. The settlement monitoring parameters had a much smaller range of results and as such were considered to more accurately represent the peat mass as a whole.

5 ESTIMATING POST SURCHARGE CREEP SETTLEMENTS

5.1 Mesri Cα/Cc Relationship

There is a well-documented relationship between Compression Index (C_c) values and the Secondary Compression Index Value (C_α) for all soil types. This relationship is also known as the Law of Compressibility and simply states that the trend of primary compression and re-compression observed within a soil is closely linked to the behaviour of a soil undergoing secondary compression. Published values from Mesri et al (1997) of C_α/C_c for peat soils are typically between 0.06 +/- 0.01. A conservative value of 0.07 was used for back analysing C_α for this project.

5.2 Surcharge to reduce secondary compression

Creep settlement in peat comprises a large component of its total settlement due to several reasons. Its hollow cellular structure and high initial water contents, results in large initial void ratio, which has a high potential to undergo significant settlements over time. The porous nature of the peat also provide a relative short duration of primary consolidation, with primary consolidation typically completed in field trials typically between 2 weeks to 2 months. The breakdown of the organic cell structures through biodegradation of the plant cell walls further compounds the secondary compression.

The application of a surcharge (i.e. increase in effective stress) will increase both the rate of primary consolidation and secondary compression. Subsequent permanent removal of part of this load will cause the underlying soil to go through a phase of primary rebound before then continuing to undergo a slightly lesser rate of secondary compression, denoted C'_α. Post-surcharge creep settlements can then be analysed by estimating the secant secondary compression index C''_α for a given time from primary rebound. Based on the following Mesri relationship the creep settlements post surcharge removal can be estimated by Equation 4.

$$S = \frac{C''\alpha}{1+e_0} L_o \log\frac{t}{t_l} \quad (4)$$

Where C''_α = Post-surcharge Secant Secondary Compression index, L_o = preconstruction thickness of compressible layer with initial void ratio e_0, t = time, t_l post surcharge time at which secondary compression appears.

The largest reduction in creep settlement can be achieved by ensuring the preload effective stresses are significantly higher than the post-surcharge final effective stresses. The time related values in equation 4 above are related to the ratio of preload effective stress to final effective stress (Rs), i.e. the magnitude of over-consolidation induced preload governs creep.

6 COMPARISON OF LABORATORY AND SETTLEMENT MONITORING DESIGN HEIGHTS

The use of equation 4 above has been used to determine a suitable pre-load height, which limits post-surcharge creep settlements to within a nominal 50mm total settlement and 25mm differential over a 50 year design period. Creep settlement of this magnitude are not considered likely to affect the proposed residential dwellings constructed on top of the minimum 1.0m of structural filling.

An iterative design process was implemented to determine the preload design. Varying surcharge heights were selected relative to the pre-filling and post surcharge fill conditions until the long-term creep settlements were reduced to less than 50mm over 50 years.

Surcharge heights were also varied to cover the range of peat thicknesses (2m, 4m, and 6m) to sufficiently reduce the differential creep settlements for different areas. Using the back-calculated parameters surcharge heights of 1.0m, 1.5m and 2.0m were estimated for the respective peat thicknesses. The preload design heights derived from laboratory test data were 0.5m, 1.0mm and 1.5m higher than those predicted using the back-calculated values. Durations for the preloads were also given for the various peat heights of between 3 months and 9 months.

7 CONCLUSIONS

The resulting preload design heights for the laboratory parameters are between 50% and 75% greater than those predicted from the back calculated parameters. Significantly higher construction costs would have been incurred if the surcharge design heights were solely based on laboratory derived parameters.

It is likely that a combination of factors has contributed to the difference between the laboratory and settlement monitoring derived parameters:

- Firstly, the soils samples within the laboratory environment may have undergone an increased rate of decomposition due to the exposure of the sample to oxygen, therefore a higher rate of settlement may be predicted, as suggested by Van der Heijden et al. (1994).

- Secondly, the difference in values may be due to highly variable components within the peat. As seen within the site investigation the peat comprised both fibrous plant / wood materials that were suspended within an amorphous matrix of more compressible organic material. Both of these components have very different properties in terms of long-term settlements. The push-tube soil samples retrieved from the field were relatively narrow (50mm in diameter) and did not allow for large inclusions of organics. It is likely that the samples primarily comprised amorphous peat, and therefore in general provided Cc and Cv values that were much higher than those seen within the back-calculated parameters. In contrast the settlement monitoring data derived parameters as a result of a widespread load which affects a much larger area and may therefore present more realistic values. The difference in settlement parameters could therefore be explained by the presence of less decomposed wood fragments / fibrous materials generally not accounted for within the laboratory samples.

- Thirdly, it is reasonable to also conclude that the number of samples may have not adequately picked up the variability within the peat soil. A small sample size will not take into account discontinuities, lenses, roots, or fissures of a macro scale and therefore the permeability provided by the laboratory is typically considered to provide a lower bound estimate. Further, the laboratory testing only considers vertical permeability and in reality the horizontal permeability will govern as is typically at a faster rate due to the fabric of the soil contributing to secondary compression.

- Fourthly, the lab samples were not undertaken in the same location as the trial embankment and therefore ground conditions beneath the trial embankment may differ slightly from those obtained within the test samples.

A larger laboratory test data set may have provided a more representative average, which would have more accurately reflected the back-calculated values. Future laboratory testing may be better to target more frequent tests within a single profile to obtain a more reliable average of the peat matrix throughout its vertical extent. It is recommended that a trial embankment is undertaken where practical to validate laboratory testing.

REFERENCES

Asaoka, A. (1978). “Observational Procedure of Settlement Prediction.” *Soil and Foundations*, 18(4), pp. 87-101

Mesri, G, Stark, T.D, Ajlouni, M.A.M, Chen C.S (1997). “Secondary Compression of Peat with or without surcharging.” *Journal of Geotechnical and Geoenvironmental Engineering*, 411 - 421.

Mesri. G, Ajlouni, M.A.M (2007). “Engineering Properties of Fibrous Peats”. *Journal of Geotechnical and Geoenvironmental Engineering*, 850 - 866.

Terzaghi, K., and Peck, R. B. (1967). *Soil mechanics in engineering practice*. John Wiley and Sons, New York.

Van der Heijden, E. Bouman, F., and Boon, J.J (1994). “Anatomy of recent and peatified Calluna vulgaris stems: implications for coal maceral formation. *Int. J. Coal Geol.*, 25, 1-25.

Proceedings of the 11th ANZ Young Geotechnical Professionals Conference – 11YGPC
Queenstown, New Zealand
25 – 28 October 2016

Embankment Failures – Local Experiences

E. G. Maynard[1], BE (Hons) Nat Res, MEM, GIPENZ

[1]Geotechnical and Water Resources Engineer, GeoSolve Ltd, Level 1, 70 Macandrew Road, Dunedin; PH (03) 466 4024; email: emaynard@geosolve.co.nz

ABSTRACT

There have been six embankment dam failures, 40 notices issued for non-compliance with the Building Act (2004), and five abatement notices issued under the Resource Management Act (1991) in respect to small irrigation dams in Otago since 2011. Investigations into three failures in Otago, and one access embankment on the West Coast, are used to illustrate common mechanisms of failure and how these could have been mitigated by good engineering practice. Each case study is summarised, a probable failure mechanism postulated, and remedial measures to avoid recurrence identified. These case studies present common examples from the spectrum of failures associated with these structures, including: foundation/fill contact piping, spillway failure, piping of the conduit, and overtopping. Common design elements to prevent, minimise the likelihood of, or safeguard against failure are introduced, and the challenges of implementing these post-failure emphasized. Because failures tend to develop very rapidly, the importance of getting the right level of design input and QA with any potentially hazardous water retaining structure, irrespective of the size of the structure, is emphasized.

Keywords: embankment dam failure, earth dams, small dams dam failure, dam failure statistics

1 INTRODUCTION

Agricultural intensification and over-allocated water resources have resulted in increased demand for decentralised irrigation water storage across Otago. Earthfill dams are a popular choice because they have comparably low operating costs, can supplement water rights by harvesting catchment runoff, and can be built at relatively low cost from on-site materials. They are, however, potentially hazardous structures should their contents be released in the event of a failure, and thus require sound engineering knowledge and construction experience to minimise the risk to downstream receptors.

This paper discusses recorded small dam failure experiences in Otago since 2011, focusing primarily on the technical aspects such as mechanisms of failure, remedial options, and consequences.

2 IRRIGATION DAMS IN OTAGO AND NON-COMPLIANCE ENFORCEMENT

Otago is the second biggest irrigated region in New Zealand, contributing 15% (c.86,000ha) of the overall irrigated land (Heiler, 2014). Farms are often remote, have intermittent or unreliable water supply, and lie within ephemeral catchments. These factors make them good candidates for a dam.

In the author's experience, a typical farm dam would be ~2-4m high, have batter slopes of 3:1 (H:V), a 3m crest width, include a low-level pipe conduit, be constructed of homogeneous alluvial/aeolian/lacustrine silt and have the potential to store <50,000m^3. In fact, many are intentionally built below the 'large dam' threshold (being dam height ≥4m high and potential to store ≥20,000m^3 of water or other fluid, (Building Act, 2015)) to avoid the requirements for a building consent and for a code compliance certificate (CCC). Many are constructed without specific engineering design, construction supervision, or compaction verification.

Irrespective of the location, size, purpose, or need for a consent, dam construction is building work and must comply with the Building Act (2004) and relevant provisions of the Resource Management Act (RMA) (1991) and Regional Plan: Water (ORC, 2015). The New Zealand Dam Safety Guidelines (NZSOLD, 2015) are the most common means of demonstrating compliance with the building code.
The Otago Regional Council (ORC) is responsible for issuing building consents for large dams and compliance matters for all dams in Otago. Since 2011, the ORC has documented six dam failures, issued 40 notices to fix for non-compliance with the building code, and five abatement notices for

dams in breach of the RMA (refer Figure 1). These equate to approximately one incident per month. The most precarious dams in the database are summarised in Table 1.

In some cases, the dam was in the process of failure at the time of inspection. In others, the dam failed a short time after the notice to fix was issued. Some owners were issued with multiple notices to fix for the same non-compliance before the dam was removed or certified. One owner was prosecuted for repeated non-compliance.

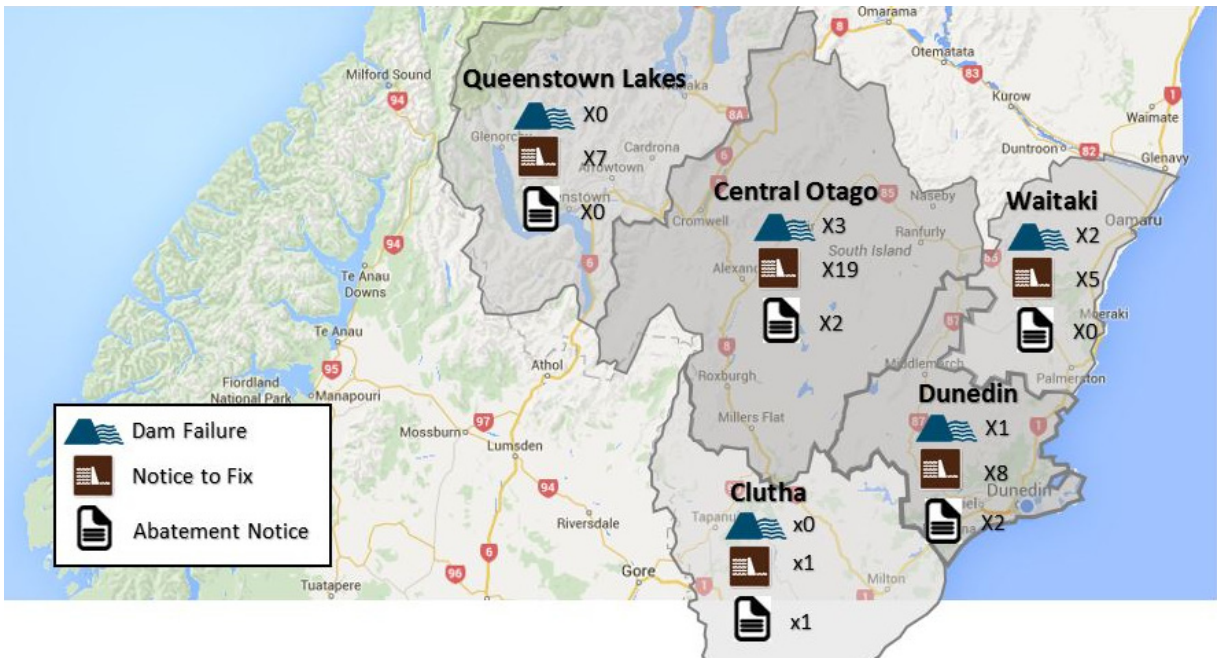


Figure 1. Failure rates and dam enforcement for dams in Otago since 2011.

Table 1. Dam Enforcements in Otago since 2011 (case studies 12 to 14 included in Section 3)

Ref.	Date NTF issued	Location	Stage			Non-compliance					
			Imminent risk	Incipient	Failure	Compaction	Fill Materials	Pipe conduit	Erosion Protection	Spillway	Seepage
1	Mar 2011	Dunedin		X						X	
2	Mar 2011	Waitaki			X				X		
3	Mar 2011	Waitaki			X		X		X		
4	Apr 2011	Queenstown Lakes	X							X	
5	May 2012	Queenstown Lakes	X							X	
6	May 2012	Waitaki	X			X	X		X		X
7	Aug 2013	Dunedin	X				X			X	
8	Aug 2013	Dunedin	X		X				X	X	
9	Dec 2013	Central Otago							X	X	
10	Mar 2014	Queenstown Lakes		X		X	X		X		
11	Apr 2014	Central Otago	X			X	X			X	
12	Oct 2014	Central Otago			X	X	X				
13	Feb 2015	Central Otago			X	X	X	X	X		X
14	Oct 2015	Central Otago			X			X			
15	Mar 2016	Dunedin	X			X	X	X	X	X	X
16	Mar 2016	Clutha District	X			X	X		X	X	
Total			8	2	6	7	9	3	9	9	2

The case study database indicates:

- Non-compliant dams are a widespread issue across Otago rather than isolated to one location;
- Improper fill materials, poorly designed or inadequate erosion protection, and inadequate spillway provisions are the most common non-compliant features of these dams;
- The majority of non-compliant dams were deficient for more than one reason; and
- Intervention by ORC may very well have prevented or reduced further damage.

3 CASE STUDIES

The following case studies illustrate the four of the most common mechanisms of failure from the Otago record: foundation piping, spillway erosion, piping along the conduit, and overtopping. These are consistent with international experiences of embankment dam failures (Table 8.1. Fell et al. 2015).

Each dam/embankment discussed is classified as small and low potential impact (PIC). Three of the four had no specific engineering design, construction supervision, or compaction verification. Failures were initiated rapidly, occurring under normal operating or flood conditions, often shortly after construction upon first filling. All have since been remediated with no signs of ongoing distress reported.

Discussions with contracting staff and owners, combined with information sourced from post-failure inspection of the dam and surrounding environment, were used to postulate probable failure mechanisms. Remedial measures to avoid future such failures are then identified with concluding remarks summarising the key lessons learnt.



Figure 2.



Figure 3.



Figure 5.

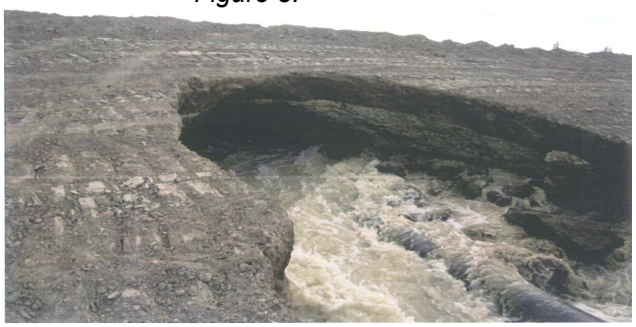


Figure 4.

Figure 2. Case Study A – Foundation piping failure at downstream dam toe immediately post failure;
Figure 3. Case Study B – Erosion of spillway throat and deposited sediment down plain post failure;
Figure 4. Case Study C – Piping failure around conduit viewed from the downstream toe during failure;
Figure 5. Case Study D – Crest overtopping during flood.

3.1 Case Study A: Foundation Piping - DS0172 *(Figure 2)*

This dam was constructed to provide short-term irrigation storage while a larger dam was constructed downstream. Compaction was stated in 300mm lifts using scrapers and a smooth drum roller.

Dam type: Homogeneous earthfill of non-plastic silty gravel/gravelly silt materials
Maximum dam height: 3.95m **Storage potential:** ~30,000m^3
Upstream batter slope: 3:1 (H:V) **Downstream batter slope:** 2.5:1 (H:V) **Crest width:** 3m
Geological setting: shallow alluvial and lacustrine sediments overlying sedimentary rock (mudstone)

Failure mechanism: Seepage at the foundation contact leading to headward void migration and subsequent piping failure soon after first-filling. This is one of the most common form of distress on initial filling of a reservoir.

Principal contributors to the failure include:

- Planar compaction surfaces with rare clumps of turf that would tend to facilitate piping
- Permeable gravel lenses providing an environment that readily transmits high pore water pressures at the foundation interface
- Sinkholes observed in the reservoir floor suggesting permeable gravel lenses do not meet filter compatibility with overlying silt

Downstream consequences: Erosion of pasture; scour of an unsealed public road; damage to a buried power cable; floodwaters approached within 5-10m of an occupied dwelling; discharge of sediment into receiving waterways.

Remediation: Undertake engineering inspection of the stripped foundation, investigate the persistence of permeable strata at/near foundation level, reduce compaction thickness, utilize a sheepsfoot roller. A new keyway and additional shoulder material was formed on the upstream dam slope.

Lessons learnt: Foundations preparation should include: 1) removal of all organic/soft materials, 2) scarification, and 3) moisture conditioning, and use of a sheepsfoot or padfoot roller to ensure a good bond between the embankment fill and foundation materials. A rigorous ground investigation should identify the potential for high-permeability conduits near the foundation, and a sufficiently deep cut-off included in the design as appropriate. Construction plant should be suitable for the soil type and fit for purpose.

3.2 Case Study B: Spillway Failure - DS0173A *(Figure 3)*

This dam was constructed progressively over three years using predominantly site-won loess soils. Water enters the upper dam via. a 32ha upstream catchment and from neighbouring irrigation races.

Dam type: Twin homogeneous earthfill ring dams of non-plastic silt (loess), connected in series
Maximum dam height: ~3m **Storage potential:** ~20-30,000m^3
Upstream batter slope: 3-4:1 (H:V) **Downstream batter slope:** 3-4:1 (H:V) **Crest width:** 3m

Geological setting: alluvial and lacustrine sediments overlying sedimentary and volcanic rock
Failure mechanism: Erosion of the spillway lining and part of the embankment during sustained rainfall of moderate intensity (20-30mm of rain over 24hrs).

Principal contributors to the failure include:

- Incompatible liner materials, being coarse graded riprap overlying erosive/dispersive silt
- Coarse riprap tending to induce turbulence causing entrainment of finer soils
- Hydraulically steep spillway (embankment slope ~15-20°)
- Flows of damaging magnitude entering the reservoir from an external source, possibly from sidling runoff beyond the natural catchment conveyed into the reservoir via a water race

Downstream consequences: Erosion of pastures; discharge of sediment into multiple receiving waterways.

Remediation: A new spillway with riprap liner and geotextile underlay was formed into natural soil.

Lessons learnt: Spillways are high energy environments where scour is often exacerbated by steep hydraulic gradients and liner roughness. Riprap is a suitable means of erosion protection, but should include appropriate bedding or geotextile at the embankment interface. Wherever possible, spillways should be formed away from the dam into competent erosion-resistant material. Inflow design floods, on which spillway capacity is designed, should be based on hydrological study which includes all contributions.

3.3 Case Study C: Piping of the Conduit - DS0176 *(Figure 4)*

This dam had typical geometry, fill compaction, and wave protection. Two concrete seepage collars (~1.2m cube) were installed around the low-level pipe conduit, presumably as a defence against piping.

Dam type: Homogeneous earthfill dam constructed of non-plastic clayey silt with minor gravel
Maximum dam height: 3.95m **Storage potential:** ~45,000m^3
Upstream batter slope: 3:1 (H:V) **Downstream batter slope:** 3:1 (H:V) **Crest width:** 3.5m
Geological setting: shallow lacustrine and alluvial sediments over sedimentary and metamorphic rock

Failure mechanism: Piping of soils along the outside of the conduit caused by tractive hydraulic forces from the reservoir leading to erosion of the downstream toe and subsequent headward breach migration, i.e. FEMA's Failure Mode 3 (Federal Emergency Management Agency FEMA, 2005). Failure occurred shortly after first filling.

Principal contributors to the failure include:

- Lack of provisions for the safe passage of seepage along the pipe without entraining fines
- Accounts from the contractor are of the inlet screen displacing laterally under high wind causing uplift, permitting water ingress along the conduit
- Trenching method and inability of compaction plant to suitably compact fill around the conduit
- Fill around the pipe being potentially dispersive and/or erosive
- Silty gravel layers near the foundation toe

Downstream consequences: Erosion of pasture; flooding of multiple public roads and closure of the state highway; floodwaters approached residential dwellings and a disused hotel.

Remediation: The pipe was re-laid with the inlet screen secured. A filter diaphragm and filter drain was installed for the downstream pipe section. New clayey silt was imported and compacted around the pipe by a small mechanical tamper.

Lessons learnt: Piped conduits through water retaining structures should be avoided wherever possible. If unavoidable, special design and construction attention should be applied. Compaction is difficult and often impaired around pipe haunches. Some degree of seepage is inevitable, hence a good design will include provision for both the mitigation and safe passage of seepage water. In this situation, international best practice has discontinued the use of concrete seepage collars in favour of filter diaphragms and filter drains (Damwatch, 2006).

3.4 Case Study D: Embankment Overtopping *(Figure 5)*

An access embankment structure was constructed to support a piped aqueduct and permitted construction traffic to cross the confluence of two streams.

Dam type: Access embankment constructed of crushed sandstone with sandstone block slope facing
Maximum dam height: ~7m **Storage potential:** N/A
Upstream batter slope: 1:1 (H:V) **Downstream batter slope:** 1:1 (H:V) **Crest width:** 4m
Geological setting: The site lies within a steep incised gorge of sedimentary rock (sandstone)

Failure mechanism: A significant rain event overwhelmed three bypass culverts, causing water to build up behind the embankment resulting in subsequent crest overtopping and scour to the downstream slope.

Principal contributors to the failure include:

- Hydraulically steep slope batters (embankment slope ~45°)
- Insufficient pipe strength resulting in at least one bypass culvert being crushed under the embankment weight
- Debris from upstream clogging the bypass culverts
- Significant rainfall, probably in excess of the design event expected for this structure

Downstream consequences: Minor sedimentation of the waterway.

Remediation: The culverts were upgraded with stronger, larger pipes with debris screens. A new high-level spillway was provided at the true left abutment. Embankment slopes were eased.

Lessons learnt: While embankment batter slopes might be geotechnically stable, they are hydraulically steep causing high-velocity water flow and scour in the event of overtopping. Design of access embankments should include provision for culvert blockage or failure, and incorporate a debris screen and high-level spillway as a last defence against overtopping.

4 CONCLUSION / DISCUSSION

Every 1-2 months a dam in Otago is identified as potentially dangerous due to a known or suspected breach of the Building Act or the Resource Management Act (1991), sometimes a combination of both. ORC records indicate about one of these fails each year on average. None of the dams that failed had building consent, and no dam that obtained building consent and a code compliance certificate has failed.

The dam failure record in Otago reflects international embankment dam failure experiences. Failures are often an unfortunate combination of substandard design and poorly understood geological conditions that require close quality control procedures during construction, commissioning and operation. It is likely the aspects attributed to the failures would have been effectively addressed through the involvement of a dam professional either at the design, regulatory review, or construction phase. The absence of observable critical features once the dam is constructed, such as foundation condition and internal drainage provisions, along with the difficulty in applying corrective action following the onset of failure, easily justify the costs associated with seeking the correct level of professional input. Inevitably, many small dam owners may be unaware of the danger presented by their dam, and often omit seeking professional advice due to limited budgets or lack of perceived value.

The lessons learnt from four representative dam failures provide a concise summary of good small dam practice:

- A rigorous ground investigation is needed to identify any adverse conditions at the dam site
- Thorough foundation preparation is essential. This should include removal of all organic/soft materials and scarification to ensure a good bond between the embankment and foundation
- Construction plant should be suitable for the soil type and fit for purpose
- Dam building materials need to be carefully selected and compatible with surrounding soils
- Spillways should be formed away from the dam, preferably in competent erosion-resistant material, at shallow bed grade, and be sized to accommodate floods from external contributions in addition to the dam catchment
- Special design and construction attention is warranted for piped conduits. Compaction is often impaired around haunches leading to preferential seepage. Modern designs include provisions for the mitigation and safe passage of seepage water via filter diaphragms and drains

Consequences of failures are rarely contained within Owner's property, and impact: pastures, infrastructure including roads and powerlines, dwellings and other buildings, and receiving waterways.

5 ACKNOWLEDGEMENTS

I would like to thank the Otago Regional Council, in particular Peter Kelliher and Dr Gavin Palmer, for providing access to their dam enforcement records and encouraging this paper to be published.

REFERENCES

Damwatch. (2006). *Review of the use of Seepage Collars in Small Dams.* Environment Bay of Plenty.
Federal Emergency Management Agency FEMA. (2005). *Conduits through Embankment Dams. Best Practices for Design, Construction, Problem Identification and Evaluation, Inspection, Maintennance, Rennovation, and Repair.*
Fell, R., MacGregor, P., Staledon, D., Bell, G. and Foster, M. (2015). *Geotechnical Engineering of Dams, 2nd Edition.*
Heiler, T. (2014, December 16). *Irrigation and drainage - Regional characteristics*. Retrieved from Te Ara - the Encyclopedia of New Zealand: URL: http://www.TeAra.govt.nz/en/map/19597/irrigated-land
New Zealand Government. (1991). *Resource Management Act.*
New Zealand Government. (Amended 4 April 2016). *Building Act 2004 No 72.*
New Zealand Society on Large Dams (NZSOLD). (2015). *New Zealand Dam Safety Guidelines.*
Otago Regional Council (ORC). (2015). *Regional Plan: Water for Otago.*

This page intentionally left blank

Proceedings of the 11th ANZ Young Geotechnical Professionals Conference – 11YGPC
Queenstown, New Zealand
25 – 28 October 2016

Liquefaction Resistance of Hamilton Pumiceous Sands

E. E. Jacobs[1] and D. L. Dennison[2]

[1]Opus International Consultants Ltd, Opus House, Princes Street, Hamilton, 3240, Private Bag 3057; PH (021) 872 663; FAX (07) 838 9324; email: emily.jacobs@opus.co.nz
[2]Opus International Consultants Ltd, Opus House, Princes Street, Hamilton, 3240, Private Bag 3057; PH (027) 476 6451; FAX (07) 838 9324; email: david.dennison@opus.co.nz

ABSTRACT

Conventional empirical methods used to assess the liquefaction resistance of soils from in situ tests, such as CPT and SPT, have been developed for hard-grained sands, and may not accurately characterise the liquefaction resistance of sedimentary pumiceous sands. The NZ Transport Agency commissioned a programme of cyclic triaxial laboratory testing, to better understand the liquefaction resistance of pumiceous sands local to the Hamilton Basin. The results of this testing confirm that the pumiceous sands in the Hamilton area are susceptible to liquefaction, and that the risk of liquefaction cannot be ruled out by the observation that the sand is pumiceous. When compared to similar testing on relatively hard-grained sands found in geotechnical literature, the results show that Hamilton pumiceous sands are generally more resistant to liquefaction than hard-grained sands of the same relative density. Current empirical methods for estimating liquefaction resistance from common field tests (SPT, CPT, Shear wave velocity) are mainly based on data from hard-grained sands, so these may underestimate the resistance of pumiceous sands to liquefaction.

Keywords: liquefaction, pumice, volcanic soils, cyclic triaxial testing, Waikato Expressway

1 INTRODUCTION

Alluvial soils within the Waikato basin contain a significant proportion of sedimentary pumiceous soils derived and transported from the Taupo Volcanic Zone. These pumiceous sands are a mixture of pumice sand and quartz sand particles. Pumice sand particles are characterised by highly porous grains with high crushability. These properties give pumice sand high void ratios, high compressibility, and low density. As a result, their behaviour may be very different to that of hard-grained soils when subject to cyclic loading (Orense and Pender 2013).

Researchers at the University of Auckland (Wesley, et al. 1998) carried out CPT testing on pure pumice sand and regular quartz sand at different relative densities (RD), and an effective overburden pressure equal to 200 kPa. Cone penetration resistance of both the loose and dense pumice sands are very similar, showing that the CPT does not distinguish very well between dense and loose states of pumice sand. Both pumice sand traces are also similar to results for loose hard-grained sand. This implies that a liquefaction assessment using the Cyclic Resistance Ratio (CRR) based on empirical correlations developed for CPT results in hard-grained sands (Boulanger and Idriss 2014) may underestimate the liquefaction resistance of dense pumice sands.

This paper describes the results of a cyclic triaxial laboratory testing programme, commissioned by the NZ Transport Agency, aimed at better understanding the liquefaction resistance of alluvial pumiceous sands. This assessment was done by the comparing the results of cyclic triaxial testing of pumiceous soils from the Hamilton Section of the Waikato Expressway to those of relatively hard-grained sand soils found in geotechnical literature.

2 TESTING METHODOLOGY

2.1 Scope

In order to better understand the liquefaction resistance of the alluvial pumiceous sands found within the Waikato Basin, we have carried out a series of consolidated undrained cyclic triaxial tests on re-constituted samples. The samples were prepared with a range of gradings and densities as follows:

- Loose, coarse pumiceous sand
- Loose, fine pumiceous sand
- Dense, coarse pumiceous sand
- Dense, fine pumiceous sand

The test specimens are re-constituted in order to isolate the effect of pumiceous particles on liquefaction resistance. As a result, the effects of in-situ soil structure, cementation, and aging are nullified. These factors would tend to increase the resistance of the soil (CRR) to liquefaction.

2.2 Sample Soils

Pumiceous sands in the Hamilton area are re-deposited sedimentary soils, with a mixture of hard-grained (quartz) and pumice particles. The coarse and fine samples were obtained as bulk samples from test pits located along the designation of the Hamilton Section of the Waikato Expressway, and are representative of the pumiceous sands typically found in the Hamilton Basin. Properties of the sample soils are summarised in Table 1.

Table 1. Pumiceous sand samples soil properties

Sample	Grading					Solid Particle Density (t/m^3)	D_{50} (mm)	ρ_{max} (t/m^3)	ρ_{min} (t/m^3)
	Gravel (%)	Coarse Sand (%)	Med. Sand (%)	Fine Sand (%)	Fines (%)				
Coarse	5	46	36	10	3	2.54	0.6	1.58	1.3
Fine	0	1	24	56	19	2.48	0.15	1.38	1.12

Scanning Electron Microscope (SEM) imaging was performed on two of the test specimens to assess pumice content. The term “pumiceous” covers a large range of pumice content, and liquefaction resistance may be affected by the relative abundance of pumice particles and hard-grain particles within the soil. Figure 1 shows two of the produced images.

It is difficult to quantitatively determine the pumice ratio from the photos alone, however these images confirm that the sample contains a substantial percentage of pumice, of the order of 20%-30%. This is illustrated in Figure 1 below.

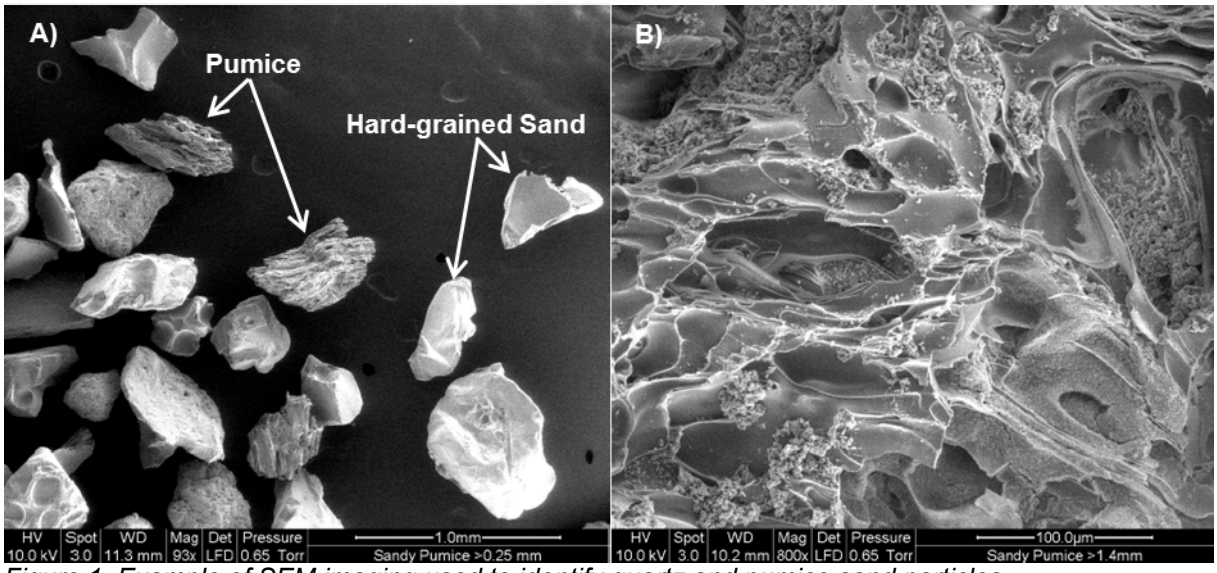


Figure 1. Example of SEM imaging used to identify quartz and pumice sand particles

Analysis of the apparent solid particle density of the pumiceous sample, relative to that of hard-grained silica sands (2.65 t/m^3) and pure pumice (~ 2.10 t/m^3), also indicates a pumice grain to hard-grained sand ratio of around 20%-30%.

2.3 Cyclic Triaxial Testing

Triaxial specimens were prepared within a cylindrical split mould, with a height to diameter ratio of 2:1 (63 mm diameter, 126 mm height). Before the placement of any soil, the split mould was lined with an impermeable membrane, which contained the test specimen during the triaxial test.

Each specimen was prepared using the technique of moist tamping. Moist tamping consists of placing 5 equal soil lifts of known mass in the mould, and compacting using a small weight to achieve the required lift thickness.

For the loose specimens, only slight re-arranging using the spoon (no tamping) was required to remove gaps in each lift and to smooth the surface.

The dense samples were compacted by tamping with a small weight. Because pumice particles are more susceptible to crushing during tamping, only a moderate level of tamping using the weight was carried out, to avoid undesirable levels of particle crushing. The maximum relative density of the coarse sample achieved using this method was 70-75%, and a relative density of 80-85% was achieved in the fine sample.

Undrained cyclic triaxial testing involves the initial consolidation of the specimen under an isotropic confining pressure (σ'_c) of 100 kPa. This consolidation pressure was selected to be consistent with a large body of similar testing in the literature.

The cyclic loading was applied in a stress-controlled manner using a pressurised load cell. Axial loads were applied alternately in compression and extension according to the specified Cyclic Stress Ratio (CSR), $\pm\Delta\sigma_1/2\sigma'_c$.

There are two alternate criteria for liquefaction in the cyclic triaxial test: when pore water pressure first reaches 95% of the initial confining pressure, or the double amplitude axial strain reaches 5%. For each cyclic triaxial test, the cyclic load was applied in compression and extension until both of these criteria were reached.

3 CYCLIC TRIAXIAL TESTING RESULTS

For the loose specimens, the two failure criteria were reached at approximately the same number of loading cycles. However, the dense specimens reached the pore pressure liquefaction criteria before reaching the strain-based liquefaction criteria.

The strain-based liquefaction criteria appears more common in the literature and will therefore be used for analysis of the current results. For each test, the number of cycles to achieve 5% double amplitude shear strain under each cyclic stress ratio are shown in Figure 2.

In the context of cyclic triaxial testing, Seed and Idriss (1982) published a curve representing the equivalent number of uniform loading cycles corresponding to various earthquake magnitudes. From this data, 15 cycles of uniform loading is taken as equivalent to shaking from a magnitude 7.5 earthquake, for comparison to standard liquefaction methods which contain magnitude weighting factors to normalise the hazard to a magnitude of 7.5.

To determine the CSR at which liquefaction would occur in 15 uniform load cycles (equivalent to a 7.5 magnitude earthquake) we fitted a power curve to the data for each grading and relative density. The resulting cyclic resistance ratios (CRR_{tx}) for a 7.5 magnitude earthquake are listed in Table 2.

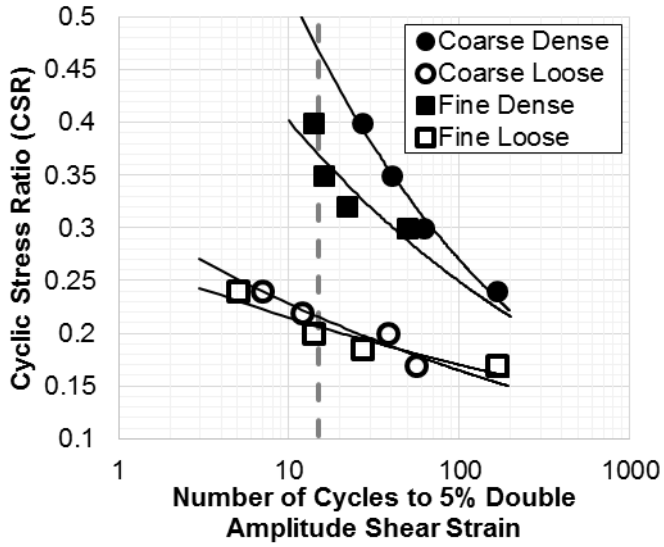


Figure 2. Cyclic triaxial testing results

Table 2. CRR_{tx} for 7.5 magnitude shaking

Sample	Relative Density (%)	CRR_{tx}
Coarse	73	0.47
	22	0.22
Fine	85	0.37
	25	0.21

4 EVALUATION OF THE CYCLIC RESISTANCE

4.1 Comparison to Published Cyclic Triaxial Results

In this study we have compared the results of the cyclic triaxial tests on Hamilton pumiceous sands to results for various hard-grained sands identified in the literature. The results from the literature (Yamamoto et al., 2009; Hosono and Yoshimine, 2004; Ishihara et al., 1980; Yoshimi et al., 1994; Thomas, 1992; Mulilis et al., 1976; and Hyodo et al., 2012) provide a benchmark for typical results to be expected for various hard grained sand materials at different densities. Each of these tests were performed on reconstituted samples at an effective confining pressure of 100 kPa.

In addition to test results on hard-grained sands, Orense and Pender (2013) performed a series of cyclic triaxial tests on commercially available pumice sand. This sand was derived from the Waikato River, and sorted into various different gradings. The sample Pumice-A is uniformly graded, and made up almost entirely of coarse sand-sized pumice particles. The Pumice-A sample is therefore coarser than both Hamilton pumiceous sand samples.

Figure 3 displays CRR_{tx} results from different published studies, for various different sands at various relative densities, along with all the cyclic triaxial testing performed in this study (labelled HamSec).

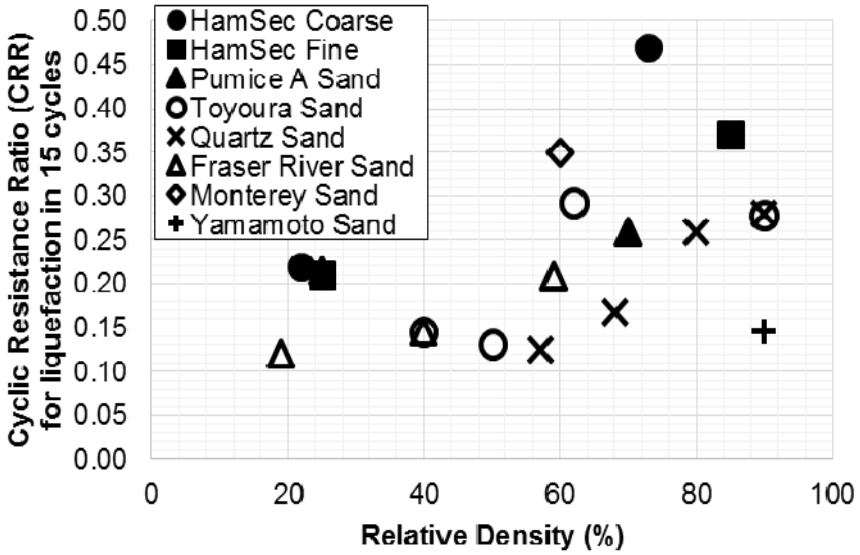


Figure 3. CRR_{tx} results compared with results from published studies for pumice and quartz sand

The cyclic triaxial results for the Hamilton pumiceous sands and the pure Pumice-A sands generally lie on the upper edge of liquefaction resistance spectrum, which suggests that the pumice and pumiceous sands are generally more resistant to liquefaction than hard-grained sands of the same relative density.

4.2 Influence of Grading

When subjected to shear forces in the cyclic triaxial test, highly crushable weak pumice grains may break down into finer particles, increasing the fines content and the liquefaction resistance (Orense, et al. 2012). Lui et al. (2015) concluded that the liquefaction response of pure pumice sand is more dependent on particle crushability during cyclic shearing than relative density.

However, unlike results of these studies on pumice sands, the pre-test and post-test particle size distributions of Hamilton pumiceous sands showed little evidence of particle crushing as a result of the cyclic triaxial testing. This is likely a result of the dominant proportion of hard-grained sands in the Hamilton pumiceous sands tested, demonstrating that the liquefaction resistance of Hamilton pumiceous soils is largely dependent on relative density.

4.3 Comparison to Inferred CPT Results

4.3.1 Conversion of Triaxial CRR to Equivalent In-Situ CRR

The stress conditions within the cyclic undrained triaxial tests are different to those experienced by soil in situ, therefore the CRR determined from cyclic triaxial testing is not equivalent to the CRR in the field. As result, conversions have been developed to relate the CRR_{tx} as determined from cyclic triaxial testing to the equivalent in-situ CRR_{field} which would be expected for a sand at a similar relative density. One such relationship is defined by Kramer (1996) as the equation below (Equation 1), with the c_r for testing in the triaxial space approximately equal to 0.69 (Kramer 1996).

$$CRR_{field}=0.9\ c_r\ (CRR_{tx}) \quad (1)$$

4.3.2 CRR from Inferred CPT Results

Robertson and Cabal (2015) published correlations to infer relative density from CPT results. This relationship was used to infer typical CPT resistances for the relative densities of the cyclic triaxial specimens, at a depth equivalent to the 100 kPa confining pressure used in the lab tests. These correlations are based on coarse hard-grained sand normalised to an overburden pressure of 100 kPa, therefore the inferred cone resistance (q_c) were converted to an equivalent $(q_{c1}N)_{cn}$ using an assumed I_c value.

Using the empirical correlations for the CRR based on CPT output published by Boulanger and Idriss (2014), the CRR_{CPT} corresponding to each relative density was calculated.

Table 3. Equivalent in situ CRRs from cyclic triaxial results compared to CRRs based on inferred CPT output

Sample	Relative Density (%)	Measured		Inferred
		CRR_{tx}	CRR_{field}	CRR_{CPT}
Coarse	73	0.47	0.29	0.13
	22	0.22	0.14	0.08
Fine	85	0.37	0.23	0.35
	25	0.21	0.13	0.08

In all but one case, the equivalent in-situ CRRs obtained from the cyclic triaxial testing of Hamilton pumiceous sand (CRR_{field}) are higher than those estimated from CPT correlations for hard-grained soils of the same relative density (CRR_{CPT}). Therefore a similar CPT response in the field, and the corresponding CRR according to conventional empirical methods, would underestimate the liquefaction resistance of pumiceous sands and therefore overestimate the liquefaction hazard. These discrepancies are further exaggerated by the tendency of the CPT test to underestimate relative density of pumice sands, as shown by Wesley, et al. (1998).

5 CONCLUSION

The conclusions resulting from this study are as follows:

- The pumiceous sands tested are susceptible to liquefaction.
- Greater cyclic liquefaction resistance was obtained in specimens of higher relative density.
- Sample grading had less effect on the liquefaction resistance than expected, however coarse sands appeared to be more resistant to liquefaction than fine sands when dense.
- Pumiceous sands of a given relative density appear more resistant to liquefaction than hard-grained sands of the same relative density.
- Empirical correlations for estimating liquefaction resistance from common field tests (SPT, CPT, V_s) are mainly based on data from hard-grained sands, and may significantly underestimate the resistance of pumiceous sands to liquefaction and therefore overestimate the liquefaction hazard.

6 ACKNOWLEDGEMENTS

The authors would like to thank the NZ Transit Agency and project manager Jo Wilton for commissioning this study and allowing its publication. The authors would also like to thank Professors Mick Pender and Rolando Orense of the University of Auckland for their assistance, and Sadeq Asadi for carrying out the experimental works.

REFERENCES

Boulanger, R. W., and Idriss, I. M. (2014). *Report No. UCD/CGM-14/01 - CPT and SPT Based Liquefaction Triggering Procedures*. Center for Geotechnical Modeling - University of California, Davis, California, 134 pp.

Hosono, Y. and Yoshimine, M. (2004). "Liquefaction of sand in simple shear condition." *Proceedings of the International Conference on Cyclic Behaviour of Soils and Liquefaction Phenomena*, Bochum, Germany.

Hyodo, M., Orense, R.P., Noda, S., Furukawa, S., and Furui, T. (2012). "Slope failures in residential land on valley fills in Yamamoto town." *Soils and Foundation*, 52(5), 975-986.

Ishihara, K., Troncoso, J., Kawase, Y., and Takahashi, Y. (1980). "Cyclic Strength Characteristics of Tailings Materials." *Japanese Society of Soil Mechanics and Foundation Engineering*, 20(4), 127-142.

Kramer, S. L., (1996). *Geotechnical Earthquke Engineering*. Prentice Hall, Upper Saddle River, New Jersey, 653 pp.

Mulilis, J. P., Horz, R. C., and Townsend, F. C. (1976). *The effects of cyclic triaxial testing techniques on the liquefaction behaviour of Monterey No. 0 sand.* U.S. Army Engineer Waterways Experiment Station, Soils and Pavements Laboratory, Vicksburg, Mississippi.

Lui, L., Orense, R.P., and Pender, M.J. (2015). "Crushing-induced liquefaction characteristics of pumice sand." *Proceedings of the New Zealand Society for Earthquake Engineering Technical Conference, NZSEE*, Rotorua, New Zealand, Paper Number O-57.

Orense, R. P., and Pender, M. J. (2013). "Liquefaction characteristics of crushable pumice sand." *Proceedings of the 18th International Conference on Soil Mechanics and Geotechnical Engineering*, Paris, 1559 - 1562.

Orense, R. P., Pender, M. J., and Tai, A. (2012). "Undrained Cyclic Shear Behaviour of Pumice Sand", *11th Australia-New Zealand Conference on Geomechanics – Ground Engineering in a Changing World*, Melbourne, Australia, pp. 858-863.

Robertson, P. K., and Cabal, K. L. (2015). *Guide to Cone Penetration Testing for Geotechnical Engineering*, 6th ed. Signal Hill, California, Gregg Drilling & Testing Inc, 133 pp.

Seed, H. B., and Idriss, I. M. (1982). *Ground Motions and Soil Liquefaction during Earthquakes.* Earthquake Engineering Research Institute, Oakland, California, 134pp.

Thomas, J. (1992). *Static, Cyclic and Post Liquefaction Undrained Behaviour of Fraser River Sand*, The University of British Columbia, Vancouver, 117 pp.

Wesley, L. D., Meyer, V., and Pender, M. J. (1998). "Cone Penetrometer Tests in Pumice Sand." *N.Z. Geomechanics News*, June, 57-61.

Yamamoto, Y., Hyodo, M., and Orense, R. P. (2009). "Liquefaction Resistance of Sandy Soils under Partially Drained Condition." *Journal of Geotechnical and Geoenvironmental Engineering*, 135(8), 1032-1043.

Yoshimi, Y., Tokimatsu, K., and Ohara, J. (1994). "In situ liquefaction resistance of clean sands over a wide density range." *Geotechnique*, 44(3), 479-494.

Proceedings of the 11th ANZ Young Geotechnical Professionals Conference – 11YGPC
Queenstown, New Zealand
25 – 28 October 2016

Seismically induced land damage on Whitewash Head, Christchurch, New Zealand

Charles. C. Mangos[1]

[1]Graduate Engineering Geologist, Infrastructure, Aurecon NZ, Unit 1, 150 Cavendish Road, Casebrook, Christchurch 8051, New Zealand, PO Box 1061, Christchurch 8140, New Zealand; email: Charles.mangos@aurecongroup.com

ABSTRACT

On 14 February 2016 a M5.7 earthquake, now commonly referred to as the Valentine's Day Earthquake, struck off the coast of Christchurch city causing land damage in the Port Hills. This earthquake follows almost five years after the M6.3 earthquake that struck the city on 22 February 2011 that caused extensive cliff retreat and ground cracking near the cliff edges. Another significant earthquake with a magnitude of 6.3 struck the same year on 13 June. This caused the cliffs at Whitewash Head in the east of the Port Hills to retreat along already mapped tension cracks and created new cracks up to 10m from the cliff edge. Currently, the structures on 'red-zoned' properties on Whitewash Head are being demolished as part of the land clearance works undertaken by Land Information New Zealand. The demolitions are in geotechnically high risk areas and strict monitoring controls are in place. The recent Feb 14 earthquake was the largest since monitoring was installed, thus enabling the engineering geologists to observe how these monitoring systems performed during a significant seismic event. This paper presents the response of the monitoring networks and aerial photograph review following the 2016 Valentine's Day earthquake; discusses possible failure modes and implications of further land deformation in the Port Hills and concludes by providing options for management of future land clearance sites affected by geotechnical hazards.

Keywords: Cliff collapse, Christchurch, Earthquake, Valentine's Day Earthquake, GNS

1 INTRODUCTION

On 14 February 2016 a Magnitude (M) 5.7 earthquake struck 2km off the coast of Christchurch city, New Zealand, approximately 8km deep, causing further land damage in the Port Hills. Cliff collapse was observed at Whitewash Head, Godley Head, Wakefield Avenue and Shag Rock Reserve, (Figure 1). These are areas of present-day or former sea-cliffs (Massey, et al., 2012) with the exception of Wakefield Ave which is an old quarry site. With exception of Godley Head, all areas are currently part of clearance and remedial works undertaken by Land Information New Zealand (LINZ) on 'red-zoned' land. The focus of this paper will be based on two properties at Whitewash Head, where the largest volume of cliff collapse debris fell, herein referred to as 'Property A' and Property B' (Figure 2).

Cliff collapse is referred herein as "rock fall failure characterised by large volumes of debris (thousands of cubic metres). The hazards associated with these cliff collapses included incipient cracking, often with differential vertical displacement and minor extension behind the top of the failed cliff faces, as well as a debris inundation hazard at the base of the cliff face" (Dellow et al. 2011).

On some areas of Whitewash Head there is an immediate risk to life based on modelling by the Institute of Geological and Nuclear Sciences (GNS) (Massey, et al., 2012). The Crown purchased the land and all the buildings and fixtures. 'Red-zoned' means the property is in an area where there is an unacceptable risk to life safety from geotechnical hazards. Demolition of the structures on a 'red-zoned' property begin once it is vacated, settlements are finalised and insurance assessments are complete (New Zealand Government, 2015, 2016a, 2016b). At Whitewash Head, properties A and B were part way through the long process of being demolished when the Valentine's Day Earthquake struck. Fortunately, the event occurred on a Sunday when no site works were being undertaken by the Contractor.

Due to the large amount of land damage caused by the 2010-2011 Christchurch Earthquake Sequence, over five years ago, a monitoring network was installed around 'red-zoned' areas in the Port Hills. Part of this network uses basic techniques that can be accessed on short notice and provide instant results for the Consultant. Tell-tales (point to point measurements that indicate movement)

were installed in areas where cracking in the soil, pavement and structures had occurred and created offsets. These were installed and monitored on a daily basis during the demolition process on Whitewash Head.



Figure 1. Areas where cliff collapse caused by the Valentine's Day Earthquake (GoogleEarth 2016)

2 RESPONSE

2.1 Monitoring Networks

In the days following the earthquake, monitoring controls and detailed field mapping of observed cracking were undertaken by engineering geologists from Aurecon and the Institute GNS. The data collected from Whitewash Head showed movement on existing and additional cracking ranging from 1mm to >150mm horizontally and up to 25mm vertical displacements in the soil, pavement and foundations of Property A and B. Nestled behind the structure on Property B is a 10m high shotcrete wall that is severely cracked.

A Digital Laser Rangefinder provides a relatively fast and reliable way of measuring distance to an object. Baseline distance tell-tale measurements using the rangefinder were established months before the demolitions began and these were compared to daily measurements taken on site, refer to Figure 2. More tell-tales were installed as the demolitions progressed, exposing more cracks that could be monitored. However, as structures became demolished, the monitoring points often had to be relocated or abandoned the number of monitoring points over time.

Table 1 lists tell-tales measurements four days prior and three days after the Valentine's Day earthquake (VDE). Since the VDE most tell-tales measurements have remained the same post VDE, however one particular measurement showed a significant change (point 'WWH_M'). This particular tell-tale was set up to measure over a >100mm crack in a stone and concrete patio on Property A (Figure 2). This crack runs sub-parallel to the cliff face and is the closest tell-tale to the cliff edge while just outside of the second cliff collapse event line, see Figure 2.

Measurements from another Tell-tale 'WWH_W', positioned to measure between the concrete block retaining wall and ring foundation on Property A. It too indicated some movement with a 4mm increase in the baseline measurement. This movement vector aligns with the tilted pile in Figure 5(a).

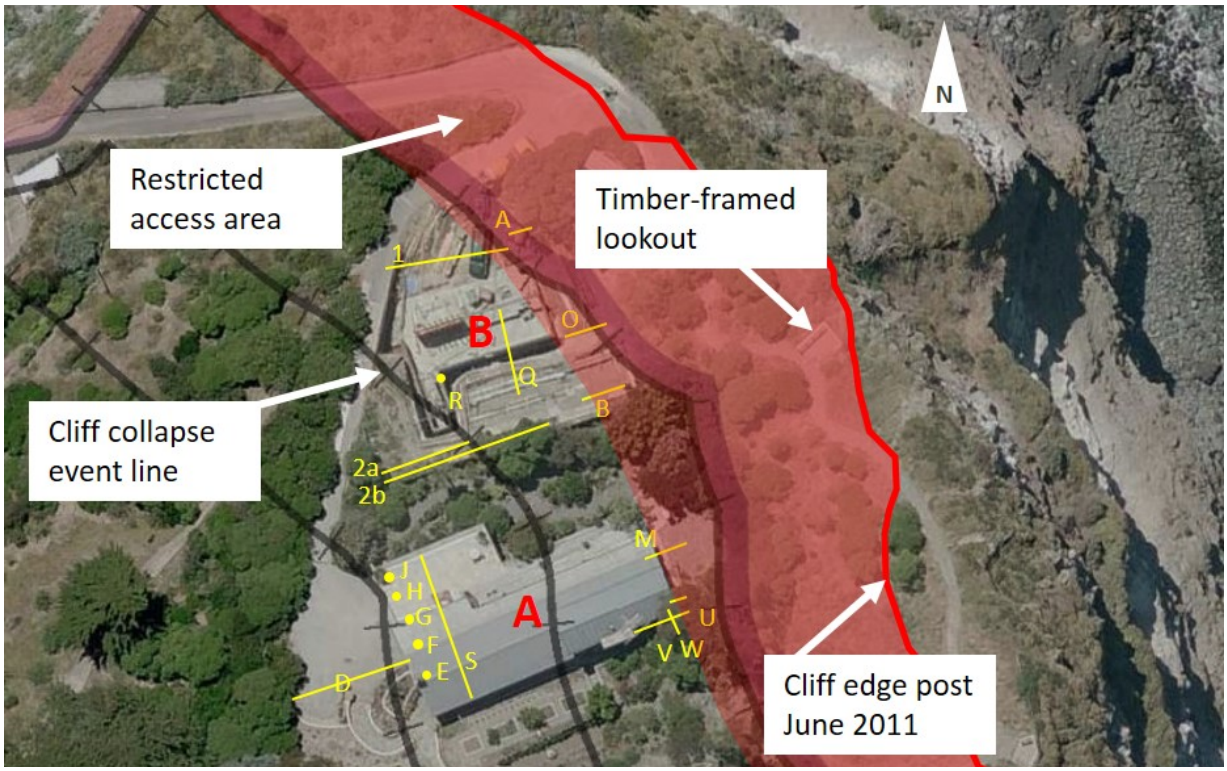


Figure 2. Tell-tale locations at Property A and B. Tell-tales are shown in yellow. The dots are vertical measurements and the lines are horizontal measurements. The 'cliff collapse event line' is defined as the point which the cliff may retreat up to in a significant seismic event. (Aurecon GIS base imagery 2009/2010).

Table 1. Tell-tale measurements (mm) taken before and after the Valentine's Day aftershock.

Location ID	Baseline Readings (mm)	04/02/2016		09/02/2016	10/02/2016		17/02/2016
		0800hrs	1200hrs	1015hrs	0800hrs	1530hrs	1030hrs
WWH_A	1546	1546	1547	1574	1546	1547	1547
WH_1	12347	–	–	12348	12346	12348	12346
WH_2a	7802	7803	7804	7803	7802	7803	7803
WH_2b	16836	16835	16835	16834	16834	16833	16834
WWH_B	3325	3328	3328	3327	3327	3329	3331
WWH_O	3784	3785	3785	3785	3784	3785	3785
WWH_D	12977	12974	–	12973	12973	12974	12975
WWH_E	3566	3563	3565	3565	3563	3566	3565
WWH_F	3569	3567	3568	3568	3567	3570	3568
WWH_G	3573	2570	3572	3573	3570	3574	3572
WWH_H	3570	3569	3569	3571	3568	3571	3570
WWH_J	3574	3574	3574	3574	3572	3575	3574
WH_4	3901	3902	3904	3903	3900	3903	3901
WWH_M	6530	6528	6528	6527	6527	6527	6535
WWH_3a	4731	4733	4732	4732	4732	4732	4733
WWH_P	2821	2821	2822	2822	2821	2820	2822
WWH_Q	8580	8580	8581	8582	8580	8582	8583
WWH_R	3349	3349	3350	3349	3348	3345	3349
WWH_S	9014	9013	9014	9014	9013	9014	9014
WWH_U	6363	6363	6362	6363	6362	6363	6361
WWH_V	1923	1924	1922	1925	1922	1922	1926
WWH_W	4444	4445	4445	4446	4446	4446	4449
WWH_X	7815	–	–	7815	7815	7815	7815
WWH_Y	7011	7010	7011	7011	7010	7010	7011
WWH_Z	2706	2707	2707	2708	2707	2707	2707

2.2 Photo Review

Hours after the 14 February 2016 earthquake, members of the LINZ Rapid Response Team comprising of geotechnical experts from Aurecon, and the demolition contractor surveyed the cliffs at Whitewash Head from a helicopter refer to Figure 3(a) and (b). Following this, further inspections were conducted using an unmanned aerial vehicle (UAV). The use of the UAV meant additional aerial reconnaissance could take place on multiple days at a fraction of the cost and allow a closer look at the cliff. The Gimbal-stabilised camera allowed high resolution photos to be taken in close proximity to assess land damage where parts of the cliff had cracked or collapsed while keeping personal out of high geotechnical risk areas.

Figures 3(a) and (b), taken before and after the 14 February 2016 aftershock, show how the cliff face below Property A and B has further retreated. The majority of material has fallen from the upper third of the cliff and it has accumulated down the bottom, see Figure 4. This same area of the cliff retreated in the February and June 2011 events.

A UAV was flown on the 17 and 18 February 2016 to assess the land damage in an area where, as described by Kupec (2016) "4 to 8m of cliff was lost (during the VDE), with cracking occurring in Property A and in the reinforced foundations of Property B. Although the cracking appears to be about 25m from the current cliff edge we need to consider that in February 2011 about 15 to 20m fell off and in June 2011 about 25m of cliff edge retreated (at different areas along the cliff). Hence the cracking does provide a credible scenario for upcoming cliff edge retreat." One landmark, a timber-framed viewing platform perched on an overhanging section of the cliff, was lost over the edge. During the earthquake a pair of surfers were floating in the water below Whitewash Head, they observed boulders as large as cars falling into the sea from the cliff and a large dust cloud was seen from as far away as New Brighton, over 2km away.



Figure 3(a). 65 – 85 m high sea cliff below Property A and B Whitewash Head, Scarborough. Note: timber framed lookout (24/09/2016 Aurecon).



Figure 3(b). 65 – 85 m high sea cliff below A and B Whitewash Head, Scarborough. Note: missing timber-framed lookout, vegetation, and visible crack sub-parallel to cliff face (14/06/2016 Aurecon).

Further inspection with a UAV showed large (>1m³) size rocks precariously perched on the cliff with daylight showing between them and the cliff, see Figure 3(b). This means there is the potential for more boulders to fall and the cliff to retreat in future seismic event. However, it is possible that "fretting

and crack width could increase under normal climatic conditions and be exacerbated by prolonged precipitation" (Kupec 2016).



Figure 4. Talus at the base of approx. 100 m high sea cliff and sediment in the sea below Searidge Lane, Scarborough (14/02/16 Aurecon).

Observations made by Engineering Geologists during a site walkover four days after the event revealed a tilted concrete pile on Property A, refer to Figure 5(a), although this may have already been tilted in an event prior to the VDE as it was in an area recently exposed by the Contractor. However, this pile does indicate movement on the site. It appears there has been vertical displacement and horizontal movement towards the cliff edge. This hypothesis is supported by evidence from the aerial photo showing a series of cracks in structures on Property A that run sub-parallel to the cliff, see Figure 5(b).



Figure 5(a). Tilted >10° concrete pile (P) on Property A (18/02/2016 Aurecon).

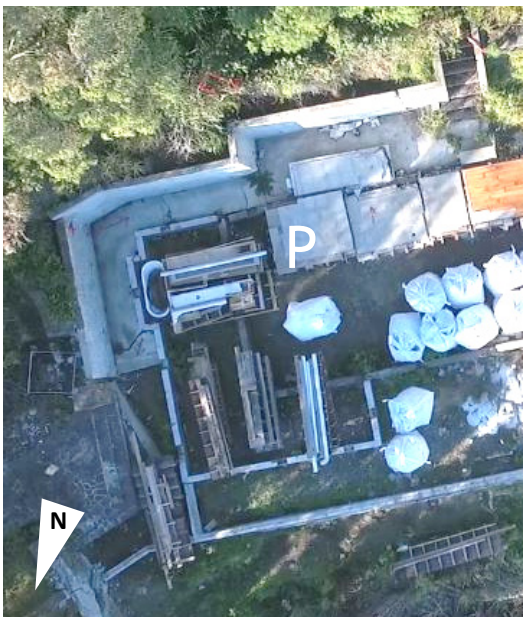


Figure 5(b). Cracked and displaced reinforced concrete ring foundations and retaining walls on Property A (18/02/2016 Aurecon).

2.3 Possible failure modes and implications for further land damage

It has become apparent in each M5+ earthquake centred near the Port Hills of Christchurch that some land damage is expected to occur along the already damaged sea cliffs at Whitewash Head. In the

February 2011 earthquake approximately 42,000m³ of material fell from the slope and over 150,000m³ in June 2011 (Massey et al. 2012). The level of shaking from the VDE caused new cracks to appear in the cliff face, released large volumes of rock and soil and has created new rock blocks that are susceptible to failure in future earthquakes.

It appears that each event is causing either further cracking and weakening of the rock with some retreat of the cliff as seen in February 2011, or a significant retreat of the cliff edge as seen in June 2011. Following this trend, a large volume of material could fall from the slope in the next M5+ earthquake.

2.4 Options for management of future land clearance sites affected by geotechnical hazards

The risk management of the long term effects of these events has already lead to the 'red-zoning' of properties in these geotechnically high risk areas. The cliff-collapse that occurred on Whitewash Head on February 2011, June 2011 and February 2016 demonstrated the necessity for these mitigation measures.

Further destabilization of the cliff caused by the VDE has led to the necessity for the demolition methodology for these two structures to be changed. Based on the deformation observed by members of Aurecon and GNS, amendments include an already restricted access area near the cliff edge, see Figure 2, to be brought further back and the requirement for a larger specialized remote controlled excavator with greater reach that can bring down the structures from a greater distance than required before the VDE. Current monitoring techniques have proven to be effective at documenting movement on Whitewash Head and can continue to be utilised in the new methodology.

3 CONCLUSION

On 14 February 2016 a M5.7 earthquake struck 2km off the coast of Christchurch city approximately 8km deep, causing further land damage in the Port Hills. The damaged areas included already 'red-zoned' properties causing cracking and collapse of sea cliffs. This has resulted in a further destabilized slope where failures can occur under normal climatic conditions. Luckily, there were no fatalities from this event. Engineering geologists from Aurecon and GNS observed movement on Whitewash Head demolition sites using monitoring techniques installed prior to the aftershock. A Digital Laser Rangefinder provided measurements of tell-tales placed over known cracks that recorded movement towards the cliff edge with mm accuracy. This is also evident in the concrete piles that have been tilted, indicating vertical displacement and horizontal movement in the same direction. A UAV proved to be an effective tool for aerial reconnaissance of the sites that showed cracks sub-parallel to the cliff and in the cliff face, and retreat of the cliff edge shown with the loss of landmark structures. These techniques when used together were effective tools for displaying seismically induced land damage on Whitewash Head.

4 ACKNOWLEDGEMENTS

The author would like to thank Aurecon for providing funding, the LINZ Rapid Response Team, Chris Massey, Camilla Gibbons for her guidance, and in particular Richard Heritage for suggesting this submission.

REFERENCES

Dellow, G., Yetton, M., Massey, C., Archibald, G., Barrel, D. J., Bell, D. and Walsh, I. (2011, December). Landslides caused by the 22 February 2011 Christchurch Earthquake and management of landslide risk in the immedite aftermath. *Bulletin of the New Zealand Society for Earthquake Engineering, 44*, pp. 227 – 238

Kupec, J. (2016, March 24). Whitewash Head Preliminary Assessment. (C. Mangos, Interviewer)

Massey, C. I., McSaveney, M. J., Yetton, M. D., Heron, D., Lukovic, B. and Bruce, Z. R. (2012). *Canterbury Earthquakes 2010/2011 Port Hills Slope Stability: Pilot Study for assessing life-safety risk from cliff collapse.* GNS Science Consultancy Report 2012/57.

New Zealand Government. (2015, August). *Crown offer for uninsured improved properties in the residential red zone*. Christchurch, Canterbury, New Zealand.

New Zealand Government. (2016a, June 30). *Demolitions and clearances*. Retrieved from Land Information New Zealand: http://www.linz.govt.nz/crown-property/types-crown-property/christchurch-residential-red-zone/demolitions-and-clearances

New Zealand Government. (2016b, June 30). *Red Zone information*. Retrieved from Canterbury Earthquake Recovery Authority: http://cera.govt.nz/land-information/red-zone

Proceedings of the 11th ANZ Young Geotechnical Professionals Conference – 11YGPC
Queenstown, New Zealand
25 – 28 October 2016

Liquefaction potential of the micaceous lake sediments in the Queenstown area

A. S. Awad[1] and J. Searle[2]

[1] Coffey International Ltd, 131 Wrights Road, Addington, Christchurch 8024, New Zealand; PH +64 (0) 3 336 5472; email: Andrew.Awad@Coffey.com
[2] Coffey International Ltd, Level 19, Tower B, Citadel Towers 799 Pacific Highway Chatswood NSW 2067, Australia; PH +61 (0)2 9406 1014; email: James.Searle@Coffey.com

ABSTRACT

Queenstown is a known seismically-active area. Following the September 2010 Canterbury earthquake, the local authorities in Queenstown have taken more initiative to improve their knowledge of the regional subsoils in order to better determine the liquefaction risk and the potential impact posed to the functionality of buildings and infrastructure should liquefaction-induced ground deformation occur. The authors carried out in-situ and laboratory testing and evaluated the liquefaction risk of the inter-bedded silt/ sandy silt laminated lake sediment layers overlying the schist bedrock. Despite a comprehensive list of assessment methods used, the data retrieved from conventional liquefaction analysis did not neatly consolidate towards a definitive conclusion and engineering judgement was needed to better interpret the body of evidence. In this paper, the authors present their liquefaction assessment and outline their findings. This paper is intended to provide readers an introduction to the topic and recommendations are given for further research to better understand the cyclic behaviour of these soils.

Keywords: Liquefaction, Queenstown, micaceous soils, lake sediments

1 INTRODUCTION

Located in the southern part of South Island, Queenstown is important to the New Zealand tourism industry and its local population also continues to grow. The nearby mapped active faults – the Alpine Fault, Nevis Fault and Cardrona Fault – are all capable of producing earthquakes greater than M_w 7. According to the recent seismic hazard study undertaken by the Otago Regional Council for the Queenstown Lakes District, the primary seismic hazard facing the region is an Alpine Fault earthquake; which is predicted to have a 30% probability of rupturing in the next 50 years. However, the modern buildings and infrastructure in the area are yet to be tested by such an event.

Given the seismological setting, we sought to evaluate the liquefaction potential of the horizontally inter-bedded silt/ sandy silt laminated lake sediment soils (lake sediments). In order to provide a measureable benchmark we carried out our liquefaction assessment in accordance with the simplified procedure set out in Modules 1 and 3 of the New Zealand Geotechnical Society (NZGS) Modules for Earthquake Geotechnical Engineering Practice (2016). Additional methods to assess liquefaction triggering were also utilised.

Conventional industry-approved procedures of determining liquefaction potential have been mostly derived from earthquake case histories of sites where the soils comprise Holocene uncemented alluvial soil deposits, and quartz is likely a dominant mineral in the soil composition. However, the microstructure of the Queenstown lake sediments, which is dominated by platy minerals, does not meet this criterion and engineering judgement was required to interpret the findings.

This paper presents our liquefaction evaluation of the lake sediments and provides recommendations for further research.

2 GEOLOGICAL SETTING

Queenstown and the surrounding Wakatipu Valley are underlain by schist of the Caples and Rakaia Terranes. The schist is actively being folded, faulted and eroded in response to regional compression and strain distributed across the mid to lower South Island. Much of the fault activity and uplift in the

area has occurred over the past five million years, which is reflected in the ruggedness of the local mountain ranges.
Repeated glaciations have carved deep troughs into the landscape, with Lake Wakatipu occupying the largest trough in the area. Lake Wakatipu covers an area of approximately 290 km^2 and is over 370 m deep. Furthermore, during the last glacial (Otira) period, the glacial lake covered a much larger area and was significantly deeper.

The surficial materials are likely to have been deposited at the end of the most recent (Otira) glaciation (i.e. late Pleistocene / early Holocene deposits).The Otira glacial period ended about 15,000 to 18,000 years ago; late and post-glacial events were marked by widespread erosion along the tributaries of Lake Wakatipu (particularly the Shotover River). The resulting sediment was deposited in Lake Wakatipu, forming deep deposits of inter-laminated silt and sandy silt.

3 GEOTECHNICAL PROPERTIES OF LAKE SEDIMENT SOILS

We carried out geotechnical investigations at four locations adjacent to Lake Wakatipu. The geotechnical investigations comprised piezocone penetration testing (CPTu), sonic-cored boreholes with Standard Penetration Tests (SPTs) and down-hole shear-wave velocity (V_s) testing. We note that the lake sediments were a minimum of 25 m thick at the investigation locations and the sites were classified as Class D - deep or soft soil sites - in accordance with NZS1170.5.

Fourteen target-soil samples were retrieved from the SPTs at depths ranging from approximately 2 m to 27 m below ground level and sent for laboratory testing to determine the soil composition and material properties. The results are presented in Table 1.

Table 1. Index properties of Queenstown lake sediments

Parameter	Value	Comment/s
USCS	ML	-
Unit weight (γ)	17.6 kN/m^3	These are averaged values, but the dataset range is not too dissimilar.
Fines content (FC) [<75 µm]	90%	
In-situ water content (w_o)	38%	
Plasticity index (PI)	8 to 15%	Few samples were simply recorded as 'non-plastic).
Liquid limit (LL)	37 to 46%	Not applicable for 'non-plastic' samples.
Overconsolidation ratio (OCR)	1.8 to 3.6	The lake sediments are in an overconsolidated stress-state as the loads of glaciers had previously been applied over them.
Compression index (C_c)	0.16 to 0.17	

Figure 1 provides the median CPT-derived profile down to 34 m below ground level and Figure 2 provides the median V_s-derived profile. It should be noted that fine to coarse grained beach gravel was encountered at the surface overlying the laminated lake sediments, and this is reflected in the upper 1.5 m of the ground profile.

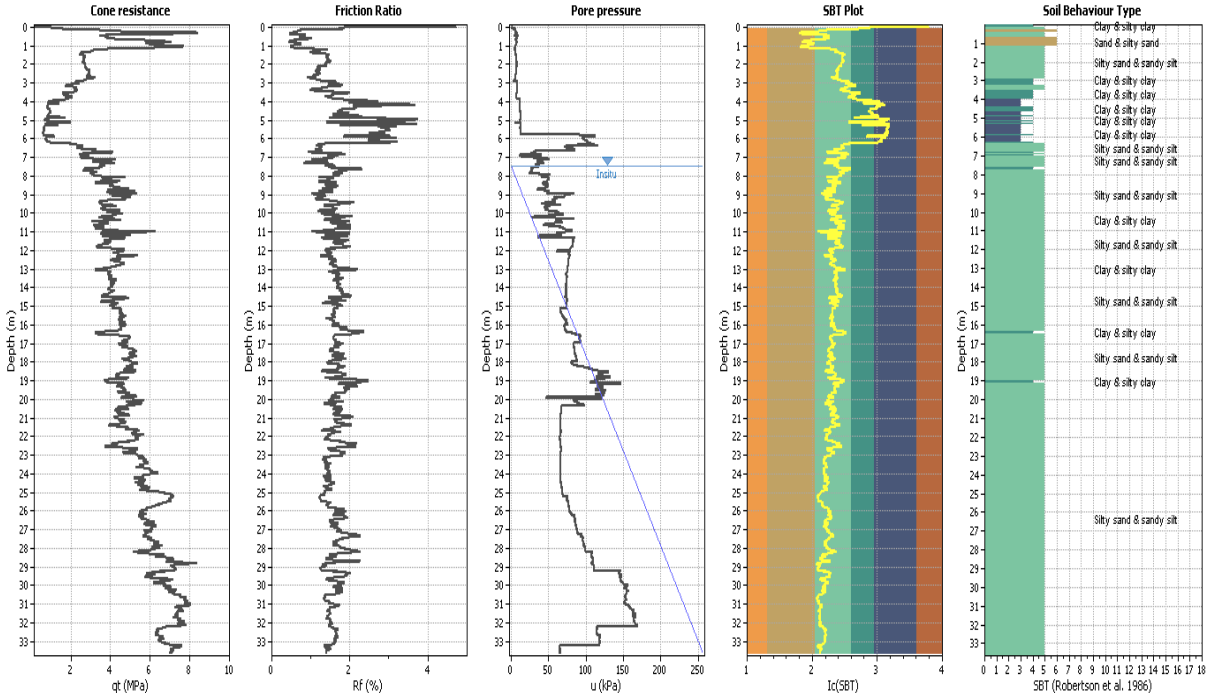


Figure 1. Median profile (design groundwater table taken at 7.5 m)

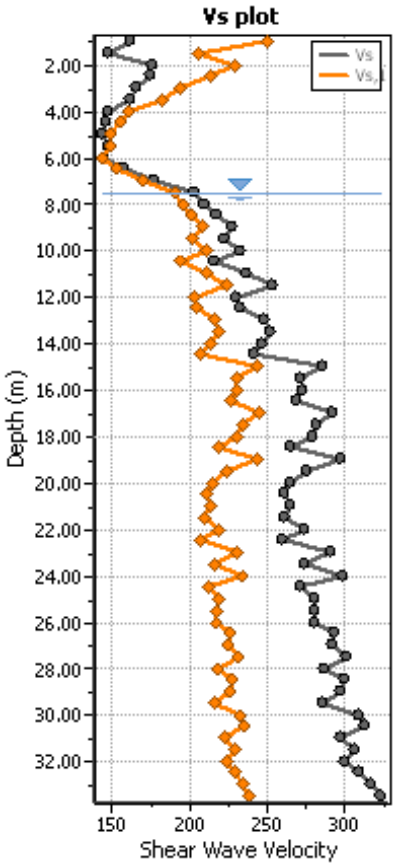


Figure 2. Median V_s and V_{s1} profile (design groundwater table taken at 7.5 m)

The laminated lake sediments in the Queenstown area are primarily derived from the schist bedrock, which contains platy mica minerals and other clay-size (i.e. finer than 75 μm) minerals. Samples were tested for mineralogy using the X-Ray Diffraction (XRD) method. It was found that the laminated lake sediments are rich in mica and chlorite (~ 84% by weight; mica and chlorite are approximately in equal amounts). Quartz makes up only 10% of the mineralogical composition and feldspars make up the remainder. Figure 3 shows the XRD patterns and their interpretations retrieved from two tests.

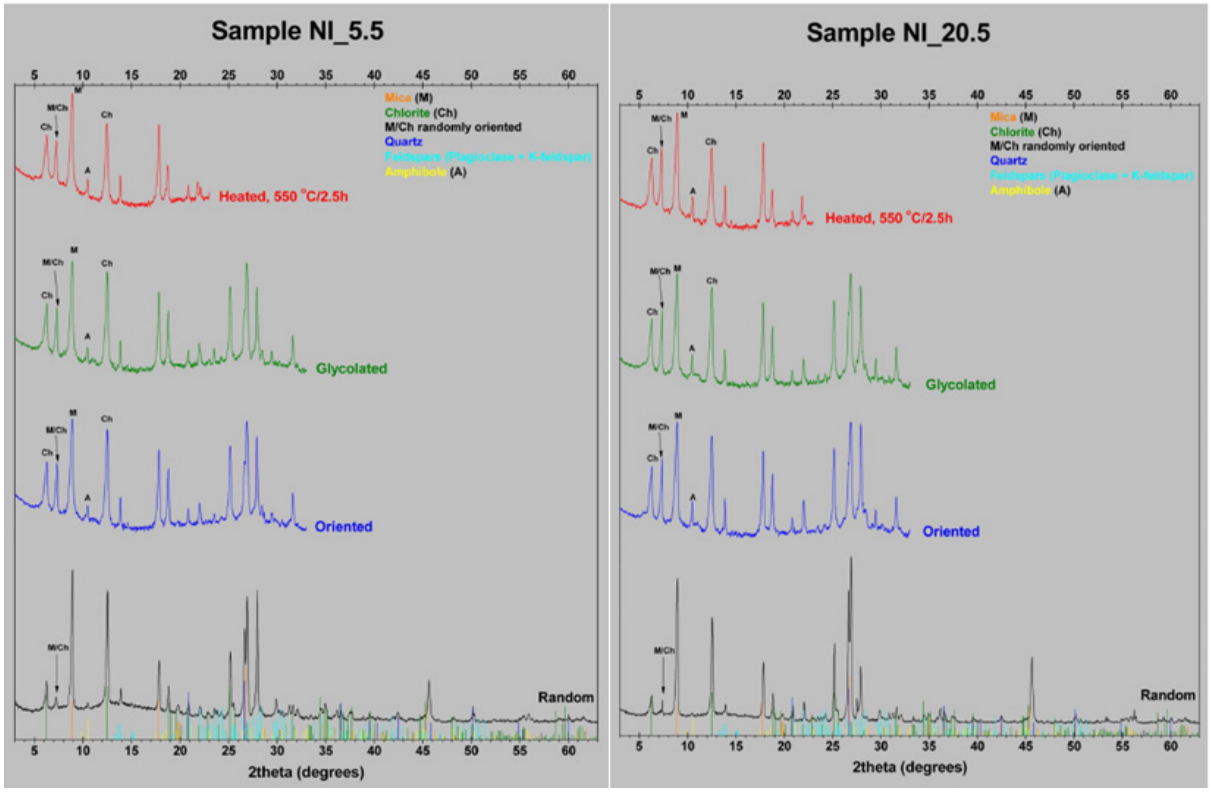


Figure 3. XRD patterns and their interpretation

4 SOIL ANISIOTROPY DUE TO MICA PARTICLES

Lee et al (2007) discusses and summarises previous research as to how the presence of platy mica particles affects the packing of soil grains and alters the mechanical behaviour of sandy soils. One of their observations is that increased mica content in sandy soils correlates with decreasing measured V_s. Even though the Queenstown lake sediments are more silty than sandy, most of the soil profile and tested samples are considered to have a 'sand-like' behaviour (I_c < 2.6) so the findings presented in Lee et al (2007) appear useful in providing an initial understanding. However, more research regarding the influence of mica in silty soils is needed to better understand the soil anisotropy.

5 ASSEESSMENT OF LIQUEFACTION POTENTIAL

5.1 Previous research

The seismic hazard report by Otago Regional Council indicates that there is little geologic evidence of widespread liquefaction for sites underlain by lake sediments, despite the area having experienced multiple Alpine Fault earthquakes over its geological history. Considering the geologic timeframe, Alpine earthquakes occur frequently in the Queenstown area (every ~ 340 years).

Bowen et al (2015) carried out 13 cyclic triaxial tests on low plasticity micaceous lake sediments in Central Otago which have similar properties to the soils we assessed in Queenstown, but with a lower plasticity range – PI = 0 to 7%. The lab testing observed cyclic mobility behaviour (gradual increase of pore pressure with increasing shear strains) but not liquefaction-type behaviour (rapid increase in pore pressure leading to complete loss of shear strength).

5.2 Liquefaction susceptibility assessment

In accordance with NZGS Module 3 (2016) we utilised the liquefaction susceptibility criteria set out in Bray and Sancio (2006). Our results showed that most of the soil samples did not meet the definitive categories of 'susceptible' or 'not susceptible' to liquefaction, but mostly lie in the region that recommends more testing be undertaken to verify the liquefaction susceptibility. The results are shown in Figure 4. (We also note that the few non-plastic samples, which are not shown in Figure 4, are considered 'susceptible to liquefaction').

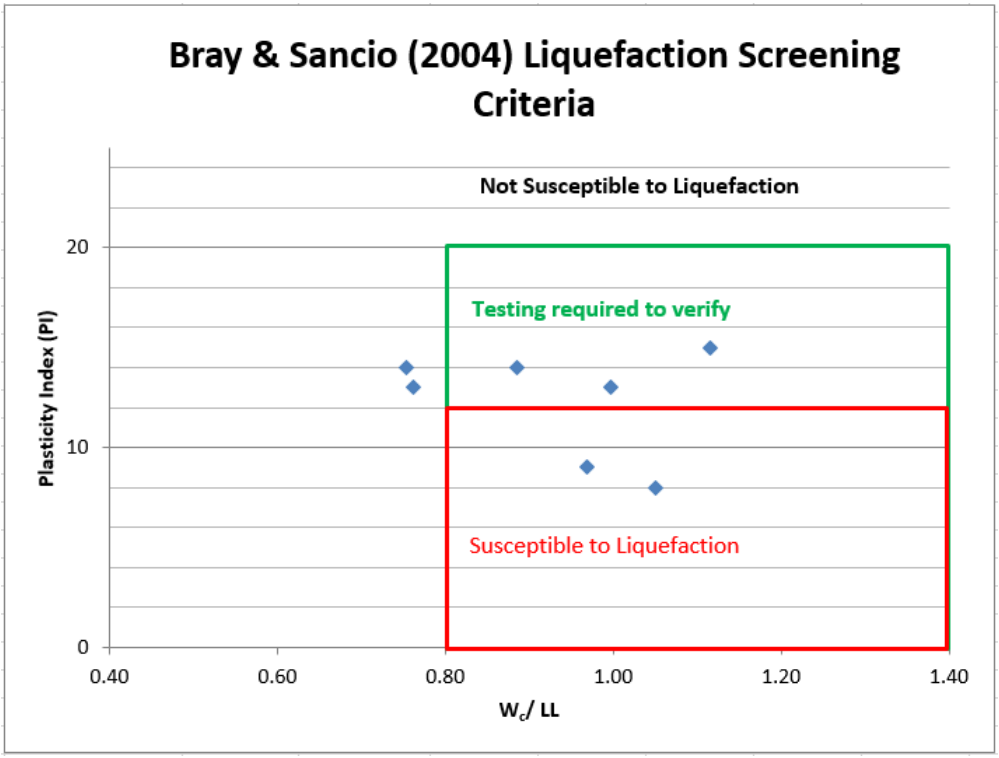


Figure 4. Liquefaction susceptibility

Overall, the results derived from the standard tests of determining liquefaction susceptibility were inconclusive.

5.3 Liquefaction triggering assessment: methodology and results

In accordance with NZGS Module 3 (2016), we adopted the procedures given by Boulanger and Idriss (2014) to assess liquefaction triggering for the CPT profiles down to 15m and applied the appropriate corrected fines content (CFC).

The ultimate limit state (ULS) ground motion parameters for a Class D sub-soil site were derived from the NZTA Bridge Manual (2014); a α_{max} of 0.4g and M_w of 6.5 (an approximate the effective value for the Queenstown area for 1000yr earthquake return period). Our investigations encountered groundwater between 3 m and 15 m, so we adopted an intermediate groundwater level at 7.5 m for the purpose of this study.

In addition, we also adopted the following methods to assess liquefaction triggering;

- Robertson and Wride (1998) analysis procedure for CPT data.
- Andrus and Stokoe (2000) analysis procedure for the small-strain V_s recorded at 0.5 m intervals.

The results of the liquefaction triggering analyses significantly varied because;

- The CPT-based methods predicted that the majority of the soil profile below the water is triggered below the water table. (It should also be noted for CPT-based methods that the Robertson and Wride [1998] procedure had slightly lower CRR profile values than the Boulanger and Idriss [2014] method).
- The Vs method considers the analysed soil profile to be non-liquefiable.

We also carried out a preliminary analysis to model an Alpine earthquake scenario. An anticipated M_w of 8.1 was adopted and in the absence of a site specific hazard assessment we adopted a large unweighted α_{max} of 1g. Our findings were the same as those outlined above.

6 DISCUSSION REGARDING RESULTS AND CURRENT INDUSTRY PRACTICE

The results from the standard tests to determine liquefaction susceptibility were inconclusive and the methods of assessing liquefaction triggering significantly varied. However, the published literature records little geologic evidence of widespread liquefaction for sites underlain by lake sediments. Based on our work, we consider that this may be due to the combination of the microstructure (i.e. the platy mineral structure), laminated layering and age of the deposits (i.e. cementation properties and overconsolidated stress state) which make the lake sediments less susceptible to liquefaction (in comparison with Holocene uncemented quartz-rich soils).

The results of our assessment identified the V_s method as the most-aligned with the geologic record and cyclic traxial test results presented in Bowen et al (2015). V_s testing estimates the small-strain shear modulus (stiffness) of the soil and as noted by Andrus and Stokoe (2000); *"V_s and liquefaction resistance are similarly influenced by many of the same factors (e.g., void ratio, state of stress, stress history, and geologic age)"*. These factors are not necessarily accounted for by penetration-based methods. It should also be noted that even though the lake sediments have high mica content (which decreases measured V_s), the measured V_s values were still high enough to predict a low risk of liquefaction.

We consider that the routine penetration-based procedures used throughout New Zealand to assess liquefaction triggering may lead to overestimating the liquefaction risk for sites in the Queenstown area. Even for sites in earthquake-damaged Christchurch, the routine evaluation procedures extensively used do not always correspond with the actual observed site performance. One example of this disparity is presented in Beyzaei et al (2015) where a certain Christchurch site has a silty profile (average FC: 82.1%, average PI: 5%) and the cyclic resistance of the soil estimated by both CPT methods and cyclic triaxial testing indicate that soil liquefaction was triggered following the 22 February 2011 earthquake event; but no surface manifestation of liquefaction was observed following the earthquake. Beyzaei et al (2015) hypothesise that the stratified profile of liquefiable and non-liquefiable soils and the sub-angular particle shape may have limited the pore water pressure redistribution and the formation of sediment ejecta. They are continuing further research to better understand this phenomenon and propose to carry out nonlinear effective stress analyses. Even though it has taken decades to develop widely accepted liquefaction evaluation procedures for Holocene deposits, this example is a reminder that the while science and practice of liquefaction assessment has advanced significantly, it still has not reached perfect maturation.

7 AREAS OF FURTHER RESEARCH

This paper was prepared based on a limited number of geotechnical investigations, in-situ tests and laboratory tests. To more accurately characterise the liquefaction potential of the inter-bedded silt/ sandy silt laminated lake sediment soils, we recommend more area-wide geotechnical investigations, in-situ and laboratory testing (including more cyclic triaxial testing) be carried out throughout the Queenstown region on similar soils.

Even if further investigations and testing shows that the lake sediments do not reach a specified condition of liquefaction, the cyclic strain softening behaviour of these fine-grained soils would need to be further researched. This was not the topic of this study but we recommended more undrained shear strength testing be undertaken to better understand the sensitivity of the cohesive soils in order to adopt suitable N_{kt} values, which are needed to establish the shear strength profiles and CRR in accordance with Boulanger and Idriss (2007).

Additionally, even though there is little geological evidence of widespread liquefaction, previous earthquake events have caused landslides and river banks to collapse throughout the Queenstown Lakes District. The stability analysis undertaken by Bowen et al (2015) predicted horizontal and vertical displacements resulting from large earthquakes but demonstrated that this mechanism was unlikely the result of a sudden flow-type failure which is associated with liquefiable soils. We therefore recommend more research be undertaken to better understand how the quantity, distribution and orientation of the mica particles influence the monotonic and cyclic behaviour of the silty soil and how this might affect slope instability.

8 CONCLUDING REMARKS

Based on our investigations and assessment, it appears that the results derived from V_s testing were the most-aligned with the geologic record. However, we recommend further investigations, testing and research be carried out.

Following further research and data collection; Correlations regarding the material properties and the liquefaction potential of the Queenstown lake sediments can be established, liquefaction hazard maps can be updated, and depending on the findings the current local practices for evaluating liquefaction risk of these soils may need to be modified accordingly. We recommend the findings of this research be readily accessible on an updated searchable database, such as the New Zealand Geotechnical Database. This type of work would provide more insight to the local geotechnical community who are likely to utilise more cost-effective methods of site investigation for small-scale projects. Furthermore, this type of work would allow more informed 'day-to-day' decisions be made by the local authorities regarding the development of the typical small-scale projects in the Queenstown area.

9 ACKNOWLEDGEMENTS

The authors would also like acknowledge the various feedback provided by their colleagues Andreas Giannakogiorgos, Ioannis Antonopoulos, Joseph Byron-Joyce and Kah-Weng Ho.

REFERENCES

Andrus, R.D. and Stokoe II, K. (2000). "Liquefaction resitance of soils from shear wave velocity", *Journal of Geotechnical and Geoenvironmental Engineering*, 126(11):1105-1025.

Barrell D., Riddolls B., Riddolls P. and Thomson R. (1994). *Surficial geology of the Wakatipu Basin, Central Otago, New Zealand*, Institute of Geological and Nuclear Sciences Report 94/39.

Bayzaei, C.Z., Bray, J.D., Cubrinovski, M., Riemer, M., Stringer, M.E., Jacka, M. and Wentz, F.J. (2015). "Liquefaction resistance of silty soils at the Riccarton Road site, Christchurch, New Zealand", *6th International Conference on Earthquake Engineering*, Christchurch, New Zealand.

Boulanger, R.W. and Idriss, I.M. (2006). "Liquefaction susceptibility criteria for silts and clays", *Journal of Geotechnical and Geoenvironmental Engineering*, 132(11), pp.1413-1426

Boulanger, R.W. and Idriss, I.M. (2007). "Evaluation of cyclic softening in silts and clays", *Journal of Geotechnical and Geoenvironmental Engineering*, 133(6), pp.641-462

Boulanger, R.W. and Idriss, I.M. (2014). *CPT and SPT liquefaction triggering procedures*, Report No. UCD/CGM-14/01, Centre for Geotechnical Modelling, Department of Civil and Environmental Engineering at the University of California, Davis, California

Bowen, H.J., Ashby, G.L. and Strigner, M.E. (2015). "Case study – Undisturbed sampling, cyclic testing and numerical modelling of a low plasticity silt", *6th International Conference on Earthquake Engineering*, Christchurch, New Zealand.

Bray, J.D., Sancio, R.B., Reimer, M. and Durgunoglu, H.T. (2004). "Liquefaction susceptibility of fine-grained soils", *Proceedings in the 11th International Conference on SDEE and 3rd International Conference on Earthquake Engineering*, pp. 655 – 662

Bray, J.D. and Sancio, R.B. (2006). "Assessment of liquefaction susceptibility of fine-grained soils", *Journal of Geotechnical and Geoenvironmental Engineering*, ASCE, pp. 1165 – 1177

Lee, J-S, Guimaraes, M. and Santamarina, J.C. (2007). "Micaceous sands: Microscale Mechanisms and Macroscale Response", *Journal of Geotechnical and Geoenvironmental Engineering*, 133(9), pp. 1136-1143.

Ministry of Business, Innovation and Employment (MBIE), (2012). *Repairing and rebuilding houses affected by the Canterbury earthquakes*.

New Zealand Geotechnical Society (NZGS) and Ministry of Business, Innovation and Employment (MBIE), (2016). *Earthquake geotechnical engineering practice Module 1: Overview of the guidelines*

New Zealand Geotechnical Society (NZGS) and Ministry of Business, Innovation and Employment (MBIE), (2016). *Earthquake geotechnical engineering practice Module 3: Identification, assessment and mitigation of liquefaction hazards*

Otago Regional Council (2015). *Seismic Hazard in Queenstown Lakes District: Study Report.*

NZ Transport Agency (2014). *Bridge manual*, Third Edition, Manual Number - SP/M/022

Robertson, P.K. and Wride, C.E. (1998). "Cyclic Liquefaction and its Evaluation based on the CPT", *Canadian Geotechnical Journal*, 35.

Robertson, P.K and Cabal K.L. (2014). *Guide to Cone Penetration Testing for Geotechnical Engineering* (6th Ed), Gregg Drilling & Testing, Inc., California, USA

Stuff (2016). *Queenstown council starts liquefaction project,* Available at: http://www.stuff.co.nz/southland-times/news/4318210/Queenstown-council-starts-liquefaction-project. [Accessed 14 June 2016]

This page intentionally left blank

Proceedings of the 11th ANZ Young Geotechnical Professionals Conference – 11YGPC
Queenstown, New Zealand
25 – 28 October 2016

A Comparison and Review of the Field Logging Standards and Guidelines in Australia and New Zealand

Katherine Farry[1]

[1]Jacobs Engineering Group, 32 Cordelia Street, South Brisbane, QLD. 4101, Australia; email: katherine.farry@jacobs.com

ABSTRACT

With the increased need for a flexible work force, labour mobility between regions and countries has become a necessary and normal practice for many geotechnical professionals. Engineers and geologists are required to work to country specific standards for the logging of soil and rock cores. The Australian Standard, AS1726-1993 aims to standardise logging procedures in Australia, and like many other countries, New Zealand has their own guidelines for logging, which differs from AS1726-1993. The purpose of this paper is to outline the similarities and differences between the Australian Standard AS1726-1993 and the New Zealand Logging Guideline, "Field Description of Soil and Rock, New Zealand Geotechnical Society, 2005". These comparisons are discussed both from a review of the standard and guideline, and further based on the author's experience of geotechnical field investigations in both Australia and New Zealand. The need for these variations is explained and any potential impact of these differences on the overall geotechnical interpretation and subsequent design is evaluated. Some advice is given to help practitioners easily adapt their logging style between the two countries.

Keywords: weathering, rock material strength, defect discontinuity spacing

1 INTRODUCTION

A comparison of significant descriptors outlined in the Australian Standard, AS1726-1993 and in the "Field Description of Soil and Rock, New Zealand Geotechnical Society, 2005" will be made. Due to changes being made to the current Standard AS1726-1993, a review of the draft standard (AS1726-2016 (DRAFT)) will also be made (at the time of publication of this paper, only a draft revision was available). In this draft revision there has been a shift from the Australian Standard being used as a "guideline", to a mandatory standard. This change in emphasis has been achieved by moving the majority of the content of the appendices into the main body of the text. The New Zealand guidelines have been prepared with the intention of reducing the 'subjective' use of terms, with an emphasis on the "describing properties that are for engineering significance" (NZGS-2005). Both publications have been written with the intention of an assessment of material classifications to be made in the field.

Not all aspects are able to be addressed in this paper; therefore what is believed to be some of the key descriptors used in engineering interpretation will be reviewed. This includes a review of rock weathering, rock strength, and discontinuity spacing. References to other literatures will be included in this paper, for comparison and therefore a more informed assessment may be made of the publications being reviewed.

2 COMPARISON OF FIELD DESCRIPTIONS

2.1 Rock Weathering

Rock weathering classification is an important descriptor for distinguishing changes to the rock fabric. Weathering describes the process of alteration of the rock's structure, (Geological Society Engineering Group Working Party Report, 1995), caused by physical, chemical and biological processes. The dominant process is dependent on the stage of weathering and type of rock; such processes are often governed by the presence of water (Clayton et al. 1995).

Chemical weathering involves the breakdown of minerals by the action of chemical agents, such as acids in the air or water (Blyth et al. 1984). As such the process is dependent on the solubility of the rock type and presence of water. Physical or mechanical weathering process involves the breakdown of rocks into smaller particles by temperature, rain, ice and abrasion, and is therefore dependent on

the weather or climatic conditions (Blyth et al. 1984). Biological weathering includes the changes made to the ground through the activities of animals and plants (Blyth et al. 1984).

Weathering is best described by its visible effects which include changes in colouring, overall staining, staining along joints and changes in strength to the rock. Often strength changes in a rock can be used as an indication of the degree of weathering; on assessment this is often the case, but should not necessarily be assumed. Before making a full assessment of the weathered state of a section of rock it is helpful to see the rock in its unweathered or fresh state. This allows the geotechnical professional to make a more informed assessment by using the rock's unweathered state as a benchmark for the remainder of the strength and weathering classification. If possible, observations from outcrops in the vicinity of the site should be investigated.

The New Zealand Guideline, NZGS-2005, outlines the weathering terms and a corresponding description that can be used in the field to interpret the weathered state of the rock. A grade number is also given for each term (see Table 1). The rock mass weathering has been described as a scale. The definition of a scale is a number or amount, used to measure or to make a comparison from a reference level. This means that a reference point, in this case the rock's unweathered state, is required in order to make a more confident assessment of the corresponding weathered state. The descriptions refer to changes in rock strength, discolouration, defect aperture width and defect spacing. This can be used to assess the process of weathering that has taken place, for example physical processes in moderately weathered rock, chemical processes in highly weathered rock and physical and chemical in completely weathered rock.

Table 1. Extract from NZGS-2005 (Table 3.1 Scale of Rock Mass Weathering)

Term	Grade	Abbreviation	Description
Unweathered (Fresh)	I	UW	Rock mass shows no loss of strength, discolouration or other effects due to weathering. There may be slight discolouration on major rock mass defect surfaces or on clasts.
Slightly Weathered	II	SW	The rock mass is not significantly weaker than when unweathered. Rock may be discoloured along defects, some of which may have been opened slightly.
Moderately Weathered	III	MW	The rock mass is significantly weaker than the fresh rock and part of the rock mass may have been changed to a soil. Rock material may be discoloured, and defect and clast surfaces will have a greater discolouration, which also penetrates slightly into the rock material. Increase in density of defects due to physical disintegration process such as slaking, stress relief, thermal expansion/ contraction and freeze/thaw.
Highly Weathered	IV	HW	Most of the original rock mass strength is lost. Material is discoloured and more than half the mass is changed to a soil by chemical decomposition or disintegration (increase in density of defects/fractures). Decomposition adjacent to defects and at the surface of clasts penetrates deeply into the rock material. Lithorelicts or corestones of unweathered or slightly weathered rock may be present.
Completely Weathered	V	CW	Original rock strength is lost and the rock mass changed to a soil either by chemical decomposition (with some rock fabric preserved) or by physical disintegration.
Residual Soil	VI	RS	Rock is completely changed to a soil with the original fabric destroyed.

In comparison, Table 2 outlines the Australian Standard's, AS1726-1993, weathering terms that are to be used, which have been referred to as a classification. The definition of classifications is the act or process of dividing things into groups according to their type. Some of the definitions for the weathering terms rely on the understanding and definition of a soil. This is defined as 'it either disintegrates or can be remoulded in water'. A soil description and rock description is often given for the XW term, due to the material behaving more like a soil then a rock. Staining, discolouration and

strength are also descriptors used to define a weathered state. Unlike NZGS-2005 there are no terms used in the Australian Standard to describe the weathering processes (physical, chemical, biological), but these are implied in some of the descriptions. AS1726-1993 differs from NZGS-2005, by using the terms XW and DW. In comparing the descriptions, it can be seen that XW can be equated to CW, as both terms describe the 'rock mass changed to a soil' or as 'having soil properties'. The DW term, is essentially a combination of HW and MW, as both are described as having significant changes in rock strength. It has however been observed that both the highly and moderately weathered terms are often used in Australia, over the distinctly weathered term, due to this being a broad descriptor. The new revision to AS1726 incorporates both the highly and moderately weathered terms, giving the geotechnical professional the option to distinguish between the two. There is no reference made to discontinuities, in the rock material weathering definitions, as this is only assessed in the rock mass weathering grades.

Unlike NZGS-2005, AS1726-1993 gives a separate table for rock mass weathering grades; with grade separation from I-VI. This is convenient for use and classification on large scale excavations. Rock mass weathering grade considers the rock mass as a whole, taking into account the effect of the individual discontinuities and how the whole block is weathered. This differs from the rock material weathering classification; the classification looks at the rock and intact material weathering. The draft revision to AS1726 has kept the table for rock mass weathering grades.

Table 2. Extract from AS1726-1993 (Table A9 Rock Material Weathering Classification)

Term	Symbol	Definition
Residual soil	RS	Soil developed on extremely weathered rock; the mass structure and substance fabric are no longer evident; there is a large change in volume but the soil has not been significantly transported.
Extremely weathered rock	XW	Rock is weathered to such an extent that it has 'soil' properties, i.e. it either disintegrates or can be remoulded, in water.
Distinctly weathered rock	DW	Rock strength usually changed by weathering. The rock may be highly discoloured, usually be ironstaining. Porosity may be increased by leaching, or may be decreased due to deposition of weathering products in pores.
Slightly weathered rock	SW	Rock is slightly discoloured but shows little or no change of strength from fresh rock.
Fresh rock	FR	Rock shows no sign of decomposition or staining.

AS1726-1993 and NZGS-2005 use different descriptors for the weathering of rock; a classification compared with a scale. The fundamental difference between these two concepts is that a scale describes the degree of the weathering, but the classification requires the geotechnical professional to choose one category to describe the weathering. It is observed that each publication has listed the terms in opposite orders; AS1726-1993, lists from a residual soil to fresh rock, whereas NZGS-2005 lists the terms from unweathered to residual soil. Nonetheless both publications rely on an understanding of the unweathered state of rock before an accurate assessment can be made.

The understanding of soil-rock boundary interface is an important factor, especially for design implications. The draft revision to AS1726 includes an important change, by incorporating both the HW and MW terms, as many projects rely on distinguishing MW rock, as this is often taken as the level for competent rock for foundation design purposes. NZGS-2005 also outlines that "in very general terms the boundary between a rock mass being more 'rock like' than 'soil like' is the boundary between moderately weathered and highly weathered."

Weathering is an important factor in assessing the geotechnical properties of rock, as it encompasses strength changes, fabric and colour changes. Care should be taken to understand the difference between describing the material weathering and the rock mass weathering. Although it is not detailed in the publications, an understanding of the type of weathering processes that are likely to have occurred on the rock unit and an understanding of the processes that would have occurred to the rock resulting in its current weathered state may both help with the assessment.

2.2 Rock Material Strength

Field strength descriptions are important and necessary to provide a complete representation of the in situ strength of the rock material. Any testing, over and above field descriptions, is only carried out in discrete locations and is not necessarily representative of the rock material strength. Overall in a highly fractured rock the behaviour may be governed by discontinuities (Clayton et al. 1995), but is important that the rock material strength is described and care should be taken not to describe the rock mass strength, which encompasses the strength loss due to discontinuities.

As presented in Table 3, the guidance from NZGS-2005 is to use the terms weak and strong, to describe the rock material strength, as the terms of high or low strength are felt to be indications of the rock mass strength. The field identification indicators use simple techniques to distinguish between the terms which include using your thumb, pocket knife and a geological hammer on the rock core. Strength indicators for unconfined compressive strength (UCS) and point loads are given, however correlations made should be site, rock type and weathering grade specific. These relationships are significant for design implications.

Table 3. Extract from NZGS-2005 (Table 3.5 Rock Strength Terms)

Term	Field Identification of Specimen	Unconfined uniaxial compressive strength q_u (MPa)	Point load strength $I_{s(50)}$ (MPa)
Extremely strong	Can only be chipped with geological hammer	>250	> 10
Very strong	Requires many blows of geological hammer to break it	100 – 250	5 – 10
Strong	Requires more than one blow of geological hammer to fracture it	50 – 100	2 – 5
Moderately strong	Cannot be scraped or peeled with a pocket knife. Can be fractured with single firm blow of geological hammer	20 – 50	1 – 2
Weak	Can be peeled by a pocket knife with difficulty. Shallow indentations made by firm blow with point of geological hammer	5 – 20	< 1
Very weak	Crumbles under firm blows with point of geological hammer. Can be peeled by a pocket knife	1 – 5	
Extremely weak *(also needs additional description in soil terminology)*	Indented by thumb nail or other lesser strength terms used for soils	< 1	
Note: No correlation is implied between q_u and $I_{s(50)}$			

The Australian Standard, AS1726-1993 has based the strength description on a scale and point load correlation, outlined in Table 4. It is suggested that a correlation to point loads should be undertaken to provide more credibility to the field descriptions. Guidance for the field indications includes using hand tests or a knife and a pick on the rock core. The use of a hammer for a sound description when hit should also be used to give an indication of the rock's material strength. As for NZGS-2005, the descriptions relate to the rock material strength and not the rock mass strength.

Table 4. Extract from AS1726-1993 (Table A8 Strength of Rock Material)

Term	Letter symbol	Point load index (MPa) $I_{s(50)}$	Field guide to strength
Extremely low	EL	≤0.03	Easily remoulded by hand to a material with soil properties
Very low	VL	>0.03 ≤0.1	Material crumbles under firm blows with sharp end of pick; can be peeled with knife; too hard to cut a triaxial sample by hand. Pieces ≤ 3cm thick can be broken by finger pressure

Term	Letter symbol	Point load index (MPa) $I_{s(50)}$	Field guide to strength
Low	L	>0.1 ≤0.3	Easily scored with a knife; indentations 1mm to 3mm show in the specimen with firm blows of the pick point; has dull sound under hammer. A piece of core 150mm long 50mm diameter may be broken by hand. Sharp edges of core may be friable and break during handling
Medium	M	>0.3 ≤1.0	Readily scored with a knife; a piece of core 150mm long by 50mm diameter can be broken by hand with difficulty
High	H	>1 ≤3	A piece of core 150mm long by 50mm diameter cannot be broken by hand but can be broken by a pick with a single firm blow; rock rings under hammer
Very high	VH	>3 ≤10	Hand specimen breaks with pick after more than one blow; rock rings under hammer
Extremely high	EH	>10	Specimen requires many blows with geological pick to break through intact material; rock rings under hammer

In the 2016 draft revision of AS1726, the extremely low strength boundary has been removed and the user is advised that any material considered to have less than a 'very low' strength should be described as a soil. It is noted that in NZGS-2005 the boundary between soil and rock is often taken as being between very weak and extremely weak. It is further noted that the British Standard, BS5930-2015, makes use of the terms weak and strong, with similar indicators as those used in NZGS-2005.

Care should be applied when switching between publications, NZGS-2005 and AS1726-1993, as the terms and boundaries used to describe the rock material strength do not align, and there is a difference between the field descriptions for classifying material strength. For example in the two upper strength boundaries for both publications; in NZGS-2005 for the extremely strong boundary, the rock material can only be "chipped at", however in AS1726-1993, for the extremely high strength boundary, the rock material can be broken with "much force". This demonstrates different upper bounds, with NZGS-2005 having a higher strength boundary.

2.3 Defect Discontinuity Spacing

Varying definitions of discontinuity spacing exist depending on the publication, and before making an assessment of this property it is important to understand the assumptions of the definition to be used. NZGS-2005 defines discontinuity spacing as the perpendicular distance between adjacent discontinuities. The terms used by the New Zealand guidelines to group spacing sets are outlined in Table 5. In cases where there are a number of parallel discontinuities it is the expectation that these are grouped into sets. It should be noted that there are other terms to describe bedding spacing, which has not been discussed in this paper.

Table 5. Extract from NZGS-2005 (Table 3.7 Spacing of Defects or Discontinuities)

Term	Spacing
Very widely spaced	>2m
Widely spaced	600mm – 2m
Moderately widely spaced	200mm – 600mm
Closely spaced	60mm – 200mm
Very closely spaced	20mm – 60mm
Extremely closely spaced	<20mm

The Australian Standard, AS1726-1993 does not present such a table with spacing terms, and advises against the use of descriptive terms. The definition that AS1726-1993 gives to describe discontinuity spacing is simply the 'spacing of defects', without advice of where this measurement should be taken from. It suggests that sets may be grouped, but does not give any clear advice on how to do so or how to determine the appropriate spacing boundary. AS1726-1993 also advises to use other indirect indicators for discontinuity spacing, such as rock quality designation (RQD). Caution is also advised in this standard, indicating that boreholes only provide one dimensional data on spacing.

In the 2016 draft revision for AS1726 the guidance has changed from the previous version to indicate that the measurements of discontinuity spacing are to be made perpendicular to the joint set and a suggestion is made that these spacing's can be grouped into appropriate numerical categories, but leaves it to the engineer or geologist to decide what grouping is appropriate for the project requirements.

It is presumed that AS1726-1993 recommends against the use of subjective descriptive terms, as geotechnical professionals can have different perceptions of what might constitute 'widely spaced' over other terms. As a comparison, the British Standard, BS5930-2015, has also chosen, like NZGS-2005, to use descriptive terms from '*extremely closely'* up to '*extremely widely'* spaced. There is also some important advice in BS5930-2015, which aligns with the caution given in AS1726-1993; that consideration of the distribution of discontinuities in three-dimensions should be made, which cannot be interpreted from a cored rock sample.

Discontinuity spacing is a measure of the degree of fracturing of a rock mass (Clayton et al.1995). Different descriptive terms have been developed in the context of different codes of practice, with varying emphasis and boundary definitions for the grouping of discontinuity spacing into sets. Regardless of the country, in all cases the investigation purpose should be understood and the use of discontinuity spacing for engineering purposes appreciated to allow a judgement to be made by the geotechnical professional as to the most appropriate way to communicate the discontinuity spacing as well as the level of detail required.

3 CONCLUSION

There are many aspects of field logging, both of soil and rock, which have not been covered in this paper, which would equally benefit from a close assessment. However, as demonstrated in this paper, switching between the Australian Standard and New Zealand Guidelines, requires careful consideration of all aspects, and may require geotechnical professionals to reconsider their interpretation of geological conditions to ensure records conform to the relevant standard or guideline.

With regard to the descriptions of rock weathering, rock material strength and defect discontinuity spacing, there are some differences between the publications which must be understood before commencing field logging. These differences are of particular importance when field descriptions are used as a basis for design, as misunderstandings would introduce margins of error in the interpretation. It is important to understand what is to be described; characteristic from the rock mass or rock material. It is always advised, when possible, to see the rock in its unweathered state to ensure a more accurate reflection of the weathered state. Whichever standard or publication the geotechnical professional is logging to, the professional must be consistent in their logging style and manner to avoid any confusion or misinterpretation, remembering that the data presented is a key input into associated designs. When the geotechnical professional is using a standard or guideline that they are not familiar with they should ensure they consider the publication carefully and not have a bias towards their more accustomed standard or guidelines. They should also use their professional judgment as to the level of detail required for the design.

4 ACKNOWLEDGEMENTS

I would like to acknowledge my colleagues from Jacobs who I have both worked with in New Zealand and Australia for sharing their advanced geotechnical and geological knowledge with me.

REFERENCES

AS1726-1993: *Geotechnical Site Investigation*, Australian Standard.

AS1726-2016 (DRAFT): *Geotechnical Site Investigation, (19th February 2016), Draft for Public Comment*, Australian Standard", (Revision of AS1726-1993).

New Zealand Geotechnical Society, (December 2005), *Field Description of Soil and Rock: Guideline for the field classification and description of soil and rock for engineering purposes*.

Clayton, C.R.I., Matthews, M.C. and Simons, N.E., (1995). *Site Investigation*, Department of Civil Engineering, University of Surrey, 2nd Edition.

BS5930-2015: *Code of Practice for Site Investigation,* British Standard.

Blyth, F.G.H. and de Freitas M.H. (1984). *Geology for Engineers*, 7th Edition.

Proceedings of the 11th ANZ Young Geotechnical Professionals Conference – 11YGPC
Queenstown, New Zealand
25 – 28 October 2016

Sydney Metro site investigation for the Sydney Harbour tunnel crossing

N. J. C. Byrne[1], and D. J. Och[1,2].

[1]WSP|Parsons Brinckerhoff, Level 27, Ernst & Young Centre, 680 George Street, Sydney NSW 2000, Australia; PH +61 2 92725310; email: NByrne@pb.com.au
[2]School of Biological, Earth and Environmental Sciences, University of New South Wales, Australia email: DOch@pb.com.au

ABSTRACT

Sydney Metro is Australia's biggest public transport project. Stage 2 of the program, the Sydney Metro City & Southwest project, will extend metro rail from Sydney's North West, under Sydney Harbour, through new underground CBD stations and beyond to the South West. A critical element of this project is tunnelling beneath Sydney Harbour. At the commencement of the concept design development, very little geophysical, geological and geotechnical information was available that covered the area of interest in Sydney Harbour. The harbour geology was therefore identified as a critical design risk, and geological information was urgently required to inform the tunnel and track alignment designs. The metro alignment and tunnelling approach were progressively refined during the site investigation stages, as the geological model was developed. This paper summarises the site investigation stages (desktop analysis, geophysical testing, cone penetration testing and boreholes with HQ coring) and describes the implications for the design development of both the tunnel alignment and metro stations, as the harbour geological model was established and refined. It highlights the importance of good coordination between all design disciplines and the geotechnical team during the site investigation process, to ensure that both the site investigation is adequate for the design and that the design can capture and guide the site investigation.

Keywords: Sydney Harbour, site investigation, geophysics, paleovalley

1 INTRODUCTION

The Sydney Metro City & Southwest will consist of two 15.5 km rail tunnels running from Chatswood to Sydenham. At the commencement of the Scoping Design phase for Sydney Metro City & Southwest, it was anticipated that the tunnels would be driven through rock using tunnel boring machines. A critical element of this project is the Sydney Harbour crossing, between Blues Point, on the North Shore and Walsh Bay at the north of the Sydney CBD (Figure 1).



Figure 1. Location plans: City section of Sydney Metro tunnel alignment & harbour crossing alignment between Barangaroo North and Blues Point.

Parsons Brinckerhoff and Aecom formed a design joint venture (PBAJV) and were engaged as the technical advisors for Transport for New South Wales (TfNSW) on the Sydney Metro City & Southwest project in 2014. The objective was to develop a Scoping, Definition and finally a Reference Design for the Sydney Metro City & Southwest, connecting to Sydney Metro Northwest at Chatswood

At the commencement of the Scoping Design, the Desktop Study highlighted a lack in previous geotechnical data that covered this part of Sydney Harbour, and therefore identified the need for a phased geotechnical investigation to adequately inform the Sydney Metro Design. One stage of geophysical testing and one stage of over water borehole drilling was planned for the harbour area in order to develop a geological model to inform the scoping/reference design.

This paper presents the development of the geological model for the tunnel alignment beneath Sydney Harbour as additional geotechnical investigation stages were performed. A series of potential alignments were investigated that attempted to take best advantage of the sea bed and bedrock profiles in order to minimise the depth of the running tunnel alignment level, to ensure that the station platforms could be located as shallow as possible. This paper reflects on how the progressive site investigation results allowed continued refinement of the geological model, and how the tunnel alignment design was refined to accommodate the development of the geological model. Furthermore it discusses how continual design re-assessments and constant communication between the geotechnical and track/tunnel design teams was required during the site investigation to relocate and refine borehole test locations to ensure an adequate site classification was achieved.

2 STAGES OF SITE INVESTIGATION AND DESIGN IMPLICATIONS

2.1 Scoping design stage

A key design objective for the project was to minimise the station platform depths below street level as the depth of platform impacts on the total passenger travel time from street to platform. A general principal for the station design was that a concourse level deeper than 35 to 40 metres below street level would reduce ease of use of the station for the customer.

An existing design constraint that influenced the station depth at Victoria Cross Station (North Sydney) was the rapid topography level change between Sydney Harbour and North Sydney (Figure 2), rising approximately 70 to 80 metres above sea level at North Sydney. The metro trains are designed to operate at a maximum gradient of 4.5%, which limited the vertical change that could be achieved over a specific length of track, (note that in comparison Sydney Trains rolling stock are typically limited to an ultimate maximum gradient of 3.3%).

As the preferred location for Victoria Cross Station had been identified, and the distance between the tunnel's inflection point (deepest point) beneath the harbour and the Victoria Cross station was fixed (approximately 2.5 km), the tunnel's deepest point beneath the harbour would directly impact on the Victoria Cross Station depth, as depicted in Figure 2.

The following criteria governed the vertical alignment for the Sydney Metro tunnels:

- A maximum grade of 4.5% on straight track and compensated horizontal curvature (i.e. flatter grade for a tighter horizontal curve).
- Minimum total cover above tunnel crown (rock + sediments) of 1.5 tunnel diameters (i.e. 11.0 m).
- Minimum rock cover above crown of 1.0m.
- 7.0 m diameter tunnel with tunnel crown 5.5 m above rail level.

The initial design study that assessed the harbour crossing, had a direct route from Martin Place Station to Victoria Cross Station, and was based on an initial geophysical survey of Sydney Harbour by Lean (1973) which was refined by Harris et al. (2001). It also referenced sections that profiled areas in Sydney Harbour in the Sydney 1:100,000 scale Geological Sheet Explanatory Notes of Herbert (1983).

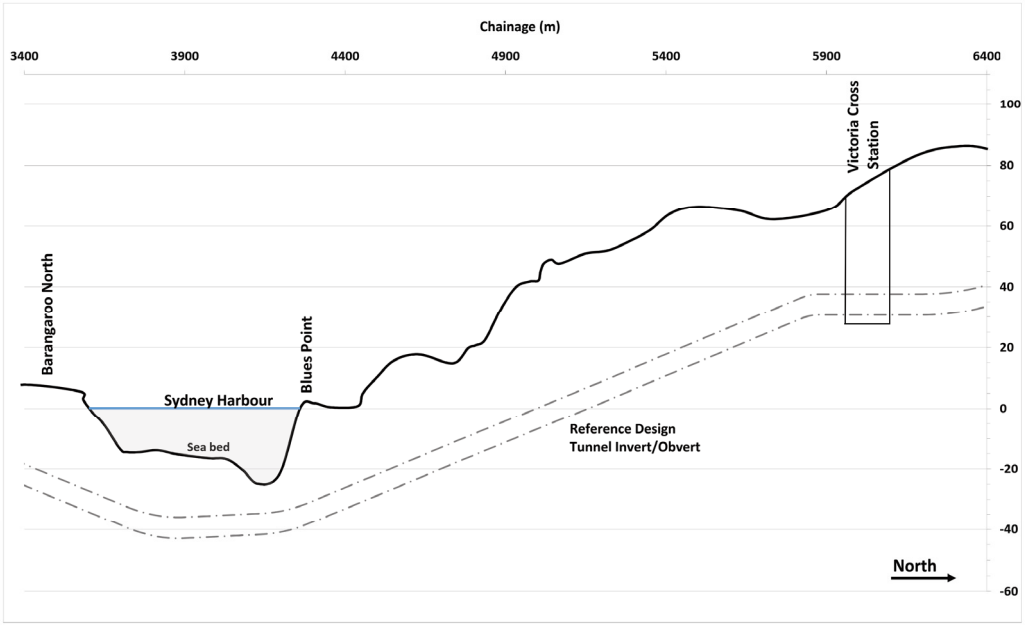


Figure 2. Section between Barangaroo and North Sydney which shows the substantial ground level change between Sydney Harbour and the Victoria Cross Station (North Sydney).

A top of rock contour model was developed from the Lean (1973) information and geological long sections were cut from this model. These sections were used to develop an early version of the Scoping Design tunnel vertical alignment. The deepest rock level, along the proposed alignment, inferred from the Lean (1973) data was approximately RL -34.5m AHD. The tunnel alignment which maintained the required rock cover resulted in the Victoria Cross Station platform level being located some 35 metres below street level.

During the Scoping Design in 2014, the Sydney Metro design technical advisor coordinated a project specific geophysical investigation to refine the available geophysical information. This geophysical survey covered an extended zone reaching from the Sydney Harbour Bridge in the east, to Goat Island in the west. The large area was surveyed to allow for the assessment of multiple alignment options to find the most suitable tunnel alignment.

The initial geophysical survey included:

- Echo sounding/bathymetric survey to provide a map of sea bed levels, and to provide accurate sea bed levels for the seismic survey results
- Side scan sonar survey to map sea bed features
- Marine magnetometer survey to locate ferrous objects over the investigation area and to attempt to delineate geological features such as faults or dykes
- Seismic reflection profiling survey to map subsurface layers across the site to assess geological conditions, in particular the depth to top of rock, and allow spatial coverage to produce a bedrock contour plan
- Seismic refraction survey focused on Scoping Design alignment to map the subsurface seismic velocity distribution to confirm the depth to rock and identify any significant variations in seismic velocity to at least 20 m below top of rock.

The geophysical investigation defined the palaeogeographical rock surface (2014 inferred rock level) and identified the existence of a NW to SE trending palaeovalley crossing the scoping design alignment approximately 11 metres deeper than indicated by the earlier geophysical data. Thus, in order to maintain the 7 metre rock cover for the tunnel crown, as required by the design criteria, the Scoping Design vertical alignment would have to be lowered by 11 metres. The Victoria Cross platform level would have to be lowered by a similar amount.

The project team was encouraged to investigate alignments that would maximise customer outcomes and reduce the depth of the station platform depth approximately 45 m below street level back to the target station depth.

In an attempt to restore the Victoria Cross station depth to the original design level, the geotechnical and track design teams investigated approximately 12 different tunnel alignments based on the revised palaeogeographical rock profile yielded by the geophysical investigation. An additional station at Barangaroo was also included in the project at this stage and hence the tunnel alignment was adjusted to incorporate this new station.

An alignment option slightly further west than the Scoping Design alignment focused on an inferred palaeogeographical rock surface which was approximately 2 m shallower than along the original alignment. Other tunnel alignment changes were also incorporated to reduce the Victoria Cross station depth which included increasing the tunnel length with a sweeping curve north of the harbour and moving the Victoria Cross station 150 metres north. The adoption of these opportunities and focusing on the alignment option with shallower rock allowed the platform depth at Victoria Cross to be lifted to approximately 40 m below street level.

2.2 Definition design geotechnical investigation

Following the Scoping Design, the Sydney Metro design team began the Definition Design and coordinated the development of a geotechnical investigation which included a suite of marine borehole investigations, which were commenced in April 2015. The marine investigation incorporated the revised tunnel alignment and the borehole locations were planned to target geophysical refraction velocity anomalies observed in the inferred rock contours.

The initial boreholes close to the shore on both the southern and the northern side of the harbour crossing correlated well with the geophysical investigation, with encountered rock levels very closely matching the rock levels predicted from the geophysical investigation. Surprisingly some of the boreholes located in the area of the identified palaeovalley encountered rock substantially deeper than anticipated from the geophysical model.

The boreholes encountered rock between 5 and 10 metres deeper than inferred on the geophysical interpreted palaeogeographical surface. The results led to the postulation that an incised valley existed within the palaeovalley perpendicular to the design alignment, which accounted for the substantial rock depth change observed. Such a structure was comparable to upstream valleys formed within Hawkesbury Sandstone rock materials that are currently visible across the Sydney region today.

Due to the unexpected borehole results, regular discussions between the site investigation and geotechnical design teams were required. As each borehole result became available, the information was incorporated by the geotechnical design team into the developing geotechnical model. Each additional result was used to inform and refine the selection of the remaining test locations to ensure a thorough and optimised site investigation was completed.

As a result of rock levels encountered in the marine boreholes being deeper than inferred in the geophysical palaeogeographical surface, an additional geophysical seismic reflection survey was carried out in May 2015 and focused on characterising the region of the deeper palaeovalley along the new alignment. The results of this geophysical survey is shown in Figure 3.

The borehole and additional geophysical investigation identified that the palaeovalley contains a deeper incised valley approximately 20 m wide and an additional 10 m deeper than anticipated. The identification of this incised rock valley lowered the minimum level of the geological rock profile an additional 10 m from the Scoping Design rock level assumptions, totalling approximately 21 m reduction from the initial rock level assumption. To comply with the design criteria of maintaining a one tunnel diameter rock cover above the tunnel crown, such results would mean that the tunnel would have to be lowered a further 10 metres. Consequently the Victoria Cross Station would further deepen to approximately 50 metres below street level.

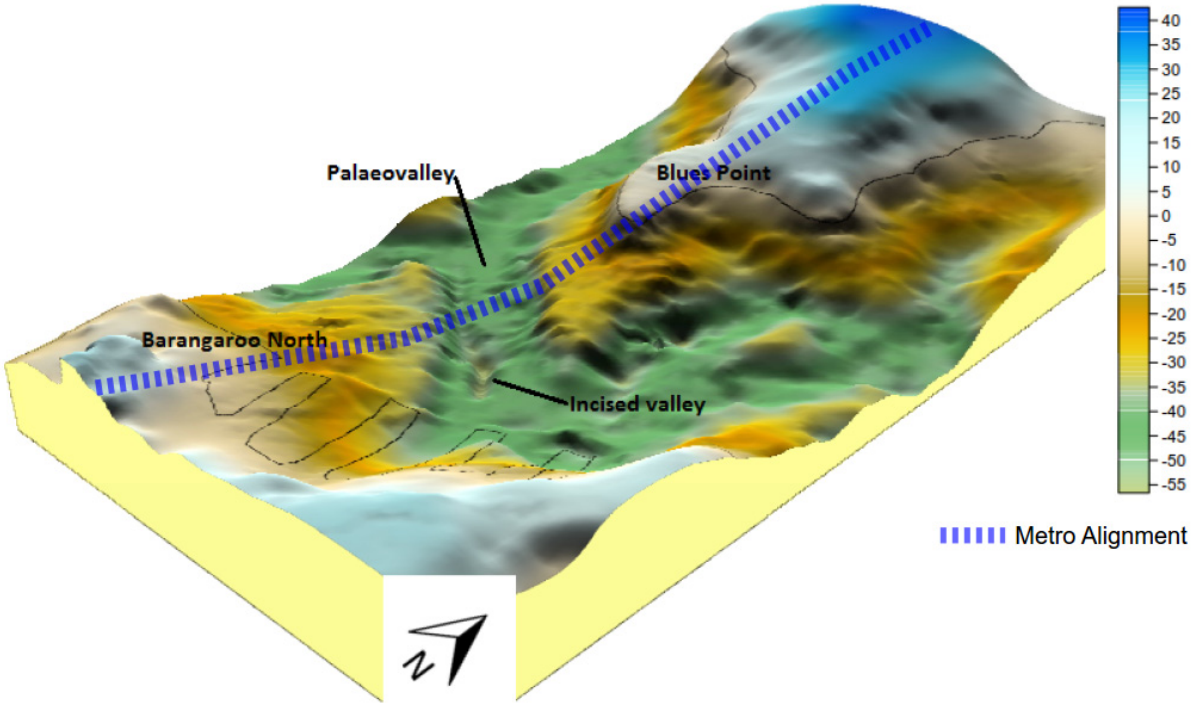


Figure 3. This 3D projection illustrates the palaeogeographical surface (top of rock) that defines the palaeovalley between Barangaroo North and Blues Point.

Discussion with the architectural and product teams concluded that a station at this depth could potentially reduce ease of use of the station for the customer and that alternative vertical alignments should be considered.

Due to the deeply incised palaeovalley crossing the proposed tunnel alignment, it was proposed that instead of lowering the tunnel alignment to keep the tunnel within rock, a tunnel alignment that passed through the soils that had infilled the palaeovalley be adopted. An alignment through soil, would introduce new tunnelling risks such as the potential need for cutter head interventions (manual replacement of drill bits) during the transition between rock and soil, and tunnelling through soil materials where tunnel blow-outs (tunnel boring machine pressure balance failures) could occur. However, it was agreed that the provision of such an alignment which would result in an ideal Victoria Cross Station depth, and thereby greatly improve the product outcome for the commuter.

To inform the tunnel design and help quantify the risks associated with construction through the soil materials, additional geotechnical investigations were performed to refine the geological model for the harbour sediments. A third seismic refraction investigation was performed along the preferred alignment and Cone Penetration Tests (CPTs) and Denison Sampler coring were also performed.

With reference to the refined geotechnical model, the tunnel alignment was adjusted to be aligned roughly perpendicular to the main axis of the palaeovalley. This minimised the distance the tunnels would be required to be bored through both soils and mixed face consitions (where the top portion of the cutter head is in soil and the bottom portion is cutting through rock).

At the completion of the harbour crossing site investigation program: 22 boreholes, 30 CPTs, 1 cross hole seismic survey, and 3 rounds of geophysical testing had been performed. The finalised tunnel alignment proposed for the project's Reference Design contained approximately 150 metres portion of tunnel through harbour sediments and located the Victoria Cross station approximately 30 metres below the entrance street level. Figure 4 presents a long section through the Sydney Harbour crossing, and details the inferred palaeogeographical profile interpreted at the various stages of the design / site investigation.

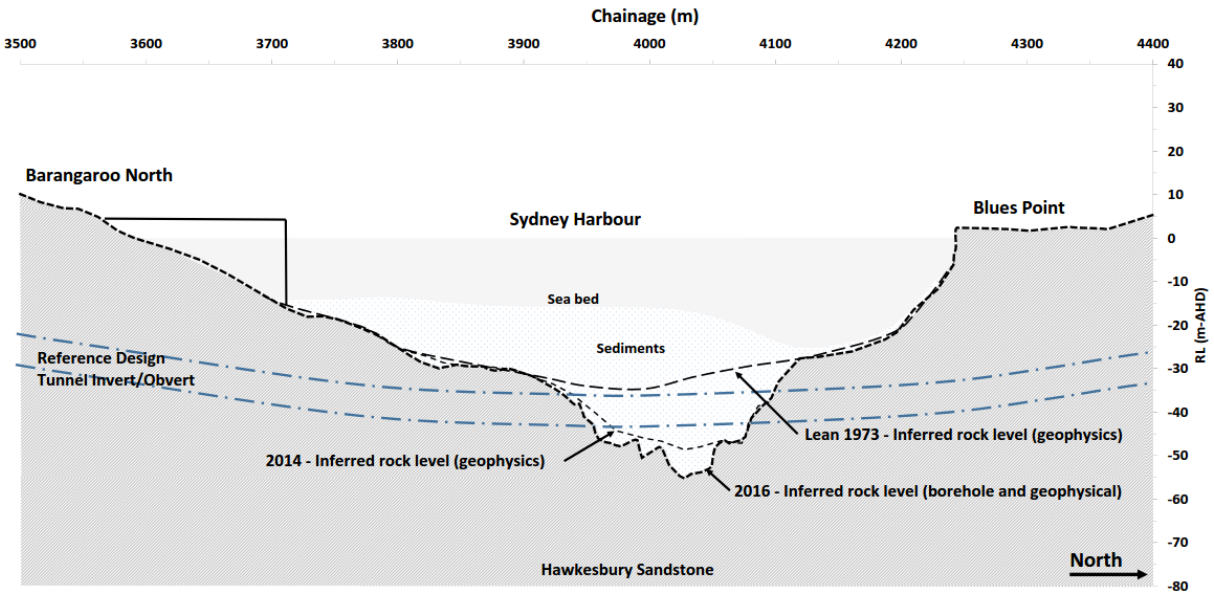


Figure 4. Geological section through Sydney Harbour, showing the inferred top of rock profile based on the initial information (Lean 1973), the 2014 geophysical investigation and the 2016 geotechnical investigation results.

3 CONCLUSION

This paper has summarised the steps taken during the site investigation for the Sydney Harbour crossing of the Sydney Metro City & Southwest project. Multiple stages of alignment redesign were performed as the geological model was developed. The close interactions between the track design, tunnel design and geotechnical teams ensured that the site investigation was able to prepare a geological model suitable for the tunnel alignment and tunnel structural design. The geological section was constantly revised upon receipt of each additional borehole log, and was used to inform the design teams and alter the locations of the remaining site investigations. The design teams worked closely together sharing draft sections and models to speed up design assessment and ensure the site investigation program was not delayed.

This paper has demonstrated the value of communication and interaction between the site investigation team, the geotechnical design team and the project design teams, so that impacts of an evolving geological profile can be appropriately assessed and addressed. This communication and interaction identified the likely negative outcome of a deep station and instigated the change to a construction method to allow for a tunnel alignment through both rock and soils.

Finally it is noted that the site investigation during this program was more extensive than originally planned. However the comprehensive geological model prepared from the site investigation is expected to greatly reduce the construction risks for the tunneling contractor.

4 ACKNOWLEDGEMENTS

The author wishes to thank TfNSW/Sydney Metro for permission to produce this technical paper. The authors also wish to thank Bill Luders, Antoni Kuras, Nagen Loganathan, Sven Thorin and Geoff Bateman from the Sydney Metro project for their assistance with the preparation of this paper.

REFERENCES

Lean, J. (1973). *Marine Investigation in Port Jackson*. Geological Survey of NSW, GS1973/059

Harris G. A., Vrbancich, J., Keene, J. and Lean, J. (2001). "Interpretation of Bedrock topography within the Port Jackson (Sydney Harbour) Region using Marine Seismic Reflection", *ASEG 15th Geophysical Conference and Exhibition*, Brisbane (DSTO 2001)

Herbert, C. (1983). Sydney 1:100,000 scale Geological Sheet 9130, 1st Edition

Proceedings of the 11th ANZ Young Geotechnical Professionals Conference – 11YGPC
Queenstown, New Zealand
25 – 28 October 2016

Geotechnical design challenges associated with construction of the new AMCOR paper mill in Botany, NSW

T. G. Cuniowski[1], B.E. (Hons), Dip. Eng. Prac., MIEAust CPEng

[1]Golder Associates, 124 Pacific Highway, Greenwich NSW 2065 Australia, PH 0412 293 734, email: tcuniowski@golder.com

ABSTRACT

The new Amcor B9 paper mill in Botany, NSW, involved the design and construction of pile and slab foundations, temporary and permanent retaining structures, deep excavations, dewatering and ground improvement. There were numerous technical and design challenges, including tight settlement tolerances, significant cyclic loads, adjacent heritage structures and uncontrolled fill material. Construction staging meant that settlement sensitive infrastructure was constructed simultaneously with and adjacent to dewatering, excavation and dynamic ground improvement activities. Geotechnical design included the derivation of realistic and workable soil parameters from a combination of laboratory testing and *insitu* soil testing. Analysis and design was carried out using a combination of empirical calculations, slope stability, settlement and finite element software, while movement monitoring was carried out to compare predicted and actual displacements.

Keywords: piles, displacements, ground improvement, monitoring, dewatering, excavations

1 PROJECT AND GEOLOGICAL SETTING AND DERIVATION OF SOIL PARAMETERS

The project involved the construction of the largest recycled paper machine in Australia. The paper machine is 330 m long, 22 m high, and capable of producing 1.6 km of paper per minute. Construction commenced in early 2011 and new paper mill officially opened in early 2013. The early works contract was awarded to Baulderstone Construction Pty. Ltd. (now part of Lend Lease Corp. Ltd.), with the D&C contract awarded to a consortium headed by Leighton Contractors Pty. Ltd. (now CPB Contractors Pty. Ltd.), which included Golder Associates Pty. Ltd. as the geotechnical designer.

The site was underlain by uncontrolled fill materials, overlying quaternary deposits, overlying bedrock, further outlined in Table 1. Due to the depositional nature of the marine materials, and the uncontrolled nature of the fill materials, the ground profile was variable and presented significant foundation engineering challenges. This risk was managed through the use of deep foundations and ground improvement, as discussed further in this paper.

Table 1. Stratigraphic units

Unit	Depth (m)[a]	Description
1 – Uncontrolled fill	1 to 4	Construction rubble, pulped paper, excavated natural materials, including infilled ponds and old waste storage areas.
2 – Botany Basin sediments[b]	25 to 35	Fine to medium grained, loose to very dense sand and silty sand (strength generally increasing with depth), with occasional peat, clay, silt and cemented zones
3 – Bedrock	N/A	Generally sandstone, with laminate and siltstone zones

[a] Approximate depth below existing surface level to base of unit.
[b] Quaternary age deposits overlying bedrock, which can comprise up to four sub-layers; marine/estuarine/aeolian sands with clay and peat lenses, overlying aeolian sands, overlying estuarine/fluvial sands and clays, overlying marine/estuarine/fluvial/aeolian sands, clays and gravels (Hatley 2004).

The derivation of suitable soil parameters for these geological units, and their sub-units, was critical for the project, to ensure safe yet economic design. Parameters were derived from the results of geotechnical test investigation data and laboratory testing, carried out during preliminary investigations prior to detailed design. For critical construction activities, additional investigations, where possible through fill, were carried out to enable design efficiencies to be realised.

2 PAPER MACHINE

The operation of the paper machine produces high frequency and varied cyclic forces. Ongoing operation of the paper machine requires a stable foundation, as small differential settlements could result in poor paper production. This resulted in the requirement for strict settlement (<6 mm settlement) and differential settlement tolerances (<0.5 mm/m between adjacent foundations). Pile foundations were chosen to provide the necessary settlement control for the paper machine.

2.1 Pile design

The paper mill machine and associated housing facility, was constructed on impact driven 350 mm square segmental precast concrete piles. This type of foundation was chosen so that pile structural strength could be controlled and standardised. Geotechnical design required piles to be driven specific depths below ground surface level and achieve prescribed blow count/penetration ratios. In addition, the pile design had to be checked to ensure that the vibration frequency of the paper machine did not match the internal dynamic frequency of the piles, which could lead to spalling, cracking, reduced pile capacity and ultimately, foundation failure. Penetration depths were generally between 9 and 12 m.

2.2 Pile testing

All piles were impact driven under the supervision of a geotechnical engineer, to record blow counts and make recommendations for further driving or pile testing. This method of installation allows for checking that the pile bearing capacity is achieved through the correlation of blow counts and penetration. In addition, the following pile tests were carried out:

- Static load test (one pile from critical pile group tested)
- Dynamic load tests with CAPWAP signal matching (approximately 50% of piles)
- Re-strike tests (minimum one pile per pile group)

This testing regime allowed for an increase of the geotechnical strength reduction factor (Φ_g) from 0.54 to 0.70, in accordance with AS2159-2009, resulting in significant construction cost savings. The results of static load test recorded 6 mm settlement under 2000 kN loading (approximately double the ULS design load), indicating settlement limits should not be exceeded during paper machine operation. It is noted that the results, analysis and conclusions from these tests are not the purpose of this paper.

3 REJECTS SUMP PIT

A rejects sump pit was constructed after the piled foundations had been installed and construction of the main housing facility had commenced. The purpose of this pit was to allow temporary storage and dry out of reject pulp material from paper production.



Figure 1. Rejects sump pit construction

3.1 Effect of excavation on adjacent pile cap

The rejects sump pit was a 3 m deep excavation carried out a horizontal distance of 0.5 m from a pile and pile cap at the eastern end of the housing facility. A finite element model using 2D-PLAXIS software was created to simulate the construction sequence to obtain movement predictions. To confirm local soil stiffness, multiple dynamic cone penetrometers were carried out at the location of the excavation.

Once the model was created, it was used to assess movement effects of various sheet pile types with various embedment depths, in order to find the most cost effective sheetpile system, to control displacements at adjacent pile cap during subsequent excavation. Figure 2 showed that 7 m long, GU7N-D sheetpiles, with 3.5 m embedment below excavation, would result horizontal displacement at the top of sheetpile between 22 and 24 mm. Modelling showed maximum horizontal and vertical pile cap movements of 10 mm and 1 mm, which were within structural and serviceability tolerances.

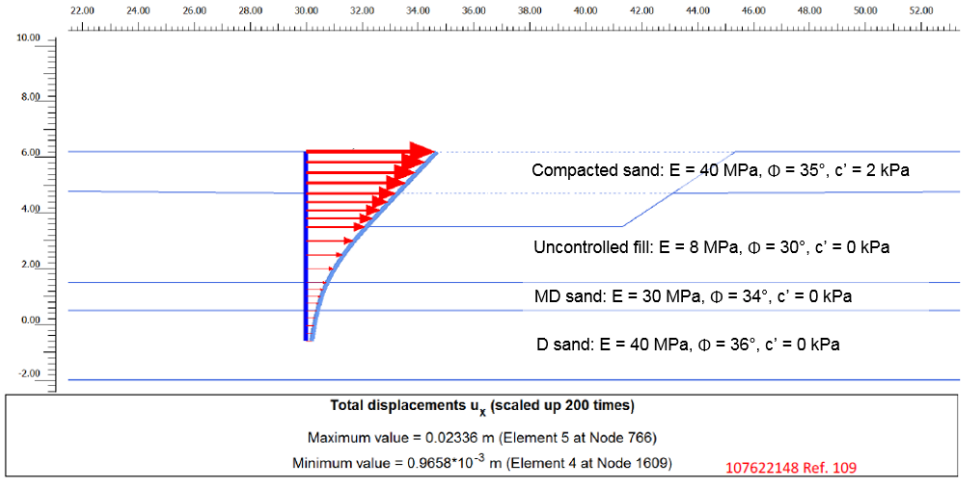


Figure 2. PLAXIS predicted movement of sheetpile

3.2 Monitoring and construction considerations

It was also recommended that the vibrations during construction should not exceed a Peak Particle Velocity of 20 mm/sec, to reduce the likelihood and proliferation of vibration induced densification of the sand and subsequent settlement below the housing facility (Gaba et al. 2003). Vibration and displacement monitoring devices were installed on the existing housing facility before sheetpile installation. Displacement monitoring was installed on the sheetpiles after installation and before excavation commenced. Displacements from the excavation are summarised in Table 2. The good match between predicted and recorded shows again the importance of realistic soil parameter derivation, to reduce the construction costs associated with overly conservative design.

Table 2. Displacement monitoring during rejects sump pit excavation

Survey mark location	Predicted (mm)	Recorded (mm)
Housing facility (average, horizontal)	3-5	2-3
Top of sheetpile wall (horizontal)	22-24	17-19

4 TEMPORARY DEWATERING

Temporary dewatering, required for the construction of three underground storage tanks, was carried out after piled foundations had been installed and construction of the main housing facility had commenced. These tanks were to temporarily store excess stormwater captured on site during high rainfall events, to reduce the impact on the surrounding stormwater system. It was necessary to assess the effects that dewatering activities would have on the recently constructed and existing infrastructure.

4.1 Effects on piles, local infrastructure and heritage structures

The location of the stormwater tanks were close to settlement sensitive infrastructure, services, heritage structures and critically, the recently installed piles of the housing facility. A finite element model using 2D-PLAXIS software was created to simulate the effect of dewatering and excavation activities. From this model, horizontal proliferation of water draw-down could be modelled, and induced settlement predicted. A series of groundwater monitoring wells and survey marks were installed, with trigger levels set up, so to monitor the effects of dewatering, as shown in Table 3 and Figure 3.

4.2 Effects of cohesive lenses and rainfall

A CPT was carried out at the location of each stormwater tank, identifying occasional clay and peat lenses within the silty-sands at each location. From this, the natural sand unit was modelled with a lower hydraulic conductivity value, and isolated bands of clay and peat were included in the model. Without reducing the hydraulic conductivity of the sand unit or modelling cohesive zones, the predicted groundwater drawdown and associated settlement were assessed to be close to allowable limits of surrounding infrastructure.

Table 3. Vertical settlement during dewatering

Survey mark location	Predicted (mm)	Recorded (mm)
Heritage structure	5	<3
Paper machine housing facility	5-7	<2
Local infrastructure and utilities	5-10	<8

This modelling methodology produced reduced groundwater drawdown adjacent to the dewatering site. Results from movement monitoring (refer Table 3) justified this assumption as predicted settlements were not exceeded. Figure 3 shows that even with the reduced conductivity and influence of cohesive zones modelled, the recorded groundwater drawdown was still less than predicted. It also shows that rainfall events resulted in groundwater recharge. The proximity to the ocean and associated tidal movements are likely to have also increased groundwater recharge rates (Somerville 2005).

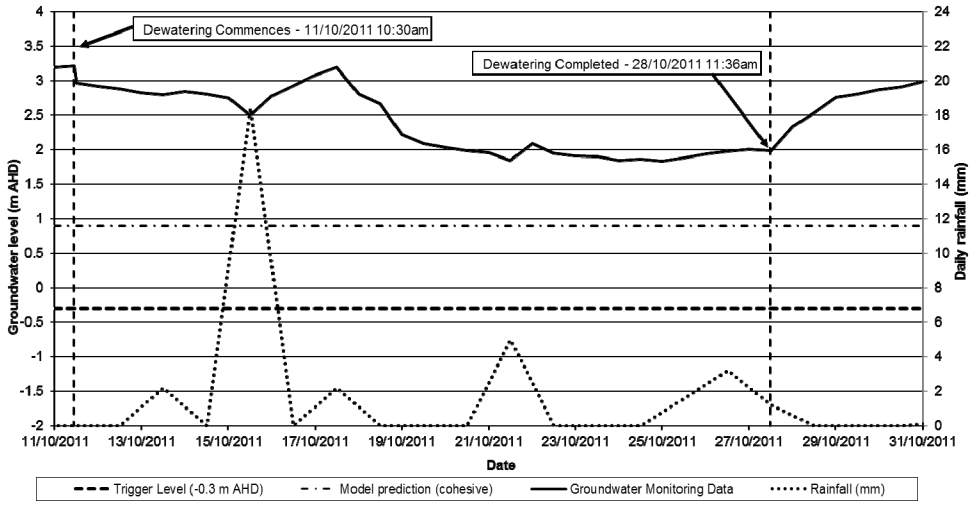


Figure 3. Groundwater drawdown during dewatering

4.3 Construction notes

Initially, geotechnical input was not requested for dewatering design and structural design of temporary shoring. However, during the initial dewatering and excavation activity, localised liquefaction was occurring at the base of excavation. Geotechnical assessments of the as-constructed excavation concluded that there were inadequate spacing of spearpoints and capacity of groundwater pumping system. In addition, the geotechnical assessment indicated that there was insufficient strutting and bracing of temporary shoring. It was therefore recommended to the client to increase the

number of spearpoints, the capacity of the pumping system, and the number and capacity of struts/bracing.

This resulted in construction delays, and could have been avoided if geotechnical input was requested during excavation and dewatering planning.

5 STORAGE FACILITY

The paper and equipment storage building, located immediately north of the paper mill machine, was not subjected to the same high, cyclic and dynamic loads as the paper mill. The main design loads were dead loads, associated with the storage of paper rolls (weighing up to 47 tonnes) and equipment. Although not as stringent as the paper mill building, settlement (<15 mm settlement) and differential settlement tolerances (<1 mm/m between adjacent and orthogonal foundations) were still strict. Shallow foundations following ground improvement was chosen for the storage facility building.

5.1 High energy impact compaction (HEIC)

Based on preliminary geotechnical investigation data available during tender and detailed design, it was inferred that uncontrolled fill consisted predominantly of granular materials, including sands, gravels and construction rubble. Investigation data also indicated that fill material within the footprint of the storage facility extended to depths of about 2.5 m. HEIC was therefore the preferred method to improve the subsurface materials in this area, as this was deemed to be the most cost effective option.

During HEIC, there was a localised area at the southern section of the storage facility where the HEIC results were not satisfactory. Subsequent proof rolling of the area confirmed inadequate compaction of the subsurface materials. Further investigation was recommended, with CPTs and GPR carried out to define and delineate the substandard subsurface materials.

5.2 Preload

From the results of CPTs and GPR, numerous isolated and one extensive unsatisfactory layer, inferred to be either cohesive materials or old pulped paper, were identified. It was therefore recommended that a 3 m high preload be constructed on site, with monitoring plates installed to monitor and assess vertical displacement. Preload was constructed in two stages; an initial 1.3 m high preload in place for 5 weeks, and full height (3 m) preload in place for 5 weeks. Figure 4 shows the predicted vs recorded settlement at the centre of preload, showing a good correlation. Preload was removed after 12 September.

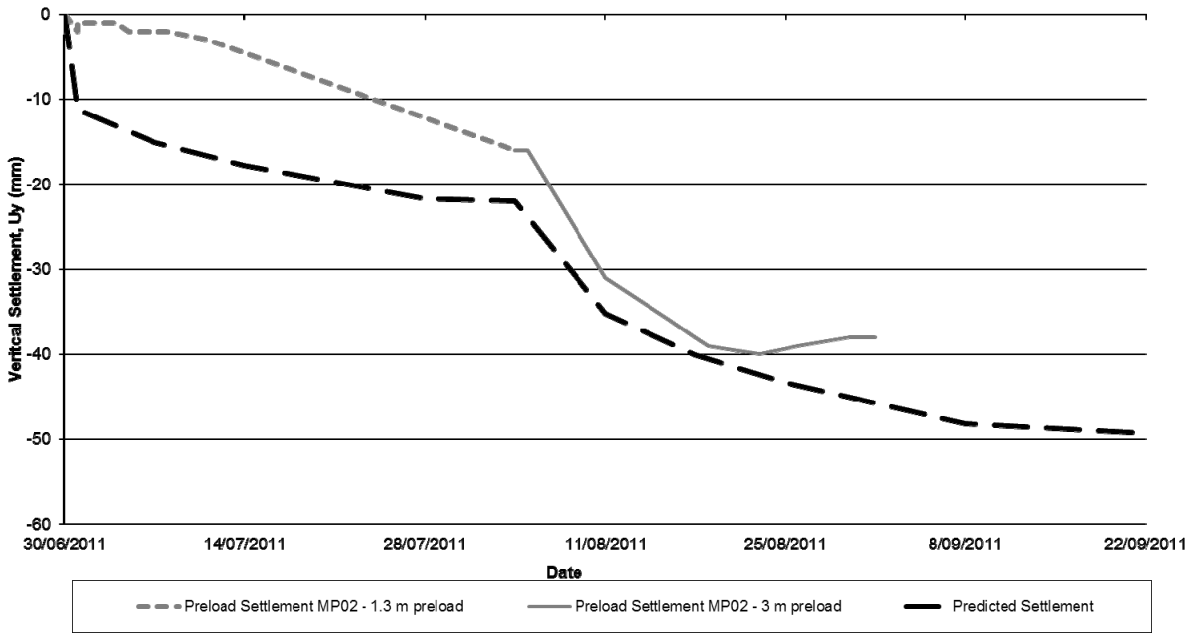


Figure 4. Settlement monitoring results from preload

The settlement data shown in Figure 4 indicate that the unsatisfactory layers were likely reworked cohesive material, not pulped paper. Settlement behaviour of pulped paper would mimic very soft and soft clays, with a high coefficient of secondary consolidation (0.03 to 0.06). This is due to pulped paper not only undergoing primary and secondary consolidation, but also degradation (or decomposition), which is time dependant. The graph indicates predominantly immediate settlement and primary consolidation, indicating well drained and thin cohesive materials. The small settlement under 1.3 m preload indicates the material was likely a reworked, firm to stiff clay, with a preconsolidation pressure of approximately 25 kPa.

5.3 Lessons learnt

During tender and detailed design, limited investigation data was available. An additional investigation was not carried out, due to the assumption of the homogeneous nature of fill materials in this area. Supplementary investigations in this area at pre-construction stage would have allowed for a better strategy for ground improvements in this area, reducing construction costs. However, D&C contracts are often structured with milestone payments and funds released only after certain construction activities are complete, meaning approval of funds for preliminary activities is often hard to justify.

6 MULTIPLE CONSTRUCTION ACTIVITIES

This project highlights some of the challenges associated with multiple construction activities occurring simultaneously on a reasonably small construction site. Early engagement with clients, as well as geotechnical input to construction staging, is critical. Construction staging is often decided through a critical path strategy, with critical activities and paths decided logistically and with contractual requirements.

It is necessary therefore, as geotechnical consultants, to ensure that construction staging allows for consideration of the effects certain activities will have on ground conditions, which may affect the long term performance and serviceability of built infrastructure. However, as this is not often the case, as geotechnical consultants, it is necessary to be able to propose construction methods that will reduce these potential impacts.

7 CONCLUSION

This project highlights the importance of three things which can overlooked by contractors:

1. *Sufficient preliminary investigations:* If additional geotechnical investigations were carried out during pre-construction, costs incurred during construction could have been reduced.
2. *Geotechnical input to construction staging:* Some of the construction activities discussed in this paper, could have been carried out prior to the installation and construction of settlement sensitive infrastructure. Although this resulted in some interesting geotechnical analysis; it could have reduced design and construction costs incurred by the contractor.
3. *Derivation of realistic geotechnical parameters:* Over-engineered and conservative design can result in unnecessary and avoidable construction costs. This is often due to the reliance on empirical data and conservative design parameters. This can be avoided by carrying out targeted and specific laboratory testing, the right suite of investigation methods and using the results obtained in creating good quality models.

There were also interesting facets of this project, which as consultants, we can learn from:

- The awareness that frequency of cyclical and dynamic loading, should be checked against proposed foundations internal frequency.
- Recommending extensive pile testing, although costly, can result in a much greater cost saving during construction due to the increase of Φ_g.
- The influence of clay and peat lenses in quaternary deposits, can help reduce the hydraulic conductivity of these materials, influencing analysis results and construction methodology.
- The effect of tidal water movements on dewatering activities, and the need for collaborative design, including geotechnical input to dewatering, shoring and bracing design.

- The behaviour of landfill materials, such as pulped paper, exhibit settlement characteristic akin to soft to very soft clay due to degradation/decomposition. It is therefore important to identify areas where these materials may be present, during early design stages.

8 ACKNOWLEDGEMENTS

The author would like to thank the wider project team; specifically the Amcor Ltd and Leighton Contractors. Secondly, the author would like to thank his colleagues at Golder Associates, for their assistance in writing this paper. Finally, the author would like to thank his wife, for her encouragement and understanding while this paper was written.

REFERENCES

Gaba, A. R., Simpson, B., Powrie, W and Beadman, D. R (2003). *Embedded retaining walls – guidance for economic design*, CIRIA C580, London, 390pp.
Hatley, R. K. (2004). "Hydrogeology of the Botany Basin." *Australian Geomechanics*, 39 (3), 73-90.
Somerville, S. H. (2005). *Control of groundwater for temporary works*. CIRIA Report 113, London, 87pp.

This page intentionally left blank

Proceedings of the 11th ANZ Young Geotechnical Professionals Conference – 11YGPC
Queenstown, New Zealand
25 – 28 October 2016

Timber Piles for Ground Improvement in Fiji's Liquefiable Soil

A. Pereira[1] and I. McPherson[2]

[1]Geotechnical Engineer, MSc in Geotechnics, www.linkedin.com/in/anacatarinapereira, email: acatarina@gmail.com
[2]Aurecon New Zealand Ltd, PO Box 1061, Christchurch, New Zealand, PH (64) 21 783 194, email:Ian.McPherson@aurecongroup.com

ABSTRACT

This paper presents the design of the ground improvement for the abutments of four bridges in Fiji, where the earthquake induced liquefaction and cyclic softening could cause slope instability. A geotechnical investigation with boreholes and Cone Penetration Testing (CPT) was undertaken to define the ground model at the eight abutments. Liquefiable sand was identified at four abutments and very soft clay up to 50m+ depth was logged under all of the considered bridge abutments. The available machinery and material supplies dictated using driven timber piles as a solution for ground improvement, as the crane on site for piling the foundations could also drive the timber piles, and treated timber piles could be easily imported from New Zealand. The slope stability analysis comprised four load cases for the eight abutments: static, earthquake Serviceability Limit State, earthquake Ultimate Limit State and Maximum Credible Earthquake (MCE) with the soil properties (drained and undrained) modelled according to the load case. The ground improvement design was based on the timber piles densifying potentially liquefiable sand and strengthening the soft clays. Swedish screw testing was used as a cost effective method to assess the post treatment densification within the sand layers as neither Standard Penetration Testing (SPT) nor CPT were readily available in Fiji. The required densification was achieved within the costs and timeframes required for the project.

Keywords: liquefaction, ground improvement, timber piles

1 INTRODUCTION

This paper presents the design of the ground improvement for the abutments of four bridges in Fiji Islands. Vunivaivai and Vunidilo bridges were near to Suva, Lomowai Bridge was near to Nadi, both in Viti Levu Island and Cogeloa Bridge was near to Labasa in Vanua Levu Island (refer to Figure 1).

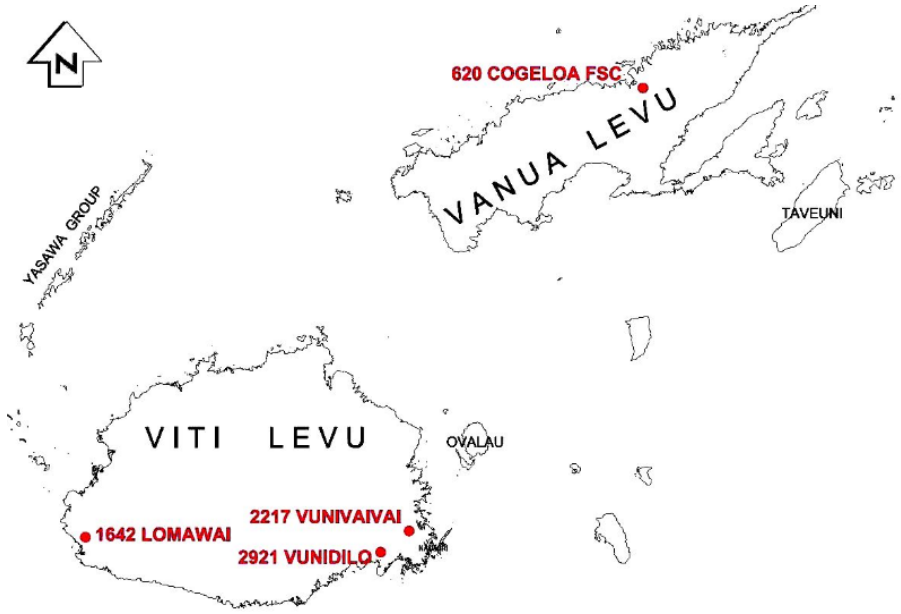


Figure 1. Bridges location plan, Fiji

There were old bridges at the same location as the new bridges in very poor condition (see Figure 2), requiring replacement. These bridges are important to the local community and economy as they are the only way to cross large rivers in the vicinity to connect villages, access schools and markets.



(a) (b)

Figure 2. View of the old bridges: (a) Vunivaivai bridge and (b) Cogeloa Bridge.

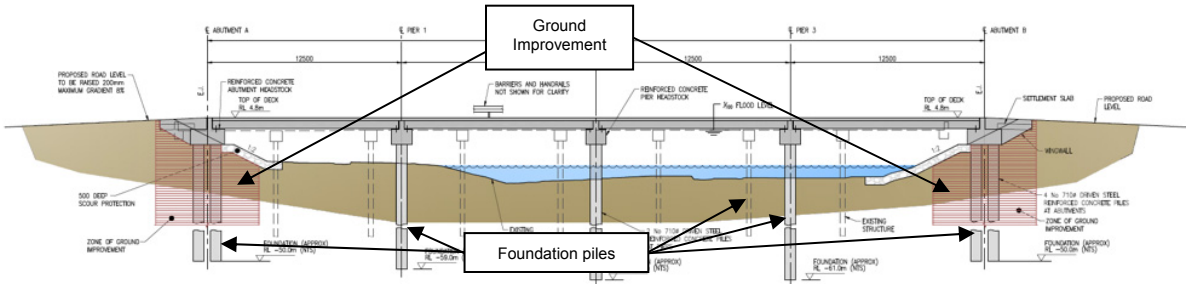


Figure 3. Long section of the new Vunivaivai Bridge

Lomowai and Cogeloa bridges also serve the sugar industry and have tracks for sugar cane trains. The sugar railway is crucial for the local economy as trains ship most of the sugar and this is the most important export item for the Fiji's economy.

The Fijian government let a design build tender for the four bridges which was won by Fletcher Construction. The design was based on the New Zealand and Australian Standards.

The construction program considered the need of a temporary pedestrian bridge to allow access to schools and markets, and the timing when the railway was needed for the sugar crop.

The design of the bridges started with an initial ground investigation with CPT and boreholes, and further shallow investigation with hand augers and shear vane testing. The geotechnical design of each bridge included the stability analysis of the abutments, ground improvement within the abutment and analysis of the foundation piles (see Figure 3). This paper will focus in particular on the ground improvement required for the abutments stability considering the particular conditions and available local Fijian resources.

2 GROUND CONDITIONS AND SEISMIC HAZARD ASSESSMENT

The geotechnical design of the four bridges in Fiji followed the traditional geotechnical design approach with an initial deep investigation comprising, three to four boreholes with SPT and two Cone Penetrometer Testing in each bridge location. Later in the project additional shallow investigation was undertaken with hand augers boreholes and shear vane testing at each bridge abutment.

The investigations indicated that the shallow ground condition at all bridges were similar with alluvial layers of interbedded soft silty clay and loose sand which required particular care for the performance of the abutment either in terms of bearing capacity or stability for static and seismic conditions. These soft and loose soils extended to:

- 55m in Vunivaivai, where no dense soils or rock was found to the depth investigated (55m);
- 18m bgl, underlain by weathered sandstone in Vunidilo
- 10m bgl underlain by weathered basalt in Lomowai
- 15m bgl underlain by weathered siltstone in Cogeloa

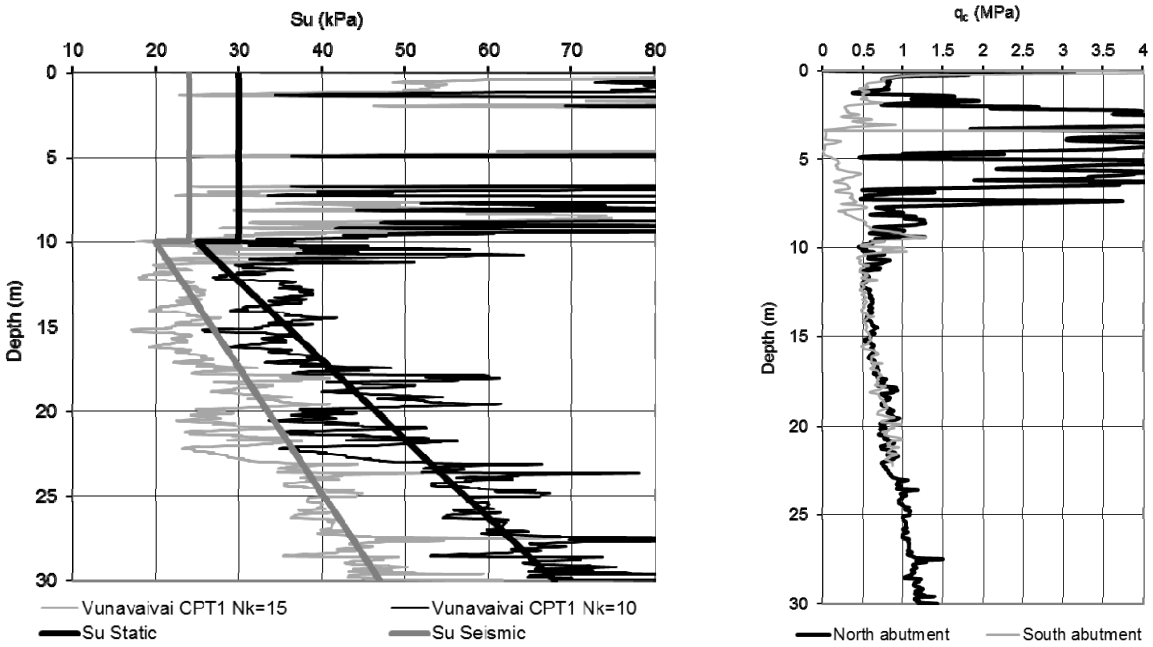


Figure 4. Vunivaivai Bridge (a) Adopted static and seismic shear strength profile; (b) CPT profile

2.1 Soil properties

Cohesive soil strengths have been assessed primarily from the CPT logs and the shear vane results from the 4m deep hand auger bore holes (Figure 4). Typically soil undrained shear strength is assessed based on the following: $S_u = (q_c-\sigma_v)/N_{kt}$, where σ_v is the total effective stress and N_{kt} is the cone factor (Robertson, 2012). Based on a comparison of undrained shear strengths from the hand auger investigations with the undrained shear strength inferred from the q_c profile, we have taken a N_{kt} value of 10 for the design of bridge foundations and ground improvement at the bridge abutments for the static case.

Cohesive soils are not expected to liquefy due to their plasticity but the laboratory test information indicates that the soil water content is close to the liquid limit, therefore it could incur cyclic mobility in the cohesive soils with a resulting loss of strength.

The residual shear strength was determined based on the hand auger logs, particularly the residual vane shear strengths, and have been taken as lower bound strengths. The adopted static and seismic strength profiles with depth are presented in Figure 4.

Sand was modelled with a friction angle of 35° based on the CPT logs for the static case. For the seismic case, it was assumed that the sand liquefies with an average residual undrained strength of 5kPa based on the SPT blow counting in the logs and the method of Idriss and Boulanger (2008).

Given the presence of loose sand layers at shallow depth and shallow water table the liquefaction risk and subsequent lateral spreading and displacements were an issue addressed in the geotechnical design. These displacements could be significant and therefore affect the global bridge stability.

The slope stability analysis of the abutments was undertaken for all eight abutments to better understand the extent of the potential liquefaction induced ground damage, along with the loss of shear strength of the soft soil under seismic conditions. This paper will focus upon liquefaction and lateral spreading mitigation. Since the liquefaction mitigation design approach was similar for all four bridges, this paper only details the analysis completed for the North abutment of the Vunivaivai Bridge.

2.2 Seismicity of Fiji

Fiji lies in a complex tectonic setting along the boundary between the Australian Plate and the Pacific Plate. Southwards from Fiji the Pacific Plate is subducting beneath the Australian Plate along the

Tonga Trench forming the Tonga Ridge island arc system and the Lau Basin back-arc basin. To the southwest of Fiji, the Australian Plate is subducting beneath the Pacific Plate forming the Vanuatu Ridge island arc system and the North Fiji back-arc basin.

For this project the seismic hazard was considered for the ground improvement design, and seismic loading has been calculated in accordance with NZS1170.5, New Zealand Transport Agency Bridge Manual (NZTABM) and Fiji Roads Authority (FRA) standard using the following parameters: Class D site; Seismic hazard factor (Z) 0.23; Ru (SLS 1/50 year return period) 0.35; Ru (ULS 1/1000 year return period) 1.30; Soil factor (Class D or E) 1.12; PGA (SLS) 0.09g; PGA (ULS) 0.33g.

3 DESIGN ASSUMPTIONS

The geotechnical design of the four bridges comprised the design of the foundation system, ground improvement and engineered fill on top of the ground improvement.

The pile analysis / design considered a number of load cases including, traffic load, flooding with scour, seismic load, with both the lateral and vertical capacity of the piles checked for geotechnical and structural issues. Given the specific topography, ground conditions, flood conditions, road and rail traffic of each bridge, the piles design was carried out for each bridge and slightly different solutions were chosen.

The ground improvement design included liquefaction, lateral spreading and slope stability assessment, which indicate the need of ground improvement for the bridges abutments stability during a major seismic event. The ground improvement design itself followed an empirical method, described in the subsequent items, and proof tests were undertaken to verify the design assumption.

3.1 Slope stability analysis

The slope stability analysis undertaken for the Vunivaivai Bridge comprised a static load case and three seismic load cases: serviceability limit state (SLS), ultimate limit state (ULS) and Maximum Credible Earthquake (MCE). The flooding load case was also modelled for assessment of scour but without seismic load, as flooding and earthquake cases are unlikely to happen simultaneously.

The North abutment of Vunivaivai Bridge had the thickest sand layer of the eight abutments, therefore it is likely to be the most vulnerable to liquefaction of the eight abutments, and will be the example used in this paper. The ground profile was defined based on the geotechnical investigation and indicates approximately a 5m thick liquefiable sand layer (Figure 5).

The failure surface geometry can have a significant effect on the calculated factor of safety against failure particularly for seismic analyses where failure surfaces are much deeper than the static case.

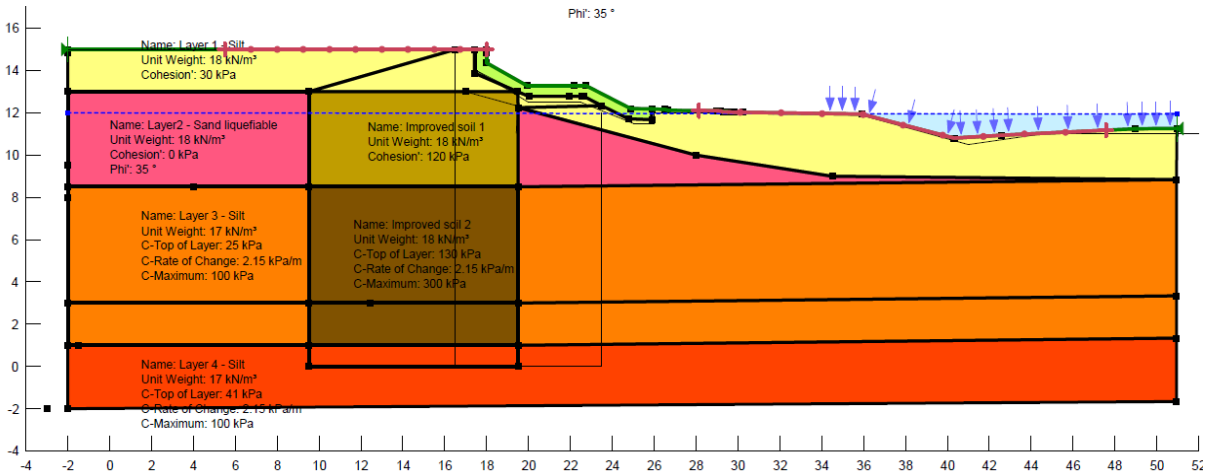


Figure 5. Geotechnical ground model for slope stability analysis (reference: SlopeW Software)

The failure surface was assumed to be constrained to 12m depth, which is considered to be the deepest credible surface. This assumption is based on Idriss and Boulanger (2008) who recommend limiting a lateral spread analysis to 2H depth where H is the height of the free face.

The analysis indicated that the slope would not be stable under a SLS earthquake therefore the following step was to find the appropriate ground improvement for the local ground conditions and local ready available materials and machinery.

3.2 Ground densification for liquefaction mitigation

Liquefaction occurs when loose sand is subject to vibration/ shaking, as it happens during an earthquake. Therefore, densifying loose sand would mitigate the liquefaction effects. The selected method to densify the loose and liquefiable sand was to drive piles into the ground, as replacing volume of soil and vibration during the driving piles process would densify the sand layers, and subsequently would increase the factor of safety against liquefaction. The effect of densification and stiffening on the soil liquefaction resistance was assessed based on the methods outlined by Baez and Martin (1993) and Rayamajhi et al (2012), where it is provided densification targets (N1(60)) according to the ground conditions and Stress Ratio to supress liquefaction. For this particular case the method indicates that a N1(60)=22 would supress liquefaction for a replacement ratio of approximately 8%. The design relied primarily on ground densification as the mechanism for ground improvement as the latest information indicates that relatively stiff inclusions such as timber piles do not increase significantly the liquefaction resistance.

As result of this analysis it was proposed to reinforce each abutment with 300mm SED timber piles at 1.2m centres. The average diameter of the piles was approximately 350mm at the depth of the sand layer therefore the replacement ratio is approximately 8%.

3.3 Ground improvement verification

During design, assumptions were made on the densification target using empirical methods and applying them to the local ground conditions. As the design would need confirmation of the assumptions made, post piles installation tests were undertaken. The verification tests were to demonstrate proof that the driven piles had sufficiently densified the soil to supress the liquefaction potential. Initially SPT was the preferred proof test because could be directly compared to the required target SPT-N value derived from literature (N1(60)=22) , however a SPT rig was not available in the islands when needed, hence the effectiveness of driven piles in densifying the ground was assessed using the Swedish Screw Test and use a correlation to N60 (SPT N-value corrected for field procedures and apparatus). The study undertaken by Habibi et al. (2006) presented a correlation from SWT to N60 that worked well for this project.

Swedish tests were undertaken prior to and post pile installation as this would allow a comparison pre installation between SPT/CPT and Swedish tests working as calibration. The tests indicated that a significant level of densification of the sand was achieved by the installation of the timber piles and largely exceeded the required N(60)=22. Figure 6 presents the results of tests in two locations pre and post installation of the timber piles. And indicates that a significant densification was achieved within the sand layer in the top 4m exceeding the target.

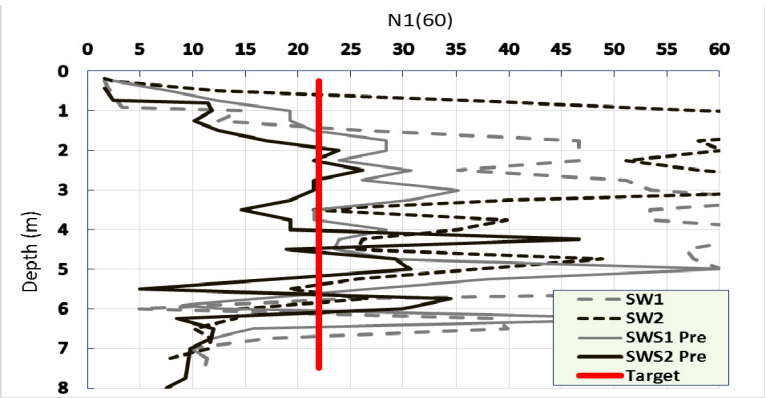


Figure 6. Swedish weight sounds for the North abutment, based on Habibi (2006)

4 CONCLUSIONS

The design of the ground improvement for the four bridges considered in Fiji was a challenge given the ground conditions and limited availability of heavy plant for pile driving and ground improvement.

The design had to comply the New Zealand and Australian Standards and at the same time be cost-effective accounting with the resources available in Fiji such as materials and machinery. The preferred type of inclusions in the ground was driven elements. Timber was known as available in the islands or easily shipped from New Zealand, therefore would be a cost-effective and sustainable solution. The technical solution of densifying the loose sand as a liquefaction mitigation method was considered to be the most appropriate for the local ground conditions. The inclusions in the ground would also strengthen the soft clays providing extra shear capacity for the slope stability.

The proof testing required to assess the level of densification induced by the timber inclusions was another challenge for the project as the usual testing equipment (CPT and SPT) was not available, therefore Swedish Screw testing was considered for that purpose and appropriate correlations had to be used and calibrated to the local ground conditions.

The success of the design and following construction stages of the new bridges was based on collaboration between design team, client and contractor to achieve a common goal of building new bridges in Fiji under the Australian and New Zealand design standards.

5 ACKNOWLEDGEMENTS

The authors would like to acknowledge and thank FRA, MWH and Fletcher Constructions Pacific for allowing them to present the above case study into the liquefaction mitigation measures applied at the four long bridges in Fiji replacement.

REFERENCES

Ambraseys, N. and Menu J. (1988). “Earthquake-induced ground displacement”. *Earthquake Engineering and Structural Dynamics,* 16, pp. 985-1006.

Ambraseys, N. and Srbulov, M. (1995). “Earthquake induced displacement of slopes”. *Soil Dynamics and Earthquake Engineering*, 14, pp. 59-71.

AS2159:2009. *Australian Standard Piling – Design and installation*. Standards Australia, Sydney, NSW, Australia.

Baez, J.I. and Martin, G. (1993) “Advances in design of vibro Systems for the improvement of liquefaction resistence” *Proceedings of the Symposium on Ground Improvement*, Canadian Geotechnical Society, Vancouver.

Habibi, M., Cheshomi, A. and Fakher, A. (2006), “A case study of liquefaction assessment using swedish weight sounding”*, 4th International Conference on Earthquake Engineering*, Taipei, Taiwan, October 12-13, 2006.

Idriss, I.M. and Boulanger R.W. (2008). *Soil Liquefaction during Earthquakes*. EERI Monograph Series MNO-12

Jibson, R. W. (2007). “Regression models for estimating coseismic landslide displacement.” *Engineering Geology*, 91, pp. 209–218

NZ Transport Agency (2013). *Bridge manual SP/M/022*

NZS 1170.5:2004. *Structural Design Actions Part 5: Earthquake actions – New Zealand*, Wellington, New Zealand: Standards New Zealand

NZS1170.0:2004. *Australia/New Zealand Standard, Structural Design Actions, Part 0: General Principles*. Standards New Zealand, Wellington, New Zealand.

Rayamadhi, D. et al. (2012). “Effect of discrete columns on shear stress distribution in liquefiable soil”, *Proceedings of GeoCongress 2012*, Oakland, California, March 25-29, 2012

Robertson, P.K, (2012). *Guide to Cone Penetration testing*, Gregg Drilling & Testing, Inc., California, USA

Proceedings of the 11th ANZ Young Geotechnical Professionals Conference – 11YGPC
Queenstown, New Zealand
25 – 28 October 2016

Capping of Tailings Deposits: Analysis, Design and Implementation

W. M. Piper[1], MIEA and D. R. Anderson[2], MIEA, CPEng, RPEQ

[1]Pells Sullivan Meynink, G3, 56 Delhi Rd, North Ryde NSW 2113; PH (02) 9812 5000; email: william.piper@psm.com.au
[2]Pells Sullivan Meynink, G3, 56 Delhi Rd, North Ryde NSW 2113; PH (02) 9812 5000; email: derek.anderson@psm.com.au

ABSTRACT

Un-rehabilitated, large coal tailings deposits present a safety and environmental risk to current and ceased coal operations. Capping of tailings deposits, involving the spreading of granular mine waste over the surface of the tailings using heavy machinery is often undertaken to rehabilitate such sites. There is often uncertainty about the risks associated with the capping works due to a lack of understanding of the condition and strength of the tailings at depth, as well as likely failure mechanisms. This paper presents a design methodology for final capping of deep, unconsolidated soft coal tailings deposits. The approach outlines a testing, analysis and construction sequence to minimise risk during capping works. A case study of the method is presented for a coal mine in the Hunter Valley of New South Wales (NSW), Australia. The design process presented in this paper outlines the significance of appropriate site investigation works required to assess the undrained shear strength profile of the tailings, which often varies considerably with depth, location and time. The results of the investigation form the basis for analysing the stability of the capping works, where heavy machinery pushing material across the surface of the tailings creates a short-term unbalanced load. Global stability due to unbalanced loads as well as local bearing capacity are considered. The analysis is then used to develop limiting fill thickness and machinery loads for the works, with consideration given to subsequent capping layers. Implementation of the capping methodology is also discussed.

Keywords: tailings dam, coal tailings, capping

1 INTRODUCTION

Following the processing of run-of-mine coal, the fine-grained residual “tailings” are typically deposited in surface storages or into available mining voids in a high moisture state. As such, the tailings often take many years to reach a state of normal consolidation. Mining voids are generally deep and large, making tailings deposited into them a considerable safety and environmental hazard until they can be rehabilitated. Rehabilitation by “capping” of these areas comprises heavy machinery spreading fill material on the surface of the tailings in layers, until a final landform height is reached. There is often little consideration given, during deposition and storage of the tailings, to the time taken for the tailings to reach a normally consolidated and desiccated condition adequate to facilitate the capping works.

Figure 1 shows a deep slip failure at a NSW coal mine which occurred during the capping of a surface Tailings Storage Facility (TSF). It is understood that the slip occurred during the placement of the third layer of capping fill due to excessive out of balance loads from the second and third layers. Insufficient investigation works also led to uncertainty about the shear strength of the tailings at depth.



Figure 1. Large scale slip failure during capping works at a NSW coal mine

2 BACKGROUND

The specific coal tailings deposit discussed in this paper is located at a coal mine in the Hunter Valley of NSW and is referred to as Tailings Dam 'A'. Tailings Dam 'A' is a surface TSF and covers an area of approximately 330,000 m^2 with a depth of tailings of generally greater than 20 m.

Tailings deposition ceased in June 2010. Since that time the tailings have undergone consolidation due to overburden pressures, and desiccation within the surface material due to evaporation.

Rehabilitation of the TSF is a requirement of the ongoing operations of the coal mine. As such, a capping design that would facilitate placement of readily available granular mine waste on to the surface of the tailings was required. The development process for the capping design is presented in the following sections.

3 INVESTIGATION

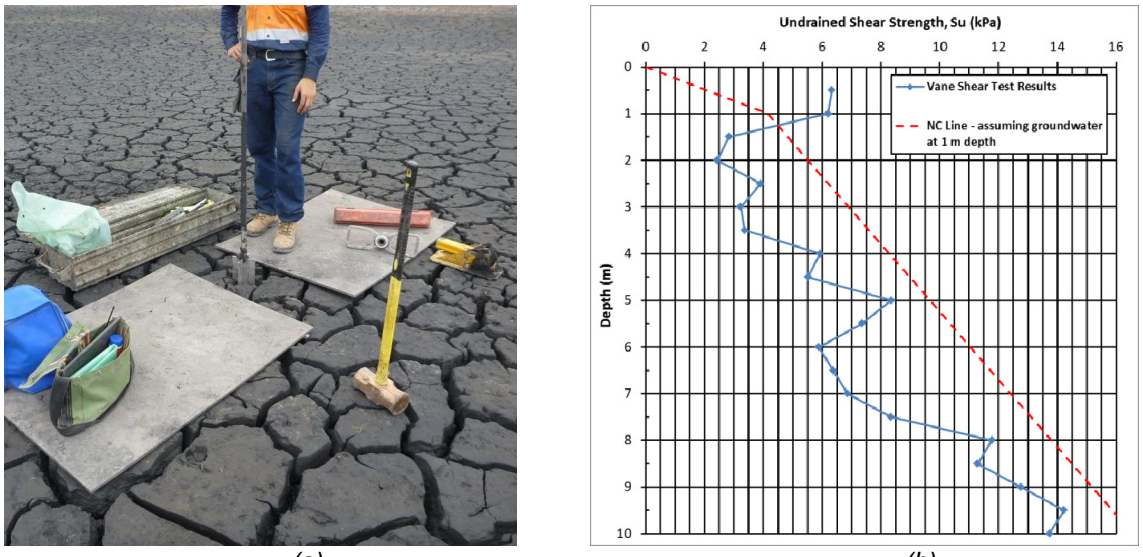
The saturated, fine grained tailings are subjected to rapid loading during capping works and so an understanding of the undrained shear strength of the tailings was required for stability analysis.

The generally "soft" nature of the deposited tailings limits the loads that can be placed directly onto the surface of the tailings, making it difficult and dangerous to traverse vehicles across the deposit. This ultimately limits the investigation techniques to either hand-held tools or machinery specifically designed to access soft areas. The latter is expensive and so simple hand-held vane shear tools were used within Tailings Dam 'A'. Vibrating wire piezometers and a soil sampler were also used.

3.1 Vane Shear Testing

Vane shear testing comprised the use of a Geonor H-70 vane shear tester and torque wrench. The Geonor H-70 incorporates a coupling system just above the steel vane, allowing a 180° turn with the torque wrench before the vane is engaged. This facilitates the recording of skin friction on the rods which is particularly useful at depth and prevents the over-estimation of shear strength values.

Testing was undertaken in 2014 at twenty-eight locations across Tailings Dam 'A' at 0.5 m depth intervals to a maximum depth of 10 m. The deep vane shear testing is considered to be vitally important for understanding the variability of shear strength with depth which reduces uncertainty and improves confidence in the design. Deep slip failures can and will develop as the height and extent of capping fill and machinery loads increase. Readings recorded by the torque wrench produced an undrained shear strength profile at each test location. Figure 2 shows the equipment used as well as the recorded undrained shear strength profile at one test location. The normally consolidated (NC) line also shown in Figure 2 adopts a groundwater depth of 1 m as measured at this location.



(a) (b)

Figure 2. (a) Vane shear testing equipment; (b) Indicative undrained shear strength profile

3.2 Sampling

A piston soil sampler was used to obtain numerous samples at varying depths and locations across Tailings Dam 'A'. The retrieved samples were tested in the laboratory to obtain information on specific gravity (G_S), moisture content (w), and dry density (ρ_d).

Moisture content results were correlated with recorded undrained shear strength values. Figure 3 shows an indicative relationship between gravimetric moisture content and undrained shear strength for the tailings sampled from Tailings Dam 'A' and other coal tailings deposits within the mine.

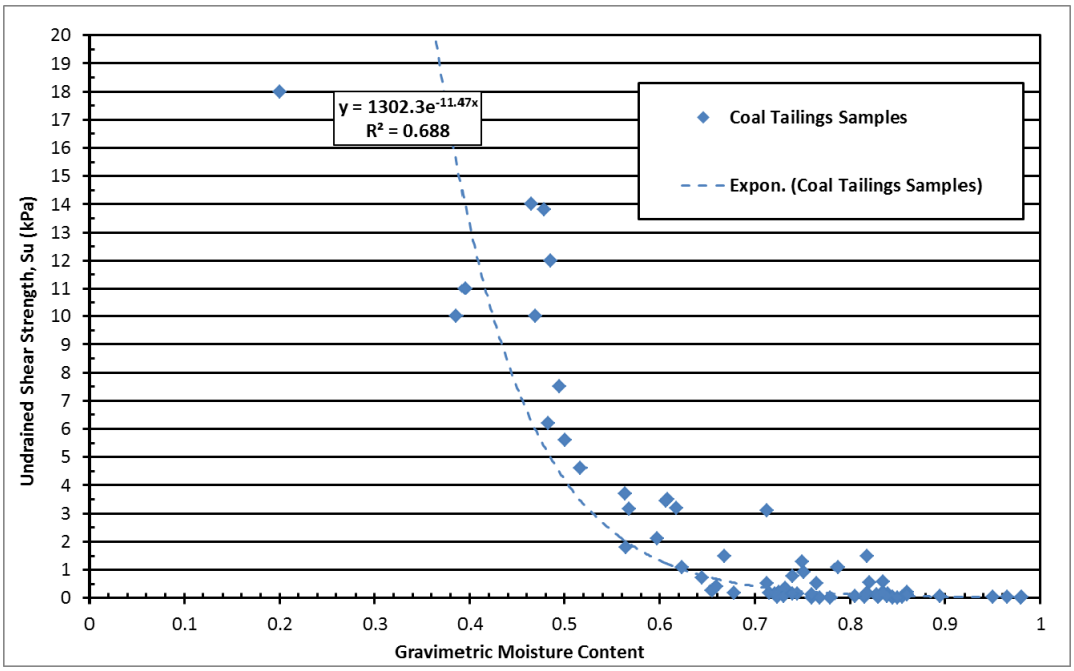


Figure 3. Undrained shear strength vs gravimetric moisture content plot

3.3 Vibrating Wire Piezometers

Vibrating wire (VW) piezometers were installed at three locations to assess the distribution of pore pressures with depth. The results indicated that at the locations examined the excess pore pressures due to overburden weight had not dissipated and the tailings had not reached normal consolidation.

4 ANALYSIS

The results of the investigation techniques discussed in Section 3 were used as the basis of the analysis for the stability of potential capping works. Two failure mechanisms likely to impact the heavy machinery spreading the capping fill were considered:

- Global stability – failure along a circular slip surface due to short-term unbalanced loads.
- Local bearing capacity – bearing failure through the capping layer into the soft tailings.

The failure mechanisms were analysed separately. Each analysis technique is discussed below.

4.1 Global Stability

The global stability of heavy machinery placing the capping fill on the surface of the tailings was analysed using the limit equilibrium computer program Slide. The input components were as follows:

- Design undrained shear strength profile of tailings derived from vane shear testing.
- Mass of the capping fill. Analysis indicated that an initial capping layer of no more than 0.5 m thickness could be placed onto the tailings surface.
- Loading from the machinery used to place the capping fill, with consideration given to the possible 3-dimensional load spread through the overlying capping material.

The stability assessment considered two types of machinery – a D6R Bulldozer and a tracked bobcat. A critical Factor of Safety (FoS), taken as the first circular failure surface extending through the tailings and impacting the machinery, was computed at each test location. Figure 4 shows a contour plot of FoS for the D6R bulldozer at the southern end of Tailings Dam 'A', computed from the limit equilibrium analysis completed at each test location.

It is noted that management protocols for Tailings Dam 'A' required the minimum FoS for the works to be 1.3. The results of the analysis indicated that the capping works could not be undertaken (FoS less than 1.3) at the northern end of the deposit with the current methodology.

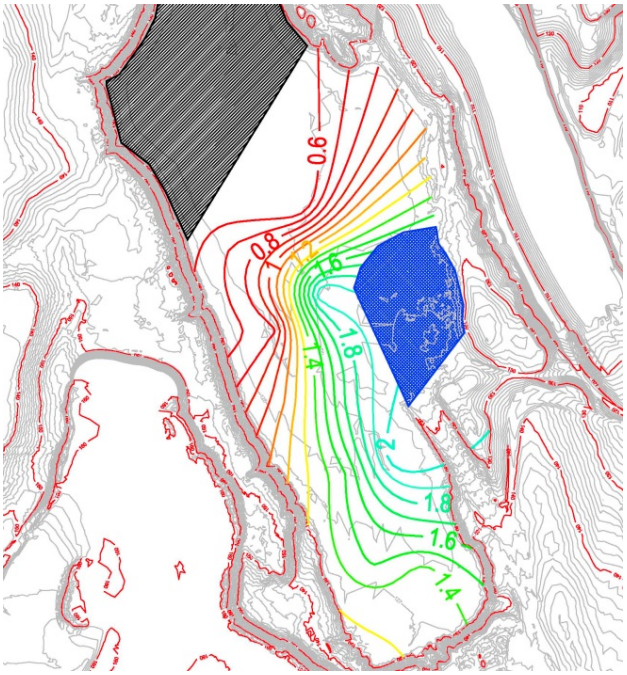


Figure 4. FoS Contour Plot – D6R Bulldozer and 0.5 m Capping Layer

4.2 Bearing Capacity

The bearing capacity of the tailings profile beneath the machinery was also considered. This is a difficult failure mechanism to analyse quantitatively due to the layered ground profile (granular material overlying soft tailings) with significantly different strength and stiffness properties.

A number of analytical methods to compute the local stability of the works in bearing were considered:

- Bearing capacity of clays with increasing shear strength profile, as presented by Davis and Booker (1973)
- Bearing capacity of granular material overlying soft clays, as presented by Hanna and Meyerhof (1980)
- Axi-symmetric modelling using the finite element analysis program Phase^2

Singularly, the computation methods above were not considered to provide a definitive answer. However, a combination of the methods gave an indication of whether the proposed machinery would be suitable for the capping works, in conjunction with the results of the global stability assessment.

The results of the analyses generally indicated global stability to control machine size and fill height.

5 DESIGN

The results of the stability analysis indicated that the capping works at the northern end of Tailings Dam 'A' could not be completed with the current methodology. This resulted in the approach where the southern end would be capped first, and various other options examined to improve the density and shear strength of the tailings at the northern end.

The southern capping area was split into two zones based on the FoS plots produced by the analyses:

- Zone 1 – a D6R Bulldozer would be used to place a 0.5 m initial capping layer
- Zone 2 – a tracked bobcat (CAT 299D or similar) would be used to place a 0.5 m initial capping layer

The spreading of subsequent capping allows increasingly thicker fill layers and possibly larger machines as the initial layers of granular material provide additional confining stresses to resist slip failure development. It is important to ensure that the initial fill layer is sufficiently developed prior to commencing the secondary layer. The secondary capping layer design was as follows:

- Zone 1 – a D6R Bulldozer would be used to place a 1.0 m secondary capping layer no closer than 50 m behind the face of the initial layer.
- Zone 2 – a tracked bobcat (CAT299D or similar) would be used to place a 0.5 m secondary capping layer no closer than 50 m behind the face of the initial layer.

A D8 Bulldozer could be used in Zone 1 and Zone 2 to spread 1.5 m to 2 m thick fill layers to a final landform height of approximately 5 m, after a 1.5 m thick capping has been established.

5.1 Design Uncertainties

There is a number of uncertainties inherent in the overall analysis process, as discussed below:

- Use of a 2-dimensional analysis technique to model a 3-dimensional problem: A 3-dimensional load spread of the plant through the capping layer was adopted for the analyses as an attempt to incorporate 3-dimensional effects.
- Assumption of the plant load as a static, concentric load: The machinery loading will be subject to some eccentric effects during pushing, turning and movement on uneven ground. It is considered that the applied FoS will accommodate these effects.
- The extent of excess pore pressures in the tailings beneath the capping fill and their rate of dissipation: Review of monitoring results during the capping works will help develop a better understanding of pore pressure reactions to loading.

6 IMPLEMENTATION

The implementation of the capping design requires the analytical design to be incorporated into real-world construction procedures. The following sections discuss the factors considered to be important for the effective implementation of the design, including hazard training of personnel, an appropriate monitoring regime, and ongoing inspections and review of the capping works.

6.1 Hazard Training

Operators and supervisors undertaking the works need to be aware of the inherent risks and hazards as well as the limitations put in place to prevent failures developing. A training document was developed prior to the commencement of capping works to outline the specific limitations to the works and the visible signs for the onset of failure. A few key points are as follows:

- Tolerances on capping fill thickness:
    i. + 200 mm
    ii. – 50 mm
- Signs of instability:
    i. Look for cracks parallel to the advancing face behind the capping crest
    ii. Look for heaving or mud-waves in the tailings in front of the advancing face
- Operation of plant:
    i. Maintain separation of plant a minimum of 20 m
    ii. Do not push out material more than 2 plant lengths from the advancing face
    iii. Avoid working on wet spots following rainfall
- Monitoring:
    i. Use survey pegs in tailings to monitor movement for onset of failure
    ii. Use spotters to monitor plant movements and to look for signs of cracking

6.2 Monitoring

VW piezometers were installed at three locations prior to commencement of the capping works as a way of assessing the pore pressure response during placement of the capping fill and the rate of dissipation of the excess pore pressures. PVC pipes of 100 mm diameter were placed over the top of the piezometers to prevent them being damaged during the placement of the capping fill and allow access once the capping fill had been placed. Additional PVC pipes were installed adjacent to the piezometers to allow further vane shear testing to be undertaken in the tailings following placement of the capping fill.

Piezometer readings taken before, during and after placement of the first capping fill layer indicated rapid increase in pore pressures up to 4 m depth, with very slow dissipation of excess pore pressures.

6.3 Design Review and Inspections

Additional vane shear testing was undertaken at the beginning of 2016 and indicated improvement in the undrained shear strength profile at a number of test locations. Review of the capping design with the new test data, in conjunction with inspection of the current capping progress, allowed the extent of the D6R zone and the overall works to be extended, improving the efficiency of the project. A D4K LGP Bulldozer was also recommended to replace the tracked bobcat within Zone 2.

At the time of writing this paper the capping works at the southern end of Tailings Dam ‘A’ are still in progress. The works are at approximately 50% completion of the second capping layer. Inspection of the works indicated no signs of heaving or displacement of the tailings or cracking of the capping fill.



Figure 5. Capping works progress - secondary 1.0 m capping layer (August 2016)

7 CONCLUSION

The investigation, analysis and design process discussed in this paper presents a systematic approach to developing and implementing a suitable capping works design that minimises the risks and hazards associated with spreading fill on the surface of deep coal tailings deposits. The author considers that a successful capping design is reliant on all steps of the discussed process.

The initial investigation works should be completed to an appropriate depth and density to capture possible deep slip failure mechanisms and zones of weaker/softer tailings. Suitable hazard training of the machine operators completing the works, as well as monitoring and review of the ongoing capping works are also considered vital to the success of the project.

REFERENCES

Davis, E. H., and Booker, J. R. (1973). “The effect of increasing strength with depth on the bearing capacity of clays” *Geotechnique*, 23(4), pp. 551-563.

Hanna, A. M. and Meyerhof, G.G. (1980). “Design charts for ultimate bearing capacity of foundations on sand overlying soft clay.” *Canadian Geotech. Journal*, 17, pp. 300-303.

Proceedings of the 11th ANZ Young Geotechnical Professionals Conference – 11YGPC
Queenstown, New Zealand
25 – 28 October 2016

Interpreting geotechnical measurements and observations: Does one size fit all?

R. E. Kristinof[1], MSc. DIC CPEng MIEAust

[1]Jacobs Engineering, PO Box 312 Flinders Lane Melbourne, VIC, 8009 Australia, PH (+61 3 8668 3372; email: ross.kristinof@jacobs.com

ABSTRACT

This paper illustrates via simple real life examples, the constraints and limitations of three common geotechnical assessment techniques. The purpose of these case studies is to highlight the need for geotechnical engineers to not only choose the right tool for their analysis, but also to fully understand and appreciate the limitations of these techniques in the context of the project requirements. In the first example, a borehole and test pit excavated within close proximity to one another is shown to lead to different interpretations of stratigraphy, and potential implications for the project in question are discussed. In the second example, PDA tests undertaken on the same driven pile at the same time are shown to result in inferred pile capacities which vary by over 20%, as a consequence of the way the data is processed and assumptions made, highlighting the need to avoid 'black box thinking' when interpreting geotechnical observations and measurements. Finally, an example is presented of an assessment of "native soil modulus" in the context of flexible pipeline design. Conventional methods of assessing the stiffness of the ground, which may be conservative for the design of a foundation, are shown to be potentially unconservative for the purposes of design of the pipeline. In this case, it is necessary to understand the wider project context and performance criteria of the pipeline, in order to provide appropriate geotechnical design advice.

Keywords: geotechnical investigation, PDA testing, native soil modulus, observations, interpretation

1 INTRODUCTION

Geotechnical engineering practice requires the application of theories and techniques which are usually based on empiricism and observation. Rarely are situations encountered where completely unambiguous ground conditions exist, such that a single, closed-form solution can be applied to solve a geotechnical problem. Geotechnical solutions require the synthesis of a ground model, selection of design parameters based on predicted material behaviour and ultimately an engineering solution based on inferences made from a finite array of data points. If over-conservative design approaches are to be avoided, then observation during construction and/or operation of the design is necessary to obtain pragmatic solutions. Burland (1987) discusses the importance of understanding the ground profile, soil behaviour and applied mechanics and design model, and stresses the need for "empiricism and well-winnowed experience" in order to reliably apply these skills to a geotechnical problem. The interplay between these aspects of geotechnical engineering is illustrated in Figure 1 as a triangle, with empiricism and experience common to the correct application of each. In this paper, the importance of experience and judgement in interpreting 'each point of the triangle' using common geotechnical tools and techniques will be explored, using case studies from the author's recent project experience.

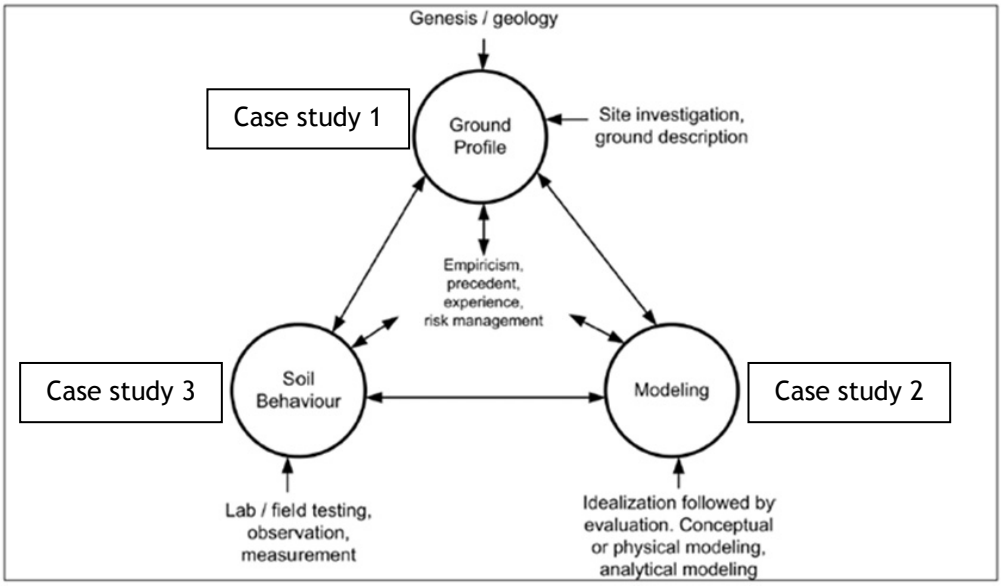


Figure 1. Ground engineering triangle (after Burland, 1987)

2 CASE STUDY 1: ENGINEERING IMPLICATIONS OF DIFFERENT GROUND PROFILES INFERRED FROM TEST PITS AND BOREHOLES

When planning and undertaking site investigations, it is important to select appropriate investigation techniques to suit the anticipated ground conditions, and also the design intent and purpose of the investigation. Use of different techniques can skew one's understanding and interpretation of the ground profile. How data is recorded and reported, particularly when it will be passed on to someone with without a primary background in geotechnics, can affect the correct application of the information at subsequent stages of a project.

At a site north of Melbourne, a geotechnical investigation was undertaken to assess ground conditions for new water-reticulation infrastructure. The investigation needed to assess conditions for a shallow slab footing and several hundred metres of trenches to allow installation of new buried pipes. The investigation comprised two shallow boreholes (drilled using a combination of auger and HQ coring techniques) at the site of the slab footing, and several mechanically excavated test pits (excavated using a 6t tracked excavator) along the route of the proposed trenches. The boreholes and test pits were logged by different geotechnical engineers at different times, and therefore at the time of logging, no direct comparison between logs produced from the test pits and boreholes was made. One borehole and one test pit however were located adjacent to each other (within 5m), and inferred ground conditions from each are illustrated in Figure 2.

Depth mbgl	BOREHOLE	TEST PIT
0	**Silty Clay (CH)**	**Silty Clay (CH)**
0.1	dark brown, trace fine sand	brown, some rootlets in top 200mm
0.2		Basalt fragments to 75mm
0.3		
0.4		
0.5		
0.6		
0.7		
0.8		increasing basalt cobbles
0.9		
1	**Basalt (MW)**	
1.1	grey, dark grey, slightly vesicular	
1.2	medium to high strength	
1.3	RQD = 12%	
1.4		Refusal at 1.4m
1.5	(hole continues to 5m)	

Figure 2. Comparison of inferred ground profile from borehole and test pit

The borehole log identified medium to high strength basalt at 0.9m below ground level, whereas the adjacent test pit identified clay with basalt fragments and cobbles to 1.4m depth. Whilst neither interpretation is incorrect when considered in isolation, it is important to consider which interpretation is the *most suitable* to include in an interpretative report. Figure 3 shows the core box retrieved from the borehole, and one of the basalt fragments retrieved from the test pit. The defect spacing and RQD of the rock means that it was easily excavated. During excavation, some mixing of soil with the rock fragments (possibly along with crushing of extremely weathered and residual material), gave the appearance of rock fragments within a clayey matrix, rather than material that was indeed mostly rock, as was inferred from the borehole.

The observations arising from the different investigation techniques have important implications in the engineering design for which the investigation was intended, noting that subsequent stages of the design would be undertaken with limited direct input by a geotechnical engineer:

- If only boreholes were undertaken, rock core similar to that shown in Figure 3 would likely have been retrieved at all investigation points. An empirical assessment of excavatability could be made based on personal experience or published approaches but would likely be quite cautious, without direct evidence of the excavatability of the material;
- If only test pits were undertaken at the site, a sound understanding of excavatability across the site would be obtained. Bearing capacity assessments in the vicinity of the footings would however tend to be more cautious, and would likely infer lower allowable bearing capacities and higher shrink-swell potential, owing to the engineering logs suggesting a mostly soil-like profile.

Thus, this case study highlights the need to apply different investigation techniques to achieve different design outcomes, and being careful to interpret and report data in a way that is not misleading or ambiguous.



Figure 3. Rock encountered in borehole and test pit

3 CASE STUDY 2: INTERPRETING PDA TESTS ON DRIVEN PILES

Dynamic pile testing by way of the pile driving analyser (PDA) is a commonly used tool with which to directly verify the capacity of driven piles. Whilst most commonly used for verification during construction, the technique can be used to refine designs and to design remedial solutions to rectify problems encountered at difficult sites (Reed et al, 2016).

At a site where multiple testing contractors were engaged to undertake PDA and CAPWAP testing, a reference pile was selected to benchmark and compare the results of two of the testing contractors. A single steel 1500mm diameter tubular pile was selected, and two testing contractors were invited to instrument and take readings from the pile during testing, and subsequently provide a recommended 'as-built' capacity for the pile. Both contractors instrumented the pile with their own strain gauges and accelerometers and used their own testing kit; however both contractors recorded and independently interpreted the same sequence of hammer strikes on the pile.

Table 1 compares the results for the same hammer strike which was reported by the two contractors. Hammer blow 2 was agreed by the contractors to be the blow of comparison; other blows were reported by Contractor A but not by Contractor B, and therefore a more thorough comparison is not possible.

Table 1. Difference in test results between testing contractors

Contractor	Hammer blow	Inferred shaft resistance (kN)	Inferred base resistance (kN)	Inferred total resistance (kN)
Contractor A	2	7312	1400	8712
Contractor B	2	5779	1368	7147
Difference between A and B on Blow 2		26.5%	2.3%	21.9%

The difference in test results are negligible when base resistance is considered, however the differences happen to be considerable on shaft resistance. This is particularly important for piles which rely on shaft resistance as a significant portion of their design capacity, such as tension piles. In this instance, the differences between the results from Contractor A and Contractor B were attributed to apparently poor correlation between force and velocity measurements, thought to arise from nearby sheet piles, which in turn were dealt with in slightly different ways by the two testers. There was also some confusion over the average set and temporary compression measured by the piling contractor and used in the analysis, and also whether or not paint was scraped off the pile prior to the gauges being attached.

Table 2 shows interpreted results from different hammer blows from the same testing sequence on the test pile at the site, which were provided by Contractor A. The earlier, 1st hammer blow shows significantly higher resistance, whereas the later blow shows values more consistent with those shown in Table 1. The higher resistance on the 1st blow is attributed to more "undisturbed" ground conditions; each hammer blow moves the pile and leads to some breakdown of shaft resistance along the pile.

Table 2. Difference in PDA test results between different hammer blows on the same pile

Contractor	Hammer blow	Inferred shaft resistance (kN)	Inferred base resistance (kN)	Inferred total resistance (kN)
Contractor A	1	9062	2800	11862
	4	6127	1000	7127

Whilst this author places no judgement on either contractor for the results provided, it is nevertheless concerning that such variability could occur under highly controlled circumstances for what is normally considered a relatively routine test procedure. It is therefore important for a geotechnical engineer to have at least a basic understanding of how tests like PDA tests are undertaken and interpreted, before using the results to validate or calibrate their designs. A PDA test, not unlike other geotechnical tests, is a measurement which must be interpreted within the context of the ground model, expected soil behaviour, and sound engineering principles. Such a test is a measurement of the resistance of the pile in the ground subjected to a certain hammer blow, and it follows that a test result could be unrepresentative of the true ultimate geotechnical capacity of the pile if hammer energy is too low

(which usually manifests in very low set readings) or too high (which can lead to inaccurate velocity or force measurements), if there is interference in the readings (which may have been the case in this example), or if set and temporary compression is recorded incorrectly.

As discussed by Reed et al (2016), understanding how to interpret a measurement such as PDA testing whilst not relying on it solely as a pass/fail result can prove invaluable in identifying and rectifying problems on site. At another location at the same site, piles were being installed with recorded final driving sets of between 20 to 45mm, which suggested ultimate geotechnical capacities of less than 2MN by application of the Hiley formula for piles requiring a design geotechnical capacity in excess of 5MN. Inspection of the ground model in the area suggested that the subsurface profile should be horizontally bedded and similar to the adjacent piling zone where piles were driven to the same toe level with a final set of 3 to 4mm. The discrepancy was resolved by reallocating a planned PDA test to the pile with the worst (highest) recorded set value. A conservative interpretation of the PDA testing on this pile (taking into consideration the factors discussed earlier) proved a design capacity of over 6MN for this pile. Together with the ground model, this data was subsequently used to demonstrate acceptance of all the piles with high sets in that zone. The data was also a trigger to review record keeping and quality procedures on site, as it suggested the recorded sets were likely too high.

4 CASE STUDY 3: NATIVE SOIL MODULUS FOR BURIED FLEXIBLE PIPES – WHICH MODULUS IS WHICH?

The design of non-rigid pipes (for example, HDPE) for many water infrastructure projects in Australia and New Zealand is governed by AS/NZS 2566.1 – 1998 Buried flexible pipelines Part 1: Structural design (Standards Australia, 1998). According to this standard the support provided to the pipe by the ground depends on the geometry of the trench, the properties of the embedment fill within the trench and the stiffness of the natural soil, which is defined by the parameter referred to as *Native Soil Modulus*, E'$_n$. AS2566.1 recommends values of E'$_n$ based on soil type and SPT N value, replicated in Figure 4. Unfortunately, the standard does not differentiate between the stiffness of embedment material (which includes the deformation of the pipe itself) or natural material. These differences are discussed by ATV-DVWK (2000) and Howard (1996) which provide details on the derivation of these values via plate load testing or direct measurement of model pipe deformations.

Materials			Moduli E'_e and E'_n MPa				
Description	Classification		Uncompacted	R_D (%)			
				85	90	95	100
				I_D (%)			
	AS 1726 †	AS 2758.1		50	60	70	80
				Standard penetration test ‡ Number of blows			
				≤ 4	> 4 ≤ 14	> 14 ≤ 24	> 24 ≤ 50	> 50
Gravel— single size	—	Coarse aggregate	5§	7§	7§	10§	14
Gravel— graded	GW	Coarse aggregate	3§	5§	7§	10§	20
Sand and coarse-grained soil with less than 12% fines	GP, SW, SP and GM-GL, GC-SC etc.	—	1	3§	5§	7§	14
Coarse-grained soil with more than 12% fines	GM, GC, SC SM and GM-SC, GC-SC	—	NR	1§	3§	5§	10
Fine-grained soil (LL<50%) with medium to no plasticity and containing more than 25% coarse-grained particles	CL, ML, mixtures ML-CL and ML-MH	—	NR	1§	3§	5§	10
Fine-grained soil (LL<50%) with medium to no plasticity and containing less than 25% coarse-grained particles	CI, CL, ML, mixtures ML-CL, CL-CH and ML-MH	—	NR	NR	1	3	7
Fine-grained soil (LL>50%) with medium to high plasticity	CH, MH and CH-MH	—	NR	NR	NR	NR	NR

Figure 4. Recommended E'$_n$ values based on AS2566.1

"NR" in Figure 4 implies "no reliable modulus" can be ascertained from the simple correlations used to derive the table. How then, can a designer evaluate E'_n for a pipeline through high plasticity (CH) clays, or if test results other than SPT values are available? This author has seen various approaches to solving this problem, many of which involve estimating "equivalent SPT values" from vane shear, pocket penetrometer or DCP data, so that Figure 4 (Table 4.2 in the standard) can be used. Such approaches introduce considerable error and uncertainty to the project, and still do not provide a solution for CH soils. This author has seen, on several occasions, geotechnical reports of 'NR' for very stiff CH soils, which provides the designer with absolutely no information with which to design the pipe. To overcome these shortcomings, this author recommends a somewhat expedient approach based on first principles and related to back-calculating the effective or constrained soil modulus beneath a footing, which has proved valuable on a number of project sites.

Review of recommendations by several pipeline manufacturers suggests that lateral movements of the pipe should be limited to less than 10 to 15mm to prevent damage to collars or joints. If one considers that a shallow footing loaded to its allowable bearing capacity can be assumed to settle by as much as 25mm (Look, 2014), then limiting deformation to these magnitudes for a flexible pipe requires conventional estimates of stiffness to be modified by a factor of at least 2.0 in order to derive a value of E'_n. Thus, an estimate of E'_n can be found by increasing a global factor of safety from 3.0 to 6.0, and otherwise adopting typical correlations between E' (not E_u) and undrained shear strength, noting that Howard (1996) states that "…there are various opinions for the relationship between E_s, M_s and E' and in light of the variability of SPT results, the terms may be considered interchangeable". Consideration of these factors allows the derivation of parameters in natural soils which are not accommodated in the standard (such as CH soils) or where SPT testing is either unavailable or unreliable.

5 CONCLUDING REMARKS

This paper has provided case study examples which exemplify the need to critically analyse and consider the results of three investigation and design approaches used routinely in geotechnical practice. Common to all three case studies is the risk of misinterpreting observations if the engineer fails to understand the 'bigger picture' of the works taking place, or the assumptions on which the technique being used is based. It is necessary for all geotechnical engineers to avoid learning and applying techniques by rote, and consider first principals at all times when undertaking geotechnical work.

6 ACKNOWLEDGEMENTS

The author wishes to thank Jacobs for the opportunity to attend this conference and present this paper, my clients from whom these project examples have been drawn, and my mentors and peers throughout my career to-date who have impressed upon me the importance of developing and applying sound engineering judgement.

REFERENCES

ATV-DVWK [German Association of Water, Wastewater and Waste], (2000). *Standard ATV-DVWK-A 127E Static calculation of drains and sewers.*

Burland, J.B. (1987) "Nash Lecture: The teaching of soil mechanics: A personal view", *Proc. 9th European conference on soil mechanics and foundation engineering*, Dublin, Ireland.

Howard, A. (2006). "The reclamation E' table, 25 years later", *Proc. Plastics Pipe XIII International Conference*, Washington DC, USA.

Howard, A. (1996). *Composite E Prime – Tech note suppliment to Pipeline Installation 2.0*, www.amsterhoward.com [accessed on 19 July 2016]

Look, B.G., (2014). *Handbook of geotechnical investigation and design tables*, 2nd Ed., Taylor & Francis, London, UK.

Reed, R.J., Kristinof, R.E., Carter, A.T. (2016) "Adapting a driven pile design to meet the challenges encountered during construction", in Neeson, F., Lacey, D., Buxton. D. and Storie, L. (eds.), *Proceedings of 11th ANZ Young Geotechnical Professionals Conference (11YGPC)*, 25 – 28th October, Queenstown, New Zealand, pp. 275 – 280

Standards Australia (1998). *AS2566.1:1998 Buried flexible Pipelines Part 1: Structural design*, Homebush, Australia

Proceedings of the 11th ANZ Young Geotechnical Professionals Conference – 11YGPC
Queenstown, New Zealand
25 – 28 October 2016

Rockfall Protection Structures on a Critical Lifeline in Christchurch

J. M. Engel[1]

[1]Engineering Geologist, Jacobs New Zealand Limited, P.O. Box 1147, Christchurch 8140; PH (03) 940 4914; email: matthew.engel@jacobs.com

ABSTRACT

Following the 2010/11 Canterbury Earthquake Sequence in Christchurch, significant rockfall, cliff collapse and mass movement features occurred around the Port Hills. The Sumner-Lyttelton Corridor is a critical link between Lyttelton Port and Christchurch CBD for transportation of oversized and hazardous goods and suffered extensive rockfall and slope failures from the earthquakes. Sections of the Sumner-Lyttelton Corridor have been kept operational through the use of temporary rockfall protection measures in the form of ballasted shipping containers. The Wakefield Avenue section of the Sumner-Lyttelton Corridor had three areas affected by rockfall and cliff collapse, which were temporarily protected by ballasted shipping containers. This paper focuses on the design of the permanent rockfall protection structures at two sites along Wakefield Avenue which will allow the removal of the shipping containers and mitigate the rockfall and cliff collapse geo-hazards in the long term. The project involved carrying out geotechnical investigations, identifying the rockfall sources, mapping existing rockfall, modelling rockfall trajectories, ground truthing modelling outputs, design of rockfall protection structures and providing assistance to the client during consenting and construction. It is concluded that important considerations for the design and construction of rock fall protection structures include detailed topographic surveys, stormwater management, service clashes and safe construction methodology.

Keywords: rockfall, protection, critical lifeline, Canterbury Earthquake Sequence

1 INTRODUCTION

The 22 February 2011 M6.3 earthquake event in Christchurch, part of the 2010 – 2011 Christchurch earthquake sequence (CES), caused significant damage to the Christchurch area with damage and collapse of buildings in the city centre and significant rockfall, cliff collapse and landslides in the Port Hills south to southeast of Christchurch's CBD. The 13 June 2011 M6.4 aftershock had peak ground accelerations (PGAs) exceeding 2g at a seismograph in the Heathcote Valley(Geonet 2011) which created considerable rockfall and cliff collapse especially around the Sumner area. A critical link between Lyttelton Port and Christchurch CBD, referred to as the Sumner-Lyttelton Corridor, was affected by cliff collapse, rockfall and mass movement. Temporary protection in the form of ballasted double and single stacked containers was put in place in the highest risk areas to allow use of the road until permanent remediation or protection measures could be implemented.

This paper will focus on the site work carried out, including shallow investigations and mapping, rockfall modelling and design of the rockfall protection structures for the two highest risk sections along a 1.1 km section of Wakefield Avenue. Jacobs developed a concept design involving two rockfall bunds along Wakefield Avenue to reduce the risk of rockfall to the road corridor for Christchurch City Council (CCC). The concept design was then taken through to a detailed design solution for tendering and construction.

2 SITE DESCRIPTION

2.1 Geology and Topography

Wakefield Avenue runs approximately north-south along the western side of Sumner at the base of Richmond Hill as shown in Figure 1. The slope above Wakefield Avenue rises from approximately 3 m above sea level (masl) at Wakefield Avenue to 170 masl at the crest of the slope. The site geology is typical of the Port Hills and predominantly consists of loess (wind-blown silt), underlain by the Lyttelton Volcanic Group basaltic to trachytic lava flows interbedded with breccia and tuff (Forsyth, P.J. et al, 2008). The joints and defects within the basalt and pyroclastic deposits generally form tabular or

equidimensional blocks, however the jointing is irregular and generally does not form persistent joint sets. The northern end of Wakefield Avenue is dominated by cliffs approximately 60 m tall below Richmond Hill while the majority of the site is typically moderately steep slopes (25-30°) with discrete bluffs along the slope (Engel, 2015). Where the basalt and pyroclastics outcrop on the slopes they form prominent rock bluffs that run across the slope. The loess slopes have developed shallow soil failures, tunnel gullies and debris flows predominantly along ephemeral drainage lines.

2.2 Geohazards

The three main geo-hazards affecting Wakefield Avenue are rockfall or boulder roll, cliff collapse and debris flow. During the 2011 CES, notably the 22 February and 13 June aftershocks, over 15,000 m^3 of debris (Massey et al. 2014) fell from the cliff collapse at the northern end of Wakefield Avenue (Figure 1). Significant ground cracking was mapped through the properties above the cliffs extending up to 50 m back towards Richmond Hill Road (Massey et al. 2014). The results of GNS mapping, modelling and investigations of the area identified 10 debris avalanche (cliff collapse) sources and thus the area was designated a Class 1 Mass Movement Area (Massey et al. 2014). The modelling of the 10 debris sources by GNS identified that only two of the sources have the potential to impact Wakefield Avenue.

At the southern end of Wakefield is a 170 m long continuous bluff below Richmond Hill Road and a smaller mid-slope bluff that were sources of a significant amount of rockfall during the CES (Figure 1). The majority of boulders that fell from these sources during the CES accumulated on the slope and park area at the base of the slope, however approximately 20-25 discrete boulders and some fly rock came to rest on the road with at least 7 boulders rolling across Wakefield Avenue into properties on the eastern side of the street.



Figure 1. The rockfall and cliff collapse hazards affecting Wakefield Avenue are indicated in yellow and red respectively. (Image courtesy of Google Earth Pro, 30 June 2016).

A risk assessment of future rockfall to the Wakefield Avenue portion of the Sumner-Lyttelton Corridor was undertaken (Swatton 2014) and identified four sections where the risk was classed as high to very high. GNS undertook research (Massey et al. 2012) and provided advice to CCC on acceptable levels of risk for different activities to allow CCC to identify what an acceptable level of risk for normal use of Wakefield Avenue would be. The sections of the Sumner-Lyttelton Corridor where the risk was assessed to be higher than medium, some form of remediation or rockfall protection structure was required. This paper focuses on two of the high risk sections on Wakefield Avenue (below the highlighted areas in yellow and red in Figure 1).

3 FIELD INVESTIGATIONS

The majority of the work undertaken on site prior to Jacobs's involvement centred around GPS mapping of rockfall boulders and some at source remediation of rockfall hazards. After the 22 February 2011 event, contractors undertook at source remediation of the continuous bluffs at the southern end of the site, including blasting and rolling loose boulders to the bottom of the slope. The highly fractured nature of the bluffs made this kind of at source remediation difficult, as removing unstable material at the surface often uncovered more unstable material behind. Jacobs mapped fallen boulders – refer Figure 2(a) and (b) – to identify run out distances and sizes of the boulders which were compared to the information used in the GNS pilot study (Massey et al 2012a) to determine what size boulders the remediation solution would be required to stop. It was difficult to determine which boulders fell as a result of the earthquakes and which had fallen from the source treatment works. Regardless, they all provided information on the size of boulders and run out distances that could be expected at road level.



(a) (b)

Figure 2. (a) This boulder is approximately 3 m^3 and is the result of rockfall from the continuous bluffs at the southern end of Wakefield Avenue; (b) This boulder fell as a result of the cliff collapse at the northern end of Wakefield Avenue. The boulder has landed at the base of the cliff immediately below where it was located; it has not rolled out towards Wakefield Avenue.

4 ROCKFALL ANALYSIS

Rocscience ® RocFall 5.0™ software was used to analyse the rockfall hazard along seven cross sections at the two locations where rockfall protection structures were proposed. Ground profiles were generated using LiDAR data flown by the Earthquake Commission (EQC) with the slope surface material properties used in the model based on information published by GNS (Massey et al. 2012a, Townsend et al. 2012a) and from Jacobs's site investigations. RocFall™ models rockfall trajectories from designated sources on the slope profile and considers how the boulders interact with the materials they impact on the slope and calculates bounce heights, kinetic energy (translational and rotational) and velocity (translational and rotational). Multiple boulder paths can be analysed simultaneously with the software (in our case 2000 boulder paths per model run). The modelling requires a design boulder size to be defined; for this project the design boulder size was assumed to be the 95th percentile, i.e. only 5% of the boulders that could fall from the site have the potential to exceed that size. In our area there were two different scenarios, cliff collapse and rockfall so two different boulders sizes were used for the modelling.

GNS carried out slope stability modelling of the cliff collapse hazard at the northern end of the site for the 10 individual cliff collapse sources (red and black areas in Figure 1) and identified the potential run out distance of slip material and debris. To determine the energy level and bounce height of boulders that could impact a protection structure during a cliff collapse event, rockfall modelling was undertaken. The 95th percentile boulder for modelling the cliff collapse scenarios was assumed to be the largest mapped boulder that was generated from the cliff collapse, which was 8 m^3.

CCC engineers (Port Hills Geotechnical Group) mapped the boulders that fell as a result of rockfall or boulder roll during the Canterbury earthquakes and aftershocks to produce a database of boulder sizes and run out distances. Based on the database of mapped boulders, GNS determined the 95th

percentile boulder size for the rockfall hazard in Sumner (yellow areas in Figure 1) was 3 m^3 (Massey et al. 2012a).

The results of the modelling were compared to onsite observations of rockfall run out and the mapped boulder database to calibrate the modelling. In general there was good agreement between the modelling and the mapped rockfall giving us confidence the modelling was realistic. A boulder in the order of 3 m^3 was identified in an aerial photo taken after the 13 June earthquake on Wakefield Avenue against a container which compared well with run out distances identified in the modelling. Discussions with residents suggested that the boulder may have been rolled by contractors remediating source material however it provided valuable information on expected run out distance and the size of boulders that could be released from this source. A summary of the modelling results taken approximately from the back (slope side) of the protection structure footprint are provided in Table 1.

Table 1. Summary of modelling results

Location	Bounce Height (m)[a]		Total Kinetic Energy (kJ)[a]	
	Minimum	Maximum	Minimum	Maximum
Cliff Collapse Northern End	1.0	1.5	2,200	2,600
Rockfall at Southern End	1.4	4.4	800	1,200

[a]Bounce height and total kinetic energy values are taken at the back of proposed rockfall protection structure locations.

5 ROCKFALL PROTECTION STRUCTURES

Two options were considered for remediating the cliff collapse and rockfall hazards above Wakefield Avenue: 1) at source treatment, 2) rock fall protection structures, including rockfall bunds and rockfall catch fences. At source treatment of the hazard was ruled out at the cliff collapse site due to the scale of the tension cracking behind the crest of the bluff and the high risk environment for any workforce. At source treatment of the rockfall hazard had been trialled on the continuous bluffs previously and was judged to be unsuccessful.

Both the cliff collapse and rockfall sources have the potential to release multiple boulders in a single event therefore a rockfall protection structure (RPS) in the form of a bund or a fence would provide the most efficient method of reducing the risk to the road. A key requirement of any RPS at this site is the ability to withstand multiple impacts during a single event plus further impacts during aftershocks or prolonged weather events following the main event, before being repaired or cleared. Other important requirements set by CCC for RPS on this project included the design life of the structures to 100 years and the consideration of ongoing maintenance and repair costs in the overall cost of the structure.

5.1 Green Terramesh Bunds

A comparison between rockfall bunds and fences was undertaken to look at the best option for this site. The advantages of a bund over a rockfall catch fence included its ability to withstand multiple impacts without losing too much capacity or height, installation and maintenance did not require specialist contractors or plant, and the costs and time associated with repairing the structure after an impact were lower in most cases. Based on these advantages a decision was made to go with a rockfall bund which could withstand multiple impacts before requiring repair. Research into the type of rockfall bunds typically used for this sort of environment and hazard was undertaken and Green Terramesh (GTM), a product supplied by Geofabrics used both locally and globally to form reinforced rockfall bunds, was identified. The manufacturer of GTM bunds have undertaken full scale field tests on the bunds and the results have been modelled and analysed using Finite Element Method (FEM) to support the design philosophy based on boulder energies and bounce heights. Two options were considered for the finished face of the bund; 1) vegetating the face with grass or native plants to give a more natural, softer appearance, 2) facing the bunds with larger rocks.

Jacobs worked with Geofabrics to design the rockfall bunds using their GTM units. GTM bunds are a modular design meaning they can be scaled to suit the requirements for each site and can be constructed across uneven terrain. The modular nature of the GTM units means that individual sections can be repaired without deconstructing large sections of the bund to make repairs. Repair in a lot of cases, is as simple as stitching a new double twist mesh section and edge cables across the damaged area.

Jacobs worked with Geofabrics to design the bunds to meet the height and impact requirements identified in Table 1. The height of the bund was determined by assuming the modelled impact point occurs at the midpoint of the boulder, then adding the radius of the boulder (to get to the top of that boulder impact) plus a minimum "freeboard" equivalent to one boulder radius above the top impact point of the boulder (Maccaferri 2012). For example, if the boulder is 3 m^3 with the dimensions 2 m x 1.5 m x 1 m and a bounce height of 1.2 m, 1 m is added to get the top point of the boulder that impacted the bund half the longest side of the boulder) then 1 m freeboard is added for the radius of the boulder, meaning the minimum bund height needs to be 3.2 m tall. The minimum crest width of a GTM bund is determined by the amount the design boulder would penetrate into the bund and the modelled bounce height. The minimum width at the point of impact recommended by Geofabrics is 2 times the penetration depth determined from a correlation between boulder radius and energy level (Maccaferri 2012).

5.2 Cliff Collapse Hazard

A rockfall bund at this location would need to withstand bounce heights up to 1.5 m above ground level (magl) with a total kinetic energy up to 2,600 kJ as indicated in Table 1. The RPS designed for the cliff collapse hazard was a 3.6 m high GTM bund 132 m long with 70 degree slopes. A minimum crest width of 1.5 m was specified to accommodate the high energy levels and maintain the minimum width of the bund at the location of a boulder impact. Based on feedback from the community, this rockfall bund was to be faced with greywacke cobbles.

5.3 Rockfall Hazard

The length of area affected by rockfall hazard is 252 m and the distance the road is from the base of the slope varies considerably. As indicated in Table 1, the bund would need to be able to accommodate boulders with bounce heights between 1.4 and 4.4 m and with a total kinetic energy up to 1,200 kJ. At the northern end of the affected section, the road is as close as 5 m to the base of the slope, compared to up to 55 m at the southern end. At the northern end, the boulders are modelled as bouncing off the steep rock and soil faced bluffs and impacting the bund at 4.4 magl, these boulders aren't actually bouncing 4.4 m. At the southern end of the section the bounce heights are up to 1.4 magl.

The GTM bund designed to mitigate the rockfall hazard at this area is 3.6 m high with 70 degree slopes and a minimum crest width of 1.5 m from the southern end until the bund is 10 m from the toe of the slope. When the bund was within 10 m of the toe of the slope, the bund is stepped up to 6 m high to accommodate the higher bounce heights. Due to the limited space between the base of the slope and the road, the sides of the bund needed to be steepened to 80 degrees to minimise the footprint and still maintain the minimum crest width of 1.5 m. Based on the consent requirements, this bund needed to have a vegetated face where possible. Where the bund has 70 degree slopes, the face was to be vegetated by native plantings. Where the bund face is stepper than 70 degrees, to maintain stability, the face was finished with greywacke cobbles.

6 IMPORTANT CONSIDERATIONS FOR ROCKFALL BUNDS

Through the process of designing and constructing the rockfall bunds a few key design considerations and lessons were learnt. A detailed topographic survey of the bund footprint and the surrounding area is recommended as small variations in topography along the length and width of the bund can have a significant impact on the volume of soil to be excavated. As rockfall bunds are typically installed at the base of, or on a slope they will affect stormwater flow. Stormwater design is important to ensure the bunds don't start acting as a dam, retaining water. This is also where a detailed topographic survey becomes important. As the bunds can cover a large area, both in length and width, it is crucial to identify any services in and around the bund location. Both underground and overhead services can have an impact on the bund location or, if the location can't be altered, relocating affected services which can lead to significant programme delays and costs if not addressed early in the design.

Rockfall bunds are only constructed in areas where there is a risk of being hit by boulders, therefore developing appropriate construction, maintenance and repair methodologies during the design phase is important. Safe construction methodologies, reducing the risk to the construction team, may impact the layout of the bund and should be considered early in the design.

7 CONCLUSION

The 2010/11 CES, notably 22 February and 13 June 2011, created significant instability in the Port Hills and along the Sumner-Lyttelton Corridor. The Wakefield Avenue section of the Sumner-Lyttelton Corridor was affected by cliff collapse, in particular at the northern end of Wakefield Avenue and rockfall or boulder roll, in particular at the southern end. Jacobs were involved in taking a concept design of mitigation measures to reduce the risk to Wakefield Avenue and develop it into a detailed design and supporting the client with construction supervision. Rockfall modelling of the 95th percentile boulder for the two different hazards was undertaken to determine the bounce height and energy levels of boulders that could impact Wakefield Avenue. The results of the modelling were compared to mapped boulders (i.e. real data from the earthquakes), to check that the results were realistic.

After considering remediation options including at source treatment of the hazard, rockfall catch fences and rockfall bunds, it was determined rockfall bunds would best meet the design life and multiple impact requirements. Jacobs worked with Geofabrics to design GTM bunds for the cliff collapse hazard and rockfall hazard. The results of the modelling of the energy levels at the cliff collapse were used to design a 132 m long, 3.6 m high rockfall bund with 70 degree, rock faced slopes to reduce the risk to an acceptable level. The results of the modelling for the rockfall hazard indicated higher bounce heights at the northern end due to the closer proximity to the bluffs at the base of the slope. The rockfall bund at the southern end is 252 m long, 3.6 m high with 70 degree slopes until the boulder gets 5 m from the base of the slope where it steps up to 6 m high with 80 degree slopes.

Important considerations identified during the design of the rockfall bunds were that a detailed topographic survey is required, stormwater needs to be managed and that service clashes need to be identified early to allow changes to the design or relocating the services. Safety in construction, maintenance and repair in case of impact needs to be addressed early during the design phase.

8 ACKNOWLEDGEMENTS

This project was undertaken for CCC and NZTA as part of their Sumner-Lyttelton Corridor reopening. The collaborative and open approach by all parties through the design process and managing challenges on site allowed a quick and successful delivery of the project. The author would like to thank all those involved in the project.

REFERENCES

Engel, J. M. and Watts, C. (2015). *Sumner-Lyttelton Corridor: Wakefield Ave Design Report*. October 2015, Jacobs New Zealand Limited.

Forsyth, P.J., Barrell, D.J.A and Jongens, R (compilers) (2008). *Geology of the Christchurch Urban Area Map*: scale 1:25,000. Lower Hutt: GNS Science. Institute of Geological & Nuclear Sciences 1:25,000 geological map.

Geonet (2011) "June 13 2011 - Large earthquakes strike south-east of Christchurch: Peak Ground Accelerations for the magnitude 6.3 earthquake." <http://info.geonet.org.nz/display/home/2011/06/13/Jun+13+2011+-+Large+earthquakes+strike+south-east+of+Christchurch>

Maccaferri (2012). *Green Terramesh® Rockfall Protection Embankments, Technical Note*, Rev 02. April 2012.

Massey, C.I., McSaveney, M.J. and Heron, D. (2012). *Canterbury earthquakes 2010/11 Port Hills Slope Stability: Life-safety risk from cliff collapse in the Port Hills*. GNS Consultancy Report 2012/124. May 2012 FINAL ISSUE 2.

Massey, C.I. McSaveney, M.J; Heron, D. and Lukovic, B. (2012a). *Canterbury Earthquakes 2010/11 Port Hills Slope Stability: Pilot study for assessing life-safety risk from rockfalls (boulder rolls)*. GNS Science Consultancy Report 2011/311. March 2012 FINAL ISSUE 2.

Massey, C.I.; Taig, T.; Della Pasqua, F.; Lukovic, B.; Ries, W.; Archibald, G. (2014). *Canterbury Earthquakes 2010/11 Port Hills Slope Stability: Debris avalanche risk assessment for Richmond Hill*. GNS Science Consultancy Report 2014/34, August 2014 FINAL.

Swatton, L. (2014). *Sumner Corridor Route Assessment, Detailed DDSRA – Wakefield Avenue*. Aurecon New Zealand Limited, 30 June 2014.

Townsend, D.H. and Rosser, B. (2012). *Canterbury Earthquakes 2010/211 Port Hills Slope Stability: Geomorphology mapping for rockfall risk assessment*. GNS Science Consultancy Report 2012/15, September 2012 FINAL.

Proceedings of the 11th ANZ Young Geotechnical Professionals Conference – 11YGPC
Queenstown, New Zealand
25 – 28 October 2016

Soil-Pile-Structure Interaction at Lyttelton Oil Berth

A. D. Wallace[1] and H. J. Bowen

[1]Tonkin & Taylor Ltd, 33 Parkhouse Road, Wigram, Christchurch, NZ, PH (03) 363-2440, email: awallace@tonkintaylor.co.nz

ABSTRACT

The Oil Berth at the Lyttelton Port is a critical infrastructure link for the South Island which suffered extensive damage due to the Canterbury Earthquake Sequence of 2010/2011. A replacement Oil Berth is proposed. Design of a new wharf presents three key challenges: (i) keeping the existing wharf operational during construction to maintain a steady supply of oil and petroleum products to the upper South Island; (ii) meeting the seismic design criteria for critical post-disaster infrastructure, and (iii) significant dredging of the berthing pocket to future proof the Oil Berth for larger ships.

A finite element slope stability model was created to assess the stability of the slope and to estimate the bending moments, shear forces and displacements of the wharf piles. A back analysis of the slope was undertaken using surveyed slope movements recorded during the Canterbury Earthquake Sequence to establish baseline seismic soil parameters and validate the model. These parameters were used to complete a seismic slope stability analysis for the proposed breakwater. Soil-pile-structure interaction analysis was undertaken to determine the pinning effects of the wharf piles on the slope. The wharf piles were then analysed to determine the demands imposed on the piles by the expected slope movements. Incorporating the pinning effects of the wharf piles in our analysis increased the calculated seismic factor of safety for the existing breakwater to a level acceptable to the client. This work has resulted in the new berthing line being closer to shore without the need for expensive ground improvement works.

1 INTRODUCTION

The Oil Berth at the Lyttelton Port provides petroleum products to a significant portion of the upper South Island and is a critical infrastructure link. The existing Oil Berth is located on the southern side of Lyttelton harbour close to the harbour entrance.

The site is situated on reclaimed land that overlies harbour deposits consisting of soft to stiff silts with medium dense to very dense sands from approximately 40 m depth and volcanic boulders and rock at approximately 50 m depth. The reclamation process involved construction of a breakwater by end dumping quarried basalt gravel on top of the natural sedimentary deposits. Progressive slope failures were reported during construction. Reclamation of land behind the breakwater was then carried out with hydraulic fill dredged from the harbour bed. The reclaimed land overlies harbour deposits consisting of soft silt, which overlies volcanic rock at depth. The volcanic rock consists of basaltic to trachytic lava flows of the Lyttelton Volcanic Group interbedded with breccias and tuff.

The existing Oil Berth suffered significant damage during the Canterbury Earthquake Sequence. Damage was primarily caused by slope movement of the existing breakwater affecting both shore based infrastructure such as oil pipes and the existing wharf structure. The Oil Berth has been deemed uneconomical to repair and a replacement Oil Berth has been proposed. The existing Oil Berth must be retained in an operational manner until the replacement Oil Berth is able to receive oil shipments to maintain a continuous supply of petroleum products to the upper South Island.

At the time of this analysis the proposed location for the replacement Oil Berth was 100 m west of the existing Oil Berth location shown in Figure 1. The water in this area is shallower than in the existing Oil Berth location. Additionally, the replacement Oil Berth is proposed to have a final depth greater than the existing Oil Berth to allow for larger ships with greater drafts to dock. To deepen the berthing pocket adjacent to the proposed replacement Oil Berth location significant dredging must be undertaken.

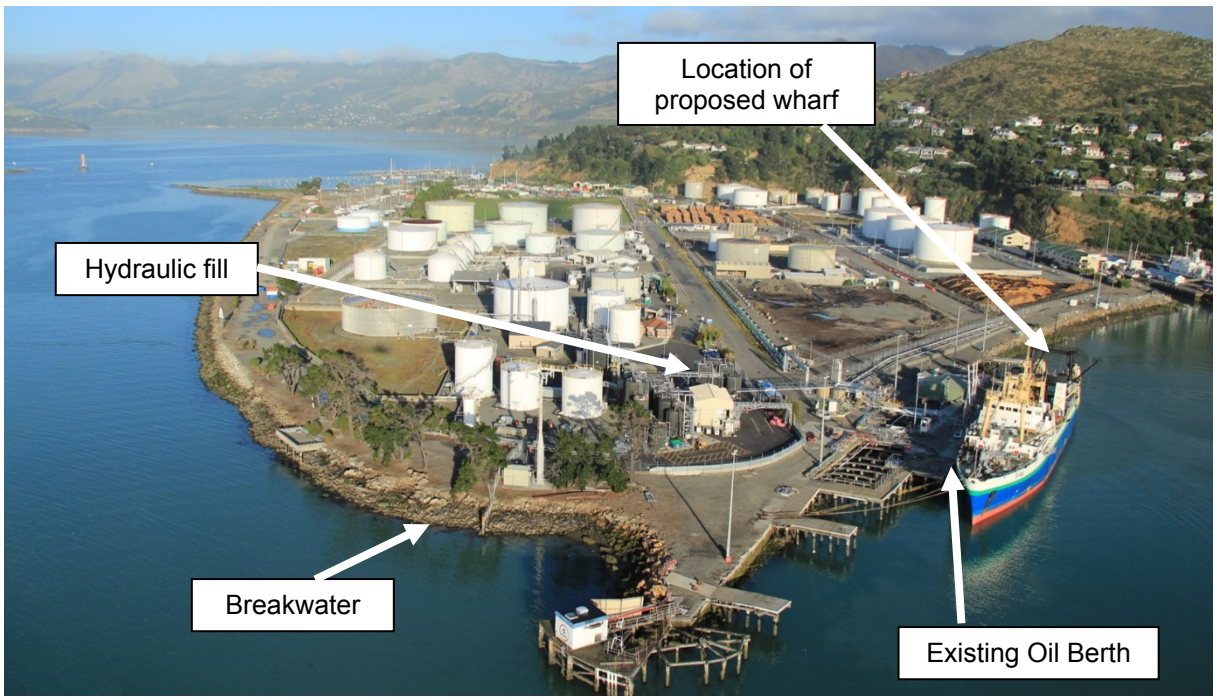


Figure 1. Proposed Oil Berth Location

The replacement Oil Berth and associated breakwater slope must be designed to provide acceptable performance under both static and seismic conditions. Difficulties in achieving acceptable performance include weak natural soils, potentially variable fill material, poor existing slope performance and an increase in slope height through dredging. The berthing line must be kept as close as practical to the shore to reduce congestion within the harbour. Slope stability analysis showed that the static stability and seismic stability of the breakwater are significantly below the level required for critical infrastructure with post- disaster functions.

To tackle this problem we incorporated soil-pile-structure interaction to determine the pinning effects of the wharf piles on the slope and the loads imposed on the piles due to slope movements. This paper presents a summary of the soil-pile-structure analysis.

2 DESIGN METHODOLOGY

2.1 Analysis methods

The analysis was undertaken using the finite element analysis program Plaxis 2D. Factor of safety is calculated in Plaxis using a strength reduction method and seismic yield acceleration was modelled with a pseudo-static acceleration. A Mohr-Coulomb soil model was used within Plaxis.

Seismic slope displacements were estimated from the yield accelerations calculated within the finite element analysis using the method described in Jibson 2007.

Pile demands were calculated based on the soil displacement profiles from the finite element model using the analysis program LPile 2012.

2.2 Design inputs

2.2.1 Performance requirement and design earthquake

Replacement wharf design was undertaken to meet ASCE 61.14. This comprised three design cases Operating level earthquake (OLE), Contingency level earthquake (CLE) and Design earthquake (DE). The seismic performance level considered in this paper is the CLE which requires a similar seismic performance to a Serviceability Limit State (SLS2) earthquake under NZS1170.5 for an Importance Level 4 structure. Following a CLE event the structure must have repairable damage which results in a loss of serviceability for no more than several months.

NZS1170 was used to calculate the design earthquake shaking for a CLE event which results in a horizontal peak ground acceleration (PGA_H) of 0.35g and a moment magnitude (M_w) of 7.5. The target static factor of safety for the slope is 1.5 and the maximum slope displacement is limited by the allowable curvature within the wharf pile elements.

2.2.2 Back analysis of existing slope

The existing breakwater profile was estimated based on the available Lyttelton Port records and the breakwater profile used in the analysis is presented in Figure 2. All levels presented are in metres Chart Datum (mCD).

The yield acceleration of the existing slope was estimated as ky = 0.053g using the slope displacements and strong ground motions recorded during the Canterbury Earthquake Sequence (CES). Soil properties were varied within the finite element analysis until the model matched the estimated yield accelerations. Figure 3 shows a comparison between the measured and modelled displacements during the 22 February 2011 earthquake.

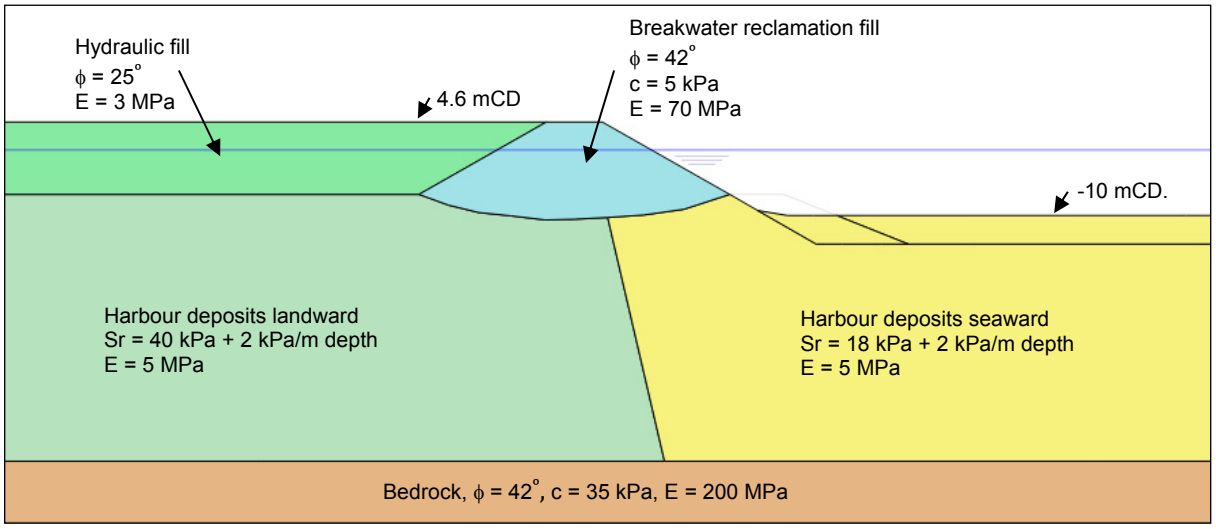


Figure 2. Existing breakwater profile

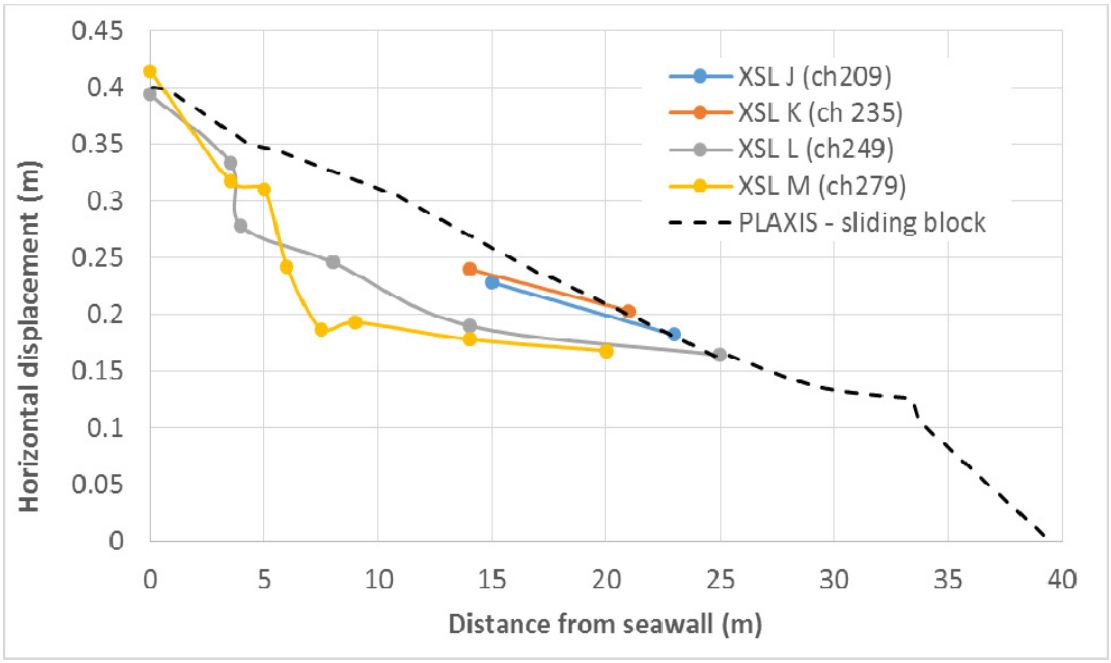


Figure 3. Existing breakwater profile

2.3 Proposed development

2.3.1 Proposed slope profile

The design requires dredging at the harbour to a level of -15.0 mCD. A number of embankment profiles were investigated to improve the slope stability following dredging while minimising the distance between the crest of the seawall and the toe of the embankment. The final embankment configuration consisted of a soil buttress at the toe of the breakwater slope comprising approximately 3 m of fill and 5 m of soil retained from the existing seabed. The soil buttress has an approximate width of 29.0 m.

2.3.2 Proposed wharf pile layout

The oil wharf must be designed to resist vertical loads from the wharf structure and oil distribution infrastructure. Bored concrete piles with permanent steel casings were proposed to transfer vertical loads to rock below and resist lateral loading from docked vessels and seismic slope displacements. The proposed pile layout comprised four rows of 1.2 m diameter piles at a spacing of 6.7 m beneath the approximately 60 m long wharf with a total of 36 piles.

To maintain the berthing line as close as practical to the toe of the embankment the piles were located within the soil buttress. Locating the piles within the slope results in kinematic soil loading on the piles when the slope displaces. The soil loading on the piles is also a load resisting slope movement. The proposed pile layout within the embankment is presented in Figure 4.

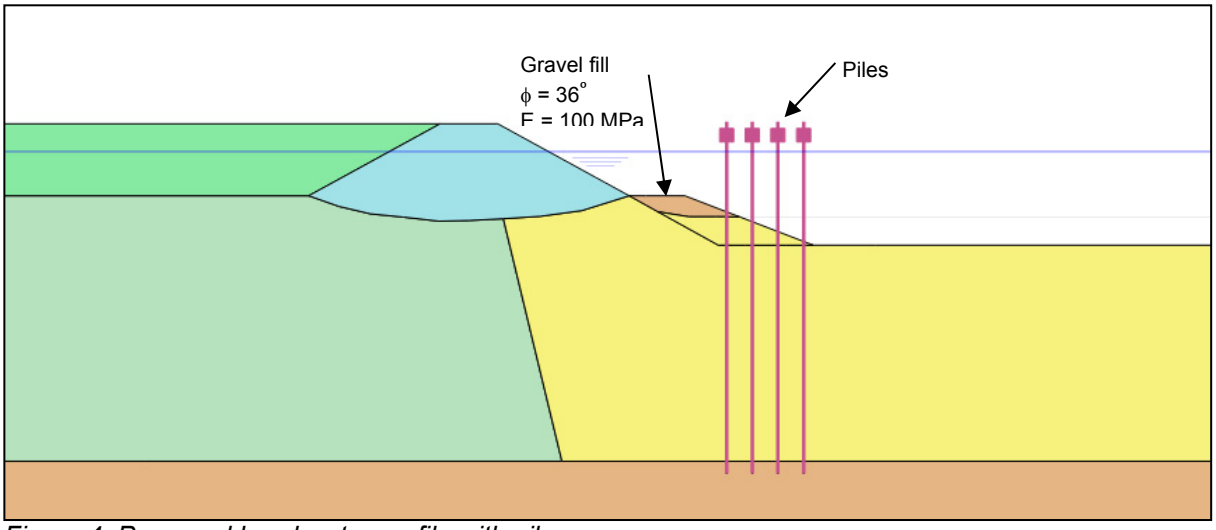


Figure 4. Proposed breakwater profile with piles

3 RESULTS

The predicted failure surfaces of the proposed breakwater profile generated from the finite element model with and without piles effects are presented in Figure 5 and Figure 6. The contours in Figure 5 and Figure 6 show the approximated failure surface only and their magnitudes are not intended to be estimates of seismic slope displacement. Red coloured contours represent larger displacements.

The results of the slope stability analysis include the static factor of safety, slope yield acceleration and predicted displacement under CLE level seismic shaking with 50% and probability of exceedance (POE). The analysis results are presented in Table 1 for the existing breakwater slope, the proposed dredged slope with a fill buttress and the proposed dredged slope including the pinning effects of the piles.

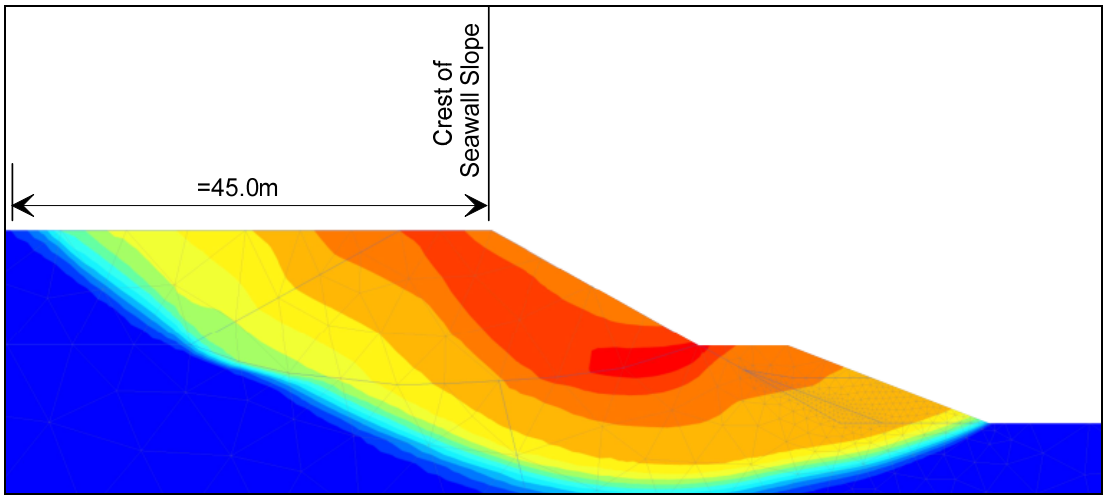


Figure 5. Predicted failure surface without pile effects

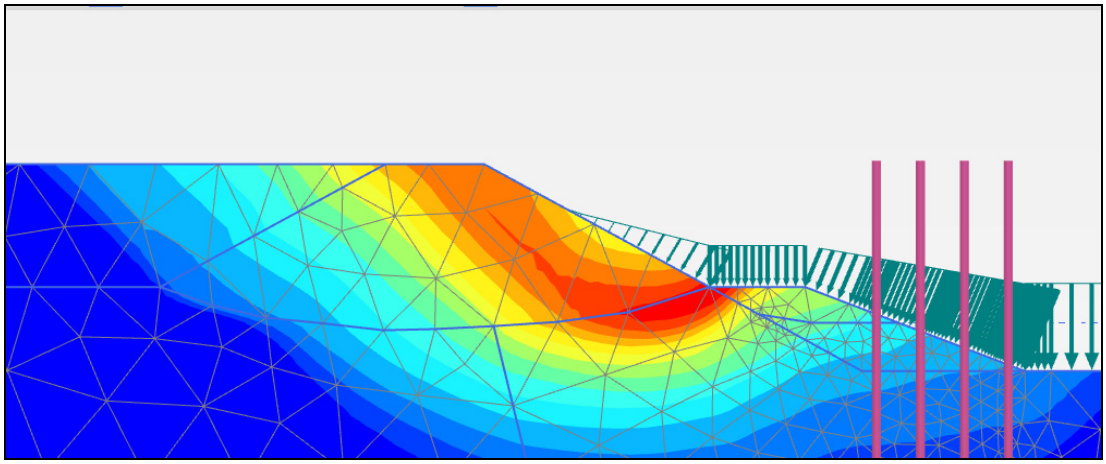


Figure 6. Predicted failure surface including pile effects

Table 1. Summary of existing breakwater analysis results

Design case	Static factor of safety	Yield acceleration	Predicted displacement of breakwater under CLE earthquake 50% POE
Existing Slope of 1V:1.8H	1.21	0.053g	0.33m
Dredging with fill buttress	1.40	0.068g	0.20m
Dredging with fill buttress incorporating soil-pile-structure interaction	1.5	0.070g	0.19m

4 DISCUSSION

When pile pinning effects are included we can see that the critical failure surface becomes a smaller localised failure. This altered critical failure surface results in smaller predicted slope movements at the pile locations as well as a reduction in the shoreward effect of the slope failure.

Restraining effects of the wharf piles were successfully modelled in Plaxis which showed:

- Increase in slope FOS from 1.4 to 1.5.
- Decrease in slope displacement at the pile location from 0.16 m to 0.11 m.
- Reduction in pile bending moments and curvatures, such that they meet CLE requirements in the ASCE code.

If pile pinning effects had not been considered we would have required:

- Additional piles to meet the ASCE curvature requirements
- Ground improvement at the base of the slope to achieve the static FOS of 1.5 required by the ASCE code.

5 CONCLUSION

This case study presents the successful application of advanced analysis techniques to solve a complex geotechnical problem. Using finite element analysis we can estimate the shape of any slope failure and use this to refine our design.

Consideration of soil structure interaction has allowed us to meet the requirements of the ASCE code without resorting to ground improvement. This has resulted in significant economic benefits to the client.

6 ACKNOWLEDGEMENTS

We wish to thank the Lyttelton Port of Christchurch for permitting us to publish the results of our studies.

REFERENCES

American Society of Civil Engineers. (2014). *Seismic Design of Piers and Wharves*, ASCE/COPRI 61-14.
Standards New Zealand. (2004). *Structural Design Actions Part 5: Earthquake actions – New Zealand*, NZS1170.5:2004.
Tonkin & Taylor Ltd (2016). *Lyttelton Port Replacement Oil Berth – Geotechnical Factual Report*, June 2016.
Tonkin & Taylor Ltd (2016). *Lyttelton Port Replacement Oil Berth – Geotechnical Interpretive Report*, August 2016.

Proceedings of the 11th ANZ Young Geotechnical Professionals Conference – 11YGPC
Queenstown, New Zealand
25 – 28 October 2016

Managing Client Expectations for Central North Island Infrastructure Designs

J. Kelly[1], B. A. Curley[2] and B. Simms[3]

[1]GHD Limited, PO Box 1746 Wellington, 6140, New Zealand; PH (04) 495 5416; email joe.kelly@ghd.com
[2]GHD Limited, PO Box 1746 Wellington, 6140, New Zealand; PH (04) 495 5832; email: beverley.curley@ghd.com
[3]GHD Limited, PO Box 1746 Wellington, 6140, New Zealand; PH (04) 495 5831; email: bruce.simms@ghd.com

ABSTRACT

As geotechnical professionals, we are often constrained by our client's expectations of timeframes, fees and scope, along with their physical works budget. Often the fees and scope don't match up. We are required to manage our client's expectations, whilst understanding their project objectives and level of knowledge. This paper looks at the challenges of designing mechanically stabilised embankments for road widening projects whilst not being able to directly interface with the client. The two example projects covered in this paper are roading projects and both based in the central North Island of New Zealand.

Case study 1 involves a 400 m section of SH1 with a maximum embankment height of 5 m. Case study 2 comprises an 80 m long embankment with a maximum height of 8 m, and a client requirement to use material excavated from site for fill. Both projects have geogrid reinforcing and subsoil drainage, and both require large undercuts for shear keys. This paper follows these projects through investigation, testing, analysis and detailed design, and highlights challenges faced by client management and design as a young geotechnical professional.

Keywords: Client Communication, Workshop, Ground Investigation.

1 INTRODUCTION

Mechanically Stabilised Embankments (MSE) are often seen as an economically viable solution for large stabilising or retaining problems. Our client's project managers required the design of MSE for both of the following road widening case studies. With the desirable outcome being the design and build of an MSE using locally sourced backfill material for a cost effective solution.

Two case studies are discussed in this paper. Both are located within the central North Island with varied natural and anthropogenic hazards, and with different geotechnical risks due to geological settings. Global stability analyses for each stage of the proposed construction were carried out for each site. In both case studies initial client communications were not direct to the designers. See Figure 1 for communication hierarchy.

The initial project understanding for Case Study 1 was detailed design of an MSE to span the entire 400 m section of State Highway 1 (SH1), with no indication of capital cost requirements expressed through the communication hierarchy to the design engineers. Detailed design was to be completed by 24 December 2015 and built within the 2015/2016 financial year.

For Case Study 2 the City Council (CC) project manager initially wanted quick, cheap and minimal ground investigation immediately preceding the detailed design on an MSE. The design engineers advised through the client relationship manager (CRM) the likely over conservative design risk and potential redesign cost implications if a thorough ground investigation was not completed. The scope changed from a detailed design to a preliminary design without ground investigation data, to be let for tender. The CC project manager wanted the ground investigation completed during the tender period, immediately followed by the detailed design of a MSE. Construction of the MSE was intended for early 2016.

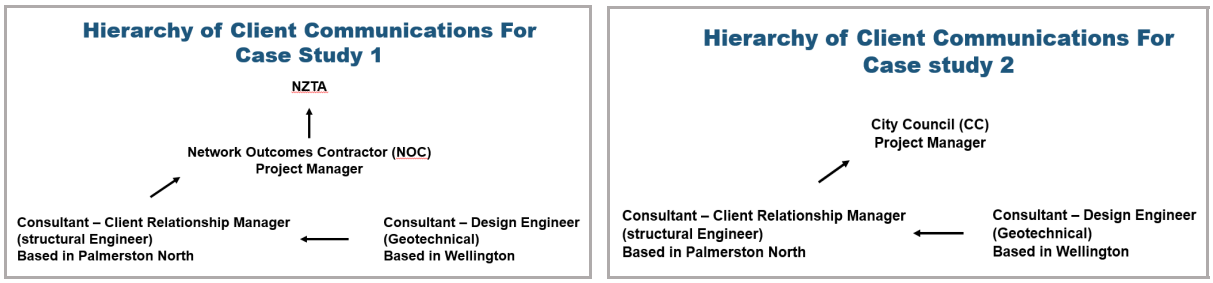


Figure 1. Hierarchy of client communications for case studies 1 and 2.

2 CASE STUDY 1 - SH1 ROAD WIDENING

It was proposed to widen SH1 by 2-4 m over a 400 m length of road. This was to be achieved by extending, steepening, and reinforcing an existing 5 m high embankment while also installing a road safety barrier. A two-week period was allowed to complete the geotechnical investigation, desktop study, slope stability assessment, detailed design of MSE, construction drawings, specification and schedule of quantities.

The existing slope was a raised fill embankment with steep slopes (max 55°) and up to 5 m in height. The existing road height was to be maintained but the slope steepened to 65° using MSE techniques.

2.1 Geology and Topography

The existing road embankment is partially located on Quaternary aged undifferentiated landslide deposits underlain by Pleistocene age river gravels and fan deposits (Townsend and Kamp 2008). The existing road is constructed on a raised fill platform in most areas along the 400 m section for stabilising which falls towards neighbouring rural properties and the local sewage treatment plant. The 400 m section of road is mostly comprised of locally sourced fill with areas in the northern section which alternates from natural ground to fill.

2.2 Geotechnical Investigation

The ground investigation was heavily constrained by the tight timeframe and budget. The investigation points were determined where changes in height, slope angle, and signs of instability were present. A series of nine hand augers and associated Scala Penetrometer tests (scalas) were conducted with an additional five scalas being carried out independent of the hand augers. The general stratigraphy across the embankment can be described as fill consisting of silt with trace sand and silty sand. Organic silty material was encountered at the toe of the embankment slope in a number of places.

2.3 Geotechnical Analysis

As no laboratory testing was carried out the material geotechnical properties were assumed based on experience and published values for similar materials. To assess the stability of the existing and proposed embankment, stability analysis was carried out using Slope/W software on a series of cross sections. The Morgenstern-Price method was adopted due to its applicability to the failure mechanisms expected from the ground model (Fedlund and Krahn 1977).

The asset (new embankment) was assigned an Importance Level (IL) of 3 in accordance with NZS 1170.0:2004 and the New Zealand Transport Agency's (NZTA) Bridge Manual SP/M/022, 3rd Edition. The peak horizontal ground acceleration (PGA) was taken as 0.63 g, calculated using both NZS 1170.0:2004 and the NZTA Bridge Manual (3rd Edition). A reduction factor of 0.5 was used to reduce the PGA to 0.32 due to both the existing embankment and proposed MSE being classed as non-rigid/flexible structures where the reduction factor levels off the over-conservative and overestimated PGA calculations for (rigid) retaining structures (NCHRP Report 611 2008).

Due to the shallow very limited ground investigation and lack of reliable in situ geotechnical data, a conservative design approach was employed to minimise the resultant risk. The proposed MSE was assessed for global stability for drained and undrained seismic and static load cases similar to the

pre-excavation analysis. The results of the stability analysis indicate that the existing slope would fail under seismic conditions.

The stability analysis was carried out on five cross sections chosen to assess the more geologically challenging sections while providing coverage of the site. The existing embankment cross sections were analysed under static conditions with 12 kPa traffic surcharge, and seismic conditions with the applied PGA. The factor of safety (FoS) results were below equilibrium (1.0) and would be subject to some degree of failure during a seismic event under the modelled conditions. The failure in seismic conditions and the requirement for additional width justified the reinforcement of the carriageway verge to stabilise the slope.

2.4 Embankment Design

The 400 m chainage site area was broken up into three sections (A, B, C) based on the pre-excavation analysis, different slope geometry and soil parameters. The designs varied based on face height, available space, soil conditions and material encountered during the ground investigation.

An undercut / shear key was required due to poor founding conditions, and to reduce the length of geogrid in tight areas. Subsoil drains installed parallel to the back cut would effectively drain the subgrade material with the pipes draining the flow past the toe of the MSE to reduce the risk of erosion or subgrade softening. The proposed MSE increased the existing FoS to above the design threshold of >1.0 under seismic conditions, and >1.5 under static conditions for a slope in equilibrium.

2.5 Design Outcomes

Detailed design for the proposed MSE was completed within the extremely tight timeframes as required by the client. Given the limited timeframe and geotechnical investigation, the client accepted the residual risks relating to deep seated instability, temporary works stability, culvert design, guardrail design, amendments to the design as a result of utility company requirements, and lack of settlement and liquefaction analysis. A number of these issues could have been addressed with a more comprehensive investigation phase and a longer analysis and design timeframe.

Ideally in addition to a more reasonable timeframe, a workshop between the design engineer, the CRM, and the Network Outcomes Contractor (NOC) project manager would have been very beneficial as other types of retaining structures could have proved suitable. Also geotechnical risks could have been explained directly to the client, and the client's risk profile could be better understood by the design engineer. However, the request for a workshop was declined. The MSE design met the client's requirements and design criteria, but it was later deemed by the CRM to be too expensive, specifically the volume of backfill for the shear key undercut.

Communication between the NOC project manager, design engineers and CRM opened up following the completion of the MSE detailed design. A new design was requested, that of a retaining wall, which would be more in line with the client's budget. The proposed design life was discussed with a view to be more flexibility. It was intended by the CRM and the NOC project manager that reducing the design life and subsequently the PGA would allow for the design of a less robust structure at a higher risk profile and hence a reduced construction cost. The CRM pushed for the lower of the design life, resulting in the design engineers request for written approval from the asset owner (NZTA) that reduction in design life was acceptable.

Three design options were presented to the client:

i. 100-year design life for the majority of the site;
ii. 25-year design life for the majority of the site: and,
iii. 50–year design life for critical areas were remediation and upgrade where most required.

Option (iii), the critical areas option, was chosen by the client as it addressed the high risk areas and was constructible within the available budget. The NOC project manager had the opinion that a letter allowing the design life reduction would not be attainable from the NZTA. Had this conversation been able to be had between the designers and the client earlier in the project, the subsequent redesign could have been avoided.

2.6 Tied Back Retaining Wall

The critical areas consisted of three retaining walls totalling 50 m in length at areas where shallow seated failures had occurred previously. The tied back retaining wall maximum face height was 1.50 m.

The critical sections were re-analysed using the same soil parameters with changes in the geometry and design life. The Importance Level was brought down to IL 2 due to the reduction in area and height of the structures. This allowed for a lower PGA of 0.32, and with an applied 0.5 reduction factor the PGA was reduced to 0.18 g. Slope/W was used to check the global stability of the proposed retaining wall design. WALLAP software was used to design the retaining walls. The model was analysed using undrained (long term) and drained (short term) seismic conditions for all of the sections.

2.7 Case Evaluation

The design brief provided to the design engineers via the CRM changed significantly from the start of the project to the end tied back retaining wall design. The second design allowed for direct contact through workshops between the NOC project manager and the design engineers to establish the design parameters, tie in the re design scope of works, total capital cost, and new timeline.

Construction of the critical areas tied back retaining walls was completed within the financial year and well within the available budget of the NOC project manager. The tied-back retaining wall construction fees were 60% less than the initial MSE design, plus there was the addition of re-design fees.

3 CASE STUDY 2 – LOCAL ROAD WIDENING

Case study 2 was located in an area undergoing a transformation from a rural setting to more urbanised. The road widening was required for a new footpaths and cycleway. Several retaining structures including an 80 m section were required along with an existing unreinforced embankment with height varying between 8 m to 2.5 m.

The scope of the work was preliminary design and detailed design, followed by tender. The preliminary design was completed prior to any ground investigation, due to the client's desire to go to tender so that works could be completed within the financial year. The detailed design phase incorporated the geotechnical investigation and allowed for a refined ground model and robust design.

3.1 Site Description

The site is situated on an old river terrace 1.7 km north of the Manawatu River in a rural setting outside the flood risk zone. The terrace edge riser crosses the design area, resulting in predominantly flat land on either side of the steep terrace slope. A drainage pond and ephemeral stream were present at the base of the slope. At the toe of the embankment was moderately to well sorted alluvial flood plain gravel, commonly overlaid by over bank deposits and, poorly to moderately sorted gravel with minor sand or silt sometimes weathered, underlying a terraced surface, and/or overlying loess/paleosol couplets (Lee and Begg 2002). Gravelly silts were exposed in the terrace slope. The slope steeply dips between 25° - 40°, towards the alluvial flood plain deposits. The southern section of the widening area was underlain by fill placed at the time of the road construction.

3.2 Preliminary Analysis

The design soil parameters were determined (in absence of field and laboratory test data) by utilising the strength parameters for similar geological units based on experience, local knowledge and published values for similar materials.

The slope stability analysis was carried out using Slope/W. The importance level for this structure was determined to be Level 2 due to its intended road user volume and in accordance with NZS 1170.0:2004 and NZTA's Bridge Manual (3rd Edition). A traffic surcharge of 12 kPa was applied on the top of the embankment. For seismic conditions a PGA of 0.35g was applied to calculate the

embankment's FoS against global stability. The PGA was further reduced by 0.5 to 0.18 g as the embankment was classed as a non-rigid/flexible structure (NCHRP 2008).

The existing unreinforced embankment global stability results were found to be >1.5 FoS under static conditions, however FoS under seismic conditions were <1.0 FoS warranting the design and construction of a slope retention measure for the widening. The proposed preliminary MSE design with a shallowing in slope angle, benched shear key undercut and reinforced geogrid with site sourced material as fill was required to achieve >1.0 FoS under seismic conditions.

3.3 Preliminary Design

The client's timeline required a preliminary MSE design to be completed prior to a ground investigation being carried out. The preliminary ground model for this was generated using desk study, aerial photographs, site photos and information gathered by the CRM local consultancy staff. Material outcrops observed along the terrace and around the site were also used in the absence of intrusive geotechnical data. The main slope stability problem centred on the existing uncontrolled fill at the top of the embankment on the southern section, poor existing stormwater infrastructure off the road above where the embankment was proposed, along with steep slope gradients along the entire existing embankment.

The completed design was required to widen the road by up to 10 m with a face slope angle of 30°. A benched undercut up to 5.2 m deep with 300 mm compacted GAP 65 was designed with geogrid layers. A subsoil drainage network to drain the back cut of the embankment out to the ephemeral stream was designed. Conservative parameters were adopted in lieu of real investigation data.

The use of site fill was not included in the preliminary design due to the risk involved with the unknown properties of an untested material only sparsely seen on site. The CC project manager through the CRM expressed hope for the available site fill to be utilised in the embankment following confirmation during detailed design.

3.4 Ground Investigation

Once the preliminary design had been issued for tender, there was time to complete the ground investigation. This consisted of a total of five cored machine boreholes with Standard Penetration Tests (SPTs) to update the existing ground model. Following the ground investigation, laboratory testing was carried out (Atterberg limits, Particle Size Distribution (PSD), and Standard Compaction Test. The laboratory testing enabled adjustment of phi and cohesion soil parameters previously adopted and indicated that gravelly silt terrace material could be utilised as fill in the proposed MSE.

3.5 Detailed Design

The stability analyses were run again with the refined soil parameters. Stability analysis results indicated that the proposed embankment configuration satisfied the global stability requirements under all load case previously analysed during the preliminary design phase.

Internal stability analyses were also conducted during the detailed design phase to assess the internal stability of the embankment for the proposed 14 m length geogrid configuration and check for pull out and sliding of the structures under static and seismic conditions.

A liquefaction assessment indicated that for liquefaction to occur, both a seismic and storm event would need to coincide. However, accepted industry standard and convention applies the use of one or the other and not a combination of seismic and 100-year storm event. Therefore, the potential for liquefaction under design criteria is considered negligible.

Finite element (FE) analysis was used to model soil behaviour. A staged construction sequence was modelled to capture realistic deformation behaviour of the embankment. Both static and seismic conditions were analysed using the refined soil parameters. In addition, an FoS using *phi - c* reduction technique was calculated (Khabbaz et al. 2012). The analysis results of the proposed MSE indicated that the deformation under static and seismic condition could be approximately 25 mm and 90 mm respectively. Most of the deformation under static condition is expected to occur during construction.

3.6 Case Evaluation

The communication hierarchy allowed for the early clarification change in the scope and timeline requirements before the design phase had commenced. Ongoing communication between the CRM and CC project manager during the preliminary and detailed design phases allowed information to filter through to design engineers to comprehend the client's risk profile, design parameters and objectives, and budgetary requirements. The detailed design was completed early 2016. Tender was awarded within the financial year, however the construction for the MSE has been delayed until summer 2017.

4 DISCUSSION AND CONCLUSION

Case Study 1's low cost, extremely restricted ground investigation only provided for a limited shallow ground model and a conservative MSE design which also resulted in a design that exceeded the available budget for construction. Case Study 2's lack of preliminary ground investigation, resulted in the design features the CC project manager initially wanted, but at much higher construction cost than initially anticipated, mainly due to the limited geotechnical data used to formulate a detailed ground model. Had sufficient investigations and adequate ground models been able to be produced before design in both cases, this may have saved costs on the design and construction phases of the project.

The client's project manager's design expectations in both case studies were received second hand through the CRM from a non-geotechnical discipline for a large portion of the projects. The level of technical understanding of the CRM, CC and NOC project managers were unknown until well into the design process when conference calls with all parties involved in the designs were approved to clarify design queries including risk profile, design life, importance level, budget, and type of retaining structure.

The CC project manager for Case Study 2 was made fully aware (by the CRM) of the additional cost involved in producing a preliminary design for tender to be updated with a detailed design during the tender period. The intended haste to complete preliminary design in line with letting an early tender to save time, may not have paid off considering the project did not start construction within the originally intended timeline.

The MSE and eventual tied back retaining wall design for Case Study 1 also required additional design fees. The tight timeframe and instructions through indirect communication ultimately led to a design for the MSE with recommendations stating that other retaining structures would offer a cheaper solution (construction), and that construction costs (of the embankment) would likely overrun any reasonable budget. However, the project was successful in completing the construction of the tied-back walls within the financial year as planned and within the available budget.

A direct line of communication with the client was missing in both case studies until well into the design phase, despite being requested several times. A simple meeting between the designers and the end client at the start of the project and at designated hold points, would have provided the clarification required to successfully deliver to the client's expectations. such meetings will be non-negotiable moving forward and will be used to confirm the scope, client's risk profile, design parameters and objectives, and importantly the client's design and construction budget to make sure the resultant design meets the client's expectations.

REFERENCES

Fredlund, D. G. and Krahn, J. (1977). "Comparison of slope stability methods of analysis", *Canadian Geotech. Journal*, 3, pp. 429-439

Khabbaz, H., Fatahi, B. and Nucifora, C. (2012). "Finite Element Methods against Limit Equilibrium Approaches for Slope Stability Analysis", *11th Australia-New Zealand Conference on Geomechanics – Ground Engineering in a Changing World*, Melbourne, Australia, accessed 26 June 2016, http://opus.lib.uts.edu.au/bitstream/10453/19297/1/2011004689.pdf

Lee, J.M. and Begg, J.G. (compilers) (2002). *Geology of the Wairarapa Area*, 1:250,000 scale Geological Map 11, Institute of Geological and Nuclear Sciences Limited, Lower Hutt, New Zealand, 1 sheet + 66 p

National Co-operative Highway Research Program (NCHRP) (2008). *Report 611 - Seismic Analysis and Design of Retaining Walls, Buried Structures, Slopes and Embankments*.

Standards New Zealand (2004). *NZS 1170.5.2004 Structural Design Actions. Part 5 Earthquake Actions – New Zealand*.

NZ Transport Agency (2013). *Bridge Manual* SP/M/022, Third Edition.

Townsend, D., Vonk, A. and Kamp, P.J.J. (compilers) (2008). *Geology of the Taranaki Area*, 1:250,000 scale Geological Map 7, Institute of Geological and Nuclear Sciences Limited, Lower Hutt, New Zealand

Proceedings of the 11th ANZ Young Geotechnical Professionals Conference – 11YGPC
Queenstown, New Zealand
25 – 28 October 2016

The Value of Interpersonal Skills in Geotechnical Projects: a Millennial's Four Year Experience

J. J. Lees, GIPENZ[1]

[1]Tonkin & Taylor Ltd. P.O. Box 5271, Wellesley Street, Auckland, PH (09) 355-0729; email: jlees@tonkintaylor.co.nz

ABSTRACT

As young professionals gaining experience we are faced with greater levels of responsibility. Client interactions, field investigations, preparation of formal documents and drawings, project management and construction supervision are all tasks that come with a myriad of challenges. Add in the complexity of geological materials and it becomes clear why many geotechnical leaders say that the learning curve in geotechnical engineering is steep. The geotechnical engineering world is generally fast paced and opportunities to reflect are fairly rare. When opportunities do present themselves, the focus is often on sharing technical lessons learnt and advancements. This paper is written from a different perspective. It discusses three projects on which the author learnt the value of maintaining a focus on interpersonal skills. From these experiences the author was led to ask: with the first crop of Millennials transitioning into professionals, how could the geotechnical field change with the latest generation? This paper suggests that with the unprecedented level of connectivity in today's world, the current crop of young professionals should put a heightened focus on interpersonal skills like communication, empathy and self-awareness. These skills each help us better understand our clients and can help our clients better understand what geotechnical professionals do. It will also go a long way in helping the young professionals of tomorrow get a stronger foothold on the geotechnical learning curve.

Keywords: Young Professional, Millennial, Geotechnical Experience, Communication, Self-awareness, Empathy.

1 INTRODUCTION

Learning from experience is a cornerstone of personal development in geotechnical engineering. Burland *et al.* (2013) describe how Karl von Terzaghi's fundamental theories of soil mechanics initially developed from learning about the geological conditions at sites where failures had occurred. This principle formed the foundation of his work whereby he kept his theories grounded in experience and observation. Numerous developments have occurred since then but many widely used theories and applications are still based at least partially on empirical evidence. This paper summarises some of the author's key lessons which have been accumulated as a developing young geotechnical engineer in New Zealand since late 2010.

Geotechnical engineering is often described as being part science and part art. Covering a wide range of subject matter, the learning curve for young professionals is steep. A lot of a young geotechnical professional's effort is focussed on avoiding mistakes and there is a heavy reliance on the support from senior practitioners especially as geological challenges vary from project to project. While the author's experience has been no different (with a broad range of technical skills being developed) upon reflection many of the key lessons learnt have been in relation to interpersonal skills like communication, self awareness and empathy. These skills relate to an individual's ability to work successfully with other people and have been applicable across projects.

The author falls into a generation referred to as the "Millennials": a term coined by Howe and Stauss (2009) for people reaching adulthood post 2000. This paper has been prepared to ask: if the latest generation of geotechnical engineers were to place a heightened importance on interpersonal skills, what effect would it have on the geotechnical workplace of tomorrow?

2 BACKGROUND

2.1 Today's Young Professionals – Millennials

Generational researchers study groups of people whose birth dates fall into a particular range of years that cover defining events and related societal changes. Studies often focus on defining 'generation gaps' which are intergenerational differences in mindset and opinion. Howe and Strauss (2009) summarise approximate bounds of birth years for different generations based on the demographic research they carried out. The generations are summarised in Table 1 below.

Table 1. Generational bounds in chronological order (as defined in Howe and Strauss, 2009)

Generation Name	Range of Birth Years	Description
The GI Generation	1901 to 1924	The generation born over the period spanning World War I (WWI)
The Silent Generation	1925 to 1942	A comparatively small generation who were born amongst the great depression and World War II (WWII)
Baby Boomers	1943 to 1960	Widely known term for those born during the post WWII baby boom which lasted approximately 20 years
Generation X	1961 to 1981	Generation defined as those being born after the baby boom
Millennials	1982 to present	Defined by researchers William Strauss and Neil Howe and often described as the offspring of the baby boomer generation

Millennials have a grown up in a period of rapid technological development and are often defined by their unprecedented level of connectivity (with the development of the internet and social media). Millennials are also the young geotechnical professionals of today. Engenerate, the Institution of Professional Engineers New Zealand's young professionals programme is targeted towards graduate engineers under the age of 35. At present that would mean the eldest Engenerate member was born in 1981 (corresponding with Howe and Strauss's generational bounds). Any "generation gaps" are likely to develop over the next few years as the profession's demographic changes and the proportion of professional Millennials increases.

2.2 Interpersonal Skills

2.2.1 Communication Skills

Ashkenas (2011) suggests that organisational inefficiencies associated with poor communication are widespread (particularly for those larger in size). In geotechnical engineering, inadequate communications are often the principal source of problems in both design and construction. With there now being numerous platforms to communicate on than was traditionally the case, effective communication is becoming an ever important skill for workers in any sector. For better or for worse, communication is now expected to be frequent, rapid and not limited to traditional working hours. Hewlett (2014) describes effective communication as one of three fundamental leadership traits. No matter how technically sophisticated an individual is, if they are unable to communicate that to anyone else they are working with then this ability can become redundant. Effective communication does not just allow knowledge to filter through an organisation but it can improve an individual's performance through understanding. Ashkenas details three key development areas for individuals to better communicate through any mode: (1) Providing a clear context (2) Making allowances for a dialogue to occur and (3) Connecting and understanding your audience.

2.2.2 Empathy or "Emotional Intelligence

"People are your greatest asset". Butler and Chinowsky (2006) quote this commonly used phrase in the services industry which is particularly true for engineering consultancies. The understanding of a person's suitability for a position has broadened over time to include a wider range of attributes (beyond the intelligence quotient – IQ). This includes what has been termed emotional intelligence (EI or EQ). The core idea is an individual's ability to empathise. The Oxford dictionary defines empathy as

the ability to understand and share the feelings of another (i.e. an emotional intelligence). Wilson (2015) and Wilcox (2015) describe their research which indicates that empathy is becoming and increasingly valuable attribute for career success.

"Empathy enables those who possess it to see the world through others' eyes and understand their unique perspectives"

2.2.3 Self-Awareness

Self-awareness is the understanding of one's own motivations and behaviours and it is strongly linked the ability to empathise (Wilcox, 2015). This idea is linked to two competing parts of the brain – the neocortex (a part of the brain linked to the IQ and memory) and the amygdala (part of the brain associated with emotions which has a faster response time). Wilcox describes how an individual's level of self-awareness determines the ability for emotions (and the amygdala) to override ones logical ability (the neocortex). In a video interview co-produced by the New Zealand Herald and the Auckland University Business School, leadership expert Dr Lester Levy discusses a regular ritual of self-checking by which people can keep themselves self-aware in the face of challenging situations.

3 KEY EXPERIENCES AND INTERPERSONAL LESSONS LEARNT AS A YOUNG PROFESSIONAL

3.1 General

Uncertainty, risk and variability are all characteristic of the geotechnical projects. The author has learnt many geotechnical lessons on successful projects but the valuable ones have often come when things have not gone to plan. The most widely applicable have been those related to understanding and working with other people (one of the few constants between geotechnical projects). The following sections summarise the main geotechnical projects on which the author learnt the value of effective communication, empathy and self-awareness.

3.2 Lesson 1: Learn to communicate in ways that others understand

It would be short sighted to say geotechnical engineering can be completely explained to people with any level of experience. However, to a degree, complex concepts can be made accessible to people of varying levels of expertise. The liquefaction studies carried out in the aftermath of the Canterbury earthquakes are an example of how a deliberate effort to communicate a complex subject in as simple terms as possible can (a) engage a wider audience and (b) lead to technical advancement.

The author has had extensive exposure to liquefaction research including the involvement in the Canterbury liquefaction vulnerability study for New Zealand's Earthquake Commission and the subsequent ground improvement trials. While some amazing technical insights have been gained from the case studies assessed in Canterbury, what was equally impressive was the widespread uptake of liquefaction theory and the interest that generated amongst the geotechnical community in New Zealand. In the not so recent past, programmes for geotechnical conferences in New Zealand were inundated with papers related in some way to seismic ground response or liquefaction.

The author's experience in this domain developed over approximately three years (including two as a student) and it reached the point where the author could participate at conferences with leading academics from around the globe. It was realised very early on that developments during the recovery would need to reach a wide audience (ranging from residential property owners with no experience to global geotechnical experts). A lot of academic effort went into effectively communicating research findings for widespread understanding. This was large reason why the author had the ability to rapidly develop a comprehensive understanding of liquefaction in Canterbury. Figure 1 below is an example of figures from the Earthquake Commission's residential ground improvement report where complex ground improvement methods were communicated to the reader in a readily consumable way.

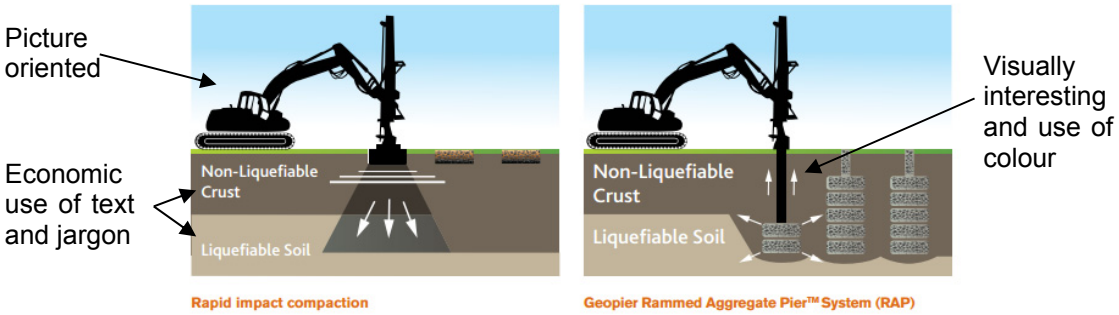


Figure 1. Figures used in the Earthquake Commissions ground improvement trials report which simplify ground improvement techniques for consumption by audiences of various experience levels (reproduced from Earthquake Commission, 2015).

3.3 Lesson 2: Empathise with those that surround you

In June 2015 the Whanganui region was hit with severe weather causing widespread flooding and landslips (Figure 2). The author travelled down in the immediate aftermath to assist with assessing the damage and reporting back to the Earthquake Commission. Seven out of the eight properties visited on that project were 'red-stickered' by the Whanganui District Council to signal that the dwellings on the site were unsafe to enter because of structural damage and the high risk of additional land movement. Upon arriving at each property you would hear a new story of people being forced from their homes and being left with the uncertainty of whether they would be able to return to their homes as they knew them. By visiting each property and listening to each story first-hand you could get a small sense of the fear, loss and helplessness that people were experiencing. It is in these situations that empathy is so important because it is what motivates geotechnical engineers (or other professionals) to use their expertise to help people in need and contribute to the greater good of society. In the case of the Whanganui flooding recovery, the reconnaissance team went above and beyond the call of duty for the residents, by working late into the night to maximise the number of visits undertaken.



(a) *(b)*

Figure 2. Photographs of the damage observed during the reconnaissance in early July 2015. (a) Debris which had inundated dwelling and accessway; and (b) landslip headscarp observed within a few metres of a dwelling.

In events like the one experienced in Whanganui, emotions can run so high that anyone would be able to empathise with the people in need. What is often neglected though is that there is no limit to our capability to better understand the people that we interact with. Whether it is assisting a colleague who is learning a difficult geotechnical lesson on a challenging project; a structural engineer needing geotechnical input to complete a design in a tight time frame; or even the client who is chasing you for a deliverable the week before you planned to have it finished; we can always exercise more empathy as people and as geotechnical engineers. Furthermore, putting empathy into action makes our work better-fulfil a specific need and makes us easier to work with.

3.4 Lesson 3: Be actively self-aware

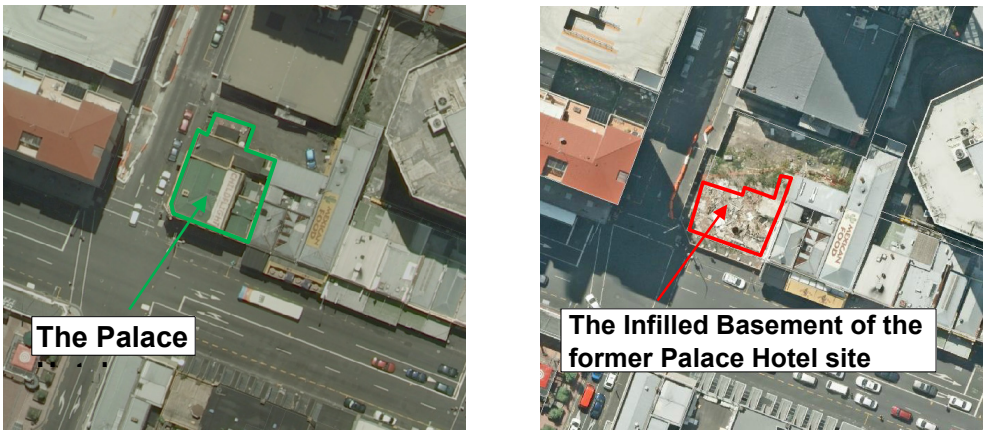
The author discovered the value of being self-aware while volunteering in the 2014 New Zealand General Election. The mandatory initial training session was taken by the manager of polling for the

electorate. This person was responsible for coordinating an extremely diverse workforce. What was immediately evident was the manager's ability to convey a common message to such a diverse group and the patience with which she explained things to those who did not understand. During question time at the conclusion of training one colleague asked: "How hard is it to bring together people with such different backgrounds to carry out a common task?" Her reply was incredibly insightful.

"In my experience, not many people come to work with the intention of doing a bad job"

It was clear that this mantra was the reason why she deeply understood how her behaviour could influence others. This epiphany caused the author to take a step back to assess how daily interactions with people in the geotechnical field were taking place. This was initially a very unnatural 'self-check and self-correction' process.

The process of maintaining self-awareness was particularly challenging on a residential apartment project at the site formerly occupied by Auckland's historic Palace Hotel. Whilst under renovation in November 2010 the structure began showing distress. In the end, the structure needed to be demolished to protect the public and the neighbouring buildings. Figure 3 shows the site's state before and after the demolition (note: much of the debris was loosely placed into the basement void to prevent further short-term damage to the neighbouring road reserve and buried services).



(a) 2008 *(b) 2010*

Figure 3. View of the 75 Victoria Street West site before (2008) and after (2010) the emergency demolition (aerial imagery sourced from the Auckland Council GIS viewer)

The site was acquired by residential property developers who proposed 24 storey apartment tower be constructed on the site. The author was involved delivering the geotechnical aspects of the project from investigation through design and construction. The challenges at the site included:

- The presence of highly variable demolition rubble across the southern half of the site;
- Potentially explosive acetylene welding tanks left within the basement prior to demolition;
- A sensitive cast iron water main in the Victoria Street West road reserve;
- Remnant foundation piles buried under the access way on the northern half of the site;
- A tight site geometrically which affected construction.

The fact that these challenges each came amongst the usual financial and time pressures of geotechnical projects meant maintaining an awareness of my own biases and drivers proved difficult at times. However, over the project the author learnt to take challenges as they came and developed an improved awareness of when short-term emotional responses (typically associated with stress) threatened to override a reasoned response. For a time this process required deliberate self-discipline but it eventually became reflexive. It also became easier to connect other people's needs and drivers (i.e. by better understanding how we react to challenging situations, it frees us up to better understand others). Making an effort to be actively self-aware in the face of geotechnical problems resulted in noticeably improved collaboration with the wider team of engineers and contractors and allowed the project to keep progressing. With the help of senior geotechnical staff, the author was able to play a part in completing the ground works earlier this year despite the many challenges faced.

4 PERSPECTIVES ON THE FUTURE FROM A MILLENNIAL

Whether societal changes are 'pre-programmed' based on the time in which people grow up or if a generation can make a concerted effort and create a change, what is the next genuine generation gap going to be? Modern day technology has made it possible to communicate in an abundance of ways and made Millennials the most connected generation there has been. The key finding from the author's experiences is that there is untapped value to be gained by prioritising the development of interpersonal skills in the geotechnical engineering field. With the increased level of social connection in the world, Millenials can be the generation which puts a greater emphasis on developing interpersonal skills like effective communication, empathy, self-awareness.

In geotechnical engineering, these skills are independent of the typical project variability and can help:

- Foster an inclusive learning culture;
- Project work better suit a given need;
- Make us easier to work with;
- Avoid instinctive emotional responses when faced with challenges, and;
- Develop collaborative and inclusive multidisciplinary project teams;

While these skills are regularly exemplified by established practitioners, in some cases they can be taken advantage of or discouraged in the heat of the competitive business world. In the field of geotechnical engineering where uncertainties and risks are so common these skills take on even greater importance. Interpersonal skills balance the enjoyment of facing geotechnical challenges with the need to be great people to work with.

5 CONCLUSIONS

If people truly are the greatest asset in the geotechnical industry, putting greater importance on interpersonal skills has the potential add substantial value. The philosophy of continually learning from experience (the basis for modern geotechnical practice) is paralleled in this paper whereby the author has learnt about the knowledge to be gained from our social experiences. Through an analysis of three of the author's geotechnical projects, this paper details the benefits of: focussing on effective communication; empathising with people around you and maintaining self-awareness. The key conclusion of this paper is that the current crop of young professionals – Millennials – can be the generation that puts a greater emphasis on interpersonal skills as they balance the demands associated with modern communications technology.

6 ACKNOWLEDGEMENTS

The author wishes to acknowledge Tonkin & Taylor Ltd for their support during University and over the first four years as a geotechnical engineer. Particular thanks are attributed to Nick Speight, Sjoerd Van Ballegooy and Grant Loney for their impact on my experiences as a geotechnical engineer. Thanks are also extended to those who contributed to the development of this paper.

REFERENCES

Ashkenas, R. (2011). "Your Communications May Not Be Communicating", Havard Business Review Blog [URL: https://hbr.org/2011/02/your-communications-may-not-be.html]

Burland, J., Chapman, T., Skinner, H. and Brown, M. (2013). *ICE manual of geotechnical engineering: Volume 1 – Geotechnical Engineering Principles, Problematic Soils and Site Investigation*, ICE Publishing (London), pp. 11-15.

Butler, C.J. and Chinowsky, P.S. (2006). "Emotional Intelligence and Leadership Behaviour in Construction Executives", *Journal of Management in Engineering*, 22(3)

Hewlett, S.A. (2014), "As You Start Your Career, Focus on People Skills". Havard Business Review Blog [URL: https://hbr.org/2014/04/as-you-start-your-career-focus-on-people-skills/]

Howe, N., and Strauss, W. (2009). *Millennials Rising: The Next Generation*, Vintage [Published as an E-book]

Stuart, S. (2014), Video - 12 Questions with Lester Levy. "Charismatic leaders need a psychologist." [New Zealand Herald Online, URL: http://www.nzherald.co.nz/university-of-auckland/news/article.cfm?c_id=1503679&objectid=11369513]

The Earthquake Commission (2015), *Residential Ground Improvement: Findings from trials to manage liquefaction vulnerability*, Prepared by Tonkin & Taylor Ltd and the Earthquake Commission

Wilcox, L. (2015). "Emotional Intelligence is No Soft Skill", The Language of Business Blog [URL: http://www.dce.harvard.edu/professional/blog/emotional-intelligence-no-soft-skill]

Wilson, E. J., III. (2015), "Empathy is Still Lacking in the Leaders Who Need it Most", Leadership and Managing People Blog [URL: https://hbr.org/2015/09/empathy-is-still-lacking-in-the-leaders-who-need-it-most]

Proceedings of the 11th ANZ Young Geotechnical Professionals Conference – 11YGPC
Queenstown, New Zealand
25 – 28 October 2016

Back Analysis and Closure Considerations for the North-East Pit Wall at the Globe Progress Gold Mine, Reefton, New Zealand

Dylan Meehan[1]

[1]Department of Geological Sciences, University of Canterbury, 20 Kirkwood Avenue, Christchurch, New Zealand;
Now at: Engineering Design Consultants Ltd; PH 021 959 732; email: dylanm@edc.co.nz

ABSTRACT

In April 2015 a kinematic slope failure occurred on the north-east (NE) pit wall at the Globe Progress gold mine in Reefton, New Zealand. The failure involved planar sliding, toppling and translational slumping through the entire height (220 m) of the wall. A probabilistic back analysis using Rocscience's 2D limit equilibrium software, Slide, was undertaken to determine rock mass strength parameters that led to failure. Back analysis results were then carried into a post closure model, also using Slide. The post closure model examines how the stability of the NE pit wall will respond to increasing pit water levels as the mine is transitioned into a pit lake. The back analysis found that to replicate the April failure, the greywacke – argillite bedding planes required an apparent cohesion of 32 kPa and a friction angle of 28°. It is interpreted that these strength parameters are a result of a period of heavy rainfall prior to failure. Post closure modelling concluded an increase in pit water level is not expected to induce instability of the NE wall, given no other external conditions occur in conjunction with pit water rise.

Keywords: Slope stability, Kinematic failure, Back analysis

1 INTRODUCTION

The Globe Progress gold mine (mine) operated by OceanaGold is 6 km south of the Reefton Township on the South Islands West Coast (Figure 1). The mine area receives an average precipitation of 2,000 mm per year, which plays a role in decreasing stability of the pit walls (Kennedy 2009). Mining in the pit was completed in September 2015. At this time the pit was put into a care and maintenance (C&M) phase for two years, during this period the water in the pit will be kept approximately 30 m deep. Following this phase the pit will fill with 124 m of water.

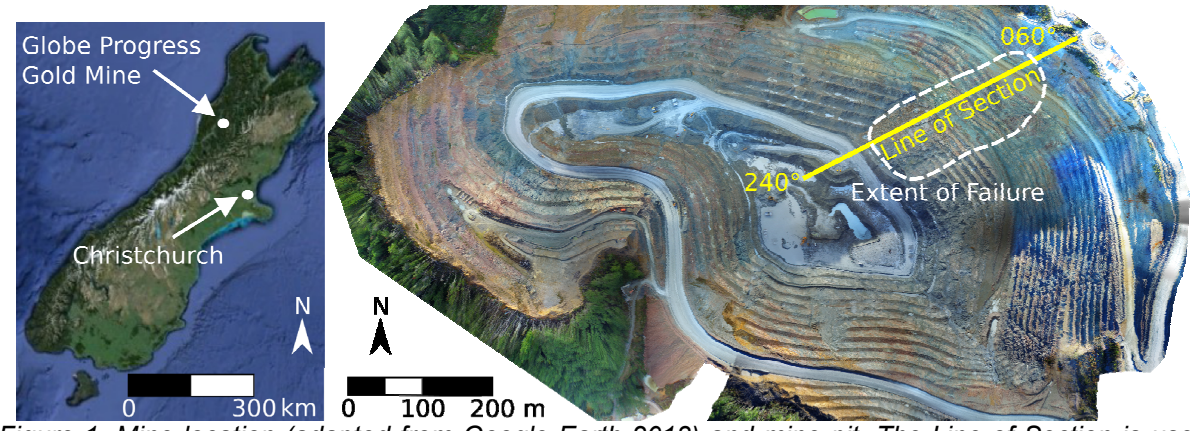


Figure 1. Mine location (adapted from Google Earth 2013) and mine pit. The Line of Section is used for stability modelling throughout this research (adapted from OceanaGold 2015)

This paper aims to describe a back analysis of the stability of the NE pit wall to determine the internal rock mass strength parameters that led to the April 2015 failure. The other aim of this paper is to analyse how the NE pit wall will respond to increased saturation as pit water levels rise following closure of the mine. Both the back analysis and the post closure analysis are important due to the potential for loss of life and damage to infrastructure in the event of a collapse of the pit wall.

1.1 Geological Setting

The geology of the Globe Progress pit is interbedded greywacke and argillite Greenland Group sediments. The argillite beds may be as thin as 30 mm (Clark 1996) with the greywacke beds ranging from 5 m - 10 m thick (Wells 2010). Two Shear Zones are also present; The Globe Progress Shear Zone runs north-west to south-east and the Oriental Shear Zone traces along the base of the NE wall from north to south. The NE pit wall is dominated by an anticline – syncline fold sequence (Figure 2). Descriptions of the geological units on the NE pit wall characterised using New Zealand Geotechnical Society (NZGS, 2005) guidelines are given in Table 1.

Table 1. Engineering geological descriptions of the rock units on the NE pit wall

Rock Unit	Engineering Geological Description
Greywacke	Slightly weathered, blueish grey, fine – medium sand, massive, weakly metamorphosed, GREYWACKE, very strong, moderately thick, narrow, inclined, undulating smooth bedding, two joint sets (Greenland Group)
Argillite	Slightly weathered, dark grey, fine grained, massive, ARGILLITE, strong, thin, very narrow, inclined, undulating smooth bedding (Greenland Group)
Oriental Shear Zone	Sandy SILT with minor fine gravel and trace clay, dark blueish grey, massive, soft, moist, non-plastic, (sheared and hydrothermally altered Greenland Group)

1.2 Kinematic Failure

On 24 April 2015 a significant slope failure occurred on the NE wall of the pit, following two months of heavy rain. A schematic engineering geological model of the wall was developed (based on scanline structural data and mapping), that illustrated the April 2015 failure was structurally controlled (Figure 2). Beds dipping into the pit on the western limb of the anticline resulted in planar sliding from the lower parts of the slope. This induced toppling on the eastern limb of the anticline where the beds above the sliding failure are dipping out of the pit. Translational slumping was also initiated at the top of the pit wall due to relaxation of the beds below. During the failure OceanaGold staff reported hearing cable bolts snapping, indicating the failure plane was within the cable bolts 15 m deep operational zone (PSM 2015). The 90 m wide failure is bound on the northern side by the Oriental Shear Zone and on the southern side by an unknown structural feature.

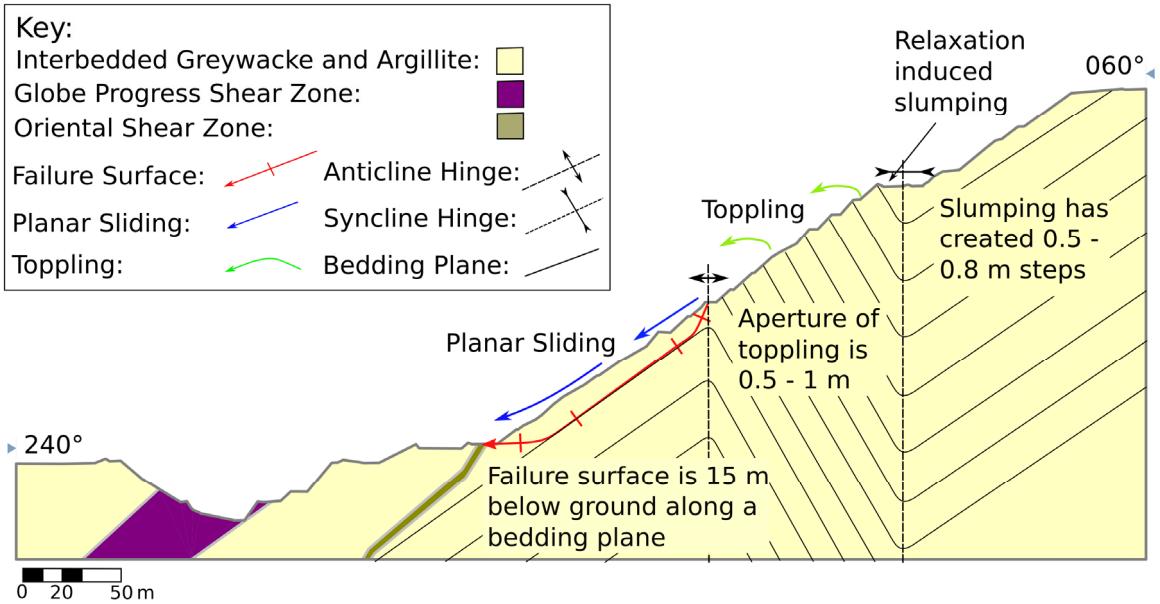


Figure 2. Schematic engineering geological model through the NE pit wall

2 STABILITY ANALYSIS

2.1 Rock Strength Quantification

Laboratory testing was used to identify rock strength parameters of the different geological units within the pit. The units were analysed with various failure criteria based on the best testing methods available for the rock type. Tables 2 to 4 summarise the strengths derived from the laboratory testing and the failure criterion used.

Table 2. Rock strength parameters using Mohr-Coulomb failure criterion

Sample	Testing Method	Apparent Cohesion (kPa)	Friction Angle (°)
Bedding plane	Direct shear box	0	25
Oriental Shear Zone pug breccia	Direct shear box	6	30

Table 3. Rock strength parameters using the Generalized Hoek-Brown (Hoek, Carranza-Torres and Corkum 2002) failure criterion

Sample	Testing Method	UCS (MPa)	GSI	Mi	D
Greywacke	UCS	150	55	19	0
Argillite	Point load	31	55	6	0

Table 4. Rock strength parameters using the Barton-Bandis failure (Barton and Bandis 1990) criterion

Sample	Testing Method	JRC	JCS (MPa)	Residual Friction Angle (°)
Bedding plane	Schmidt hammer	7	38	25

The friction angle of the bedding plane (Table 2) was inputted into the Barton-Bandis failure criterion along with Joint Roughness Coefficient (JRC) derived in the field and Joint Compressive Strength (JCS) taken from Schmidt Hammer testing (Table 4). This calculated the apparent cohesion and friction angle of the bedding plane to be 90 kPa (standard deviation = 35 kPa) and 30° (standard deviation = 2°), respectively.

2.2 Back Analysis

The back analysis model (Figure 3) was established in slope stability software using topography obtained from a Digital Terrain Model (DTM) of the NE pit wall taken in March 2015. The argillite bedding failure surface (enlarged section of Figure 3) was set as a 200 mm thick zone 15 m below ground, using structural data (Figure 2). The water table was allowed to vary between 2 m and 7 m below ground (OceanaGold 2013). The rock strength parameters used in the model were taken from Tables 2 – 4 apart from the bedding plane data. The bedding plane parameters were reduced from the laboratory obtained results to the lower bound of one standard deviation. This was due to the model not corresponding to the observed failure with the laboratory tested rock strength parameters. The reduced bedding plane mean cohesion and friction angle used were 50 kPa and 25°, respectively.

The back analysis focuses on the failure plane along the argillite bedding. It is inferred that following heavy rainfall, water would have infiltrated the bedding planes along joints through the rock mass. The model ran the analysis 1000 times within the range of cohesion (40 kPa – 110 kPa) and friction angle (15° – 36°) bedding plane parameters, determining which combinations of parameters would lead to failure of the pit wall within the defined constraints. The failure toe exit angle was chosen as 180° (from horizontal) to replicate what was observed in the pit.

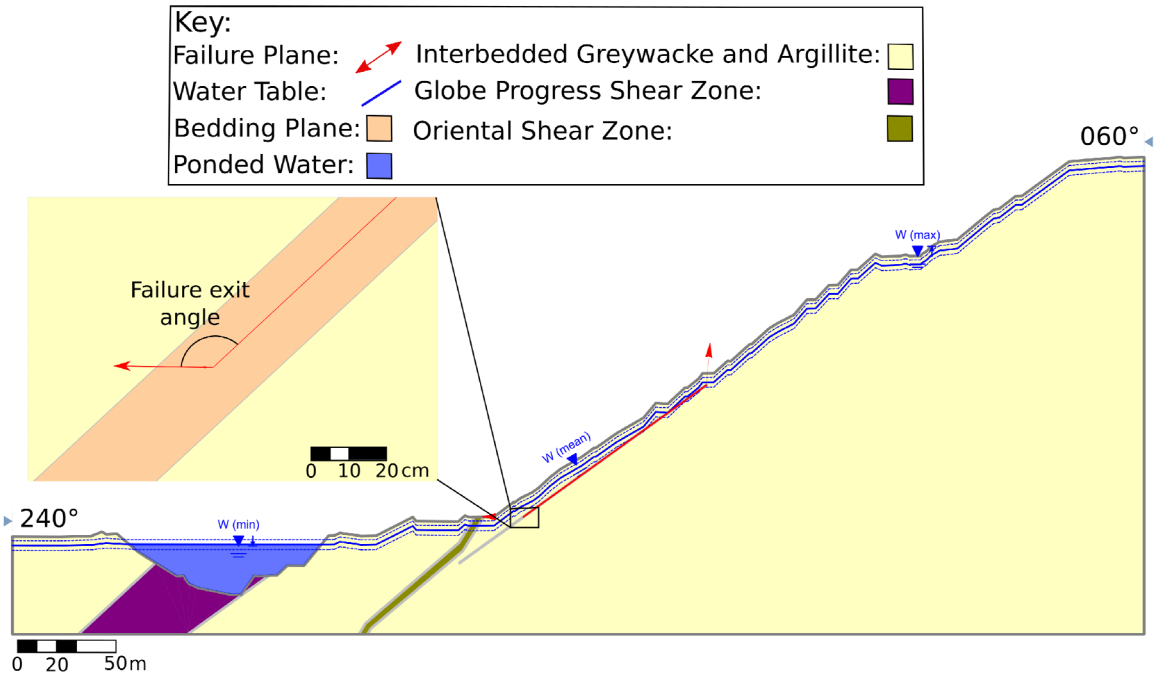


Figure 3. Stability model used to perform a back analysis of the kinematic failure on the NE wall. Enlarged section shows failure surface along the bedding plane interpreted to have failed

2.3 Post Closure Analysis

The post closure model (Figure 4) was produced from a June 2015 DTM. The area of planar sliding was inserted using a failure surface block search allowing the software to choose the most likely place of failure within the block. Failure was constrained to a dip of 36° along the bedding planes. The exit angle of the failure was set to choose the most likely angle between 170° and 250° from horizontal.

An increasing water depth to a maximum of 124 m was modelled. The models began with a water depth of 30 m, as this is the water depth during the C&M period. The rock strength parameters used in the post closure model were calculated from back analysis modelling (Table 5).

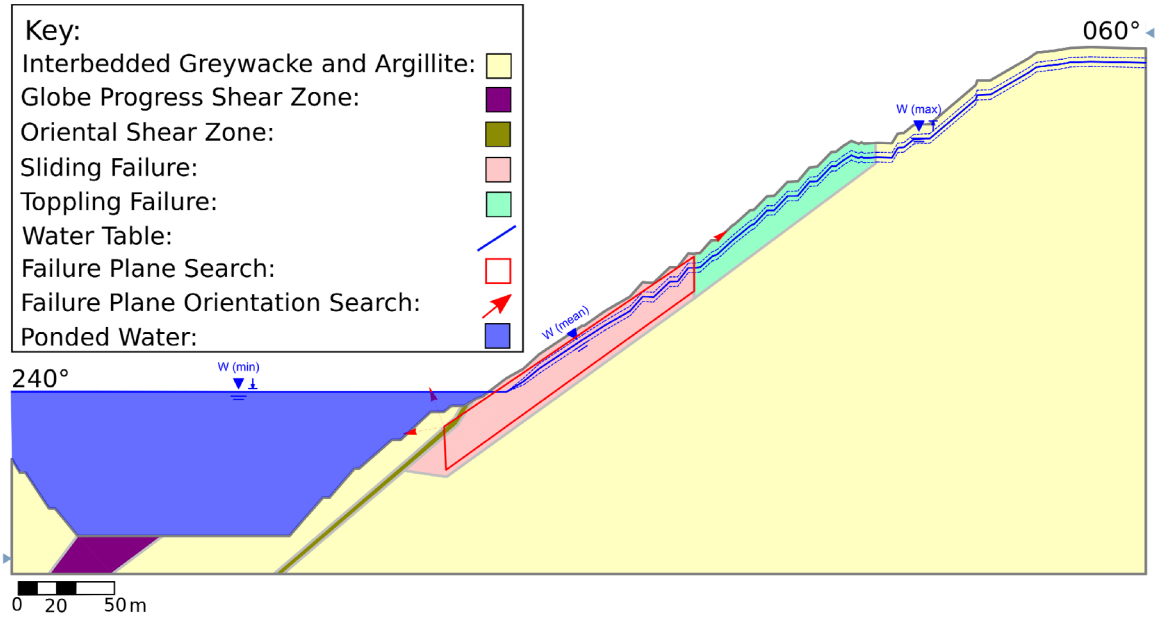


Figure 4. Representative model (75 m water depth) to analyse the post closure water table

3 BACK ANALYSIS

3.1 Results

From 1000 model iterations, 54 models resulted in a factor of safety of 1.0 and thus gave parameters for the April pit wall failure to occur. These results averaged to an apparent cohesion of 32 kPa and a friction angle of 28° along the bedding plane. The results plus the strength of the Oriental Shear Zone and the greywacke at failure are shown in Table 5.

Table 5. Rock strength parameters that resulted in failure of the NE pit wall derived from back analysis

Sample	Apparent Cohesion (kPa)	Friction Angle (°)
Bedding Plane	32	28
Oriental Shear Zone	6	30
Greywacke	2710	54

3.2 Discussion

The shear strength of the bedding plane established by the back analysis is weaker than was determined from laboratory testing. Intact shear and Schmidt hammer tests on the bedding plane found the apparent cohesion to be 90 kPa and friction angle to be 30°. Results of the back analysis indicate for failure to occur, the apparent cohesion is 32 kPa and friction angle is 28°. These parameters denote the average required strength of the bedding plane for planar failure to occur with the modelled pit wall geometry.

The results of laboratory testing were reduced in the stability model due to ground truthing. It was found that a probabilistic analysis with the initial laboratory tested strength parameters resulted in no failure of the wall. The rock strength parameters were therefore reduced to a mean cohesion and friction angle of 50 kPa and 25°, respectively to allow failure to occur as was observed in the mine. It can be inferred that heavy rainfall caused increases in pore pressure within the bedding planes. This combined with the unfavourable dip into the pit and the mass of the overlying rock, resulted in the planar sliding failure that then migrated up the pit wall inducing toppling and translational slumping.

Shear strength reduction modelling was undertaken using Rocscience's Phase^2 software for comparison; however being a finite element program neither structural data nor a failure surface could be input into the model. This resulted in a large-scale rotational failure occurring through the NE wall. Given the structure of the wall this was considered infeasible and the model was disregarded. This gives confidence in the structurally controlled stability model providing an accurate representation the observed failure in the mine.

The results of the back analysis are important because they can be carried forward to determine how the wall will respond to post closure water rise. Continued work would be to calibrate both laboratory tested and modelled results. This would require further laboratory testing on a range of samples from the NE pit wall as well as stability modelling in other software packages.

4 POST CLOSURE IMPLICATIONS

4.1 Results

The post closure model outputted eight factors of safety for the NE pit wall during the two year C&M period and subsequent filling of the pit (30 m – 124 m water depth). The different models effectively determine how the wall would respond over the filling period (Figure 5).

4.2 Discussions

The lowest factor of safety during filling of the lake is 1.2 at 75 m water depth, the factor of safety then increases as water level increases. This implies rising pit water levels are not expected to induce pit wall failure under the saturated conditions modelled, without other external factors. There are two possible reasons for failure not being induced as compared to the April 2015 failure. The first is the weight of water within the pit will buttress the pit wall. Figure 5 supports this by illustrating the pit wall is least stable when the water depth is 75 m, which corresponds to the pit water saturating the toe of the

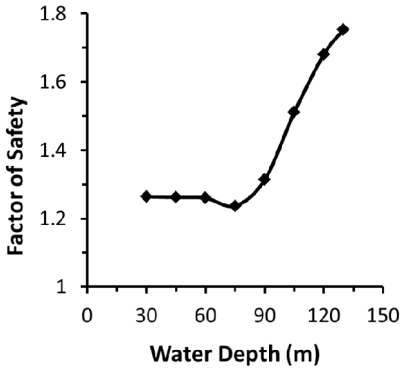


Figure 5. Plot of factor of safety versus water depth

slide only, with very little buttressing support force (Figure 4). As the water fills above 75 m the factor of safety increases due to a corresponding increase in buttressing force. The second possible reason for a stable post closure wall is the altered geometry. Since April 2015, due to both the failure that occurred and further mining within the pit the shape of the wall has changed favourably.

Additional work should examine other external conditions that could induce failure. Given the mines location, the main external condition to be researched is instability of the wall during seismic activity.

5 CONCLUSIONS

Back analysis effectively determined the rock strength parameters of the bedding plane that resulted in failure of the NE pit wall at the mine on 24 April 2015. It is inferred that the bedding planes dipping on limbs of an anticline within the NE pit wall experienced a loss of strength resulting in planar sliding into the pit. The loss of toe support then produced toppling through the mid – upper pit wall and relaxation induced translational slumping along the upper wall as illustrated by the engineering geological model. These results are important for understanding how prone to failure other sections of the pit wall with similar geomorphologies are and how they may react given comparable conditions.

Post closure models carried forward from the back analysis found that with no other external factors, pit water level rising is not expected to induce pit wall instability. This is important because of the potential negative consequences to both life and infrastructure in the event of further failure of the NE pit wall. Further research should be undertaken to better categorise the normal conditions rock strength and assess the effects of seismic loading on the pit wall using the parameters derived from the back analysis.

6 ACKNOWLEDGMENTS

Thank you to David Bell, OceanaGold, Luke Matheson, Marlene Villeneuve, Cathy Higgins, Sarah Pope, Ashley Coutts, Timothy Howard and Sunny Kalidas for your various help throughout this project.

REFERENCES

Barton, N.R. and Bandis, S. (1990). “Review of predictive capabilities of JRC-JCS model in engineering practice.” In *Rock Joints, Proceedings of International Symposium on Rock Joints*, Loen, Norway, pp. 603-610.

Clark, P. B. (1996). *Rock Mass and Ripbability Valuation for a Proposed Open Pit Mine at Globe Progress, near Reefton* [Masters thesis], University of Canterbury, Christchurch, New Zealand

Golder Associates (2014). *Reefton Gold Project Closure: Globe Pit Closure Initial Assessment*.

Google Earth [v 7.1.5.1557] (17 August, 2013). Globe Progress gold mine, Reefton, New Zealand. 42°09’57.67” S 171°50’28.68” E, DigitalGlobe 2015. www.earth.google.com [18 November, 2015].

Hoek, E., Carranza-Torres, C. and Corkum, B. (2002). “Hoek-Brown Failure Criterion – 2002 Edition”, *5th North American Rock Mechanics Symposium and 17th Tunnelling Association of Canada Conference: NARMS-TAC 2002*, Toronto, Canada, pp. 267-271.

Kennedy, G. D. (2009). *Geotechnical investigation of the Footwall Zone, Globe Progress Open Cut Gold Mine, Reefton, New Zealand* [Honours thesis], University of Canterbury, Christchurch, New Zealand.

New Zealand Geotechnical Society Inc (2005). *Field Description of Soil and Rock*.

OceanaGold (2015). UAV transparent mosaic image of Globe Progress pit.

OceanaGold (2013). Technical Report for the Reefton Project. Melbourne.

Pells Sullivan Meynink (PSM) (2015). May 2015 Site Visit: NE Wall.

Wells, A. J. (2010). *Geotechnical Investigation of the Hanging Wall Zone, Globe Progress Open Cut Gold Mine, Reefton, New Zealand* [Honours thesis], University of Canterbury, Christchurch, New Zealand.

Proceedings of the 11th ANZ Young Geotechnical Professionals Conference – 11YGPC
Queenstown, New Zealand
25 – 28 October 2016

Challenges and Experiences of Site Investigations Abroad

H. L. McEwan[1] and R. B. Graafhuis[2]

[1]AECOM NZ Limited, 121 Rostrevor Street, Hamilton, PO Box 434 Waikato MC Hamilton 3240 ; PH +64 21 567 261; FAX +64 7 834 8981; email: hamish.mcewan@aecom.com; mcewanhamish@gmail.com
[2]AECOM NZ Limited, 8 Mahuhu Crescent, Auckland, 1010; PH +64 21 645 097; FAX +64 9 967 9201; email; rhys.graafhuis@aecom.com

ABSTRACT

Site investigations abroad offer opportunities to learn about a region's geology and to experience cultures different to our own. More importantly, challenges working in remote conditions and developing countries require adapting to local environments and using a diverse range of investigation methods. This paper discusses the challenges and experiences while undertaking geotechnical site investigations in the Middle East. It outlines the processes we put in place to ensure consistent and usable geological data was collected so that a workable ground model could be established. As the investigations were located abroad, it was critical that the data obtained was usable for interpretation once back in our home country of New Zealand. This requires a clear understanding of the local geological environment and geotechnical risks to the specific projects. In addition, local workers, many of whom spoke little English, added a further dynamic to the investigations and a window into their own culture. The lessons learnt while abroad have improved our site investigation methodologies and techniques, and have been an excellent personal opportunity to develop technically and visit places otherwise inaccessible.

*Keywords: S*ite Investigations, Middle East Geology, Data Management, Limestone Breccia

1 INTRODUCTION

The investigations were undertaken for a metro rail project proposed to service a major city in the Middle East. Due to client considerations, the name and location of the project cannot be revealed. AECOM provided geotechnical design services for two of the metro rail lines which included tracks and stations underground, above ground and at-grade, and depots and shafts.

Our key task was to undertake geotechnical studies to inform detailed design and construction. Initially, field mapping of building excavations throughout the city provided the basis of our geological and geotechnical models. Consequently investigations were scoped and undertaken by three separate geotechnical contractors in a staged approach. These investigations included 333 drillholes, 284 surface geophysical lines, laboratory testing and a wide range of in situ testing including wireline geophysics, downhole seismic geophysics, televiewer and lugeon testing. To ensure the investigations were of sufficient quality and consistency to inform our analysis we worked closely with the contractors to achieve the best result possible.

This paper discusses the challenges and experiences while undertaking the site investigations in the Middle East. While the geotechnical contractors were responsible for undertaking the investigations and producing a factual report we maintained a presence on site to ensure the results were of sufficient quality and consistency to inform our analysis and interpretation. The key challenges in undertaking the investigation include:

- Understanding a unique geological terrane
- Ensuring quality and consistent investigation results were delivered by the contractors
- Managing the vast amount of geotechnical information gathered from the investigations

2 SITE GEOLOGY

2.1 General

The geology at the project area typically comprised fill and alluvium overlying regionally consistent layers of bedded limestone and brecciated limestone dipping 1° to the east. Within the limestone,

voids and infilled cavities were common. Initially, a geological model for the site was established by undertaking geological mapping of exposed outcrops and building excavations throughout the city and from literature study. This model was then developed as further investigations were undertaken.

The brecciated limestone was an unusual geological material, as will be explained in the next section and we needed to develop a clear understanding of its formation and implication on geotechnical behaviour.

2.2 Formation of limestone breccia

Brecciated limestone observed at the project area was formed from the preferential dissolution of beds of anhydrite between limestone layers causing collapse of the limestone layers. The layers of anhydrite and limestone were deposited during the Late Jurassic to Early Cretaceous in upward cycles of shallowing marine and tidal flat environments (USGS, 1985 and Farooq A. Sharief, 1991). The anhydrite beds, which are formed from hyperconcentrated marine environments, are especially susceptible to dissolution and are easily dissolved in acidic groundwater derived from rainfall. Tectonic uplift during the Miocene and wet climactic conditions during the Pliocene (Vincent, 2008) resulted in dissolution of the anhydrite beds and an estimated vertical thickness up to 250m removed (Farooq A. Sharief, 1991).

Following dissolution, the remaining limestone beds then collapsed, slumped and contorted forming breccia with clasts ranging from mm's to 10m's in size. Between the clasts, various amounts of clay matrix and calcite cement are observed with voids and vugs often present. This process is complex and can be seen at scales of cm's to km's, Figure 1 and Figure 2.

Dissolution of the anhydrite beds had already occurred in the project area leaving two distinct brecciated units approximately 20m thick separated by bedded limestone. Approximately 20kms east of the city, active dissolution could be seen at a nearby escarpment and is analogous of past conditions on site (Vaslet, 1991), Figure 1.

3 FIELD LOGGING GUIDANCE

3.1 General

The local geotechnical contractors undertook the investigations and also logging of the drill core. From previous reports and initial meetings with the contracting geologists it became apparent we needed to provide clear logging guidance so consistent results were provided that could be correlated during analysis. This was particularly important because there were three separate contractors involving approximately 10 site geologists and a consistent approach to geological descriptions was required. In addition, many of the field staff had variable English language skills which added to the challenge. We provided the following guidance:

- Logging help sheets
- On site guidance to the site geologists
- Project specific geotechnical database template and library

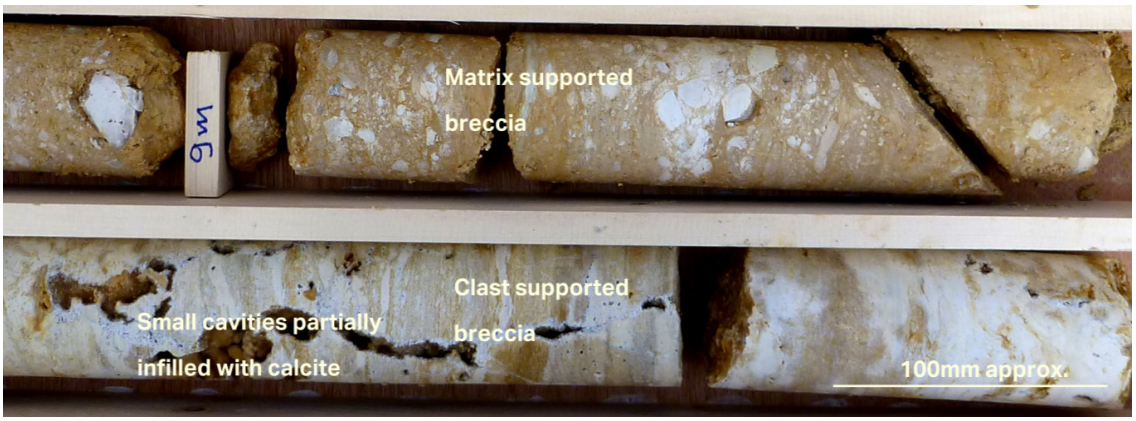


Figure 1. Core sample of limestone breccia. This breccia has likely undergone several cycles of brecciation and dissolution.



Figure 2. Escarpment showing large scale collapse of bedded limestone. Sinkholes were encountered at the foot of this escarpment in several locations.

3.2 Logging help sheets

The project was to be undertaken using British Logging Standards (BSI, 1999) where applicable or otherwise American Society for Testing and Materials (ASTM) Standards. The initial logging help sheet for the site geologists included extracts from relevant British Standards, however as the investigation progressed the consistency and quality of the logs did not improve. It seemed there were too many options for the geologists to describe essentially very similar materials and it was likely they could not read English to the level required to understand the standard. A standout example from one log is London Clay being used as a description for highly weathered limestone breccia. When queried, the geologist pointed out London Clay is an example given in the British Standard for soil description!

To overcome the problem described above and as our understanding of the local geology and of the important differences between geological units improved, we developed and provided to the field geologists a logging memorandum, shown in Figure 3. The memorandum highlighted key aspects of the core that needed to be differentiated between the various geological units during the analysis.

The memorandum to the geologists presented in Figure 3 explains what was adopted as logging requirements of limestone breccia for this project and broadly follows British Logging Standards. By providing this guidance and working very closely with the site geologists we were able to improve the consistency and quality of the logs. The wider project team also benefited from the memorandum and adopted a consistent approach during the interpretation stage.

3.3 Onsite guidance to the site geologists

Our team comprised approximately 4 to 7 staff working abroad at any one time and were from New Zealand and Australia. Typically our onsite geologists and engineers supervised two to three drill rigs / site geologists each. On site, this entailed discussing the recovered core samples, checking their field log, specifying and overseeing in situ field tests and ensuring operations were undertaken safely. The drillhole locations were positioned throughout the city which meant we were able to experience difference parts of the city daily. We were able to get to know the contracting geologists, who being ex-pats from various Middle Eastern countries, had had little contact with New Zealander's before. They were very interested to know the differences between their home countries and ours –which they

thought was probably like Hobbiton! For us, it was a great opportunity to learn more about cultures different to our own.

A high turnover of the contractor's geologists resulted in inconsistencies in many logs which required re-logging by our staff. However, the quality of the logs from the geologists who remained on the project improved significantly.

3.4 Consistent geotechnical databases

It was critical we were provided geotechnical data in an electronic format by the three contractors to prevent manual re-entry of the information when it came to analysis at later project stages. The widely recognised AGS file format (AGS4) provides an electronic format to transfer geotechnical data (AGS, 2010). Although we specified AGS4 files of the geotechnical data to be provided, it appeared the contractors did not have the capability to produce them. To ensure we were delivered usable electronic data, we prepared a project specific geotechnical database template in gINT, a geotechnical database software package which each of the contractors had. The database was designed to be simple and easy to use for people who have not used the program before. It also featured dropdown lists based on the relevant British Standard for logging, e.g. strength, weathering, piezometer installation. This meant the contractors could send us their database files and we could read and incorporate them without any issues. By using dropdown lists based on British Standards, we would prevent the contractors logging to other standards or using terms that were not defined. The database had capability to export/import in AGS3.1 and AGS4 however these formats were not needed to transfer the information by using a consistent project database approach.

Laboratory results were expected to be entered into the database by the contractors however this did not happen and they preferred to enter results on pdf reports or spreadsheets. This meant there was still some manual data entry to be undertaken and the provided spreadsheets had to be massaged into a format which could be imported into the project database.

4 INVESTIGATION DATA MANAGEMENT

During the site investigations a vast amount of information was produced and needed to be shared between the wider project team. This information was not the finished reports, which would be later filed in project specific file management tools such as ProjectWise and ACONEX, but working files which were integral in making decisions as the investigations progressed. The project team included other consultants and contractors and AECOM staff including up to 4 field staff working between the various contractors on site, 2-3 staff based in a project office and additional teams in Auckland, Christchurch and Wellington, New Zealand, and Melbourne and Brisbane, Australia. Typical office based networks proved to be slow and difficult to use across the globe and an alternative cloud based file management tool was implemented.

The cloud based file management tool Dropbox was used to collaborate and share information between the teams effectively. While file management tools mentioned above were used for project deliverables, these packages proved to be cumbersome for working documents. Using a cloud based tool enabled us to improve the speed of our file sharing and better manage who could access the files. The tool could also download and synchronise data to user's computers allowing staff on site to access stored files without being online. When the field staff regained internet connection, either via mobile, at the hotel or office, their work from that day was automatically uploaded to the project cloud and shared among users across the globe, Figure 4.

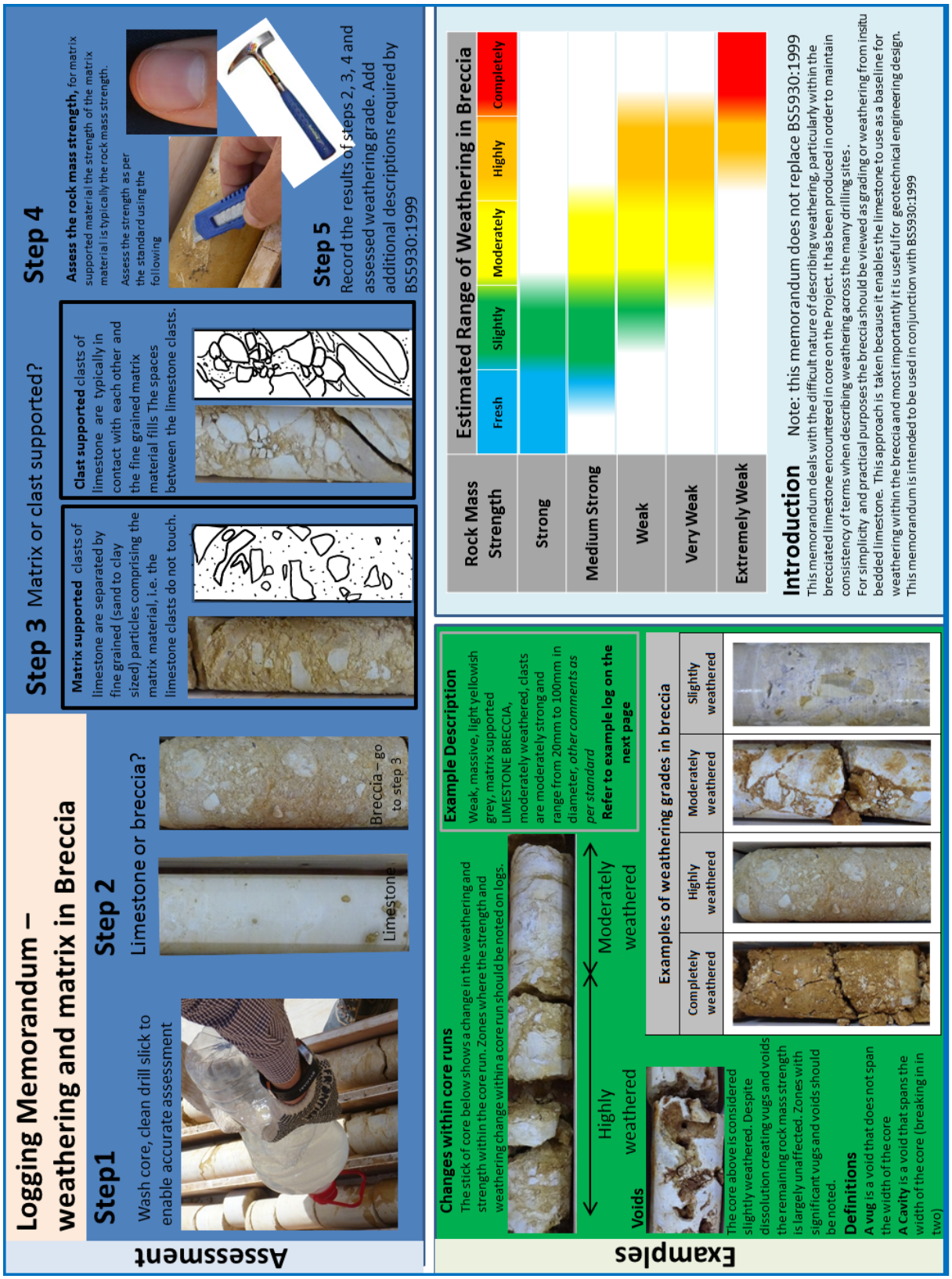


Figure 3. Logging help sheet. This sheet was provided to the site geologist to ensure a consistent approach in logging limestone and limestone breccia.

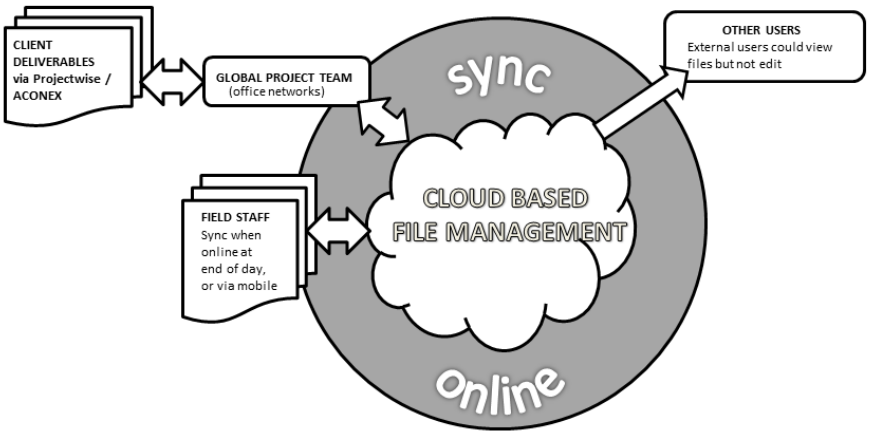


Figure 4. Diagram of the data management structure used on the project. The use of a cloud based system ensured files from field staff and the global project team were shared efficiently.

5 CONCLUSION

Investigations for the project in the Middle East offered a range of challenges and experiences which were unique to the region.

By establishing the geological model early we were able to provide clear guidelines to the contracting geologists to ensure quality and consistent investigation results. The development of the logging memorandum went some way to improving logging consistency and ensured that critical geological information (matrix support, strength and weathering) was captured in the field. It did not replace adequate training of geologists. A high turnover of contractor geologists resulted in logging inconsistencies that were not able to be remediated by the logging memorandum alone. Geologists who remained on the project for a significant period and received adequate training were able to be produce consistent logs. The memorandum also ensured consistent approach from the wider project team.

The project specific geotechnical database streamlined the transfer of investigation data in lieu of using AGS file format and ensured key data was entered consistently between contractors. By simplifying the database structure little training was needed for the contractors to use the database.

Using a cloud based file management tool effectively shared information between the wider project team working from a range of locations across the globe where regular company networks proved slow or inaccessible. Field staff utilised the system to synchronise their field work daily without the need to return to a project office, saving time and improving data management.

Field work overseas and getting to know local workers provided insight into different cultures. This experience and the challenges of the site investigations were an excellent platform to improve our investigation skills for future projects.

6 ACKNOWLEDGEMENTS

We would like to thank the project team who all played a part in the success of the project and especially those who shared the experience abroad. Thank you also to Debbie Fellows for reviewing the paper and challenging us to be a part of the conference.

REFERENCES

The Association of Geotechnical and Geoenvironmental Specialists (AGS), (2010). *Electronic Transfer of Geotechnical and Geoenvironmental Data: AGS4.* Kent, England.

British Standards Institution (BSI), (1999). *BSI BS 5930: Code of practice for site investigations.*

Farooq A. and Sharief, M. S. (1991). "Outcrop-Subcrop Sequence and Diagenesis of Upper Jurassic Arab-Hith Formations", *Earth Science*

United States Geological Survey (USGS), (1985). *Sedimentary Geology of Saudi Arabia.*

Vaslet, D. (1991). *Explanatory Notes to the Geological Map of Ar Riyadh Quadrangle*, Sheet 241, 1:250,000. Kingdom of Saudi Arabia: Ministry of Petroleum and Mineral Resource.

Vincent, P. (2008). *Saudi Arabia Environmental Overview.* London: Taylor and Francis.

Proceedings of the 11th ANZ Young Geotechnical Professionals Conference – 11YGPC
Queenstown, New Zealand
25 – 28 October 2016

Determination of Effective Stress Parameters for Clayey Silt Using a Borehole Shear Test

J. B. Fairhall[1]

[1]Geotechnical Engineer, Jacobs Engineering Group, Queensland, email:Joshua.fairhall@jacobs.com

ABSTRACT

The determination of shear strength parameters for use in geotechnical analysis is integral to safe and cost effective design. In general practise, shear strength parameters are frequently determined using published correlations and relationships with insitu field tests that are highly variable and are not intended to be used to develop shear strength relationships. Laboratory testing for measuring shear strength parameters is often minimal due to the inherent expense. Commercial drivers, sample quality assurance and turnaround timeframes greatly influence the quantity and quality of laboratory testing which is used to directly measure the shear strengths of soils. The Borehole Shear Test (BST) is an insitu testing apparatus that provides near instantaneous shear strength parameters, directly measured by shearing the side walls of a borehole at various normal stresses. Peak shear stresses are used to develop a Mohr Coulomb failure criterion and provide a direct measurement of shear strength. This paper summarises the results obtained from a series of Borehole Shear Tests undertaken on clayey silt in South East Queensland. Shear strengths were measured at various depths using the BST and were used to develop shear strengths parameters for the tested material. Thin walled Shelby tubes were used to recover insitu material samples which were used to determine the laboratory shear strength of the material. Consolidated Undrained Triaxial tests, Index testing and Standard Penetration Testing (SPT) were compared with the field BST results to assess relationships between the different testing methods. Results of the BST agree well with those tested in the laboratory. Results suggest that the BST could be an effective and alternative, cost efficient investigation tool which can be used to assess insitu strength parameters in conjunction with traditional laboratory testing.

Keywords: Borehole Shear Test, Effective Stress, Insitu Testing, Shear Strength

1 INTRODUCTION

Geotechnical design frequently requires the interpretation and assignment of ‘characteristic’ soil strength parameters for the various subsurface materials encountered during site investigations. Subsurface materials are generally classified using insitu exploration methods and typically involve a series of penetration tests (Standard Penetration Test and Cone Penetration Test) being undertaken to measure soil strength with depth.

Laboratory testing is undertaken on recovered disturbed samples, with a general focus on material classification and development of characteristic design parameters. Insitu Shelby tube samples collected during an investigation yield undisturbed samples that can be used to determine material shear strength; however results may be significantly altered from their insitu state by sample disturbance. Stiff to hard clay samples can be difficult to sample and require special tools to successfully obtain insitu samples. Similarly, the shear strength of granular dominated material samples is seldom determined within a laboratory due to difficulty in retaining insitu conditions when extruded. To accurately replicate the insitu conditions and determine suitable shear strength parameters using laboratory testing methods, high quality (undisturbed) sampling is required.

Laboratory testing is often seen as an excessive expense, and to people with limited geotechnical knowledge, it can be seen as an unnecessary cost burden to a project, as similar material parameters can be determined using correlations with penetration tests. Commercial drivers dictate the quantity and types of laboratory testing that can generally be accommodated on a project. The cost of site investigation generally increases significantly when laboratory shear strength testing is specified. This adversely increases the reliance on empirical relationships to determine characteristic shear strength parameters.

Common geotechnical engineering practice involves using correlations with empirical relationships of soil parameters with insitu tests; such as Standard Penetrations Tests (SPT) and Cone Penetration tests (CPT). Such empirical relationships have been derived from comparison between field and laboratory tests. These generic relationships are often deemed acceptable for use in geotechnical design, but can be highly variable and do not always account for the intrinsic nature of a specific soil. Although often universally applied, generic relationships are a direct production of the data available to the author at the time of their derivation. Accordingly, the results of the 'blind' application of such a generic relationship may be highly variable and may not account for the site specific nature of a soil (e.g. Application of a correlation upon alluvial / transported soils compared with a residual soil). Adopting empirical relationships may provide a design approach to determining material strength characteristics; however the accuracy of a geotechnical design is best defined by a direct measurement of the soil strength characteristics.

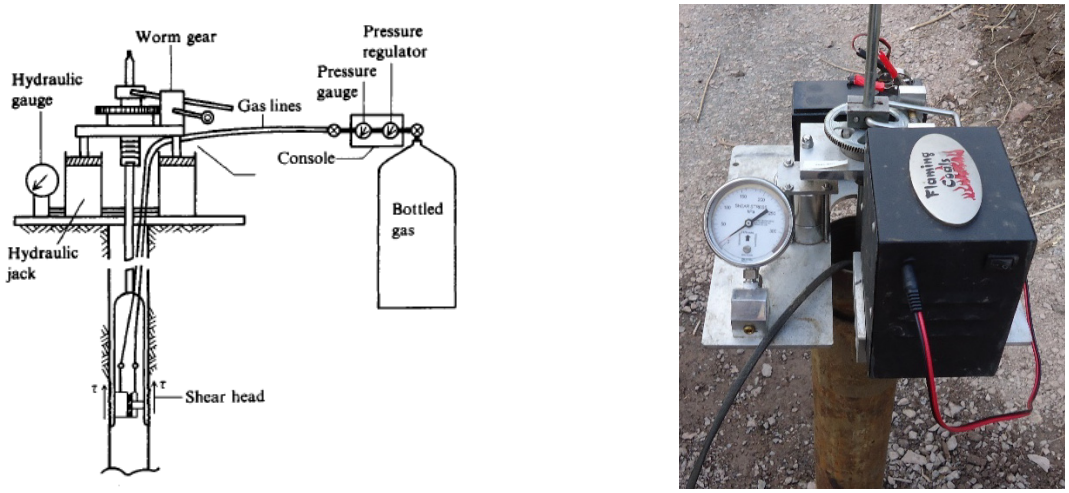
The BST is a unique tool that can be used to directly measure the shear strength of a soil within an open borehole. The BST uses a retractable shear head that can expand within a borehole to allow shearing of the encountered material on the side walls of a borehole. The BST can be used to test subsurface material at any depth below the ground surface, limited only by the number of extension rods and length of pneumatic tube used to control the shear head.

The BST presents numerous advantages when complementing a typical site investigation due to its ability to directly measure Mohr Coulomb shear strength parameters without the need for direct correlation. The test can be undertaken during borehole advancement and is intended for use within the void created from thin walled Shelby (u75) tube sampling. As the BST is undertaken insitu, it is likely to provide improved representation of actual shear strength parameters due to minimisation of sample disturbance compared with traditional laboratory sampling methods. A complete test can usually be completed within one hour with results providing instantaneous shear strength parameters. This can be advantageous for projects, providing both cost and time efficiencies.

This paper provides detail of a case study in which the BST has been used to obtain shear strength parameters. The Borehole Shear Test is an additional field investigation tool that can be used to obtain direct measurements of a soils shear strength.

2 BOREHOLE SHEAR TEST APPARATUS

The BST is undertaken by lowering a bilateral expandable shear head into a carefully drilled borehole or open cavity resulting from thin walled Shelby tube (u75) sampling. The test proceeds by expanding the shear head so that it engages the soil on the walls of the open borehole. A normal force is firstly applied to the shear head through pneumatic pressure plates that are controlled from the ground surface. The shear head is then axially pulled in the direction of the base plate with measurements of the shear force recorded at time intervals until peak failure is observed. Figure 1 shows the major components of the BST apparatus.



(a) (b)

Figure 1. (a) Typical Borehole Shear Test Apparatus (Handy, 2013); and (b) Photo of the BST with retrofitted motorised crank during a trial test in a cased borehole.

2.1 Test Methodology

The BST operation is undertaken in two phases:

- A seating / consolidation phase – A normal pressure is applied to the side wall of a borehole and then left for a duration of time to allow surrounding material to consolidate and for any excess pore water pressures to dissipate prior to commencement of the shear phase; and
- Shearing phase – A shear force is applied by rotating the crank attached to the base plate at a constant rate (typically 2 revolutions per second). The shear force is transferred along the pull rods to a dynamometer fitted with a hydraulic shear gauge. Results on the gauge are recorded until the soil material is observed to reach its peak shear strength. The peak shear strength is recorded and plotted against its corresponding normal stress.

Both testing phases are repeated for increases in normal stress. The test is typically repeated four to five times with the individual data points used to plot measurements of shear stress against normal stress. Figure 2 shows a typical BST data plot.

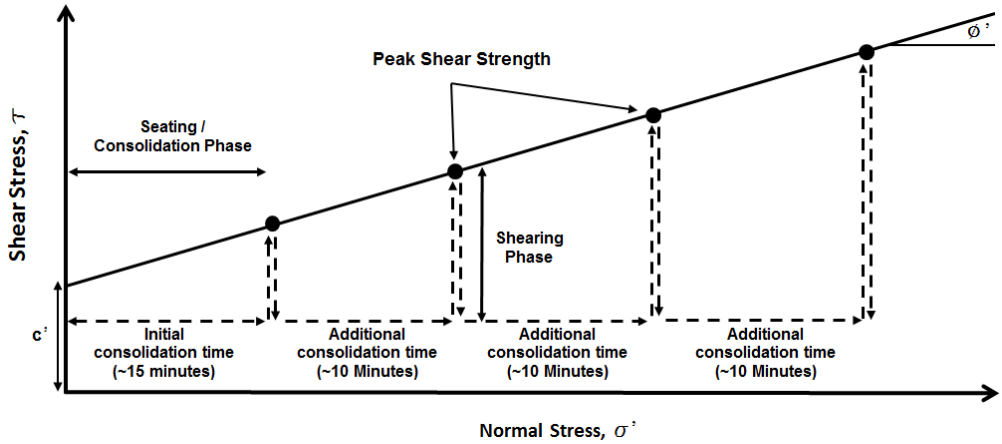


Figure 2. Typical borehole shear testing procedure for clayey silts (Bechtum, 2012)

With sufficient time allowed for consolidation and drainage, the slope of the line passing through each of the 'peak' shear strength points should be linear and conveniently plot a Mohr Coulomb failure plane. A line of best fit is applied to the data points with the characteristic strength parameters determined from the fitted lines slope and y-axis intercept. Consolidation times vary between material types, with granular soils typically requiring a shorter consolidation durations.

The shear head plates are equipped with grooved teeth that engage the material on the walls of the borehole and force the failure plane to occur within the surrounding soil material rather than at the shear head interface. Each repetition of the shearing phase shifts the shear surface radially outwards into virgin material and as such, consolidation and dissipation of pore water pressures are considered to be cumulative for each test (Lutenegger and Tierney, 1986). When an increase in normal stress is applied, the previously sheared material will reconsolidate and increase in strength. This causes the shear plane to move outwards into weaker undisturbed material. The radial geometry of the shear head distributes stresses away from the surface of the borehole walls such that consolidating pressures are highest in the soil closest to the shear plates. Successive shear failure readings are therefore able to be obtained without relocating the shear head or releasing the normal stress between each test interval.

The Borehole Shear Test has been well documented as a successful insitu test that can determine shear strength parameters for all soil types. Historically the BST has been compared with direct shear tests which force failure through a horizontal failure plane with results suggesting that the BST produces similar strength parameters.

3 SOUTH EAST QUEENSLAND CASE STUDY

A case study undertaken using the BST at a site in South East Queensland (SEQ) is presented to demonstrate the effectiveness of the BST. A borehole was undertaken and advanced using a 75 mm

tungsten carbide tipped auger to a depth of 10m below the existing ground surface. The site comprised primarily of alluvial clayey silt extending to a depth of 9.5m below the existing ground surface.

SPT tests were undertaken at 1.0m intervals with 50mm diameter (U50) Shelby tube samples recovered at alternating 1.0m sample depths. The consistency of the soil was assessed as 'firm' (as per AS1726-1993) within the top 4.5m and improved in stiffness thereafter. Laboratory index test results for the clayey silt are provided in Table 1 and confirm the consistency of the material within the depth intervals subsequently tested by the BST.

Table 1. Laboratory Test Results

Depth (mbgl)	Sample Classification (USCS)	Moisture Content (%)	Particle Distribution			Atterberg Limits			
			Sand (%)	Silt (%)	Clay (%)	LL (%)	PL (%)	PI (%)	LS (%)
1.00–1.45	clayey silt (ML)	20.2	13	60	27	35.2	21.6	13.6	5.2
2.00–2.45	clayey silt (ML)	20.4	–	–	–	33.0	20.6	12.4	5.6

A total of six multistage BST's were undertaken at various depths within the top 2.0m of the borehole. As per Table 1, all tests were undertaken within 'firm' clayey silt. Swelling of the borehole after excavation limited the test depth to 2.0m, as the shear head could not progress further to promote testing at greater depths. The shear head of the BST was inserted to the desired test depth, with an initial normal stress of 20kPa applied to the shear head. A ten (10) minute consolidation period was allowed between each increase in normal stress test to allow for equalisation of pore pressures. An applied shearing force was standardised using a retrofitted motorised crank that rotated at a constant rate of 2 revolutions per second (0.05 mm/s). The shear stress was recorded at 15 second time intervals. Once the peak shear stress was observed, rotation of the BST crank was stopped and the shearing force reduced until the shear stress gauge returned to a zero reading. The normal stress was then increased by increments of 20kPa, with the test repeated until four successful peak shear stresses were obtained.

Three Consolidated Undrained (CU) Traixial tests were undertaken on samples extruded from the recovered Shelby tubes. The triaxial tests were undertaken at normal forces similar to those applied during the BST field investigations. A Mohr Coulomb failure envelope was developed for each triaxial test, with the results summarised in Table 2.

Table 2. Consolidated Undrained Triaxial Test Results

Sample ID	Depth (mbgl)	Sample Classification	Description	SPT 'N' Value	Effective Stress Parameters	
					c'	Ø'
CU-01	0.00 – 0.50	clayey silt (ML)	Soft - Firm	–	4	34
CU-02	1.00 – 1.50	clayey silt (ML)	Firm	5	1	34
CU-03	2.00 – 2.50	clayey silt (ML)	Firm	5	8	30

4 RESULTS

The peak shear stress and the corresponding normal stress were recorded and graphed to produce a Mohr Coulomb failure criterion. Each BST result was plotted in terms of normal and shear strength relationships and compared with the nearest CU triaxial test result. One BST results has been excluded from further analysis due to data irregularities - likely due to the over extension of the shear head during the completion of the test. Table 3 shows the peak failure shear stresses for each corresponding normal stress. Figure 3 shows the peak BST results compared with the laboratory triaxial tests undertaken on extruded samples.

Table 3. Peak Shear Results

Normal Stress (kPa)	Peak Shear Strength (kPa)				
	BST-01 (0.50mbgl)	BST-03 (1.00mbgl)	BST-04 (1.00mbgl)	BST-05 (1.80mbgl)	BST-06 (2.00mbgl)
20	17	19	20	16	25
40	30	40	40	30	38
60	44	52	55	46	52
80	58	64	70	60	69

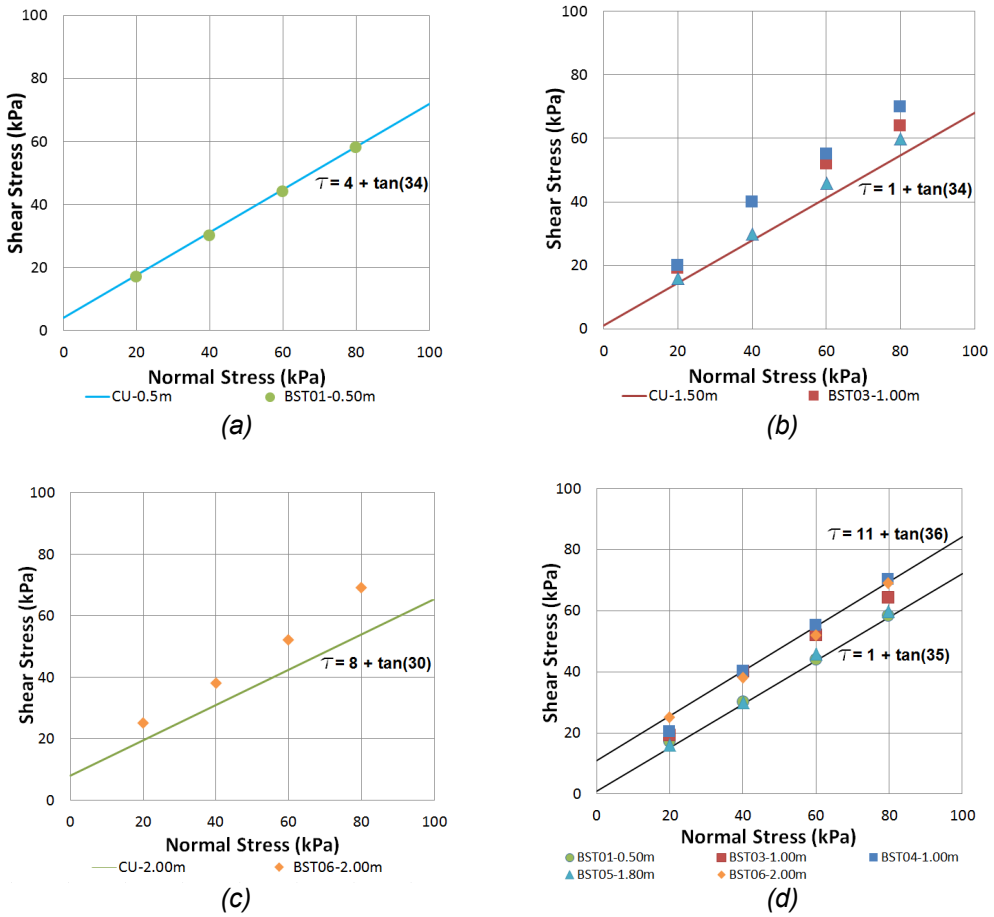


Figure 3. Comparison of Individual BST data points and laboratory triaxial failure envelope – (a) Comparison of BST and CU test between 0.50m and 1.00m depth; (b) Comparison of BST and CU test between 1.00m to 1.80m depth; (c) Comparison of BST and CU test between 2.00m and 2.50m depth; and (d) All data points for Borehole Shear Tests undertaken in clayey silt.

The results of the BST compared with the effective stress parameters determined from the CU Triaxial tests are summarised in Table 4.

Table 4. Effective stress comparison between BST and CU triaxial tests

Sample ID	Depth (mbgl)	BST		Triaxial Compression	
		Effective Cohesion (kPa)	Effective Friction Angle (°)	Effective Cohesion (kPa)	Effective Friction Angle (°)
BST-01	0.50	3	34	4	34
BST-03	1.00	16	31	1	34
BST-04	1.00	10	37		
BST-05	1.80	1	37		
BST-06	2.00	11	34	8	30
Mean		8.2	34.6	–	–
Standard Deviation		6.1	2.5	–	–
COV		75%	7%	–	–

5 DISCUSSION

The BST results observed within the clayey silt material agree well with the shear strength parameters derived from laboratory triaxial test results. Comparison of the results show that the BST achieves similar friction angles compared with the CU triaxial test results, with the effective friction angle calculated to be typically within ± 3° (±10%) of the corresponding laboratory test result. The apparent cohesion determined by the interpretation of the BST was observed to be approximately equal or greater than that observed in the laboratory test results. Comparison of the shear strength failure plots suggests that the BST generally provided equal or higher shear strengths than those observed in CU

triaxial tests. When comparing the results of the BST and the triaxial tests, it is important to consider the different failure paths which can occur for each test method. The BST forces failure to occur in a plane that is approximately parallel to the shear head. Conversely, a triaxial test induces a compressive force that encourages a failure plane to develop anywhere within a soil sample. It is likely that this variation in failure mechanism could contribute to variances in shear strengths between the two test methods.

Laboratory test results can be adversely impacted by sample disturbance compared with their insitu counterparts. Insitu tests typically experience less disturbance than those extruded from a Shelby tube as the sampling and extrusion process may create variances in the soils microstructure. In some cases, these processes may impact on the observed shear strength of a material. Similarly, any variance in moisture content between the insitu samples and those tested in a saturated triaxial test is likely to have an impact on the apparent cohesion for a tested material. The influence of matric suction on an unsaturated soil is not captured in a standard consolidated undrained (cu) triaxial test, and therefore such tests discount any apparent cohesion that may exist within the unsaturated zone. The strength anisotropy of a soil may also have an impact on the soil shear strength. Further research comparing the results of the BST and unsaturated triaxial test results should be considered to assess the suitability of the BST in estimating the increase in apparent cohesion due to matric suction within the unsaturated zone.

The presented results compare CU triaxial tests and BST's within close depth proximity to one another. It is possible that there is a slight variation between the tested triaxial samples and that of where the borehole shear tests were undertaken. However, due to the encountered subsurface profile and the repeatability of the triaxial test results, this is not considered to be of significant impact. As expected with geotechnical testing, some variability between test results can be expected. This is demonstrated by comparison of the laboratory triaxial test results which were undertaken on three samples considered to be of the same material unit. Due to the inherent nature of the soil, slight variations in the microstructure of the soil matrix are likely to exist between the tested samples. Phoon et al, 1999 suggested that the friction angle of clayey silt broadly has a coefficient of variation (COV) of less than 20%, typically with a measurement error between 5% and 15%. Considering this, the results of the triaxial tests appear to correlate well with one another. Similarly, it can be expected that there will be a certain degree of difference between the laboratory test results and those measured in the field due to reasons mentioned above. Analyses of the BST effective friction angles provide a COV of 7%. This is within the typical measurement error range suggested by Phoon et al (1999). Generally the results obtained from the BST appear to provide a good correlation with those calculated from laboratory CU Triaxial tests. Small variations in friction angle and apparent cohesion can be expected and attributed to measurement error, sample disturbance and matric suction.

6 CONCLUSION

The case study undertaken on clayey silt soils supports the existing literature, such that a BST can be used on clayey silts to determine effective stress parameters. The BST can provide insitu measurements for both the effective friction angle (Ø') and the apparent cohesion (c') of a soil without the need for laboratory testing. The results of the friction angle are expected to be within 10% of comparative laboratory test results, whilst the apparent cohesion appears to capture the additional strength gains associated with matric suction and insitu conditions. The BST provides an effective and alternative tool capable of determining direct insitu strength parameters in a time and cost effective manner which are comparable to CU triaxial tests.

REFERENCES

Australian Standard AS 1726. (1993). *Geotechnical site investigations*, Standards Australia

Bechtum, T. (2012). *Automation and further developments of the borehole shear test*, Iowa State University

Handy, R.L. (2013). *Borehole Shear Test Manual*, Handy Geotechincal Instruments Inc., Madrid, IA.

Lutenegger, A.J. and Tierney, K.F. (1986). "Pore Pressure Effects in Borehole Shear Testing", *Use of In Situ Tests in Geotechnical Engineering*, ASCE, pp. 752-764.

Phoon, K. and Kulhawy, F.H. (1999). "Characterisation of Geotechnical Variablility", *Canadian Geotechnical Journal*; ProQuest Science Journals, pg. 612.

Proceedings of the 11th ANZ Young Geotechnical Professionals Conference – 11YGPC
Queenstown, New Zealand
25 – 28 October 2016

Deep Excavation Impact Assessment in Urban Environments: Predictions versus Reality

G. Chan[1], MIEAust CPEng

[1]Geotechnical Engineer at Jacobs (formerly Coffey), 177 Pacific Highway, North Sydney NSW 2060, Australia; email: Geoffrey.Chan@Jacobs.com

ABSTRACT

To cater for the increasing population in Australia, we have had a property boom for several years. This has resulted in the demand for high-rise buildings with deep basement space. Within the Sydney metropolitan, these are preferably founded in rock strata. Invariably, proposed building developments are in close vicinity to other high-rise buildings, services and tunnels. In order to satisfy council's Development Approval (DA) requirements for new developments, rigorous and sophisticated numerical analyses are commonly executed to assess potential induced deformation and its consequent damage risks. Predictions of such performances require a sound understanding of rock behaviour and their defects; these include the appreciation of locked in-situ stresses and relief mechanism, defect orientations, inclusions and presence of fault zones. This is better understood by creating geotechnical models based on appropriate geotechnical site investigations and interpretation by geotechnical professionals. During construction phase, specific monitoring plans are implemented whilst bulk excavation is progressed to verify the design assumptions. This is achieved by providing monitoring equipment including the installation of geophones, inclinometers, extensometers and survey targets. This paper attempts to provide an insight into the geotechnical project life cycle for deep excavations in an urban environment from design phase to construction support and implementation of monitoring measures.

Keywords: Deep excavation, impact assessment, field monitoring, numerical model, rock engineering

1 INTRODUCTION

Studies to understand rock mechanics and its applications with deep excavation near tunnels have been a popular topic in Sydney since the late 1990s. Early texts have summarised case studies relating to the impact assessments of past building developments including the Genting Centre, Shangri-La Hotel and Green Square Station (Nye 2005). A more recent case study has also discussed the different approaches used to assess the proposed York & George building development which lay within a fault zone (Oliveira et al 2014).

The creation of a geotechnical ground model enables the design and development of economical solutions for ground bearing and underground infrastructures. This involves geotechnical site investigations to provide data to assist in developing the site geotechnical conditions. Inferred geological units are then adopted by understanding the regional geomorphology, geological setting and groundwater. To classify the different units, rock quality in the Sydney region is interpreted based on the Sydney Rock Mass Classification System (SRMCS) (Pells et al. 1978 and Pells et al. 1998). Appropriate design parameters are then carefully derived based on this classification system, which requires the understanding of rock behaviours and their defects; these include the appreciation of in-situ stress of rock and its relief, defect orientations, inclusions and presence of fault zones. Typical design parameters for tunnels and deep excavations are presented in Bertuzzi (2014) and Oliveira (2014). Oliveira and Wong (2012) have also provided a detailed discussion on relevant mechanisms that should be accounted for in deep excavation projects in Sydney. These papers emphasize the importance for designers to conduct their own assessment and adjustments to reflect the adopted method of analysis.

For geotechnical professionals, the services they provide to the principal contractor may vary dependent on the phase of involvement in the project life cycle. With deep excavations, it typically includes the design phase, construction monitoring planning and construction support services. The design phase may include the design of retention systems, remedial works and planning of construction methodologies. Whilst construction monitor planning assesses the impact of excavation

methods by installing instrumentation to measure movements, vibrations and noise. The scope and requirements are usually based on criteria specified by local authorities and key infrastructure asset owners (i.e. Sydney Trains and Roads and Martine Services).

Comparisons of predicted rock behaviour and actual performance are presented, based on experience on various projects.

2 GEOTECHNICAL PARAMETERS AND NUMERICAL MODEL

Geotechnical parameters used in numerical models are assessed based on a combined approach involving the understanding of the site geological history and processes, compilation of a geotechnical model, interpretation of in-situ tests from geotechnical site investigation and laboratory tests. Empirical methods from published text such as Carter and Bentley (1991) and Look (2007) are then commonly used to assist in deriving appropriate soil and rock parameters, which are consistent with previous experience in similar design conditions. The most influential engineering parameters on the behaviour of rock masses in deep excavation requires further calibration based on the results from the monitoring program.

Typical in-situ geotechnical parameters used in design of deep excavations are then assisted by processes of determining rock mass classes such as the SRMCS, which the author has used on projects in the Sydney region. Typical rock parameters for Sydney sandstone and shales can be interpreted from publications such as Bertuzzi (2014) and Oliveira (2014) for preliminary assessment. For other regions other than Sydney, the Q-system or RMR (Rock Mass Rating) system and local published research papers should be used.

Other considerations include interpreting the relationship between "*at-rest*" ground conditions and the in-situ stress relief during excavation of the deep basement. Especially with deep excavation in Sydney, the assumption of a single linear relationship with depth may not be appropriate. This is due to the existence of high tectonic locked-in horizontal stress at shallow depths (Oliveira and Parker 2014) and the influence of rock masses of varying stiffness.

Simulation of the excavation processes can be replicated by commercially available Finite Element Analysis (FEA) software with geotechnical capabilities. In Sydney, extremely weathered sandstone (i.e. rock mass with soil like properties) are modelled as isotropic elastic – perfectly plastic materials following the Hoek-Brown failure criterion, whilst weathered to fresh sandstone are modelled as transversely isotropic elastic – perfectly plastic material with failure through either the intact rock (matrix) or ubiquitous joints. An example of a numerical model is depicted in Figure 1. Emphasis should be placed on adopting appropriate engineering design parameters to determine ground deformation and relevant structural actions.

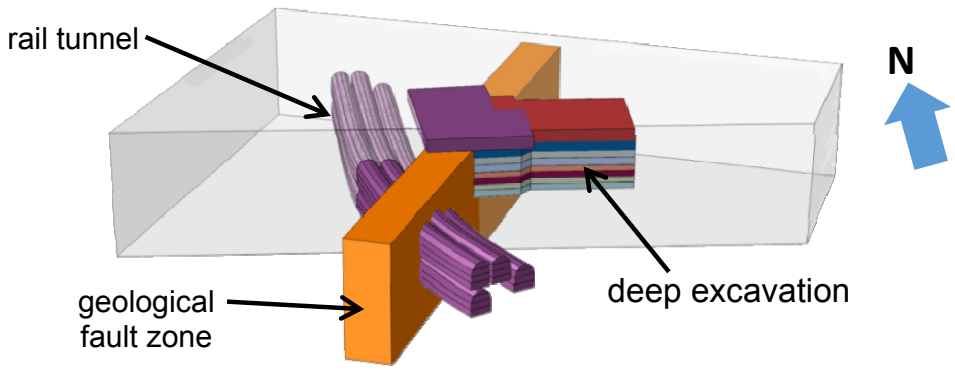


Figure 1. Typical 3-dimensional numerical model used to predict excavation performances on the York & George Street project site (after Oliveira et al. 2014)

3 EXCAVATION AND VIBRATION MONITORING PLAN

Deep excavations in urban areas can be relatively complex due to the presence of existing services, adjacent building structures and/or tunnels. To protect these assets and to verify the design, monitoring plans are devised including Geotechnical Excavation Monitor Plan (GEMP) and Vibration Monitor Plan (VMP).

The objectives of both GEMP and VMP are to monitor the behaviour of the excavation and its effects on adjacent infrastructures and services. These are then validated with predicted performances of the deep excavation considered during DA stages. Certain limit criteria are set so that excavation procedures can be tracked and modified if recordings exceed acceptable levels. These monitoring plans are primarily in place to provide safety during construction and to the public, and mitigate risk of damages to adjacent structures and infrastructures.

3.1 Geotechnical Excavation Monitoring Plan

GEMP involves various tasks to satisfy the objectives of the project. The procedures can be described in conjunction with excavation processes of the development. The excavation processes include pre-excavation works, installation of geotechnical instrumentation, performing geotechnical monitoring throughout the bulk excavation period, reporting as excavation progresses and conclusive summary. This is depicted on Figure 2. To confirm anticipated lateral displacement performances, geotechnical monitoring is assessed at each incremental drop of bulk excavation and compared to a set of criterions. The set of criterions can be in the form of excavation deformation trigger levels and response as listed below:

- *Alert level (or green light):* Safe working value less than the agreed level;
- *Alarm level (or amber light):* Working value where caution is advised but less than the agreed level. Frequency of monitoring to be increased;
- *Action level (or red light):* Value where agreed level has exceeded. Works will stop, monitoring will continue and a tailored contingency action plan will be devised.

The agreed level is semi-empirical method derived from a combination of numerical predictions and tolerable displacement limits from adjacent structures/services. Based on semi-empirical methods and past experience with deep excavations in Sydney, has shown that lateral deformations in deep basement excavations typically vary between 0.5-2 mm/m of rock depth excavation in practice (Pells 1990, Walker 2004 and Oliveira and Wong 2012).

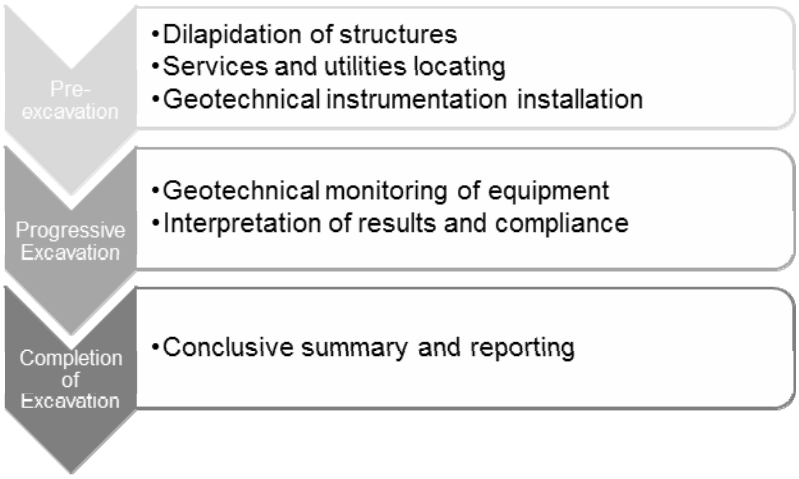


Figure 2. Construction excavation process with GEMP and VMP involvement

3.2 Vibration Monitoring Plan

Similarly, VMP's utilised during bulk excavation, may work in conjunction with the GEMP. The works involve the monitoring of peak particle velocity (PPV) caused by heavy machinery during deep excavation. By doing so, the procedure provides a measure of risk mitigation and early warning signs of potential damages. BS 5228-4:1986 *Noise and vibration control on construction and open sites* recommends a set of trigger level range between 10-25 mm/s and values may be tailored to specific projects. In some instances this may be low as 6.5-12.5 mm/s for structures over or adjacent to tunnels. This is in accordance with Transport for NSW Standard for *Miscellaneous Structures*: T HR CI 12070 ST to prevent the potential damages to rail tunnel lining. If recordings surpass the trigger level, modification of equipment and excavation methodology would be required.

4 CASE STUDY PERFORMANCES

Three projects are presented where deep excavation induced movements have been assessed by FEA for the purpose of 'Class A' predictions (i.e. prior to construction and based on inferred models and parameters). Lateral displacements are horizontal movement occurring near top of a deep excavation face. These are presented in conjunction with results from geotechnical monitoring summarised in Table 1 and Figure 4. The below mentioned cases were assessed and designed by Coffey Geotechnics Sydney Office. Details of each case study have been summarised with the following key points; site description, excavation support, types of monitoring plans and field measurement results.

4.1 York and George Street, Sydney

- *Site description*: The York and George Street project is a mixed use development located within the Sydney CBD. The geological units vary across the site and can be separated into two zones. The rock mass on the York Street side lies within a fault zone and comprises low quality rock to great depths. The rock mass along the George Street comprises of fill overlying weathered to fresh sandstone with rock mass quality increasing with depth.

- *Excavation support*: Lateral support comprised of soldier pile walls with a combination of anchoring and propping support along York Street (refer Figure 3) and deep open cut along George Street. These were devised to address the variable quality of rock mass encountered, from poor to good. Sensitive neighbouring structures in close vicinity to the project site included adjacent commercial buildings, frequently used roads (York Street and George Street) and existing rail tunnels. Further details of the project are presented in Oliveira et al (2014) and Oliveira and Chan (2016).

- *Monitoring plans*: A VMP was developed with vibration monitoring in the rail tunnel and neighbouring building. The tolerable surface vibration limit near commercial building was determined from an acoustic logic assessment with references to BS 5228-4:1986. This assessment enabled the development of vibration trigger levels for alert and action of 15 and 25 mm/s respectively. The neighbouring rail tunnel is an asset of Sydney Trains (Transport for NSW) and required to comply with alert and action trigger levels of 6.5 to 12.5 mm/s respectively from T HR CI 12070 ST. Geophone sensors with monitor readout unit were installed at the north-west (near a commercial building) and south west corner (near the rail tunnel) and maintained throughout the excavation period. GEMP was also enforced with two inclinometers in the soldier pile walls (Spiden and Carlton House), survey monitoring at 10 m centres located at the top of the capping/excavation and a horizontal extensometer installed along the excavation face closest to the rail tunnel. The excavation monitoring plan regime was to ensure that behaviours were as predicted with numerical model and within tolerable limits.

- *Field results:* A maximum PPV occurrence of 11 mm/s near the commercial building and 1 mm/s within the tunnel was recorded during the bulk excavation period. This was considered to be within acceptable levels. Construction inspections were also called upon for observation of ground conditions of the excavation face, piles and footings to ensure compatibility with design. With an approximately 15 m excavation depth, the predicted performance from FEA indicated lateral displacements between 10-22 mm acting at the top of the open excavation and soldier pile walls. Results from inclinometer measurement indicated a maximum lateral displacement of 14 mm (i.e. were well within the expected movement range for deep excavations).



(a) *(b)*

Figure 3. View of excavation faces for the York and George Street project – (a) York and George, Sydney – Carlton House; and (b) York and George, Sydney – Spiden House

4.2 Epping Road, Lane Cove

- *Site description*: This is a property development running adjacent to Epping Road located in Lane Cove. The geological unit of the site typically comprised fill overlying slightly weathered to fresh sandstone at shallow depths.

- *Excavation support*: Contiguous pile walls were used to retain all side of the basement excavation with anchoring support. The site is bounded by a busy road, commercial buildings and in close vicinity to a road tunnel.

- *Monitoring plans*: A VMP was developed for the project and geophones installed on the excavation face closest to the road tunnel. An initial VMP advising vibration triggers for alert and action levels of 10 and 25 mm/s respectively were issued to the respective stakeholders of the project. This was later reduced to 7.5 and 10 mm/s at the request of the asset owner of the road tunnel. These geophones were installed and monitored for the duration of the bulk excavation to ensure risk was limited as a result of the vibration by heavy machinery. A GEMP was also utilised during the bulk excavation of the site to confirm typical lateral behaviours based on experience of sites with similar conditions. To satisfy Roads and Martine Services (RMS) requirements, three inclinometers along the northern boundary were installation closest to the RMS road (Epping Road). These were accompanied with survey points at 25 m nominal centres. Measurements were to be recorded and assessed at each 1.5 m depth of excavation.

- *Field results:* For an approximate 15 m deep of excavation, the actual lateral displacements were 8 mm from the top of the excavation face. Vibration monitors at the north-east corner of site, located closest to the road tunnel recorded a maximum PPV of 4 mm/s. Both vibration and lateral displacement were within anticipated and tolerable limits.

4.3 Pacific Highway, Lane Cove

- *Site Description*: A property development located in close vicinity to a major intersection, along Pacific Highway in Lane Cove. The geological units comprised fill overlying residual soil, and then weathered to fresh shale whose rock mass quality increased with depth.

- *Excavation Support*: Soldier Pile Walls were used to retain all side of the basement. Anchoring was predominately used, with propping support used in areas with boundary restrictions. This development lay in close vicinity to a busy highway, existing neighbouring structures and road tunnel.

- *Monitoring plans*: As proposed in the VMP, an in-ground geophone sensor was installed at the site closest to the road tunnel to ensure vibration trigger levels of 10 and 25 mm/s for alert and action levels is not exceeded. A base station connected to the sensor included the functionality of housing the monitoring unit, remote access and alarm capabilities. This

enabled real-time monitoring and efficient response if trigger levels were exceeded. In accordance with the project specific GEMP, the plan aimed to reduce the risk in damaging adjacent structures. The setup included two inclinometers (along adjacent property and Pacific Highway), survey monitoring at 10 m centres along the pile cap and a vertical extensometer closest to the road tunnel were installed. Initiating the plan allowed the designers to verify its compliance with numerical predicted behaviours between 10-15 mm.

- *Field results:* The maximum recorded lateral displacement was 14 mm from top of the excavation for a 9.5 m deep excavation. Based on the inclinometer results, this occurred along the Pacific Highway alignment. The maximum recorded PPV was 13 mm/s during an isolated incident were daily assessment of vibration data subsequently carried out and the incident did not reoccur. Overall the vibration and displacement were well within tolerable limits.

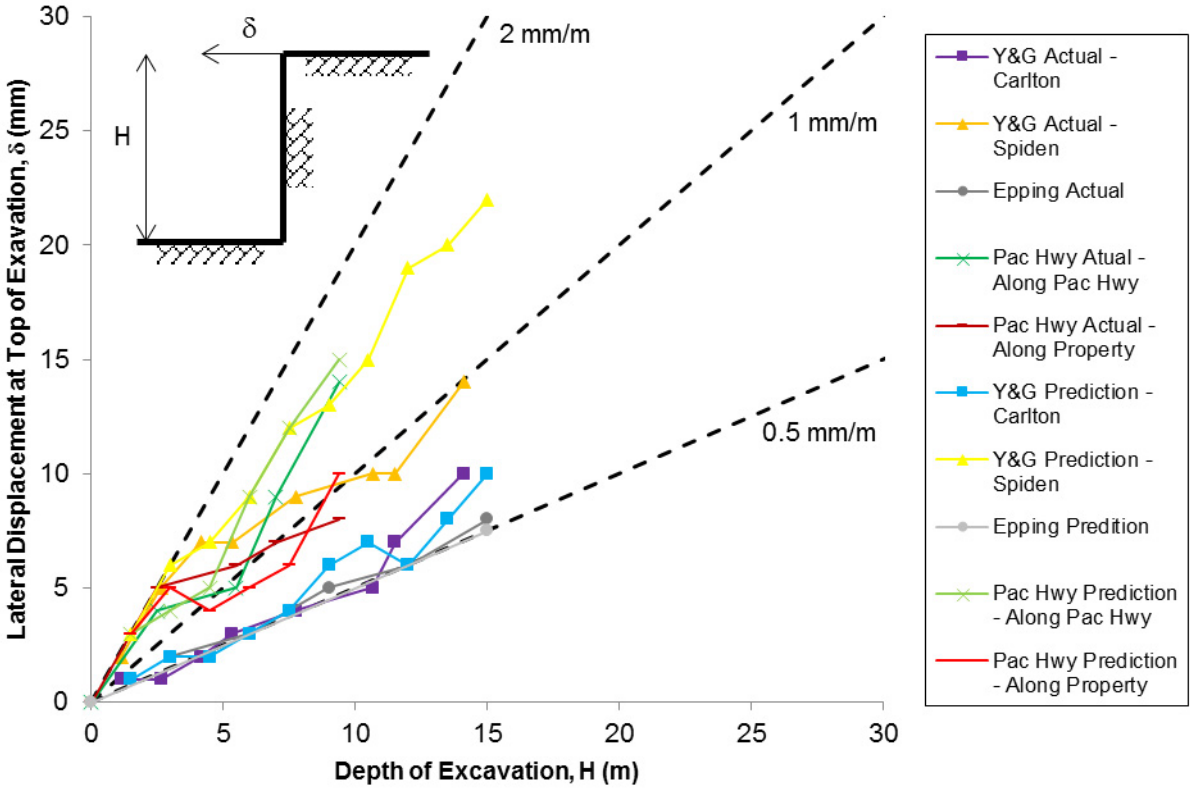


Figure 4. Summary of lateral displacement at top of excavation depth and length of excavation

Table 1. Summary of lateral performances and vibrations from case study

Site Location		Predicted Lateral Performance[a] (mm/m)	Actual Lateral Performance[a] (mm/m)	Vibration Limit[b] (mm/s)	Actual Vibration (mm/s)
York & George St, Sydney	Carlton House	0.6	0.6	15/25	11
	Spiden House	1.5	1		
Epping Rd, Lane Cove		0.5-2[c]	0.5	7.5/10	4
Pacific Hwy, Lane Cove	Along Pacific Hwy	1.4	1.3	10/25	13
	Along Property	1	1		

[a] Average lateral displacement interpolated from line of best fit and intercepting the origin.
[b] Two values shown, provides a lower bound and upper bound vibration limit.
[c] Lateral displacement range based on experience

5 SUMMARY AND CONCLUSIONS

An insight into deep excavation construction has been presented in the form of case studies within this paper. To predict its impact to important assets, FEA are carried out to assess the behaviours of deep excavation faces and its compliance with tolerable limits. Their performance is then confirmed by field measurements.

The variations in lateral displacement, especially where the differences are at the same site can be attributed to the changing geology, influences of high locked-in stress in rock masses from a dominate direction, changes to excavation sequence and the type of retention system (e.g. anchored Soldier Pile Walls, propped Soldier Pile Walls or open cut excavation) which can deviate the outcomes of the predictions.

A well-developed excavation plan is essential in mitigating risk associated with the deep excavation. It also provides a strategy and contingencies if limits are reached. Plans such as VMP and GEMP were used across all sites mentioned in this paper.

Measured displacements in the three case studies presented confirmed past experience in Sydney. The 'Class A' predictions have also generally confirmed the anticipated behaviour despite some over-predictions. It is important to note that these over-predictions are generally a result of some degree of conservatism in the assessment and considered beneficial to the project as no "factor of safety" are applicable for such serviceability assessment. Measurements of actual displacement below predictions allow for an excavation progress without the need for interventions and therefore beneficial from a construction program viewpoint. Nevertheless, some of the discrepancies between predictions and actual measurements are typically related to discrete features that are often difficult to capture in numerical models. These include uncertainties in the assessment of both in-situ stress conditions and rock mass deformation parameters which largely rely on engineering judgment to choose appropriate values.

6 ACKNOWLEDGEMENTS

The work reported in this paper was carried out during studies by Coffey Geotechnics on a number of property projects in Sydney. The author wishes to gratefully acknowledge the colleagues who were heavily involved on those projects and this paper including David Oliveira, Helen Chow and Pawan Sethi. In addition, the primary contractor for York and George project, Watpac Pty Ltd for generously allowing publication of their project and photos.

REFERENCES

Bertuzzi, R. (2014). "Sydney Sandstone and Shale Parameters for tunnel design", *Australian Geomechanics*, 49(1), March 2014, 1-104.

Carter, M. and Bentley, S. P. (1991). *Correlations of soil properties*, Pentech Press, London.

Look, B. (2007). *Handbook of Geotechnical Investigation and Design Tables*, Taylor & Francis, Balkema.

Nye, T (2005). "Building Around Tunnels – Case Histories", *AGS AUCTA Mini-Symposium: Geotechnical Aspects of Tunnelling For Infrastructure Projects*, October 2005, pp. 1-11.

Oliveira, D. A. F. and Wong, P. K. (2012). "Selection of Rock Mass Design Parameters for Assessing Excavation Induced Movements in the Sydney CBD." *11th Australia-New Zealand Conference on Geomechanics – Ground Engineering in a Changing World*, Melbourne, Australia

Oliveira, D. A. F., Badelow, F. and Wong, P. K. (2014). "Assessing the impact of a deep basement excavation on old rail tunnels in Sydney, Australia." *Proceedings of the World Tunnel Congress 2014*, Foz do Iguacu, Brazil, pp. 1-11.

Oliveira, D. A. F. (2014). "An alternative view on geotechnical parameters for tunnel design in Sydney." *Australian Geomechanics*, 49(3), September 2014, pp. 1-14.

Oliveira, D. A. F., Parker, C. J. (2014). "An alternative approach for assessing in situ stresses in Sydney", *Proceedings of 15th Australasian Tunnelling Conference 2014*, Sydney, NSW, 17-19 September 2014.

Oliveira, D. A. F. and Chan, G. (2016). "Ground control for a deep basement excavation in Sydney's GPO fault zone". *Proceedings of the AGS 2016 Sydney Symposium: Ground Stabilisation Techniques for Problematic Soils and Unstable Rocks*, (submitted)

Pells, P. J. N. (1990). "Stress and Displacement around Deep Basements in Sydney Area", *Proceedings of 7th Australian Tunnelling Conference: the underground domain*, Sydney, Australia, 11-13 September 1990.

Pells, P. J. N., Mostyn, G. and Walker, B. F. (1998). "Foundations on Sandstone and Shale in Sydney Region." *Australian Geomechanics*, 33(3), December, pp. 17-29.

Walker, B. F. (2004). "Stress Relief on Hillside and Hillside Excavations", *Australian Geomechanics,* 39(3), September 2004.

This page intentionally left blank

Proceedings of the 11th ANZ Young Geotechnical Professionals Conference – 11YGPC
Queenstown, New Zealand
25 – 28 October 2016

The Use of Engineering Index Correlations with the Shrink-Swell Test

J. Johnston[1] and S. Fityus[2]

[1]Geotechnical Engineer, Snowy Mountains Engineering Corporation (SMEC) Australia, 74 Hunter Street, Newcastle, 2300, NSW, Australia, email: John.Johnston@smec.com
[2]Professor in Geotechnical Engineering and Assistant Dean Research – FEBE, The University of Newcastle, University Drive, Callaghan, 2308, NSW, Australia, email: Stephen.Fityus@newcastle.edu.au

ABSTRACT

Expansive soils are a very common in many parts of the world and are often a direct cause of damage to housing, through their tendency to undergo significant volumetric change in reaction to changes in moisture content. The shrink-swell test (AS1289.7.1.1-2003) has become a widely adopted laboratory test in Australia for estimating the degree of reactivity of an in-situ soil due to its simplicity, low cost and ability to generate relatively reliable data which is independent of soil suction and initial water content. Anecdotal reports indicate that it has become increasingly common to use engineering index properties such as the Liquid Limit (LL), Plasticity Index (PI) and Linear Shrinkage (LS) in place of a shrink-swell test, with the results being correlated to a Shrink-Swell Index (I_{ss}) value, using a variety of published correlations. This is typically occurring both in response to cost and time pressures placed on the geotechnical consultant, as well as in certain situations where an undisturbed sample (required for the shrink-swell test) is not able to be obtained in the field. However, the use of such correlations without regard for the context in which they were developed, together with conservative interpretation, can have a significant effect on the resulting site classification and construction cost. This paper examines and discusses the use of these correlations in Australian geotechnical consulting practice within the context of site classification to AS2870-2011. It is demonstrated that using a non-geologically specific correlation between I_{ss} and engineering index in the calculation of ground surface movement and subsequent site classification is not able to be achieved without an unacceptable likelihood of significant error and adverse cost implications.

Keywords: expansive soils, engineering index properties, Atterberg limits, site classification, AS2870

1 INTRODUCTION

Reactive soils are one of the most common causes of damage to engineering works and residential structures in the world, with projected costs of remediation in the billions of dollars annually (eg. Zhao et al. 2013). Reactive soils, commonly known as expansive soils or swelling clays, are clay soils that exhibit significant volumetric change in response to a change in moisture content. This extreme volume change in response to moisture content variation is typically attributable to a high proportion of certain types of clay minerals present, such as those of the smectite group that produce this effect in the soil (e.g. Fityus et al., 2005, Johnston et al., 2015).

While the damage due to reactive soils has long been recognised, the history of treating or designing for the movements of reactive soils in Australia is relatively recent. The first Australian Standard to provide methods of estimating and designing for the effects of reactive soils was issued as recently as 1986 (AS2870-1986, Residential Slabs and Footings). Preliminary experimental methods to quantify expansive soil movements due to reactive clays specific to Australia and subsequently used in AS2870 are detailed in Cameron and Walsh (1984). In that study, several test methods were used to derive an “instability” index, used as a quantitative measure of a soil’s expansive potential, for input into the calculation of the free surface movement due to reactive soils expected at a particular site. Of these early test methods, the shrink-swell test has been most widely adopted as a measure of soil reactivity due to its relative simplicity and cost effectiveness as much as for the quality of data that is able to be obtained (Johnston et al. 2015, Fityus et al. 2005).

The current version of Australian Standard 2870 (Standards Australia, 2011) allows for design according to a site classification. Site Classification is based on an estimated characteristic surface movement (y_s) which assesses the reactivity of the soil profile. Methods to assess instability index that are currently permissible by AS2870 include direct laboratory tests (such as the shrink swell test),

correlations between the instability index and other clay index tests for the soil type (with which this paper deals) or visual-tactile identification of the soil by an engineer or engineering geologist having appropriate expertise and local experience.

It is generally considered that the visual-tactile method is appropriate for simple geological situations, however when the visual-tactle method is applied in complex geological sequences, it is highly unreliable (Fityus and Delaney, 1995; Jayasekera and Mohajerani, 2003). However, estimations of shrink-swell potential via the results of engineering index property tests are considered by some consulting geotechnical engineers to be useful for estimation of instability index (Mitchell and Avalle 1984, Davenport 2007).

Engineering index property tests, for the most part, are able to adequately characterise soils for use in geotechnical works and enjoy widespread acceptance within the geotechnical community for this purpose. However while these engineering index tests are able to provide a general indication of the degree of reactivity, there is a view that they are able to provide quantitative data for direct use in the classification of residential building sites in accordance with AS2870-2011 without significant risk or conservatism. This paper tests this view.

2 REVIEW OF CURRENT CORRELATIONS

Eleven consultancies, predominantly practicing in NSW, were contacted regarding relationships between the shrink-swell index and engineering index properties. Typical published correlations between shrink-swell index and LS, PI and LL currently in general use by consulting geotechnical engineers in Australia are those presented by Cameron, and Walsh, (1984); Earl, (2005); Reynolds, (2013) and Davenport, (2007). These correlations, together with a number of other studies that have been reported in the literature, are presented in Table 1. The table also summarises the number of data used in the development of the correlation and the region from where the data was derived.

Table 1. Correlations Analysed and Used in this Study

Correlation	PI	LL	LS	Geological Origin
Cameron (1989)	0	0	55	Nonspecific Geological Formations Throughout Australia
Davenport (2007)	64	0	0	Various formations (Guildford formation, Darling Range Region, Goldfields Region, Wheatbelt region, Southwest Region), WA.
Delaney (2005)	43	42	44	Nonspecific Geological Formations, Sydney Basin, NSW
Earl (2005)	29	29	29	Quaternary basalt, Shepparton Formation, Vic
Jaska (1997)	0	4	0	Geological Formations Throughout Metropolitan Adelaide, SA.
Jayasekera (2003)	9	9	0	Remoulded Basaltic Clay of Unknown Origin
Reynolds (2013)	66	63	65	Nonspecific Geological Formations, Queensland
Seo and Mersne (2014)	0	37	32	Various formations throughout Brisbane (Ipswitch), Qld
Zou (2015)	44	44	44	Geological formations Throughout Metropolitan Melbourne, Vic
Total	255	228	269	

In analysing the above correlations and accompanying literature, it was found that while index property tests generally show a visual correlation with shrink-swell index, significant uncertainty is associated with the correlation relationships for all correlations with large data, with coefficient of correlation (r^2) values ranging from 21% (Delaney, 2005, PI vs. Iss) to 65% (Zou, 2015, LL vs Iss). No study reported a consistent, viable correlation for shrink-swell index with any single engineering index property test for natural soils that could be used without likelihood of significant error.

The geologically-specific correlations contained in Zou (2015) and Davenport (2007) in some cases showed a decrease in uncertainty in the correlation compared to other methods. Importantly though, these methods still result in correlations between engineering index properties and the shrink-swell index that cannot be utilised with sufficient confidence that a reliable prediction of instability index can be achieved. It was also noted during the literature review that despite a common view that a geologically-specific correlation improved the reliability of estimated ground movements (e.g. Davenport (2007), the most commonly referenced correlation by the consultants contacted was the

Australia-wide correlation provided by Cameron (1989), and subsequently reproduced in Fityus (2005), that did not limit the scope of the study to any regional geological formation or soil type.

3 EVALUATION OF CORRELATIONS WITH ENGINEERING INDEX PROPERTIES

In response to the above review findings, an evaluation of correlations between I_{ss} and the three commonly adopted engineering index properties (LS, PI and PI) was undertaken. Despite the commonly-held belief that geologically-specific correlations are likely to be more reliable, there is also a general principle that more statistically-reliable correlations can be established for larger data sets. To evaluate the potential for reliable index-based predictions, three general non-regional and non-geology-specific correlations have been generated based on the data contained in all the studies referenced in Table 1. The combined data are presented in Figure 1, Figure 2 and Figure 3 with the best fit linear regression lines and the 10th and 90th percentiles shown.

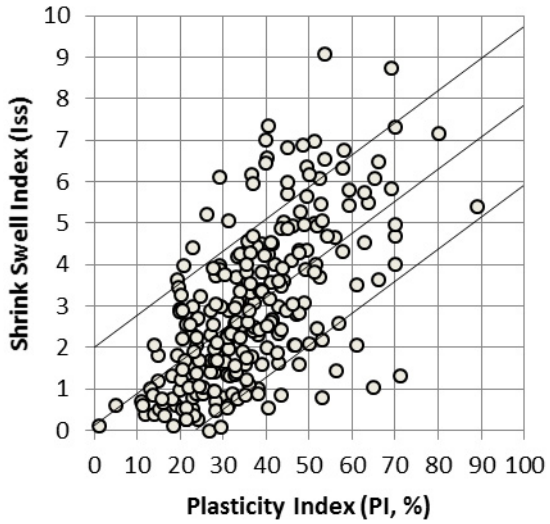


Figure 1. Shrink-swell index (I_{ss}) vs. Plasticity Index (PI)

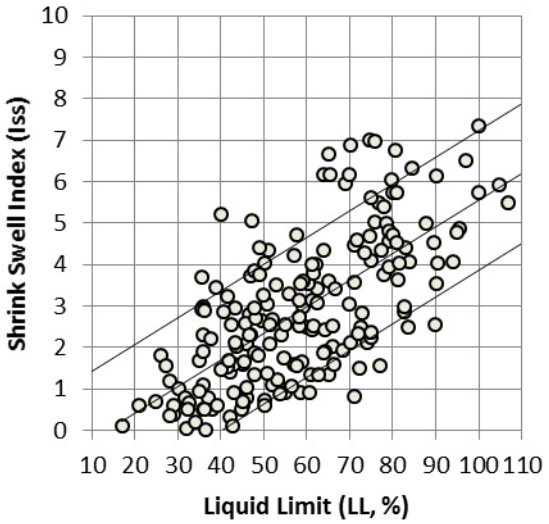


Figure 2. Shrink-swell index (I_{ss}) vs. Liquid Limit (LL)

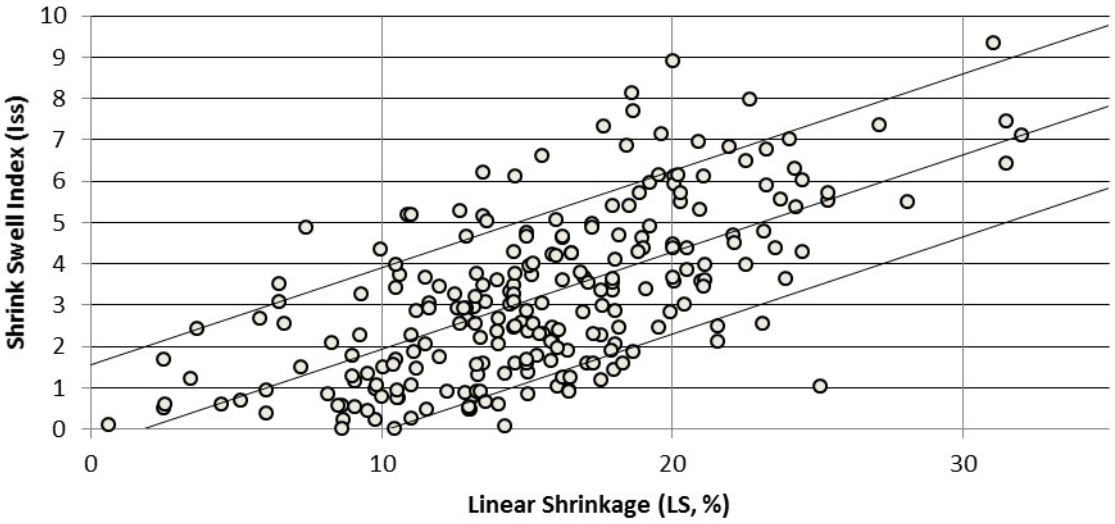


Figure 3. Shrink-swell index (I_{ss}) vs. Linear Shrinkage (LS)

General equations for each of the three engineering index property tests and the shrink-swell index for the data shown in Figures 1 to 3 are given below in Equations 1, 2 and 3.

I_{ss} = 0.0774 x PI + 0.1041	R^2 = 0.3733	N = 255	(1)
I_{ss} = 0.0538 x LL – 0.0248	R^2 = 0.3353	N = 228	(2)
I_{ss} = 0.2382 x LS – 0.4493	R^2 = 0.4121	N = 269	(3)

Where:

I_{ss} = Shrink-swell Index;
PI = Plasticity Index;
LL= Liquid Limit;
LS = Linear Shrinkage; and
N is number of data used.

As can be seen from the correlations for each engineering index property test, a visual trend is indicated in each figure, implying a valid and expected general correlation between each engineering index property and shrink-swell index. However there is significant variation in the data, which can produce errors in the assessment of shrink-swell index (or instability index).

To quantify the nature of the possible error associated with each correlation, and to assess if any one index is able to give a more reliable correlation than the others, the possible cumulative error associated with each correlation is plotted against its likelihood of occurrence in Figure 4. Similarly, an example case in which the full range of I_{ss} values and their likelihood of occurrence has been normalised to a total range of 1.0%strain/pF is presented in Figure 5.

Figures 4 and 5 indicate that the reliability of correlations based on any of three commonly adopted indices is approximately the same. For example, regardless of the index correlation used, there is only an 82-85% chance that the predicted value of I_{ss} will be within a range of 2 I_{ss} units of the actual value of I_{ss}, either positively or negatively. This can be seen clearly in Figure 5 which shows that approximately 80% of the probable values lie over approximately 55% of the total range of values for each correlation.

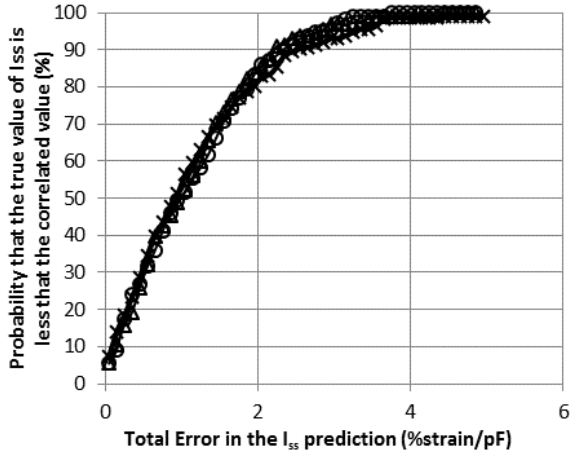


Figure 4. Error in the Prediction of the Shrink-swell index (I_{ss})

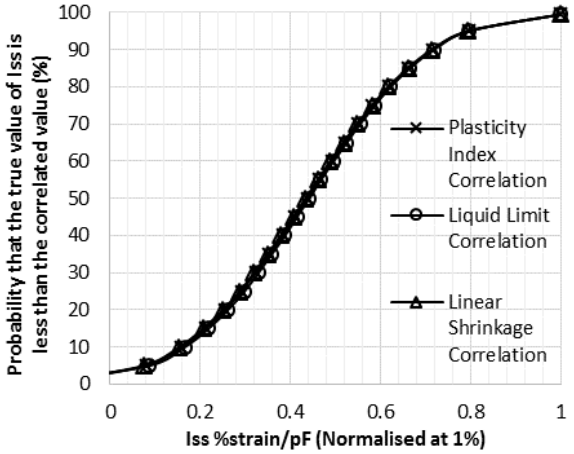


Figure 5. Probability that the actual value of Shrink-swell index (I_{ss}) is obtained

4 SIGNIFICANCE FOR GROUND MOVEMENT PREDICTION AND SITE CLASSIFICATION

Using the developed engineering index correlations, an attempt has been made to quantify the magnitude of the error implicit in each correlation in practice, and show the effect using the correlations has on a typical site classification.

An example relationship showing potential effect of the error implicit in the use of the developed correlations is shown in Figure 6. For the purposes of illustration, the relationship used was normalised around predicted values of 1%, 3% and 5%strain/pF. The site classification ranges have been based on the predicted ground movement calculated in accordance with AS2870 assuming a depth of suction change of 1.8m, a crack depth of 0.9m, and a uniform clay profile.

From Figure 6 it can be seen that the range of possible site classifications resulting from a single engineering index test are large. It can be observed that the “middle value” correlation for 3.0%strain/pF returns the potential for the full range of possible reactive site classifications (from Class S to Class E), indicating that a large amount of uncertainty exists in the developed correlations. Whilst the range of possible site classifications is large for the 3%strain/pF case, it can be seen that the most likely site classification (with a probability of occurrence of approximately 30% each), was Class M and Class H1.

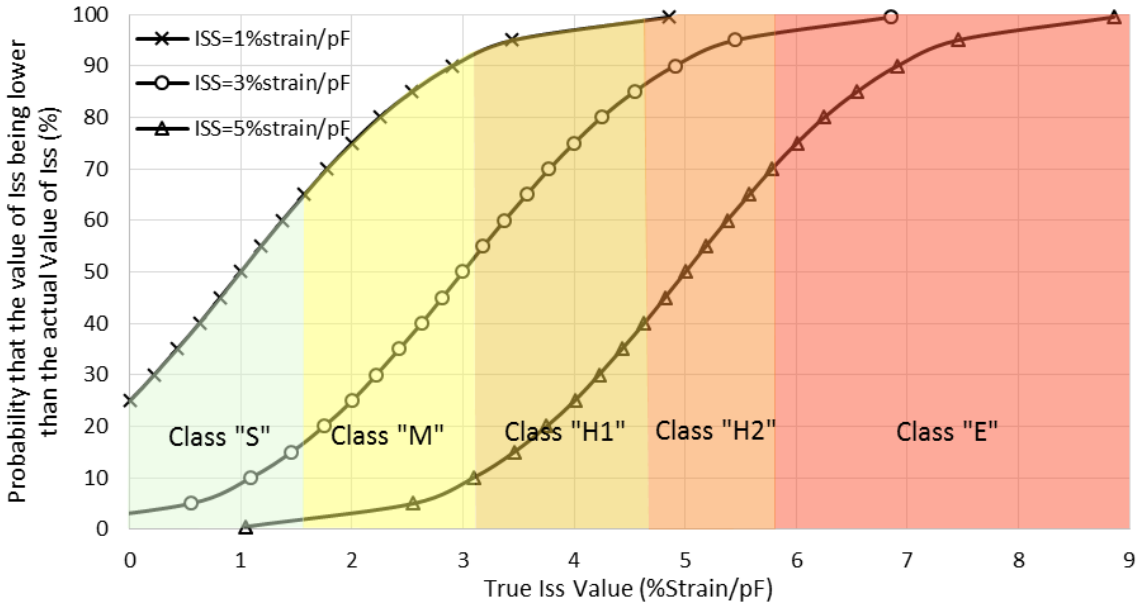


Figure 6. Probability that the Correlated Value of I_{ss} is lower than the Actual Value of I_{ss}

Interestingly, at the lower end value of 1%strain/pF, there is a greater potential of a particular site classification (in this case an approximate 65% chance of Class S) due to the lower bound of the correlation returning a negative (and therefore 0%strain/pF) result.

5 DISCUSSION AND CONCLUSION

As can be seen from Figure 5, it was found that an estimation of shrink swell index using any of the three developed correlations was extremely similar (generally with a final difference of less than 0.1%strain/pF in practice). However the error in the various engineering index properties is large and the correlation coefficient for each index method is relatively low. As displayed in Figure 6, the use of these correlations with any percentile greater than 70% results in an increase in predicted site classification for the examples given. A typical confidence limit of 90% results in a site classification of between one and two classes higher than what the mean value of shrink swell index would give.

There are good reasons why an accurate correlation between I_{ss} and indices based on engineering index properties may not achievable. To a large extent, the Plastic Limit, Liquid Limit and Linear Shrinkage limit can be generally correlated to the clay content in the sample. Generally, the higher the clay content, the higher the plastic and liquid limit values will be. While clay content undoubtedly contributes to the overall reactivity of a soil, the degree of reactivity is heavily dependent on the clay soil's specific minerology. A clay soil that has a relatively high proportion of kaolinite in its makeup may hardly swell at all, while a clay with a relatively small proportion of smectite may be highly reactive. Both soils may exhibit similar plastic and liquid limits due to the trade-off between proportion and type of clay in the samples.

Another reason that there may not be a reliable correlation of shrink-swell index to any engineering index property test is due to the nature of the laboratory tests themselves. A shrink-swell test is performed on an "undisturbed" specimen of soil from a site. While there is invariably some measure of sample disturbance from driving a sampling tube and then extruding the sample prior to testing, the sample still retains most of the soil structure and fabric throughout the testing regime. In contrast, all engineering index property tests are completed on a screened and remoulded soil specimen, where no trace of the original soil fabric or structure remains. Johnston et al. (2015) found that even when all other variables were controlled, altering or remoulding the structure of a clay specimen resulted in significantly higher reactivity when tested over its undisturbed counterpart.

In addition to the complete destruction of the soil structure, the sample preparation for all engineering index property tests assessed in this paper requires the removal of all soil particles greater than 425µm, which in cases of gravelly or sandy clays, means that significant inert material is removed from the soil, greatly affecting its reactivity when compared to its in-situ state. Removal of inert material in performing index tests is likely to concentrate the amount of the remaining clay material,

and hence, will tend to indicate higher reactive potential. The significance of destroying the soil's fabric is much harder to evaluate, and it is uncertain as to whether a soil in its remoulded condition will consistently reflect greater or reduced reactivity. Regardless of this, Figures 4 and 5 seem to indicate that there is roughly equal likelihood that predictions made using any index value assessed in this study will overestimate or underestimate the true value by the same amount.

In considering the above, it must be remembered that, implicit in this assessment and any correlation that is produced, there is an assumption that both the shrink-swell test and its corresponding index test were correctly carried out and that the results obtained are fully valid for that particular soil unit. Invariably, the standard and quality of laboratory testing varies between laboratories, and so it is likely that, for at least some of the data, either the I_{ss}, or its corresponding index value (or both) are not truly representative of the material tested. Unfortunately, the assumption is unavoidable, as it is not possible to verify the integrity of the data from many sources quoted for this work.

The use of a correlation between I_{ss} and engineering index in the assessment of site classification is not able to be achieved without an unacceptable likelihood of error. This has large ramifications for residential construction cost. Conversely the repair costs for damage to a building for an under-designed residential structure, such as the repair of cracked/warped slabs/walls and other structural elements, would likely be greater than the initial construction cost of the foundation system. Considering the cost of a shrink/swell test is relatively minor and comparable to that of an Atterberg Limit test suite (approximately $150 / test AUD, 2016 dollars), the economics of carrying out Atterberg Limit testing instead of Shrink-swell index testing is questionable.

Whilst in some situations, such as a particularly hard, dry soil where an undisturbed sample cannot be obtained, the general correlations defined herein (Figures 1 to 3) may prove useful to provide a 'somewhat informed' design value. However for general use they are a poor and demonstrably unreliable substitute for the shrink-swell test. Utilisation of the developed correlations requires significant consideration be given to the risk level a geotechnical consultant is prepared to accept, and the large increase in foundation cost associated with unnecessary increases in resulting site classification.

REFERENCES

Cameron, D. A. and Walsh, P. F. (1984). "The Prediction of Moisture Induced Foundation Movements Using the Instability Index", *Australian Geomechanics*, 8, 5-11.

Cameron, D. A. (1989). "Tests for Reactivity and Prediction of Ground Movement" *Australian Civil Engineering Transactions*, Institution of Civil Engineers Australia, Volume CE31, No 3, pp 121-132.

Davernport, F. (2007). "Problem Soils – A Western Australian Perspective", *Australian Geomechanics*, 42(3), pp 1 - 20.

Delaney, M., Li, J. and Fityus, S. (2005). "Field monitoring of expansive soil behaviour in the Newcastle-Hunter region", *Journal of Australian Geomechanics*, 40(2), pp. 3-14.

Earl, D. (2005). *To Determine if There is a Correlation Between the Shrink-swell Index and Atterberg Limits for soils Within the Shepparton Formation*, Undergraduate Research Project, University of Southern Queensland, Australia.

Fityus, S. G., Cameron, D. A. and Walsh, P. F. (2005). "The shrink-swell test", *Geotechnical Testing Journal*, 28(1).

Fityus, S. G. and Delaney, M. D. (1995). "The Unique Influence of Lower Hunter Coal Measures on Reactive Soil Phenomena in the Newcastle area", *Proceedings of the 28th Symposium on Advances in the Study of the Sydney Basin*, UoN, 167-174.

Jaska, M. B., Cavagnaro, R. L. and Cameron, D. A. (1997). "Uncertanties Associated with the Visual-Tactile Method for Quantifying the Reactivity of Expansive Soils", *Autralian Geomechanics*, 31, pp. 84-91.

Jayasekera, S. and Mohajerani, A. (2003). "Some Relationships between Shrink-Swell Index, Liquid Limit, Plasticity Index, Activity and Free Swell Index", *Australian Geomechanics*, 38(2), pp. 53 – 58.

Johnston, J., Fityus, S., Buzzi, O., Rodgers, C. and Kingsland, R. (2015). "Engineering properties of Permian clay tuffs", *Engineering Geology for Society and Territory*, 6(2), Springer International Publishing, Switzerland, 273-278.

Johnston, J., Cavicchia, J., Hosking, T. and Thomson, R. (2015). "The effect of sample remoulding on the shrink-swell test." *Proceedings of the 12th Australia New Zealand Conference on Geomechanics (ANZ 2015)*, Wellington, New Zealand.

Mitchell, P. And Avalle, D. (1984). "A technique to predict expansive soil movements", *Proceedings of the Fifth International Conference on Expansive Soils*, Adelaide, South Australia, 21-23 May, 1984.

Reynolds, P. W. (2013). *Engineering Correlations for the Characterisation of Reactive Soil Behaviour for Use in Road Design*, Undergraduate Research Project, University of Southern Queensland, Australia.

Seo, B. and Mersne, T. (2014). *Development of Soil Property Database for the Brisbane Area and Empirical Correlations between I_{ss} and Atterberg Limits for Brisbane Soils*, Queensland University of Technology (AGS Society Presentation)

Standards Australia (1986). *Australian standard AS 2870-1986: Residential slabs and footings*, SAI Ltd, Sydney, 60 pp.

Standards Australia (2003). *Australian Standard AS 1289.7.1.1-2003: Methods for testing soils for engineering purposes: Method 7.1.1: Determination of the shrinkage index of a soil - Shrink-swell index*, SAI Ltd, Sydney, 8 pp.

Standards Australia (2011). *Australian standard AS 2870-2011: Residential slabs and footings*, SAI Ltd, Sydney, 176 pp.

Zhao, H., Ge, L., Petry, T. M. and Sun, Y. (2014). "Effects of chemical stabilizers on an expansive clay", *KSCE Journal of Civil Engineering*, 18(4), pp. 1009-1017.

Zou, Z. (2015). *Assessment of the reactivity of expansive soil in Melbourne metropolitan area*, Masters of Engineering Thesis, RMIT Univesity, Australia.

Proceedings of the 11th ANZ Young Geotechnical Professionals Conference – 11YGPC
Queenstown, New Zealand
25 – 28 October 2016

Monitoring geohazards and trigger level response on Deans Head in the Port Hills, Christchurch

Z. J. Pletz[1]

[1]Aurecon Ltd., Unit 1, 150 Cavendish Road, Casebrook, Christchurch 8051, New Zealand; PH 03-366 0821; email: zoe.pletz@aurecongroup.com

ABSTRACT

Following the recent Canterbury Earthquake, GNS Science have identified numerous mass movement areas in the Port Hills with a potential risk to nearby infrastructure and life lines. Deans Head, a Class I mass movement area near the Sumner suburb, comprises of an approximate modelled 46,000m^3 soil (loess) landslide on a steep sloping site. Different to other mass movements, the Deans Head landslide could be triggered by relatively frequent rainfall events. During the land clearance phase of works carried out by Land Information New Zealand (LINZ; formerly Christchurch Earthquake Recovery Authority, CERA), the Deans Head project has proven to be challenging including overcoming the multiple site constraints. These constraints include CERA Red Zoned structures, a key lifeline route below the site, cliff collapse and landslide hazards both susceptible to weather. During the land clearance phase, mass movement hazard monitoring has formed an integral part of the health and safety for personnel working on site. This paper will identify the numerous site hazards on Deans Head and provide an overview of the hazard monitoring techniques including ground movement, laser scan monitoring and groundwater monitoring used during LINZ's land clearance phase of works. An overview will be provided on the emergency management if trigger levels are exceeded and the importance of procedures and reporting during hazard monitoring throughout the project.

Keywords: monitoring, landslide, Deans Head, ground movement, ground water, laser scan.

1 INTRODUCTION

The Deans Head site area is located in the Christchurch suburb of Sumner and covers an area of approximately >8,300m^2. The site is located on a gentle to steep sloping hillside (averaging 20°-30°) above Main Road. Main Road forms a key lifeline route between the Lyttelton Port and Christchurch. The site comprises two main geohazards, cliff collapse (and retreat) along the northern fringes of the site (mainly Shag Rock Reserve) and a mass movement (landslide) area containing an estimated 46,000m^3 of soil material that could be triggered by potential rainfall events (Massey et al., 2014). From surface movement and slope displacements, landslide direction has been modelled in a northwest direction (in relation to the site). The site features and indicative landslide direction is outlined in Figure 1.

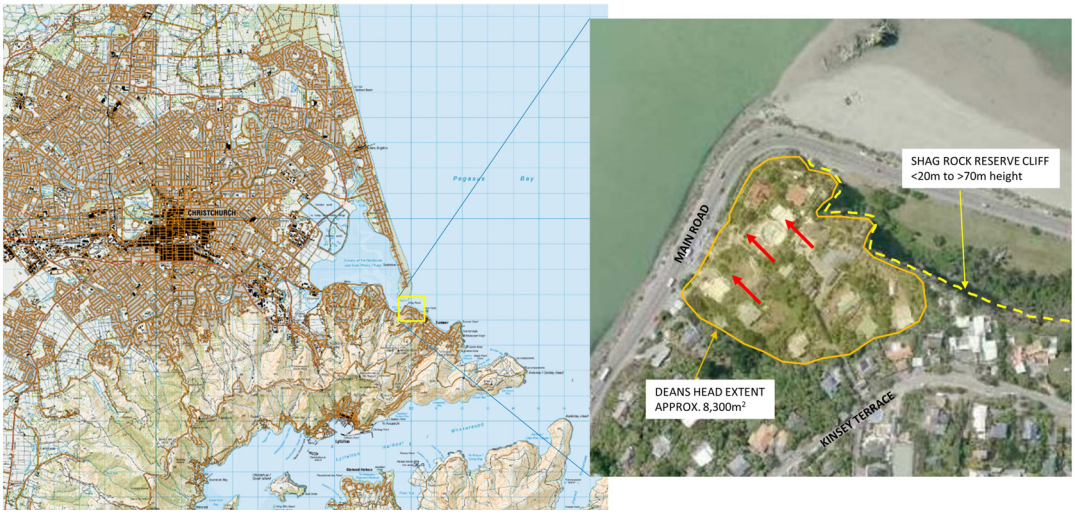


Figure 1. Deans Head site area, extent & indicative landslide direction (in red), LINZ and LiDAR, 2011

In addition, properties within the Deans Head mass movement area were deemed high risk and have been CERA Red Zoned following the recent Canterbury Earthquakes. Through involvement on the Deans Head Project; how do you manage the geohazard risks when working on site, became the focus for establishing a monitoring network during site works on Deans Head. With multiple site features, removal of these properties has proven to be complex, requiring in depth monitoring and establishment of trigger level thresholds to undertake works safely. A brief outline of the main geohazard monitoring techniques used on the project and trigger thresholds are outlined below.

2 MONITORING

Several monitoring techniques have been implemented on Deans Head for ground movement, ground water, rainfall (weather), seismic and laser scan monitoring in Shag Rock Reserve. Addressing key site constraints and site features was important when selecting the most appropriate monitoring technique for Deans Head. These were identified and discussed in risk workshops with the project geotechnical team, survey team, project managers, client and key stakeholders so all hazards were covered and a robust monitoring network established. Some of the main constraints discussed during the Deans Head project included; the type of geohazards (and hazards) on site, mode of failure, likely triggers, access to the site (and reducing people in high risk areas), how often data is required, what cost effective equipment is available and proposed works on site. During the Deans Head project, each monitoring technique was run through a simple what are we trying to carry out (purpose), the aim of the technique and how would this be measured to identify if the main modes of failure and geohazard have been covered. An overview of the purpose, aim and how data was collected for each monitoring technique is outlined in Figure 2.

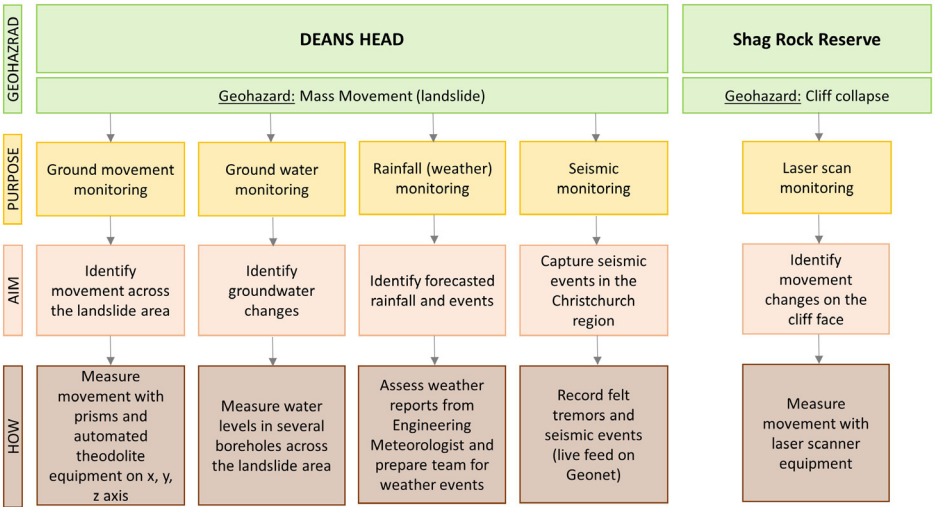


Figure 2. The main geohazards (mass movement and cliff collapse), monitoring technique (purpose), aim and how data was collected is outlined for Deans Head and Shag Rock Reserve.

Details on each monitoring technique including an overview of the setup is outlined below.

2.1 Ground movement monitoring

Ground movement monitoring was undertaken to identify the surface changes across the Deans Head mass movement area. A series of prisms and a theodolite total station was established on Reserve Spit (adjacent to the site) to remotely measure prism movement in the X, Y and Z axis, 24 hours a day, 7 days a week. Prior to survey establishment, several issues arose including limited suitable locations for equipment set up, security of equipment, powering the equipment, how will data be received and stabilising equipment (a low movement tolerance).

With Main Road and the Avon Heathcote Estuary below, suitable site locations were limited. A raised sandy beach area was selected across from the site, accessed via a 4WD track. Equipment was housed in a purpose built container for security and protection from the elements. A viewing window and series of backsight windows were fabricated on the front of the container and around the side to measure monitoring and control prisms. A concrete plinth and footing was fabricated for equipment mounting. The footing was buried in the underlying sand prior to container placement. The container

was mounted over the plinth so the container and plinth could move independently. Two control prisms were installed on Reserve Spit in a similar manor except control prisms did not require container housing. The total station was linked to solar power and battery units to power the equipment continuously. The theodolite and monitoring computer in the project office was linked by radio communication via a radio repeater located on an adjacent site. Photographs of the ground movement monitoring set up and view from the container towards Deans Head are shown in Figure 3.

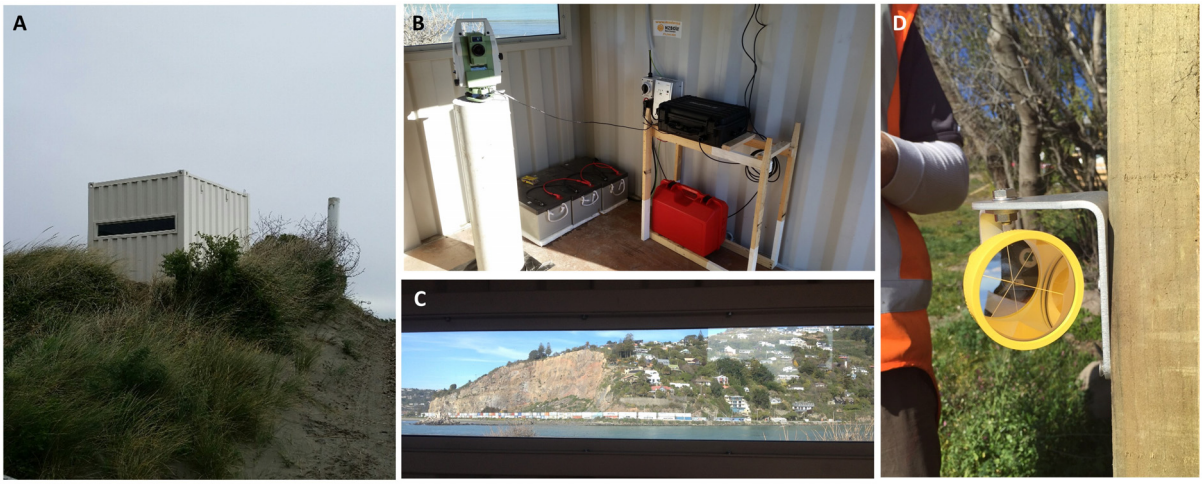


Figure 3. Ground movement monitoring set up; A, monitoring container on Reserve Spit, Southshore; B, equipment set up in the container; C, view from monitoring container looking towards Deans Head area; D, monitoring prism installed on Deans Head. Photographs taken 20.7.2015.

Across from the container on Deans Head, a series of prisms (up to 50) were installed on structures, retaining walls and permanent posts in the ground. Throughout the project, prisms could be relocated depending on the project phase of works. Data is collated using Geomos software to capture and track prism movements. Displacement movement relative to the total station is measured on three axis, that is transverse (left and right), longitudinal (in and out) and height (up and down). Aerial imagery and graphs could then be created to model and present prism changes. Prism data could be accessed remotely on smart phones and laptop devices in the field using TeamViewer software. Prism data for each axis was displayed for the week, month, cumulative and issued to the project team in the Deans Head Weekly monitoring update. Following baseline studies, a series of trigger level thresholds were loaded into the software program to send text alerts to a designated list of people on the project.

2.2 Cliff face monitoring

Cliff face monitoring was undertaken to identify cliff face changes below the site in Shag Rock Reserve. A laser scan MS50 laser scanner was established adjacent to Main Road to remotely measure cliff face changes using a mesh comparison model full time. Similar to the set up of the ground movement monitoring system as outlined in Section 2.1 above, several issues arose prior to equipment establishment, including limited suitable locations for equipment set up, security of equipment, powering the equipment, how will data be received and stabilising equipment (a low movement tolerance).

With Main Road and the Shag Rock beach area below, suitable site locations were limited. Equipment was housed in a purpose built container along Main Road and in alignment with other temporary containers protecting the road against potential rockfall. Equipment was secured on a thick steel pole that was welded to the top of a container. The internal area of the container was reinforced below the steel pole to reduce warping of the container and equipment movement. One of the control prisms on reserve Spit (from the ground movement monitoring) were referenced as a control prism and an additional prism was mounted in Shag Rock Reserve. The laser scanner was linked to solar power and battery units to power equipment continuously. Data was relayed to the project office via the same radio communication system used for ground movement monitoring. Photographs of the laser scan monitoring set up and aerial of the Shag Rock Reserve cliff face area are shown in Figure 4 (overleaf).

Laser scan data is processed to create a mesh that can be overlayed and compared to daily scan and baseline data. For presenting and reporting the cliff face was divided into quadrants and scans could be undertaken for each quadrant. Laser scan data could be accessed remotely on smart phones and laptop devices in the field. Laser scan data was displayed for the day and month (baseline comparison model) and was issued to the project team in the Deans Head Weekly monitoring update.



Figure 4. Laser scan monitoring Shag Rock Reserve, Sumner; A, aerial of Shag Rock Reserve cliff face and reserve area, the monitoring container location is shown with the red arrow; B, laser scan unit in monitoring box mounted in the monitoring container (as indicated by red arrow in photograph A).

2.3 Piezometer (ground water) monitoring

A series piezometers were installed across the Deans Head including four vibrating wire piezometers and a levelogger. Piezometer locations were based on an even spread across the mapped mass movement area and included parts of the lower, middle and upper areas of the slope. When selecting suitable piezometer locations on Deans Head, drainage paths and features, site access and known areas of localised instability were given consideration. Although modelling has indicated the likely slip surface to be between the loess colluvium and underlying volcanic bedrock. A response zone from bedrock to ground level was installed in all piezometers as modelling indicated complete ground saturation could cause instability.

Given the site is susceptible to water level changes, retrieving ground water data was important during periods of heavy rainfall. Where practical, piezometers were linked to a vibrating wire logger and mobile network so data could be remotely accessed from the project office. This reduced the time people were on site, in particular during periods of heavy rainfall when the site was most at risk. Cumulative rainfall and ground water level responses were graphed and issued to the project team in the Deans Head Weekly monitoring update.

2.4 Rainfall monitoring

Understanding weather patterns and forecasted rainfall events were used to manage site access, schedule site visits and walkovers. Rainfall forecasts were a key component in ground water monitoring and allowed the project team to identify early, be alert and prepare in case of an emergency event. Rainfall and ground water monitoring were closely linked during trigger level monitoring on the Deans Head project.

Weather forecasting was undertaken by an Engineering Meteorologist, providing information on weather forecast and patterns to the wider team throughout the project. Weather events such El Nino often lead to periods of dry weather and adverse or abnormal rainfall events. Although uncommon for such events to occur, they have been noted in areas of the Port Hills such as the 1 in 100 year rainfall event that occurred during August 2014. Rainfall measurements were collected locally in a rain gauge during works on site.

2.5 Seismic monitoring

With the recent Canterbury earthquakes, regional seismic activity in Christchurch was monitored on Geonet (refer www.geonet.org.nz). Seismic monitoring is the most passive of all the monitoring techniques used on Deans Head as you cannot predict (day to day) a seismic event happening and it is assumed an aftershock may occur at any time. Throughout the Deans Head project, seismic activity was monitored on Geonet (via local seismometers) and reported during the Deans Head weekly monitoring updates. During the Deans Head project, the most notable earthquake was the Valentines earthquake (Ma5.7 on the 14.2.2016). Following the earthquake, site works were put on hold for a few days while assessments, data analysis and walkovers were undertaken across the site area before works recommenced. Earthquake trends in the Christchurch area can be viewed on the GNS website (refer to 'recent aftershock map', refer www.GNS.cri.nz).

3 MONITORING TRIGGER LEVELS

A series of trigger levels were developed for each monitoring aspect to identify if thresholds had been exceeded or if there is a heightened risk of failure. This section provides an outline of the trigger level system developed on the Deans Head project and does not go into detail on the individual trigger level thresholds for each monitoring technique.

Thresholds were implemented for ground movement, ground water, seismic, weather and laser scan monitoring to advise the project team if trigger level thresholds have been exceeded or are likely to be exceeded. Depending on the monitoring technique, data was reviewed at different intervals during the day. Deciding when to review data was important throughout the project as data may need to be reviewed prior to works or specific tasks.

During ground movement monitoring, an automated text alert system was implemented so alerts could be sent if pre-recorded trigger level thresholds were reached or exceeded. This reduced human error however it was important to understand if a text alert was received, why changes have occurred as the text is computer generated. Three trigger thresholds were developed for ground movement monitoring (low, moderate, high) following baseline assessments. A text alert stated which threshold had been exceeded and to contact the project engineer. Although the project did not have an on-call roster, an overlap type system was developed so multiple personnel were on the text list at any given time. As the site was more susceptible to failure during periods of heavy rainfall, an on-call system could be implemented if deemed appropriate by the project engineer. System checks were carried out randomly including manually covering up prisms to confirm the automated system was operating correctly and the proper lines of reporting were followed by the monitoring team.

A monitoring status system was established on the project and was issued following review of the monitoring data each working day. A simple 'green' and 'amber' light system was created and issued in email format to notify the project team, client, key stakeholders and contractor(s) of the daily status update. It was important to undertake briefings on these systems to communicate a clear understanding to the wider team. The monitoring status system formed a key component of the contractor's methodology and for the health and safety of personnel working on a high risk geohazard site. Geohazard monitoring and systems in place were discussed during project meetings, site prestarts and site toolbox talks.

Another key component of monitoring was the stipulation of when monitoring will be undertaken, will monitoring be undertaken on non-work days, weekends, public holidays. This became important in managing project expectations and keeping a clear communication about when data was monitored. Data may be collected outside work times but may not be reviewed till the following day. A hierarchy of who to contact was developed as part of the monitoring management. Texts alerts were issued to a list of people from the project geotechnical and survey team. From a technical aspect, understanding why texts have been generated was important as often data can be miss leading and false alarms can be generated. This was highlighted when a prism was being measured through an earthquake event causing an inaccurate measurement to be recorded and a false alarm text alert issued. Managing who is on the text alert system is important, so they are clear on what they need to do, who they need to contact or report to and what happens next. Not having a clear line of communication and instructions could lead to a chaotic response. A clear communication line proved fundamental in managing, prioritising, assessing and reporting following the recent Valentines earthquake in Christchurch.

4 CONCLUSION

The main geohazards on Deans Head include a Class I Mass Movement area (landslide) and cliff collapse. Several monitoring techniques have been implemented on the Deans Head project, including for ground movement, ground water, rainfall (weather), seismic and laser scan monitoring in Shag Rock Reserve. These techniques have been adapted around the many site constraints and site features on Deans Head. During the Deans Head project, each monitoring technique was run through a simple what is the purpose of the technique, the aim of the technique and how would this be measured to identify if the main modes of failure and geohazards have been addressed.

Monitoring trigger level thresholds were implemented on the project including a text alert system for ground movement (prism) monitoring. When establishing an emergency management system, clear communication between the team is fundamental in creating a robust system. Who is on the text alert system is important as miss interpreting data and receiving false alarm texts may lead to a chaotic response.

5 ACKNOWLEDGEMENTS

I would like to acknowledge Aurecon and Land Information New Zealand (LINZ) for supporting me write this paper and allowing me to use the Deans Head project as a case study. I would also like to thank Calum Marshall for taking the time to review my paper.

REFERENCES

Aurecon (2015). *Monitoring photographs of Deans Head.*
Aurecon (2016). *Monitoring photographs of Shag Rock Reserve.*
Aurecon (2016). *Monitoring Phase 4 Deans Head, memorandum, (Rev. 1).*
Geonet (www.geonet.org.nz).
GNS Science, Recent aftershock map (www.GNS.cri.nz).
Land Information New Zealand (2011). NZ Topo 50-BX24. Edition 1.02 Published 2011.
Massey C. I, Della Pasqua F., Taig. T, Lukovic. B., Ries. W. and Heron D. (2014). *GNS Canterbury Earthquakes 2010/11 Port Hills Slope Stability: Risk assessment for Deans Head*. GNS Science Consultancy Report 2014/77.

Proceedings of the 11th ANZ Young Geotechnical Professionals Conference – 11YGPC
Queenstown, New Zealand
25 – 28 October 2016

The Undrained Cyclic Response of Monterey Sand in Direct Simple Shear

C. Cappellaro[1] and M. Cubrinovski[2]

[1]PhD Student, Department of Civil and Natural Resources Engineering, University of Canterbury, Private Bag 4800, Christchurch 8140, New Zealand PH (64) 3-3642987; email: claudio.cappellaro@pg.canterbury.ac.nz
[2]Professor, Department of Civil and Natural Resources Engineering, University of Canterbury, Private Bag 4800, Christchurch 8140, New Zealand PH (64) 3-3642251; email: misko.cubrinovski@canterbury.ac.nz

ABSTRACT

The high impact that earthquake-induced liquefaction has on the New Zealand economy, as observed during the 2010-2011 Canterbury Earthquake Sequence in the Christchurch urban area, requires a better understanding of the undrained response of silty sands to cyclic shear loadings. This problem remains still difficult to address because progresses are hindered by the paucity of laboratory experimental data regarding silty sands. In order to address this issue, a series of triaxial tests have been performed at the University of Canterbury since 2011 on undisturbed samples recovered from seven sites in Christchurch. This study aims at using a direct simple shear device for improved evaluation of earthquake and liquefaction response of silty soils. In the first phase of the experimental programme, comprehensive calibration of the testing device and testing procedures has been performed. This paper summarizes key aspects of this important preparatory phase of the testing including description of testing procedures. Reliability of testing procedures and obtained results are assessed by means of a series of simple shear tests performed on a clean sand, whose results are compared against data from the literature.

Keywords: liquefaction, direct simple shear, cyclic, undrained, Monterey sand

1 INTRODUCTION

1.1 Recent studies on soils from Christchurch

Earthquake-induced liquefaction damage is one the principal seismic hazards in New Zealand, and it is responsible for significant socio-economic costs. For instance, soil liquefaction can be accounted for approximately 50% of the NZ$ 40 billion losses caused by the 2010-2011 Canterbury Earthquakes, in which severe damage to roads and bridges, residential houses, commercial buildings, lifeline facilities and levees was widely observed (Cubrinovski et al., 2014).

Early studies on soil liquefaction essentially focused on loose clean sands (i.e. sands with less than 5% particles smaller than 75 μm), as the first well-documented case histories reported liquefaction in this type of soils (Seed, 1979). Recent experience suggests that liquefaction, lateral spreading and flow failure involve sands with fines (Cubrinovski and Ishihara, 2000). Within this list of recent evidence is also the urban area of Christchurch, where liquefaction-related phenomena have been observed in sandy silts deposits of fluvial origin (Bray et al., 2015; Cubrinovski and Robinson, 2015). This implies the need to establish a reliable basis for liquefaction evaluations of silty sands (fines-containing sands) rather than always referring to idealized clean sands.

Fabric, i.e. the arrangement of soil grains in the packing (skeleton), and structural features such as soil layering are the product of processes leading to the formation of natural soil deposits, and are unique to the depositional environment. The liquefaction strength of cohesionless soils has been shown to be strongly influenced by fabric (Ladd, 1977; Mulilis et al., 1977) and layered structure (Verdugo et al., 1995). In order to capture these effects, ideally one should test undisturbed specimens collected from the field. However, sampling of cohesionless soils without significant disturbance is a difficult and expensive task. This is the main reason why research in the past has often made use of reconstituted specimens prepared in the laboratory. Obviously, in order to get a better picture of the liquefaction behaviour of natural soil deposits, one has to reproduce in the lab a fabric similar to that encountered in the field. There exist several specimen reconstitution techniques, each one of them resulting in a different fabric. Among them, moist tamping has been widely used by researchers as it allows to easily

prepare either loose or dense specimens (Ishihara, 1993). Fabric obtained with moist tamping, however, is not representative of fabric of natural soils. Although it is more difficult to employ than moist tamping, the water sedimentation technique is considered to result in a fabric more closely resembling that of fluvial soil deposits (Vaid and Sivathayalan, 2000).

Previous research performed at the University of Canterbury includes investigations of different aspects of the undrained cyclic and monotonic triaxial response of fines-containing sandy soils from Christchurch, and also undisturbed specimens have been used to account for the effects of natural fabric. Rees (2010) focused on moist-tamped specimens with various fines contents, while Taylor (2015) presented comparisons between undisturbed and moist-tamped specimens of another set of Christchurch soils. Additional advanced laboratory testing of undisturbed specimens from two different sites are presented by Stringer et al. (2015) and Beyzaei et al. (2015).

This study represents a continuation of these efforts, as it aims to assess how fabric and layered structure influence the undrained cyclic response of sandy soils from Christchurch in direct simple shear (DSS) conditions. This will be achieved by performing comparative tests on undisturbed specimens, collected with the Gel-Push and Dames & Moore samplers, and on water sedimented specimens of the same soils prepared in the laboratory. This experimental series is preceded by calibration and verification tests on moist-tamped specimens of Monterey #0/30 sand presented in this paper. As this material has been extensively employed in past laboratory studies on liquefaction, it provides a good benchmark in the development of testing protocols for subsequent investigations on Christchurch natural soils.

1.2 Features of cyclic DSS for liquefaction studies

Past laboratory studies on the undrained cyclic behaviour of cohesionless soils have made extensive use of the triaxial device because of its common availability in research facilities and of its relative simplicity in use. Nevertheless, as level-ground free-field response involves simple shear mode of deformation, the DSS test is capable of reproducing the field conditions of deformation more rigorously. The conversion of triaxial test data to simple shear mode of deformation, as encountered in level-ground free-field conditions, has traditionally been described in terms of cyclic stress ratio (CSR) using Equation 1:

$$CSR = [\tau / \sigma'_v]_{field} = (1 + 2K_0) / 3 \cdot [|\sigma_a| / (2 \cdot \sigma'_c)]_{TX} \quad (1)$$

where the stress terms are defined in Figure 1. Stress induced in triaxial testing are very different from stresses imposed by earthquakes to soils in level-ground free-field deposits. The actual relationship between liquefaction resistance in triaxial and simple shear conditions is a complex function depending on the tested soil, amplitude of imposed cyclic stresses, and soil fabric, among others, and these aspects are not captured by Equation 1 (Tatsuoka et al., 1986). Direct simple shear (DSS) testing was conceived as a means to overcome this shortcoming of triaxial testing. Ideal undrained DSS loading conditions correspond to a planar state of strain: a soil element undergoes shear strains in the vertical plane while subjected to shear stresses in the horizontal plane; constant height, volume and total vertical load are enforced during the shearing.

Over the years, different procedures and designs of testing apparatuses have been developed in order to overcome several technical difficulties in achieving DSS conditions in the practice, as explained by Boulanger (1990) and Kammerer (2002). Tested specimens can have rectangular or circular cross-section. The states of stress and strain across the specimen are highly non-uniform, especially for specimens with circular cross-section. This induces rocking in the loading system, which represented a major issue for early DSS devices (e.g. Ishihara and Yamazaki, 1980). Also, in order to overcome potential scale effects, tested specimens should have a large diameter-to-height ratio (≥ 4), as opposed to triaxial specimens. Lateral confinement to the specimen can be provided in different ways, for example by means of a wire-reinforced membrane (NGI-type devices), by a stack of rigid rings (SGI-type devices), or by applying a lateral pressure to a specimen surrounded by a plain latex membrane, similarly to a triaxial test.

This experimental study makes use of a custom-designed DSS device built at the University of California, Berkeley (refer Figure 2). Tested specimens are cylindrical in shape, 61 mm in diameter and 15 mm in height, and laterally confined by a plain latex membrane. The device is provided with a

pressure chamber, where compressed air is used to apply confining stresses to the specimen, and makes use of back pressure for saturation. The upper and lower faces of the specimen are in contact with two porous stones fitted in the recesses of two aluminium caps. These provide a means to realize a firm connection between the specimen and the horizontal and vertical loading systems. The bottom cap is clamped to a sliding table mounted on track bearings and connected to a servo-controlled pneumatic actuator. The top cap is connected, via an analogous sliding block on track bearings, to a manually-controlled pneumatic actuator. The systems of track bearings are designed to minimize rocking of the top cap and friction. An array of transducers is employed to measure and record vertical and horizontal loads and displacements, pore water pressures, and volume changes.

2 EXPERIMENTAL SETUP

2.1 Test material

The test material used in this study is Monterey #0/30 sand, a clean, uniform, medium grain-sized sand with sub-rounded particles from Monterey, California. Several studies on the undrained cyclic behaviour of coarse-grained soils made use of either Monterey #0 or #0/30 sands, which differ for the method used to separate the extracted material based on grain size (Kammerer, 2002). The two sands, however, are very similar to each other (Wu, 2002), and references describing tests on either one or the other material represent a good reference for comparison with this study. Relevant index properties for Monterey sand are listed in Table 1. Minimum and maximum dry densities for the present study were determined according to the Standard for soil testing of the Japanese Geotechnical Society (JGS 0161-2009). Particle size distribution was determined from five different samples of oven-dried material using the laser diffraction method (ASTM C1070-0).

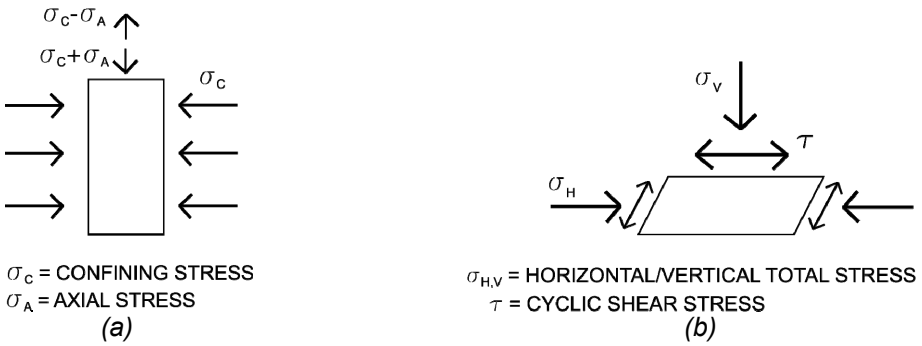


Figure 1. Triaxial (left) and idealized simple shear (right) cyclic loading conditions.

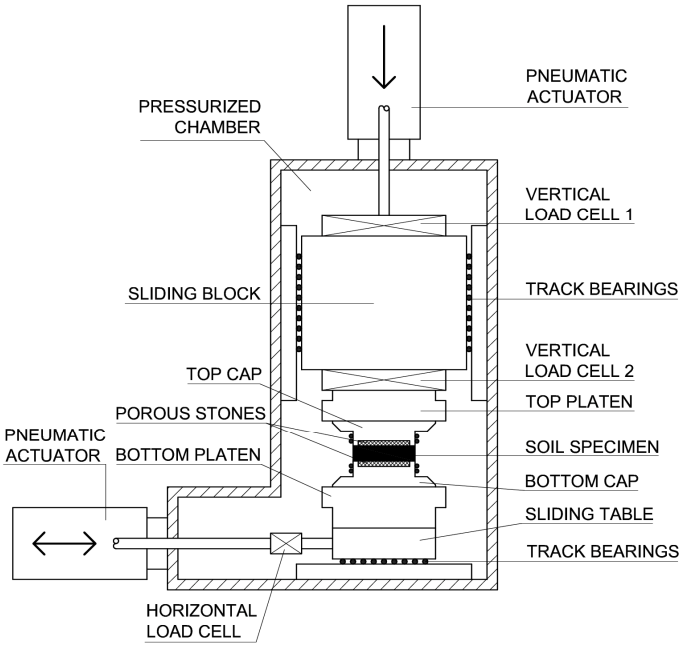


Figure 2. Schematic diagram of DSS device used in this study (modified, after Boulanger, 1990).

Table 1. Index properties of Monterey #0 and #0/30 sand.

Type of sand	G_s	e_{min}	e_{max}	D_{50} [mm]
Monterey #0 Sand (Silver et al., 1976)	2.65	0.56	0.85	0.36
Monterey #0/30 Sand (This study)	2.64	0.585	0.837	0.59

2.2 Testing programme and procedure

This paper reports test results from five cyclic DSS tests performed on moist-tamped Monterey #0/30 sand specimens. Testing on a clean sand is deemed to provide a useful basis to validate testing procedures and assess capabilities of testing equipment before further testing is carried out on soils from Christchurch. This is ensured first by evaluating consistency and repeatability of test results within this experimental series, while test results from literature studies performed in similar conditions provide an additional and independent basis for comparison and results evaluation.

Specimens were prepared by the moist tamping technique (Ishihara, 1993). Moist sand, mixed at 8% water content, is tamped in a single layer using a tamping rod. The top cap is then placed on top of the specimen, and a vacuum of 30 kPa is applied.

Carbon dioxide is percolated through the specimen for 90 minutes, followed by percolation of de-aired water, in order to improve subsequent saturation. Back pressure is increased to 50 kPa before the vertical effective stress is increased to σ'_v = 60 kPa, with σ'_h / σ'_v = 0.5. A subsequent increase of σ'_v to 100 kPa takes place at the same (constant) σ'_h / σ'_v ratio. This consolidation ratio corresponds to average K_0 conditions across a specimen for Monterey sand (Riemer, 1992). Back pressure is finally raised to 250 kPa while keeping the effective stress constant. For these tests, pre-shearing B-values ranged between 0.91 and 0.94, which indicate nearly fully saturated soil. Height and volume changes were monitored during all these preparation stages, and were found to be very small for this material.

Before shearing, the vertical piston is clamped in position to enforce a constant height condition, and undrained conditions are then imposed. A sinusoidal cyclic shear load of pre-determined amplitude is applied by the servo-control system at a frequency of 0.05 Hz. The cyclic shearing phase takes place at constant total horizontal stress, σ_h.

Although the target dry density was 1.57 g/cm^3 (D_R = 62%), initial densities of specimens ranged between 1.55 and 1.60 g/cm^3 (D_R = 54-73%). Both the small size of the specimen and the relatively narrow range of limiting void ratios of Monterey sand (which is used in computations of relative density) contributed to the dispersion in the initial relative density. Use of larger specimens would have certainly minimized this effect. However, future planned tests on Christchurch soils will be constrained by the diameters, respectively 70 mm and 61 mm (Beyzaei et al., 2015) for the Gel-Push and Dames & Moore samplers, using 61 mm specimens for testing after careful trimming the soil. For this reason, testing of larger reconstituted specimens of clean sand was not a priority in this study.

3 ANALYSIS OF EXPERIMENTAL RESULTS

Figure 3 shows typical time histories of shear stress, shear strain and excess pore water pressure for a DSS test. Figure 4 plots the experimental results in terms of number of cycles necessary to develop 10% double amplitude (DA, i.e. peak-to-peak) axial strain (triaxial tests) or 15% DA shear strain (DSS tests) against imposed CSR. Specimens subjected to higher CSR reach a condition of initial liquefaction in a smaller number of cycles, demonstrating internal consistency for this test series. These results can be compared with those performed at 60% relative density by Tatsuoka et al. (1980), who employed an experimental setup analogous to that of this study. The good agreement between the two DSS datasets is encouraging, as it confirms the quality of test results obtained by this study.

On the same plot are shown also cyclic triaxial data for Monterey Sand at 60% relative density (Markham, unpublished data; Silver et al., 1976). The tests by Markham were performed at UC Berkeley with the same batch of Monterey #0/30 sand employed in this study. The test results from Markham and Silver et al. (1976) suggest that no discernible difference can be inferred between the cyclic liquefaction strength of Monterey #0 and #0/30 sands. Comparison between triaxial and DSS test results also provides further evidence of the absence of significant difference in the liquefaction resistance between these two test conditions.

4 CONCLUSIONS

A series of cyclic DSS tests on moist-tamped specimens of Monterey #0/30 sand was performed for comprehensive calibration of the testing device and testing procedures developed as part of a study on the liquefaction behaviour of Christchurch natural soils. Mutual consistency among test results, and good agreement with data from the literature for the same soil support validity and reliability of adopted testing procedures. Before effective testing of fines-containing soils from Christchurch is undertaken, testing of Monterey sand will be extended to water sedimented specimens, so as to establish a rigorous protocol for preparation and testing of also this type of specimens.

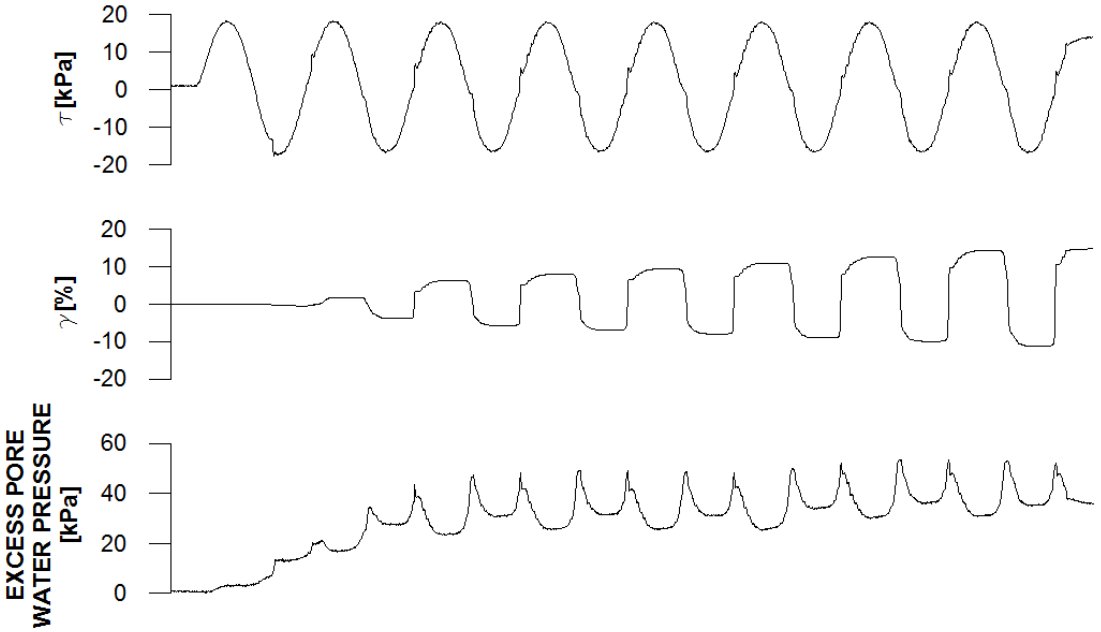
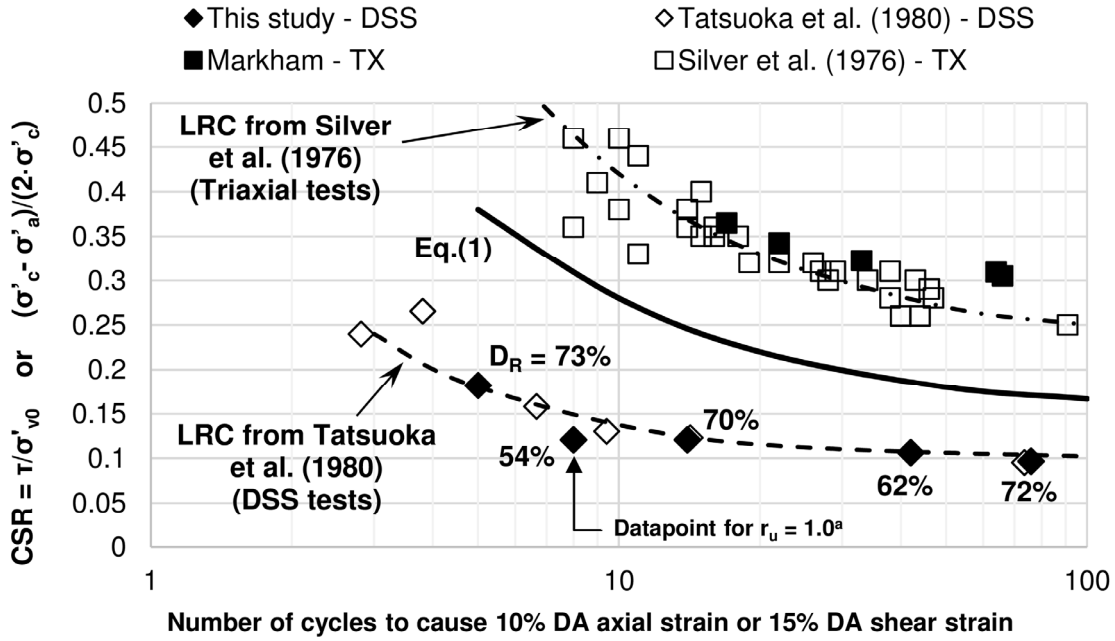


Figure 3. Typical time histories of shear stress, shear strain, and excess pore water pressure for DSS test (Test MTS_SM16, D_R = 73%, CSR = 0.18).



[a] Sudden loss of stiffness at the attainment of r_u = 1.0 (i.e. state of zero effective stress) prevented recording of any additional shear strains.

Figure 4. Liquefaction Resistance Curves of moist tamped Monterey #0/30 (filled points) and #0 (empty points) sand at 60% relative density from DSS and triaxial tests.

5 ACKNOWLEDGEMENTS

The contributions of Dr Gabriele Chiaro from the University of Canterbury, and Professors Jonathan D. Bray and Michael Riemer from UC Berkeley, in the development and implementation of the testing procedures is gratefully acknowledged. Permission from Dr Chris Markham to use of triaxial data is also acknowledged. The first author wishes finally to thank the support to his studies provided by the UC Doctoral Scholarship, the NHRP research grant, and the EQC Capability Funding.

REFERENCES

ASTM C1070-01(2014). *Standard Test Method for Determining Particle Size Distribution of Alumina or Quartz by Laser Light Scattering*, ASTM International, West Conshohocken, PA, 2014, www.astm.org.

Beyzaei, C. Z., Bray J. D., Cubrinovski, M., Riemer, M., Stringer, M. E., Jacka, M. and Wentz, F. J. (2015). "Liquefaction Resistance of Silty Soils at the Riccarton Road Site, Christchurch, New Zealand", *Proc. 6th ICEGE*, Christchurch, New Zealand, Paper No 616.

Boulanger, R. W. (1990). *Liquefaction Behaviour of Saturated Cohesionless Soils Subjected to Uni-Directional and Bi-Directional Static and Cyclic Simple Shear Stresses*, PhD Thesis, University of California, Berkeley.

Bray, J. D., Markham, C., and Cubrinovski, M. (2015). "Liquefaction Assessments in the Central Business District of Christchurch, New Zealand", *Proc. 6th ICEGE*, Christchurch, New Zealand, Paper No 791.

Cubrinovski, M. and Ishihara, K. (2000). "Flow Potential of Sandy Soils with Different Grain Compositions", *Soils and Foundations*, 40(4), pp. 103-119.

Cubrinovski, M. and Robinson, K. (2015). "Lateral spreading: evidence and interpretation from the 2010-2011 Christchurch earthquakes", *Proc. 6th ICEGE*, Christchurch, New Zealand, Paper No 792.

Cubrinovski, M., Taylor, M., Robinson, K., Winkley, A., Hughes, M., Haskell, J., Bradley, B., Bray, J. D., O'Rourke, T. D. and Wotherspoon, L. (2014). "Key Factors in the Liquefaction-Induced Damage to Buildings and Infrastructure in Christchurch: Preliminary Findings", *2014 NZSEE*, Auckland, New Zealand.

Ishihara, K. (1993). "Liquefaction and Flow Failures during Earthquakes", *Géotechnique*, 43(3), pp. 351-415.

Ishihara, K. and Yamazaki, F. (1980). "Cyclic simple shear tests on saturated sand in multi-directional loading", *Soils and Foundations*, 20 (1), pp. 45-59.

JGS 0161-2009 (2009). *Test Method for Minimum and Maximum Densities of Sands*, Japanese Geotechnical Society.

Kammerer, A. M. (2002). *Undrained Response of Monterey 0/30 Sand under Multidirectional Cyclic Simple Shear Loading Conditions*, PhD Thesis, University of California, Berkeley, USA.

Ladd, R. D. (1977). "Specimen Preparation and Cyclic Stability of Sands", *Journal of the Geotechnical Engineering Division*, 103(6), pp. 535-547.

Mulilis, J. P., Seed, H. B., Chan, C. K., Mitchell, J. K. and Arulanandan, K. (1977). "Effects of Sample Preparation on Sand Liquefaction", *Journal of the Geotechnical Engineering Division*, 103(2), pp. 91-108.

Rees, S. (2010). *Effects of Fines on the Undrained Behaviour of Christchurch Sandy Soils*, PhD Thesis, University of Canterbury, Christchurch, New Zealand.

Riemer, M. F. (1992). *The Effects of Testing Conditions on the Constitutive Behavior of Loose, Saturated Sands under Monotonic Loading*, PhD Thesis, University of California, Berkeley.

Seed, H. B. (1979). "Soil Liquefaction and Cyclic Mobility Evaluation for Level Ground during Earthquakes", *Journal of the Geotechnical Engineering Division*, 105 (2), pp. 201-255.

Silver, M. L., Chan, C. K., Ladd, R. D., Lee, K. L., Tiedemann, D. A., Townsend, F. C., Valera, J. E. and Wilson, J. H. (1976). "Cyclic Triaxial Strength of Standard Test Sand", *Journal of the Geotechnical Engineering Division*, 102(GT5), pp. 511-523.

Stringer, M., Beyzaei, C., Cubrinovski, M., Bray, J., Riemer, M., Jacka, M. and Wentz, F. (2015). "Liquefaction Characteristics of Christchurch Silty Soils: Gainsborough Reserve", *Proc. 6th ICEGE*, Christchurch, New Zealand, Paper No 726.

Tatsuoka, F., Ochi, K., Fujii, S. and Okamoto, M. (1986). "Cyclic Undrained Triaxial and Torsional Shear Strength of Sands for Different Sample Preparation Methods", *Soils and Foundations*, 26(3), pp. 23-41.

Tatsuoka, F., Silver, M. L., Phukunhaphan, A. and Avramidis, A. (1980). "Cyclic Undrained Strength of Sand by Simple Shear Test and Triaxial Test II", *Seisan Kenkyu*, 32(2), pp. 24-27.

Taylor, M. (2015). *The Geotechnical Characterization of Christchurch Sands for Advanced Soil Modelling*, PhD Thesis, University of Canterbury, Christchurch, New Zealand.

Vaid, Y. P. and Sivathayalan, S. (2000). "Fundamental Factors Affecting Liquefaction Susceptibility of Sands", *Canadian Geotechnical Journal*, 37, pp. 592-606.

Verdugo, R., Castillo, P. and Briceño, L. (1995). "Initial Soil Structure and Steady State Strength" in Ishihara, K. (ed.) *Proceedings of 1st International Conference on Earthquake Geotechnical Engineering*, Tokyo, Japan, 209-214.

Wu, J. (2002). *Liquefaction Triggering and Post-Liquefaction Deformation of Monterey 0/30 Sand under Uni-Directional Cyclic Simple Shear Loading*, PhD Thesis, University of California, Berkeley, USA.

Proceedings of the 11th ANZ Young Geotechnical Professionals Conference – 11YGPC
Queenstown, New Zealand
25 – 28 October 2016

Modelling Behaviour of Soft Estuarine Clay in Newcastle using Soft Soil Creep Model

R. C. Tanuwidjaja[1]

[1]Arup, Level 10, 201 Kent Street, Sydney, NSW 2000, Australia; PH (+61) 2 9320 9320; FAX (+61) 2 9320 9321; email: renardi.tanuwidjaja@arup.com

ABSTRACT

Soil behaviour is complex, non-linear and very much dependent on its stress state conditions. Advanced constitutive soil models have become more commonly used in an attempt to come closer to simulating realistic soil behaviour. This paper looks at the use of Plaxis Soft Soil Creep model to develop an appropriate representation of the soft Estuarine Clay soil behaviour found at Kooragang Island, Newcastle for the optimisation of a rail embankment design. A review of field/laboratory tests and back analysis of field monitoring data from a trial embankment were undertaken to derive design parameters of the Estuarine Clay. Site history and ageing of the Estuarine Clay were modelled using Soft Soil Creep model in Plaxis, which allows calibration of the stress state conditions at present time with field conditions. The calculated soil strength profile and ground movements in the past were able to be correlated with available data including CPTs, shear vanes, inclinometer and extensometers. Predictions from the Soft Soil Creep model demonstrate a more sensible representation of current site conditions compared to using basic soil models. This realistic design approach assures confident in optimising the rail embankment design, which brings massive potential savings on construction costs. The use of an appropriate advanced constitutive soil model, combined with a rigorous study of site specific data, has proven to reduce conservatism and substantially benefit real projects.

Keywords: consolidation, soft soil creep, Kooragang Island, Newcastle

1 INTRODUCTION

Soil behaviour is very much complex and often difficult to predict. It is common to use conventional soil models in order to simplify the interpretation of material properties and predictions. In doing so, conservatism is frequently introduced leading to a costly over-design. Whilst it is often justifiable and beneficial to simplify the analysis, there are situations where this is not possible due to project specific constraints. This paper looks at a rail project at Kooragang Island, Newcastle as a case study where the advanced Plaxis Soft Soil Creep model, combined with targeted site investigation and rigorous site specific study, were utilised to more realistically simulate the behaviour of the soft Estuarine Clay, overcoming project constraints and reducing construction costs.

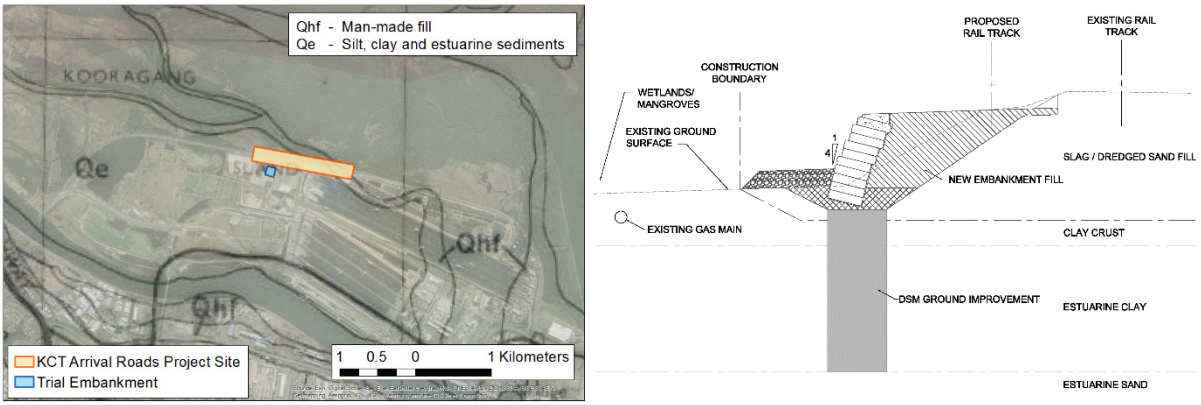
The current rail configuration of the Kooragang Coal Terminal (KCT) Arrival Roads is not capable of processing the required volume of trains to meet demands. An additional rail track is required adjacent to existing rail tracks in order to improve the operational capacity. At the location of this case study, there are currently two existing rail tracks situated on an approximately 2 m high embankment consisting of slag material. This existing rail embankment was constructed in the early 1980's and has been operating for over 30 years, withstanding the 1989 Newcastle earthquake.

Several constraints complicate the construction of the proposed rail embankment. These include:

- Presence of very soft to soft Estuarine Clay, which may cause excessive settlements beyond rail operation tolerances and trigger a global slope instability shearing through this soft layer;
- Existing high pressure gas pipeline runs parallel along the existing rail embankment, limiting construction area and allowable stress/deformation effects on the pipeline;
- The variability of the existing dredged sandfill, slag and mixed fill reclamation;
- Construction of the new embankment adjacent to live operating rail traffic;
- Endangered ecological communities in the wetlands area;
- Low lying swamp bounded by the existing reclamation and rail infrastructure;
- Natural watercourses and creeks; and
- Potential asbestos contaminated material within the existing embankment.

2 GEOLOGY OF KOORAGANG ISLAND IN NEWCASTLE

Kooragang Island is located north of Newcastle near the mouth of the Hunter River estuary extending upstream to Hexham. Originally Kooragang Island was subdivided into smaller former islands by mud flats and various subsidiary channels. Industrial development in the 1960's led to dredged sand fill reclamation, which amalgamated the former islands into the current larger Kooragang Island. The project site area – refer Figure 1(a) – for this case study comprises a section of land reclamation abutting natural swamp area and mangroves. The site covers channel infill, including the truncated Moschetto Channel and an old paleo-channel along a buried previous course of the Moschetto Channel.



(a) (b)

Figure 1. (a) Project site location and geology; (b) Illustration of original ground improvement design

A series of ground investigations have been undertaken at the project site, including conventional borehole drilling, test pit excavation, Cone Penetration Test (CPT) and hand shear vane test. The existing rail embankment is situated on recent soft Estuarine Clay deposits, known to be up to 14 m thick at the old paleo-channel. Towards the Moschetto Channel, the embankment sits on dredged sand fill, which overlies the Estuarine Clay. The rail embankment itself is made of a mixture of very dense slag and reclamation fill material. Since the 1960's, the existing ground is expected to have undergone considerable consolidation under the existing rail embankment and live heavy rail loads.

3 ORIGINAL DESIGN: GROUND IMPROVEMENT OF SOFT ESTUARINE CLAY

3.1 Ground Improvement by Deep Soil Mixing (DSM)

The philosophy of the original earthworks design was to adopt deep soil mixing (DSM) using dry soil mix technique to improve shear strength and limit compressibility of the Estuarine Clay under the proposed embankment extension, as illustrated in Figure 1(b). A gravity retaining structure constructed on the improved ground will support the proposed rail embankment. The ground improvement would: 1) provide a suitable foundation for the proposed retaining structure and proposed rail embankment extension; 2) achieve acceptable ground deformations and embankment stability; and 3) limit the impacts of the proposed embankment on the existing gas pipeline. Ground improvement would normally have been appropriate, as have been previously utilised on Kooragang Island including the Newcastle Coal Infrastructure Group (NCIG) projects (Hawkins et al., 2008 and Chua et al., 2008). However, the constraints discussed in Chapter 1 limit the constructability of the original ground improvement scheme and another design solution had to be put forward.

3.2 Conservatism in the Original Design

Ground improvement was initially proposed following slope stability analysis of the proposed rail embankment using simple Mohr-Coulomb soil model. The analysis indicated that the proposed embankment without any ground improvement would have factors of safety (FOS) less than 1.5 (minimum required for the project). Based on this finding DSM was proposed.

This modelling approach relies on available CPTs and in-situ shear vanes to determine the undrained shear strength parameter of the soft Estuarine Clay. However, these tests were restricted to locations

at the wetlands or near the toe of the existing embankment. The Estuarine Clay immediately beneath the existing embankment is expected to have higher shear strengths due to consolidation over time from the rail and embankment surcharge, decreasing further away from the embankment toe. The simple slope model was not able to utilise this strength gain to accurately capture this gradient shear strength profile due to limitations of available testing and soil model applied. The conservatism was confirmed when the stability analysis resulted in factors of safety between 1.1 and 1.2 for the existing embankment, when site observations suggested the slope had been performing well and had withstood the 1989 Newcastle earthquake measuring 5.6 on the Richter scale (McCue et al. 1990).

4 MODELLING WITH SOFT SOIL CREEP MODEL

4.1 Plaxis Soft Soil Creep Model

The Plaxis Soft Soil Creep model is an advanced constitutive soil model which differentiate the soil behaviour under primary load and unload/reload, similar to Hardening Soil and Soft Soil models (Waterman and Broere 2004). The Soft Soil Creep model applies a cap in the stress space to delineate the limit stress state. The initial cap is first established by the pre-consolidation stress, and expands over time due to the creep component being modelled. The cap is hence a function of the soil stress state and time. Any change in the soil stress state will affect the rate at which the cap expands. The cap, however, will always continue to expand (at a decreasing rate) simulating the improvement effect of the soft soil from creep over time.

The key parameters used in the Soft Soil Creep model include the modified Cam-Clay parameters, i.e. modified compression index (λ^*), modified swelling index (κ^*) and modified creep index (μ^*). These parameters are related to common soft soil compressible parameters C_c, C_s and C_α respectively as presented in equations (1), (2) and (3). In addition, the Soft Soil Creep model is also dependent on the permeability (k) and change of permeability (C_k) of the material, as further discussed in Chapter 4.2.2.

$$\lambda^* = \lambda / (1+e) = C_c / [2.3(1+e)] \quad (1)$$

$$\kappa^* = \kappa / (1+e) = 2C_s / [2.3(1+e)] \quad (2)$$

$$\mu^* = C_\alpha / [2.3(1+e)] \quad (3)$$

$$\log(k / k_0) = \Delta e / C_k \quad (4)$$

With consideration of the above, it is paramount that the site history is well understood and modelled in order to develop the correct soil stress state at the present time. For this project, firstly the Soft Soil Creep parameters were calibrated with monitoring data recorded from a trial embankment – Figure 1(a) – and secondly the site history was modelled to reach a soil stress state and strength profile that matched existing conditions from available ground investigations.

4.2 Validation with Trial Embankment Study

A trial embankment was constructed in 2011 in close proximity to the project location, as shown in Figure 1(a), with the purpose of studying the magnitude and rate of settlement of the Estuarine Clay at Kooragang Island. Monitoring systems including settlement measurement plates (SMP), inclinometers, vibrating wire piezometers (VWP) and extensometers were installed. Monitoring was undertaken for an approximate two year period. A back-analysis based on interpretation of available monitoring data was carried out in Plaxis 3D to calibrate and validate the Estuarine Clay parameters for the Soft Soil Creep model. Compressibility parameters (λ^*, κ^* and μ^*) and permeability parameters (k and C_k) of the Estuarine Clay were assessed in this study. Initial parameters used in the model were derived from available laboratory and in-situ test results.

In order to simulate the ageing of the estuarine sediments, an initial period of 1100 years consolidation of natural sediments only (particularly the Estuarine Clay), followed by a 40 year consolidation period of the reclamation in the 1960s were modelled in Plaxis 3D. Sensitivity assessment demonstrated that the initial ageing periods beyond 1100 years made negligible difference. The subsequent construction of the trial embankment was modelled based on the embankment geometry, estimated fill loadings (periods and lifts) and available monitoring data. The Estuarine Clay parameters were then adjusted to

match with monitoring results of the trial embankment. The set of parameters demonstrating sensible results in the Plaxis 3D model of the trial embankment were then adopted in the Plaxis 2D model for the alternative design solution.

4.2.1 Compressibility

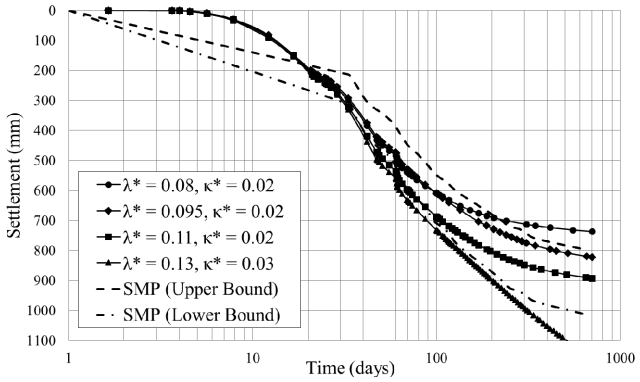


Figure 2. Comparison of overall actual recorded settlements and predicted settlements by Plaxis 3D model with varying compressibility parameters

Compressibility of the Estuarine Clay was investigated in relation to available oedometer tests. The oedometer tests undertaken on the Estuarine Clay samples provide reasonably similar results. All oedometer results were plotted on a stress-strain curve (void ratio, e, against effective vertical load) in natural logarithm scale. These provided a range of values for C_c, C_s and C_α, which were then adjusted to the modified equivalents λ*, κ* and μ* for input into the Soft Soil Creep model. Note the unload portion of the curve was used for κ* calculations. A sensitivity analysis was subsequently undertaken on the range of λ*, κ* and μ* values, and are compared in Figure 2. λ* = 0.095 to 0.11, κ* = 0.02 and μ* = 0.002 were deemed most appropriate for the Estuarine Clay at Kooragang Island.

4.2.2 Permeability

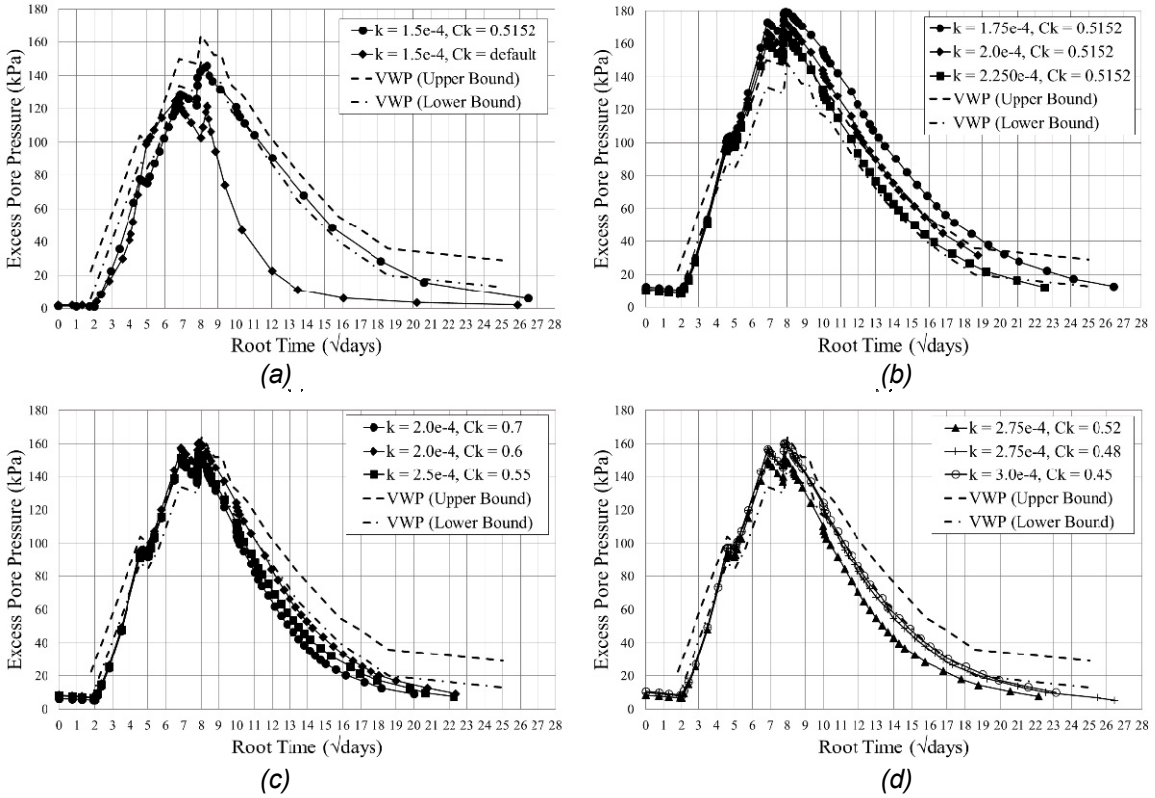


Figure 3. Plots of excess pore pressure of the Estuarine Clay against root time showing: (a) effects of C_k; (b) sensitivity of k; and (c) and (d) calibration of varying k and C_k

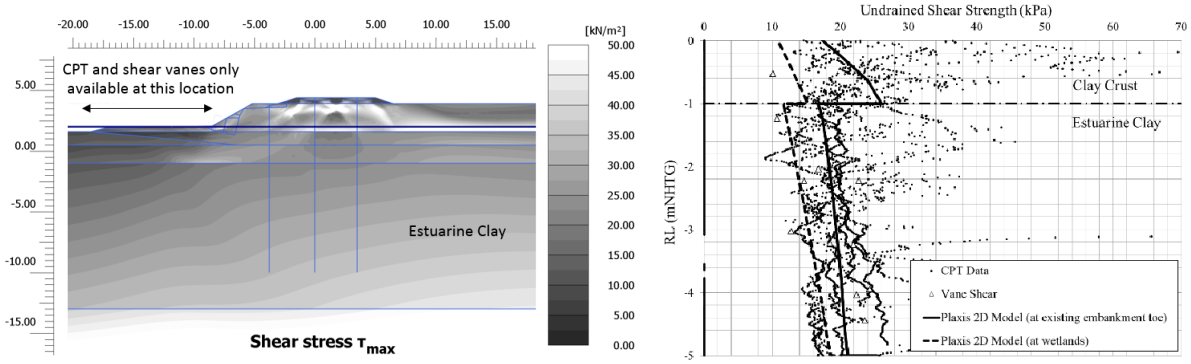
The permeability of the Estuarine Clay was calibrated against VWPs. The construction staging of the trial embankment was similarly calibrated as above. Initially, it was noted that the magnitude of pore water pressure generated during construction was best corresponded with permeability between $1.0x10^{-4}$ m/day and $3.0x10^{-4}$ m/day. It was discovered that the rate of dissipation of pore water pressure was too rapid and as such, a change in permeability with compression, C_k, was implemented. Based on the assumption that the change in permeability is approximately equivalent to the change in void ratio, $C_k = C_c = 0.5152$ was initially adopted with $k = 1.5x10^{-4}$ m/day. This provides excellent correlation with VWP measurements as shown in Figure 3(a). It should be noted that when using the C_k parameter, recalibration is required if the compressibility of the soil is altered.

In the final iteration of the trial embankment study, $\lambda^* = 0.11$, $\kappa^* = 0.02$ and $\mu^* = 0.002$ were considered to be most appropriate for the Estuarine Clay at Kooragang Island. Figures 3(b), 3(c) and 3(d) show the sensitivity of varying permeability parameter k and calibration of C_k with k respectively. Permeability parameters $k = 2.0x10^{-4}$ m/day to $2.75x10^{-4}$ m/day and $C_k = 0.45$ to 0.55 were deemed appropriate and hence adopted in the alternative design solution.

5 ALTERNATIVE DESIGN SOLUTION: PRELOADING AND STAGED CONSTRUCTION

The Soft Soil Creep parameters of the Estuarine Clay validated by the trial embankment study were then applied to a Plaxis 2D model of the proposed rail embankment design. Similar to the Plaxis 3D model, the site specific history was modelled to develop the current soil stress state. That is, the ageing of the Estuarine Clay was first modelled, followed by the reclamation and construction of the existing rail embankment approximately 40 years ago. At this stage, prior to further modelling the construction stages of the proposed rail embankment design, the resulting undrained shear strength profile (Figure 4(a)) and OCR were assessed with available investigation of the existing ground. The undrained shear strength is compared with CPT and hand shear vane tests that are available at the wetland side and at the toe of the existing embankment, as displayed in Figure 4(b). Calculated settlements over the last 40 years and FOS of the existing embankment were also assessed by comparing with field observations. The results of modelling the site history generally agrees with available data and field observations. This further validates the reliability and accuracy of the model, in particular the Estuarine Clay parameters used in the Soft Soil Creep model. The construction phases of the alternative design solution is subsequently modelled to assess its acceptability.

As discussed in Chapter 3.2, relying on only the limited CPTs and hand shear vane tests available towards the wetlands side is likely conservative. Figure 4(a) demonstrates how the Soft Soil Creep model has taken advantage of the expected strength gain in the Estuarine Clay immediately beneath the existing rail embankment from consolidation and creep over time.



(a) *(b)*

Figure 4. (a) Calculated undrained shear strength profile of current site condition after site history phases modelled in Plaxis 2D; (b) Comparison of undrained shear strength profile of the Estuarine Clay generated by the Soft Soil Creep model against available CPT and vane shear results

With the understanding of the site specific study and the use of the more advanced Soft Soil Creep model, acceptable global stability and settlements were able to be demonstrated with no ground improvement; hence, the alternative design solution (Figure 5). The philosophy of the alternative earthworks design is to undertake preloading and stage the construction to limit post-construction settlements within allowable limits, and implement sufficient instrumentation and monitoring to control

the construction and operation of the proposed rail embankment. A gravity retaining structure would then be constructed on the improved ground to support the proposed rail embankment.

Caution should be exercised when using the Soft Soil Creep model. The results of using the Soft Soil Creep model is very much sensitive to the input parameters and construction phases developed in Plaxis. In the case of KCT Arrival Roads, the combination of a sound knowledge of the site history, available in-situ and laboratory tests, and trial embankment monitoring contributed to validating the reliability and accuracy of using the Soft Soil Creep model.

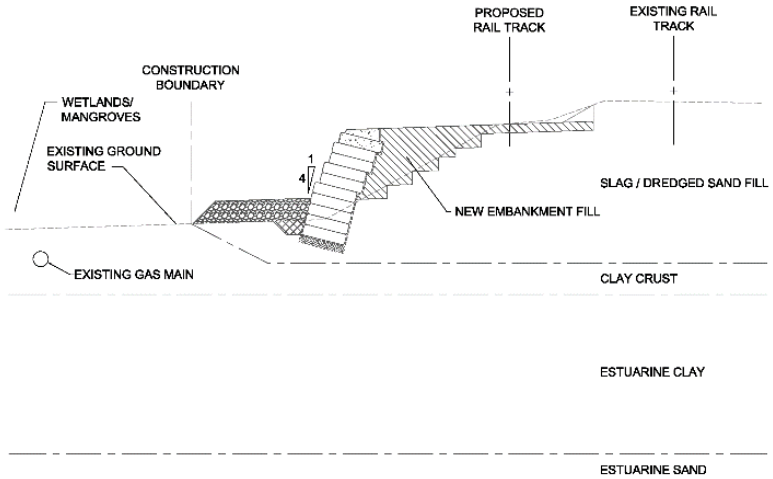


Figure 5. Illustration of revised earthworks design

6 CONCLUSION

The design of the KCT Arrival Roads has undergone significant geotechnical engineering design development in order to overcome numerous project constraints. It has involved rigorous site specific study and the use of the advanced Soft Soil Creep model to demonstrate a more sensible representation of current site conditions. This realistic design approach not only allowed for improvement of the constructability, but also assures confidence in optimising the rail embankment design without DSM ground improvement, bringing massive potential savings on construction costs on this project.

This alternative design solution of the KCT Arrival Roads is currently being constructed at the time of writing this paper. The construction of the new rail embankment is closely monitored and valuable data is continually collected from the instrumentation and monitoring regime implemented. Recorded movements are within predicted thus far.

7 ACKNOWLEDGEMENTS

The author would like to express his gratitude to Greg Cavanagh, David Buttenshaw, Aaron Manderson and the Australian Rail Track Corporation for their kind permission to publish this paper. Much appreciation is given to Sergei Terzaghi and Karen Oj, whom without their knowledge and guidance, the design of KCT Arrival Roads and this paper would not have been possible. Lastly, a special thanks is given to Hui Ling Lim for her encouragement and review of this paper.

REFERENCES

Chua, C. C. H., Lai, M., Hoffmann, G. and Hawkins, B. (2008). "Ground Improvement using Dynamic Replacement for NCIG CET3 Coal Stockyard", *Australian Geomechanics*, 43(3), pp. 63-74

Fityus, S., Hawkins, G., Delaney, M. and Morton, S. (2005). "An overview of engineering geology and geotechnical challenges in the Newcastle Region", *Australian Geomechanics*, 40(1), pp. 5-28.

Hawkins, B., Chua, C. C. H. and Niu, J. (2008). "NCIG CET3 Project", *Australian Geomechanics*, 43(3), pp. 53-62.

McCue, K. F., Wesson, V. and Gibson, G. M. (1990). "The Newcastle, New South Wales, earthquake of 28 December 1989." Bureau of Mineral Resources, *Journal of Australian Geology and Geophysics*, 11, pp. 559-567.

Terzaghi, K. and Peck, R. B. (1967). *Soil mechanics in engineering practice*, 2nd Edition, John Wiley and Sons, New York.

Waterman, D. and Broere, W. (2004). *Practical Application of Soft Soil Creep Model*, Plaxis.

Waterman, D. and Broere, W. (2004). *Practical Application of Soft Soil Creep Model Part II: Undrained Behaviour*, Plaxis.

Waterman, D. and Broere, W. (2005). *Practical Application of Soft Soil Creep Model Part III: Parameter Determination*, Plaxis.

Proceedings of the 11th ANZ Young Geotechnical Professionals Conference – 11YGPC
Queenstown, New Zealand
25 – 28 October 2016

Seismic Ground Response at a Deep Soft Soil Site: Comparing 1D Numerical Solutions with Observed Data from the Christchurch Earthquakes

J. K. Lim[1], GIPENZ, A.M. ISSMGE

[1]Tonkin and Taylor Ltd, 105 Carlton Gore Road, Newmarket, Auckland 1023, New Zealand; PO Box 5271, Wellesley Street, Auckland 1141; PH (+64-9) 355 6000; email: jlim@tonkintaylor.co.nz

ABSTRACT

The earthquake hazard for an engineered structure is influenced by the dynamic response of the soils that underlie the site. During seismic shaking, bedrock motions are altered when travelling through surficial soils. Analytical methods to model these effects have developed over the last few decades. This paper compares the observed ground response at a deep soil site at Lyttelton Harbour, Christchurch with the calculated response using both equivalent-linear and non-linear 1D analytical methods. Ground motion records from two seismographs were utilised; one located on a nearby rock outcrop and the other at the surface of a 60m deep soft soil profile. The observed ground response indicates the presence of non-linear, hysteretic and 3-dimensional effects at the site. Comparisons between the observed and calculated acceleration response spectra, peak ground accelerations and site periods are made. The non-linear analysis demonstrates an overall good fit to the observed data, and is shown to outperform the NZS1170.5 subsoil class method for most periods, emphasising the importance of carrying out a ground response analysis for important structures.

Keywords: site response, ground response, deep soils, soft soils, seismic hazard, local site effects

1 INTRODUCTION

When a rupture occurs along a fault line, energy waves are released that travel in all directions through the bedrock. When these energy waves reach the softer surficial soils they begin to slow and travel towards the surface. Depending on the ground profile, the physical characteristics of each soil layer and the strength and direction of shaking, the resulting ground motions and forces on a structure at the surface can be very different to a rock outcrop site or even another nearby soil site.

The 1985 Mexico City earthquake is an example of when ground response played a significant part in the destruction of a populated area. The unconsolidated deposits within the City Lake Zone had a natural site period of about 2 seconds, resulting in amplification of earthquake waves at this period. The 6- to 15-storey structures that had been built upon the lakebed also had a fundamental period near 2 seconds. This aligning of the structural and site periods created the ‘double-resonance effect’ and the large seismic forces that resulted in the collapse or irreparable damage to many of the buildings in the area, and the deaths of thousands (Seed 1989).

Over the last few decades, analytical solutions to estimate site specific ground response have evolved and many numerical codes are available to the engineering industry. Although these codes are readily available, they are not commonly used within New Zealand due to the requirement of additional ground information that is not routinely investigated and the provisions of the New Zealand loadings standard NZS1170.5 (2004) which provides a simplified method for estimating design spectra based on discrete “subsoil classes”.

The existing literature has reported on case studies comparing 1D ground response analyses with observed motions (e.g. Rollins, et al. 1994; Baturay and Stewart 2003). Varying success of the analyses have been reported often depending on the presence of 2D/3D physical effects that cannot be captured in the assumptions of the analytical codes.

This paper uses strong ground motion records from Lyttelton Port, Christchurch collected from the Canterbury Earthquake Sequence of 2010-2011 to compare the ground response measured at the port with the predicted ground response using common 1D equivalent-linear and non-linear codes.

2 BACKGROUND

2.1 Lyttelton Port

Lyttelton has long been the main port of the Christchurch area and is located on the southern slopes of the Port Hills, which effectively separate Lyttelton Harbour from the city of Christchurch. The port overlies deep marine sediments that in turn overlie the volcanic basalt and andesite bedrock that form the Port Hills to the north. Much of the port development has also been constructed on reclaimed land.

2.2 NZS1170.5 site subsoil classification

The New Zealand Standard NZS1170.5 incorporates ground response into design spectra by means of Spectral Shape Factors, $C_h(T)$ for different subsoil classes. These subsoil classes range from Class A/B (rock) to Class C (shallow soils), Class D (deep/soft soils) and Class E (very soft soils). Sites are classified based on either the shear wave travel time to bedrock, the undrained shear strength or SPT-N values of the soils, or simply the depth to rock. Based on low SPT-N values for the marine sediments, the subject site is Class E (very soft soils). These shape factors consider the ground response for a large number of sites that fit within each classification 'bucket' and therefore provide an average response that may not adequately represent the site specific response.

Additionally, unlike other international standards (e.g. IBC 2009; NBC 2015) NZS1170.5 keeps a constant shape factor regardless of the level of shaking. As a result, the shape factors are required to envelope the non-linear response of both low and high levels of shaking, often leading to significant over-prediction of large amplitude motions for soft soil sites.

2.3 Common ground response analytical methods

The most common methods of ground response analysis are based on the assumption of one-dimensional propagation of shear waves. For sites where 2D/3D effects are considered not to be significant, this assumption is broadly valid due to the refraction of shear waves towards the ground surface as they travel through increasingly softer surficial soils. The two most common methods are summarised below and in Figure 1.

1D equivalent-linear (EL) analyses are the easiest to implement and work by analysing ground motion records in the frequency domain. Irregular input bedrock motions are deconvoluted (by way of Fourier transform) into a series of harmonic sinusoidal waves. A closed-form solution and linear-elastic model (a constant value of soil stiffness and damping is assumed for each layer) is then used to calculate the amplification/damping for each harmonic load. The calculated responses are combined to obtain the irregular response at the ground surface. The assumed constant stiffness and damping values are then updated based on the calculated soil shear-strain history and the process is repeated until strain compatible stiffness and damping constants are obtained.

1D non-linear (NL) analyses require additional input parameters and work by solving the dynamic equation of motion at each time step to model the propagation of shear waves through the soil profile (i.e. in the time domain). The soil column is discretised into individual layers using a multi-degree-of-freedom lumped parameter model. A corresponding mass and non-linear hysteresis spring represent each layer. The instantaneous spring stiffnesses are updated at each time increment to incorporate soil non-linearity and damping.

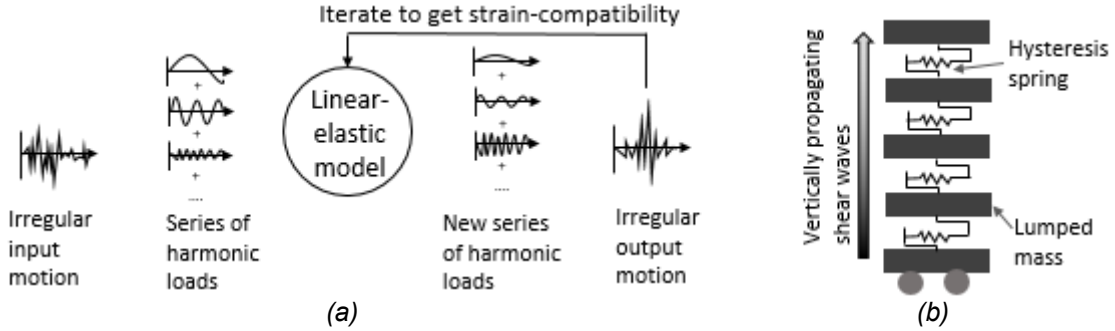


Figure 1. Diagram of (a) equivalent-linear (EL); and (b) non-linear (NL) ground response analysis methods

3 GROUND MOTION RECORDS

Ground motion records from three earthquakes were sourced from the GeoNet (2016) database and are summarised in Table 1. Each earthquake record was analysed separately for its orthogonal horizontal directions. i.e. a total of six outcrop motions and six deep soil profile motions from the three earthquakes were used.

Rock outcrop ground motions were obtained from the *"LPCC"* record station located east of the port at the base of the Port Hills. The *LPCC* record station is located on a shallow weathered rock profile and the ground motions were accordingly deconvolved to bedrock motions using an equivalent-linear analysis.

The deep soil profile motions were obtained from the "*LPOC"* record station located near the western end of the port on reclaimed land. The accelerograms at both stations are roughly aligned north-south and east-west.

Table 1. Earthquake ground motion records

Earthquake	Magnitude, M_w	Epicentral distance and bearing from *LPOC* station
22 February 2011 (Christchurch)	6.2	4km NW
13 June 2011 (Christchurch)	6.0	5km N
23 December 2011 (Christchurch)	5.9	10km N

4 SITE CHARACTERISATION

4.1 Small-strain shear modulus and shear wave velocity

The geological profile beneath the Lyttelton Port *LPOC* record station has been obtained from borehole logs and CPT soundings and is summarised in Table 2.

Characterisation of the small-strain shear modulus, G_{max} of the soils and rock underlying a site is an integral part of ground response analysis. Data from a downhole shear wave velocity survey at a nearby location was used to estimate the average shear wave velocity, V_s (which is directly related by $G_{max} = \rho V_s^2$) for each soil unit. These shear wave velocities were compared with published CPT-V_s correlations (PEER 2012) which were found to be in relative agreement with the adopted values.

Table 2. Ground profile and soil parameter values

Layer No.	Unit	Soil description	Depth of unit (m)	V_s (m/s)	Non-linear G/G_{max} and ε curve
1a	Reclamation fill	Loose silty GRAVEL	0 to 6	130	Vucetic and Dobry (1991) PI=15
1b	Reclamation fill	Medium dense silty GRAVEL	6 to 13	230	
2a	Harbour muds	Soft to firm SILT	13 to 27	180	
2b	Harbour muds	Firm to stiff SILT	27 to 35	250	
2c	Harbour muds	Stiff SILT	35 to 43	230	
3	Harbour sands	Medium dense to very dense SAND	43 to 61	420	Vucetic and Dobry (1991) PI=0
4	Colluvium	COBBLES and BOULDERS	61+	830	EPRI (1993) Rock – 37m to 76m depth

4.2 Non-linear parameters

Geotechnical input parameters required for ground response analysis include modulus degradation (G/G_{max}) and damping (ε) curves. These curves define the non-linear soil stiffness and hysteretic damping behaviour as a function of the shear strain of the soil. Vucetic and Dobry (1991) showed that the plasticity index (PI) is the main factor controlling the G/G_{max} and ε curves for a wide variety of soils ranging from clays to sands. The published curves in Figure 2 have been selected based on soil descriptions in borehole logs as well as historic atterburg limit tests of the soils. Curves adopted for each soil layer are summarised in Table 2.

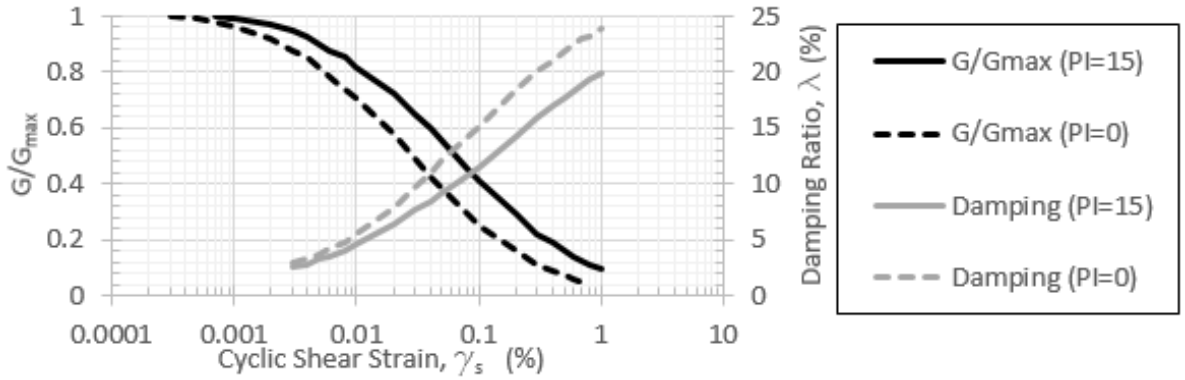


Figure 2. Non-linear G/G$_{max}$ and damping (ε) curves assumed for the reclamation fill and harbour sediments (after Vucetic and Dobry 1991).

5 METHODOLOGY

The SHAKE2000 and DMOD2000 program codes were used for the EL and NL analysis respectively. A 'blind' analysis was undertaken (i.e. no calibration of the input parameters was carried out against the observed motions). The *LPCC* rock motions were applied as outcrop motions to the base of the 1D soil columns.

The non-linear DMOD2000 analysis assumed a total-stress analysis without cyclic softening or build-up of pore-water pressures. The DMOD2000 code can account for cyclic stiffness degradation, however Vucetic and Dobry (1991) showed that generally, the G/G$_{max}$ curve is affected far more by a variation in the assumed PI of the soil. Given the lack of cyclic loading test data and the relative uncertainty in the assumed G/G$_{max}$ and ε curves for the soils, approximation and modelling of cyclic degradation in DMOD2000 was considered unnecessary and was not investigated further.

6 RESULTS AND DISCUSSION

6.1 Peak ground accelerations (PGA)

The EL and NL analyses both predicted soil hysteretic damping for PGAs (Figure 3), as shown by the EL/NL data points plotting below the grey dashed line. The observed PGAs were similar to those predicted, with the NL method generally giving slightly better predictions.

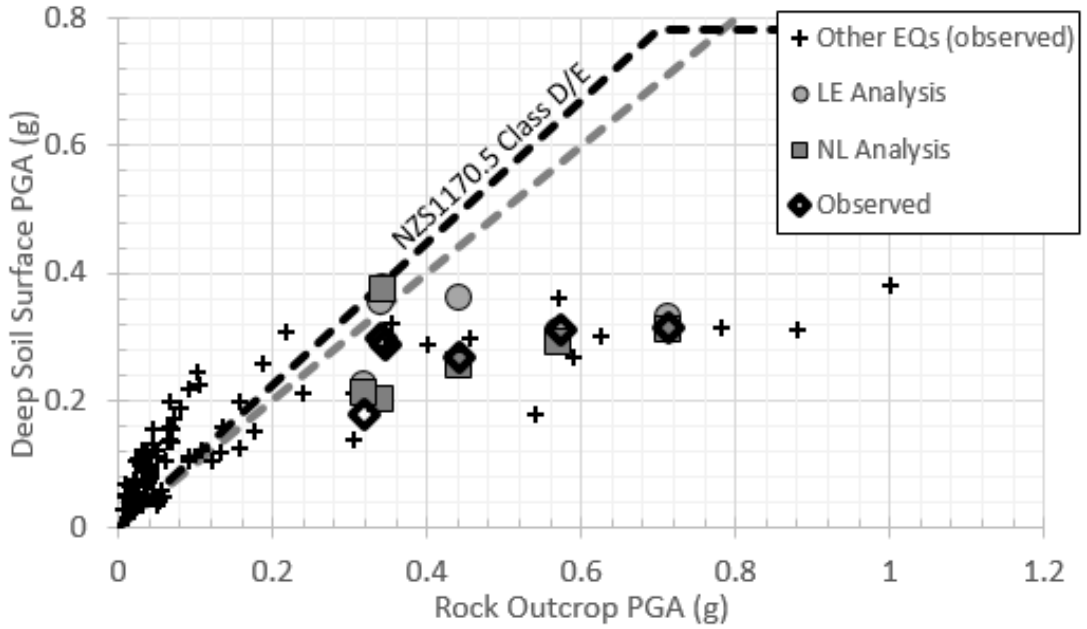


Figure 3. Non-linear response in peak ground accelerations (PGA) at the Lyttelton Port site.

These non-linear ground response effects are supported by the PGA records from other earthquakes recorded between 22 February 2011 and 30 September 2013, which are included in Figure 3. The observed data show clear non-linear effects at the site beyond an outcrop PGA of approximately 0.2g.

It is worthwhile to note that NZS1170.5 Class D/E ($C_h(0)$=1.12) under-predicts PGA for low levels of shaking and over-predict PGA for large levels of shaking at the site. This is partly because NZS1170.5 considers a spectral shape factor independent of the level of shaking. This may have consequences for assessments based on PGA such as liquefaction triggering, seismic earth pressures on retaining walls or slope stability.

6.2 Acceleration response spectra

Although de-amplification of PGAs is observed in these results, ground response effects may result in amplified spectral accelerations at periods greater than T=0. The 5%-damped acceleration response spectra from the EL/NL analyses are presented in Figure 4(a) together with the observed ground motion response spectra. The observed ground response was slightly different in each direction, as discussed later. Figure 4(a) therefore presents the geometric mean spectra for comparison.

The calculated response for both the EL and NL methods provide reasonable visual matches to the observed spectra for periods shorter than about one second. For periods longer than one second the June record provided a very close fit however the February and December records both under-predicted the observed response.

The larger observed response for periods beyond one second may be due to the occurrence of liquefaction or physical processes that are not captured within the simplifications of a 1D analysis, such as topographical or basin effects (Baturay and Stewart 2003; Afshari and Stewart 2015). However, they may also be a result of the uncertainties in the soil and rock model. Most notably the assumed shear wave profile and non-linear G/G_{max} and ε curves. A parametric study or calibration of the input parameters would need to be undertaken to confirm if the 1D analysis is capable of capturing the observed response.

6.3 Ratio of response spectra and site period

Ratio of response spectra (RRS) are plots of the ratio between the ordinates of the surface response spectra (with ground response effects) and the ordinates of the outcrop spectra i.e. $SA_{site}/SA_{outcrop}$. They provide a means of investigating the ground response at each spectral period. The geometric mean RRS for the Lyttelton Port analysis are presented in Figure 4(b), and several observations are made from them.

6.3.1 Site period

The high-amplitude site period (as shown by the peaks in the RRS) is the period at which the maximum amplification of ground response is observed during a large earthquake. This can vary from the low-amplitude site period calculated as ‘four times the shear wave travel time to rock’ due to the non-linear softening of soils under high strains. Correctly predicting this site period is critical to ground response analysis as was shown in the 1985 Mexico earthquake. Structures with periods at or near the site period can expect to attract potentially significant seismic forces. Calculated high-amplitude site periods agree well with the observed data. For both the February and June records a period at about 1.7 seconds (based on the geometric mean) is observed. For the December record, it is less clear due to different values depending on the direction of shaking, as discussed later. It is evident from the RRS that the NL method provides a closer fit to the observed data for most periods and for all three earthquakes.

Although the calculated site period provides a close match to the observed data, the magnitude of the amplification was under-estimated in all cases. This may be due to topographical or basin effects as previously mentioned; although it would be expected that any resonance of motions due to 3D effects would likely be at a period different to that of the 1D site period, but not necessarily.

6.3.2 Non-linear effects at periods T>0

Non-linear effects at high frequencies (i.e. PGA) have already been discussed. However, it can also be observed by way of the RRS that these non-linear effects extend to periods up to about one second (both observed and calculated). This is evident in the smaller short period RRS values for the February record which had the highest level of shaking, and the largest short period RRS values for the December record which had the lowest level of shaking. It is interesting to note however that the peaks of the RRS curves appear to increase with increased levels of shaking.

6.3.3 Comparisons with NZS1170.5

Because NZS1170.5 assumes a shape factor, $C_h(T)$ for ground response effects that is independent of the level of shaking, it is possible to plot the equivalent RRS curve that is assumed for each subsoil class. This is simply the shape factor ordinates for the Site Class divided by the ordinates for a Class B (rock) site. The equivalent RRS curve for a NZS1170.5 Class E site is included in Figure 4(b) for comparison with the site specific ground response.

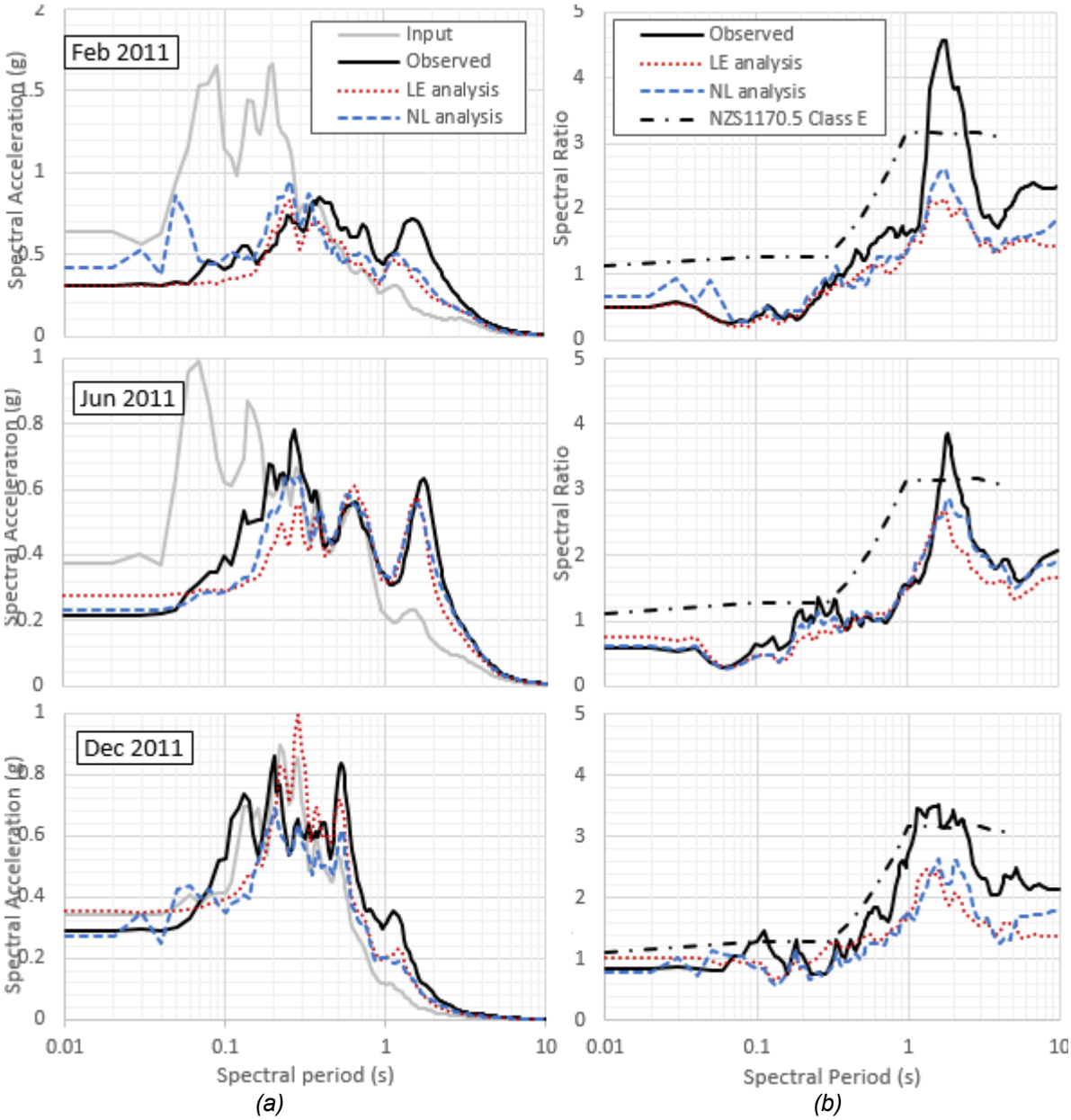


Figure 4. (a) 5% damped geometric mean acceleration response spectra. (b) Geometric mean ratio of response spectra ($SA_{site}/SA_{outcrop}$).

For the December record, the site specific RRS appears to be similar to the NZS1170.5 Class E curve for periods shorter than 3 seconds. For the larger February and June records, the observed site specific RRS are lower than the Class E curve (for periods other than the site period). This is also the case for the calculated responses which provide a much better fit to the observed data over the NZS1170.5 Class E shape factor. This is likely due to the non-linear effects as discussed previously, that NZS1170.5 does not provide for.

6.4 Topographical and basin effects

The ground response analysis presented here has assumed one-dimensional propagation of shear waves only. In reality, the ground response will be influenced by three-dimensional factors such as earthquake source or directivity effects, surface waves, topography or basin effects. However, the extent of these effects are difficult to estimate without detailed investigations and models. The observed ground motion data shows some variation in the ground response in each direction of shaking and this may indicate the presence of 3D effects which could account for some of the differences between the calculated and observed ground responses.

The RRS from the observed ground motions is presented in Figure 5 for the two orthogonal directions of motion recorded. If the ground response was truly one dimensional, it would be expected that the peaks for each direction would be about equal. However, it is observed that the spectral peak in the east-west direction of shaking is at a longer period than for north-south shaking.

The difference might be the result of topographical effects at either the *LPCC* or *LPOC* stations. The *LPOC* station is located on a quay made of reclaimed land behind a rock-fill buttress that runs roughly north-south. If ridge amplification effects due to the elevated land were present, it would be expected that the natural period in the east-west direction would be longer than the north-south direction, and this is what is observed in Figure 5.

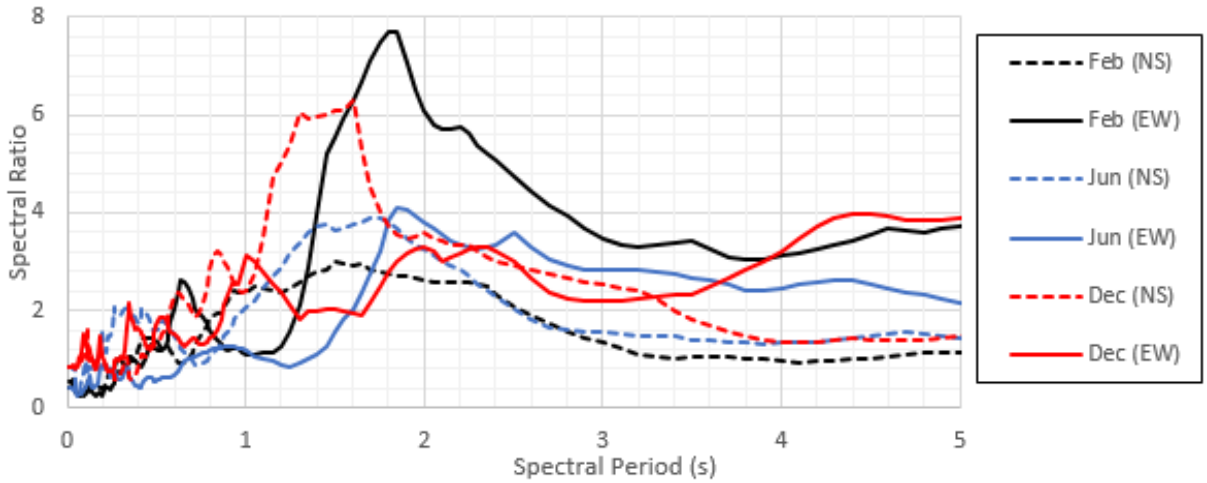


Figure 5. RRS for observed ground motions in each direction of shaking (SA_{LPOC}/SA_{LPCC}).

It is also interesting to note that the February record results in the largest amplification across the three records for the east-west direction, but shows the smallest amplification in the north-south direction. The converse is true for the December record. The reason for this is unknown but could be due to earthquake source or directivity effects.

7 CONCLUSIONS

i. Non-linear effects at short spectral periods occur at the port for high levels of shaking. Both the EL and NL methods are able to capture these observations unlike NZS1170.5, which significantly over-predicts PGAs and short period responses for high levels of shaking such as the February 2011 earthquake.
ii. The observed response at the port site varies between the north-south and east-west directions of shaking. This variation was not seen in the EL and NL methods and indicate the presence of some 2D/3D effects, although the significance or cause of the variation is unclear.

iii. The calculated response using both the EL and NL methods resulted in acceleration response spectra that provides reasonable matches to the observed spectra for periods less than one second. For periods greater than one second the observed response is generally larger, possibly due to liquefaction or 2D/3D effects not captured in the 1D analysis. A parametric study or calibration of the assumed input parameters would need to be undertaken to confirm if the 1D analysis is capable of capturing the observed response.

iv. The high-amplitude site period during large levels of shaking corresponds to the period of maximum response amplification and is critical for the design of structures with a similar period. The EL and NL methods both show good agreement with the observed site period, with the NL method providing a slightly better fit. However, both methods under-estimate the maximum amplification at this period.

v. The site specific ground response analysis provides a much better fit to the observed response when compared with the NZS1170.5 subsoil class method for all periods except near the site natural period (although this may be able to be improved with calibration of the model). This is particularly the case for high levels of shaking (with non-linear effects) such as the February and June 2011 earthquake, and is due to the inherent simplifications within the subsoil class method. NZS1170.5 significantly over-predicts the seismic hazard at the Lyttelton Port deep soft soil site (Class E) for long return period earthquakes. It is recommended that a site specific ground response study be considered for important structures at sites with similar conditions.

8 ACKNOWLEDGEMENTS

The author would like to acknowledge Tonkin+Taylor for their support and the Lyttelton Port Company for providing the investigation data.

REFERENCES

Afshari, K. and Stewart, J. P. (2015). “Uncertainty of Site Amplification Derived from Ground Response Analysis”, *Proceedings of 6th International Conference on Earthquake Geotechnical Engineering*, Christchurch, New Zealand.

Baturay, M. B. and Stewart, J. P. (2003). “Uncertainty and Bias in Ground-Motion Estimates from Ground Response Analyses”, *Bull. Seismol. Soc. Am.*, 93(5), pp. 2025-2042.

Bradley B. A. (2012). “Ground Motions Observed in the Darfield and Christchurch Earthquakes and the Importance of Local Site Response Effects”, *New Zealand Journal of Geology and Geophysics*, 55(3), pp. 279-286.

Bradley B. A. (2015). “Benefits of Site-Specific Hazard Analyses for Seismic Design in New Zealand”, *Bulletin of the New Zealand Society for Earthquake Engineering*, 48(2), pp. 92-99.

Electric Power Research Institute (1993). *Guidelines for determining design basis ground motions*, Palo Alto, Calif: Electric Power Research Institute, Vol. 1-5, EPRI.

GNS Science (2016). “GeoNet Strong-Motion Data”, <http://info.geonet.org.nz/display/appdata/Strong-Motion+Data> (Mar. 15, 2016).

Hashash, Y. M. A., Phillips, C. and Groholski, D. R. (2010). “Recent Advances in Non-linear Site Response Analysis.” *Proceedings of Fifth International Conference on Recent Advances in Geotechnical Earthquake Engineering and Soil Dynamics*.

International Code Consortium (2009). *ICC IBC (2009): International Building Code*, International Code Council, Inc., USA.

Kwok, A. O. L., Stewart, J. P., Hashash, Y. M. A., Matasovic, N., Pyke, R., Wang, Z. and Yang Z. (2007). “Use of Exact Solutions of Wave Propogation Problems to Guide Implementation of Nonlinear Seismic Ground Response Analysis Procedures”, *J. of Geotech. Geoenviron. Eng.*, 133(11), pp. 1385-1398.

NRC (2015). *National Building Code of Canada 2015, Volume 1*, National Research Council Canada, 708pp.

Pacific Earthquake Engineering Research Center (2012). *Guidelines for Estimation of Shear Wave Velocity Profiles*, PEER 2012/08.

Rollins, K. M., Mchood, M. D., Hryciw, R. D., Homolka, M. and Shewbridge, S. E. (1994). “Ground Response on Treasure Island”, *US Geological Survey Professional Paper*, 1551 A, pp. 109-121.

Seed, H. B. et al. (1988). “Ground response effects in the Mexico City earthquake of September 19, 1985”, *Reducing Earthquake Hazards: Lessons Learned from the 1985 Mexico Earthquak*e, pp. 74-77.

Standards New Zealand (2004). *Structural Design Actions, Part 5: Earthquake Actions – New Zealand*, Standards New Zealand, Wellington, New Zealand. 82 pp.

Van Houtte, C., Ktenidou, O. J., Larkin, T. and Kaiser, A. (2012). “Reference Stations for Christchurch”, *Bulletin of the New Zealand Society for Earthquake Engineering*, 45(4), pp. 184-195.

Vucetic, M. and Dobry, R. (1991). “Effect of Soil Plasticity on Cyclic Response”, *J. Geotech. Enginerring*, 117(1), pp. 89-107.

Proceedings of the 11th ANZ Young Geotechnical Professionals Conference – 11YGPC
Queenstown, New Zealand
25 – 28 October 2016

Topographic amplification on steep slopes during seismic events

D. Gainsford[1] and G. Salt[2]

[1]Geosolve Limited, 70 Macandrew Road, South Dunedin 9012; PH (03) 466-4024; email: dgainsford@geosolve.co.nz
[2]Geosolve Limited, 8 Pinot Noir Drive, Cromwell, 9310; PH (03) 445-0061; email: gsalt@geosolve.co.nz

ABSTRACT

The geomorphology of New Zealand has dictated that many transport corridors and residential areas have been formed on, or adjacent to, steep slopes and undulating terrain underlain by variable geology. Observations of the seismic behaviour of cliff-top properties in the Port Hills during the Canterbury earthquakes suggests the current approach recommended in NZS 1170.5 and the NZTA Bridge Manual may be unconservative at estimating the design peak ground accelerations (PGA's) for sites influenced by topographic amplification. A number of sites may pose a higher risk of seismic failure, with potential to cause damage to dwellings and infrastructure, if topographic amplification effects were to be considered under the current codes. It is fundamental to design success that accurate design PGA's are estimated for assessments of existing slopes, design of slope stabilisation works near steep slopes, and design of structures near the crests of slopes. This is particularly relevant in view of the high probability of an Alpine Fault earthquake of Mw8 and the relative vulnerability of large metropolitan areas like Wellington to seismic events. Eurocode 8 appears to be an exception to existing literature in that it is a code that provides a readily implementable criterion for estimating topographic amplification. A similar, albeit interim, simplified method for estimating topographic amplification factors in New Zealand is proposed, based on back-analysis of observed movement at the Port Hills of Christchurch during the 22 February 2011 earthquake.

Keywords: seismic performance, topographic amplification, seismic design, slope stability analysis

1 INTRODUCTION

The geomorphology of New Zealand has dictated that many transport corridors and residential areas have been formed on steep slopes and undulating terrain underlain by variable geology. The geological setting of New Zealand on the Australian and Pacific plate boundary causes tectonic deformation with frequent seismic events of varying and frequently damaging magnitudes.

For geotechnical engineering, evaluating the effects of seismic events in terms of shaking duration, magnitude, and amplitude of ground shaking, are the key inputs to most design procedures in New Zealand. Two probabilistic methods are commonly applied in practice, being the New Zealand Transport Agency (NZTA) Bridge Manual and NZS1170.5:2004. The Bridge Manual is currently favoured among geotechnical practitioners as unweighted PGA-Mw pairs can be readily estimated. At present, the Bridge Manual allows derivation of these inputs for any site in the country, although potential influences on the input values due to external factors such as topography and shallow geology are neglected. The Bridge Manual also currently specifies that slopes should be designed to a lower level of earthquake performance compared to bridges and other structures (Opus, 2014).

Topographic amplification of seismic shaking is a widely recognised phenomenon (Ashford, 1997 and Jeong, 2013), but has not been accurately quantified, presumably due to difficulties in identifying either the zone of influence or the degree of amplification. The issue affects the hazard risk of steep, vulnerable slopes, and damage from seismically induced rockslides and rockfalls. These effects need to be taken into account during design of slope stabilisation works, retaining walls, and foundations on steep slopes, particularly in view of the 30% probability of a large (likely to be Mw8) Alpine Fault earthquake in the next 50 years, based on a mean occurrence interval of 330 years (Berryman et al, 2012).

Observations following the Canterbury earthquakes has shown that steep slopes in the Port Hills area of Christchurch were subjected to high degrees of localised damage due to mass movement along with infrastructure and residential dwellings built on them (Massey et al, 2012). Damage assessments by geotechnical staff along ridgelines and around cliff tops in the Port Hills of Christchurch following

the Mw6.3 earthquake on February 22 2011 recorded prominent evidence of well demarked zones of heightened damage, later attributed to the effects of seismic amplification.

It is clear that design criteria appropriate to New Zealand conditions which account for the interrelation of seismic events and topographic amplification effects need to be quantified more appropriately. The purpose of this paper is to examine current practice in New Zealand and overseas and to present an interim simplified method for determining appropriate factors based on back-analysis of measured amplification factors determined from observed damage of the 22 February 2011 Christchurch earthquake.

2 LITERATURE REVIEW

The results of Kaiser, et al (2014) from studies in the Port Hills showed measured amplification factors of up to 2.7 times horizontal and 3.7 times vertical for shallow soil sites, with up to 2.5 times for horizontal and 3.0 for vertical accelerations for sites on rock. Many of the events measured in their datasets were from small to medium earthquake events (i.e. high-frequency ground motions) which do not necessarily represent the effects of larger earthquake events due to nonlinear site responses. The importance of source seismic event back-azimuth in relation to the site was also noted, with amplification shown to increase or decrease depending on the slope azimuth in relation to the strike of the fault rupture (Section 4, Kaiser et al (2014). As a result, their field trials are too limited to accurately define the nature or extents of amplification in comparison to field observations but do allow useful insight into the amplification range resulting from low amplitude seismic events recorded from the after-shocks. The results can only reasonably be applied to the discrete location of the instruments used to gather the data, a limitation overcome by the proposed new method in Section 3.

Modelling amplification of seismic waves by surface topographic irregularities was addressed by Paulucci (2002) through analytical and numerical investigations, similar to the suggested approach. Firstly, a closed-form expression for estimating the fundamental vibration frequency of homogeneous triangular mountains was obtained using Rayleigh's method. Subsequently, numerical modelling based on the spectral element approximation was used to study the 3D seismic response of several steep topographic irregularities excited by vertically propagating plane S-waves. The topographic amplification factor is obtained for each case by a suitable average of the ratio of acceleration response spectra of output motion to input motion. The 3D amplification factors are then compared with those derived by 2D slope stability analyses as well as with the topographic factors recommended in Eurocode 8 for seismic design. A factor of >=1.7 was derived for slopes of similar height to width ratio and of slope angles between 30° and 60°, although the simplified method proposed in this article seeks to provide an interim factor for a wider range of parameters.

Laboratory testing by Jeong (2013) demonstrated the results of testing physical models such as compacted sand layers in a laminar box and derived numerical finite element models. This showed complex wavefields that characterise the response of topographic features with non-homogeneous soil cannot be predicted by the superposition of topography effects and site response - a common assumption in engineering and seismological models. Nonlinear soil response was observed to increase amplification effects due to low velocity layers intensifying the impedance contrast and accentuate energy trapping and reverberation in higher velocity layers. Topographic amplification was shown to vary with changes in soil type, indicating that both phenomena need to be accounted for in seismic code provisions and ground motion predictive models. ‘Parasitic’ waves (interactions between vertically propagating S-waves and non-flat ground surfaces) were also outlined as a site-specific factor. No method for calculating site-specific factors was given, although the complexities of doing so were outlined.

Studies by Cauzzi et al, 2012 sought to include topographic amplification factors in ground motion prediction equations (GMPEs) by assessing the results of numerical models against measured slope displacements in selected field areas in Italy and Switzerland. The Italian Building Code was referenced in this paper which provides topographic amplification factors based on slope angle (0-15, 15-30, 30+) and geometry, (flat, slope, ridge). Results showed large errors can affect predictions when site effects are not directly related to the reduction in seismic impedance in near-surface layers. Topographic amplification factors from a numerical model calibrated to a site in Italy shows topographic amplification factors of 0.5-3.0, with a mean value of approximately 1.4 and a standard

deviation of 0.5. Practical flaws in the dataset include non-representative slope geometries, inaccuracies in the geological model, and complex 2D and 3D topography not being characterised.

Case studies such as that presented by Sepulveda, 2005 document seismometer readings at a hydro-dam site during a Mw=6.7 quake in Pacioma Canyon, California in 1994. A clear correlation between increased measured ground motions and differing topography is made – peak accelerations at the base of the canyon of 0.5g and nearly 1.6g on the dam abutment (Sepulveda et al, 2005). As with GNS (2014) however, the analysis and conclusions are limited to that of the immediate study area and do not present a method immediately applicable to other sites without having the pre-requisites of well-defined geology, accurately measured seismic data at the slope location and back-analysed slope movements with inputs from precedent performance.

An assessment of worldwide standards and literature on the subject of topographic amplification of cut slopes is presented by Opus (2014). Key findings of their literature review indicate that topographic crests are where seismic ground motion amplification is generally greatest, with several topographic and geological factors making numerical methods inaccurate. Key aspects of New Zealand geology and seismicity are characterised as landform categories, approximations of geological properties and earthquake probabilities. It outlines key research areas for NZ practice and makes suggestions for the formation of future seismic guidelines, but does not present a means to derive topographic amplification factors for New Zealand geotechnical conditions.

Overall, it can be seen that work to date has mainly been directed towards modelling and identifying the underlying mechanics and spatial variations of the effects of topographic amplification (Caruzzi, 2012 and Jeong 2013). Several authors have highlighted that spatial variation of the degree of amplification is common in virtually all sites which indicates that using a fixed value to represent amplification across an entire slope may be problematic. It has also been identified by (Opus, 2014) that applying overseas research may also be inappropriate for use in New Zealand given the disparities of terrain and geology when compared to their countries of origin.

The only published reference for deriving amplification factors for seismic design actions was given in Annex A of Eurocode 8: Design of structures for earthquake resistance, Part 5 Foundations, Retaining Structures, Geotechnical Aspects, despite over-simplification of amplification and de-amplification mechanisms and slope geometry. It is clear that at least a simplified method should be available to practitioners in New Zealand in the interim until more rigorous analysis are developed. This will ensure that topographic amplification effects do not continue to be ignored in practice.

3 BACKGROUND AND RATIONALE FOR PROPOSED METHOD

The site seismic performance observations from Glendevere Terrace, Redcliffs provided a geotechnically fascinating case history of the style of damage that extreme accelerations can cause on cliff-top properties. Figure 1 shows a very low angle landslip that developed within loess overburden a short distance from the cliff crest. The static safety factor for the shown slip was calculated at over 3. The observed displacement was attributed to:

i. either very large horizontal accelerations or, more likely,
ii. moderately high horizontal accelerations in phase with large downward vertical accelerations due to the overburden that has a moderately high frictional component of strength.

Of interest here was that the direction of movement of the slip was strongly oblique to the slope direction. Much more displacement would have resulted had the earthquake acceleration vectors been more directly aligned in the direction of steepest slope (normal to the cliff face) as mentioned in Kaiser et al, (2014).

The approach used by this new topographic amplification factor derivation method is seen as one step towards limiting future recurrences of seismic damage in the study area, or other residential areas with steep terrain - particularly Wellington, Queenstown or coastal land where relatively recent shoreline erosion has formed steep cliffs.



Figure 1. Low angle slip in loess affecting 3 houses in a clifftop seismic amplification zone. Slip has displaced 500 mm horizontally with only minor vertical displacement despite having a back-calculated sliding FOS = 3. Most distant house has collapsed; central house has rafted en masse with shear passing underneath. Seismic amplification factor for this slide (from back-calculation) comes to over 1.6.

4 OVERVIEW OF PROPOSED METHOD

The proposed method was developed primarily on the wealth of empirical evidence (observed land deformation, structural damage, measured accelerations and detailed profiles from several hundred cross sections developed from accurate LiDAR data) accompanied by limit equilibrium back-analysis of damage at known sites within the Port Hills as a result of the Canterbury Earthquake sequence.
Much of the dataset was from the worst affected clifftop areas such as Mt Pleasant, Redcliffs, Richmond Hill, and Whitewash Head. The observed behaviour and information collected (including ground accelerations almost an order of magnitude higher than the customary ultimate design accelerations) provided a rare opportunity to appreciate topographic effects and the need to address a significant technical omission in the current standard (NZS 1170.5).

An informative example of the observed behaviour is provided in Figure 1, which illustrates the movement of a very low angle landslide in the loess overburden encompassing three houses on the top of Redcliffs. Having determined the applicable strength parameters for these materials and the slide profile, back-analysis using widely recognised limit equilibrium analyses confirmed peak accelerations must have been significantly higher than those reported by instrumentation in the valley floor. After collating the field evidence, a spreadsheet was developed to enable more robust design for (i) consideration of zoning for building on cliff-top sites based on potential seismic performance, and (ii) what amplification factor should be applied in design for any given location where a building site on or above a steep slope is proposed.

4.1 DESCRIPTION OF METHOD

The proposed methodology acknowledges the practicalities of determining appropriate design parameters for seismic code accelerations bearing in mind the uncertainties which are associated with quantifying topographic amplification.

It uses the factual information from extensive observed performance to establish the extent of the amplification zone and the relevant amplification factor. This approach is considered more robust at quantifying area-wide vulnerabilities when compared to discrete instrumentation methods.

At present the method has been set out with a practical spreadsheet interface as shown in Figure 2. It consists of an eight-step procedure using a representative cross section through any site of interest.

Outputs for the model include a site amplification factor for inclusion in all earthquake related requirements (geotechnical and structural design), as well as the distance from the cliff edge to the end of the amplification zone. Additional inputs are required compared to the Eurocode but are all readily estimated by a representative cross section.

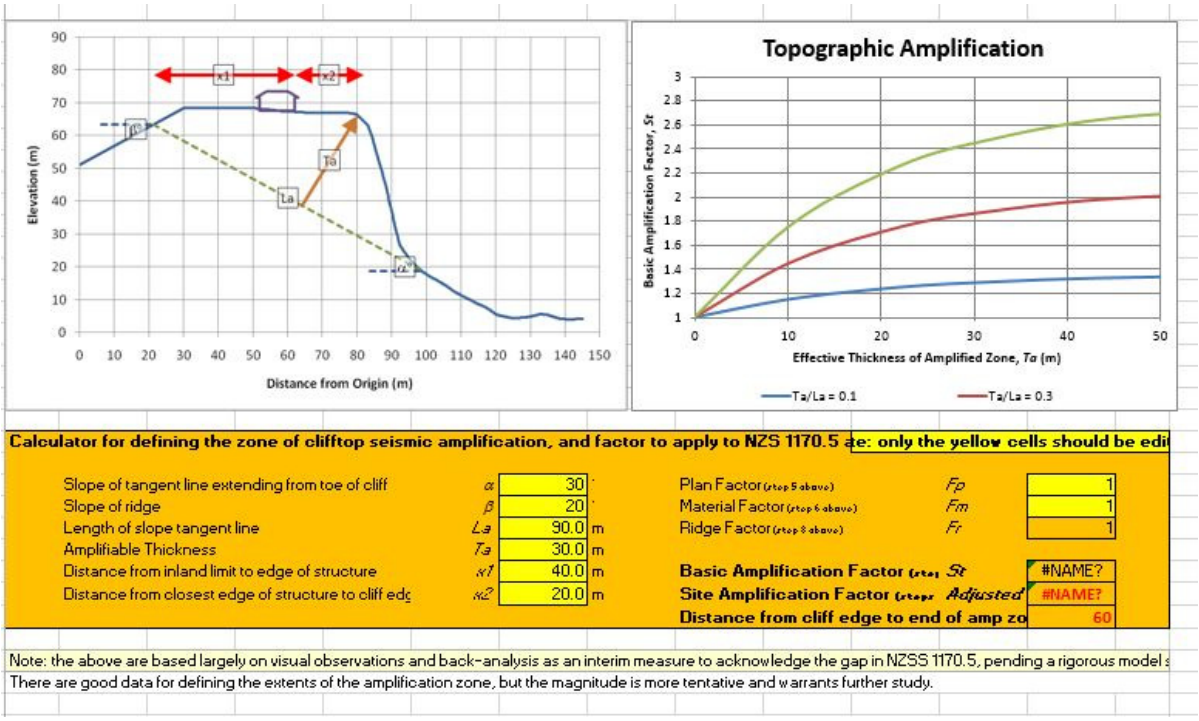


Figure 2. Screenshot of spreadsheet used for calculation of topographic amplification factors using proposed new method.

Typical amplification factors of 1.2 to 2.8 are output from the model, which are then directly multiplied by the PGA determined in accordance with NZS1170.5 or NZTA Bridge Manual to give an estimate of the amplified PGAs likely to be experienced at the site. These factors are generally in accordance with those measured by Kaiser, et al, (2014, p13). Adopting amplification factors for design are not necessarily onerous, for example, some sites developed near the crest of cliffs in areas of low reported seismic risk will only be designed to the same PGAs as similar structures in areas of higher seismic risk.

4.2 METHOD REFINEMENT AND FORMAL REVIEW

The fundamental reason for proposing a rapid analysis method using a calibrated spreadsheet calculation of amplification based on slope geometry and other parameters, (rather than a full dynamic analysis), is the uncertainty associated with the base motion (prior to amplification). The Port Hills study made it very clear that in practice, the magnitude of deformation or displacement that will occur in an earthquake as a result of topographic amplification is not a simple parameter that can be calculated deterministically, because as well as magnitude of the seismic event itself, some of the evident variables were:

i. Profile, i.e. steepness of the cross section through the slope
ii. Height relative to crest of profile
iii. Distance back from the crest
iv. Lithology
v. Overburden depth or weathering profile and strength parameters
vi. Focal depth
vii. Distance from epicentre
viii. Scale effect (out of phase effects minimise deformation on long, gradual slopes)
ix. Phase of vertical versus horizontal accelerations
x. Direction of the predominant acceleration vector relative to the direction of steepest slope

Because all of the above factors will interact to allow only a probabilistic assessment of seismic deformation, it may be argued that in practice, comprehensive dynamic analyses are unlikely to provide a more reliable or more cost effective evaluation than a simplified approach such as the proposed spreadsheet collated from the Port Hills observations.

Accordingly, the Redcliffs research is proposed for interim application as a pragmatic step towards a more conservative amplification factor. This can be applied in addition to current code requirements to meet what appears to be a significant shortcoming. It needs to be considered only where unusually steep slopes or cliffs are involved and the situation presents safety or serviceability issues, but where more sophisticated methods are not warranted. It is not intended to be a substitute for a critical situation where more formal dynamic modelling of seismic amplification with sensitivity analyses would be appropriate.

The model could be readily upgraded to 3D, by further adaptation using GIS software. This could be undertaken by collating any series of adjacent cross sections, to presenting the data as a 3D contour model. The output from a series of spreadsheets can then be automatically presented as colour coded topographic amplification factors superimposed on a standard topographic contour drawing. This would allow the practitioner a convenient overview of the critical areas that can be readily transferred to common GIS packages.

The variation of seismic shaking over the height of the slope can be explored in further detail and become supplementary as a standard model output. The focus is primarily on providing a simple procedure, not dependent on a rigorous model, in view of the uncertainties in the seismic accelerations prior to amplification as referenced as limitations by Jeong (2013) and Cauzzi (2012).

5 FUTURE WORK

Further work is required to define quantitative analytical models of the mechanics of amplification in two-dimensional and three-dimensional space. Refinement could also include taking on board the slope performance and earthquake parameter information from studies of NZ events such as that by Kaiser et al, (2014). Model validation for dynamic analysis is expected to use primarily the well-recognised GeoStudio Suite, as that is most likely to be used by other practitioners, although an assessment of whether there is any more suitable software for this specific purpose would consequently be required.

These further studies will also identify areas for calibrating the model for variations in slope characteristics (lithology, weathering, water table level etc). Robust guidelines appropriate to derive equivalent pseudo-static loads for topographic amplification zones could then be provided for other sites throughout New Zealand.

Where necessary, this method is intended to be adapted in line with international best practice. The intention is that once appropriate validation has been completed, the existing spreadsheet would be used for sites by engineering practitioners and infrastructure asset managers where the consequences of failure are low to moderate. For more critical sites, the spreadsheet would still be useful as a screening tool to decide whether a full dynamic analysis model is warranted based on derived amplification values and potential site complexities.

6 CONCLUSIONS

This paper presents a review of literature on the derivation of site-specific topographic amplification during earthquakes on steep slopes. Slope stability problems remain prevalent in geotechnical and earthquake engineering due to the desirable real estate or strategic infrastructure attributes of sites on or at the crest of steep slopes. Key limitations of current practice are a narrow scope of field studies, the requirement for detailed site knowledge (in excess of that normally available outside of well-studied areas) and a lack of availability of readily-usable methods with an acceptable degree of approximation. This paper presents the background for a geometrically-based spreadsheet method of deriving a topographic amplification factor for slopes in New Zealand. This is intended, with refinement, to enable more efficient seismic design practices in the future and act as a pragmatic interim measure until more rigorous methods become developed.

7 ACKNOWLEDGEMENTS

The authors are indebted to the staff at GeoSolve and external colleagues for their assistance and support during the production of this paper.

REFERENCES

Ashford, S. A., Sitar, N., Lysmer, J. and Deng, N. (1997). "Topographic Effects on the Seismic Response of Steep Slopes", *Bulletin of the Seismological Society of America*, 87(3), pp. 701-701

Berryman, K. R., Cochran, U. A., Clark, K. J., Biasi, G. P., Langridge, R. M. and Villamor, P. (2012). "Major earthquakes occur regularly on an isolated plate boundary fault", *Science, 336(6089),* pp. 1690-1693; doi: 10.1126/science.1218959

Cauzzi, C., Fäh, D., Pessina, V., Faccioli, E. and Smerzini, C. (2012). Topographic amplification from recorded earthquake data and numerical simulations. In *15th World Conference on Earthquake Engineering*, Lisbon, Portugal

CEN (European Committee for Standardisation) (2004). *European Standard EN1998-5 – EuroCode 8: Design of structures for earthquake resistance, Part 5: Foundations, retaining structures and geotechnical aspects*, CEN, Brussels, Belgium, https://law.resource.org/pub/eu/eurocode/en.1998.5.2004.pdf

Jeong, S. (2013). *Topographic amplification of seismic motion including nonlinear response*, PhD thesis, Georgia Institute of Technology, 2013, https://smartech.gatech.edu/bitstream/handle/1853/50325/JEONG-DISSERTATION-2013.pdf

Kaiser, A., Massey, C., Holden, C. (2014). *Site amplification and topographic effects in the Port Hills during the Canterbury Earthquake sequence,* GNS Science Consultancy Report 2014/121 (EQC Research Report 12-626)

Massey, C., Yetton, M., Carey, J., et al (2013). *Canterbury Earthquakes 2010-2011 Port Hills Slope Stability: Stage 1 report on the findings from investigations into areas of significant ground damage (mass movements)*, GNS Science Consultancy Report 2012/317, Final Issue 1

New Zealand Transport Agency (2013). *Bridge Manual*, SP/M/022*,* https://www.nzta.govt.nz/resources/bridge-manual/

Paolucci, R. (2002). "Amplification of earthquake ground motion by steep topographic irregularities", *Earthquake engineering & structural dynamics*, Vol. 31 (10), pp. 1831-1853.

Sepúlveda, S. A., Murphy, W., Jibson, R. W. and Petley, D. N. (2005). "Seismically induced rock slope failures resulting from topographic amplification of strong ground motions: The case of Pacoima Canyon, California", *Engineering Geology*, 80(3), pp. 336-348.

Standards New Zealand (2004). *NZS 1170.5: 2004 Structural design actions – Part 5: Earthquake actions*, Technical Committee BD-006-04-11, 22 December 2004

This page intentionally left blank

Proceedings of the 11th ANZ Young Geotechnical Professionals Conference – 11YGPC
Queenstown, New Zealand
25 – 28 October 2016

Estimating Geotechnical Parameters in Highly Heterogeneous Material Including Peat Deposits using Trial Embankment Data.

J. Leeves[1]

[1]Jacobs New Zealand Ltd, 12-16 Nicholls Ln, Parnell, Auckland Carlaw Park Avenue Parnell, Auckland, 1010 New Zealand, PH (+64 9 928 5500); email: Jack.Leeves@jacobs.com

ABSTRACT

When designing high embankments over compressible material it is important to have a sound understanding of the characteristics of the materials in question. When dealing with soils that are highly heterogeneous and consist of many layers of different compressibility it becomes difficult to reliably estimate soil parameters from conventional sampling and laboratory testing. In particular, assessing the magnitudes of primary, secondary and immediate settlement can be difficult as the various layers within the soil consolidate at different rates. This can be further complicated by the presence of peat materials which tend to undergo significant amounts of settlement. An instrumented trial embankment was built over a significant thickness of soft material comprising amorphous peats, organic silts, silts and clays. Soil parameters were back-calculated from monitoring of the trial embankment and these were subsequently used to model the embankment's behaviour using the software package *Settle3d*. The results of the modelling were then calibrated to create a set of parameters which match the settlement data from the trial embankment.

Keywords: Trial Embankment, Settlement, Consolidation, Peat, Settle3d, Compressibility

1 INTRODUCTION

When evaluating geotechnical parameters for the purpose of design, geotechnical engineers typically rely upon laboratory testing data or inferred properties based on site investigations. In larger projects where more accurate soil parameters can represent large costs savings, full scale testing in the form of trial embankments can be an economical method of determining soil parameters and reducing project risk. Primary and secondary consolidation settlements are often difficult to accurately predict and on large highway projects involving soft soils they are a significant risk to both the programme and budget. Indeed, a great proportion of the geotechnical design effort is focused on mitigating and monitoring the effects of settlement. Trial embankments provide a continuous set of data that fully captures all of the various influences on the settlement that cannot be picked up in small scale oedometer testing. However, surface settlement readings from trial embankments do not differentiate between the settlement characteristics of the various discrete soil layers in the same way that a series of oedometer tests can. The primary focus of this paper is to evaluate soil parameters from trial embankment data and the use of Settle3D to model and calibrate these parameters.

2 TRIAL EMBANKMENT

2.1 Description of the Trial Embankment

The trial embankment is 3.3m high and is made out of a compacted sand fill material with a unit weight of around 18kN/m^3. The trial embankment was constructed over a period of 34 days, the exact methodology of construction is unknown to the author and it has been assumed that the trial embankment has been constructed at a steady rate. The top of the embankment measured 18m by 18m with 3H:1V batter slopes.

2.2 Ground profile

The subsurface conditions at the trial embankment were assessed using data from boreholes (BH) and cone penetration tests (CPT) undertaken at the location of the trial embankment. The ground investigation indicated that the trial embankment is directly underlain by a thin stiff crust around 0.5m thick and soft compressible layer around 6.0m thick. Below the soft compressible layer are medium dense sands; the borehole was terminated in this layer at 9m bgl due to the presence of high artesian

pressures. For the purpose of this paper the sand layer is assumed to extend indefinitely. The artesian pressures appear to be confined to the sands as the soft compressible layer acts as an aquiclude. The CPT data indicated that the ground water level was at a depth of 0.9m bgl (below ground level). The CPT data can be found in Figure 1.

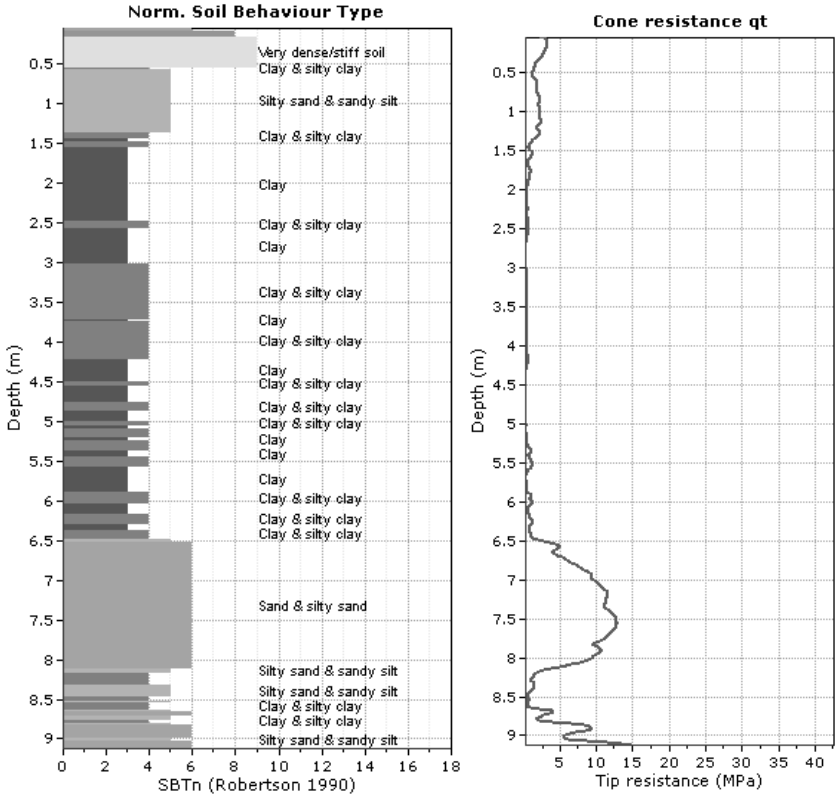


Figure 1. CPT data at the location of the Trial Embankment

The borehole adjacent to the CPT indicates that the upper 6.5m is highly variable and consists of a mix of silt, organic silt, sand, amorphous peat, wood organics, and clay. Much of the compressible layer is understood to be overconsolidated based on correlations with CPT data, this is likely due to the soil being dessicated due to a fluctuating water table. The soil is also assumed to be in double drainage conditions as the embankment above and medium dense sands below the compressible layer are reasonably permeable. A summary of the parameters used in back calculation of compressibility parameters can be found in Table 1 below. These values have been obtained based on a combination of laboratory testing, site obervations and typical values for the material types.

Table 1. Summary of soil parameters from lab testing and empirical correlations

Soil Parameters	Soft Layer (0 - 6.5m, 8.2 – 8.75)	Medium Dense Sands (6.5 – 8.2, 8.75+)	Embankment Fill
G_s (specific Gravity)[a]	2.665	-	-
Liquid Limit (%)[a]	56	-	-
Bulk unit weight (kN/m^3)[b]	15	18	18
E Young's Modulus (MPa)[b]	-	25	-
e_o (void ratio)[a]	1.8	-	-
Over Consolidation Ratio (OCR)[c]	1.5	-	-

[a] Laboratory Testing; [b] Typical soil parameters as per Look (2007); [c] Correlation with CPT data as per Robertson (2012)

2.3 Settlement Monitoring and Results

Profilometers were used to measure the amount of settlement during the trial embankment construction period. The Settlement during construction was measured using two profilometers. After construction was completed a series of survey pins were installed on the top of the fill. These pins were then surveyed continuously for a period of around 580 days at irregular intervals. The results

indicate that approximately 100 mm of settlement occurred prior to the completion of the trial embankment. After the completion of the embankment a further 160 mm of settlement occurred.

Three piezometers were installed prior to construction in the borehole undertaken at the trial embankment location at depths outlined in Figure 2. The piezometer readings indicate an increase in pore water pressure of around 47 to 26 kPa immediately after the completion of construction. This is smaller than the estimated total pressure increase due the embankment of 60kPa. The difference in pore water pressure is likely due to the presence of highly permeable layers within the material which quickly dissipate excess pore water pressure during loading. The piezometers indicate that 90% consolidation occurs around 550 days after the start of construction or 520 days after the end of construction.

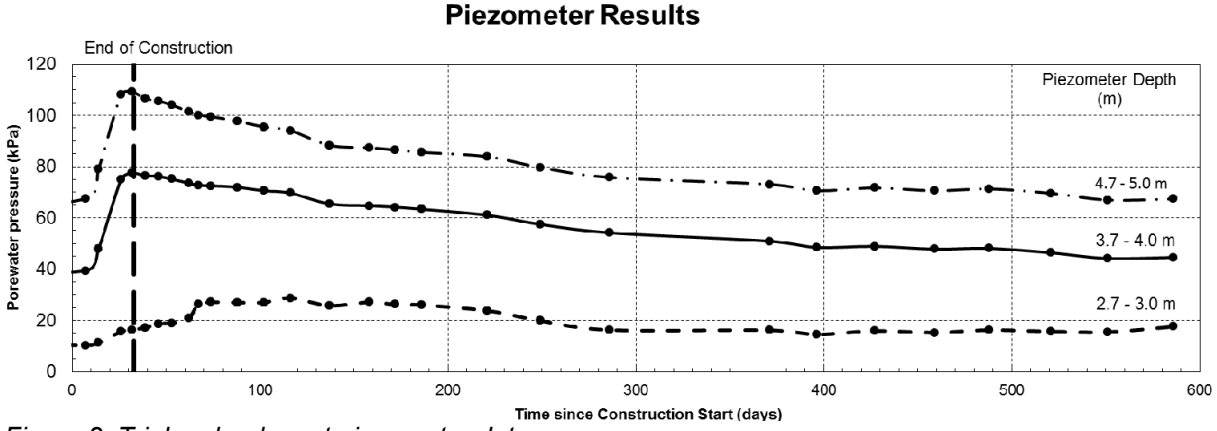


Figure 2. Trial embankment piezometer data

A slowdown in the dissipation of excess pore-water pressure occurred around day 400 and lasted for a period of 150 days. At this time the trial embankment also appears to have risen by around 10mm. This may have been caused by a rise in the water table resulting in increased pore-water pressure and some swelling of the soils as they become saturated. The influence of the rise of the water table on the dissipation of pore-water pressure could potentially have slowed the rate of primary settlement, delaying the time to 90% consolidation.

2.4 Back Calculation of Soil Parameters

To back calculate the compressibility parameters from the trial embankment it is necessary to make some assumptions around what sections of the curve are immediate, primary or secondary. For this exercise the author has assumed that all of the settlement prior to the end of construction is immediate while all of the settlement afterwards is primary settlement. The duration of the trial embankment monitoring data means there is data on the magnitude of secondary compression. The soil parameters were back calculated based on settlement magnitudes from the trial embankment data and the theoretical relationships defined in the equations in Table 2 below. The values used for G_s, w_l, and e_o were as per Table 1. The $\sigma`_{vo}$ was calculated based on the ground conditions prior to the construction of the embankment while the $\sigma`_{pc}$ was determined based on the OCR.

Table 2. Summary of settlement equations used in back analysis

Settlement Type	Equation	Equation Number	Settlement (mm)[d]
Immediate Settlement	$S_i = 1/E_s * H * \Delta\sigma$	1[a]	100
Primary Settlement (Swell Index)	$C_s = 0.0463 * w_l/100 * G_s$	2[b]	–
Primary Settlement (Compression Index)	$S_p = (C_s * H)/(1 + e_o) * \log(\sigma`_{pc}/ \sigma`_{vo}) + (C_c * H)/(1 + e_o) * \log((\sigma`_{vo} + \Delta\sigma) / \sigma`_{pc})$	3[a]	160
Secondary Settlement	$S_s = C\alpha /(1 + eo) * H * \log(t2 / t1)$	4[a]	–
Consolidation Time	$t = (d2 * Tv) / Cv$	5[c]	–

[a] Terzaghi, Peck and Mesri (1996); [b] Nagarag and Murthy (1985); [c] Terzaghi (1943); [d] Settlement magnitude as measured from the trial embankment

Where:

- H is the thickness of compressible material
- $\Delta\sigma$ is the change of stress at the centre of the compressible layer
- C_s is the swell index
- C_c is the compression index
- e_o is the initial void ratio
- $\sigma`_{pc}$ is the pre-consolidation pressure
- $\sigma`_{vo}$ is the initial overburden stress
- w_l is the liquid limit
- G_s is the specific gravity of the material
- S_s is secondary settlement
- t_1 and t_2 are the times at the start and end of the interest period
- E_s is the constrained modulus
- T_v is a non-dimensional time factor
- C_v is the coefficient of consolidation
- d is the drainage distance
- C_α is the secondary compression index

The trial embankment was never unloaded and the data cannot be used to back calculate the swelling index, hence Equation 2 was used.

The trial embankment data available does not cover a period of purely secondary settlement and therefore the author has opted to use the constant relationship between C_α and C_c based on material type. The compressible layer is largely made up of organic silt and as such as per Terzaghi et al (1996) a C_c/ C_α ratio of 0.05 has been adopted. A summary of the back calculated soil compressibility parameters determined can be found in Table 3 below:

Table 3. Summary of back calculated soil compressibility properties

Soil Compressibility Parameter	Soft Layer (0 - 6.5mbgl)	Medium Dense Sands
E_s Constrained Modulus (MPa)	3.45	25
C_v Coefficient of Consolidation (m^2/year)	6	-
C_c Compression Index	0.35	-
C_s Swelling Index	0.07	-
C_α Coefficient of Secondary Consolidation	0.0175	-

3 SETTLE3D MODELLING OF THE TRIAL EMBANKMENT

3.1 Settle3D Inputs

The compressibility parameters and the trial embankment dimensions were then input into RocScience's Settle3d software to model the trial embankment and validate the back calculated settlement parameters. The soil parameters used were as per Table 1 and Table 3 of this report with the compressible layer assumed to have double drainage conditions. The Mesri method of secondary consolidation was chosen and a value of 0.05 was adopted for the C_c/C_α ratio.

3.2 Initial Settle 3D Results and Discussion

The Settle3d results have been summarised in the graph in Figure 3. The graph shows that using the back-calculated parameters the settlement predicted prior to day 200 is overestimated when compared to the actual data, and subsequent to day 200 it is underestimated. This is likely due to the way in which in soil parameters were estimated from the trial embankment. The author has assumed that primary settlement begins at the end of construction and everything prior to that is immediate settlement. In reality, primary and immediate settlement will occur simultaneously during construction. Settle3D is an advanced settlement modelling software and can accurately model the primary settlement during construction.

The largest discrepancy between the Settle3D model and the trial embankment results is the time taken to 90% consolidation. The piezometer data indicate that the trial embankment reached 90% consolidation after 520 days while the Settle3D model indicates that the average degree of consolidation reaches 90% after about 350 days. The author has been thus far unable to exactly determine what is causing this difference in consolidation times. It is possible that this is due to using one dimensional theory to back calculate the C_v value from the trial embankment and then inputting that value into a three dimensional software analysis package.

3.3 Calibration of Settlement Parameters

It is now necessary to calibrate the soil parameters in Settle3d to separate the immediate and primary settlement during construction. The first step when calibrating the model was to establish a relationship between C_c and C_s. Murthy (2002) recommends that a ratio of between C_s and C_c of around 0.2 to 0.1 be used, these have been adopted as the upper and lower bound value. The values of C_v, C_c, C_s and E_s were continuously modified to find a combination of parameters which gives a settlement curve that conforms with the monitoring data from the trial embankment. This process resulted in the development of the soil parameters presented in Table 4.

Table 4. Table summarising calibrated soil parameters

Soil Compressibility Parameters	Soft Layer (0 - 6.5mbgl)	Medium Dense Sands
Constrained Modulus, E_s (MPa)	8.0	25
Coefficient of Consolidation, C_v (m^2/year)	3	–
Compression Index, C_c	0.28	–
Swelling Index, C_s	0.028	–
Coefficient of Secondary Consolidation, C_α	0.014	–

The major difference between the calibrated and back calculated soil parameters is the increase in the constrained modulus, E_s, and the reduction in the C_v value. The increase in the constrained modulus reflects the portion of the assumed immediate settlement which is in reality primary settlement occurring during construction. The settlement curves for both the back calculated parameters and the calibrated parameters can be found in Figure 3 below.

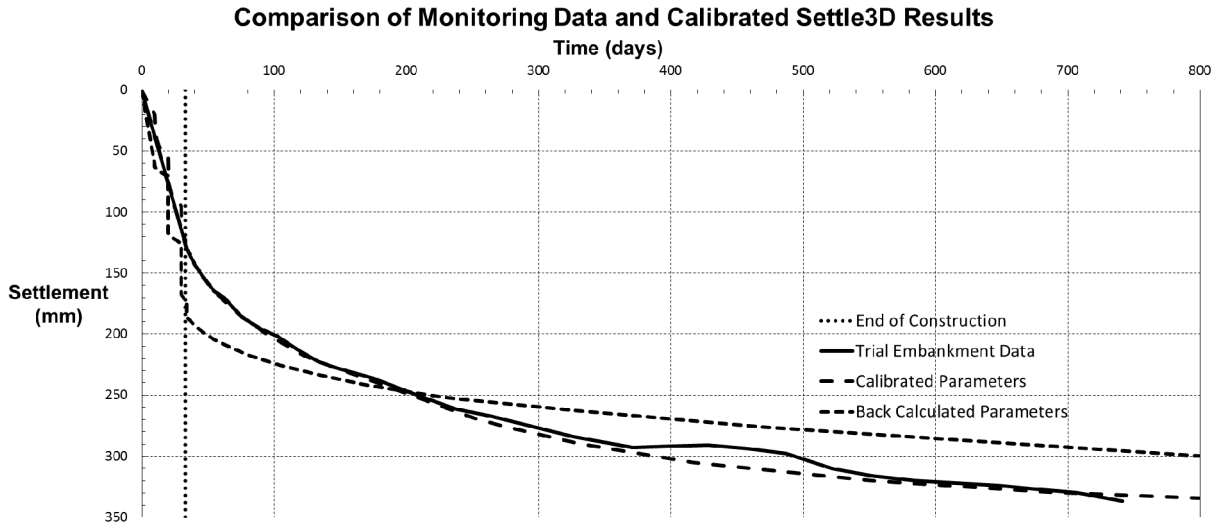


Figure 3. Measured and Settle3D total settlement values for both back calculated and calibrated soil parameters

4 CONCLUSION

Soil parameters have been back calculated from the settlement results of a monitored trial embankment on soft organic material using the standard 1D settlement equations given in Table 2. These soil parameters have been calibrated using Settle3D in an attempt to create a set of parameters that accurately model the trial embankment data.

Differentiating between immediate, primary and secondary settlement in a trial embankment is difficult, especially in soils made up of many heterogeneous layers. Layers will tend to behave differently to each other; sandier layers will tend to undergo relatively large immediate settlements but small primary and secondary settlements whilst very silty or clayey layers will tend to experience small immediate settlements but large primary and secondary settlements. This trial embankment provided settlement data which are an amalgamation of settlement in the different soil layers. This means that while trial embankments provide excellent data on the performance of embankments, they do not provide accurate soil parameters that represent the discrete layers underneath the trial embankment. This can

result in back calculated soil parameters from trial embankments giving very different parameters to those obtained from more targeted testing such as oedometers.

An important observation in this trial embankment study was the large amount of settlement prior to the end of construction. Whilst some of this is probably caused by primary settlement mechanisms, a significant portion of it appears to be immediate settlement. This immediate settlement is possibly caused by the compaction of the sandier layers interbedded with the compressible material. Separating the immediate from the primary settlement in the construction period of the curve is almost impossible. To find the portion of immediate and primary settlement during this phase of the curve an iterative process using Settle3D was adopted to determine calibrated soil parameters. The back calculated soil parameters were calibrated using the trial embankment data to come up with a set of soil parameters which the author believes to be a reasonably good approximation of the soils beneath the trial embankment. Due to the difficulties in differentiating between immediate settlement and primary during construction, back calculation of soil parameters would be very difficult in heterogeneous ground conditions without the use of analysis software such as Settle 3D.

Further analysis would be required to determine, through back calculation, the soil parameters for the discrete layers underlying the trial embankment. For the purposes of this study the soft layer was assumed to be a homogenous material. However, borehole investigations indicate that it consist of a heterogonous layer which includes a wide variety of material types from loose sandy silts to amorphous peats. These materials will behave very differently when subjected to embankment loads. A more vigorous analysis would involve separating the soft layer into discrete layers and identifying those which will behave as sand and those that will display more clay-like behaviour. Laboratory testing such as oedometers could be used to define specific soil parameters for these layers and develop a more complex and accurate ground model.

5 ACKNOWLEDGEMENTS

The author would like to thank Áine McCarthy and Ross Kristinof for carrying out the review of my paper. I would also like to thank Ian McPherson, Larry Goldfarb, Ian Froggatt, and Grant Murray for their invaluable technical support in helping me understand settlement and its myriad of complexities. Finally I would like to thank Jacobs for sponsoring my attendance of the YGPC conference and the NZGS for hosting it, this paper wouldn't be possible without both of those organisations. I also want to thank the entire Jacob's geotechnical team for providing a great work environment that has allowed me to develop as an engineer.

REFERENCES

Burka, L. P. (1993). *A hypertext history of multi-user dimensions. MUD history*, <http://www.ccs.neu.edu> (Dec. 5, 1994).

Toki, M. and Karunawardena A., (2013). "Design and Performance of Highway Embankments Constructed Over Sri Lankan Peaty Soils", *Proceedings of the 18th International Conference on Soil Mechanics and Geotechnical Engineer*, International Society for Soil Mechanics and Geotechnical Engineer (ISSMGE), Paris, France

Bowles, J. E. (1996). *Foundation Analysis and Design*, McGraw-Hill, New York.

Look, B. (2007). *Handbook of Geotechnical Investigation and Design Tables*, Taylor and Francis Group, London, UK

Mesri, G., Ajlouni, M. A., Feng T. W. and Lo, D.O.K. (2001). "Surcharging of soft ground to reduce secondary settlement", *Proceedings of the 3rd International Conference on Soft Soil Engineering*, pp. 55-56.

Mesri, G., Stark, T.D., Ajlouni, M.A. and Chen, C.S. (1997). "Secondary compression of peat with or without surcharging", *Journal of Geotechnical and Geoenvironmental Engineering*, 123, pp. 411-421

Mesri, G. and Godlewski, P.M. (1997). "Time and Stress-Compressibility Interrelationship", *Journal of the Geotechnical and Geoenvironmental Engineering Division*, 103 (GT5), ASCE (12910).

Murthy, V.N. (2002). *Geotechnical Engineering: Principles and Practices of Soil Mechanics and Foundation Engineering*, New York, USA, Marcel Dekker Incorporated.

Tan Y. Ch., Lee P. T. and Koo, K.S. (2013). "Instrumented trial embankment on soft ground at Tokai, State of Kedah, Malaysia", *Proceedings of the 18th International Conference on Soil Mechanics and Geotechnical Engineer*, International Society for Soil Mechanics and Geotechnical Engineer (ISSMGE), Paris, France

Shibata, T. and Sekiguchi, H. (1984). "Performance of trial embankment on soft clay", *International Conference on Case Histories in Geotechnical Engineering*

Robertson P.K (2012). "The James K. Mitchell Lecture: Interpretation of in-situ tests – some insights", in *Proc. 4th Int. Conf. on Geotechnical and Geophysical Site Characterization – ISC'4*, pp. 3-24.

Rocscience Inc. *Settle3D Settlement and consolidation analysis Theory Manual*

Terzaghi, K., (1943). *Theoretical soil mechanics*, New York, John Wiley and Sons.

Terzaghi, K., Peck, R.B. and Mesri, G. (1996). *Soil Mechanics in Engineering Practise*, John Wiley & Sons, Inc., Third Edition New York.

Proceedings of the 11th ANZ Young Geotechnical Professionals Conference – 11YGPC
Queenstown, New Zealand
25 – 28 October 2016

Geotechnical challenges during design of Aokautere Reservoir – Palmerston North

Ravikumar Sundar[1], GIPENZ and Mark Frampton[2], CPEng, MIPENZ.

[1]Opus International Consultants Ltd, 74 Ingestere Street, Whanganui 4500; PH +64 6 349 6600; ravi.sundar@opus.co.nz
[2]Opus International Consultants Ltd, 74 Ingestere Street, Whanganui 4500; PH +64 6 349 6600; mark.frampton@opus.co.nz

ABSTRACT

Palmerston North City Council (PNCC) is currently constructing one of two planned new 2,500m^3 reservoirs and a new 1.2km long access road on a site at 291 Turitea Road, southeast of Palmerston North city. The reservoir site is located on a hill with slopes ranging from 15^0 to 30^0. The reservoir platform is to be created by cutting the hill top down by 7 m. The reservoir will be designed to be serviceable after a major earthquake event. The reservoir, and therefore its platform is designed as an Importance Level 4 (IL4) structure with special post-disaster function requirements. Site investigation and slope stability analysis was carried out for the reservoir platform to confirm the setback distance of the reservoir from the edge of the slope. The 1.2km access road alignment, which provides the alignment for the pumped rising main supplying the reservoirs, traverses steep valley sides with high sidling cuts. The challenges encountered during the design of the high cuts included restricted availability of information and limited scope for localised site investigation necessitating the extrapolation of surface geological mapping data. Conservative cut slope batters would have required large earthwork volumes at high cost. A risk based approach to the batter design was undertaken, accepting that steeper cut batter angles may result in failures along the access route, but that these failures could be managed for a lower overall cost. Lessons from the experience are drawn for application to similar situations in the future.

Keywords: Aokautere, reservoir, platform, slope stability, seismic design, analysis

1 INTRODUCTION

Palmerston North City Council (PNCC) is upgrading the water supply for the Summerhill, Aokautere and Linton areas. The building of two water storage reservoirs at a higher elevation than the City's current reservoirs is a project that was part of the Water Supply Development Plan, adopted in 1996. When completed, the new water supply will not only allow housing developments at higher elevations, but will improve the resilience of the City's water supply network following a major seismic event.

2 SITE LOCATION AND DESCRIPTION

The Aokautere area lies within the low-lying hills and raised terraces of the western side of the Tararua Range. This reservoir site is located on the gentler foothills of the Tararua range approximately 1 km northeast of Turitea Road. The access route to the reservoir site branches off from Turitea Road before travelling northeast up an existing farm track that flanks the southern side of the gully, and winds its way up to a saddle on a ridge. Most of the access route will be subject to potential slope instability. The reservoir site is located on the ridge covered in pasture. TheTproposal is to cut approximately 7.8m from the top of the ridge to create a platform for the reservoir. The northwest and southwest hillside slope of the reservoir platform is gentle, having slope gradient of no more than 13^0. The northeast and southern slopes are steeper, typically in the range of between 20^0 and 30^0. A critical section on the southeast slope is at 42^0.

3 DEVELOPMENT PLAN

The development plan for Stage One and Two of the Aokautere Reservoir project included the construction of an access road from Turitea Road to the reservoir platform completed by the end of May 2016. The total estimated project cost is $5.4m. Stage Three of the project includes the construction of Reservoir No.1, planned to be completed by June 2017. The second reservoir is planned for construction in approximately five years' time. Due to the hilly nature and steep slopes of the existing site significant earthworks were carried out to form the roads and the reservoir platform.

Refer to Figure 1 for the locations of the access road and the reservoir platform.

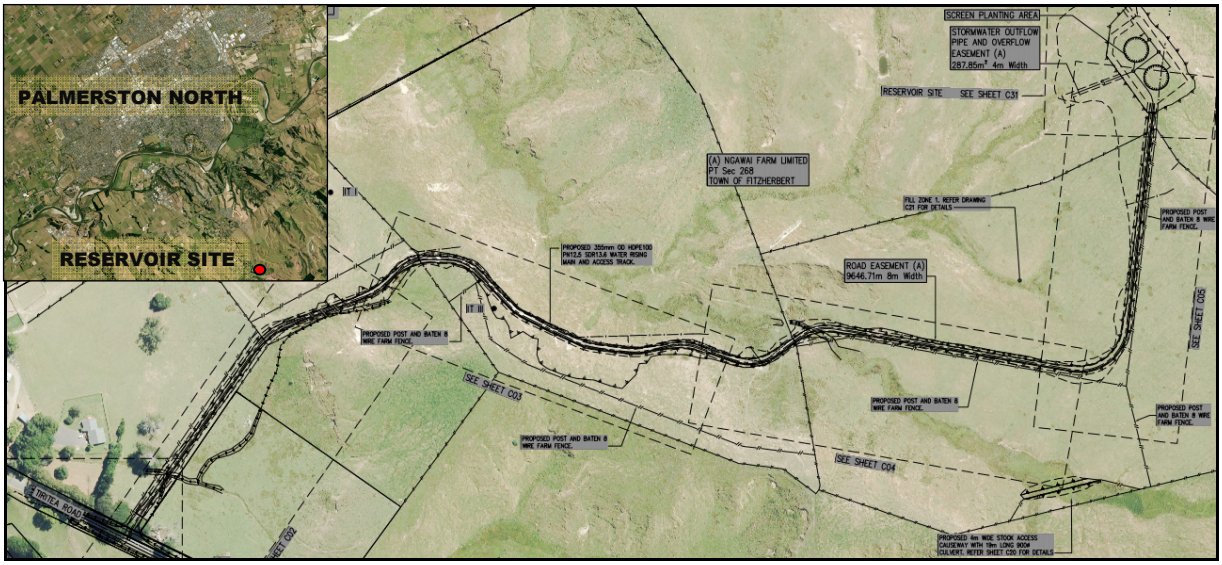


Figure 1. Site Layout Plan

4 GEOLOGIC SETTING

4.1 Geology of the Area

The geology of the area are indicated to be marine deposits of the Wanganui Series (Mid Pleistocene), which include well-weathered gravels, sands, and silts (DSIR, 1962). Wanganui Series deposits forms the highest marine terrace sequences of the Manawatu area and these unconformably overlie basement greywacke bedrock of the Tararua Range. IGNS (1994a) presented a more detailed geological map of the Palmerston North area that indicates the foothills near Turitea to be soft Plio-Pleistocene marine rock, deposited between 0.5 – 5 million years ago in shallow seas. Alluvial fan and colluvial debris flow deposits of Holocene Age, overlay the marine sediments on the foothills. A thin blanket of loess (up to 2m thick) also covers much of the area.

4.2 Seismicity

The Palmerston North region is one of the most earthquake prone in New Zealand. The active Wellington Fault lies approximately 9km southeast of the Turitea area. It presents the highest seismic hazard to the area, having a recurrence interval of between 500 and 770 years with a magnitude estimate of 7.6 ± 0.3 (Begg and Mazengarb, 1996).

4.2.1 Calculation of Peak Ground Acceleration

Based on the most conservative estimate of the SPT data (N value 30 – 50 and maximum depth of soil is 55 m) from boreholes, the site is consistent with a Class C (Shallow Soil Sites) classification. Therefore, the site is classified as Class C – Shallow Soil Site, in terms of the seismic design requirements of NZS1170.5:2004.

The client determined the proposed reservoir would be designated an Importance Level 4 (IL4) structure in accordance with NZS1170.0:2002 and will have a post-disaster function. The structure is to have a design working life of 50 years (for seismic considerations). Through application of Table 3.3 AS/NZS1170.0:2002, the earthquake annual probability of exceedances were established for the proposed reservoir. The design return periods (i.e. the inverse of the Annual Probability of Exceedance (APE)) are 25 and 500 years for SLS1 and SLS2 limit states, respectively.

NZS1170.5:2004 can be utilised to develop design magnitude-weighted PGA values (hereafter referred to as '(PGA)M=7.5') for use in the foundation design of the proposed reservoir. (PGA)M=7.5 values for the site are weighted to a magnitude 7.5 earthquake and are 0.13g and 0.51g for SLS1 and SLS2 limit states respectively. Earthquake actions for Importance Level 4 structure SLS2 limit state is

avoidance of damage to structure to the extent that they can no longer remain operational after the SLS2 earthquake motions. The horizontal seismic coefficient K_h, was taken to be equal to peak ground acceleration calculated from the SLS2 earthquake motion, used in the slope stability analysis. A design FS of 1.0 was then targeted for the slope.

5 ASSESSMENT OF THE STABILITY OF RESERVOIR ACCESS TRACK

5.1 Geotechnical Investigations

A cut batter slope was proposed into the hillside slope to upgrade the farm track to permanent access track to allow for construction and maintenance of the reservoir. The existing natural slope of the hillside along the track route is between 25^0 and 55^0, and up to 14 m high. Observations on the site indicate the slope is only marginally stable. Erosion of silt and sandy silt was observed along the existing farm track. Observations also indicated mass movement at various locations. Geotechnical site investigations were carried out to assess the ground condition for slope stability analysis.

5.1.1 Field Work

Ten mechanically excavated trial pits were conducted at the site during June 2015. Of these, four trial pits were located on the proposed access track, and six trial pits were located on the top, face and bottom of the proposed track cut slope. Scala penetrometer tests were undertaken adjacent to the trial pits from ground level to a maximum depth of 3.0m or refusal. The number of blows for each 100mm penetration was recorded. Pilcon vane shear tests were also undertaken in the near surface soils during excavation of the trial pits.

5.1.2 Geotechnical Parameters

The soils encountered in the trial pits and parameters used in slope stability analysis are presented in Table 1, and have been derived from visual description of soils encountered, in-situ soil testing and published empirical correlations with in-situ test results

Table 1. Summary of Soil Properties

USCS Soil Classification	Description	Parameters used in SLOPE/W analysis		
		Unit Weight (kN/m^3)	Φ' (degrees)	c' (kPa)
CL	Silty CLAY	17	28	20
GM	Silty GRAVEL	20	36	2
ML	Sandy SILT	18	29	5
ML	Gravelly SILT	19	34	2
MH	Clayey SILT	16	30	10

5.2 Slope Stability Assessment

The geotechnical data was used to prepare three interpretive sub-surface ground models for the proposed cuts. Refer to Figure 2 for the presentation of the interpretive ground models, which formed the basis of the slope stability assessments. The slope stability assessments were conducted utilising numerical analysis using the computer programme SLOPE/W (GEO-SLOPE, 2012). In accordance with the standard engineering practice for slopes that provide integral support for or direct loading on a structure, target factors of safety (*FS*) against failure of 1.5 was established for static loading condition.The Morgenstern-Price method of slices was utilised to determine the *FS* for each failure surface. As no groundwater was encountered in any of the sub-surface investigations, the groundwater table was assumed to be below access track level for the analysis.

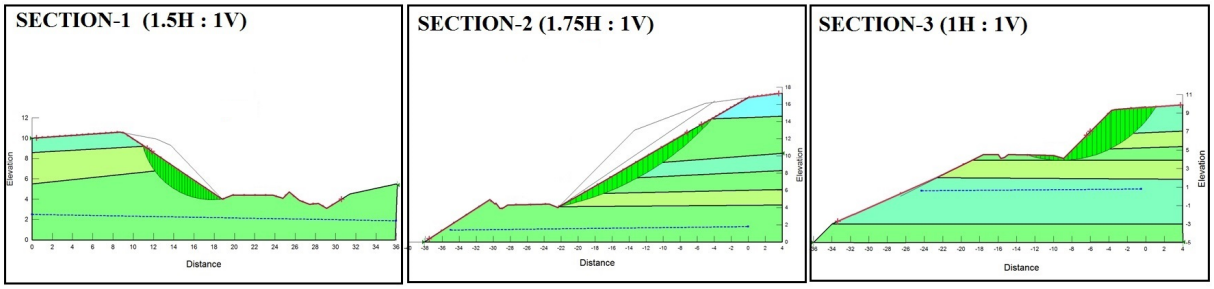


Figure 2. Access Track Analysis Models

5.3 Summary of Stability Analyses and Design of Slope Surface

The Factor of Safety for each section with different cut slopes to achieve has been briefly summarised below in Table 2.

Table 2. Summary of Analysis

Section Description	Analysis Model Chainage	Slope	Angle (^{0})	Factor of Safety (*FS*)
Section – 1	260 m to 340 m	1 H : 1 V	45	1.16
		1.5 H : 1 V	34	1.53
Section – 2	420 m to 580 m	1 H : 1 V	45	0.99
		1.5 H : 1 V	34	1.34
		1.75 H : 1 V	30	1.52
Section – 3	580 m to 660 m	1 H : 1 V	45	2.08

The cut slopes for the access road have been computed from the *FS* values returned from the slope stability analyses. All met or exceeded the target *FS* value of 1.5. Initial assessment of the cut slope for the access road using seismic case required large cuts, daylighting at the top of ridges with large earthwork quantities. After a value engineering process, the client decided to accept the risk of failure during major seismic event by assuming the access route could be reinstated quickly after the event.

6 ASSESSMENT OF THE STABILITY OF RESERVOIR PLATFORM

6.1 Geotechnical Investigations

The proposal for the reservoir platform was to cut approximately up to 7.8m from the top of the ridge to create a platform for the new reservoirs. Geotechnical site investigations, laboratory testing and slope stability analysis were carried out to confirm the setback distance from the edge of the slope to the water tank, stability of the reservoir platform and to check the bearing capacity and settlement of the ground beneath the reservoirs.

6.1.1 Field Work

Two boreholes and five static Cone Penetration Test (CPT) were conducted at the site during January 2016. Boreholes were drilled to 20m depth at the platform location before earthworks, with Standard Penetration Test (SPT) at 1.5m intervals. The core samples were logged in accordance with the Guidelines for the Field Description of Soil and Rock (NZGS, 2005). All CPT testing progressed until the cone meet refusal (was unable to penetrate the ground). CPTs meet refusal at a maximum depth of 5.3m, with further penetration retarded by dense gravel layers.

6.1.2 Geotechnical Parameters

The soils encountered in the boreholes and parameters used in slope stability analysis are presented in Table 3, and have been derived from visual description of soils encountered, in-situ soil testing and published empirical correlations with in-situ test results

Table 3. Summary of Soil Properties

USCS Soil Classification	Description	Parameters used in SLOPE/W analysis		
		Unit Weight (kN/m^3)	Φ' (degrees)	c' (kPa)
-	Fill	17	34	1
SM	Silty SAND	18	34	2
GM	Sandy / Silty GRAVEL	20	40	2
ML	SILT / Gravelly SILT	19	36	5

6.2 Slope Stability Assessment

The geotechnical data was used to prepare three interpretive sub-surface ground models for the proposed engineered cut/fill platform. Refer to Figure 3 for the presentation of the interpretive ground models, which formed the basis of the slope stability assessments. The slope stability assessments were conducted utilising numerical analysis using the computer programme SLOPE/W (GEO-SLOPE, 2012). In accordance with the standard engineering practice for slopes that provide integral support for or direct loading on a structure, target factors of safety (*FS*) against failure of 1.5, 1.0 were established for static and seismic loading conditions, respectively.

The Morgenstern-Price method of slices was utilised to determine the *FS* for each failure surface. As no groundwater was encountered in any of the sub-surface investigations, the groundwater table was assumed to be well below the reservoir platform level for the analysis.

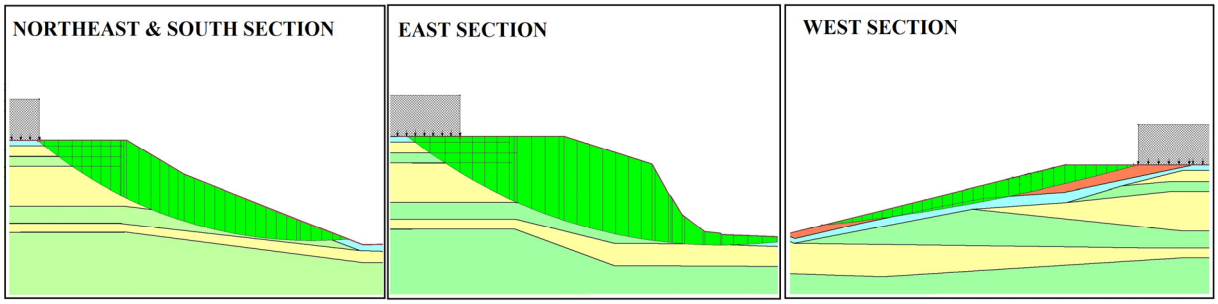


Figure 3. Reservoir Platform Analysis Models

6.3 Summary of Stability Analyses and Design of Slope Surface

The Factor of Safety for each section with different cut slopes to achieve has been briefly summarised below in Table 4.

Table 4. Summary of Analysis

Analysis Model	Analysis Type	Maximum Slope Angle	Factor of Safety (*FS*)	Distance of tank from edge of the slope[a]
Northeast & South	Static case	25^0	2.55	15 m
	Seismic case		0.87	
East	Static case	41^0	2.23	18 m
	Seismic case		0.93	
West	Static case	14^0	3.56	6 m
	Seismic case		0.92	

[a] Slip circles beyond this distance from edge of the tank are not considered in FOS calculation

Results from the stability analysis shows the slope stability of the critical section has a factor of safety of 2.23 under static condition. However, factor of safety under seismic condition is less than the recommended seismic factor of safety of one. This factor of safety is accepted considering the conservative value of K_h equal to PGA.

7 DESIGN OF RESERVOIR PLATFORM

The proposed setback distances for the reservoir could be achieved by increasing the footprint of the reservoir platform. The excavated material from the top of the ridge were used to construct engineered fill to increase the platform footprint. The development included removing a maximum thickness of

approximately 7.8 m of materials from the site to form the proposed reservoir platform. This material was placed on the western side to increase the platform area to accommodate the northern reservoir. The predominant ground conditions found on the site were that of marine deposits consisting of sand and gravel interbedded with layers of silts. The marine deposits are considered suitable for re-use as engineering fill provided the water content is controlled, adequate compaction is achieved and unsuitable material such as loess/ residual soil were cut to waste. It was recommended that, in order to achieve a stable slope, all permanent slopes be constructed at a maximum gradient of 4H:1V (14^0) and that topsoil be spread out on any disturbed areas to an even depth, grade and finish.

Reservoir–1 (Southeast Reservoir) would be built fully on the cut platform. The depth of cut within the proposed reservoir footprint varies from 1m to 7m depth. Reservoir–2 (Northeast Reservoir) would be built across a cut and fill platform, which varies in depth from approximately 2.4m depth of cut to 2m thickness of fill. The whole Reservoir–2 footprint including the in-situ ground is to undercut by 2 metres minimum and recompacted with imported AP65 material to ensure a transition in the stiffness of foundation materials, to minimise differential movement.

8 SUMMARY AND CONCLUSIONS

On the basis of the terrain evaluation, ground investigations and analysis, the conclusions on access track cut and the reservoir platform are given as follows:

- The soils were likely to be erodible and care was required on the cut batter face to avoid rilling and surficial failures. Measures to stabilise the cut batter and exposed soils were to be incorporated into the works;
- Slope angles identified for the cut batter slope for different chainage were based on the factor of safety of 1.5 for static slope stability analysis given in Table 2;
- Global stability is considered satisfactory following the construction of the reservoirs. However, appropriately sized setbacks listed in Table 4 from the reservoir and crests of slopes were incorporated in the layout to mitigate seismic slope stability hazard;
- The reservoir site is underlain by marine deposits, which include weathered dense to very dense gravels, weathered firm to stiff silt, with a thin blanket of loess deposit. The marine deposits generally have a SPT N value greater than 40;
- Foundation bearing capacities are satisfactory, but differential settlement needed to be addressed. This is because Reservoir–2 is to be partially in cut and fill so that the net loading is non-uniform. Undercutting and replacing with granular fill was recommended to ensure uniformity of subgrade conditions; and
- It was recommended that, in order to achieve a stable slope, all permanent platform fill slopes be constructed at a maximum gradient of 4H:1V (14^0) and that topsoil be spread out on any disturbed areas to an even depth, grade and finish.

9 ACKNOWLEDGEMENTS

The author thanks Palmerston North City Council (PNCC), for their permission to prepare this paper.

REFERENCES

IGNS (1994a). *Characterisation of Near-Surface Geological Conditions in Urban Areas of the Manawatu-Wanganui Region*, Institute of Geological and Nuclear Sciences. Prepared for Manawatu-Wanganui Regional Council.

DSIR (1962). *Geological Map of New Zealand at 1:250,000 scale*, Sheet 11, Dannevirke (1st Edition), Department of Sceintific and Industrial Research, Wellington, New Zealand.

Begg, J.G. and Mazengarb, C. (1996). *Geology of the Wellington area*, Geological Map 22. Scale 1:50000, Institute of Geological and Nuclear Sciences.

Standards Australia/Standards New Zealand (2002). *AS/NZS 1170.0:2002 Structural Design Actions Parts 0 - General Principle*, Standards Australia/Standards New Zealand, Wellington

Standards Australia/Standards New Zealand (2004). *AS/NZS 1170.0:2004 Structural Design Actions Part 5 - Earthquake Actions*, Standards Australia/Standards New Zealand, Wellington

GEO-SLOPE International, Ltd. 2012. SLOPE/W by GeoStudio. August 2015 release. Version 8.15.5.1177.

Opus International Consultants Ltd (2015a). *Aokautere Water Supply Reservoir Platform, Geotechnical Desktop Study Report*, Opus International Consultants Ltd. Opus Reference 5WT439.00/01

Opus International Consultants Ltd (2015b). *Aokautere Reservoir Access Track, Cut Slope Assessment Report*, Opus International Consultants Ltd. Opus Reference 5WT439.00/02

Opus International Consultants Ltd (2016). *Aokautere Water Supply Reservoir Platform, Geotechnical Assessment Report*, Opus International Consultants Ltd. Opus Reference 5WT439.00/03

Proceedings of the 11th ANZ Young Geotechnical Professionals Conference – 11YGPC
Queenstown, New Zealand
25 – 28 October 2016

Static failure mechanisms in sensitive volcanic soils in the Tauranga Region, New Zealand

P.R. Mills[1, 2] and V.G. Moon[1]

[1]School of Science, Faculty of Science and Engineering, University of Waikato, Private Bag 3105, Hamilton 3240; PH (+64) 7-8384148; email: pip.mills@outlook.co.nz; vgmoon@waikato.ac.nz;
[2]Coffey Geotechnics, Level 11, 7 City Road, Grafton, 1010: PH (+64) 9 379 9463

ABSTRACT

Sensitive soils derived from weathered rhyolitic volcanic materials have contributed to major landslides in the Bay of Plenty. Soil was sampled from sensitive layers near the failure surface of two coastal landslides bordering Tauranga Harbour. Methods were adapted from Gylland et al. (2014) including undrained, consolidated static triaxial tests at a high compression rate of 0.5 mm/min in order to replicate rapid loading during landsliding. Like sensitive materials derived from glacial till, sensitive volcanic derived material showed contractive p-q plots, strain softening stress- strain behaviour, coupled with rising pore pressures, and single or double shear band formation after peak strength was reached. Little to no cohesion or friction softening occurred between peak and residual states. This evidence indicates that like sensitive soils derived from glacial till, the low permeability of the clay allows pore pressure gradients to evolve, eventually initiating collapse of clay microstructures into shear zones, where further excess pore pressure generation within the shear zone instigates progressive failure. Shear zone development causes a rapid loss of global resistance, expressed as strain softening behaviour.

Keywords: landslide, sensitive, volcanic, shear zone, strain localisation, strain softening

1 INTRODUCTION

1.1 Problem background

It is well documented that sensitive soil failures in Tauranga occur after heavy, prolonged periods of rainfall (Moon et al., 2015a & b). The fundamental failure mechanisms relating to rising pore pressures during heavy rainfall has not been studied for these materials. The strain softening failure properties of these soils are important to understand for accurate slope stability modelling (Gylland et al., 2014; Thakur et al., 2011). Several notable large landslides attributed to sensitive soils in the Tauranga Region include (1) the Ruahihi Canal failure in 1981, (2) a significant coastal cliff collapse at Bramley Drive in 1979 (Gulliver & Houghton, 1980), and (3) numerous landslides in the Tauranga city margins after heavy rainfall in 2005.

1.2 Literature review

Sensitive soils derived from both glacial till (Bjerrum, 1955; Bernander, 2000; Locat et al., 2011; and Gylland et al. 2013), and also from weathered volcanic material (Wyatt, 2009; Cunningham, 2012) show brittle failure and a reduction in the shearing resistance following peak strength, known as strain softening (Taylor, 1937; Skempton, 1964). Recently, at a microstructural level, brittle failure and strain softening in glacial till derived sensitive materials in the northern hemisphere has been attributed to excess pore pressure generation in localised shear bands (Thakur, 2007; Thakur, 2011; Gylland et al., 2013; and Gylland et al., 2014) rather than a reduction of c' and φ'.

Recent evidence indicates that at both a macroscopic level (Skempton, 1964; Urciuoli, 2007; and Quinn et al., 2011), and microscopic level (Thakur, 2007; Thakur, 2011; Gylland et al., 2013; and Gylland et al., 2014), progressive failure, where strain softening in one soil element results in failure and strain softening in its neighbouring soil element, like falling dominoes, is a dominant process governing failure of sensitive soils. At the macroscopic level, three progressive failure mechanisms have been described: (i) upwards progressive failure, wherein a perturbation at a cut slope propagates upwards into the slope, (ii) downwards progressive failure, where a load further back from a free face, for example pile driving, initiates shear band propagation, and (iii) widespread liquefaction of the

sensitive layer. Recently, fracture mechanics principles (Rice, 1968; Palmer, 1973) have been applied to progressive (stable), and catastrophic (unstable) growth of shear bands in sensitive soils at a macroscopic scale (Quinn et al., 2011). The high liquidity index, saturation, and void ratios of sensitive material mean that a significant amount of water is released during failure, allowing the soil to transport overlying material long distances (Torrance, 2014).

During undrained compression of glacial till sensitive soils at a microscopic scale, initial strain localisation and the following strain softening, contractive response observed has been attributed to excess pore pressure generation (Thakur, 2007; Thakur, 2011; Gylland et al., 2013; and Gylland et al., 2014). Low material permeability combined with high loading rates result in pore pressure gradients, leading to localised strain and further excess pore pressure generation due to contractant microstructure within a shear band (Thakur, 2007; Thakur, 2011; Gylland et al., 2013; and Gylland et al., 2014). All plastic straining occurs within the shear band following its formation.

1.3 Aim

In this study we aim to answer whether sensitive volcanic material soils bear similar failure characteristics to glacial till sensitive soils, by relating lab observations to field observations. We studied two coastal cliff landslide sites in the Tauranga Region where sensitivity is believed to contribute to failure: (i) a significant landslide at Bramley Drive, Omokoroa, which has been the subject of ongoing research by the University of Waikato and University of Bremen, and (ii) a smaller landslide, initially investigated by Coffey Geotechnics in 2012, on the south side of Matua Peninsula within Tauranga City urban area.

2 METHODS

Geomorphic maps were drawn over aerial photographs overlain with contours during a site walkover (WBOPDC, 2014). Sampling sites of the sensitive material were chosen based on (a), safe location (b) compliance of property owners and (c) extra sensitive material in the layer suspected to contribute to failure. *In situ* peak and remoulded strength was measured with a Pilcon Geotechnics vane. Stratigraphy was described in accordance with NZGS (2005). Stratigraphic layers at the sampling site at Omokoroa were correlated with a borehole drilled behind the failure scarp in February 2012. At Matua, stratigraphy was correlated with hand auger boreholes drilled in February 2013 (Geotechnics 2013). For triaxial sampling, push tubes were chosen over block samples as the material was too brittle for carving. At each site, a bench was dug horizontally into the sensitive layer, and separate stainless steel push tubes (d=48 mm, h=148 mm) were gently tapped into the dug bench from the vertical direction. Four push tubes of Matua material (M1) were collected and three of Omokoroa material (OM1), as well as bulk samples for geomechanical properties. Field moisture was preserved by thorough plastic wrapping and storage containers. Moisture content, wet and dry bulk densities, voids ratio, and Atterberg limits all followed ISO standards (ISO/TS 17892-1:2004), undrained effective triaxial testing, and cohesion and friction angle methods followed NZS 4402 (1986) with the exception of the compression rate, where a higher rate of 0.5 mm/min was chosen over the testing time recommended, in accordance with Gylland et al. (2013), who justified using a higher rate because undrained loading occurs rapidly during landslides. All samples were saturated to B values greater than 95%. A membrane correction was applied in accordance with NZS 4402 (1986). To determine brittleness or strain softening of the soil, we used Bishops (1971) parameter:

$$\text{Brittleness} = (q_{max} - q_{residual} / q_{max}) \times 100 \quad (1)$$

where q_{max} and $q_{residual}$ are peak and residual deviator stresses respectively.

3 STRATIGRAPHY AND GEOMOROPHOLOGY

3.1 Stratigraphy

The stratigraphy of the steep to gently inclined, roughly NE aligned peninsulas around the Tauranga Harbour margins comprise a sequence of locally and distally sourced, reworked and *in situ* volcanogenic sediments (Briggs, 1996). Problem-causing sensitive layers occur within the Matua Subgroup (60 ka – 2.09 Ma), a variable fluvial sequence consisting mainly of reworked pyroclastics. The Pahoia Tephras (0.35 – 2.18 Ma), a series of air fall tephras and ignimbrites, are intercalated with

the Matua Subgroup (Briggs, 1996). Overlying the Matua Subgroup are younger airfall tephra sequences (Briggs, 1996; Lowe et al., 2001). Stratigraphic profiles and soil sample descriptions at each site are outlined in Figure 1.

3.2 Geomorphology

The Bramley Drive landslide has geomorphic features which are most similar to flow failures (Bernander, 2000; Locat et al., 2011). These features include a largely scarred, empty landslide crater, a large flowslide runout component (~160 m after 2012 event), and to a lesser degree, a narrow landslide neck (Locat et al., 2011). The approximate equidimensional and bowl-shaped scarp are similar to lump landslides (Hungr et al., 2014). Like landslides in glacial till, retrogression has occurred, but over a much longer time scale, and shorter distances (initially ~ 30 m in 1979, then 3 -5 m in 2011-2012) (Moon et al., 2015). The failure scarp of the slide at Matua is shallow relative to the surface, slightly back rotated toward the base (52º) and roughly equidimensional (11 m long, 10 m wide), indicating planar-slight rotational sliding (Hungr et al., 2014). The long runout component (~ 50 m), remoulded nature of the debris, and extra sensitive material near the base of the failure scarp at Matua indicate that sensitivity contributed to failure.

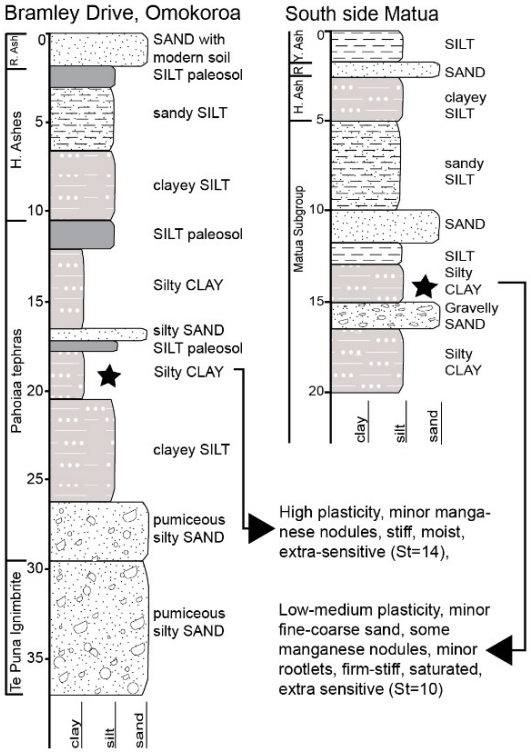


Figure 1. Stratigraphic profiles of Bramley Drive and Matua.

Table 1. Geomechanical properties of soil sampled from Omokoroa and Matua

	Omokoroa ± S. Error	**Matua ± S. Error**
Peak FS[a] (kPa)	66 ± 3	60 ± 0.4
Remoulded FS (kPa)	5 ± 1	6 ± 0.6
Moisture Content, w (%)	72 ± 1	64 ± 0.3
ρ_d (kg/m^3)[b]	1320 ± 46	1690 ± 98
Porosity, n (%)	70 ± 0	65 ± 3
Void Ratio, e (%)	2.3 ± 0	1.8 ± 0.3
Sensitivity, St (%)	15 ± 3	10 ± 1
ρ_c (kg/m^3)[c]	2517 ± 9.7	2777 ± 257
Clay (%)	63 ± 4	40 ± 11
Silt (%)	37 ± 4	23 ± 7
Sand (%)	0 ± 0	37 ± 17
Liquid Limit (%)	66 (R^2 = 0.99)	52 (R^2 = 0.87)
Plastic Limit (%)	41 ± 0.4	37 ± 2
Plasticity Index (%)	25	15
Liquidity Index (%)	2.9	1.8
Activity (%)	0.4	0.4

[a] FS = Field Vane Strength;
[b] ρ_d = wet bulk density;
[c] ρ_c = Particle Density

4 GEOMECHANICS

4.1 Standard geomechanical properties

Porosity, void ratio, liquidity indices and moisture content are high for Matua (M1) and Omokoroa (OM1) materials, in keeping with previously published research on material derived from halloysite (Table 1) (Wesley, 1977; Wesley, 2009; Wyatt, 2009; Cunningham, 2012; and Moon et al., 2015). Soils from both sites are silty clays, in contrast to most soils reported in previous publications (Keam, 2008; Wyatt, 2009; and Cunningham, 2012), which are silts or clayey silts. SEM scans suggest material from both sites to be halloysite dominated, with an open structure of point-point contacts, small, ubiquitous pore spaces, and clay mineral coatings on larger silt and sand sized grains (Moon et al., 2015). Many, saturated pores accounts for the low wet bulk densities observed in M1 and OM1. Both M1 and OM1 have high Atterberg limits, plotting below the A-line as high compressibility silts, and low activities (Table 1), in line with halloysite dominated sensitive material (Wesley, 2009; Moon et al., 2015).

4.2 Triaxial results

Triaxial results for M1 and OM1 samples are presented in Table 2, for tests a – d. At greater confining stresses, peak deviator stress, curvature of peak, and degree of strain softening increases for both M1 and OM1. Tests where pore pressure rises after peak stress correlate with a contractive, left trending curve along the CSL (critical state line) (c, d), while tests where pore pressure drops following peak stress correlate with curves that touch the CSL and trend slightly to the right. All samples failed along either one sliding plane by shear, or as a wedge, where two sliding planes occur at roughly perpendicular angles. Only sample M1a failed by barrel deformation with very minor shear zones observed. High effective friction and variable effective cohesion values are in the range of previous publications (Keam, 2008; Wyatt, 2009; and Cunningham, 2012). Effective friction angles and cohesion for samples stayed mostly consistent between peak and residual states, albeit minor reductions i.e. little to no friction and cohesion softening occurred.

Table 2. Undrained, consolidated triaxial test results for Omokoroa and Matua

Sample	Test Label	ECP (kPa)[a]	B (%)[b]	TR[c] (mm/ min)	ε_f (%)[d]	q_f (kPa)[e]	SS (%)[f]	FM[g]	c'_f[h]	c'_r[i]	φ'_f (°)[h]	φ'_r (°)[i]
OM1	a	140	95	0.5	1.9	179	14	W	26	24	31	26
	b	240	98	0.5	3.2	246	20	S				
	c	340	98	0.5	2.0	299	50	S-W				
M1	a	75	95	0.5	2.2	131	13	B-S	17	17	32	29
	b	150	98	0.5	2.3	137	29	S-W				
	c	225	98	0.5	2.2	207	33	S-W				
	d	255	96	0.5	4.4	250	29	S				

[a] ECP = Effective Confining Pressure; [b] B = Saturation; [c] TR = Test Rate; [d] ε_f = Axial strain at failure; [e] q_f = deviator stress at failure; [f] SS = Strain Softening defined by Bishop (1971); [g] FM = Failure Mode: W = Wedge, S = Shear, B = Barrel; [h] c'_f, φ'_f = Effective cohesion and friction at peak deviator stress; [i] c'_r, φ'_r = effective cohesion and friction at residual deviator stress

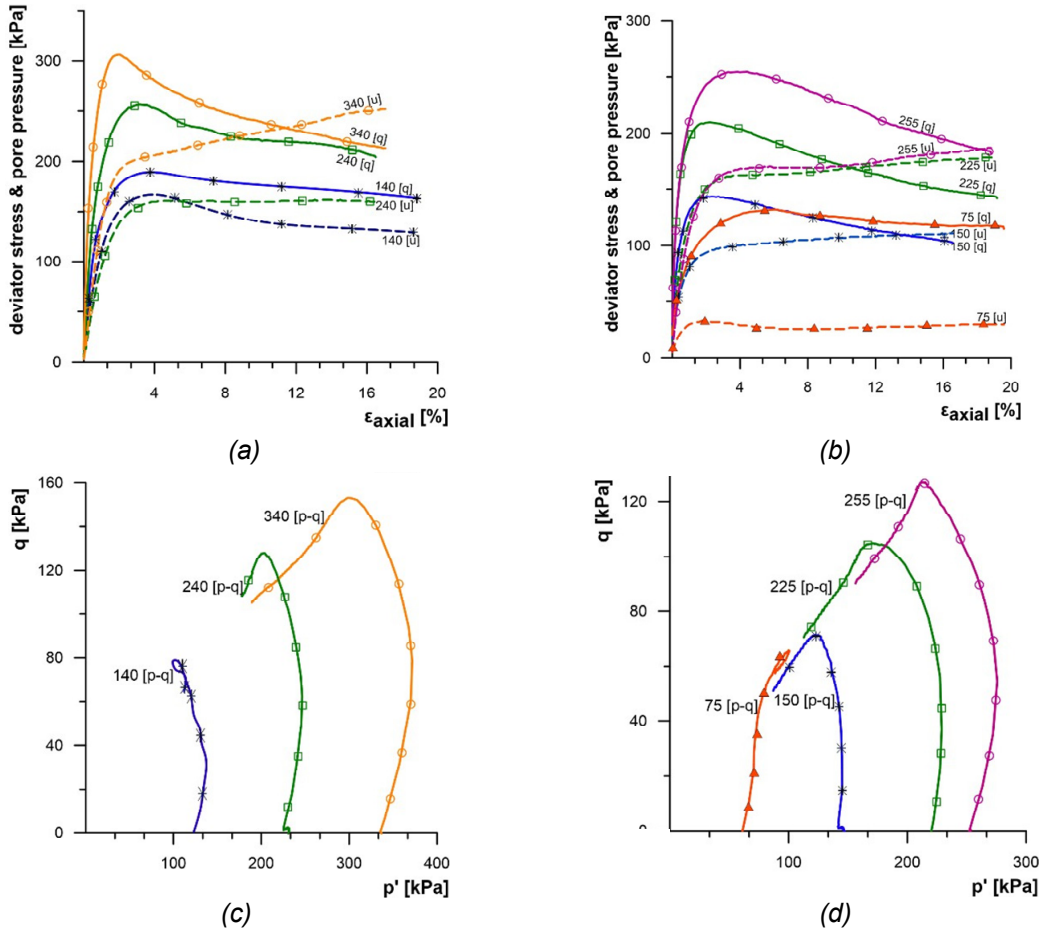


Figure 2. (a) & (b) Deviator stress & pore pressure vs. axial strain; (c) & (d) p'-q' stress path plots for Omokoroa (left – (a) & (c)) and Matua materials (right – (b) & (d)).

5 DISCUSSION

The contractive, strain softening responses observed in our volcanic material samples concurs with the observations of undrained, consolidated tests on glacial till sensitive soils (Thakur, 2007; Gylland et al., 2014; and Thakur et al., 2014). The low material permeability and high compression rate induce excess pore pressure gradients to evolve, leading to strain localisation, likely in a weak region (Zhang et al., 2015), prior to or at peak stress (Gylland et al., 2014), ending in progressive failure (Mills, 2016) within one or more shear bands. Like Gylland et al. (2013), thin section analysis of shear zones shows differential development of Riedel shears and P shears, i.e. one end of the shear zone is more developed than the other (Mills, 2016). The shear band likely creates a preferential pathway for excess pore pressure to drain, registering as a delayed response with the pore pressure base sensor as observed in the pore pressure plots (Figure 2(a) and (b)). The minor strain softening observed in samples M1a and OM1a shows that some contraction occurred, but the drop in pore pressure after peak stress shows that the majority of the sample slightly dilated. This is because the lower confining pressures allowed pore pressure to dissipate within the sample, so no gradients could evolve and induce contractive failure in a shear band.

Strain softening was initially considered by Bishop (1971) to be a reduction in stress after peak stress. Importantly, recent authors (Tavenas, 1984; Quinn et al., 2011) consider the horizontal strain or shear band displacement required to reach the residual state equally important to consider. It was not feasible to include horizontal displacement in our experimental setup, therefore the brittleness parameter we used is an estimate of strain softening. The sampling method we used may have resulted in a reduction of sensitivity of the soil, as shown by (Thakur et al., 2014).

Friction and cohesion softening was first proposed as a stress reduction mechanism by Skempton in 1964, for the case of long term stability of overconsolidated clays under drained conditions. In the range of 10 – 20% strain, or short term stability, effective cohesion and friction in sensitive glacial till soils is consistent between the peak and residual states (Gylland et al., 2013; Gylland et al., 2014; and Thakur et al., 2014). Excess pore pressure in localised shear bands has been shown to be responsible for the strain softening contractive responses observed (Gylland et al., 2013; Gylland et al., 2014; and Thakur et al., 2014). At very large strains, i.e. greater than 20%, cohesion and friction softening have been observed in sensitive glacial till soils (Stark, 1994). In our samples, little to no reduction in effective cohesion and friction angle occurred between peak and residual states (Table 2), implying that shear induced pore pressure was the governing failure mechanism.

5.1 Connecting the dots: Laboratory observations to macroscopic failure mechanism

Landslide events at both sites occurred following intense, prolonged rainfall (Gulliver & Houghton, 1980; Coffey Geotechnics, 2013; and Moon et al., 2015). We postulate that failure likely initiated within a thin layer at 23 m depth, on the basis of its extra high sensitivity (St = 130) and correlation with the base of the landslide scarp. We suggest that the high rainfall prior to the main sliding events resulted in excess pore pressure accumulation within the already saturated extra sensitive layer at 23 m, initiating strain localisation and downwards progressive failure along the extra sensitive layer at 23 m, towards the free face of the adjacent cliff. Once a critical end length of the shear band reached the residual strength, the shear band propagated through stiffer overlying tephra layers (Quinn et al., 2011). The failure mechanism that initiated the Matua slide is suggested to be similar to the Bramley Drive slip, with a tentative conclusion that the different geomorphologies are explained by the lack of a paleovalley at Matua.

6 CONCLUSIONS

Field observations of two landslides in sensitive soils in Tauranga are linked to laboratory observations of undrained, consolidated triaxial tests, in an attempt to quantify static failure mechanisms. At high confining pressures, sensitive soils sampled from the suspected failure plane of each landslide show strain softening, contractive responses coupled with rising pore pressure post peak deviator stress, and single or double shear band failure modes. Very minor effective friction and cohesion softening occurred. This evidence points to excess pore pressure gradients initiating strain localisation and progressive failure in one or more shear bands i.e. the same failure mechanism that occurs in glacial till sensitive soils. The hypothesis of excess pore pressure ties in with observed landslides at both sites occurring after heavy rainfall, whereby excess pore pressure gradients are likely to have

accumulated in extra sensitive layers at depth. The high liquidity indices and water content of the soil allows the soil to flow like a liquid, explaining the long runout distances observed at both landslides.

7 ACKNOWLEDGEMENTS

This paper was inspired by Gylland and Thakur's publications on sensitive soil failure. Research was under a partnership between University of Waikato and Coffey Geotechnics, funded by the Callaghan Innovation. Thank you to Kori Lentfer, Dave Sullivan and Max Kluger for mentoring, and Kah-Weng Ho for the constructive feedback on this paper.

REFERENCES

Bernander, S. (2000). *Progressive landslides in long natural slopes, formation, potential extension and configuration of finished slides in strain-softening soils,* PhD Thesis, Lule University of Technology, Sweden.

Bishop, A. W. (1971). "The influence of progressive failure on the choice of the method of stability analysis", *Géotechnique*, 21, pp. 168-172.

Bjerrum, L. (1955). "Stability of natural slopes in quick clay", *Géotechnique*, 5(1), pp. 101-119.

Briggs, R. M. (1996). *Geology of the Tauranga Area*. Dept. of Earth Sciences Occasional Report. Hamilton, Uni. of Waikato

Coffey Geotechnics. (2013). *Cross sections and hand auger borehole records for Matua*. Project 15730AA.

Cunningham, M. J. (2012). *Sensitive rhyolitic pyroclastic deposits in the Tauranga region: mineralogy, geomechanics and microstructure of peak and remoulded states,* MSc. thesis.

Gulliver, C. P., Houghton, B.F. (1980). *Omokoroa Point Land Stability Investigation*, Tonkin and Taylor.

Gylland, A. S., H. P. Jostad and S. Nordal (2014). "Experimental study of strain localization in sensitive clays", *Acta Geotechnica*, 9, pp. 227-240.

Gylland, A. S., H. Rueslåtten, H. P. Jostad,. S. Nordal. (2013). "Microstructural observations of shear zones in sensitive clay", *Engineering Geology*, 163, pp. 75-88.

Head, K. H., Epps, R.J., Scotland, U.K., Hungr, O., Leroueil, S. and Picarelli, L. (2014). *Manual of soil laboratory testing: Soil classification and compaction tests*, London, Pentech Press.

Hungr, O., Leroueil, S. and Picarelli, L. (2014). "The Varnes classification of landslide types, an update", *Landslides,* 11, pp. 167-194.

Keam, M. J. (2008). *Engineering geology and mass movement on the Omokoroa Peninsula, Bay of Plenty*, MSc thesis.

Locat, A., Leroueil, S., Bernander, S., Demers, D., Jostad, H.P. and Ouehb, L. (2011). "Progressive failures in eastern Canadian and Scandinavian sensitive clays", *Canadian Geotechnical Journal*, 48, pp. 1696-1712.

Lowe, D. J., Tippett, T.D., Kamp, P.J.J., Liddell, I. J., Briggs R. M., Horrocks, J. L. (2001). "Ages on weathered Plio-Pleistocene tephra sequences, western North Island, New Zealand". *Les Dossiers de l'ArcheoLogis*, 1, pp. 45-60.

Mills, P.R. (2016). *Failure mechanisms in sensitive volcanic soils in the Tauranga Region, New Zealand*, MSc thesis (Unpublished), University of Waikato.

Moon, V.G., Lowe, D.J., Cunningham, M.J., Wyatt, J., Churchman, G.J., de Lange, W.P., Mörz, T., Kreiter, S., Kluger, M.O. and Jorat, M.E. (2015a). "Sensitive pyroclastic derived halloysitic soils in northern New Zealand: interplay of microstructure, minerals, and geomechanics", in: Rotonda, T., Cecconi, M., Silvestri, F. and Tommasi, P. (eds.), *Proc. of the Int. Workshop on Volcanic Rocks and Soils*, Lacco Ameno, Ischia Island, Italy, 24-25 September, 2015, pp. 3-21.

Moon, V. G., de Lange, W. P., Garae, C.P., Mörz, T., Jorat, M.E. and Kreiter, S. (2015b). "Monitoring the landslide at Bramley Drive, Tauranga, NZ", *Proc. of 12th Australia New Zealand Conf. on Geomechanics (ANZ 2015)*, Wellington, New Zealand

New Zealand Standard (NZS) (1986). *NZS 4402: Methods of testing soil for civil engineering purposes*, The soil testing committee, (44/3), of the building and civil engineering division committee, (30/-). Wellington.

NZGS. (2005). *Guidelines for the field classification and description of soil and rock for engineering purposes*

Palmer, A. C. R. and Rice, J. R. (1973). "The growth of slip surfaces in the progressive failure of over-consolidated clay", *Proceedings of the Royal Society of London Mathematical and Physical Sciences,* 332, pp. 527-548.

Quinn, P., Hutchinson D.J., Rowe R.K. (2011). "A new model for large landslides in sensitive clay using a fracture mechanics approach", *Canadian Geotechnical Journal*, 48, pp. 1151-1162.

Rice, J. R. (1968). "A path independent integral and the approximate analysis of strain concentration by notches and cracks", *Journal of Applied Mechanics*, 35 (2), pp. 379-386.

Skempton, A. W. (1964). "Long-term stability of clay slopes", *Géotechnique*, 14(2), pp. 75-102.

Stark, T. D. and Contreras, I.A. (1994). "Drained residual strength of cohesive soils", *Journal of Geotechnical Engineering,* 120(120), pp. 856-871.

Tavenas, F. (1984). "Landslides in Canadian sensitive clays-a state-of-the-art", *Proceedings of the 4th International Symposium on Landslides*, Toronto Press, Toronto, Ontario, Vol. 1, pp. 141-153.

Taylor, D. W. (1937). "Stability of Earth Slopes", *Journal of the Boston Society of Civil Engineers*, 24(3), pp. 197-246.

Thakur, V. (2007). *Strain localisation in sensitive soft clays*, PhD. Thesis, Norwegian University of Science and Technology.

Thakur, V. (2011). "Numerically observed shear bands in soft sensitive clays", *Geomechanics and Geoengineering: An International Journal*, 6(2), pp. 131-146.

Thakur, V., Jostad, H.P., Kornbrekke, H.A. and Degago, S.A. (2014). *Landslides in Sensitive Clays: From Geosciences to Risk Management*, Netherlands, Springer.

Torrance, J. K. (2014). *Chemistry, Sensitivity and Quick-Clay Landslide Amelioration*, Netherlands, Springer.

Urciuoli, G., Picarelli, L. and Leroueil, S. (2007). "Local soil failure before general soil failure", *Geotechnical and Geological Engineering Journal*, 25(1), pp. 103-122

Wesley, L. D. (1977). "Shear strength properties of halloysite and allophane clays in Java, Indonesia", *Géotechnique*, 27(2), pp. 125- 136.

Wesley, L. D. (2009). "Behaviour & geotechnical properties of residual soils and allophane clays", *Obras y Proyectos*, 6, pp5-10

Wyatt, J. B. (2009). *Sensitivity and clay mineralogy of weathered tephra-derived soil materials in the Tauranga region*, MSc thesis, University of Waikato.

Zhang, W., Wang, D., Randolph, M.F., Purzin, A.M. (2015). "Catastrophic failure in planar landslides with a fully softened weak zone", *Géotechnique*, 65(9), pp. 755-769.

Proceedings of the 11th ANZ Young Geotechnical Professionals Conference – 11YGPC
Queenstown, New Zealand
25 – 28 October 2016

Geotechnical investigations to address Earthquake Hazards for the Petone to Grenada Link Road, Wellington, New Zealand

E. Boam[1], and P. Brabhaharan[1]

[1]Opus International Consultants Ltd, P.O. Box 12003, Wellington, 6144, New Zealand; PH +64 (04) 471 7000 ; FAX +64 (04) 471 1397; email: ella.boam@opus.co.nz

ABSTRACT

The New Zealand Transport Agency is developing a new Petone to Grenada (P2G) link between Hutt Valley and Porirua, to improve road access and reliability in the region. Resilience is a key objective for the project and for the transportation network in the Wellington region. The P2G project crosses land that has complex geotechnical issues and is exposed to significant natural hazards, and consequently a comprehensive programme of site investigation was carried out to characterise the ground conditions and inform the development of robust and resilient options for the road alignment. Particular geotechnical issues investigated for this project were the location of the active Wellington Fault, the liquefaction hazards in Petone, the slope failure hazards in the steep hilly terrain, the properties of the highly fractured and faulted greywacke bedrock and the depth and distribution of deeply weathered material. A comprehensive ground model is presented that incorporates the geomorphology and geology of the site with the geotechnical issues and hazards, and implications for the geotechnical design of the project are discussed. It is noted that the development of this project is in progress, and additional geotechnical investigations are currently being carried out to inform further development of the design.

Keywords: earthquake, hazards, site investigations, resilience, road development

1 INTRODUCTION

The New Zealand Transport Agency is developing a new link road between the Hutt Valley and the northern Wellington districts. The project area lies between State Highway 2 at Petone and State Highway 1 at Tawa/Grenada North and is called the Petone to Grenada route (P2G). The proposed link is approximately 6 km in length and proposes tying SH1 and SH2 together through new interchanges at both Petone and Tawa, as well as an interchange in the middle of the route to connect to the proposed development at the Lincolnshire Farms area and Grenada Village via Mark Avenue, see Figure 1. This project includes widening the section of SH1 between Tawa and the southern extent of the Transmission Gully expressway at Linden.

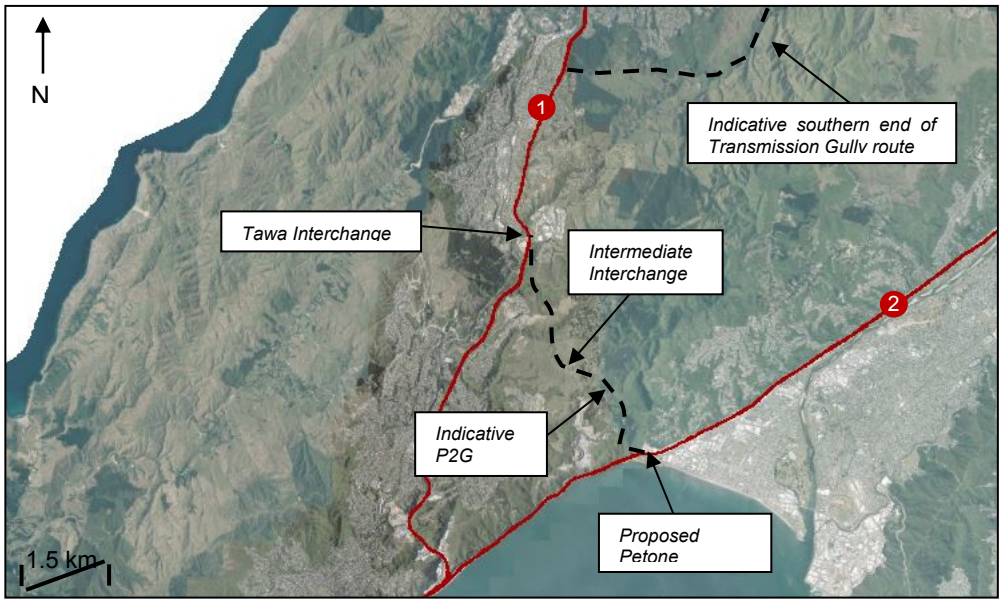


Figure 1. Location of Petone to Grenada Route (image: Greater Wellington Regional Council, n.d.)

To achieve robust and resilient alignment options for the link, a comprehensive ground model has been developed to address the complex geotechnical issues and earthquake hazards that could adversely impact the performance of the road.

2 RESILIENCE

One of the key objectives for the new road is to enhance the resilience of the Wellington state highway network. Previous assessments of the existing state highway network indicate that the region has poor resilience in the event of a large earthquake and the need to enhance resilience is of critical importance for the road controlling authorities such as the New Zealand Transport Agency and local authorities. These authorities have a responsibility to proactively manage the risks to their road networks from natural hazards and enhance resilience. A new route between SH1 and SH2 would achieve enhanced resilience of the network, as well as improve connectivity between the lower Hutt Valley and Wellington's northern suburbs and Porirua, reduce journey times across the region as well as enhance safety.

Resilience studies of the road networks in the region indicate poor resilience of access into the region in the aftermath of hazard events such as a large earthquake or storms (Brabhaharan and Mason, 2012). The loss of access will severely impact the supply of essential goods and services for emergency response and recovery. Not only will the region be cut off, the individual districts will be cut off from each other, making it difficult for the districts to help each other. In addition to this, the Wellington Region has very limited redundancy and connectivity in its network outside the city centres. The Greater Wellington area comprises only two state highways and parallel rail links providing road or rail access from outside the region, one along the western corridor (SH 1) and one from the east (SH 2) and there are very few viable alternative arterial local roads. In terms of connectivity, there are no viable connections between the cities of Wellington and Hutt Valley, and between Porirua and Hutt Valley other than SH2 and SH 58 respectively; both of which are assessed to have poor route resilience (Brabhaharan and Mason, 2012). Both these networks are expected to be cut off following a large magnitude 7.5 earthquake in the Wellington region due to their vulnerability to large landslides and liquefaction. Critical points such as Haywards Hill (SH58), Rimutaka Hill (SH2) and SH2 between Ngauranga and Petone are expected to be closed for many weeks to months due to large landslides, see Figure 2.

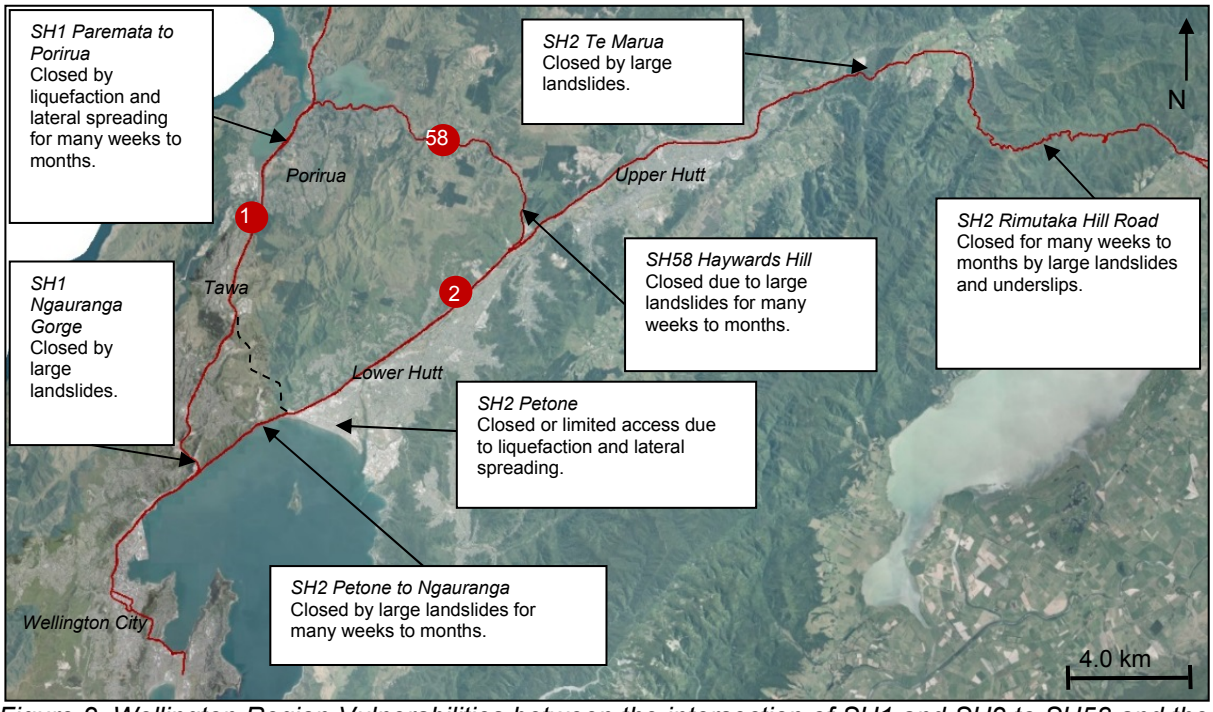


Figure 2. Wellington Region Vulnerabilities between the intersection of SH1 and SH2 to SH58 and the Rimutaka Hill (image source: Greater Wellington Regional Council, n.d.)

The Petone to Grenada route would provide an opportunity to enhance the regional resilience by providing a viable connection between Porirua and the Hutt Valley by bypassing the critical points located along SH2 and SH58. This would enhance access resilience into the Hutt Valley in the aftermath of hazard events such as earthquakes and improve redundancy of access.

The overall resilience of the P2G route will be dependent on the specific alignment selected. Understanding the vulnerabilities of each alignment to earthquake induced ground damage is critical to the overall resilience of the project and as the project area is subject is complex geotechnical issues and exposed to significant natural hazards, a comprehensive programme of site investigations has been carried out to assess these issues and inform the development of robust and resilient options for the road.

3 EARTHQUAKE HAZARDS AND GEOTECHNICAL INVESTIGATION

The Wellington Region is exposed to a high level of seismicity which is associated with a number of major active faults and the main subduction zone marking the active plate boundary between the Pacific and Australian plates. There are four major active faults within 20 km of the P2G route which represent significant earthquake sources and are capable of generating earthquakes of Mw 7.5 to 8+. These faults and their characteristic magnitudes and recurrence intervals are the Wellington Fault (M7.5, 840 years), Wairarapa Fault (M8.2, 1,200 years), Ohariu Fault (M7.4, 2,460 years) and Moonshine Fault (M7.1,12,540 years) (Stirling, et al, 2010). Earthquakes of this scale would cause strong ground shaking and induce significant ground damage in the form of fault rupture, landslides and liquefaction and associated ground subsidence and lateral spreading in the region.

To assess the vulnerability of the overall P2G route and various alignments to damage from these hazards, an extensive programme of investigations was undertaken to characterise the ground conditions and provide site specific information to inform geotechnical assessment. This assessment is critical to ensuring a resilient design. For ease of this assessment, the route is considered in two sections based on the characterisation of the geomorphology, geology and geotechnical issues; the Petone section and the hilltop section. The investigations undertaken were targeted to address the potential ground damage effects of earthquake hazards, specific to each section, as described below.

3.1 The Petone Section

The P2G route begins in Petone at the south-western end of the Hutt Valley. An interchange is proposed at Petone to tie into the existing SH2 and the local roads near the Korokoro Valley and stream, see Figure 1.

The wider area of the lower Hutt Valley is characterised by low lying, flat coastal and alluvial terraces with a naturally high water table. The geology consists of an extensive sequence of Quaternary marine and alluvial deposits which have aggraded within the Hutt Basin in excess of 300 m at the western end of the Esplanade in Petone. These deposits are described to be bound to the west by the Wellington Fault which is mapped to pass through the Petone area in the vicinity of the proposed P2G interchange. Figure 3 depicts this situation; showing the relationship of the Wellington Fault and the basin sediments (Begg et al., 2008). Fault rupture, ground shaking and liquefaction are considered to be the critical hazards in the Petone section and are described in more detail below.

3.1.1 The Wellington Fault

The influence of the Wellington Fault is considered a principal hazard to the P2G route. It represents a significant earthquake source within the Wellington Region and has been mapped in close proximity to the proposed interchange in Petone. The fault has a recurrence interval of 610 to 1,100 years and ruptures in large earthquakes of magnitude 7.5 with typical coseismic displacements of the ground surface of 5 m horizontally and 1 m vertically (Little et al., 2010). Confirming the location of the fault is imperative for the siting and resilient design of interchange structures and ensuring the fault rupture zone is avoided.

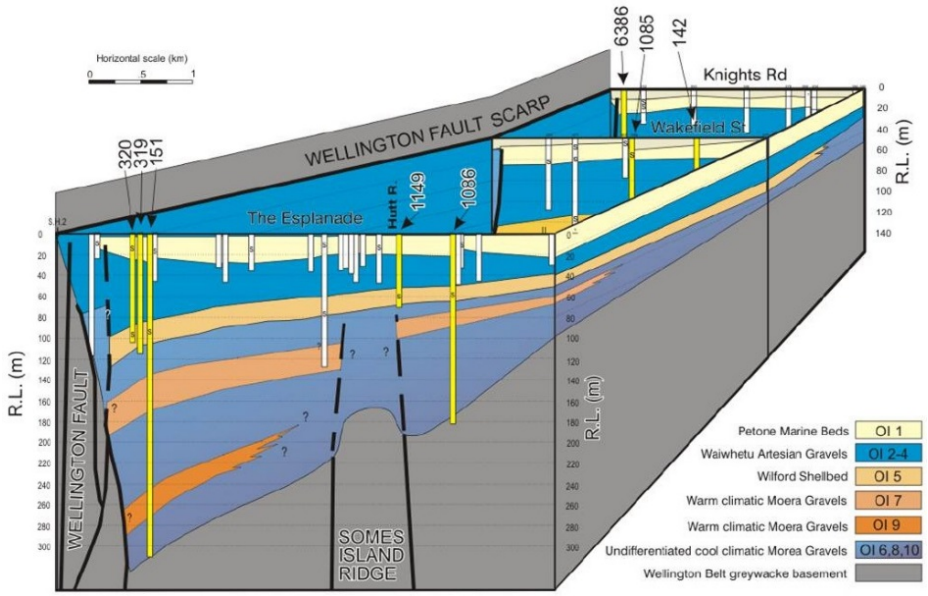


Figure 3. 3D block model of the Wellington Fault scarp and Lower Hutt Basin (Begg et al. 2008)

The location of the Wellington Fault in Petone and the Wellington Harbour is poorly constrained due to the lack of surface expression. This is apparent from differing published geological maps of the area. Prior to this study, the location of the active trace of the Wellington Fault was inferred to lie approximately 200 m from the proposed P2G interchange at Petone. This was based on geological mapping of the active fault trace north of the SH2 Dowse Interchange and on geophysical imaging of the fault zone in the harbour to the south of Kaiwharawhara (IGNS, 1996, 2000). The 1:20,000 Wellington Fault Hazard Map (Wellington Regional Council, 1991) shows the fault to have two strands and suggests a wider fault zone. The northern strand runs closer to the section of State Highway 2 between Horokiwi and Petone off-ramp. The southern strand runs parallel to the northern strand but about 550 m to the south, refer Figure 4.

Given the uncertainty in the fault's location, the width of the fault zone and the possible fault splay/s, geotechnical and geophysical investigations were carried out; targeted to refine the fault's location as well as determine the ground conditions and stratigraphy in the vicinity of the fault zone. Initially, stereo aerial photo analysis and field mapping were conducted before a series of boreholes were undertaken. The boreholes indicated a sharp change in depth across a relatively short horizontal distance indicating a steep step. To gain an understanding of the fault location, a series of seismic refraction lines were then undertaken. These were accompanied by a microgravity survey. Both these geophysical techniques are influenced by the depth to bedrock and were able to be correlated with the borehole data. These surveys indicated the presence of several steps in the bedrock between the main fault structure and the interchange area. The data from these geophysical surveys allowed for a location of these steps to be more accurately known at the ground surface and using this information, an additional, inclined borehole was undertaken in an attempt to physically observe fault disturbed material.

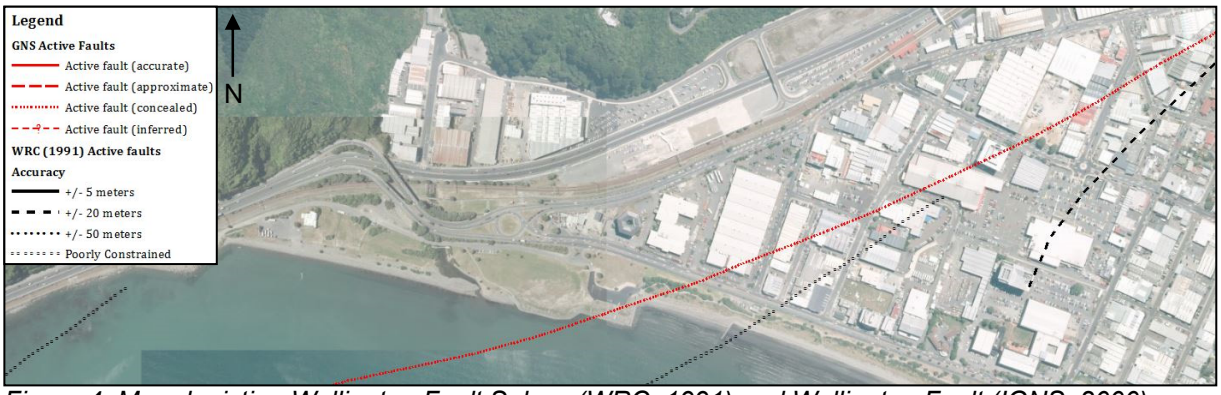


Figure 4. Map depicting Wellington Fault Splays (WRC, 1991) and Wellington Fault (IGNS, 2000)

3.1.2 Liquefaction

The close proximity of the Wellington Fault increases the risk of a higher level of ground shaking in a seismic event leading to a higher level of ground damage in both the Petone section and across the remainder of the P2G route. In the Petone section, this is particularly relevant for the assessment of potential ground damage caused by liquefaction.

It has been well documented that there is a liquefaction hazard in the Petone area due to the high water table and extensive loose alluvial and marine soils (Wellington Regional Council, 1993). Liquefaction ground damage can lead to foundation failure, subsidence and lateral spreading, which could affect any surface development and more specifically, the interchange structures. The proposed location of the Petone interchange is located in a zone mapped with a high liquefaction potential and as such, it is critical to determine the extent of liquefiable material present and to assess the potential for ground damage in a large earthquake. This information will be valuable for the design of the interchange.

Boreholes and static cone penetration tests (CPTs) were targeted across the wider interchange area to determine the depths and lateral extent of potentially liquefiable material. They were placed to cover various geological deposits such as alluvial material around the Korokoro Stream, colluvial deposits from the adjacent hillslopes and the fill, beach and marine sediments closer to the foreshore. The CPTs provided detailed information about the soil characteristics which were correlated with physical samples retrieved from the boreholes. The borehole samples were also used for laboratory testing (particle size distribution, Atterberg limits and plasticity index) to provide further site specific detail for liquefaction analysis.

The soil characteristics determined from these methods enabled an assessment of liquefaction in the Petone and Tawa Interchange areas. The assessment indicated that there would be liquefaction expected in the Petone interchange area which will be taken into consideration in the design, but not expected to be a significant issue in the Tawa interchange area.

3.2 The Hilltop Section

The hilltop section comprises the remainder of the P2G route through to Grenada/Tawa. Immediately following the Petone interchange, the link road climbs the adjacent southwestern slopes that bound the Hutt Valley. These slopes are the result of uplift associated with the Wellington Fault and represent the heavily eroded fault scarp. They are steep and are bisected by steeply incised gullies. The slopes rise from sea level at the SH2 Petone interchange, to 290 m elevation on the hilltops in Horokiwi at the summit of the route. The summit and the adjacent Lincolnshire Farms area has more gently rolling topography and is characterised by the remnants of an ancient erosion surface called a K-Surface. This surface has been subsequently uplifted and dissected so that only remnants of it are preserved; as rounded ridge crests and undulating tableland surfaces. This area is the location of a proposed intermediate interchange. From the Lincolnshire Farms area, the route continues north across a steeply sloping gully and past Grenada Village before sidling down to the existing SH1 to connect at the Tawa / Grenada North Interchange.

The hilltop section of the route is dominated by Wellington belt greywacke which comprises interbedded sandstone, siltstone and mudstone/argillite of varying proportions. These rocks have been complexly folded and faulted through numerous deformation events which have caused significant fracturing of the rock including joint sets generated due to the change in stress direction over time.
The earthquake hazards considered to be most significant in this section are earthquake induced slope instability and to a lesser extent, the presence of the Moonshine Fault.

3.2.1 Earthquake Induced Slope Instability

Moderate to large earthquakes can lead to slope failures in steep to very steep slopes, including cuttings which are generally steeper than the natural hillslopes. The P2G route crosses steep, hilly terrain, particularly at its southern end between Petone and the hilltops at Horokiwi. This area, along the western side of SH2 is characterised by steep hillslopes and deeply incised gullies of the uplifted block of the Wellington Fault. Here, the hills rise from sea level at the SH2 Petone interchange up to 290 m elevation on the hillslopes near Horokiwi. These slopes have been mapped as having high

susceptibility to earthquake induced landslides, particularly along the eroded Wellington Fault scarp along the Wellington Harbour and along the flanks of deeply incised valleys such as the Korokoro Stream valley, see Figure 5 (Brabhaharan *et al*, 1994). This is influenced by evidence of historical earthquake induced landslides, most notably 'Gold's Slide' along SH2 in close proximity to the proposed route, which was triggered during the 1855 earthquake (Brabhaharan et al, 1994). To overcome the sharp change in elevation in this area and to still achieve a design gradient for the road, significant cuts up to 70 m high are being considered. A further large cut slope north of Lincolnshire Farms in the vicinity of Grenada Village is also being considered.

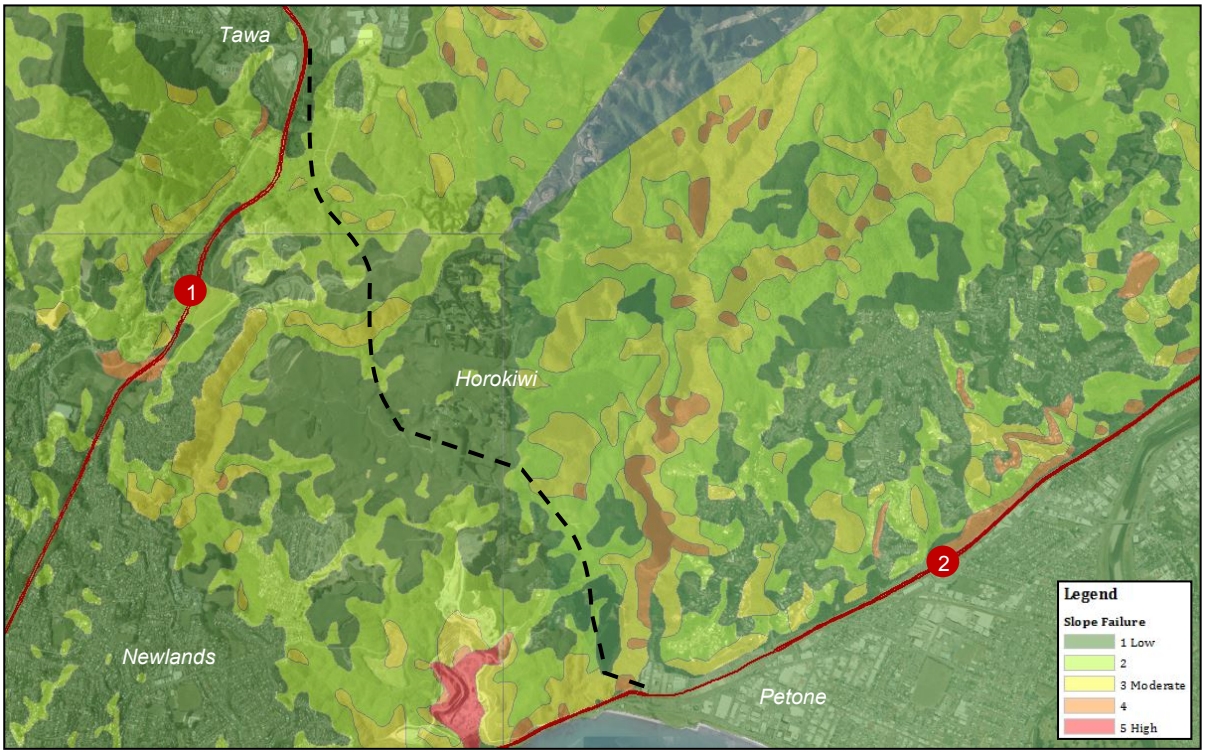


Figure 5. Earthquake induced slope failure susceptibility map (Brabhaharan et al, 1994)

The hazard of earthquake induced slope instability is strongly controlled by the level of ground shaking during an earthquake event, but also by the geology and orientation and form of the cut slope design. The areas where large cut slopes are being considered are both predominantly greywacke, however have undergone differing weathering and tectonic deformation processes resulting in highly variable rock quality. The hillslopes rising from the Petone area have undergone tectonic deformation associated with the Wellington Fault. The greywacke is generally less weathered but there are prominent zones of breccia, sheared and crushed zones and clay seams. These zones can be extremely weak and are likely to more readily fail during a seismic event, particularly if they daylight in the cut slope at an unfavourable orientation; as for any significant joint set or bedding plane which can act as a failure surface. At the summit and north of Lincolnshire Farms, processes associated with the K-Surface have had more influence over the rock mass quality. Here the weathering profile is significantly deeper (>30 m) (IGNS, 1996) below ground level, indicating a greater depth of more highly weathered and generally weaker rock exposed in the proposed cut slopes.

Initially stereo aerial photo analysis and field mapping of rock exposures and landforms were conducted. This allowed historical slope failures to be identified and enabled the expected modes of failures in individual material types and angles at which failures could be expected at along the route to be assessed. This work identified the potential for landslides in weathered bedrock along the Moonshine Fault, shallow landslides and rill-gully erosion in colluvium and residual soil on the K-surface, possible shallow landslides in colluvium and larger rock block slides on the flanks of the Korokoro Stream. The Wellington Fault scarp above SH2 was also identified as a zone of historical slope failure, as mentioned earlier. This area is important to the resilience of the P2G project as it is currently a critical point of weakness in the existing regional State Highway network. Field mapping also allowed for the identification of weathering and strength characteristics of exposed rock, as well as measurement of shear zone orientations and other surficial features.

To gather information on the subsurface ground conditions, a series of deep, cored boreholes were drilled and accompanied by down hole televiewer surveys. The boreholes were positioned along the route in the expected locations of cut slopes so that the weathering profile and changes in strength and rock mass quality over the depth of the cut could be physically examined. These also provided information on the properties and thickness of soil overburden which was identified as particularly important along the K-Surface where a significant thickness of loess had been mapped. A number of representative samples were used for triaxial and unconfined compressive strength testing to determine accurate rock properties for use in cut slope analysis. This information is critical to design to ensure the form of the cut slope (angle, height, bench width etc.) is appropriate to achieve a resilient design. The identification of critical defect orientations is also imperative to a resilient design, which were obtained both through field mapping and downhole acoustic and optical televiewer surveys. These surveys were able to be correlated to the borehole data to assess the defect orientation and differentiate defect types such as sheared zones, joint sets and bedding which could impact the slope performance. This defect data was invaluable for the subsequent assessment of the stability of the proposed 30 m to 80 m high greywacke rock cut slopes. Three mechanisms of failure; (a) failure along dominant defects (b) rock mass failure through intensely jointed rock and (c) combined failure through dominant defects and break out through rock mass, were identified, and analyses for static as well as earthquake conditions enabled the design of preliminary cut slope angle and slope configuration. This will be presented in a subsequent paper in the future.

3.2.2 Moonshine Fault

Similar to the Wellington Fault in the Petone area; the P2G route crosses the Moonshine Fault trace near the proposed interchange with State Highway 1 at Tawa/Grenada North. However, unlike the Wellington Fault, this fault has a very long recurrence interval (>11,000 years) and accordingly a very low probability of rupture. The location, width, characteristics and form of the fault zone are poorly defined. As a result, the Moonshine fault is considered of low risk to the P2G route and conceptual designs and no site investigations have been targeted to address the fault hazards.

However, notwithstanding the low level of assessed risk, the potential ground damage effects associated to a seismic event on the Moonshine Fault have been broadly considered to ensure a resilient design is maintained. The siting of the interchange structures should avoid the mapped fault rupture zone.

4 CONCLUSIONS

The existing State Highway network in the Wellington region has poor resilience in the event of a large earthquake event and the need to enhance this resilience is of critical importance to the region. The proposed Petone to Grenada link road provides an opportunity to offer a viable connection between Porirua, Northern Wellington and the Hutt Valley. This alternative route will compensate for one of the significant deficiencies in the current network; the likelihood that access into the Hutt Valley will be cut off for months, whereas the new route is likely to be able to be opened in days to 2 weeks after a large earthquake. To achieve this level of resilience for the route, it must be designed to reduce the impact of hazards associated with a large earthquake event so that it can be quickly recovered to an accessible state.

The earthquake hazards that are likely to most severely impact the route are fault rupture associated with the Wellington Fault, liquefaction in the Petone area and earthquake induced slope instability along the Wellington Fault scarp and the cut slopes. The influence of the Wellington Fault is of critical importance to the resilience of the link road. The fault represents a significant earthquake hazard and given the close proximity of the route, particularly to the Petone interchange and the adjacent cut slopes, the likely high level of ground shaking induced from such an event will intensify the amount of ground damage sustained.

The geotechnical investigations described in this paper were invaluable in selecting a suitable alignment for the project avoiding areas of major hazard such as historical slope failure sites, the Wellington Fault scarp along the Wellington harbour foreshore and the Wellington Fault strand in Petone. The investigations enabled preliminary design of the proposed major cut slopes and embankments and provide input for consideration of interchange structures. It is noted that given the nature of the project and the uncertainties a staged investigation programme was adopted and further

detailed investigations are ongoing to inform scheme assessment and assessment of environmental effects at the time of presentation of this paper.

A key lesson of this project is the importance of identifying hazards at an early stage, and to plan and implement a staged programme of geotechnical investigations that can provide an appropriate level of information at each stage as the project progresses.

5 ACKNOWLEDGEMENTS

We gratefully acknowledge the permission of the New Zealand Transport Agency to publish this paper, and thank Doug Mason for his valued contribution.

REFERENCES

Begg, J.G., Langridge, R., Van Dissen, R.J. and Little, T.A. (2008). "Wellington Fault: Neotectonics and earthquake geology of the Wellington-Hutt Valley segment. Field Trip 1", *GeoSciences '08 Field Trip Guides*, pp. 5-66. Geoscience Society of New Zealand.

Brabhaharan, P., Hancox, G., Perrin, N. And Dellow, G. (1994). *Earthquake Induced Slope Failure Hazard Study, Wellington Region. Study areas for Wellington City, Hutt Valley, Porirua and Kapiti*.

Brabhaharan, P. and Mason, D. (2012). *Wellington Region Road Netowrk Earthquake Resilience Study*. Report prepared by Opus International Consultants for Upper Hutt City Council, Porirua City Council, Kapiti Coast District Council, Hutt City Council, Wellington City Council and the New Zealand Transport Agency.

Institute of Geological and Nuclear Sciences (1996). *Geology of the Wellington area, 1:50,000 scale*, Geological Map 22, Institute of Geological & Nuclear Sciences, Lower Hutt, New Zealand, compiled by Begg, J.G. and Mazengarb, C.

Institute of Geological and Nuclear Sciences (2000). *Geology of the Wellington area, 1:250,000 scale*, Geological Map 10, Institute of Geological and Nuclear Sciences, Lower Hutt, New Zealand, compiled by Begg, J.G and Johnston, M.R.

Little, T.A.; Van Dissen, R.J.; Rieser, U.; Smith, E.G.C. and Langridge, R.M. (2010). "Coseismic strike slip at a point during the last four earthquakes on the Wellington Fault near Wellington, New Zealand", *Journal of Geophysical Research: Solid Earth*, 115 (B05403), doi:10.1029/2009JB006589.

Stirling, M., McVerry, G., Gerstenberger, M., Litchfield, N., Van Dissen, R., Berryman, K., Barnes, P., Wallace, L., Villamor, P., Langridge, R., Lamarche, G., Nodder, S., Reyners, M., Bradley, B., Rhoades, D., Smith, W., Nicol, A., Pettinga, J., Clark, K. and Jacobs, K. (2012). "National seismic hazard model for New Zealand: 2010 update", *Bulletin of the Seismological Society of America*, 102(4), pp. 1514-1542.

Wellington Regional Council (1991). *Major active faults of the Wellington Region map series: Sheet 1 Wellington Fault*, 1:20,000 scale, compiled by McMenamin, A. R. And Kingsbury, P.A.

Wellington Regional Council (1993). *Seismic hazard map series: Liquefaction hazard map sheet 3 Hutt Valley,* (first edition), 1:75,000 scale, Wellington Regional Council Publication WRC/PP-T- 93/74, Compiled by Kingsbury, P.A., and Hastie, W.J.

Proceedings of the 11th ANZ Young Geotechnical Professionals Conference – 11YGPC
Queenstown, New Zealand
25 – 28 October 2016

Counterfort Drain Performance in the Auckland Area

S. M. Torvelainen[1], GIPENZ, NZGS

[1]Riley Consultants Ltd, P.O. Box 100253 North Shore, Auckland 0745; PH (09) 489 787; email storvelainen@riley.co.nz

ABSTRACT

Counterfort drains are a method of lowering groundwater levels in soils and subsequently reducing pore water pressures on possible failure planes that can induce slope instability. This paper discusses the typical detail of counterfort drains employed and whether counterfort drains continue to be effective in reducing groundwater levels as has been demonstrated in Fitch (1990). Maintenance issues, monitoring and performance over time is outlined. Up to date costs of construction of counterfort drains are also given. The appropriateness of counterfort drain use in different types of Auckland Region Northland Allochthon geology is investigated. Counterfort drains are shown to generally have a demonstrable effect on groundwater levels. Their effectiveness is dependent on site specific geology rather than the overall geological unit present. Provided site specific factors are fully considered they can routinely be considered as a slope stability improvement option in the Auckland region.

Keywords: counterfort drain, buttress drain, trench drain, groundwater, slope stability, piezometers.

1 INTRODUCTION

Counterfort drains, also known as trench or buttress drains, are a method of lowering groundwater levels in soils and subsequently reducing pore water pressures on possible failure planes related to slope instability and thus improves the effective shear strength along such a plane. Counterfort drains have been used in New Zealand for a number of years, however, little analysis of their performance in recent projects along with their performance over time has been presented. Performance over time is important as generally counterfort drains are constructed to increase a slope's stability (quantified by a Factor of Safety (FOS)) to a sufficient level for a council to permit land development. The majority of structures and infrastructure in land development is intended to have a 50 or 100 year design life and therefore the stability of the land should also be assessed for this time.

2 TYPICAL DETAIL

The typical detail of a counterfort drain, as specified by Riley Consultants Ltd (RILEY), has had very limited changes made to it over the last 25 years. Figure 1 shows the typical cross section through a counterfort drain as specified by RILEY currently.

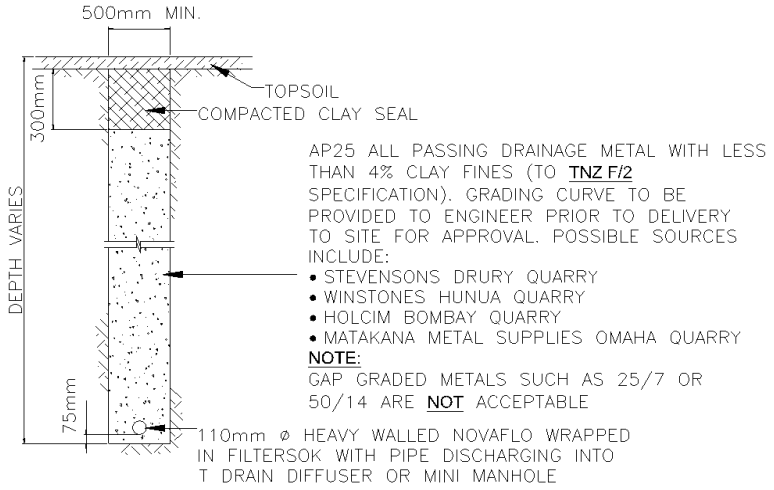


Figure 1. Typical Counterfort Drain Detail 2016 (RILEY)

The main changes to the RILEY counterfort drain detail over time as compared to Fitch (1990) are that the 110mm diameter "Novaflo" (perforated plastic pipe) is specified as heavy wall and, although the filter material is similar in composition the scoria specification is no longer used. Instead a general all passing material to Transit New Zealand F2 specification is stipulated. The appropriate scoria material typically was sourced from Three Kings Quarry in Auckland. However, the output of this material from the quarry (in particular low fines content) has now ceased as the quarry is economically at the end of its life. It is important that the grading curve of the filter material is specified by the engineer and that of the acquired material is checked before the material is delivered to site. The criticality of the low fines content is often not understood by the contractor. From some quarries a blended material or a builder's mix can produce a material similar to the F2 grading envelope.

3 THEORY AND DESIGN

A counterfort drains system's ability to reduce groundwater levels from both normal seasonal levels and storm related spikes is dependent on their depth and spacing (Cornforth, 2005). Cornforth (2005) states that theoretical research by Hutchinson (1977), Stanic (1984) and Bromhead (1986) to determine the required spacing to attain a certain drawdown is based on a number of assumptions: the infinite slope model applies, the landslide mass is homogeneous and isotropic (Bromhead's method allows some anisotropy in permeability). To encounter such conditions in the field is unlikely.

The three authors' drain spacing-depth-drawdown relationships are not dependent on landslide mass permeability coefficients with Stanic (1984) summarising that the recommended drain spacing is short enough in a trench drain system that the drainage path is of a length that allows consolidation to occur very quickly and thus pore pressure change with time to not been considered. Therefore, Stanic has not included the coefficient of permeability is the derived relationship. A notable recommendation by Stanic (1984) is that the ratio of spacing between drains relative to their depth below the original groundwater level should not be more than 4:1 as experience has indicated that sliding can occur within the landslide mass between the drains when the ratio is exceeded.

4 SPACING AND DEPTHS

Local authorities have become less stringent in recent years regarding stipulating that monitoring of groundwater must occur post counterfort drain construction. Therefore, there are limited case studies within the RILEY job records to undertake a thorough review of recent performance of the drain spacing and depths required for particular levels of groundwater drawdown in Waitemata Group soils as detailed in Fitch (1990).

Review of a counterfort drain system designed by RILEY on land at 67 to 73 and 77 to 81 West Hoe Heights Road, Orewa (Figure 2) known as West Hoe Homes (WHH) site for which an extensive period (over 15 years) of groundwater monitoring has occurred post drain construction provides insight into how counterfort drains in the wider Auckland area perform, beyond Waitemata Group geology, and allows assessment of performance over time. The WHH site is located near the east coast in the northern Auckland Council area (formerly known as Rodney District). The Rodney District has areas underlain by Northland Allochthon (historically known as Onerahi Chaos Breccia). Toan (1980), on behalf of Beca, Carter, Hollings and Ferner, provided a summary of Northland Allochthon/ Onerahi Chaos Breccia. Toan outlines that the Northland Allochthon is irregularly bedded rocks found both below and above Waitemata Group material. Toan explains that there is often a cohesive, low permeability skin of residual mudstone or siltstone in the allochthon, particularly on gentle slopes and ridges. This is different to Waitemata Group residual clays; Fitch (1990) outlines will often have major seepage path in vertical shrinkage cracks or soil creep may also open tension cracks across the slope which have high permeability's.

The 1:50,000 New Zealand Geological Survey's Geological Map shows Post Miocene Chaos Breccia underlying the WHH site. Typically this is comprised of displaced blocks of Miocene Flysch (interbedded sandstone and siltstone of the Pakiri Formation). Investigation at the WHH site in 1980 identified a sequence of deeply weathered sandstones and siltstones apparently dipping at about 10º in an easterly direction. The site was subject to instability in 1979 following earthworks in 1977 and 1978 near the toe of the slope. Heavy rainfall in 1998 triggered a secondary slip and reactivated the original instability. Post the 1998 movement groundwater monitoring was installed and approximately two years later a system of counterfort drains was constructed along with new standpipe piezometers.

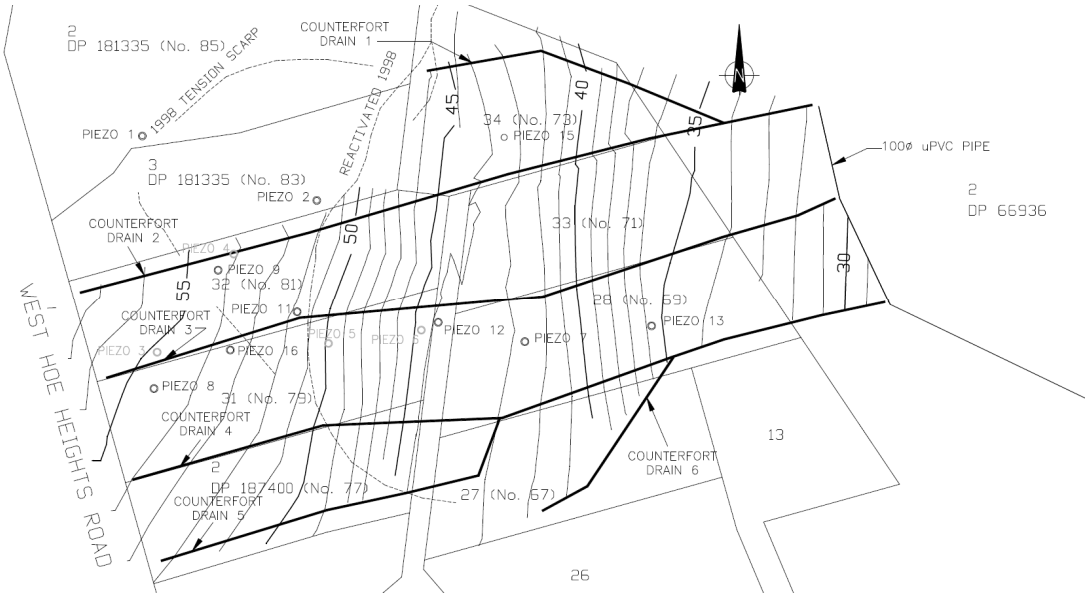


Figure 2. West Hoe Homes Site Plan

Table 1 list the counterfort drain sets at the WHH site along with their depths and spacing's. Table 2 indicates the average (over the record length) groundwater depths in standpipe piezometers (with response zones across their full depth) at WHH three drainage sets. Table 3 outlines the approximation of groundwater level for selected counterfort drain depths and spacing's calculated by Fitch (1990) based on number of case studies.

Table 1. West Hoe Homes, Orewa Counterfort Drain Performance

Drain Set	Depth (m)	Spacing (m)	Spacing/Depth
2 to 3	5	16	3.2
3 to 4	5	19	3.8
4 to 5	5	15	3.0
4,5 & 6 Lower to 3 Lower	4	18	4.5
3 Lower to 2 Lower	4	21	5.3
1 Lower to 2 Lower	4	20	5.0

Table 2. West Hoe Homes, Orewa Counterfort Drain Performance

Drain Set	Groundwater Depth Prior to drain installation (m)	Depth to groundwater with drains installed (m)	Groundwater Drawdown [a] (m)
2 to 3	1.24 (P3), 1.60 (P4)	2.86 (P11[b]), 3.32 (P9[b]),	1.7
3 to 4	0.82 (P5), 0.91 (P6)	3.65 (P8[b]), 2.56 (P12s[bc])	2.2
4,5 & 6 to 3 Lower	2.09 (P7)	2.03 (P7), 2.25 (P13s[g]), 1.84 (P14s)	0.0

[a] Difference between average groundwater levels at piezometer location before & after drain construction between drain sets
[b] P8, P9, P11 and P12s are replacement piezometers for P5, P4, P3 and P6 respectively
[c] s = the shallow screen portion at the subject piezometer location

Table 3. Fitch (1990) Counterfort Drain Performance- Reasonable approximation

Drain Depth (m)	Drain Spacing (m)	Approximate Average Depth to Groundwater Level (m)
2	5	1.5
2	10	1.0
4	10	3.0
4	15	2.5
4	20	2.0
6	15	4.5
6	20	4.0

The WHH site results agree somewhat with the Fitch (1990) and the WHH case study for the depth to groundwater level achieved by certain drain spacing's and depth's is made if linear interpolation made

between the 4m and 6m drain depths in Table 3. However, given what is known about the geology at the WHH site and that the Fitch (1990) paper is focused on drains in Waitemata Group material this is assessed to be coincidental only.

5 MAINTENANCE

Counterfort drains, if designed and constructed appropriately, are considered as generally low to no maintenance items. However, there is little evidence published the author is aware of to substantiate this. Maintenance of counterfort drain typically involves ensuring that outlets are kept clear and that flushing is undertaken at regular intervals. In general maintenance is not something that is regularly undertaken, as counterfort drains are often constructed at subdivisional stage and the lots sold soon after, with dwelling construction then following within months to a year. Thus it is assumed that the drainage is working adequately as it has typically had testing undertaken that has allowed the subdivision to be approved. Once the drains are built there is often no statutory requirement to maintain them and the lot owner is unlikely to understand the importance of the drainage to the stability of their site. Flushing of the drains via ports can occur every 5 years. There should be no sediment emanating from the drains. The effort required in flushing a counterfort drain will be dependent on whether a flushing port has been installed and whether it is easily locatable along with ability to access water for flushing.

Maintenance is often embarked on when there is redevelopment occurring on the site or the site has remained undeveloped since subdivisional stage. To gain building consent for the proposed structure(s) a geotechnical report is then required to satisfy that the stability of the site meets the required FOS (typically 1.5 for residential development). Analysing the stability of the site requires comprehension of the groundwater regime and this can be assessed by installing piezometers. If the piezometers do not show favourable groundwater levels in line with the counterfort drains performing as expected then flushing of the counterfort drains may be undertaken. The outlets would also be located, cleared of any obstructions, flow rates assessed and any remediation to ensure scouring does not occur performed so that possible de-stabilising effects such as loss of toe support do not transpire. Monitoring well maintenance issues are discussed in the following section.

6 MONITORING

As previously mentioned, its is occasionally a requirement of the local authority or a recommendation of the design engineer or peer reviewer that monitoring of groundwater levels occur post counterfort drain construction, so as to demonstrate adequate performance. Standpipes installed in boreholes allow for monitoring. The monitoring is undertaken by a range of methods depending on budget, site location and monitoring period. The most common option is to manually visit the site and use a dip meter to record the groundwater level at the time of the visit. Alternatively installation of a system of custom made devices that allow ground water level rises during extreme precipitation events between technician visits' to be captured and recorded later on a technician returns. In remote locations or large budget projects, electronic water level data loggers are installed in the piezometers to provide measurements at consistent, prescribed intervals and which can be downloaded onsite or with more sophisticated equipment transferred via wireless and internet connections.

There are a number of issues with monitoring groundwater level in piezometers that make review of the performance of counterfort drains difficult. Protection of the standpipe is often difficult as vandalism from trespassers on vacant lots can occur and destruction from mowers or vehicles is regularly a problem. Piezometers can become blocked which may necessitate new piezometers being installed. With regard to manual monitoring by dipping at the site in an extreme rainfall event it can be too dangerous to access the site at the time and therefore groundwater peaks may be missed. The more sophisticated methods of manual measurement such as customised manual devices to capture extreme events are time consuming to make. Furthermore electronic data loggers are expensive and if they do not have remote monitoring there is no way to know whether adequate data has been recorded until a visit to the site is undertaken, often after the event in question. In addition, due to their cost, often electronic monitoring cannot be left in the ground for long periods of time, although with cost reductions this is becoming more economic. A secondary issue besides the measurement technique for the water level in the piezometer is that using standpipes without selective response zones can give inaccurate reading of the true hydrostatic pressures at the critical depth as the standpipe will potentially intercept or penetrate through perched groundwater tables. WHH case study

is an example of the perched groundwater phenomenon influencing modelling and is reviewed in the next section.

7 PERFORMANCE

The performance of counterfort drains is often critical to maintaining the required margin against instability. The WHH site provides invaluable data on long term counterfort performance and performance in Northern Allochthon material due to the period of groundwater monitoring that has occurred.

7.1 Background and Initial Performance

Groundwater levels were first monitored at the WHH site after instability occurred following a heavy rainfall event in 1998 when groundwater was inferred to be close to ground surface as outlined in Section 4. Two piezometers (P1 and P2) were installed on the neighbouring adjoined properties at 83 and 85 West Hoe Heights in 1999 concurrent with installation of counterfort drains within the properties. These piezometers have been monitored since July 1999. Five piezometers (P3 to P7) were installed on the WHH site in July 1999 with monitoring commencing in August 1999. All groundwater levels have been manually dipped. After a period of six months the groundwater levels were reviewed and it was shown that groundwater levels on WHH land were on average 1.8m below the ground surface and the water level was 1.0m to 1.5m higher than at 83 and 85 West Hoe Heights Road. Furthermore certain piezometers on the WHH site showed rapid response to rainfall and this was inferred to be a result of these piezometers intercepting a permeable sand horizon between approximately 3.9 and 5.0m encountered in the boreholes before standpipe installation. The back analysis of the 1979 and 1998 failures assessed that depth of failure plane were between 6-7m and around 5m respectively. Soft soils in general were found between 3m to 5m depth. Draining the permeable sand horizon(s) was considered essential to improving stability of the site.

To improve site stability counterfort drains were installed on the site with layout and characteristics outlined shown in Figure 2 and Table 1 respectively. The groundwater levels in Table 3 indicate that the counterfort drains had a demonstrable effect on groundwater levels. Stability review of the slope from the groundwater levels recorded post construction to early 2003 indicated that under extreme levels the FOS of the slope was 1.30. Although the counterfort drainage system was primarily installed for land stabilisation purposes future development for residential dwellings was being considered. For this it would be necessary to prove that a FOS of 1.50 for the site had been attained. To clarify whether perched groundwater was potentially giving an exaggerated result of the hydrostatic pressure at failure plane level it was recommended that multiport piezometers be installed. Confirmation of such a phenomenon would indicate that the FOS in the land was higher than had been modelled under observed extreme groundwater.

7.2 Multiport Piezometers and Extended Performance

Four multiport piezometers were installed at the site; two in May 2003 (P12 and P13) and two in April 2004 (P14 and P15). Each piezometer had an upper screen from ground level to approximately 3.5 – 4.0m depth and a lower screen from below the depth of the shallow piezometer to the base of the drilled boreholes which were 6m deep. Figure 3 shows results from multiport piezometer 12 (over time period where both shallow and deep parts of the piezometers remained operational) clearly show that a downward groundwater gradient does exist at the site and hydrostatic pressure at the inferred failure surface level is less than indicated by a standpipe piezometer without a targeted response zone and may reflect a separate aquifer, a downward gradient in flow or a combination of both.

A selection of deep screen piezometers currently still in operation on site is shown in Figure 4 to assess the performance of counterfort drains on hydrostatic pressure at the depth of the inferred failure surface. No obvious trend is shown in these groundwater levels from when monitoring commenced that would indicate that the groundwater levels have risen over time. There does however appear to be some increased activity with P15/1 Deep and P16 over 2013 and winter spring 2014. However, peak groundwater levels for these piezometers coincided with their lowest recorded levels in the same period. For this period the rainfall does not follow any atypical trend. Observations on site, such as of concrete driveways and kerbings do not indicate any ground movement, however, an up to date survey of monitoring points has not recently been undertaken.

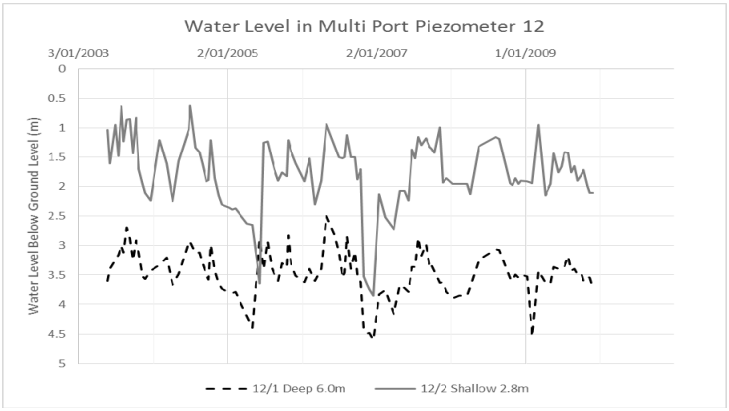


Figure 3. Multi Port Piezometer Performance

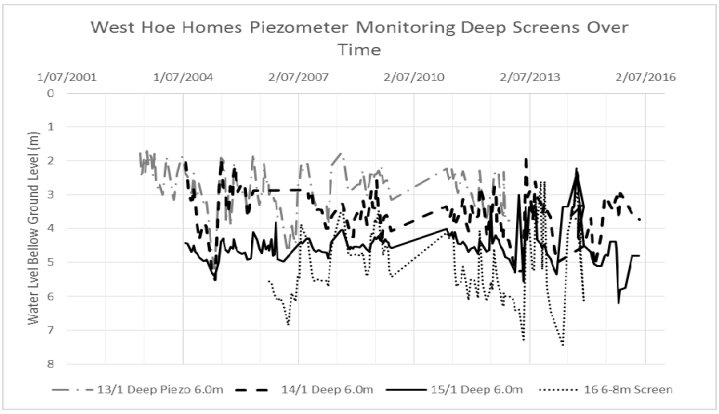


Figure 4. Ground water levels of deep screen piezometers over time

8 CONSTRUCTION COSTS

Recent (2014) costs for counterfort drain construction in Auckland is outlined in Table 4.

Table 4. Counterfort drain construction costs from 2014

Drain depth (m)	Cost (NZD)/m length of drain
0-3m	$270
Up to 5m	$480
5m to 6m depth	$780

9 CONCLUSION

Counterfort drains are shown to generally have a demonstrable effect on groundwater levels. Their effectiveness is dependent on site specific geology rather than the overall geological unit present. Understanding the response zone in a piezometer is necessary. Provided site specific factors are fully considered they can routinely be considered as a slope stability improvement option in Auckland.

10 ACKNOWLEDGEMENTS

I would like to thank the staff at Riley Consultants Ltd for their guidance in writing this paper.

REFERENCES

Cornforth, D.H. (2005). *Landslides in Practice – Investigation, Analysis and Remedial/Preventative Options in Soils*

Fitch, N. R. (1990). "Ground Stabilisation with Counterfort Drains – Design, Installation and Monitoring of Drawdown Performance", *Proceedings NZ Geomechanics Society*, 16 1(G), pp. 97 -101.

Hutchison, J .N. (1977). "Assessment of Corrective Measures in Relation to Geological Conditions and Types of Slope Movement", *Bulletin of the International Association of Engineering Geology*, No. 16, pp. 131-155

Stanic, B. (1984). "Influence of Drainage Trenches on Slope Stability", *Journal of Geotechnical Engineering*, 110 (11), pp. 1624-1636

Taon, D.V. (1980). *Report on Onerahi Chaos Breccia for Rodney County Council*, Beca Carter Hollings and Ferner Ltd Report No 130149/3

Proceedings of the 11th ANZ Young Geotechnical Professionals Conference – 11YGPC
Queenstown, New Zealand
25 – 28 October 2016

Geotechnical issues in seismic assessments: When do I need a geotechnical specialist?

B. H. Rama[1], GIPENZ and S. J. Palmer[2]

[1]Tonkin & Taylor Ltd, Level 4, ASB Tower, 2 Hunter St. Wellington, New Zealand; PH (04) 381-8560; email: BRama@tonkintaylor.co.nz
[2]Tonkin & Taylor Ltd, Level 4, ASB Tower, 2 Hunter St. Wellington, New Zealand; PH (04) 381-8560; email: SPalmer@tonkintaylor.co.nz

ABSTRACT

The Canterbury Earthquakes Royal Commission recognised the need for greater focus on geotechnical investigations and assessment as part of engineering projects. The current revision of the New Zealand Society for Earthquake Engineering's (NZSEE) guidelines document "Assessment and Improvement of the Structural Performance of Buildings in Earthquakes" June 2006 (Red Book) has no specific guidance for consideration of geotechnical aspects as part of a detailed seismic assessment and mitigation design for an existing building. NZSEE and the Ministry of Business, Innovation and Employment (MBIE) have addressed this by adding a chapter on geotechnical assessment. That geotechnical chapter (C4) is in draft and will be formally released in early 2017. In parallel to Chapter C4, the New Zealand Geotechnical Society (NZGS) and MBIE are developing guidelines to help summarise current practice in earthquake geotechnical engineering. These documents provide guidance on geotechnical input, but only provide limited guidance on the question of when to get a geotechnical specialist involved. This paper highlights issues in building assessment and design which can arise if geotechnical issues are not adequately considered. These include; variability of ground conditions, "brittle" behaviour of some foundation types, changes in soil-foundation performance under cyclic loading, and soil-foundation-structure interaction.

Keywords: geotechnical, earthquake, seismic assessment, strengthening, soil-foundation-structure

1 INTRODUCTION

The Canterbury Earthquakes Royal Commission recognised the need for greater focus on geotechnical investigations and assessment as part of engineering projects.

The current revision of the New Zealand Society for Earthquake Engineering's (NZSEE) guidelines document "Assessment and Improvement of the Structural Performance of Buildings in Earthquakes" June 2006 (Red Book) has no specific guidance for consideration of geotechnical aspects as part of a detailed seismic assessment and mitigation design for an existing building, except with regards to seismic subsoil soil class. NZSEE and the Ministry of Business, Innovation and Employment (MBIE) have addressed this by adding a chapter on geotechnical assessment. That geotechnical chapter (Chapter C4) is in draft and will be formally released in early 2017 (NZSEE 2016).

In parallel to Chapter C4, the New Zealand Geotechnical Society (NZGS) and MBIE are developing guidelines to help summarise current practice in earthquake geotechnical engineering with a focus on New Zealand conditions, regulatory framework, and practice to promote consistency and improve geotechnical earthquake aspects of the performance of the built environment. These guidelines have been split into modules and are briefly described below (text based on, and abbreviated from MBIE & NZGS 2016). Modules 1, 3 and 5A are publicly available, the remainder are in production.

- *Module 1:* Overview of the guidelines: Provides an introduction and outlines the objectives of the guidelines. Includes procedure for estimating ground motion parameters for earthquake geotechnical engineering.

- *Module 2:* Geotechnical investigation for earthquake engineering: Explains the importance of developing a geotechnical model; provides guidance on planning a site investigation; describes the advantages and disadvantages of various investigation techniques; provides guidance on the preparation and considerations for geotechnical factual, interpretive, design

and construction observation reports; recommends appropriate densities of investigation and sampling for sites; and discusses common problems encountered during investigations works.

- *Module 3:* Identification, assessment, and mitigation of liquefaction hazards: Describes liquefaction phenomena; provides guidance on identification of liquefaction hazards; discusses methodologies for assessing the risk of liquefaction triggering including a 'simplified procedure' appropriate for everyday engineering situations; discusses liquefaction induced ground deformation and procedures for assessment; discusses residual strength of liquefied soils and the effect on structures; and provides an overview of how the effects of liquefaction could be mitigated.

- *Module 4:* Earthquake resistant foundation design: Discusses building code foundation performance requirements during earthquakes; common foundation types and strategies for selection; issues affecting shallow foundation performance and appropriate design procedures; issues affecting earthquake performance, and advantages and disadvantages of various deep foundation types; and analysis and design requirements for deep foundations with earthquake loading.

- *Module 5:* Ground improvement: Considers ground improvement techniques to mitigate the effects of liquefaction, cyclic softening, lateral spreading and the partial loss of soil strength through increases in pore water pressure during earthquakes; provides guidance on the need for and extent of ground improvement required; discusses various ground improvement techniques including advantages, disadvantages and relative cost; provides design guidance for each technique; and discusses construction and verification considerations.

- *Module 5A:* Specification of ground improvement for residential properties in the Canterbury region: Provides guidance on specification requirements for selected improvement techniques for small scale works (single residential) along with preliminary and general, testing and earthworks specifications.

- *Module 6:* Retaining walls: Considers earthquake considerations for design of retaining walls.

Modules 1 to 6 provide guidance on geotechnical investigation, assessment and design, and Chapter C4 (draft) provides guidance on geotechnical input required in a seismic assessment; however only limited guidance is provided on when to get a geotechnical specialist involved in a project. Section 2 of this paper outlines scenarios which would trigger the need to engage a geotechnical specialist, Section 3 provides guidance on what should be considered in determining the level of geotechnical input that is required, and Section 4 outlines common geotechnical issues (traps) in seismic assessments and mitigation designs which geotechnical input could mitigate.

2 TRIGGER SCENARIOS FOR ENGAGING A GEOTECHNICAL SPECIALIST

There is limited guidance available on when to get a geotechnical specialist involved in a project. Although not an exhaustive list, the scenarios outlined below provides some guidance on when it would be prudent to engage a geotechnical specialist.

- Projects that have complex engineering geological considerations, and projects that have complex interaction between the structure and soils. These are discussed further in the following bullet points.

- Those undertaking the assessment:
    - do not have geotechnical skills and experience; or
    - are not experienced in the local geology and geohazards relating to that geology; or
    - are not experienced in the particular geotechnical issues relating to the site, e.g. local weak areas of soil.
    - do not have available geotechnical data relating to the site, or ground conditions could be variable.

- Geohazards are present which could materially impact on the performance of the building or the assessor is not skilled in identifying these hazards:
    - Vertical and lateral load-deformation behaviour (capacity and stiffness) of foundations[(a)]
    - Shaking hazard (seismic subsoil class not definitive)[(a)]
    - Liquefaction[(a)]
    - Lateral spread[(a)]
    - Retaining wall instability: Underslip[(a)] and overslip[(b)]
    - Slope stability: Underslip[(a)] and overslip[(b)]
    - Rockfall[(b)]
    - Fault rapture[(a)]
    - Inundation: Tsunami, dam break and tectonic lowering[(a)]

    Footnote: Based on current interpretation of the Building Act:
    [a] May be material to %NBS (New building standard)
    [b] To be reported but not material to %NBS.

- Foundation loads could exceed the dependable (reduced) bearing capacity (ϕR), i.e. load and resistance factored design (LRFD) requirements may not be met, and performance of the soil-foundation-structure beyond this limit (>ϕR) needs to be considered.

- The structure has a relatively low tolerance to foundation movements.

- Retaining structures are integral in the structure and the structure has a relatively low tolerance to movement of these walls; or loads imposed by these walls could be critical to the structure.

- If the benefits of the flexibility of the foundation soils are to be considered in assessing the structure's natural period, i.e. if anything other than rigid base is to be considered in assessing the building's period.

- Geotechnical conditions or soil-foundation-structure interaction could dominate the assessment of the building.

- New or modification to foundation elements required as part of the mitigation works. The integration of new elements and compatibility of these with existing is to be considered and understood. A critical issue is the relative stiffness of foundation elements and consequently the distribution of load.

3 COLLABORATION BETWEEN STRUCTURAL ENGINEER AND GEOTECHNICAL SPECIALIST: WHAT LEVEL OF GEOTECHNICAL INPUT IS REQUIRED?

It is recommended that the structural engineer and a geotechnical specialist have a review session early in each project to determine if further geotechnical input is required, i.e. if ground compliance and / or geohazards could have a significant impact on the assessment. If further geotechnical input is required, and once the ground model has been developed and geotechnical issues have been identified, the structural engineer and geotechnical specialist should meet again to explore the significance of these geotechnical issues (NZSEE 2016). The meeting should explore what further geotechnical and structural assessment and analysis is required considering the following (summarising information from NZSEE 2016):

- For each identified geotechnical issue, what is the likely impact of that issue on the building's seismic performance?

- Which issues could impact on the buildings % NBS?

- For those geotechnical issues which could be critical to the buildings % NBS what further geotechnical and structural analysis and assessment is required?

- What geotechnical parameters are to be provided to the structural engineer and in what form?

- Which of the following categories describes the %NBS assessment of the building (terminology taken from draft geotechnical chapter C4):
    - *Structure Dominated:* Foundations which can be relied on and unlikely to limit the seismic performance of the building.
    - *Interaction:* Possible displacement of the foundations could limit seismic performance of the building. Soil-foundation-structure-interaction is significant.
    - *Geotechnical Dominated:* A step change in the performance of the foundations limits the performance of the building.

- What is the cost / benefit of geotechnical investigations, and at what stage of the process should they be carried out.

It would be prudent to involve the client in the meeting (or a separate meeting) so that the needs and drivers for the client with respect to %NBS of the building can be understood (or discuss and agree with the structural engineer how communication with the client will happen and be disseminated).

A number of meetings with the structural engineer (and client) are likely to be required through the iterative process of the assessment.

4 COMMON GEOTECHNICAL ISSUES (TRAPS) IN SEISMIC ASSESSMENTS AND MITIGATION DESIGNS

Common traps which can be mitigated with specialist geotechnical input are briefly discussed below.

- Engineering geology skills in development of a ground model are essential. This includes consideration of land forms, geological processes, site history and geotechnical investigation data, to determine the likely site conditions and produce a ground model. Common examples of misunderstood or unforeseen ground conditions include:
    - Geological materials such as alluvium can be highly variable, both with depth and in plan. Soft silt beds and loose sand layers can exist even within thick layers of dense sand or gravel. Historic meandering rivers and streams could have been present and infilled flow channels with soft silt within a dense soil layer.
    - Unidentified infilled gulleys on a competent soil or rock surface can result in competent founding conditions being assumed when actual conditions are locally weak soil.
    - Basalt flows can be variable in extent and thickness requiring careful consideration if relied on as a founding layer.
    - In areas around faults, weak layers or fault gouge within the rock mass (being the product of tectonic shearing and/or weathering) can be present in a rock profile. These layers can have the strength of a soil, substantially reducing the capacity of foundations bearing above them.
    - Historic earthworks can modify a soil profile such that fills are present when competent natural ground is expected. Weak soil layers buried under engineered fill can also be present.
    - End bearing piles with a soft silt bed or liquefiable sand below the base can result in piles punching through and large differential displacements in the supported structure.
    - Highly sensitive soils such as Ash can have high in-situ strength but generally reduce to residual strength when reworked (e.g. during earthworks, augering for piles or under seismic loading). Design of foundations assuming peak strength values in this material can be catastrophic. These soils are subject to a step change in behaviour leading to possible poor seismic resilience.

  - Basalt and limestone can include voids making them problematic in construction of grouted anchors or piles.
  - Within alluvial soils or in terrains of historic slope movement, weak soil layers may exist allowing slope failures on relatively low slope angles in the event of seismic shaking.
  - Unfavourably oriented defects may exist in rock allowing wedge or planar failures of slopes under relatively low seismic shaking.

- Seismic subsoil class can be assessed incorrectly.
  - Published geological maps with depths to rock are available for some centres and provide a useful starting point for subsoil class assessment. It should be noted that these maps are prepared on a global scale and cannot be relied upon solely for a site specific assessment. For a site specific assessment, maps need to be used in conjunction with geological interpretation, historic investigations, prior experience at nearby sites, and if necessary physical site specific investigations. Where no site specific investigation is carried out, there should be confidence that the local geology is consistent and unlikely to vary.

- Geo-hazards such as cyclic softening or liquefaction are not identified. Presence of these hazards can result in:
  - Loss of support below shallow and pile foundations.
  - Loss of shaft / skin friction in piles or anchors.
  - Lateral loading on piles from cyclic displacement (ground lurch) or lateral spread.
  - Negative skin friction loading on piles.
  - Post-earthquake settlement.

- Unfavourable behaviour of foundations under cyclic loading.
  - Shaft resistance of piles and anchors can be significantly reduced when subject to cyclic loading.

- Anchors / micropiles are often used to supplement existing foundations and resist uplift loads from new bracing elements. Common issues around the use of these are listed below:
  - Where there has not been an appropriate ground model developed or geo-hazard assessment carried out, it is possible that these anchors could be constructed within liquefiable soils. Anchors may test up to required loads when constructed, however in a seismic event inducing liquefaction, grout to country bond strength can be significantly reduced and anchors may fail at a fraction of the design load.
  - Stiffness compatibility between existing foundations and new anchors should be considered. Anchors may be stiffer than existing foundations thus attract load in compression until they fail.
  - Reverse cyclic loading can result in substantially lower anchor / micropile capacity than that assessed by static load testing.
  - High strain and grout to country bond yielding in upper sections of bond length can occur, i.e. strain degradation of bond. A 10m bond length is unlikely to provide double the capacity of a 5m bond length. Bond lengths of greater than 10m are generally not recommended.
  - A poorly detailed or constructed test anchor can provide non-conservative and misleading results.
  - The capacity of an anchor / micropile determined by testing is dependent on the loading sequence and acceptance criteria applied. For this reason codes and guidelines specify these and should be followed.

5 CONCLUSIONS

- The Canterbury Earthquakes Royal Commission recognised the need for greater focus on geotechnical investigations and assessment as part of engineering projects.

- MBIE, NZSEE, and NZGS are addressing this by publishing guidelines (Modules 1 to 6) for earthquake geotechnical practice in New Zealand and adding a chapter on geotechnical assessment (Chapter C4) to the Red Book. Modules 1 to 6 provide guidance on geotechnical investigation, assessment and design, and Chapter C4 provides guidance on geotechnical assessment of existing buildings; however only limited guidance is provided on the question of when to get a geotechnical specialist involved.

- Section 2 of this paper outlines scenarios which would trigger the need to engage a geotechnical specialist, Section 3 provides guidance on what should be considered in determining the level of geotechnical input that is required, and Section 4 outlines common traps in seismic assessments and mitigation designs for which specialist geotechnical input could mitigate.

- It is recommended that the structural engineer and a geotechnical specialist have a review session early in each project to determine the scope of geotechnical input required, i.e. if ground compliance and/or geohazards could have a significant impact on the assessment.

6 REFERENCES

Ministry of Business Innovation and Emplyment (MBIE) and New Zeland Geotechnical Society (NZGS) (2016). *Earthquake geotechnical engineering practice, Module 1: Overview of the guidelines*

New Zealand Society for Earthquake Engineering (NZSEE) (2006). *Assessment and Improvement of the Structural Performance of Buildings in Earthquakes*

New Zealand Society for Earthquake Engineering (NZSEE) (2016). *The Seismic Assessment of Existing Buildings, Technical Guidance for Engineering Assessments (Draft for Section Briefings) – Part C4 Geotechnical Considerations*

Proceedings of the 11th ANZ Young Geotechnical Professionals Conference – 11YGPC
Queenstown, New Zealand
25 – 28 October 2016

Design and construction of a commercial building on a closed municipal solid waste landfill in Takapuna, Auckland

Nicole Li[1], GIPENZ

[1]RILEY Consultants Ltd, PO Box 100253, North Shore, Auckland, New Zealand; Ph. +64-9-498-7872; Email nli@riley.co.nz

ABSTRACT

Ground engineering works on closed municipal solid waste landfills provide challenges beyond those related to construction on other brownfield sites within the urban environment. Design and construction of a multi-level commercial building on the closed Barrys Point landfill site in Auckland presented challenges for foundation design, durability, and mitigation of hazards (refuse, gas, and leachate) related to landfill material. Geotechnical inputs for the new building included deep-piled foundations and landfill gas protection measures. Engineering observation of construction for the gas protection measures was required to comply with stringent consent conditions. This paper describes challenges, during detailed design and construction of the new building, posed by the complex ground conditions on-site. The challenges included the development of pile installation methods that would not contribute to leachate migration, and construction of the passive landfill gas protection system. Permanent design features of the building includes deep-driven steel piles, and landfill gas mitigation measures entailing a specifically designed gas manifold system and a subfloor slab with high-density polyethylene (HDPE) geo-membrane to prevent ingress of landfill gas into the new building.

Keywords: solid waste landfill, construction, excavation, pile installation, leachate migration, landfill gas mitigation measures

1 INTRODUCTION

The four-storey commercial building (known as 3 Fred Thomas Drive), located inside the eastern margin of the former Barrys Point solid waste landfill in Takapuna, Auckland, is underlain by landfill material. The closed municipal Barrys Point landfill is managed by Auckland Council and authorised by a discharge permit held by the Council. Land development within the closed landfill site is relatively slow in comparison to its surrounding areas in the Takapuna suburb due to technical challenges and high expenses for construction on landfill. The location of the site is shown on Figure 1. The building has a ground floor footprint of approximately 1,350m^2, which consists of two specific areas (Areas 1 and 2). Area 1 (western half) includes a ground floor retail tenancy, whilst Area 2 (eastern half) is a parking area occupying the balance of the ground floor footprint.

Settlement of ground surrounding buildings has been observed on neighbouring properties, and ingress of high concentration landfill gas into the neighbouring structures (detected by landfill gas alarms installed) has historically been reported. The key objectives of the 3 Fred Thomas Drive development are to prevent damage to the building due to ground settlement and to eliminate landfill gas from leaking into the retail area.

Specific site investigations were undertaken in 2014 to define the site subsurface conditions for design of the deep pile foundations and the gas protection system. The investigations included geotechnical machine boreholes, environmental boreholes, and laboratory testing on soil and groundwater samples. Geotechnical challenges of this project involved the installation of driven steel H-piles to 30m depth on average, excavations of approximately 340m^3 into landfill material, and construction of a landfill gas mitigation system.

Construction of the new building was completed in April 2016. As part of the Auckland Council consent conditions, ongoing long term landfill gas monitoring is required to ensure there is no ingress of landfill gas to the retail area.



Figure 1. Location of the site (aerial photo sourced from Google Earth)

2 GEOLOGICAL SETTING

2.1 General Site Geology and Geomorphology

The geology of the site is Pleistocene materials (alluvial sediments) of the Puketoka Formation, overlying Waitemata sandstones and siltstone. The site and its surrounding area were used as a municipal solid waste landfill prior to the opening of the Auckland Harbour Bridge in 1959. Refuse landfill (depth various) was placed directly above the alluvial sediments. Limited information obtained from the Auckland Council closed landfill register indicated that a clay landfill cap may be in place.

The site is situated on the fringe of lava flows, which originated from the nearby Lake Pupuke. Highly compressible and soft Pleistocene age alluvial and estuarine muds and peats exist over the lava flows. During glacial periods of the Pleistocene epoch, sea level was considerably lower than present. The Shoal Bay stream, a tributary of the ancestral Waitemata River, initially cut down deeply into the underlying Waitemata Group. Pleistocene silts and peats were later deposited as valley fill, leaving alluvial terraces. The valley was flooded by the sea as it is today, during inter-glacial periods.

2.2 Subsurface Conditions

The subsurface conditions were confirmed by the specific field investigations. Refuse landfill was generally encountered to approximately 6.5m depth below existing ground surface. The clay landfill cap, to variable depths, was only encountered at some test locations, indicating the capping layer is not consistently placed across the site. Firm alluvial sediments of the Puketota Formation were identified beneath the landfill to approximately 30m depth, overlying alternating layers of completely to moderately weathered Waitemata sandstone and siltstone.

Laboratory testing was carried out for contamination on soil and groundwater samples recovered from the landfill layer. The high concentrations detected from the selected chemicals (i.e. sulphates, heavy metals, etc.) would pose severe corrosion on piles and risk to construction workers.

3 LANDFILL GAS HAZARD

Landfill gas alarms were previously triggered in the neighbouring properties due to ingress of landfill gas. In order to assess the landfill gas level within 3 Fred Thomas Drive, gas readings were recorded from the environmental boreholes on completion of drilling using a portable landfill gas analyser (GA5000). The gas readings indicated that the landfill refuse was still producing landfill gas. Landfill gas is considered a high level health and safety hazard. It could migrate into structures in numerous ways, including via minor cracks in the concrete slab and services. Accumulated landfill gas in a confined space may trigger an explosion or caused an asphyxiation hazard risk.

4 DESIGN PHILOSOPHY AND FEATURES

4.1 Pile Foundation and Installation Methodology

The landfill materials and firm alluvial sediments are compressible and have high settlement characteristics. Deep driven steel UC piles, founded within the Waitemata Group sandstones/siltstones, were adopted to prevent damage to the building due to ground settlement. Driven steel piles, in this instance, had the advantage that they could be constructed relatively quickly, significantly reducing drilling spoil from pile holes, and minimising cross contamination between the landfill layer and the natural ground. Main challenges encountered during development of the pile installation methodology included the collapse of the pile hole within the landfill layer, removal of the refuse obstructions during driving, and preventing leachate migration.

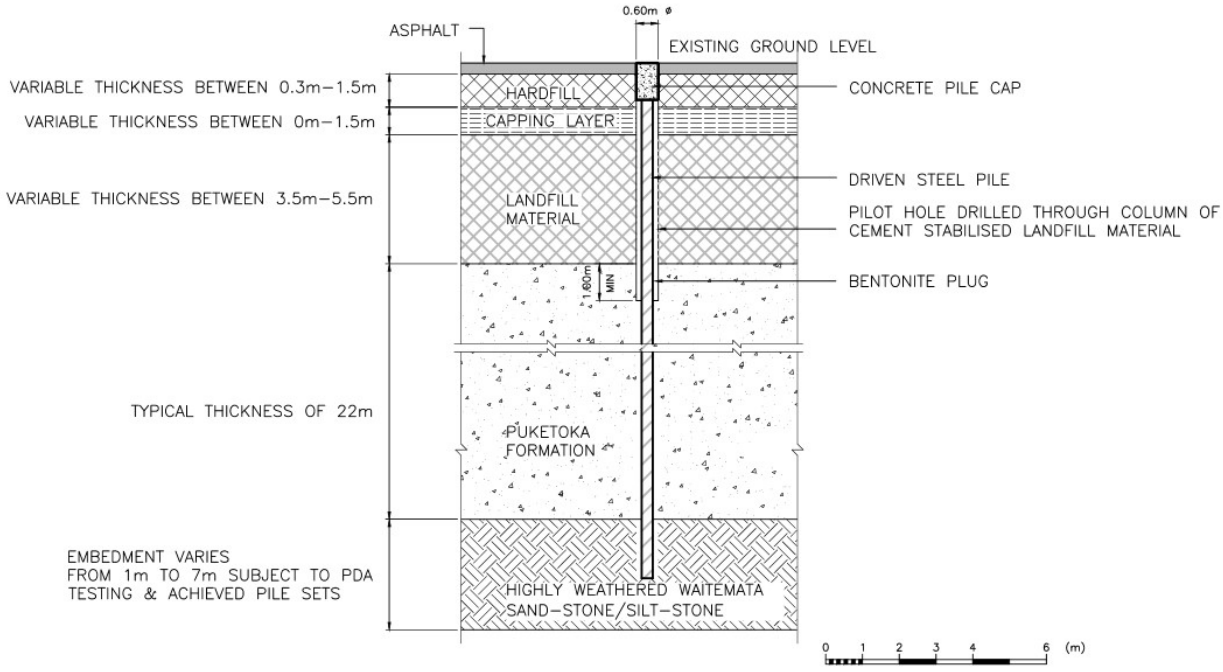


Figure 2. Typical pile cross section

In consultation with the piling contractor, an installation methodology combined of pre-drilling and driving was developed. All pile holes were pre-drilled to approximately 1m depth into the natural ground beneath the refuse (i.e. approximately 7.5m depth below the existing ground surface), and backfilled with low-strength concrete. This methodology not only provided a solution to the challenges, but also prevented both leachate entering the natural soils, and landfill gas escaping into the construction site. A smaller diameter pilot hole was then augered through the low-strength concrete to the bottom of the backfill. The steel H-pile was lowered vertically into the pilot hole, and driving commenced at 7.5m depth below ground surface. Figure 2 presents a typical pile cross section.

The foundation design involved 39 driven steel H-piles of varying size and length. The pile size ranged from 310 UC158 to 200 UC46, and extended to an average of 30m depth below the existing ground surface. All piles were connected by a network of ground beams to resist lateral loads. Pile corrosion was addressed by allowances in steel thickness for uncoated steel and coating protection systems.

The upper portion of each pile, approximately 10m in length was then painted with a high performance epoxy coating to provide protection against severe corrosion within the landfill layer. A minimum of 100mm cover of the low-strength concrete backfill was allowed around the steel piles over the pre-drilled depth to further minimise corrosion. In addition, pile driving analyser testing with CAPWAP analysis was undertaken on approximately 15% of the piles.

4.2 Landfill Gas Protection Measures

Results recorded during field investigations indicated the landfill refuse continued to produce gas. As the building and the Area 1 (retail tenancy) ground floor slab are supported on piles, ongoing settlement within the underlying landfill layer will potentially develop a void, allowing landfill gas to collect immediately beneath the building slab. Given the landfill gas hazard outlined in Section 3, it was important that a specifically designed passive venting system was constructed beneath the building to collect and discharge the landfill gas at safe locations.

The landfill gas protection measures beneath Areas 1 and 2 were designed differently. Area 1 includes a closed space retail tenancy (Area 2 is an open air car park building), hence, a more complicated passive ventilation system to fulfil the stringent consent conditions was required. This paper focuses on the design features of the Area 1 system.

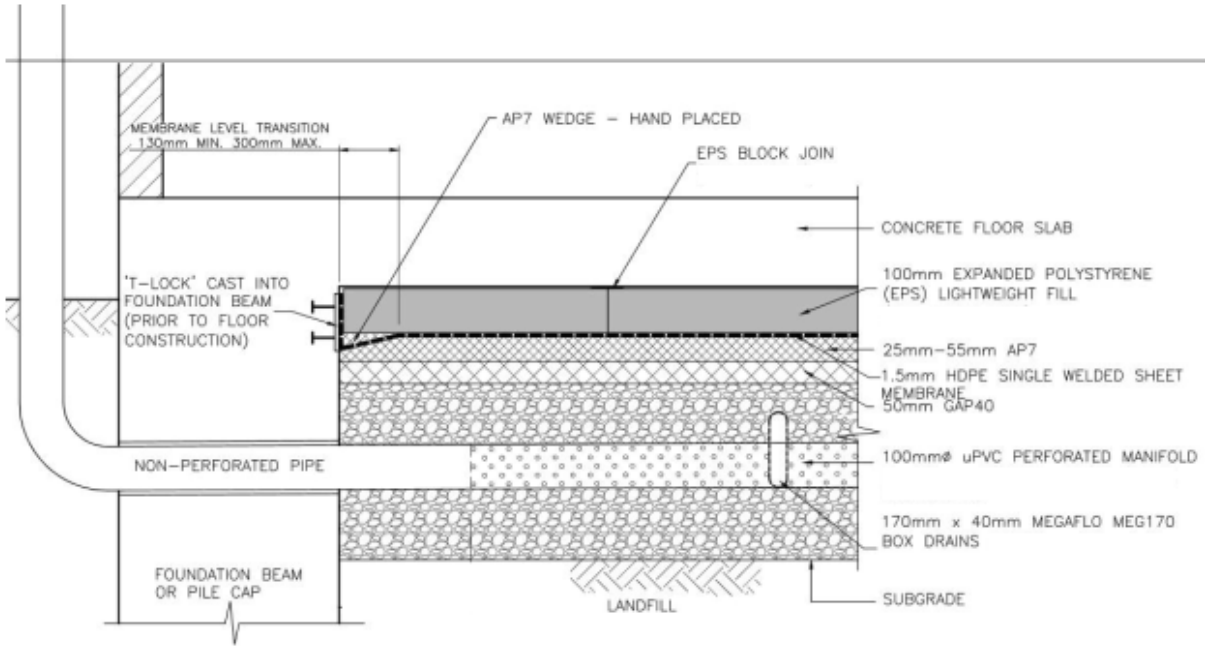


Figure 3. Typical details of Area 1 passive ventilation

Design of the Area 1 gas protection system includes a continuous subfloor passive gas collection network and an intact gas resistant HDPE membrane beneath the ground floor slab. The gas collection network consists of perforated manifold pipes, falling at a gradient of 0.5% towards vent stacks located between Areas 1 and 2. Box drains, connected perpendicularly to the manifold pipes at regular intervals, are incorporated into the design in order to maximise the area of influence. The manifold system is buried within a layer of granular materials, which provides a pathway for the landfill gas to migrate into the system. The landfill gas is directed and discharged via rotary ventilators on the building's roof. The HDPE membrane was placed above the granular layer. The membrane was designed to be welded to polyethylene brackets ('T-locks') that were pre-casted into the foundation ground beams. Figure 3 shows typical details for the gas membrane and subfloor passive ventilation within Area 1.

5 CONSTRUCTION

5.1 Excavation in Landfill

Floor levels were positioned to minimise excavation into the refuse. However, due to the highly variable thickness of the landfill cap (which is not consistently in place across the site), it was difficult to predict the volume of excavation into the refuse during ground works. Large amounts of refuse, consisting of bottles, glass, metal pieces, plastic, etc., along with a strong odour were encountered during site excavations – refer Figure 4(a) and (b).

Regular observations were undertaken by a Geotechnical Engineer during ground excavations, and geotechnical comments on the stability of trench excavation within soft refuse were provided. Where issues or conflicts arose between consented design and its constructability/excavatability, practical and cost-effective solutions were provided to the contractor.



(a) *(b)*

Figure 4. (a) Excavation within landfill; and (b) Landfill refuse observed

As part of the consent conditions, personnel working in the landfill materials were required to wear chemical resistant gloves and overalls to reduce potential contact with contaminated materials. To further minimise the landfill gas hazard, personnel was also required to wear portable gas monitors at all time during landfill excavation and pile installation. Electric fans were positioned near the landfill excavation areas to provide ventilation during excavation. Excavated materials were removed off-site as soon as possible and disposed at a licensed waste facility. Any surface water or groundwater that came into contact with refuse was treated as leachate and was removed off site, under instructions of the Engineer, by a sucker truck.

5.2 Installation of Gas Manifold System and HDPE Membrane

The subgrade for the gas manifold system was prepared by removing all sharp objects on the surface and proof-rolling. On completion of the subgrade preparation the manifold pipes were assembled within individual foundation compartments (divided by ground beams). To accommodate the slight difference in size and shape of each compartment, the length and space of the drains and pipes were adjusted on-site, under the instruction of the Engineer. Figure 5(a) shows a typical alignment of an assembled manifold system, prior to placement of the granular venting layer. The top blinding layer was hand placed to ensure a smooth finishing surface for the HDPE membrane.

The HDPE membrane was installed by a specialist contractor under full time observation of the Engineer to ensure the manufacturers' requirements for the gas membrane were correctly adopted and the membrane was undamaged. Extrusion welding, a technique that 'glues' HDPE materials together by using hot polyethylene, was utilised to weld the HDPE membrane to the T-locks. Quality control, via spark testing (electrical current passed though copper wire to generate spark), was undertaken on completion of membrane placement within each compartment, to detect if there were any unsealed/damaged spots.



(a) (b)

Figure 5. (a) Gas collection network; and (b) Placement of HDPE membrane

It was noted by the Engineer that the membrane (which had been installed and tested) was regularly damaged by site personnel. Frequent repair (in conjunction with re-testing) of the membrane was time consuming and could reduce the performance of the gas membrane. Following numerous discussions with the site contractor, placement of blocks of expanded polystyrene (EPS) lightweight fill on top of the membrane was considered the most practical solution to prevent further damage – refer Figure 6(a). The lightweight fill blocks were closely butted and taped to further minimise physical contact with the HDPE membrane, as shown in Figure 6(b). Subsequently the HDPE membrane remained undamaged.



(a) (b)

Figure 6. (a) EPS fill on HDPE membrane; and (b) Closely taped EPS fill

6 CONCLUSION

The new multi-storey commercial building at 3 Fred Thomas Drive, Takapuna has been constructed on a closed solid waste landfill. The building is supported on driven steel H piles to approximately 30m depth below ground surface to prevent damage to the structure due to ground settlement. A specially developed pile installation methodology was adopted, and landfill gas protection systems were constructed beneath the building subfloor to prevent migration of leachate and ingress of landfill gas into the new building. Construction was completed in April 2016.

7 ACKNOWLEDGEMENTS

The author wishes to thank Arthur Amputch, Technical Director at Riley Consultants Ltd for providing information and technical support, and Smales Farm Management Ltd for permission to publish this paper.

Proceedings of the 11th ANZ Young Geotechnical Professionals Conference – 11YGPC
Queenstown, New Zealand
25 – 28 October 2016

Adapting a Driven Pile Design to meet the Challenges encountered during Construction

R. J. Reed[1], GIPENZ, R. E. Kristinof[2], CPEng MIEAust and A. T. Carter[3]

[1]Jacobs New Zealand Ltd., Wynn Williams Building, Level 2, 47 Hereford Street, Christchurch, New Zealand; PH (+64) 3-940-4900; FAX (+64) 3-940-4901; email: Ryan.Reed2@Jacobs.com
[2]Jacobs Group (Australia) Pty. Ltd., Floor 11, 452 Flinders Street, Melbourne VIC, Australia; PH (+61) 3-8668-3000; FAX (+61) 3-8668-3001; email: Ross.Kristinof@Jacobs.com
[3]A. B. Investments Ltd., Level 5, 83 Victoria Street, Christchurch Central, Christchurch, New Zealand; PH (+64) 3-379-1650; FAX (+64) 3-379-0971; email: office@cartergroup.co.nz

ABSTRACT

A recent multi-storey commercial development undertaken in Christchurch, New Zealand following the 2010/11 Canterbury Earthquake Sequence presented a range of geotechnical foundation constraints. These included loose, liquefiable silts and sands layered with dense, non-liquefiable gravels; predicted large post-seismic settlements; and significant demand loads from the multi-storey superstructure; all of which had to be addressed via an economic capital cost design solution. A relatively "straightforward" driven concrete pile foundation design was designed for the development, which required adaption during construction due to latent conditions and difficulties encountered. When construction commenced, several piles refused above their target depth. Where this was due to factors such as localised variations in the soil profile, adverse pile performance during driving, or the striking of buried obstructions, automatic acceptance of these piles could not be guaranteed. Careful investigation as to the cause of these issues, and reanalysis of the piled foundation design was necessary to resolve the problems, meet the design requirements and account for the constraints of construction on the site. Various tools were used throughout this process, including high-strain dynamic PDA testing, CPT investigations and engineering judgement. The solutions ranged from acceptance of the refused piles 'as-is', to predrilling through surficial fill for the installation of remedial piles. Ongoing critique and assessment of the PDA results, including variation of the testing schedule as construction progressed resulted in value engineering opportunities, including the reduction of the overall number of piles compared to the original design. This ultimately offset the pile remediation costs such that both a successfully constructed foundation and a net cost saving on the original consented design were achieved.

Keywords: Driven concrete piles, PDA testing, construction challenges

1 INTRODUCTION

The 2010/11 Canterbury Earthquake Sequence saw extensive damage to many structures in the Christchurch Central Business District (CBD). This prompted their subsequent demolition and clearance, opening the way for new developments, albeit with a much greater awareness of the performance of buildings in seismic events. This project was a product of that redevelopment opportunity and involved the construction of a retail precinct comprising a new eight storey car park building (Building A), the extension of an existing two to five storey retail and commercial building (Building B) and two new four and three storey retail and commercial structures (Buildings C and D respectively). Due to the size of the project, the client had a strong focus on economic efficiency, in addition to meeting a rigid timeframe for the completion of the works due to their contractual obligations to the site's future tenants.

1.1 Geological Environment

Geotechnical investigations at the site comprised six boreholes to 25 metres below ground level (mbgl) depth or greater. These identified a fill layer at the surface arising from demolition of the previous structures that occupied the site, overlying layers of silt, sand and gravel of the Springston formation. The Riccarton gravels that persist across the city beneath the Springston formation were identified at a uniform depth of 23 mbgl. This soil profile is summarised in Table 1.

Table 1. Soil profile beneath the site determined from machine boreholes

Layer	Top of Layer (mbgl)	Thickness of Layer (m)	Description	Formation
1	0.0	2.2 – 3.2	Medium dense to very dense Sandy GRAVEL	Fill
2	2.8	0.0 – 1.1	Soft to firm Clayey SILT	Springston
3	3.3	1.0 – 1.3	Loose to medium dense Silty SAND	
4	4.4	3.3 – 3.7	Medium dense to very dense Sandy GRAVEL	
5	7.9	5.6 – 6.4	Loose to medium dense Silty SAND	
6	13.8	4.0 – 4.4	Medium dense to dense Silty SAND	
7	18.0	1.0	Soft SILT	
8	19.0	2.0 – 2.8	Loose to dense Silty SAND	
9	21.1	2.0	Soft to firm SILT	
10	23.1	–	Medium dense to very dense Sandy GRAVEL	Riccarton

Piezometers installed in several of the boreholes identified the groundwater table depth to vary from 3.3 to 5.0 mbgl.

Cone Penetration Tests (CPTs) were also completed across the site. These were used to investigate the liquefaction potential of the soil profile and the results were correlated against the soil layers described in Table 1. Below the non-liquefiable crust, layers 2, 3, and 5 were identified as being susceptible to liquefaction.

1.2 Foundation Design

The foundation design selected for the site consisted of 300 mm square driven precast concrete piles. The piles were arranged in square groups ranging from single piles to 16 piles, in a 4 x 4 arrangement. The piles resisted the demand loads of the superstructure and were connected on top by a concrete pile cap, with each cap linked by concrete foundation beams. The ground floor slab was structurally disconnected from the rest of the superstructure and founded on a reinforced gravel raft installed beneath it, laterally confined by the foundation beams.

To improve the constructability of the foundations, a consistent design was adopted across the site, with only the lesser demand loads on the piles of Building B enabling a shorter pile length. 15.0 – 15.5 mbgl was selected as the target depth range for Buildings A, C and D, resulting in pile cast lengths of up to 17 m, with the piles bedding within layer 6. Building B utilised a target depth range of 5.8 to 6.3 mbgl, with the piles bedding within layer 4. These target depth ranges were selected to achieve a minimum penetration of the pile within the founding layer of at least three pile diameters whilst also maximising the extent of stress bulb development within the same competent bedding material. Hence, there was minimal opportunity to reduce the pile penetration depth without promoting the risk of the piles bearing on liquefiable soils.

Each of the piles was designed to behave as an individual pile, rather than in a block mechanism, when subjected to each of the ULS loading conditions considered. These conditions included static loading in compression in both a pre and post-liquefaction environment; and seismic loading in compression and tension. The pile capacity was assumed to result from combinations of toe and shaft resistance in each case. Lateral design of the piles was completed by the Structural Engineer and so will not be commented on further.

2 PROBLEMS ENCOUNTERED DURING CONSTRUCTION

The multi-layered, liquefiable nature of the soil profile posed problems during construction of the piled foundations. The increase in density of the soil profile, both in the upper fill layer (layer 1) and the upper gravel layer (layer 4), when compared to the layers around them, meant that the piles had the potential to refuse prior to reaching their target depth range.

Pile refusal was the result of attrition on the pile during the driving process. Every time the pile head is struck, energy is transferred through the pile in the form of mechanical waves. The driving process fails the soil beneath the pile toe and along its shaft, and the pile displaces itself downwards. In instances where the strength of the soil exceeds that of the pile itself, the energy is absorbed by the pile instead, incrementally damaging it. Over the driving history of the pile, where the latter scenario

was prevalent, the pile damage accumulated to the level that the pile failed structurally, resulting in refusal of the pile to continue to drive when subjected to further hammer blows. Examples of the damage observed in the piles are included in Figure 1.



(a) *(b)*

Figure 1. Pile damage to a pile that was (a) driven to the target depth range; and (b) refused above the target depth range

Whilst driving a pile to refusal would normally imply that the pile has sufficient capacity, this capacity could only be relied upon under pre-liquefaction static conditions when the pile is subjected to compressive loading. The performance of the pile under the other loading cases could not be guaranteed, particularly when considering the effects of liquefaction, both along the installed length of the pile and of the soil immediately beneath the refused pile's toe. Liquefaction presents the risk of both nullifying the shaft capacity of layers of soil along the pile's length and of a punching failure mechanism beneath the toe of the pile. Likewise, acceptance that the pile's integrity had not been compromised during its refusal was also required.

The majority of piles on the site successfully reached the target depth; refusal was noted for only 51 of the 746 piles (6.8%) driven on the site. Those encountered in Building A are shown in Figure 2. Of those piles which refused prematurely, there did not appear to be a trend with respect to depth or location. There were instances of pile failure early in the driving process, in and immediately below the fill layer (layer 1), and at depth (in layer 4, 5 and just above the target depth range in layer 6). Sometimes it was the later installed piles in a given group that refused, which was likely due to densification of the surrounding soil by the installation of nearby piles, however, at other times, there was refusal of the first pile installed, with subsequent piles in the group driving without incident. There were instances of two piles diagonally opposite from each other refusing, while the adjacent piles reached the target depth range. Likewise, there were also instances of the majority of piles in whole groups adjacent to each other all refusing at similar depths.

3 SOLUTION METHODOLOGY

3.1 General Process

When assessing each pile which refused prematurely, it was necessary to understand the causes of pile refusal and its potential impact to the structure, through a process of data collection, review and consideration of alternative remediation options.

Central to every discussion was the significance of each refused pile. In each case it was necessary to consider:

- Did sufficient structural redundancy exist to compensate for a pile which may be under capacity?
- If not, what load cases were affected, and what was the magnitude of the potential deficiency in capacity?

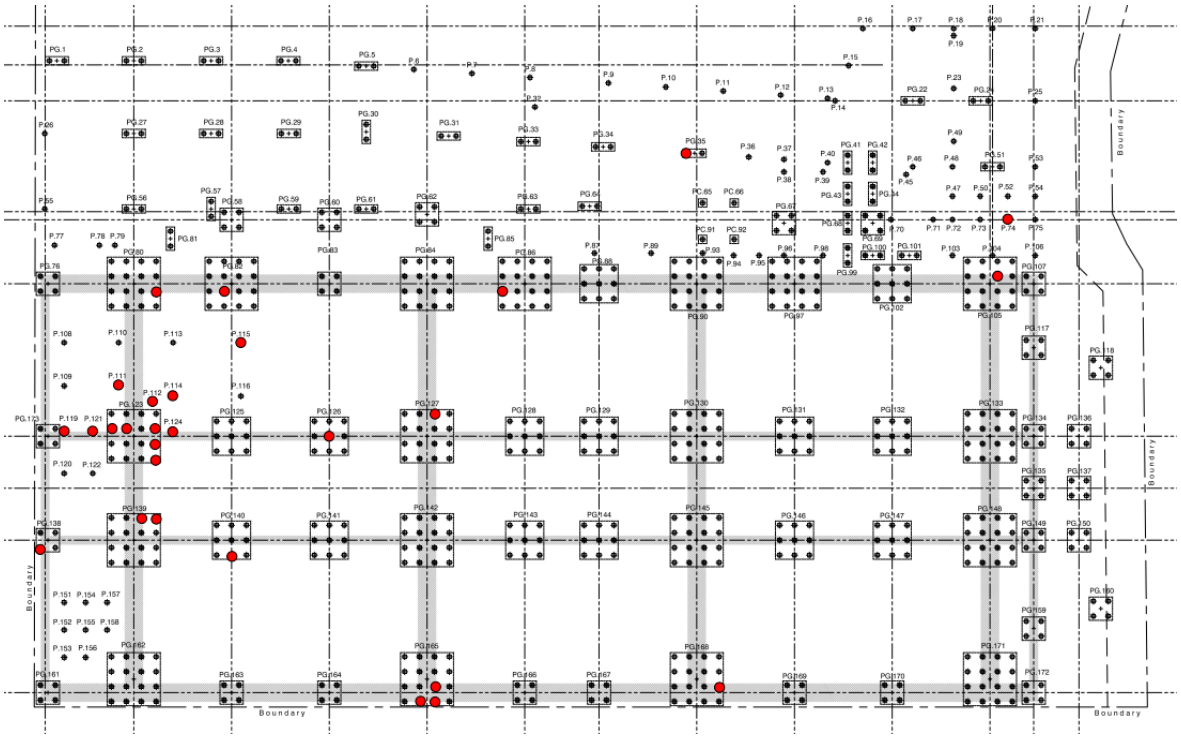


Figure 2. Locations of refused piles on Building A, shown in red; pile plan by Wilson and Hill Architects Ltd. (2015)

The answers to these questions informed the process thereafter. In some instances, the pile could be accepted 'as-is', on the basis that there was sufficient redundancy amongst nearby piles to compensate for the lower capacity of an isolated pile. Alternatively, where the refused pile was designed to carry large loads with minimal redundancy provided by surrounding piles, an evaluation of its expected performance became critical.

Communication between the client, the contractor, the geotechnical engineer and the structural engineer was also of high importance throughout the process.

3.2 Pile Driving Analyser (PDA) Testing

The main method for analysis of the expected performance of piles on the site was high-dynamic PDA testing. This was completed on 5.9 % of the number of piles in each building's foundation, with 55 tests completed in total on 44 different piles. The testing involved the attachment of two accelerometers and two strain-gauges to the top of the pile during driving. The records collected by these instruments were correlated to measurements of the pile set (depth of penetration of the pile per hammer blow); rebound (temporary compression of the pile when struck); and the driving hammer characteristics (type, weight and drop height) through a Case Pile Wave Analysis Program (CAPWAP) analysis. The results of this analysis predict the ULS capacity of the pile, the distribution of this capacity between toe resistance and shaft resistance, and the integrity of the installed pile.

The initial purpose of the PDA testing was to validate the theoretical pile capacity determined during the design phase. This enabled acceptance of the piles that successfully reached the target depth range, but didn't allow for decisions regarding remediation of the refused piles to be made. In order to address these, an explanation for the refusal of each pile had to be found, by way of examining local variability in ground conditions.

A review of PDA results during construction identified a general trend of higher pile capacities in the areas where pile refusals were encountered. Based on the assumption that two PDA tests of comparable piles in comparable soil profiles should produce comparable results, localised variations in the soil profile were inferred to be the main reason for variations in the measured PDA capacities. As these variations were also a likely cause for the early refusal of piles, it was justifiable on both a geotechnical and economic basis to consider individual PDA results to be indicative of the soil profile and the capacity of nearby piles. Thus, adjacent PDA tests were used to inform the pile remediation

process of refused piles, providing estimates of the expected capacities of the other piles in the group and therefore establishing whether there was sufficient additional capacity in additional piles to compensate for the pile which had refused prematurely.

A secondary benefit of this methodology was found through the extrapolation of it to all pile groups on the site. In many instances it was found that the pile capacities measured using PDA testing were sufficiently in excess of the demand loads on the pile group to allow for downsizing of the original group. An overall saving of 137 piles from the originally consented design was thereby achieved. This provided cost savings and reduced the foundation construction time, savings that offset the cost of the data collection and remediation of the piles for which it was still required, and the construction delays resulting from that remediation respectively.

3.3 Cone Penetrometer Test (CPT) Investigations

The secondary method for analysis of the expected performance of piles on the site was CPT investigations. The liquefaction susceptibility of the site was the primary driver for selection of the target depth range for the piles. This susceptibility was based on an average profile for the site, but as with the pile capacities, localised variations to this were possible. Furthermore, densification of the soil profile through the driving process was expected, but the benefits of this could not be quantified without supplementary CPT testing after the pile driving was completed.

CPT testing in the vicinity of the refused piles was used as a means of justifying 'exceptions to the rule' provided by the soil profile determined during the geotechnical investigations stage of the project. CPT testing was limited to areas where it was necessary to prove that ground conditions were more favourable than the site-wide ground model. Furthermore, due to their relative cost, they were used sparingly and only when other considerations, such as thicker than average gravel layers observed in the closest machine borehole, indicated a high likelihood of the method being successful.

3.4 Engineering Judgement

Applying engineering judgement and previous experience in similar conditions was a crucial element to the remediation process of every pile refusal. There were instances where it aided the decisions made using the PDA results, or the application of CPT investigations. In the former it was used to optimise the locations for the testing, to accept the test results and to determine the calculation methodology by which the raw results were transformed into estimated capacities for each of the load cases considered. In the latter it was used to interpret the results and to set limits on the zone of piles to which the results should be extrapolated to. However, there were also instances where it alone provided a means to justify acceptance of a refused pile or a recommendation for a remediation solution.

In the instance of a cluster of refused piles in Building A (seen on the left side of Figure 2), pile refusal had occurred for all piles at very similar depths and all in close proximity of the target depth range. A localised reduction of the minimum target depth by 150 mm was justified on the basis of this clustering, the nearby PDA test results and the expected soil densification in this area from the driving of many piles in close proximity to each other. This reduction enabled acceptance of 11 of the 12 refused piles in that area, avoiding the pile remediation costs and time delays that would otherwise have been required.

Likewise in Building C there were several instances of piles refusing within the demolition fill of layer 1. These piles exhibited very extreme degrees of damage, including snapping of the pile at its middle in one case and a 700 mm shortening of the pile from crushing in another. Judgement in these cases suggested that buried obstructions were the most reasonable explanation for the refusal, rather than the accumulation of variability in the soil profile. As such, excavations through the fill layer in these locations revealed a buried foundation beam and a buried concrete over-pour from construction of the previous building on the site, and a denser than expected layer of fill that a 30T excavator bucket couldn't penetrate.

3.5 Remediation Solutions

For 42 of the 51 piles which refused prematurely, close scrutiny of PDA testing and engineering judgement enabled acceptance of the refused pile 'as-is'. A further three piles refused at a shallow enough depth, including the two in Building C that struck buried obstructions, to enable them to be extracted, with subsequent driving of a replacement pile being completed without incident.

For the remaining piles, a decision was made regarding whether to undertake further CPT testing to gather additional information, or to proceed directly to the installation of remedial piles. This decision was a question of economics, scheduling and risk; weighing the potential cost-benefit of gathering further information to inform a remedial decision against the risk of the additional testing not returning favourable data. The risk of further refusal of remedial piles also had to be taken into account.

Different stages of the project called for different risk appetites. Early on in the project, the potential for decisions to have a large impact on cost or program was higher, and therefore the risk tolerance was also higher, and installing remedial piles was viewed more favourably for the construction program savings it allowed. Piles intended for use elsewhere were able to be re-purposed for installation as remedial piles without the need to delay the project, on the expectation of future pile savings from ongoing PDA testing in other areas. However, later in the project these options were not available.

In one case, predrilling was performed to aid the installation of a remedial pile and several other piles included in the original design to ensure they reached the target depth range. This could only be undertaken where there was sufficient additional capacity in the ground to compensate for the loss of shaft friction arising from the predrilling.

An additional five piles were required to provide remediation for the groups containing the six remaining pile refusals. These were installed around the group at locations chosen in consultation with the structural engineer to ensure a balanced load distribution for the group.

4 CONCLUSIONS

A redevelopment in the Christchurch CBD employed the use of a driven pile foundation solution for the structures on the site. However, pile refusals above the target depth range required adaptation of the originally consented design during construction. These refusals were managed through a process of data collection, review and alternative remediation option consideration for each pile.

Different methods were applied to justify the acceptance or rejection of each refused pile. These methods included PDA testing, CPT investigations and engineering judgement. Each method was extended beyond its usual application to understand the every refused pile and the likelihood of cumulative variations in the soil profile ("exceptions to the rule" provided by the ground model) being responsible for their refusal.

Application of these tools in this manner was proven to enable manipulation of a piled foundation design to meet the demands of construction and overcome the challenges encountered. Furthermore, in addition to minimising the extent of pile remediation, the PDA test analysis was also extended to justify downsizing of many of the original pile group designs, achieving a net cost saving for the client on the original consented design.

5 ACKNOWLEDGEMENTS

Charles Watts, Jacobs New Zealand Ltd.
Grant Murray, Grant Murray Associates
A.B. Investments Ltd.
Wilson and Hill Architects Ltd.
The Engineering Company Ltd.
Southbase Construction Ltd.
Daniel Smith Industries Ltd.
DPT Australia Ltd.

Proceedings of the 11th ANZ Young Geotechnical Professionals Conference – 11YGPC
Queenstown, New Zealand
25 – 28 October 2016

Site characterization of the area surrounding a sinkhole, a case study

M. P. Magagula[1], AMSAICE and G.R. Wardle[1], FSAICE

[1]Jones & Wagener (Pty) Ltd, Engineering & Environmental Consultants, P.O. Box 1434, Rivonia, 2128; PH (+27) 11-519-0226; FAX (+27) 11-519 0201; email: magagula@jaws.co.za or mondli1937@live.com, wardle@jaws.co.za

ABSTRACT

In 2014, a sinkhole occurred below a fuel pipeline at Tarlton International Speedway, near Johannesburg in South Africa. Following the sinkhole collapse, visual inspections were conducted to determine the direction of the throat and the probable causes of the sinkhole. Emergency backfilling of the sinkhole was undertaken, followed by site characterisation of the area comprising geophysical gravity surveys and percussion borehole drilling. The boreholes were drilled on the gravity highs and lows as per the results of the gravity surveys. The gravity survey was able to establish the shallow and deep weathering profile of the dolomite rock head, but was unable to define the cavity or subsurface receptacle. Additional boreholes were drilled in the perceived visual direction of the sinkhole throat observed from the initial inspection. This drilling defined a cavity that extended beyond the surface opening of the sinkhole. The investigation confirmed the importance of using more than just one method of ground investigation to compile an accurate geotechnical model of the site. The true extent of the subsurface cavity could only be discovered through exploratory drilling based on observations of the throat itself soon after the sinkhole was discovered. Had the cavity, that extends beyond the surface opening of the sinkhole, not been identified, it would have resulted in an underestimate of the extent and cost of the remedial works.

Keywords: Dolomite, Investigation, Sinkhole, Geophysics, Boreholes.

1 BACKGROUND

Gauteng is South Africa's smallest province, but is the country's economic hub and has drawn a large percentage of the country's population to seek work and residence on its land. With the continued growth of the province's population, real estate development is forced more and more onto dolomitic land. The dolomites are prone to sinkhole formation and are recognised as one of South Africa's main 'problem soils', Wagener (1985). This has prompted extensive research into dolomite and the development of a South African National Standard to address development on dolomitic land, i.e. SANS 1936:2012.

Dolomite is a chemical or biochemical sedimentary rock, comprising primarily of the mineral dolomite which consists of calcium magnesium carbonate $CaMg(CO_3)_2$ and secondary Silica known as chert. Although dolomite has many practical uses such as aggregate in concrete, the one drawback is that dolomitic rock is highly susceptible to solutioning by even slightly acidic water. Acidic water refers to water that has been subjected to dissolution with CO_2 in the atmosphere, with the resultant reaction creating weak carbonic acid (H_2CO_3). As this slightly acidic water infiltrates the ground and mixes with the ground water system, it causes weathering of the dolomitic rock. The rock subsequently breaks down into soluble and insoluble by-products. This chemical process is represented as follows: $CaMg(CO_3)_2 + 2H_2CO_3 \rightarrow Ca(HCO_3)_2 + Mg(HCO_3)_2$ (WRC, 2003). Solutioning of these by-products results in sub-surface cavities in the rock profile. In areas with a low or deep water table i.e. a water table below the solution cavity, where wash out of the soils within the overburden has resulted in the development of a meta-stable arch above the throat of the cavity, the downward migration of water can weaken the arch and trigger the formation of a sinkhole. In areas with a shallow water table, i.e. water table above the cavity, subsequent drawdown of the water table can similarly trigger the formation of a sinkhole. Figure 1 illustrates the idealized sinkhole formation mechanism in a low groundwater table environment as contained in SANS 1936. In Figure 1 the sinkhole is triggered by a leaking wet service. Leaking services are by far the dominant cause of sinkhole formation in built-up urban areas, whereas lowering of the water table as a result of farming and/or mining activities is often the trigger in rural areas. South African research shows that 96% of sinkholes and subsidence events recorded were man induced and resulted from the absence of appropriate risk mitigating measures.

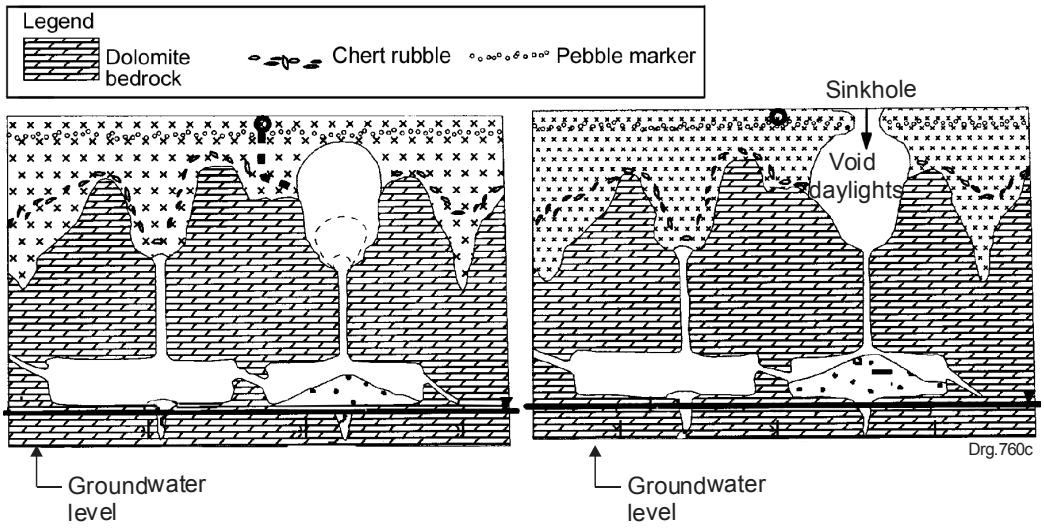


Figure 1. Sinkhole Formation (SANS 1936)

2 INTRODUCTION

In April 2014, a sinkhole formed below a fuel distribution pipeline in the Tarlton agricultural region of Gauteng. The regional geology comprises Malmani Subgroup dolomites of the Chuniespoort Group, Transvaal Supergroup. The sinkhole (left hand side of Figure 2) was about 10m to 12m in diameter at ground surface and was estimated to be about 7m deep on average. The sidewalls of the sinkhole were near-vertical with the overburden comprising mainly silty sand with fine chert gravels and ferricrete/manganocrete nodules.

A preliminary site inspection of the sinkhole was undertaken to determine the possible causes of the sinkhole, as well as to assess any damage to the fuel pipeline. During the preliminary inspection, it was noted that the fuel line had neither ruptured nor had incurred any damage, thus was most likely not the reason for the sinkhole formation. Also noted during the preliminary inspection, was that at the southern end of the sinkhole, there was an approximately 1.5m diameter “throat” that disappeared from view in a southerly direction almost immediately below the pipeline (shown in the right hand side of Figure 2). It was through this throat and lower-lying cavities that the ground that originally occupied the volume of the sinkhole had been eroded.



(a) *(b)*

Figure 2. (a) Sinkhole; and (b) 1.5m Sinkhole Throat

For safety reasons as well as to prevent water ingress into the sinkhole, which would have resulted in material washing away through the sinkhole throat, thus increasing the size of the sinkhole. Emergency backfilling of the sinkhole was recommended and carried out shortly after the initial inspection. The backfilling was a short term solution as saturation of the backfill from surface water ingress would be likely to cause the soil to start settling under its own weight and drag the pipeline down.

3 SITE CHARACTERISATION

3.1 Initial Site Visit

The initial site visit, whilst the sinkhole was open, proved to be invaluable, as information obtained from the site visit turned out to be the biggest contributor to the planning of the geotechnical investigation and subsequent remedial works.

During the site visit it was also discovered that the probable cause of the sinkhole was an existing trench, termed a “security trench”, dug to prevent vehicles entering the area on the property on which the pipeline is located. The trench facilitated collection and ponding of surface water run-off, thus resulting in infiltration into the underlying subsoil and ultimately leading to the collapse of the overburden.

Following the inspection, the sinkhole was immediately backfilled with loose spoils placed as an emergency measure for (i) safety; (ii) to prevent further concentration of surface water; (iii) to prevent enlargement of the sinkhole by choking the throat; and (iv) to provide support to the fuel line. Upon re-inspection of the site at a later stage, it was discovered that consolidation of the fill had resulted in a slight depression of the surface.

3.2 Gravity Surveys

3.2.1 Initial assessment of the site

The SANS 1936 standard stipulates that physical geotechnical investigations on dolomitic land should be preceded by a gravity survey of the area. This portion of the investigation was undertaken by a geophysicist. A total of 156 gravity stations were proposed, and data was acquired on a 180m x 165m area using a 15m grid spacing. An additional 36 stations were added in close proximity to the sinkhole on a 7,5m grid spacing to provide more detail in this area. The gravity measurements were recorded using a Scintrex CG-5 gravimeter. The gravity station coordinates and elevations were surveyed using a Trimble RTK GPS system.

The product of the gravity survey is a residual gravity anomaly map obtained by subtracting the regional influence from the measured values. The regional gravity map was obtained using a gridding algorithm where each cell is influenced by a large number of surrounding measurement points. The purpose of this is to remove deeper gravity variations and to provide a more detailed and shallower view of density variations. High residual gravity values are indicative of shallow bedrock, typically pinnacles of hard dolomite rock. Low residual gravity values, on the other hand, are indicative of deeply weathered grykes or valleys between the pinnacles, or subsurface cavities in the rock mass.

Figure 3 illustrates the results of the residual gravity survey highlighting three anomalies detected namely; Anomaly A – a very prominent gravity low, Anomaly B – a gravity low and Anomaly C – a relatively high gravity feature.

From Figure 3 it can be seen that there was no defined gravity low in the immediate area of the sinkhole that could be associated with a cavity. However, anomaly A suggested that, if anything, the cavity would be expected on the south western side of the sinkhole. A decision was taken to investigate this anomaly and the area immediately around the sinkhole by drilling percussion boreholes. It was clear that it would take an assimilation of the gravity maps, borehole information, as well as observations during the initial site visit, in order to properly classify the area.

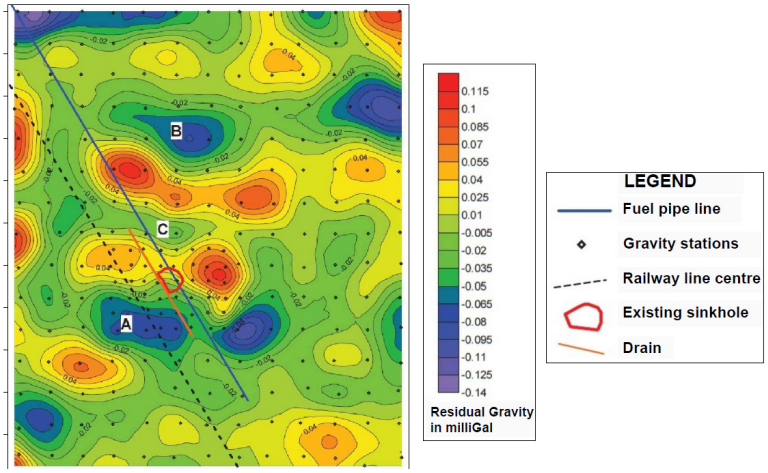


Figure 3. Residual Gravity Survey

3.3 Aerial Photo Interpretation

To better develop the geotechnical model for the area, aerial photograph interpretation (API) was applied. The API made use of 1:30 000 stereo aerial photographs flown in August 1968 and issued by the Government Printer. API is used to delineate general geological features/contacts, terrain units and linear features such as faults and dykes. A terrain unit defines a specific geomorphological landform within the broader area topography where similar geological conditions are present. Similar terrain units generally exhibit similar soil profiles and consequently geotechnical parameters.

The API indicated that, within the area of the sinkhole, a defined linear depression is evident and has been there since 1968. The main section of this depression conformed well to the gravity lows recorded during the gravity survey as shown on Figure 4. The depression is characterized by a very gentle gradient that would typically not have resulted in excessive concentration and infiltration of surface water.

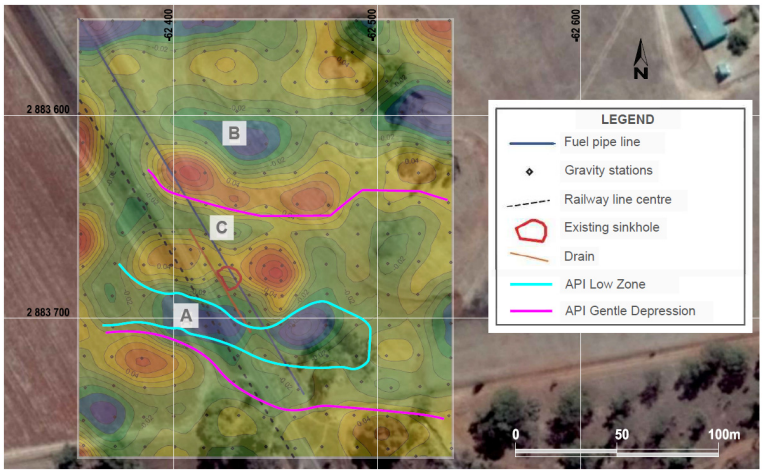


Figure 4. API Interpretation

3.4 Percussion Drilling

3.4.1 The drilling campaign

As shown in Figure 5, eleven percussion boreholes were drilled during the investigation. Boreholes BH1 to BH4 were drilled primarily for the purpose of 'proofing' the results obtained from the gravity surveys. Boreholes BH5 to BH8 were drilled around the perimeter of the sinkhole. Based on the results of these initial boreholes, three additional holes were drilled, i.e. BH9 to BH11.

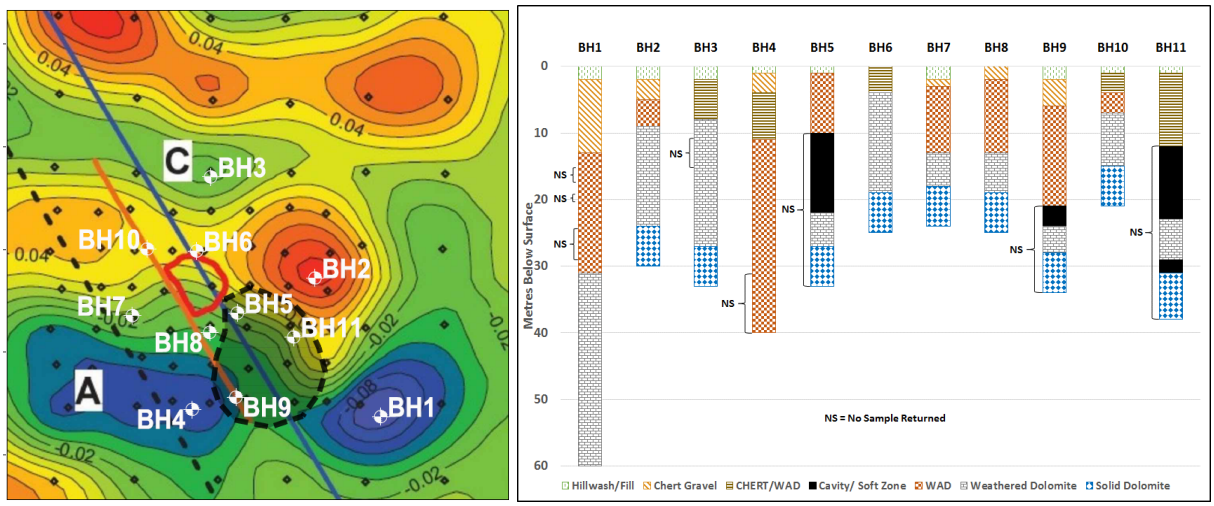
The depth of drilling was determined in accordance with the guidelines of SANS 1936-2 which requires boreholes to be drilled into dolomite bedrock on gravity high anomalies to determine the

shallowest dolomite bedrock depth, at least 6m into hard rock dolomite or 15m into non-dolomitic rock and a representative selection of boreholes to at least 60m if dolomite bedrock is not confirmed at shallower depth.

The drilling of the boreholes was conducted by geotechnical contractors and was carried out using a 116mm (4.5”) diameter down-the-hole air percussion hammer. Representative samples of drilling chips were collected at 1m intervals and placed in marked plastic bags. Drilling observations were recorded on driller’s log namely: depth, drilling rate per meter, water strikes, addition of water or drilling foam if required, air loss, potential cavities, sample return and hammer tempo.

3.4.2 Drilling Results

Following logging of the chip samples by an experienced engineering geologist, a profile log was compiled for each borehole including the drilling parameters. Figure 5(a) shows the borehole positions as well as the approximate position of the cavity, whilst Figure 5(b) shows a simplified profile summary for each borehole.



(a) *(b)*

Figure 5. (a) Borehole Positions; and (b) simplified profile of material units within each borehole

From Figure 5 it is evident that the gravity survey was able to identify the shallow (BH3, Anomaly C) and deeply weathered profiles (BH 4, Anomaly A) in the bedrock. However, it was not able to identify the cavities/soft zones around the sinkhole identified in BH5, BH9 and BH11.

Based on the drilling information the approximate extent of the cavity and its position relative to the sinkhole was established. Figure 6 illustrates the extent of the sinkhole and the approximated locations of the underlying cavities.

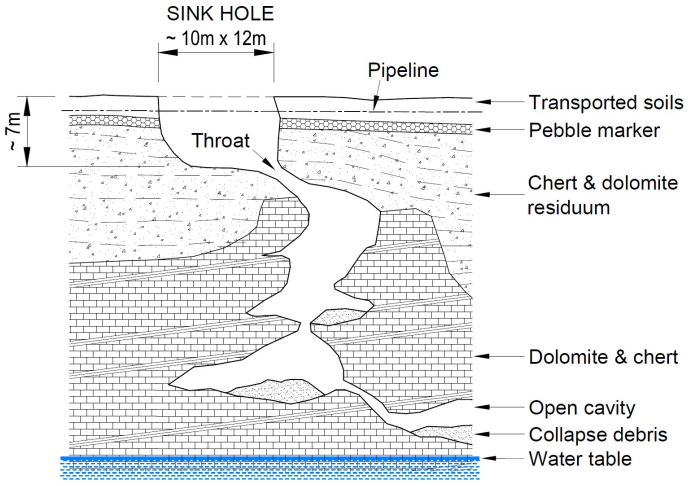


Figure 6. Sinkhole and Underlying Cavities

4 DISCUSSION

The detailed geotechnical investigation which followed the sinkhole collapse made use of a range of available methods recommended by the SANS 1936 documents. Each method contributed to the understanding and development of a comprehensive geotechnical model of the site and the sinkhole mechanism. The initial site inspection, shortly after the sinkhole was noticed, provided invaluable clues as to the location of the sub-surface cavity and the trigger for the sinkhole collapse. Gravity surveys identified the variable shallow and deep rock head topography that is so characteristic of the pinnacles and grykes in the dolomites. Physical borehole drilling, guided by the gravity anomalies, confirmed the locality and extent of the cavity/ies around the site and thus helped facilitate the final remedial works. The API revealed that the naturally occurring depressions on site did not result in the excessive ponding of surface water and that the ponding of surface water was as a result of manmade interventions, in this case the “security trench”.

An interesting and unexpected observation of this project was the offset and asymmetrical location of the surface expression of the sinkhole compared to the sub-surface cavity. In January 2004 a 20m deep, 30m wide sinkhole formed in Bapsfontein located in the east of Johannesburg. The sinkhole was also asymmetrically located from the throat; this shows that a throat asymmetrically located from the sinkhole is not a unique feature to the Tarlton Sinkhole. Most illustrations of a sinkhole model, e.g. SANS 1936, show the sinkhole developing directly above the mouth of the cavity. Recent centrifuge research at the University of Pretoria (Jacobsz, 2016) confirms the vertical chimney-like nature of the propagation of subsurface erosion mechanisms in cohesionless soils above the water table. It is important that we further develop our understanding of these mechanisms and the reasons for the sinkhole to develop off-centre with respect to the mouth or throat of the cavity.

Remedial works of the sinkhole are not discussed in this paper, suffice to mention that compaction grouting of the sub-surface void was carried out to prevent a repeat occurrence of the sinkhole. As part of this exercise, the “security” trench was backfilled and the surface levelled off to allow surface water to pass over to a nearby concrete-lined drainage channel.

5 CONCLUSIONS

It is concluded that no single investigative method can be relied upon to provide a full geotechnical characterisation of a site, especially a site with complex geology or problem soil conditions. Several methods, each acting like a piece in a puzzle, have to be assimilated to compile the full picture. In addition, this case study has also shown the value of experienced geotechnical practitioners attending to a site inspection as soon as possible after the event of the sinkhole occurrence. Had the site not been properly characterised, only partial remediation of the problem ground condition would have been achieved by the remedial works. This case study highlights the importance of using geophysical methods in conjunction with visual inspections and physical explorations (boreholes).

6 ACKNOWLEDGEMENTS

The author wishes to acknowledge the contributions of Dr Nico Vermeulen, Dr Peter Day and Mr Gavin Wardle and Dr Martin Rust all of Jones & Wagener.

7 REFERENCES

Jacobsz, S.W. (2016). “Trapdoor experiments studying cavity propagation”, in Jacobsz (ed.), *Proceedings of the first Southern African Geotechnical Conference*, pp. 159-165.

Jones & Wagener (2004). *Investigation of Dolomite Instability Bapsfontein Proposed Remedial Measures*, report no. JW21/04, prepared for Ekurhuleni.

SABS Standard Division (2012). *SANS 1936-1:2012: Development of Dolomite Land Part 1: General Principles and Requirements*

SABS Standard Division (2012). *SANS 1936-2:2012: Development of Dolomite Land Part 2: Geotechnical Investigations and Determinations*

SABS Standard Division (2012). *SANS 1936-3:2012: Development of Dolomite Land Part 3: Design and Construction of Buildings, Structures and Infrastructure*

SABS Standard Division (2012). *SANS 1936-4:2012: Development of Dolomite Land Part 4: Risk Management*

SABS Standard Division (2012). *SANS 2001-BE3:2012: Repair of Sinkholes and Subsidence in Dolomite Land*

Wagener, F. (1985). “Problem of soils in South Africa - State-of-the-art: Dolomites”, *The Civil Engineer in South Africa*, pp. 395-407.

WRC. (2003). *Understanding Groundwater: A stakeholders guide to the North West dolomite aquifer*, <http://fred.csir.co.za/project/groundwater/documents/WUAGroundwaterBooklet.pdf>, accessed Apr. 30, 2016

Proceedings of the 11th ANZ Young Geotechnical Professionals Conference – 11YGPC
Queenstown, New Zealand
25 – 28 October 2016

Arching in geosynthetic reinforced column supported embankments – recent findings from a field case study

Daniel King[1]

[1]Room G24, Building 60, Department of Civil Engineering, Monash University, Clayton, Victoria, Australia; PH (+61 3) 9905 5576; email: daniel.king@monash.edu.au / dking@golder.com.au

ABSTRACT

As part of the Regional Rail Link project in Melbourne, Australia a field case study has been undertaken by Golder Associates and Monash University that involved the instrumentation of a geosynthetic reinforced column supported embankment (GRCSE). The field case study site is located in inner Melbourne within the Yarra Delta and is underlain by Coode Island Silt, a soft soil well known to the local geotechnical profession. A number of the findings relating to the site characterisation, load transfer platform behaviour, the development of soil arching and global embankment behaviour have been published recently in several journal and conference proceedings. This paper focuses on the arching stress development in GRCSEs and compares arching stress/deformation models. The widely adopted design standards (BS 8006, 2010 and EBGEO, 2010) adopt a "two-step" design approach that de-couples the arching stress/deformation relationship. This is compared with the Ground Reaction Curve method that describes the four phases of arching: initial, maximum, load recovery and terminal phases as a deformation (and time) dependent process. The implications that these arching stress/deformation relationships presents for design is described.

Keywords: Arching, geosynthetic reinforced column supported embankment, field case study

1 INTRODUCTION

A variety of ground improvement techniques exist to support road and rail embankments constructed over soft soils. However, in recent years, GRCSEs have become an increasingly popular design solution due to the rapid speed of construction and their ability to meet stringent performance criteria. A GRCSE is supported on semi-rigid ground improvement and comprises an embankment with a geosynthetic reinforced load transfer platform at its' base. While various pile types (i.e. driven piles, timber piles etc.) can be used for ground improvement, in recent years the use of drilled displacement columns has become increasingly popular. The load transfer platform serves to transfer embankment load to the semi-rigid elements that then transfers this load to a stiffer founding unit. Over the past decade, a significant quantity of research has been reported in this area with a particular emphasis on describing the complex soil-structure-geosynthetic reinforcement interaction occurring in the load transfer platform. A key component of the load transfer platform behaviour is the load distribution mechanism that transfers embankment stresses to the stiffer columns. This mechanism is known as "soil arching" and is one of the oldest problems in soil mechanics. Soil arching is often assessed through the trapdoor test, with Terzaghi (1943) undertaking one of the earliest systematic studies of the trapdoor problem. Since this time, it has been studied extensively and the knowledge gained applied to a range of geotechnical problems, including: tunnel support in underground excavations, granular flow between vertical walls (silo problem), cave formation in karstic terrain and in GRCSEs.

The design approach adopted in the widely used German design standard (EBGEO 2010) and British design standard (BS8006-1 2010), amongst others, is a "two-step" approach (Figure 1) which utilize limit equilibrium arching models. In Step 1, a limit equilibrium arching model is adopted to assess arching stresses distribution. Based on this assessment, a constant value of "design" stress that acts in the unarched zone (Load component B + C) is used in Step 2 to calculate the load distribution between the geosynthetic reinforcement and sub-soil support. This "two-step" approach de-couples the relationship between arching stresses and base settlement as the arching stresses in Step 1 are assumed to be constant with respect to time and base settlement (sub-soil settlement and/or geogrid deflection). The relationship between trapdoor settlement and arching development is described by the Ground Reaction Curve proposed by Iglesia (1991, 2013), amongst others, and has been used herein to interpret the field behaviour. It is shown that considerable insight into the load transfer

platform behaviour can be gained when the coupled relationship between arching stresses and sub-soil settlement is considered.

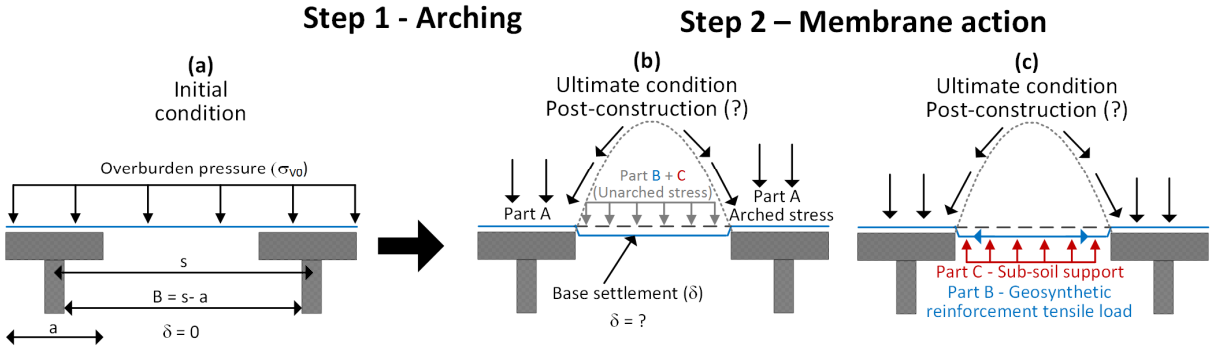


Figure 1. Conceptual load distribution (a) Initial condition (b) Arching stresses (c) Membrane action

2 BACKGROUND

As part of the Regional Rail Link project in Melbourne, Australia, a number of GRCSEs were constructed to support rail embankments underlain by Coode Island Silt. One of these embankments, the North Dynon embankment, was selected for instrumentation as part of a research project involving Monash University and Golder Associates. The North Dynon embankment is a widened embankment, approximately 180 m in total length of which a 60 m length of the embankment is designed and constructed with a lower and upper level load transfer platform (Figure 2). The split-level load transfer was required to control differential settlement across the width of the widened embankment as well as to reduce potential settlement beneath the existing embankment.

Ground improvement options including a fully piled structure, soil mixed columns and drilled displacement columns were evaluated during design, however, it was considered that drilled displacement columns would provide the most efficient and cost effective solution as columns could be installed relatively quickly and efficiently while minimizing the potential for spoil generation. The later was particularly important as the Coode Island Silt is an acid sulphate soil and offsite disposal would have been costly. The ground improvement works were completed in stages with the lower level completed as part of Stage 1 and 2 works and the upper level constructed as part of Stage 3a/b works. The analysis and interpretation of the instrumentation data has been described separately in two papers. The localized behaviour based on earth pressure cell and strain gauge data is presented in King *et al.* (2016b) and focuses on arching stress development in the load transfer platform.

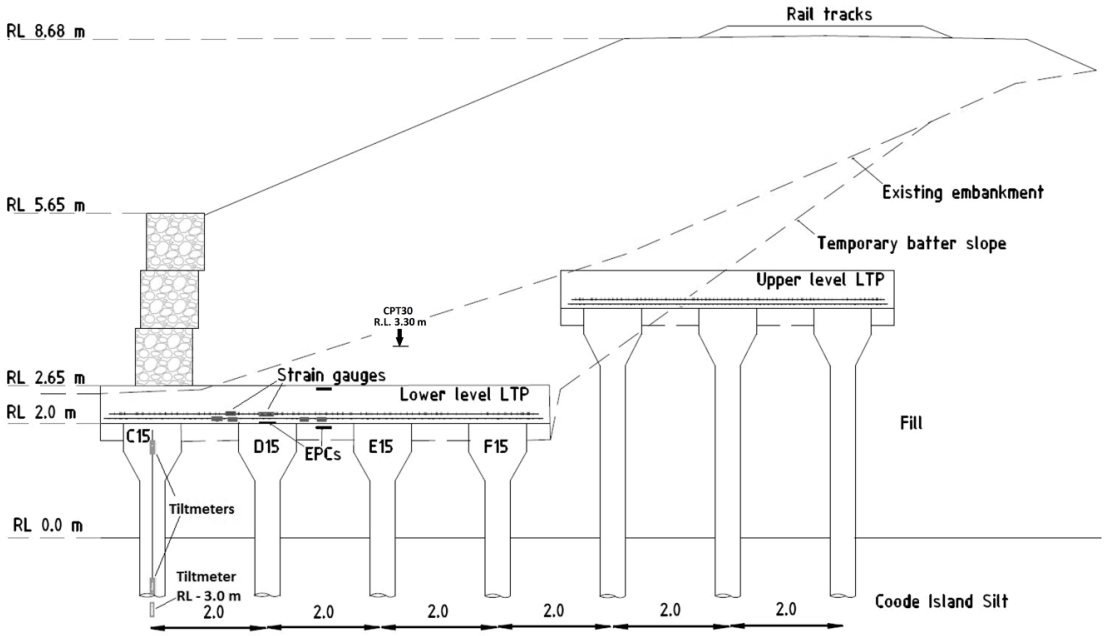


Figure 2. Cross section of North Dynon embankment at Area #2

A second paper (King *et al.* 2016c) describes the installation effects associated with the ground improvement works and their interaction with global embankment behaviour based on piezometer, tiltmeter, inclinometer and survey data. This current paper focuses on some of the design implications arising from the research findings presented in King *et al.* (2016b). Gniel and Haberfield (2015) have also described separately the GRCS approach embankment for the Maribyrnong River viaduct constructed for the Regional Rail Link project.

3 SUB-SURFACE CONDITIONS

The North Dynon embankment is located immediately adjacent to the Moonee Ponds Creek in the suburb of North Melbourne and is founded on a sequence of Quaternary aged sediments (Yarra Delta sediments) overlying the Silurian aged Siltstone/Sandstone of the Melbourne formation (Neilson 1992). The near-surface Coode Island Silt, is of particular importance owing to its wide spatial distribution, low undrained shear strength (s_u typically increases from about 15 kPa to 40 kPa at depth) and its considerable thickness of up to 25 m in parts. The geological profile is complex and highly variable, with the Coode Island Silt varying from 7 m to 15 m along the length of the embankment, the underlying stiff to very stiff clays of the Fishermens Bend Silt unit form the founding unit for the columns. As part of the site characterisation for the research case study, the site investigation information was reviewed and an extensive program of additional laboratory testing was undertaken. This was primarily focused on characterising the compressibility and time rate of settlement of the Coode Island Silt. The findings of this investigation along with a detailed description of the sub-surface conditions is presented in King *et al.* (2016a).

4 FIELD CASE STUDY RESULTS

Instrumentation was installed in two separate areas of the embankment (Area #1 and Area #2). The data from Area #2 is shown in Figure 3 along with the earth pressure cells arrangement in the figure insert. The stress acting on the column head can be seen to increase as the embankment height increases (increasing overburden stress) and as the arching develops due to sub-soil settlement. Following the completion of the embankment, the arching stresses are seen to develop progressively post-construction under a constant vertical load. The term “stress reduction ratio” is often used to quantify arching stresses and is defined as the stress acting in the zone being unloaded (i.e. EPC2 stress) divided by the overburden stress and is shown in Figure 3. The overburden stress was assessed to be 74 kPa in Area #2 based on 2D plane strain finite element analysis (see King *et al.* 2016b).

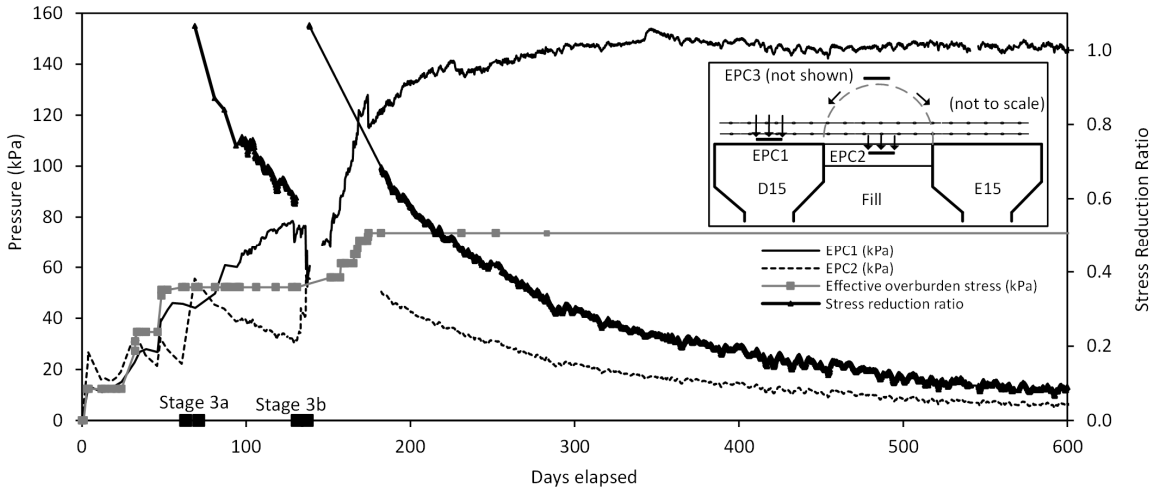


Figure 3. Earth pressure cell data and calculated stress reduction ratio

5 GROUND REACTION CURVE

The Ground Reaction Curve describes the relationship between the stress reduction ratio and the relative (normalised) displacement in a trapdoor test (defined as trapdoor displacement (δ) / trapdoor width (B)) over the initial, maximum, load recovery and terminal phases of arching (Figure 4). This method has been utilized in the current field case study to describe the development of the arching

stresses shown in Figure 3 by considering a 2D axisymmetric unit cell with parameters H (height of overburden material) and B (equivalent width of trapdoor). For the unit cell considered in the present investigation H = 3.73 m and B = 1.42 m. The material properties of the rockfill used in the load transfer platform, friction angle φ = 50° and mean particle size D_{50} = 9.7 mm, are also used to calculate the Ground Reaction Curve. The stress reduction ratio data in Figure 3 is reproduced in Figure 5 and compared with the predicted values (shown in bold) determined from the Ground Reaction Curve method. Based on the data available, the development of arching stresses up to the period of maximum arching shows good agreement with the predicted behaviour based on the Ground Reaction Curve method.

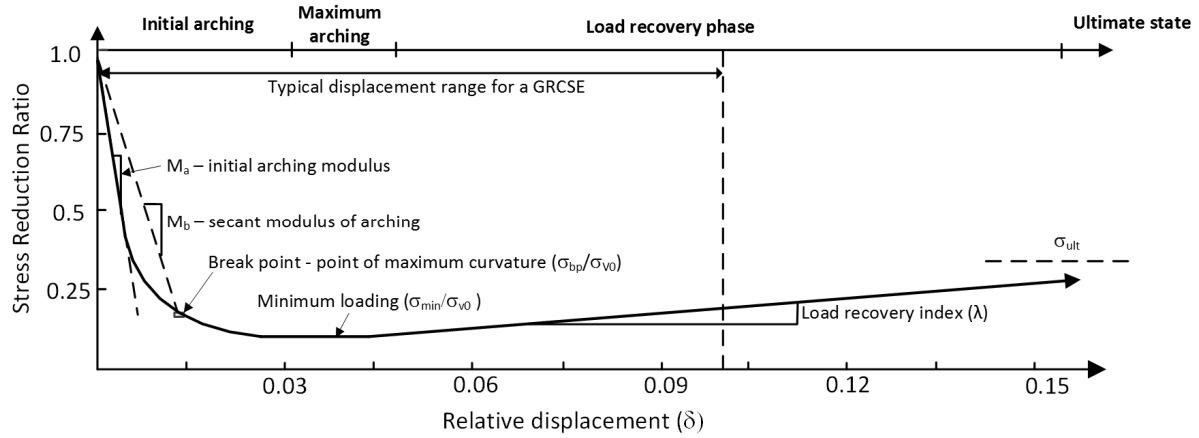


Figure 4. Characteristic Ground Reaction Curve (modified from Iglesia et al. 2013)

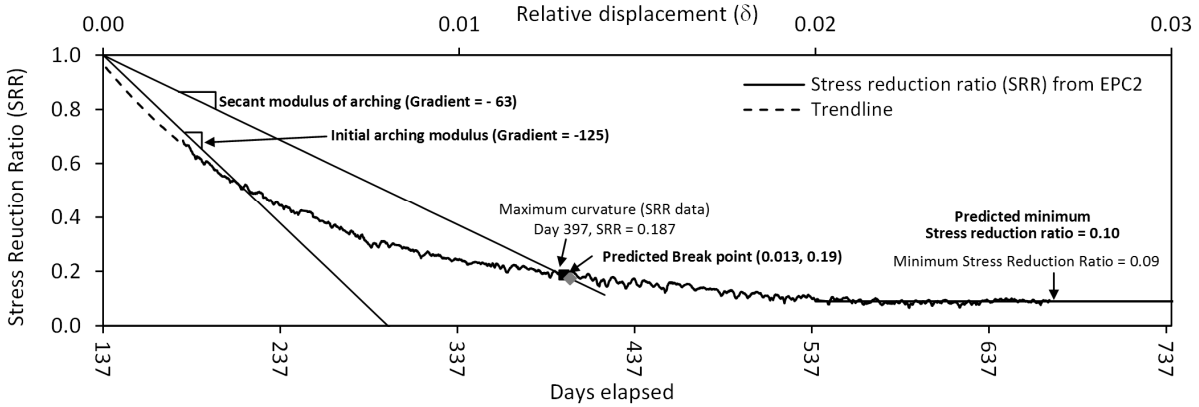


Figure 5. Area #2 – Stress Reduction Ratio based on EPC2 and predicted Ground Reaction Curve values (in bold)

6 IMPLICATIONS FOR THE DESIGN OF GRCSE

The development of arching stresses up to the period of maximum arching was found to be in good agreement with the values predicted from the Ground Reaction Curve method. This behaviour also agrees well with the settlement analysis and strain gauge data (see King *et al.* 2016b) which suggests about 30 mm to 60 mm of sub-soil settlement has occurred to date. The applied stress currently acting on the sub-soil is about 10 kPa and under these stresses acting on Coode Island Silt, on-going settlement, if it is occurring, is due to creep settlement. Rates of long-term creep settlement are described by Ervin (1992) and Srithar (2010), and on this basis, it is expected that long-term settlement of the sub-soil will continue for much of the design life of the embankment, and more importantly, will continue until the loss of sub-soil support condition occurs. The Ground Reaction Curve describes an increase in arching stresses after the period of maximum arching, i.e., increasing stresses acting on the geogrid in the long-term. On this basis, four phases of arching development as they relate to this GRCSE are outlined in Figure 6.

Based on the analysis of the arching stress development (Figure 6), the stress acting on the geogrid when the loss of sub-soil support condition occurs is predicted to be 11.4 kPa and in the load recovery

phase. This highlights two important findings relevant to the behaviour of GRCSEs: 1) the stress conditions that established shortly after construction (maximum arching condition) are not in a state of equilibrium nor are they representative of the long-term stresses (the stresses are expected to increase by 30 % over the long term) and 2) the majority of the base settlement occurs post-construction. This is due to the small amount of stress acting on the sub-soil at maximum arching. i.e. it is difficult to "impose" the loss of subsoil support condition once maximum arching develops. Whilst much of the discussion presented focuses on the stress development, it is the base settlement that governs surface settlement and serviceability behaviour. These findings have important implications for the design of shallow height GRCSEs as this post-construction base settlement can translate to surface settlement and lead to serviceability failure. The serviceability behaviour of shallow height embankments is examined further in King *et al.* (2016d).

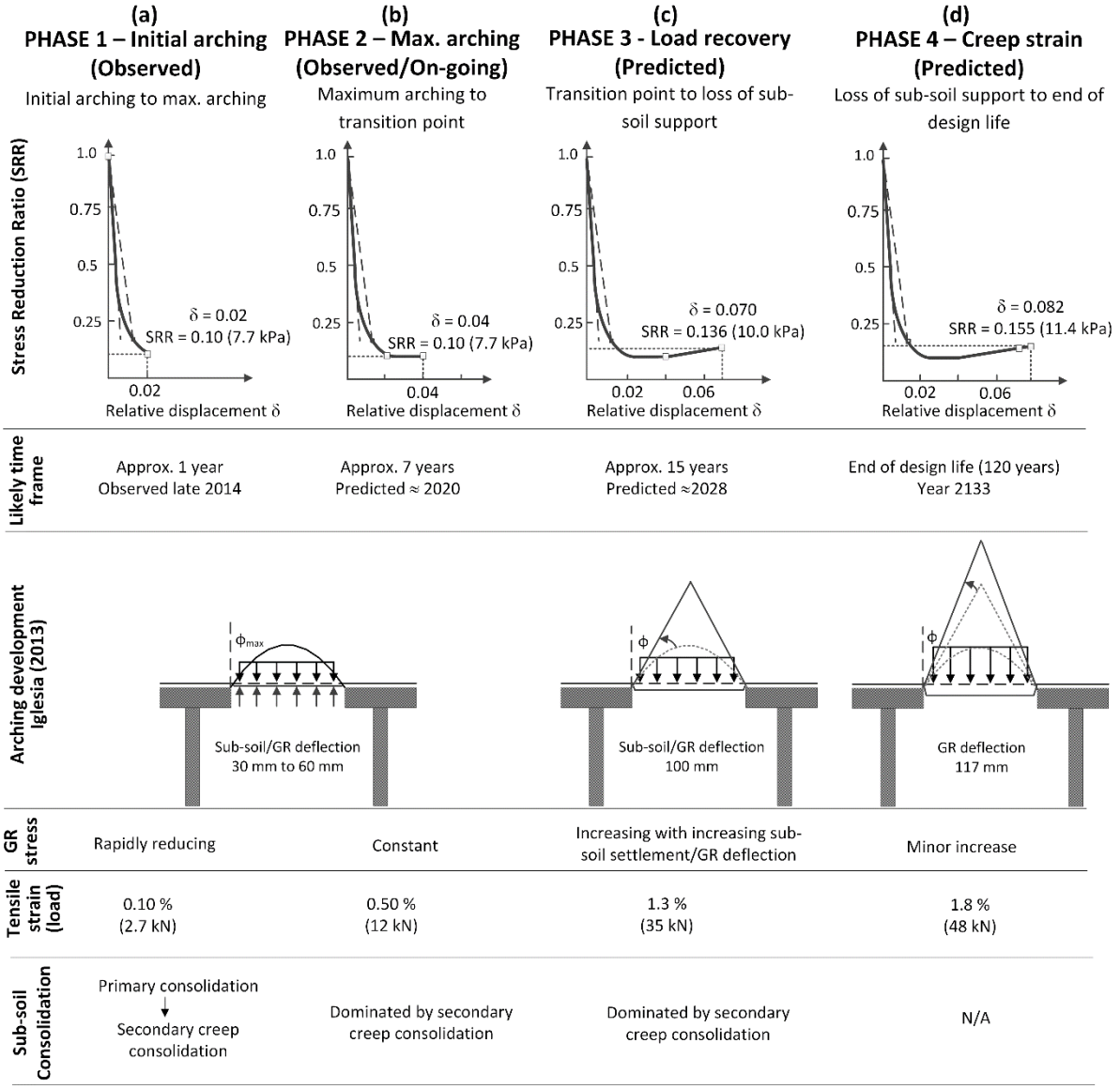


Figure 6. Four phases of arching development based on application of GRC method to Area #2 – (a) Initial arching (b) Maximum arching (c) Load recovery (d) Creep strain

7 CONCLUSION

A GRCSE has been extensively instrumented in Melbourne, Australia and monitored for nearly three years. The findings of this case study has been presented in a number of journal and conference publications and some of the implications of these research findings as they relate to the design of a GRCSE have been briefly outlined in this paper. Interested readers are referred to the authors' journal publications for further details. The key finding relating to the load transfer platform, which has been

the focus of this paper, is the relationship between the development of arching stresses and sub-soil settlement. The widely adopted “two-step” design approach for load transfer platform design, found in many design standards, has been described and compared with the four phase of arching development described by the authors (Figure 6). The limit equilibrium models used in these “two-step” design approaches describe the arching stress/deformation relationship as a constant. The authors consider that the development of arching described by an initial, maximum, load recovery and creep phase of arching is a concept that improves the understanding of load transfer platform behaviour, enables assessment of serviceability behaviour and is of great benefit to designers. Further research involving centrifuge embankment models and non-destructive imaging techniques is currently being undertaken at Monash University to develop these concepts relating to the arching stress/deformation relationship into a GRCSE design method.

8 ACKNOWLEDGEMENTS

The lead author would like to thank his co-supervisors, Joel Gniel (Golder Associates) and Ha Bui (Monash University) for their support during his Ph.D. studies, and in addition, Golder Associates and Monash University for the financial supported provided which enabled the author to pursue his PhD studies. We are grateful to the Regional Rail Link – City to Maribyrnong Alliance (RRLCMR) for supporting and providing the opportunity to undertake this field case study.

9 REFERENCES

British Standards Institution (2010) *BS 8006-1. 2010. Code of Practice for Strengthened/Reinforced Soils and Other Fills*, London, UK.

EBGEO (2010). *Recommendations for Design and Analysis of Earth Structures Using Geosynthetic Reinforcements - EBGEO* (2011), Translation of the 2nd German edition, German Geotechnical Society, Ernst & Sohn, Germany.

Ervin, M. C. (1992). "Engineering properties of Quaternary age sediments of the Yarra Delta", in Peck, W.A., Neilson, J.L., Olds, R.J. and Seddon, K.D. (eds.), *Engineering Geology of Melbourne*, A. A. Balkema, Rotterdam, Netherlands, pp. 245-259.

Gniel, J. and Haberfield, C. (2015). "Design, construction and performance of a tied-wall embankment supported on concrete column ground improvement", *Proceedings of the International Conference on Geotechnical Engineering: Soil-Structure Interaction, Underground Structures and Retaining Walls*, St. Petersburg, Russia, June 2014. IOS Press, pp. 18-27.

Iglesia, G. R. (1991). *Trapdoor experiments on the centrifuge - a study of arching in geomaterials and similitude in geotechnical models*, Ph.D. thesis, Department of Civil Engineering, Massachusetts Institute of Technology, Massachusetts, U.S.A.

Iglesia, G. R., Einstein, H. H. and Whitman, R. V. (2013). "Investigation of Soil Arching with Centrifuge Tests", *Journal of Geotechnical and Geoenvironmental Engineering*, 140(2), doi: 10.1061/(ASCE)GT.1943-5606.0000998

King, D. J., Bouazza, A., Gniel, J. and Bui, H. H. (2016a). "The compressibility, permeability and structured nature of the Coode Island Silt", *Australian Geomechanics*, 50 (2), pp. 45-62

King, D. J., Bouazza, A., Gniel, J., Rowe, K. R. and Bui, H. H. (2016b). "A new insight in the load transfer platform behaviour of a geosynthetic reinforced column supported embankment: importance and implications of the ground reaction curve", *Canadian Geotechnical Journal* (submitted).

King, D. J., Bouazza, A., Gniel, J., Rowe, K. R. and Bui, H. H. (2016c). "Geosynthetic reinforced column supported embankments and the role of ground improvement effects", *Canadian Geotechnical Journal* (submitted).

King, D. J., Bouazza, A., Gniel, J., Rowe, K. R. and Bui, H. H. (2016d). "Serviceability behaviour in geosynthetic reinforced column supported embankments", *Geotextiles and Geomembranes* (submitted).

Neilson, J. L. (1992). "Geology of the Yarra Delta", in Peck, W.A., Neilson, J.L., Olds, R.J. and Seddon, K.D. (eds.), *Engineering Geology of Melbourne*, A. A. Balkema, Rotterdam, Netherlands, pp. 223-245.

Srithar, S. T. (2010). "Settlement characteristics of Coode Island Silt", *Australian Geomechanics*, 45(1), pp. 55-64.

Terzaghi, K. (1943). *Theoretical Soil Mechanics*. John Wiley and Sons, New York.

Proceedings of the 11th ANZ Young Geotechnical Professionals Conference – 11YGPC
Queenstown, New Zealand
25 – 28 October 2016

An Assessment of Foundation Rocking Behaviour based on Field Observations

S. J. Harris[1], M.IPENZ.

[1]Geotechnical Engineer, AECOM New Zealand Limited, P.O. Box 434 Waikato Mail Centre, Hamilton 3240; PH (+64) 7 959 1766; email: sam.harris@aecom.com

ABSTRACT

Controlled foundation rocking can be considered a satisfactory response to dynamic loading, as it can reduce the stress induced in the super structure, and it can reduce the required foundation size. This paper presents the results of a geotechnical assessment into the rocking behaviour of shallow foundations of a flying fox. The foundations of the flying fox were showing considerable rocking behaviour due to the dynamic loading effect when in use. This rocking behaviour was observed in the field, and the geotechnical aspects modelled using the methods set out by Pender et al. (2014). The results are then related to a more significant structure; a 550 tonne silo store. If rocking of this foundation had been allowed, then considerable material savings in the foundation construction could have been made.

Keywords: Shallow, foundation, rocking, flying fox.

1 INTRODUCTION

Shallow foundations designed in accordance with the New Zealand Building Code (NZBC) (DBH, 2011) are designed so there is no contact pressure lost between the underside of the foundation and the subgrade under an applied moment. Typically, such applied moments arise from lateral loads (usually wind and seismic) applied to the superstructure at some height above the foundation. To ensure contact between the foundation and subgrade is not lost, these foundations are designed so the following inequality is met:

$$e \leq \frac{\mathrm{B}}{6} \tag{1}$$

Where *e* is the applied eccentricity, or point of application of the resultant force on the underside of the foundation. This eccentricity is defined as the ratio of the moment to vertical force applied to the foundation. *B* is the foundation dimension perpendicular to the axis of which the moment is applied about. Should the applied eccentricity increase beyond this equality, then contact pressure will be lost on one side of the foundation, and uplift of the foundation will occur at this side. Rocking foundations are foundations in which this contact is allowed to be lost. Under a reversing lateral load (i.e. seismic), contact is lost on one side of the foundation, re-made, and then subsequently lost on the other side of the foundation as the load reverses. Thus the foundation displays rocking behaviour.

Foundations which are designed to rock have a distinct number of advantages over traditional foundation design (Gazetas, 2015). Principal among these is the forces and stresses which are applied to the superstructure are limited by the maximum overturning moment which can be applied to the foundation. Thus the structure needs only designing for these forces (Priestley et al. 1978). This limiting force mechanism means there is less chance of damage occurring in the superstructure columns during high lateral loading. The required foundation size can also be reduced, as the inequality shown in Equation 1 no longer needs to be met. This means that construction costs and constructability issues may be greatly reduced.

The benefits of rocking foundations have long been identified in the New Zealand. An investigation into the seismic response of structures on rocking foundations was undertaken by Priestley et al. (1978), who developed a simple method for predicting the maximum displacement of a rocking foundation, and undertook shake-table testing to validate the theory. Taylor and Williams (1979) presented a procedure for the design of rocking foundations in New Zealand. More recently, the work by Pender et al. (2013) to better model soil structure interaction and rocking behaviour and Storie et

al. (2014) who studied the response of structures founded on shallow foundations has added to the state of the art and practice in New Zealand. Further afield, a comprehensive analysis of rocking foundations has been presented recently by Gazetas (2015).

The inspiration for this paper arose from the foundation design of two unique structures which the author was concurrently undertaking; one a flying fox located in a children's playground, the other a large silo store. Diagrams of these structures are presented in Figure 1. The two structures have similar engineering characteristics. Both consist of a centre of gravity situated at a centralised location above a square, shallow foundation. The foundation of the flying fox showed considerable rocking behaviour when in use. It was the author's brief to design a strengthening solution for the foundation to limit this rocking behaviour. The silo foundation was a new build and designed in accordance with the NZBC, so that no foundation soil contact would be lost during lateral loading of the silo.

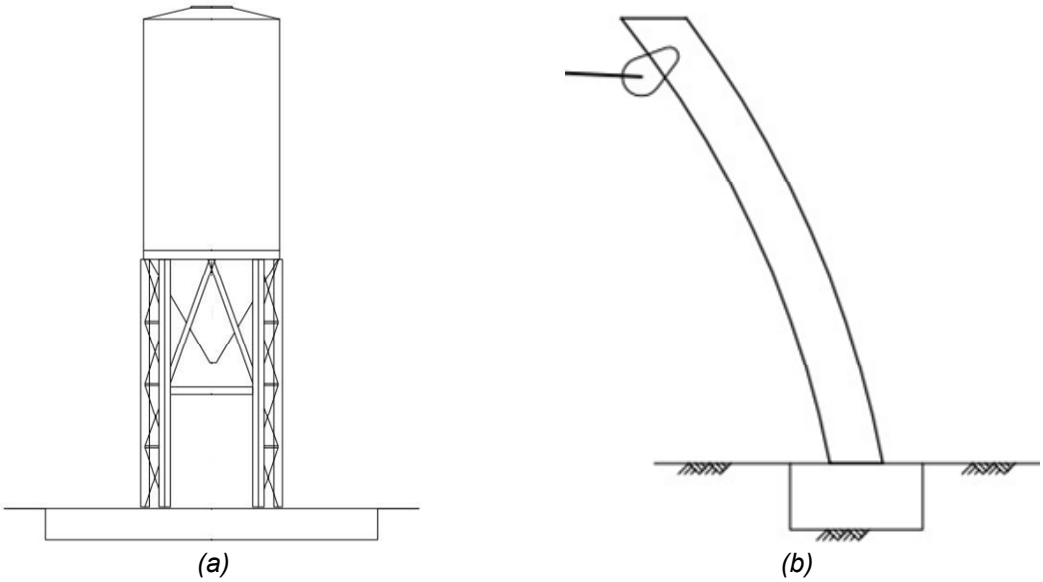
This paper focuses on simple concepts related to foundation design and foundation rocking behaviour related to the design of the flying fox and silo foundations. The intent of this paper is not to provide a new design philosophy, theory or procedure related to rocking foundations. It is acknowledged that rocking foundations have been extensively researched both in New Zealand and overseas (Gazetas, 2015, Pender et al. 2013, Priestley et al. 1978, Storie et al. 2014 and Taylor and Williams, 1979). This case study was undertaken out of interests' sake of the benefits of rocking foundations.

2 DESCRIPTION OF THE TWO STRUCTURES

The flying fox consists of a 25m long wire cable strung between two glulam timber columns. These columns are fixed to shallow foundations via a steel bracket and bolted base plate. The shallow foundations had dimensions of 1m square by 500mm deep. The wire cable is fixed to the timber columns approximately 3.8m above ground level.

The flying fox had been in use over a period of months, and worked adequately when smaller children were using it. However, when larger children (and adults) were using the flying fox, the foundations at each end showed considerable rocking behaviour. The edge of the flying fox was observed to move approximately 40mm (a rotation of approximately 5 degrees) when in use by larger children. The flying fox was a proprietary product and thus no specific engineering design was undertaken for the design of the foundation.

A cone penetrometer test (CPT) and a hand auger (HA) were undertaken to define the underlying ground conditions. The structure was constructed on a very soft Hinuera Formation organic silt layer. This organic silt was tested to have an undrained shear strength of approximately 25 kPa. This layer extended to a depth of approximately 8m; well below the zone of influence of the foundation. Underlying this material was alluvial dense sand of the Hinuera Formation. The groundwater table was measured at a depth of approximately 1m below ground surface.



(a) (b)

Figure 1. The two structures analysed in this case study – (a) a silo store; and (b) a flying fox stand.

The second structure was a large silo store. The silo consists of a steel tank supported on steel columns which were bolted onto a shallow foundation. The tank of the silo is elevated to allow trucks to fit underneath the silo for loading purposes. The silo has a design weight of 550 tonnes. This elevation and large mass means that when full, the silo has a centre of gravity located approximately 18m above ground level. It was the author's brief to design a shallow foundation that meets the NZBC. Two CPTs and two machine drillholes (DHs) were undertaken to assess the ground conditions at the silo site. Ground conditions at the silo consisted of a firm clay, which extended to a depth of approximately 8m below ground level. This clay is part of the Taumatamaire Formation, and consists of extremely weak clasts of mudstone supported in a clay matrix. This unit overlays moderately weathered mudstone of the Taumatamaire formation. The clay was measured to have an undrained shear strength of approximately 35 to 50kPa.

3 ANALYSIS OF THE FLYING FOX

The author was briefed to re-design the foundations of the flying fox so that they would not rock when in use. To do this, the foundation was enlarged to meet the requirements of the NZBC. The foundation was increased in size to 3m by 1.5m. The embedment remained the same (500mm). This increase in foundation size proved to prevent the foundation from showing any signs of rocking when in use. However, the steel base plates showed signs of overstressing (cracking and fracturing) after the foundations had been strengthened (albeit at opposite ends of the flying fox). These steel base plates thus had to be also strengthened by thickening the steel plates (Figure 2).



Figure 2. The steel base plates required thickening following the strengthening of the foundation (at alternative ends of the flying fox). The large weld on the base plate is the results of this thickening.

This example explicitly shows the benefits of a rocking foundation. Prior to the enlargement of the foundation, the moment transferred through the baseplate by the cable forces was limited by the overturning moment capacity of the foundation. When subsequently enlarged, the overturning moment capacity of the foundation was increased, and thus the stresses induced in the baseplate became larger. This eventually caused overstressing and damage to the base plate.

This rocking behaviour has been analysed using the methodology as set out by Pender et al. (2013). The vertical force, horizontal force and moment applied to the underside of the foundation at the destination end as a passenger moves along the flying fox are presented in Figure 3. These forces were derived using simplified assumptions regarding the cable behaviour. Typically this graph could be reversed if plotted for the origin end foundation of the flying fox; however in this case study the origin end foundation and destination end foundation were different sizes. As observed, the horizontal moment applied to the foundation is reasonably consistent throughout the journey, only decreasing as the passenger reaches the very end of the journey.

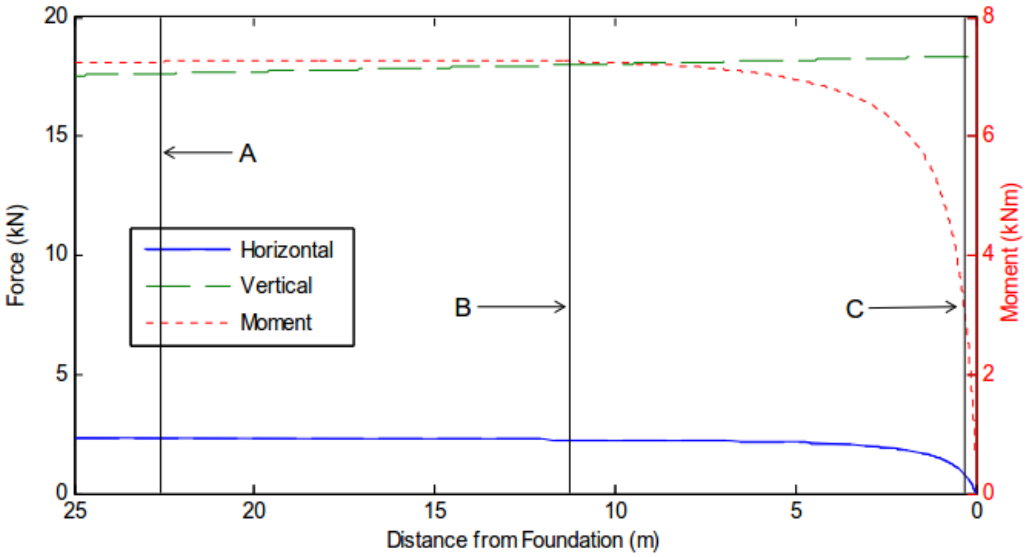


Figure 3. Forces applied to the flying fox foundation as a passenger moves towards the foundation at the destination end of the flying fox.

The applied moment is a function of this horizontal load, and thus follows a similar path. The vertical load increases linearly along the journey. This is the total load acting on the foundation, including foundation weight. The self-weight of the foundation and glulam timber column dominates the vertical foundation load. This structure is unique in that it is self-regulating with respect to overturning. As the applied horizontal load causes rotation of the foundation, the tension in the cable reduces due to rotation of the timber column. This reduces the horizontal load (the load acts more vertically) and thus the moment load applied to the foundation. At the start of the journey, the moment applied to the foundation at the destination end is largest while the vertical load is smallest, thus the eccentricity is at its largest. As the passenger moves towards the foundation, and the moment reduces while vertical load increases, the applied eccentricity decreases. Thus as a passenger gets closer to the destination end foundation, the foundation can withstand more moment capacity before the inequality requirement shown in Equation 1 is not met. The effect of this on the foundation resistance is depicted in Figure 4. These graphs were produced assuming a linear soil response until a yield limit is reached, as set out by Taylor and Williams (1979).

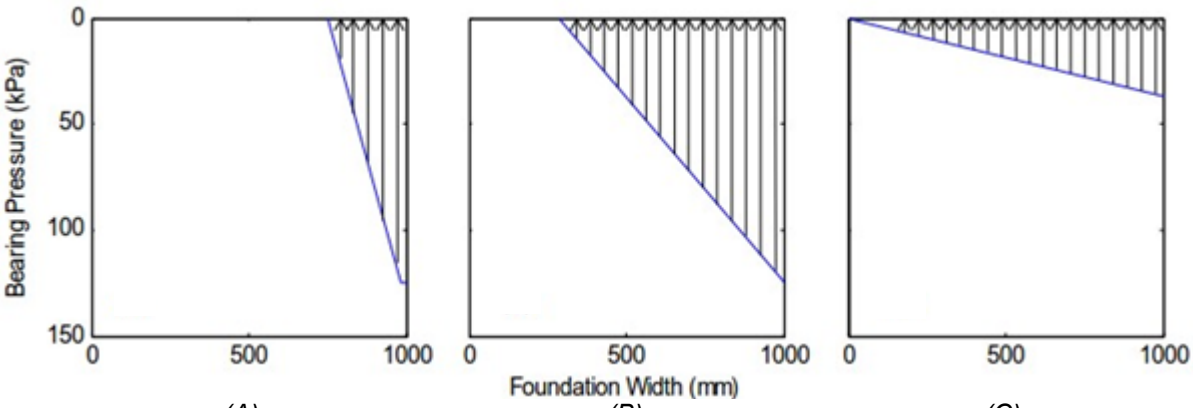


Figure 4. The soil reaction as a passenger moves along the flying fox. Graphs (A), (B) and (C) corresponding to the same points along the journey as depicted in Figure 3.

Near the start of the journey (point A), the soil is at its yielding point under one edge of the foundation. This is depicted by the flat line of the soil pressure curve. Uplift has occurred at the other side of the foundation. If further moment is applied, then the zone of soil yielding (the flat part of the curve) will increase. At point B, The soil is only just at its yielding point under one edge of the foundation. For a square shallow foundation, this occurs when the eccentricity applied to the foundation is as shown in Equation 2. At point A, the eccentricity of the foundation is equal to B/6 (Equation 1 is just satisfied), and thus no loss of contact has occurred at the edge of the foundation.

$$e = \frac{B}{2} - \frac{2V}{3L \cdot q_{ult}} \quad (2)$$

where *B* and *L* are the interchangeable plan dimensions of the foundation, *V* is the vertical load applied to the foundation, and qult is the ultimate bearing pressure of the soil. The foundation behaviour of the flying fox can be further expanded using the method set out by Pender et al. (2013). The moment – rotation relationship of the foundation obtained using this method is shown in Figure 5. Points (A), (B) and C shown on Figure 5 correspond to points (A), (B) and (C) in Figures 3 and 4. As observed, point (C), where no uplift has occurred, is located near the end of the initial linear part of the curve. Point (A) is located at the vertex of the curve. After this point, any extra moment applied to the foundation results in foundation rotation. Point (B) is located in between the two. The rotation of the foundation at point C is approximately 4 degrees, which agrees generally well with site observations. To stop the rocking behaviour of the foundation, the foundation was enlarged considerably. This results in a new moment – rotation relationship as depicted by the solid line in Figure 5. As observed, point (C) on the new foundation is now located on the linear part of the curve. Thus more moment can be applied to the foundation before rocking behaviour initiates, and thus more stress is induced in the superstructure under lateral loading.

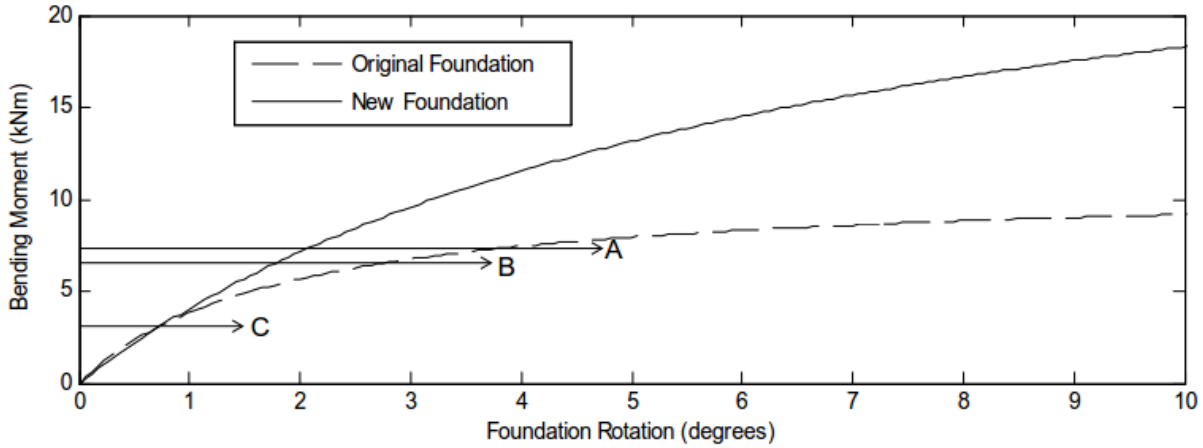


Figure 5. Moment – Rotation curve for the foundation of the flying fox.

4 IMPLICATIONS FOR THE SILO DESIGN

Due to the large mass, height of the centre of gravity and geographical location of the silo, the design moment and eccentricity acting on the foundation under ultimate limit state (ULS) earthquake loadings was large. This governed design of the foundation. The shallow foundation was designed in accordance with the NZBC. To meet static loading requirements, the foundation size was in the order of 12m x 12m by 1m deep. However, to satisfy Equation 1 during seismic events, the foundation was enlarged to 14m by 14m by 1.5m deep.

The moment-rotation curve obtained using the method described by Pender et al. (2013) for the 12m x 12m foundation is presented in Figure 6. The NZ Transport Agency (2013) defined serviceability limit state (SLS; 0.07g) and ULS (0.27g) earthquake induced moment are plotted on the curve. As observed, the SLS moment is located on the linear portion of the curve, implying that uplift of the foundation is unlikely during SLS events. The ULS induced moment plots below the vertex of the curve, which indicates that excessive foundation displacement wouldn't occur during ULS events. The estimated foundation rotation under ULS loading is in the order of 6 degrees. This is a crude estimation as it ignores the response spectra of the structure. Such rotation would not result in overturning of the structure, as the centre of mass is still located inside the foundation footprint; however it is noted that this amount of tilt is beyond reliable analysis. The soil pressure underneath the foundation (insert in Figure 6) indicates the soil pressure has not yet reached its ultimate bearing pressure underneath one side of the foundation (i.e. the eccentricity has not yet reached the limiting value as set out in equation 2). This indicates by allowing some rocking behaviour in the foundation, the amount of concrete required for the foundation would have halved. It is likely that additional savings could have been made in the superstructure if the limiting forces in the superstructure due to the foundation rocking behaviour were analysed and accounted for.

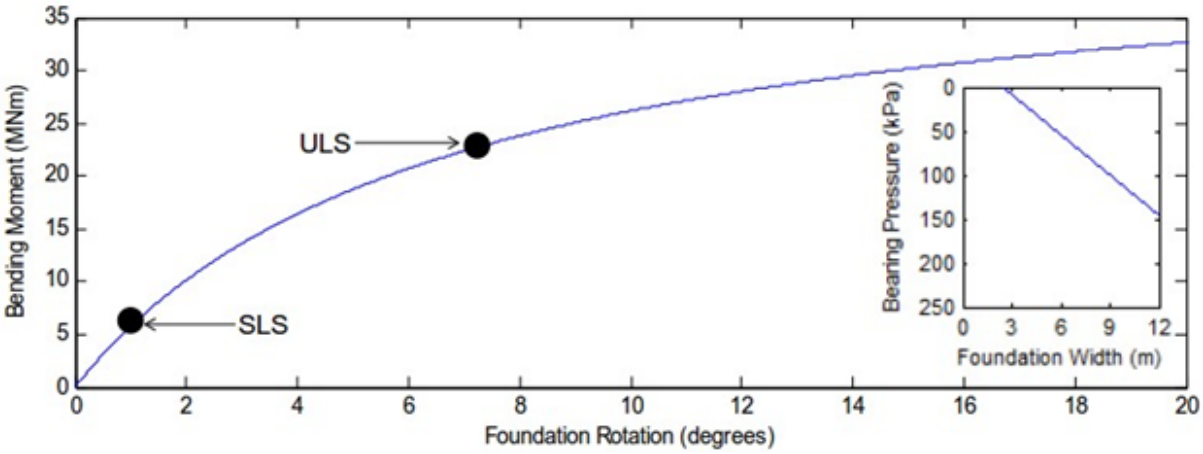


Figure 6. Moment – rotation curve for the silo foundation which satisfies static bearing capacity. The insert shows the bearing pressure reaction underneath the silo foundation under ULS seismic loading.

5 LIMITATIONS OF ROCKING FOUNDATIONS

Rocking foundations have limitations which should be factored in to the consideration of their use. Primarily, they will reduce the factor of safety against bearing capacity during static conditions, simply because of the smaller foundation size employed in rocking foundations. Also, careful analysis of the soil behaviour as it approaches its yield limit is required; strain softening behaviour may be induced and loose sand filling the void made as contact is lost can cause the foundation to 'walk out of the ground'. Also, the relationship between foundation shape and loading direction needs to be considered. Unless the foundation is circular, it will behaviour differently when loaded in different directions (orthogonal and diagonal).

6 CONCLUSION

The benefits of rocking foundations are presented here using two structures of which the author was involved in the foundation design of as examples. The first structure, a flying fox, initially displayed rocking behaviour when in use. When the foundation was subsequently enlarged to prevent this rocking behaviour, additional stresses were induced in the columns of the structure which potentially caused the base plate to fracture. The moment-rotation curve for the foundation, obtained using the method set out by Pender et al. (2013), matched well with field observations made of the flying fox. The second structure was a large silo store. The foundation for the silo was designed so that no loss of contact pressure of the foundation and the subgrade would occur during ULS seismic events. If the foundation was designed to static bearing capacity only, then the moment induced by SLS and ULS events would have been unlikely to lead to excessive foundation displacement. Thus by allowing the foundation to rock, significant material savings could have been made in the foundation construction.

7 ACKNOWLEDGEMENTS

The author would like thank Lars Schmidt of AECOM NZ for his input and advice.

REFERENCES

Department of Building and Housing (DBH), (2011). *Compliance Document for New Zealand Building Code, Clause B1, Structure*, sourced from www.dbh.govt.nz.

Gazetas, G. (2015). "4th Ishihara lecture: Soil-foundation-structure systems beyond conventional seismic failure thresholds", *Soil Dynamics and Earthquake Engineering*, 68, pp. 23-39.

NZ Transport Agency, (2013). *Bridge Manual*, (SP/M/022), 3rd Edition, Revised September 2014.

Pender, M.J., Algae, T.B., Storie, L.B. and Salimath, R. (2013). "Rocking controlled design of shallow foundations", *New Zealand Society of Earthquake Engineering Technical Conference*, Wellington, April 26 – 28.

Priestley, M. J. N., Evison, R. J., and Carr, A. J. (1978). "Seismic response of structures free to rock on their foundations", *Bulletin of the New Zealand National Society for Earthquake Engineering*, 11(3), pp. 141-150.

Storie, L. B., Pender, M. J., Clifton, G. C., and Wotherspoon, L. M. (2014). "Soil-Foundation-Structure Interaction for Buildings on Shallow Foundations in the Christchurch Earthquake", *Tenth U.S. National Conference on Earthquake Engineering*, July 21-25, Anchorage, Alaska.

Taylor, P. W. and Williams, R. L. (1979). "Foundations for capacity designed structures", *Bulletin of the New Zealand National Society for Earthquake Engineering*, 12(3), pp. 101-113.

Proceedings of the 11th ANZ Young Geotechnical Professionals Conference – 11YGPC
Queenstown, New Zealand
25 – 28 October 2016

Unmanned Aerial Vehicles: A new tool for landslide risk assessment

I. C. Jaukovic[1], BSc (Hons) and A. J. Hunter[2], BSc (Hons), MEng.Sc

[1]Coffey Services Australia Pty Ltd, Level 19, Tower B, 799 Pacific Highway, Chatswood, NSW; PH (+61 2) 9406-1000; FAX (+61 2) 9406-1002; email: isabella.jaukovic@coffey.com
[2]Coffey Services Australia Pty Ltd, Level 19, Tower B, 799 Pacific Highway, Chatswood, NSW; PH (+61 2) 9406-1000; FAX (+61 2) 9406-1002; email: andrew.hunter@coffey.com.

ABSTRACT

The use of Unmanned Aerial Vehicles (UAV), or drones, in landslide risk assessments is 'taking off'. This has been made possible by rapid advances in UAV technology in recent years that have seen the emergence of affordable and sophisticated UAV with payloads capable of carrying high resolution cameras and other remote sensing equipment. UAV provide a quick, safe and potentially superior means of inspecting large scale, remote and difficult to access landforms with significant cost benefits compared to traditional inspection methods. UAV can be mobilised quickly, require minimal human resources and facilitate rapid on-site assessment and hazard identification. Inaccessible and hazardous terrain can be inspected in real-time allowing assessment methodology to be adapted in the field. In addition, data collected by UAV can be used to produce high resolution 3D models in 'client-friendly' visualisation formats as well as accurate ground surface surveys. However, if we embrace the use of UAV, what role is left for geotechnical professionals to play? This paper attempts to answer this question and provides recent case studies to demonstrate the application of UAV technology in landslide risk assessment.

Keywords: unmanned aerial vehicles, drones, landslide risk assessment

1 INTRODUCTION

Rapid advancements in remotely-piloted technology have seen a dramatic increase in the use of unmanned aerial vehicles (UAV) for a wide range of applications. UAV, also known as Remotely Piloted Aircraft (RPA), Unmanned Aerial Systems (UAS), or drones, typically comprise an aircraft system remote-controlled by an operator on the ground or by a pre-programmed autonomous piloting system (Antonio, 2016). UAV come in a variety of forms: multi-rotor systems (Figure 1), unmanned helicopters and fixed wing aircraft.



Figure 1. Quad-rotor mini UAV system carrying a high resolution camera.

Since World War II, UAV were developed for military applications, but owing to their increased accessibility and affordability they are increasingly being used for commercial applications and by amateur enthusiasts. UAV applications are wide-ranging and include: surveying, topographic mapping, condition assessments of buildings and structures (such as bridges and seawalls), monitoring of habitats, vegetation and noxious weeds, firefighting, disaster relief, wildlife surveys, geomorphological studies, geophysical surveys and archaeological site inventories (Nardi, 2009; CASA, 2015; Bell, 2016; Walker 2016). Over the past 5 years, the popularity of multi-rotor UAV

systems has increased due to their widespread commercial availability, relatively low cost, sensor technology, ease of operation, and performance (CASA, 2015; Walker, 2016).

2 OPERATION AND LICENCING

Commercial and recreational use of UAV is currently tightly regulated in most countries; however, legislative changes are being implemented in an attempt to keep up with advances in technology. In Australia, UAV pilots must hold certificates for UAV and radio operation, obtained by passing an examination, and recording at least 5 hours of flight or simulation time in a specified UAV category. In addition, UAV pilots must also be employed by a company holding a UAV Operators Certificate. Operation of UAV is generally limited to visual line of sight. Further restrictions apply for the use of UAV in controlled airspace such as within 3 nautical miles of aerodromes, above 400ft (122m) as well as prohibited or restricted areas (CASA, 2015). Additional flight limitations may also be set by clients and public organisations that may place further restrictions on flight areas and data collection (e.g. UAV may not be operated within a certain distance of active transport corridors such as railways and motorways).

There are currently no international standards for the use of UAV for landslide risk assessment purposes, although attempts have been made to draft standards for the use of micro-UAV for rockfall emergency conditions (Giordan et al., 2015).

3 LANDSLIDE RISK ASSESSMENT APPLICATIONS

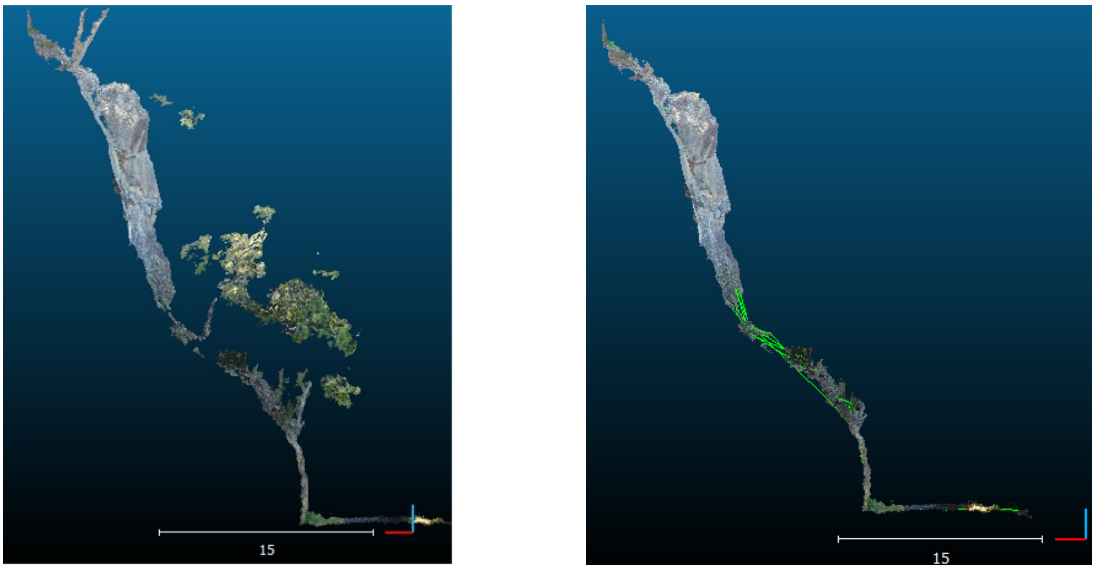
Landslide studies typically involve field mapping to characterise the geomorphological conditions and identify hazards. Depending on the scale of the problem, this can take considerable time and rugged terrain can pose access restrictions. Cliffs and steep slopes can be inspected using rope access methods (Hunter et al., 2009), however this also comes at considerable cost and productivity can be slow. Traditionally a number of remote sensing methods have been employed to complement field studies including: photogrammetry (airborne and terrestrial), stereoscopy, and terrestrial and airborne laser scanning (LiDAR). These techniques can be hindered by short timeframes, 'blind spots' / shadowing caused by slope geometry (resulting in unobserved surfaces), surface roughness and reflectivity, and vegetation screening (Neithammer et al., 2012; Lightbody and Wilkinson, 2015). In addition, captured images typically require editing using sophisticated processing software to correct for optical distortion, such as that caused by variations in relief (Niethammer et al., 2011).

Recent studies have reported on the use of UAV for photogrammetric surveys of rockfall instability, rockfall assessments and coastal risk assessments. UAV have also been used for remote sensing and object-oriented mapping of slow-moving landslides. For example, UAV-assisted monitoring of the Super-Sauze landslide in Germany detected horizontal displacements between 7m and 55m over a 17-month interval (Neithammer et al., 2012). UAV-mounted high resolution remote sensing equipment can also be used to collect subsurface data such as soil moisture and medial grain size (Neithammer et al., 2011). More recently, UAV were used to identify and monitor an emergency rockfall situation in Torino, Italy, to assist civil protection agencies with road safety assessments, by providing information on discontinuities in the rock mass and assisting with the determination of scale, dimensions and likely timing of the failure (Giordan et al., 2015).

4 3D MODELLING

Simple applications of UAV involve real time or post viewing of footage and still photographs of the study area. However, for some applications, visualisation of the terrain can be enhanced by creating 3D Digital Surface Models (DSM) from high resolution images. The DSM is created by generating a point cloud reconstruction of the captured area using image photogrammetric processing of multiple overlapping images (Figure 2). Among other factors, the accuracy of the model depends on high quality data inputs (large image overlap, no blur, similar exposure, good quality photographs and accurate ground control points) and the Ground Sampling Distance (GSD), or the distance between two consecutive pixel centres measured on the ground. Ground Control Points (GCPs) can be used to provide a higher degree of accuracy by orienting 3D models in space. The generation of 3D models using photogrammetric image processing software is possible across multiple digital platforms – for example, most smartphones can generate 3D models using freely available software.

Further processing of the point cloud can filter out or remove vegetation and artificial features to isolate the underlying terrain, producing a Digital Terrain Model (DTM). DTM can also be produced by LiDAR survey; however, these techniques can be hindered by shadowing caused by slope geometry and vegetation. UAV-assisted photogrammetric and LiDAR surveys are less prone to these effects as imagery is captured from a variety of angles.



(a) *(b)*

Figure 2. (a) Point cloud produced by UAV photogrammetry (b) Point cloud with vegetation removed.

5 CASE STUDY: RISK ZONING ALONG A RIVERSIDE ESCARPMENT

The authors have used UAV for several landslide risk studies over recent years. These studies primarily involved inspections of large rock cuts, cliffs, and rugged escarpments close to critical infrastructure. We have found UAV offer a rapid and highly flexible means of data acquisition that can be adapted in real time to suit site conditions.

One example involved the use of UAV to investigate a 30km stretch of road constructed along the foot of a sandstone escarpment adjacent to a large river system on the east coast of New South Wales, Australia (Figure 3). The escarpment reaches elevations of up to 140m above road level, comprising sheer cliffs up to 40m high, steep talus slopes and high rock cuts (Figure 4). The road had been subject to rock falls since construction about 100 years ago, with some events resulting in up to 20m^3 of debris on the road. The escarpment is heavily forested and largely inaccessible.



Figure 3. Riverside escarpment captured by UAV.



Figure 4. UAV photo showing cliffs and loose talus 40m above road (road lower right).

Due to the extent of the escarpment, a high-level risk zoning study was required to rank areas of highest risk and allow risk management works to be prioritised. An initial risk assessment was performed to identify high risk sites using traditional methods such as orthophotos, topographic maps and a walkover from road level. Following this preliminary assessment, a detailed risk assessment was complemented by UAV flyover to characterise hazards otherwise not observable from road level. UAV flyovers were performed at several of the high risk sites over one day with a total flying time of about 3.5 hours during which time approximately 4km of escarpment was inspected. The largest site comprised an 800m long, 160m high escarpment captured by a flying time of about 35 minutes. By manoeuvring the UAV to different positions, visual obstructions such as trees and topographic features could readily be overcome. A number of 3D DSM of the high risk sites were created from still photographs taken during the flights (Figure 5). These were provided to the client using on-line viewing applications and were very well received due to the ease of viewing and navigation and enhanced the decision making process.

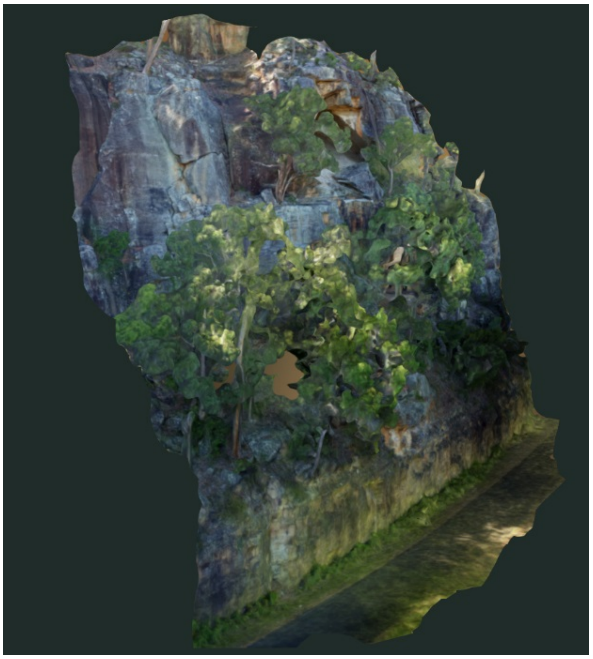


Figure 5. 3D model of cliffs captured by UAV photogrammetry

As the hazards in this study typically comprised detached boulders (talus) and rock falls associated with cliffs, traditional methods of assessment would have lacked the required resolution or been prohibitively expensive (e.g. helicopters). Even helicopters are unable to fly as close to the landform as the UAV, which was able to fly within about 1m of cliff faces and trees.

6 CASE STUDY: DISCONTINUITY MAPPING TRIAL

6.1 Background

A discontinuity mapping trial was conducted at a former quarry site in a porphyritic, columnar basalt (Figure 6). The purpose of the trial was to investigate the reliability of discontinuity orientations acquired remotely using an UAV, for use in kinematic analyses. The orientation of 20 discontinuities, all of which were joints, were measured using a geological compass. The joints were labelled in the field. Images were captured using a 'DJI Inspire 1' Mini-UAV fitted with a 'DJI X5' digital camera with 16MP resolution capability. Six GCPs were surveyed with a differential GPS to georeference the images.

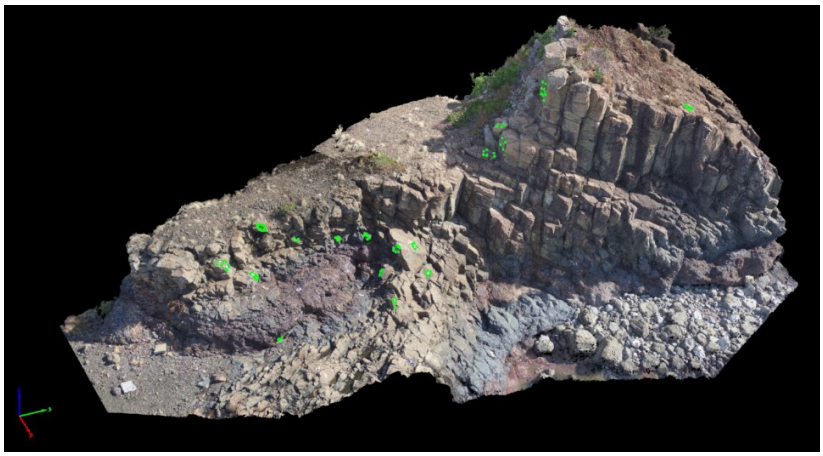
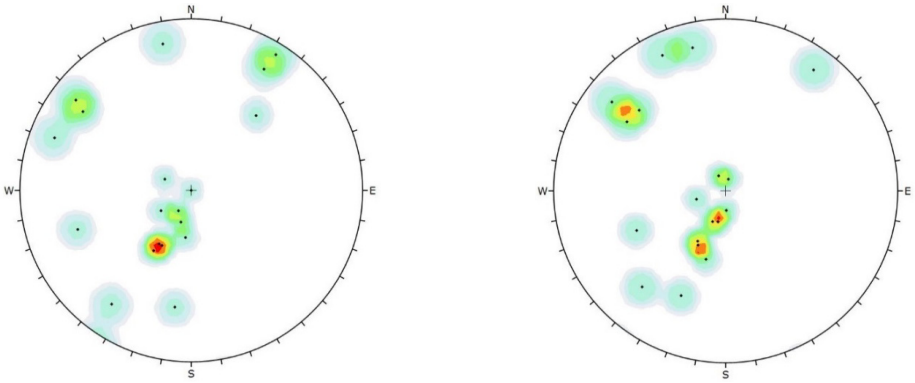


Figure 6. 3D model of case study area captured by UAV

6.2 Discontinuity Mapping

High resolution images captured by the UAV were used to create a point cloud of the study area using photogrammetric processing software. The GSD achieved was approximately 6mm, resulting in a point cloud with a confidence to about 15mm. To account for this variability, a defect surface was drawn by connecting points to form a visual plane of 'best-fit' for each joint plane. The orientation of each plane was then calculated manually using a 3D civil design software package. Field and UAV defect measurements are shown on the stereonets in Figure 7.



(a) *(b)*

Figure 7. Stereographic projections of defect orientations: (a) poles of direct measurements (b) poles of UAV-measured defect orientations.

UAV measurements were found to vary, on average, by up to 5° in dip and up to 21° in dip direction. Three joints were found to vary by up to 56° in dip direction however this appears to be due to the joints being curved or shallowly dipping. Given that the compass measurements represent the orientation of planes at a point, whereas the 3D model provides a more average representation of the plane, the trial indicates that UAV photogrammetry could be a viable alternative to other methods commonly used to collect defect orientation information such as terrestrial photogrammetry and laser scanning.

7 CONCLUSIONS

The application of UAV to landslide studies reported in the literature has increased significantly over the last 5 years, in response to advances in the technology and increased affordability. One of the greatest benefits of UAV assessments is a significant reduction in field time due to the ability to rapidly survey large areas. UAV imagery allows hazards and features to be viewed from multiple angles in almost any terrain, which is not achievable using any other single method. The flight path can be easily modified in real-time under the guidance of a geotechnical professional, typically without causing disruption to the operation of infrastructure such as roads and railways. The ability to generate accurate 3D photogrammetry models using open source software from photographs taken at multiple angles is a valuable visualisation tool that can be used by geotechnical professionals and clients alike. The discontinuity mapping trial reported in this paper indicates that these models are reasonably accurate and could offer a significantly cheaper alternative to other methods currently used to remotely measure discontinuity orientations on slopes. Due to the high repeatability of this data, such models could be used to detect creep movements in landslides and monitor rock fall history.

We have found that in some circumstances, such as high glare conditions, real time observations of site features can be hampered by reflections on the UAV controller LCD screens. This can result in longer flight times and can place a greater emphasis on review of the data following fieldwork. Advances in virtual reality headsets that allow the user to control the direction of the camera in the field have the potential to overcome this in the near future. UAV use can also be limited by wet weather, strong winds and dense vegetation. We have also experienced significant interference from aggressive birds.

In our experience it is vital that geotechnical professionals direct or control the UAV survey, due to the high possibility of important site features being inadequately captured. However, we anticipate that with time, virtual reality technology may allow an office-based geotechnical professional to observe the flight in real-time and therefore perform their role remotely.

8 ACKNOWLEDGEMENTS

The authors gratefully acknowledge Mr Zack Wasson for his comments on this paper and Diodrone for their UAV operations and photogrammetry processing of the case study data. The authors wish to thank Mr Robert Turner of Coffey Services Australia Pty Ltd and an anonymous reviewer for proof reading this paper and providing valuable comments.

REFERENCES

Antonio, A. (2016). “Drones: new tools for natural risk mitigation and disaster response”, *Current Science*, 110(6), pp. 958-959.

Bell, R.S. (2016). “The Bureau of Land Management and the use of Unmanned Aircraft Systems (UAS) for Resource Management”, *FastTIMES*, pp. 29-33

CASA (2015). Remotely piloted aircraft systems, Civil Aviation Safety Authority, accessed 6 June 2016 <https://www.casa.gov.au/aircraft/landing-page/remotely-piloted-aircraft-system>

Danzi, M., Di Crescenzo, G., Ramondini, M. and Santo, A. (2012). “Use of unmanned aerial vehicles (UAV) for photogrammetric surveys in rockfall instability studies”, *Rendiconti Online Della Società Geologica Italiana*, 24, pp. 82-85.

Giordan, D., Manconi, A., Facello, A., Baldo, M., dell’Anese, F., Allasia, P. and Dutto, F. (2015). “Brief Communication: The use of an unmanned aerial vehicle in a rockfall emergency scenario”, *Natural Hazards and Earth System Sciences*, Vol. 15, pp. 163-169.

Hunter, A. and Hendrickx, M. (2009). “Rope access methods in Slope Risk Assessment and remediation”, *Australian Geomechanics*, 44(2).

Lightbody, S.W. and Wilkinson, A. (2015). “Rockfall protection in Gibraltar”, *Proceedings of the XVI ECSMGE – Geotechnical Engineering for Infrastructure and Development*, pp. 1591 – 1596.

Nardi, D. (2009). “Intelligent systems for emergency response”, invited talk in *Fourth International Workshop on Synthetic Simulation and Robotics to Mitigate Earthquake Disaster* (SRMED 2009), 6th July, Graz, Austria

Niethammer, U., Rothmund, S., Schwaderer, U., Zeman, J. and Joswig, M. (2011). “Open source image-processing tools for low-cost UAV-based landslide investigations”, *International Archives of the Photogrammetry, Remote Sensing and Spatial Information Sciences*, Vol. XXXVIII-1/C22, pp. 161-166.

Neithammer, U., James, M. R., Rothmund, S., Travelletti, J. and Joswig, M. (2012). “UAV-based remote sensing of the Super-Sauze landslide: Evaluation and results”, *Engineering Geology*, 128, pp. 2-11.

Walker, B. (2016). “Developing high sensitivity magnetometers for unmanned aircraft”, *FastTIMES*, pp. 16-22

Proceedings of the 11th ANZ Young Geotechnical Professionals Conference – 11YGPC
Queenstown, New Zealand
25 – 28 October 2016

Analysing Slope Change at Globe Progress Open Pit, Reefton

T. Howard[1] and A. Cantwell[2]

[1]Department of Geological Sciences, University of Canterbury, 20 Kirkwood Avenue, Christchurch, New Zealand;
now at: Soil and Rock Consultants; PH 021 1164484; email: timh@soilandrock.co.nz
[2]ARANZ Geo, 41 Leslie Hills Drive, Christchurch 8011, New Zealand; PH 021 2720663; email: andrewc290@gmail.com

ABSTRACT

Airborne LiDAR and photogrammetry data collected across 2014 and 2015 was used to develop detailed digital terrain models and produce slope change models at the Globe Progress open pit mine in Reefton, New Zealand. Coupling of these slope change models with existing geotechnical data from the last eight years of mining allowed the north-east pit wall to be subdivided into four geotechnical domains, to understand the mechanism of failure and quantify the movement along the pit wall. The models were created in Leapfrog software developed by ARANZ Geo, allowing for data processing, measurements and models to be created in a single effective program. The range of maximum slope movement between the four domains is 1.6 m - 3.9 m with the volume of material loss from the pit wall in the order of 1800 m^3 - 4900 m^3. The failure across the domains is controlled by complex geology associated with the footwall of the major gold bearing shear zone. Asymmetric folds displaced by shears across the pit wall cause unfavourable bedding dip orientations, leading to the observed topple and planar failure within each domain.

Keywords: remote sensing, slope change, engineering geological model

1 INTRODUCTION

The use of remote sensing data has become common for assessing change in surface topography, for example the work undertaken by Turner et al. (2015) and Kromer et al. (2015). This work commonly uses freeware such as Cloudcompare developed by DanielGM to compare point clouds, providing the relative slope movement. A different software package known as Leapfrog developed by ARANZ Geo is used to investigate pit wall change at the Globe Progress open pit mine in Reefton, where the north-east (NE) pit wall is actively deforming.

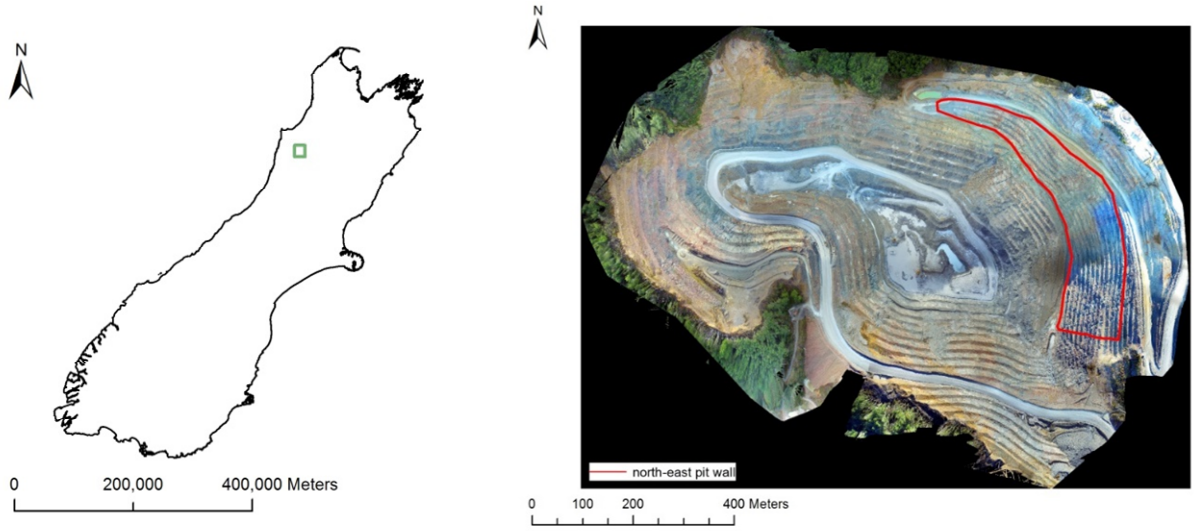
This software provides solutions to solve geological modelling problems through an implicit modelling technique (Alcaraz et al., 2015). Routinely used in the mining industry for exploration purposes, grade control (Stewart et al., 2014) and creating geological models (Rose and Ireland, 2014), the distance function is used to assess slope change between multiple point clouds.

This project aims to quantify slope change of the NE pit wall between successive 2014 and 2015 airborne Light Detection and Ranging (LiDAR) and photogrammetry surveys. A review of existing geological data coupled with the change models allows for the development of geotechnical domains.

1.1 Geological Setting

The Globe Progress open pit mine is located 7 kilometres south-east of Reefton and was commissioned by OceanaGold in 2007 (Figure 1). The goldfield is located within a highly active geological zone. Hydrothermal fluids emplaced ~65,000 kg of gold in typical quartz vein hosted deposits, associated with an east - west shortening event during the late Ordovician early Silurian approximately > 390 Ma (Clark, 1996; Kennedy, 2009).

The mine consists of several open pits developed along a regional shear structure, in intensely folded and sheared greywacke and argillite turbidite sequences (Clark, 1996; Kennedy, 2009). The region receives significant annual rainfall of around 2000 mm (Kennedy, 2009). The area of interest at the NE pit wall is approximately 7 ha, from relative level (RL) 410 to 530 within the OceanaGold co-ordinate system.



(a) *(b)*

Figure 1. (a) South Island, New Zealand; and (b) approximate 7 ha area of interest outlined, from RL 410 – 530 within the NE pit wall at the open pit mine

2 METHODS

2.1 Analysing Slope Change

Georeferenced airborne LiDAR and photogrammetry data supplied by OceanaGold consisted of dense point clouds which were reduced in size using a least squares system approach. This allowed for more user friendly datasets to be compared. The processed point clouds were implicitly modelled into detailed digitals terrain models (DTM) across 2014 and 2015.

The nearest neighbour distance between the two DTMs quantifies the surface movement between successive years and identifies areas which were prone to movement across that time period. This method was adapted for each of the two surfaces in order to measure the 'gain' and 'loss' with reference to the 2014 surface (Figure 2). The 2014 surface was treated as the lower surface, therefore anything which was above this surface was considered 'material gain' while anything below this original surface was considered 'material loss'. All changes are assumed natural in this project.

A Leica TM30 total station was installed at the open pit mine, with 22 prisms located within the area of interest. The vector distances at discrete locations along the pit wall were measured to compare with the point cloud derived model. Radar data was also available for the pit wall; however this is useful for 'real time' measurement and prediction of rockfall across hour to day time periods. A comparison cannot be made between the radar and annually acquired point cloud data due to the difference in temporal resolution.

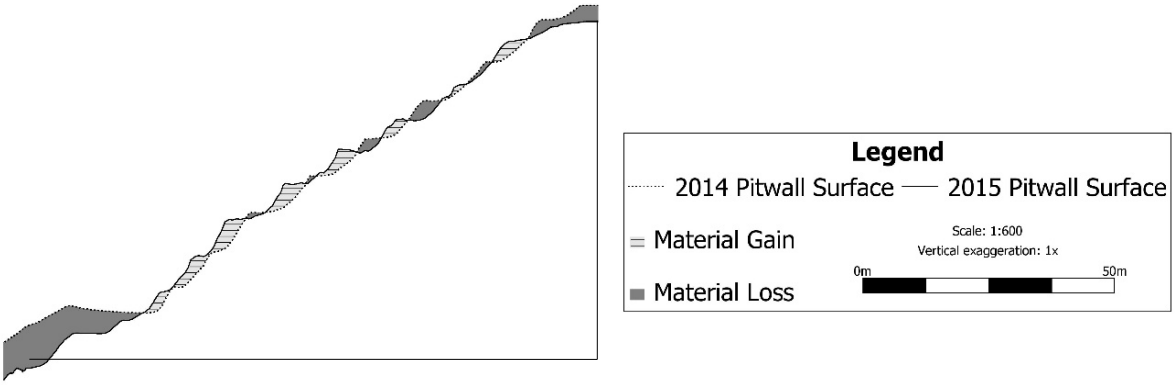


Figure 2. Nearest neighbour measurement of material loss and material gain from the 2014 pitwall topographic surface. Both the volume and distance between successive surfaces was calculated.

2.2 Geotechnical Domain Development

Georeferencing and overlaying the data in Leapfrog enabled the areas of slope change to be compared against the engineering geological review. Leapfrog Mining software was used to fit surfaces to the measured geotechnical data from 8 years of mining, including bedding and joints, to create representative 3D surfaces. This enabled the NE pit wall to be refined into domains in order to accurately represent the movement within these areas. The change, volume loss and failure mechanism could then be understood for each section of the pit wall and better describe the situation occurring.

3 CHANGE MODEL

The change model indicated the absolute loss of material from the pit wall was between 0 m - 3.6 m (Figure 3) across the NE pit wall. The volume lost across the wall is 12,850 m^3. The maximum gain of material was 3.9 m measured as the nearest neighbour distance which could also be influenced by rockfall from above. The total station prisms indicated movement of 0.3 m – 4.9 m in a direction of 150° – 270 °.

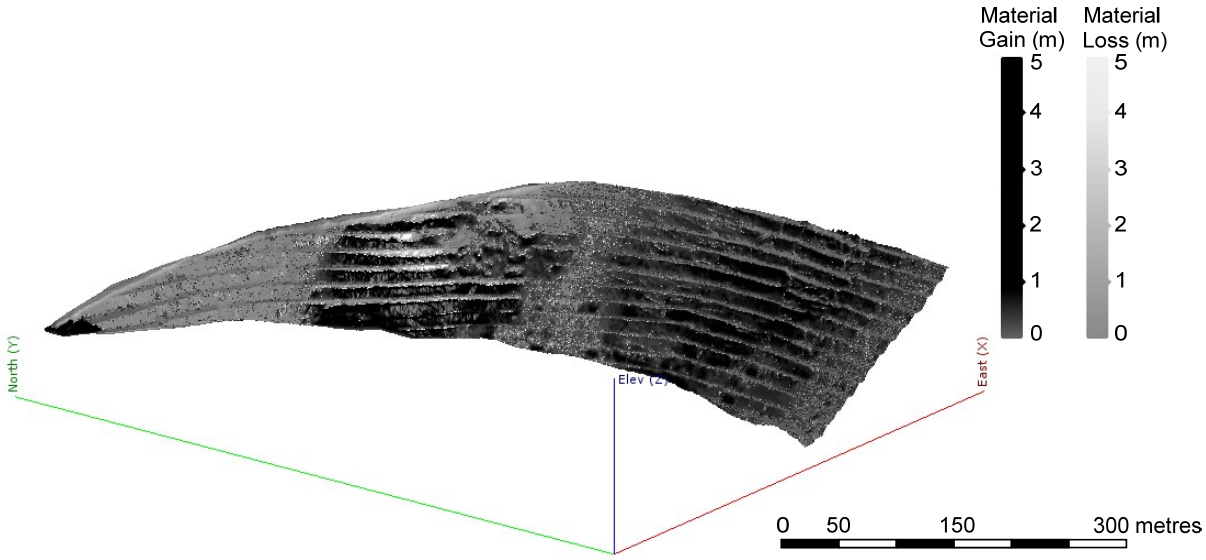


Figure 3. DTM change model developed from LiDAR and photogrammetry point clouds

A comparison of the change measured through each technique shows that similar values are observed across similar areas of the wall, validating each method of measuring the slope change. Advantages of continuous point cloud data include data across the entire pit wall and the ability to estimate volume changes. Disadvantages include shadow areas or occlusion zones through data acquisition and the computer power required for data processing. The lack of spatial coverage across the slope limits prism monitoring, as this does not assist with the interpretation of local complexities within the failure mass

The two point clouds were assumed to be georeferenced correctly with relation to one another and therefore it was deemed unnecessary to validate them as with other similar studies such as Turner et al. (2015). In the future, validation of the two point clouds could be undertaken to ensure any errors in the data are accounted for.

4 ENGINEERING GEOLOGICAL REVIEW OF THE NORTH-EAST PIT WALL

4.1 Rock Mass

The north-eastern and eastern (E) pit walls make up the footwall of the Oriental shear which is associated with greater deformation than the hanging wall with a Geological Strength Index (GSI) of 35 – 50 (OceanaGold, 2015; Golder Associates, 2014). Complex geological structures generally comprising of several tight asymmetric folds trending N – S, with a number of NE – SW striking shears and faults that offset the folds are characteristic of this area (Golder Associates, 2014). Closely

spaced bedding surfaces form the dominant structural fabric while less persistent jointing is also prevalent (Golder Associates, 2014).

4.2 Observed Failures

The majority of the NE pit wall is cut along the western limb of an anticline which results in bedding dipping out of the face at approximately 30 – 40°. The upper eastern pit wall is cut through the eastern limb of an anticline resulting in bedding dipping at 60 - 80° into the face (Golder Associates, 2014). Two zones of planar sliding and a large zone of flexural toppling have been observed in the NE and E pit walls (OceanaGold, 2015; Golder Associates, 2014). Planar sliding is associated with bedding surfaces which daylight and dip out of the batter slopes, while toppling is experienced along steeply dipping limbs (~62°) of the anticline structure into the pit wall (OceanaGold, 2015; Golder Associates, 2014).

4.3 Batter Design

The batters at the NE pitwall are designed according to the local structures and failure type. A management style approach, whereby smaller bench scale failures and prevention of deep seated failure is designed for. The areas which are considered susceptible to planar sliding have been designed with an angle of 34 – 38°, while the areas prone to topple have been designed at ~45° and cable bolted allowing a safe and easier clean-up of debris and prevention of a deeper seated failure (OceanaGold, 2015).

5 GEOTECHNICAL DOMAINS

The engineering geological review encompassing data from the last eight years of mining, site observations and associated change models enabled the NE pit wall to be further divided into four geotechnical domains (Figure 4). The domain locations are ultimately controlled by the fold hinges and shears which offset bedding. As mentioned above, the major controls on failure are closely spaced bedding surfaces forming the dominant structural fabric while less persistent jointing of the pit wall provides release mechanisms for kinematic failure. Schematic cross sections illustrating the failure mechanisms are shown on Figure 5. A summary of the change information measured in each domain along with the mechanism of failure provided within Table 1.

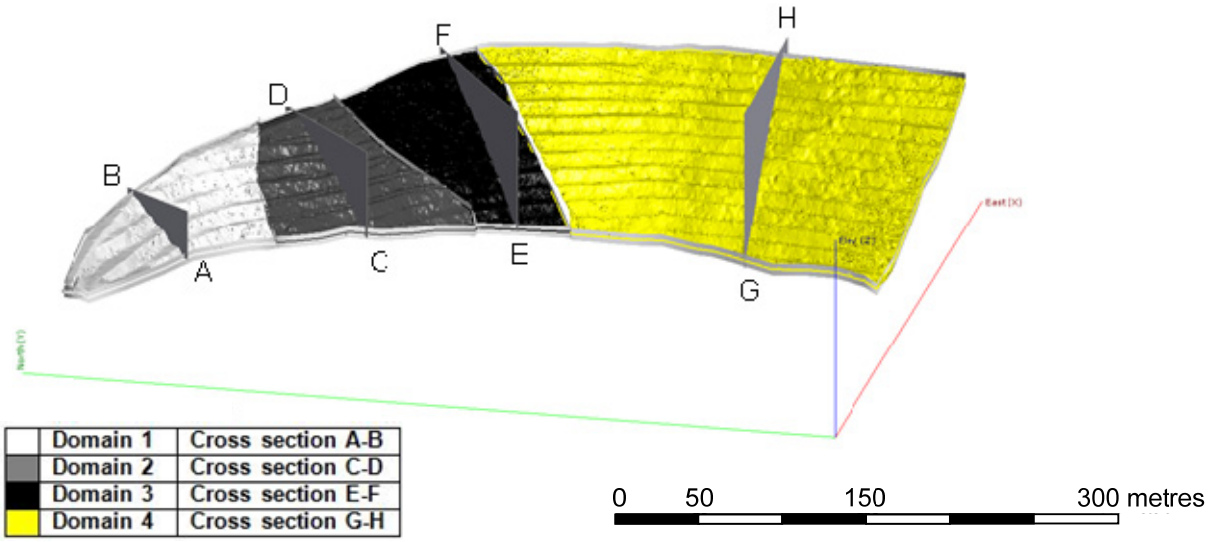


Figure 4. Geotechnical domains based upon geotechnical information and measurements of slope change. Planes show locations of cross sections through each domain.

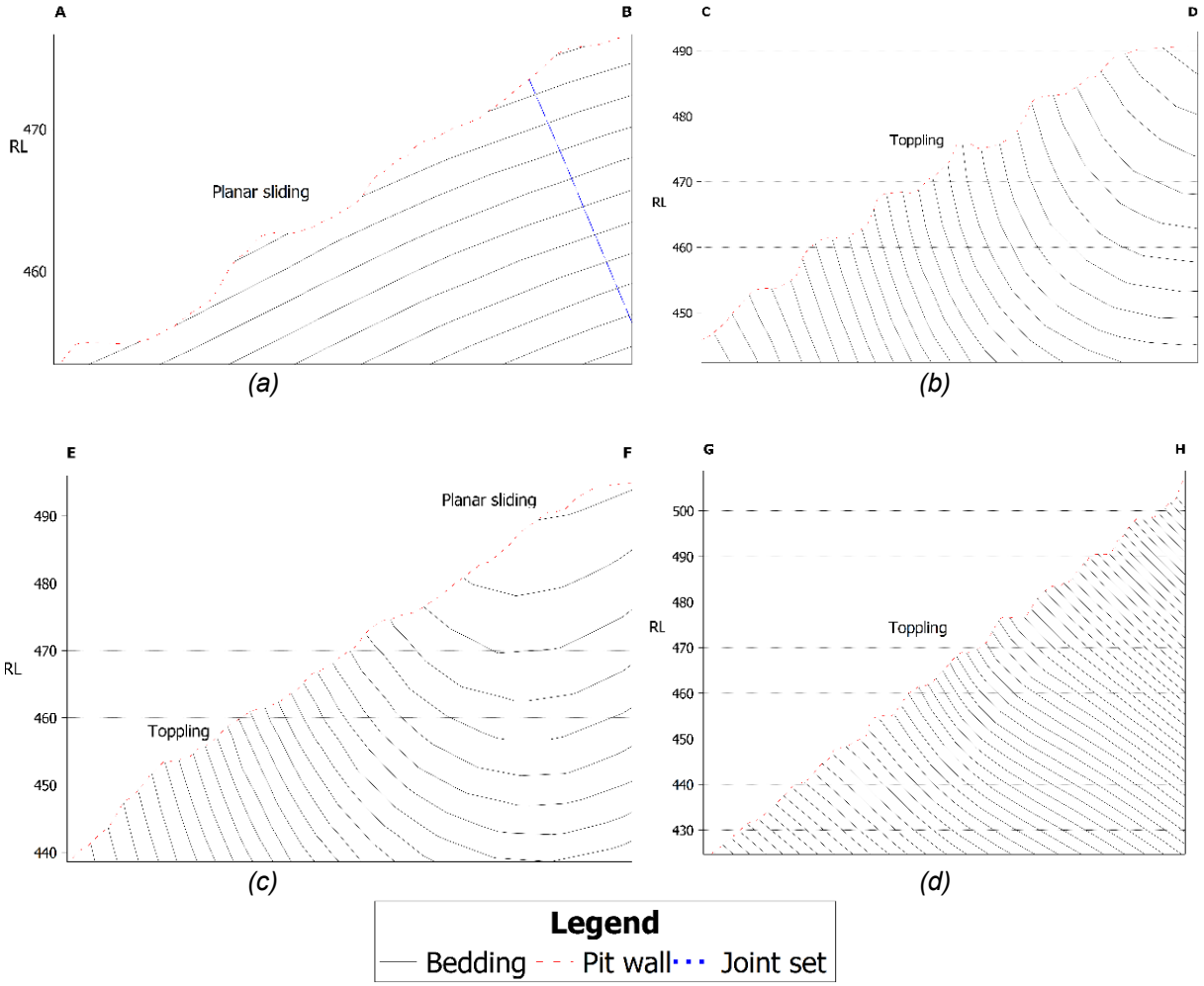


Figure 5. Schematic cross sections highlighting failure mechanisms for each geotechnical domain at the NE pit wall – (a) Domain 1; (b) Domain 2; (c) Domain 3; and (d) Domain 4.

5.1 Domain 1

The failure mechanism in domain 1 is planar sliding, giving rise to slope changes of 0.1 m – 3.6 m. Bedding dipping between 35° - 43° out of the slope, with joints dipping steeply into the slope at 56° – 88° provide release planes for planar sliding to occur. The slope change model of this area shows that the majority of the slope surface within this domain has experienced material loss.

5.2 Domain 2

Toppling is the dominant mechanism of failure in domain 2, with slope changes of 0 m – 3.9 m. Bedding dips between 37° – 90° into the pit wall. A failure at lower RL below the area of interest in April 2015 has led to the greatest movement in this zone. Slumping below has created 0.5 m – 0.8 m steps above the zone, with the aperture of toppling between 0.5 m – 1.0 m. The major control on failure is the release of this lower key block which has allowed the bedding to topple in a west direction.

5.3 Domain 3

A complex zone with both planar sliding and topple failure mechanisms present, related to the synclinal hinge intersecting the surface at 480 RL. Lower in the domain below the hinge, the major failure mechanism is toppling which can be seen in the change model with the tops of benches portraying a higher volume loss. The geotechnical model shows bedding dipping steeply into the face between 70° – 80° also corresponding with topple mechanisms. The bedding tends to dip out of the face at a shallower angle approximately 25° – 40° above 480 RL giving rise to planar sliding. We

notice on the change model that the entire surface tends to portray loss as we would expect from planar sliding with larger volumes of material moving.

5.4 Domain 4

Domain 4 is characterised by a topple failure mechanism, with movement of 0 m – 1.6 m. Bedding dips steeply into the slope between 33° – 80°. The change models show that movement generally occurs higher on the slope above 470 RL. Again the material loss occurs at the top of benches; while the most gain is found at the toe of the benches.

5.5 Geotechnical Domain Summary

Table 1. Geotechnical domain summary

Domain	Approx. RL top of zone	Approx. RL base of zone	Max. loss slope material (m)	Total volume lost (m^3)	Failure mechanism	Failure control
1	465 – 485	455 – 440	3.2	4960	Planar	Bedding / joint
2	485 – 500	440 – 432	3.9	3160	Topple	Bedding
3	500 – 510	432 – 425	2.8	1890	Planar / topple	Bedding / joint
4	510 – 530	425 – 410	1.6	2840	Topple	Bedding

6 CONCLUSION

Leapfrog software can be used to develop geological models, assess slope movement from both point cloud and discrete prism data which can be useful for volumetric calculations, mine planning and hazard assessment. Change models could be useful during mine works in order to update and develop geotechnical models, as well as contributing to rockfall and hazard assessment. Volumetric calculations could be undertaken at the same time in order understand pit wall movement.

At the north-east pit wall of the Globe Progress open pit mine in Reefton, slope change models and geotechnical information collected over the last eight years allowed for the development of geotechnical domains. Each domain has a different failure mechanism which is ultimately controlled by the complex folding within the area. The orientation of asymmetric fold structures with limbs dipping between 30° – 60° provide a mechanism for movement. Several shears and faults offset the hinges of such structures which results in the variation of failure mechanisms across each of the domains.

Future work could include comparing point cloud data with mine plans, providing feedback to mine designers as the pit is progressing. Comparison with a mine design mesh could provide valuable feedback to slope designers during mining to understand where the pit wall is different to the design.

7 ACKNOWLEDGEMENTS

I would like to thank OceanaGold, Luke Matheson, Andrew Cantwell, ARANZ Geo, Marlène Villeneuve, David Bell, Clark Fenton, Dylan Meehan and Sunny Kalidas for assisting with this project.

REFERENCES

Alcaraz, S., Chambefort, I., Pearson, R., and Cantwell, A. (2015). “An integrated approach to 3-D modelling to better understand geothermal reservoirs”, in *Proceedings of World Geothermal Congress*, Melbourne.

Clark, P.B. (1996). *Rock Mass and Rippability Valuation for a Proposed Open Pit Mine at Globe Progress, near Reefton* (Unpublished master’s thesis). University of Canterbury, Christchurch, New Zealand

Golder Associates (2014). *Review of Highwall Stability*, retrieved from OceanaGold

Kennedy, G.D. (2009). *Geotechnical investigation of the Footwall Zone, Globe Progress Open Cut Gold Mine, Reefton, New Zealand*, Undergraduate (honours) thesis, University of Canterbury, Christchurch, New Zealand (Unpublished)

Kromer, R., Hutchinson, J., Lato, M., Gauthier, D. and Edwards, T. (2015). “Identifying rock slope failure precursors using LiDAR for transportation corridor hazard management”, *Engineering Geology,* 195, pp. 93-103.

OceanaGold. (2015). *OceanaGold mapping data*, retrieved from OceanaGold.

Rose, S and Ireland, J. (2014). “Implicit modelling applied to grade control data”, in *Proceedings Ninth International Mining Geology Conference 2014*, pp. 115–122 (The Australasian Institute of Mining and Metallurgy: Melbourne).

Stewart, M., de Lacey, J., Hodkiewicz, P. F. and Lane, R. (2014). “Grade estimation from radial basis functions – how does it compare with conventional geostatistical estimation?”, in *Proceedings Ninth International Mining Geology Conference 2014*, pp 129–140 (The Australasian Institute of Mining and Metallurgy: Melbourne).

Turner, D., Lucieer, A. and de Jong, S. (2015). “Time Series Analysis of Landslide Dynamics Using an Unmanned Aerial Vehicle (UAV)” *Remote Sensing,* 7(2), pp. 1736-1757.

Proceedings of the 11th ANZ Young Geotechnical Professionals Conference – 11YGPC
Queenstown, New Zealand
25 – 28 October 2016

SH20A to Airport: New Zealand's First Project adopting Screw Piles and Diaphragm Walls as a Trench Combination

Maggie. M. Yan[1]

[1]Geotechnical Engineer, Beca Ltd, P.O. Box 6345, Wellesley Street, Auckland 1141, New Zealand; PH: (+649) 300-9000; email: maggie.yan@beca.com

ABSTRACT

State Highway 20A (SH20A) is the primary route to and from Auckland's international and domestic airports and forms a strategic link between State Highway 20 (SH20), State Highway 16 (SH16), the airport, and the greater Auckland area. The SH20A to Airport project comprises a new motorway interchange that separates the local and motorway traffic. SH20A is to be trenched below Kirkbride Road. The trench is approx. 450 m long and 30 m wide, retaining up to 7.2 m height of soil, and accommodating two carriageways with allowance for a future rail corridor. Diaphragm walls (D-walls) and screw piles are adopted as the trench supports, a combination never before used in New Zealand. This paper focuses on the trenching works, outlining the geotechnical design aspects for the trench, and the challenges through the design and construction to-date.

Keywords: Screw Piles, Diaphragm Wall, Trench, SH20A, Kirkbride Road, MHX

1 INTRODUCTION

SH20A is the primary route to and from the airport and forms a strategic link between SH20, SH16, Auckland's international and domestic airports, and the greater Auckland area. The main physical work for this project includes SH20A and Kirkbride Road widening, and grade separation of the SH20A/Kirkbride Road intersection by trenching the SH20A alignment under Kirkbride Road. The trench is some 450 m long and 30 m wide, retaining up to 7.2 m height of soil, and accommodating two carriageways and a future rail corridor. D-walls have been adopted for retaining the trench sides, and screw piles are adopted for anchoring the trench base slab down and resisting hydrostatic uplift pressures on the slab. The SH20A to Airport project is New Zealand's first project using the combination of D-walls and screw piles.

This project was initiated in 2010 with detail design commenced in May 2014. The construction started in July 2015 with project completion in 2017 by the MHX Kirkbride Alliance, consisting of alliance partners the New Zealand Transport Agency (the Transport Agency), Beca Ltd, Fletcher Construction Company (FCC) Ltd, and Higgins Group Holding Ltd. At the time of preparing this paper, the majority of the D-wall panels and screw piles have been constructed and installed, and the trench excavation between the D-walls is about to begin.

2 SITE CONDITION

2.1 Geology

The site is underlain by Puketoka Formation of the Tauranga Group, comprising of mostly light grey to orange-brown pumiceous mud, sand and gravel with black, muddy peat and lignite. The northern side of the site is underlain by undifferentiated organic-rich alluvium (Kermode, 1992). The nearest active fault is the Waiora North fault, some 30 km to the east. It is an active normal fault, dipping 60 – 70 ° to the west or northwest (Wise, 1999) with an apparent vertical slip rate of about 0.1 mm/year. The fault is a potential source for large earthquakes.

2.2 Ground and Groundwater Conditions

Between 2010 and 2015, field investigations of 28 CPTs, 27 machine boreholes, and 47 hand augers were undertaken and tested to up to 45.2 mbgl. The typical ground profile interpreted is summarised in Table 1.

The trench structure is located within the upper 4 layers identified in Table 1 with the top of the base slab positioned within soft Peat (L4), the toe of the D-wall founded on Puketoka Formation soils (varies from L5 to L7), and the toe of the screw piles founded on dense to very dense Shallow Marine Deposits (L8). Figure 1 shows the exposed Ash (L3) and Peat (L4) during the earthworks excavation.

Table 1. Typical Ground Profile

Layer Unit		Soil Description	Depth to Top of Layer (m)
1	TOPSOIL		0 (RL14.5m)
2	FILL	Stiff to very stiff, clayey SILT, minor gravel, yellow brown mottled grey, moist, highly plastic	0.1 – 0.15
3	ASH/Recent Alluvium	Loose sandy SILT; Soft to firm pumiceous sandy/clayey SILT and silty CLAY	1.5 – 2.25
4	Estuarine Deposits	Soft amorphous PEAT; very soft to firm organic SILT with minor clay, minor fibrous organics and wood pieces	2.0 – 4.4
5a[a]			8.0 – 16.2
5	Puketoka Formation	Alluvium including organics beds – Loose to medium dense silty/clayey SAND and sandy SILT, pumiceous; firm to stiff SILT-CLAY	8.2 – 9.2
6		Alluvium – Medium dense to very dense silty SAND	17.9 – 22
7		Interbedded Alluvium – very stiff to hard pumiceous sandy/clayey SILT; dense to very dense silty SAND	23.5 – 24.5
8	Shallow Marine Deposits[b]	Dense to very dense silty SAND; hard sandy SILT; trace shells	30.8 – 33.6

[a] Interbedded Peat within Layer 5 typically across the site.
[b] The soil was initially understood as "Kaawa Formation". However, the geological unit has been updated as "Shallow Marine Deposits" to reflect the fact of the absence of microfossils based on a paleontology studies of the "Kaawa Formation".



Figure 1. Earthworks Excavation Exposing Ash (L3) and Peat (L4)

Three distinct water levels are observed from monitoring: a shallow water level in Peat ranging from RL14.5 m to RL 8.5 m from south to north, an intermediate water level some 2 m to 5 m lower in the Puketoka Formation, and a deeper water level at approx. RL 5 m in the underlying sands. For design purposes, these aquifers have been assumed as all connected to produce a hydrostatic groundwater table level close to the surface.

It is understood that short-term groundwater drawdown (due to construction) would not extend beyond the construction zone. For long-term groundwater drawdown, it has been conservatively estimated up to 5 m could occur immediately adjacent to the trench, rapidly reducing to less than 2 m within 10 m to 15 m of the trench walls, and reducing to 0.25 m around 65 m from the trench walls. However, with the removal of soil from within and adjacent to the trench, static settlements due to groundwater drawdown are expected to be negligible long term. Short term drawdown measured to date has been small and less than 60% of the estimated 50mm.

2.3 Seismicity

The site subsoil class is Class E, in accordance with NZS1170.5 (Standards New Zealand, 2004). The design Peak Ground Acceleration (PGA) for the ULS case is 0.21 g for 2500 years return period with a moment magnitude of 5.8 determined by New Zealand Bridge Manual 3rd Edition Amendment 0 (New Zealand Transport Agency, 2013). A PGA 1.5 times that adopted for the ULS case is adopted for the

Maximum Considered Event (MCE) case in accordance with the Bridge Manual, and the return period of 10,000 years was probabilistically derived from a Site Specific Seismic Hazard Assessment (MHX Kirkbride Alliance, 2015). This required and received approval from the Transport Agency Scope and standards for specific use on this project.

3 TRENCH DESIGN OVERVIEW

3.1 D-Walls

Concrete D-walls are the main trench retaining structures for the project, to limit the excavation footprint and the need for groundwater dewatering during wall excavation. Bentonite slurry is utilised to maintain the stability of the existing ground during the excavation. When the excavation is complete, a prefabricated reinforcement cage is inserted into the excavated D-wall location. Concrete is then tremmied into the excavation, progressively displacing the bentonite and forming the D-wall.

Each D-wall panel is 800 mm thick and 7 m wide, retaining a soil height of 2.5 m to 7.2 m. Most of the D-walls are to be permanently propped by concrete beams. Temporary props are to be utilised during trench excavation before the base slab is cast. The D-wall throughout the trench is categorised into five types based on the structural setting (refer to Figure 2):

- *Type 1 D-Wall* – propped by bridge structures, with toe at RL -10 m, retaining approx. 7.2 m height of soil
- *Type 2 D-Wall* – propped by concrete beams, with toe at RL -10 m, retaining approx. 6 m height of soil
- *Type 3 D-Wall* – propped by concrete beams, with stormwater sump below the road base slab, toe at RL -10 m, and retaining approx. 6.5 m height of soil
- *Type 4 D-Wall* – propped by concrete beams, with shallow toe at RL -3.5 m to RL -2.8 m and retaining approx. 6.5 m height of soil
- *Type 5 D-Wall* – cantilever, with toe at RL -1.4 m to -3 m and maximum retained height of 4 m.

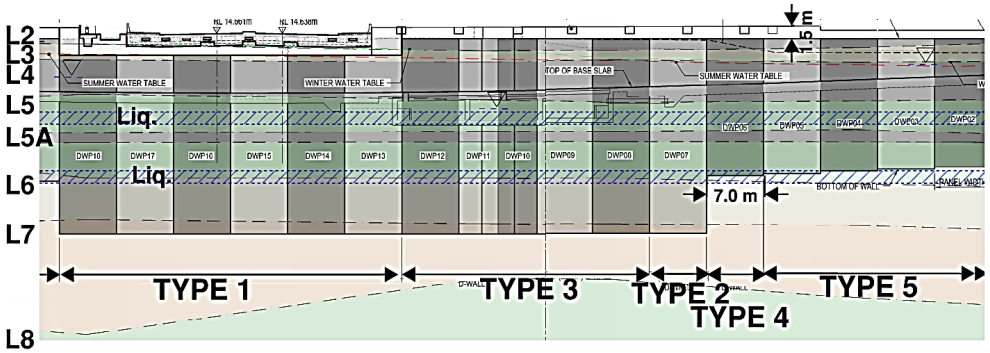


Figure 2. D-Wall Long Section (partial) and Ground Profile (screw pile not shown for clarity)

3.1.1 Liquefaction Analysis

Liquefaction potential and induced settlement have been assessed using the methods of Idriss and Boulanger (2008) and Zhang et al. (Zhang, Brachman and Robertson, 2002) in accordance with the Bridge Manual. Isolated part of the interbedded loose to medium dense silty SAND (L5 in Table 1 and Figure 1), is expected to liquefy in the ULS event at two horizons. The upper horizon is centred at an average of RL 4 m with an average thickness of approx. 1.5 m and the lower horizon is centred at an average of RL -3 m, also with an average thickness of about 1.5 m.

In an MCE event, liquefaction is also expected to occur broadly at two horizons. The upper horizon is as for the ULS event but the lower horizon is centred about a metre lower at an average of RL -4 m and has an average thickness of about 3 m.

As shown in Figure 2, Type 1, 2 and 3 walls are founded in very stiff to hard interbedded silty SAND (L7), while Type 4 and 5 walls are founded approximately at the interface of loose to medium dense sandy SILT (L5) and medium dense to very dense silty SAND (L6). The potential liquefaction induced settlements have been estimated and shown in Table 2.

Table 2. Estimated Liquefaction Induced Settlements under ULS and (MCE) cases

D-Wall Settlements (in mm)	Type 1	Type 2	Type 3	Type 4	Type 5
Above toe of D-wall	95[a] (150[a])			85[b] (100[b])	50-85[b] (60-100[b])
Below toe of D-wall	5 (30)			15 (80)	15-50 (80-120)
Adopted Wall Settl. for Slab Design	5-50 (10-90)			15-100 (20-180)	

[a] Up to half of the estimated settlements could induce settlement of the wall due to negative skin friction.
[b] Possible settlements due to negative skin friction
[c] Settlement under MCE case are shown in the brackets

3.1.2 D-Wall Analysis

Geotechnical analysis of the D-wall was carried out using Strength Reduction and 2-D Finite Element Methods in the computer program WALLAP Ver 6.05 by Geosolve Ltd. WALLAP was used to assess bending and shear demands, horizontal wall displacements, prop reactions (for both permanent and temporary props), and base slab propping reactions. The analysis took into account each stage of construction, long term static, seismic ULS, liquefaction, sequential seismic ULS (i.e. 2 x ULS case that was tested against collapse rather than controlling design), and MCE Cases. The program Plaxis 2D was used to cross-check the magnitude of demands and displacements determined by WALLAP.

The demands obtained from WALLAP were then adopted by Spacegass (a structural analysis program) to analyse the demands at the joints of the D-wall and the base slab, and of the base slab and screw piles.

3.2 Screw Piles

Screw piles are the 'Design and Construct' component of the project carried out by Piletech Ltd, a business unit of FCC. The piles have been designed to support the trench base slab as well as provide the hydrostatic pressure resistance. To date, more than half of the total 360 screw piles have been installed. Figure 3(a) shows the installation of screw piles on site. Piles have been installed with a mandrel from the existing ground level to some 39 m depth. The mandrel acts like a pile extension allowing the top of the pile to be pushed to the pile cut-off level (approx. the base slab level) from the existing ground level. The bore within the mandrel has been backfilled with sand before the mandrel was removed.

The geotechnical screw pile design, including pile helices configuration and foundation verification requirements, were carried out based on the test pile investigations in accordance with AS2159.

3.2.1 Test piles

Three piles with different number and configurations of helices were installed on site and full scale load tested in tension in 2014. The configuration of helices of Test Pile 1 (TP1) was selected with an upper helix of 650 mm diameter and lower helix of 500 mm diameter at 1.6 m spacing. It was founded at 39 mbgl and reached the ultimate test load of 2700 kN without geotechnical failure. A further 7 test piles (including one that failed to reach the geotechnical ultimate capacity of 2700 kN) were installed and tested also in tension in 2015 based on the same configuration as TP1. These 6 pile tests have confirmed a minimum tensile ultimate geotechnical capacity of 2700 kN. Piletech advised that the compressive capacity would not be less than its tensile capacity based on dense to very dense nature of the Shallow Marine Deposits. Pile demands are also mitigated by distribution of compressive loads to the base slab sharing some vertical loads.

Soil creep at the toe of the pile (100 years) has been estimated from 7 of the test piles. Deflections were obtained under a constant load of 1650 kN over a 12-hour holding period, and extrapolated and extended conservatively up to 100 years. Deflections due to soil creep have been combined with initial deflections for long term pile toe deflections. The total deflections have been tabulated in Table 3, and the 95th percentile has been considered in the base slab design.

Table 3. Summary of Pile Toe Creep from Test Piles

Test Pile	Initial Deflection[a] A (mm)	Short Term Creep[b] B (mm)	Long Term Creep C (mm)	Total Creep B+C (mm)	Total Deflection A+B+C (mm)
2014 TP1	11	3.25	5.75	9	20
2014 TP2	11	3.25	7.35	10.6	21.6
2015 TP1	6.8	4.6	7.9	12.5	19.3
2015 TP2	4.0	5.5	7.35	12.9	16.85
2015 TP3	10.5	3.1	5.5	8.6	19.1
2015 TP5	13.6	4.3	7.5	11.8	25.4
2015 TP6	18.9	3.0	8.25	11.25	30.15
				95th Percentile	28.7

[a] Load zero to 1650kN (P_s, in accordance with AS2159)
[b] Creep tested under a constant load of 1650kN for 12 hours
[c] Creep estimated based on the tested short term creep, for 12 hours to 100 years under a constant load of 1650kN

3.2.2 Pile Foundation Verification

CPT and SPT test results have been compared against the torque obtained from the test pile installation. Based on the comparison, sandy soil of SPT N = 50+ would generate a torque of some 2000 psi during the screw pile installation. During each pile installation, 5 test scenarios (A to E as shown in Figure 3(b)) are to be checked against target pressures. Our screw pile design assumption can then be validated. Scenario A is to test the geotechnical compressive capacity, while Scenarios B to E are to be considered for the tensile capacity.

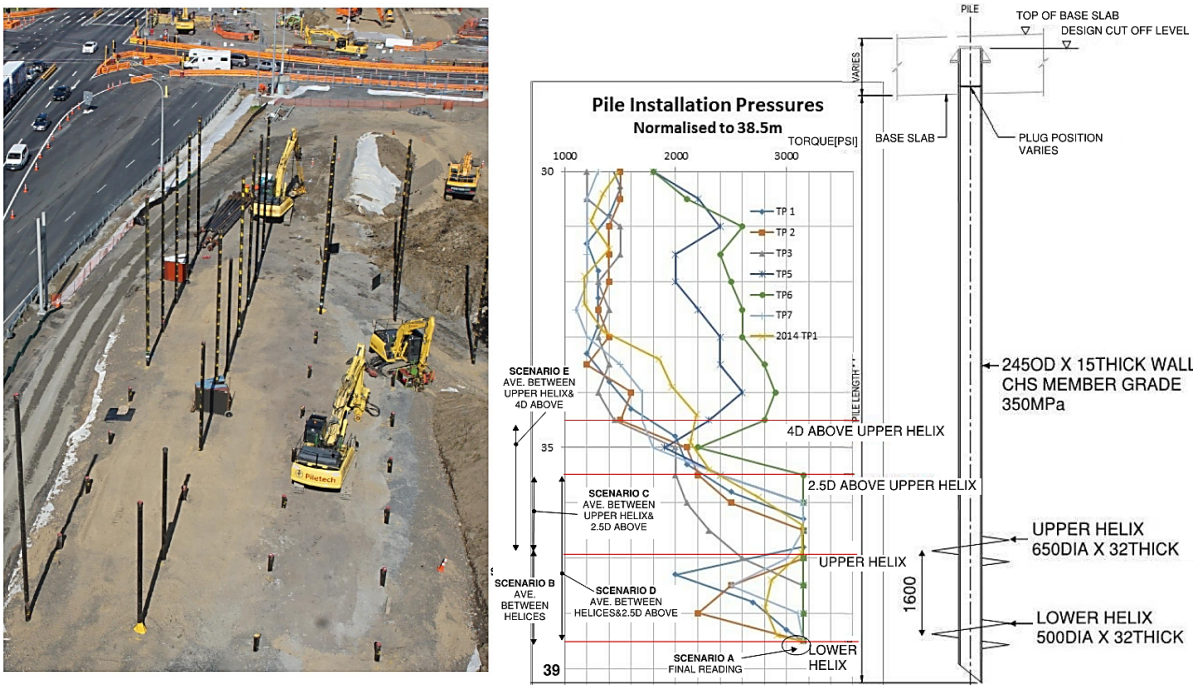


Figure 3. (a) Screw Pile Installation in April 2016; and (b) Test Pile Installation Pressures

3.3 Base Slab

The concrete reinforced base slab supported by screw piles is typically 600 mm thick between the trench D-walls. The base slab is to be connected to an edge beam on both sides of the trench. The edge beam is 1.2 m thick and 1.6 m wide accommodating the drainage pipe and catchpits along the trench. Between the edge beam and base slab, a 'soft slab' of 400 mm thick and 2 m wide is to be 'pin-connected' to the edge beam and provide the load transition between the base slab and D-wall.

4 CHALLENGES

4.1 Differential Settlement between D-Wall and Base Slab

Some of the D-walls are founded on Puketoka silty SAND and sandy SILT (L5) which are potentially liquefiable. The base slab is supported by screw piles founded on very dense Shallow Marine Deposits (L8) where liquefaction is not expected. In the seismic event especially in combination with hydrostatic uplift pressures, the D-wall is expected to settle. The 'hinge' (described in Section 3.3) between the 'soft slab' and edge beam would enable movement to prevent the main slab body and the nearest screw piles from being over-stressed. This 'soft slab' would provide more flexibility to accommodate the load demand, therefore reducing the connection demand at the joints between the D-wall and edge beam. After a major earthquake, the slab at 2 m to 3 m depth adjacent to the D-wall is expected to need to be repaired.

4.2 Use of Screw Piles

The available CPT results have been used for initial assessment to establish top of soil with an SPT N = 50+. However, linear interpolation between CPTs and BHs did not account for variations in ground conditions encountered during pile installation. So far, 44 % of the installed piles are up to 10 % longer than expected, and 4.2 % of the "longer piles" are founded in locally weaker soils than expected, which require further structural checks of the impact of the resulting reduction in ultimate capacity and pile vertical stiffness.

The increase in pile length results in an increase in the elastic displacement of the pile. The increase in elastic displacement from differential founding levels of the screw piles could over-stress the base slab. Therefore, before the mandrel is disengaged, reviewing the piling record and providing the feedback to the structural team promptly is important. The structural team then review the change and identify appropriate remedial options, such as using additional base slab reinforcement to redistribute load from the soft piles to the surrounding piles to reduce the impact on the base slab.

4.3 Cost Implication and Construction Sequences

The cost of fabricating temporary props is in the order of $150,000 each. Therefore prior to construction a value engineering exercise was undertaken to potentially reduce the required number of temporary props. This included examining the construction sequence and identifying potential impacts on the design, with new prop arrangements and rationalising the construction sequence in terms of temporary prop installation and removal staging in relation to the trench excavation. Temporary prop optimisation design has been undertaken deliberately with the involvement of Constructors, Structural and Geotechnical Designers working collaboratively. To date the outcome has been cost savings in the vicinity of $500,000 to $750,000 by lessening the number of temporary props to be fabricated.

5 CONCLUSION

The SH20A to Airport project has been successfully designed and is currently under construction. The trench has been designed with the innovations of using a D-wall and screw pile combination as the trench support, and 'soft slabs' to accommodate large load demands due to potential liquefaction induced settlements between the D-wall and base slab. The collaborative environment of an effective Alliance has allowed an innovative construction methodology, rationalised design (for example temporary prop design), rapid response to unexpected ground conditions and consequent project cost savings.

For future screw pile and base slab design, increasing the tolerance for pile lengthening shall be considered for encountering potentially significant variations in ground conditions.

6 ACKNOWLEDGEMENTS

The author would like to acknowledge the Transport Agency and MHX Kirkbride Alliance for permission to publish this paper. The author would also like to thank Sian France and Grant Newby of Beca Ltd for their help throughout the project and the review of this paper.

REFERENCES

Idriss, I. M. and Boulanger, R. W. (2008). *Soil liquefaction during earthquakes,* Oakland: Engineering Research Institute.
Kermode, L. (1992). *Geology of the Auckland Urban Area,* 1:50,000 scale, Geological Map 2, Lower Hutt, New Zealand: Institute of Geological & Nuclear Sciences Ltd.
Manukau Harbour Crossing Alliance. (2010). *SH20A Upgrade Project Geotechnical Interpretive Report*, Auckland
MHX Kirkbride Alliance (2015). *Seismic Hazard Assessment for the SH20A to Airport Kirkbride Project*, Auckland
MHX Kirkbride Alliance (2015). *SH20A to Airport Geotechnical Factual Report,* Auckland
MHX Kirkbride Alliance (2015). *SH20A to Airport Trench Structural Design Statement Detailed Design RPT019,* Auckland
New Zealand Transport Agency. (2013). *Bridge Manual Third Edition Amendment 0*, Wellington, New Zealand
Standards Australia Limited. (2009). *Australian Standard AS2159 Piling Design & Installation*, Sydney, Australia
Standards New Zealand. (2004). *NZS 1170.5:2004 Part 5:Earthquake actions-New Zealand*, Wellington, New Zealand
Wise, J. D. (1999). *A geophysical and geotechnical study of the Wairoa North Fault, South Auckland*. University of Auckland, Auckland
Zhang, G., Brachman, R. W. and Robertson, P. K. (2002). “Estimating liquefaction-induced ground settlements from CPT for level ground”, *Canadian Geotechnical Journal* , 39 (5), pp. 1168–1180

This page intentionally left blank

Proceedings of the 11th ANZ Young Geotechnical Professionals Conference – 11YGPC
Queenstown, New Zealand
25 – 28 October 2016

3D terrain and geological modelling for the design of a cut slope in Wellington

M. K. H. Brown[1]

[1]Ian R Brown Associates Ltd, 18 Park Road, Lower Hutt; PH +64 4 565 1777; email: matt@irba.co.nz

ABSTRACT

A 3D terrain and geological model has been used to assist in the design of a cut slope for a proposed house in Wadestown, Wellington. The natural slope of the site is ~30º and consists of colluvium overlying fractured greywacke. A 3D geological model was built from site investigation data, a topographical survey, and from point cloud data generated via photogrammetry (utilising photographs obtained by a UAV). The 3D model was analysed using TSLOPE; a 3D limit equilibrium slope stability package. This enabled calculation of the appropriate parameters for design of slope reinforcement.

Keywords: 3D, photogrammetry, slope stability, Wellington, geotechnical, modelling

1 INTRODUCTION

This paper outlines a methodology for deriving the design parameters for an appropriate slope retention system for a largely unmodified, north facing ridge in Upper Wadestown, Wellington. The site was originally covered by sparse bush/scrub that was cleared before investigations commenced. The site slopes much more steeply to the north-east than to the north. It is the north facing part of the site which will be excavated to accommodate a house over three levels (Figure 1).

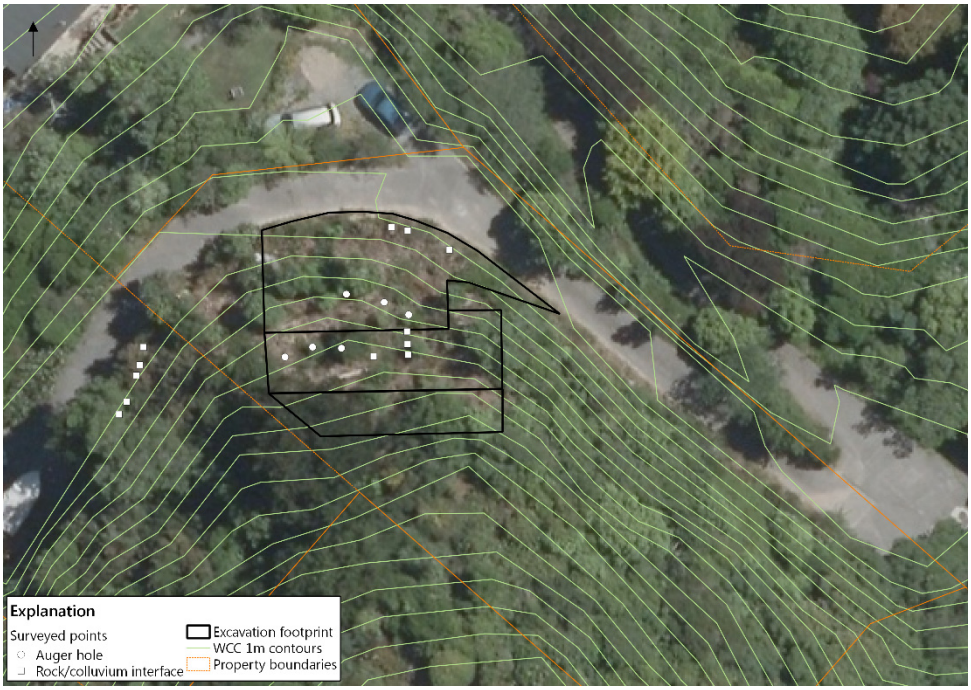


Figure 1. Topography, auger holes and surveyed rock/colluvium contacts

2 DATA ACQUISITION

A topographical survey of the pre-existing slope at the site was provided by the client. A site visit to examine the outcropping rock along the existing driveway cut revealed that as is typically found in the Wellington area varying amounts of colluvium were overlying weathered, fractured greywacke rock.

To investigate the depth and geometry of the colluvium/greywacke interface at the area of the proposed excavation, a bench was cut into the slope and rock was exposed in the southeast corner.

Following excavation, 6 holes were machine augured until at least 0.5m of rock was penetrated. The location of the auger holes and marked points along the outcropping and recently exposed rock/colluvium interface were then surveyed by a surveyor. Fracture orientation within the outcropping rock were measured with a Klaar compass.

After investigations were completed a DJI Phantom 3 advanced unmanned aerial vehicle (UAV) was deployed over the site using Pix4D capture (Pix4D, 2016) to photograph the modified topography. The UAV was flown in autonomous mode to generate an overview of the site, and in free-flight mode to better photograph the face of the cut.

3 MODELLING

The data from the original topographical survey was gridded and triangulated using TECHBASE (MINEsoft, 2016) software to populate a cell table and give an 'original' ground surface.

Using surveyed points from the greywacke/colluvium contact as seen in outcrop, the excavated cut and the augured holes, Leapfrog® (ARANZ Geo, 2016) geological modelling software was used to interpolate the top of greywacke surface.

The photos taken by the UAV were processed using Pix4D (Pix4D, 2016). This program uses geolocation data and photo stitching algorithms to generate a highly accurate 3D point cloud (Figure 2) and an orthomosaic image of the site.

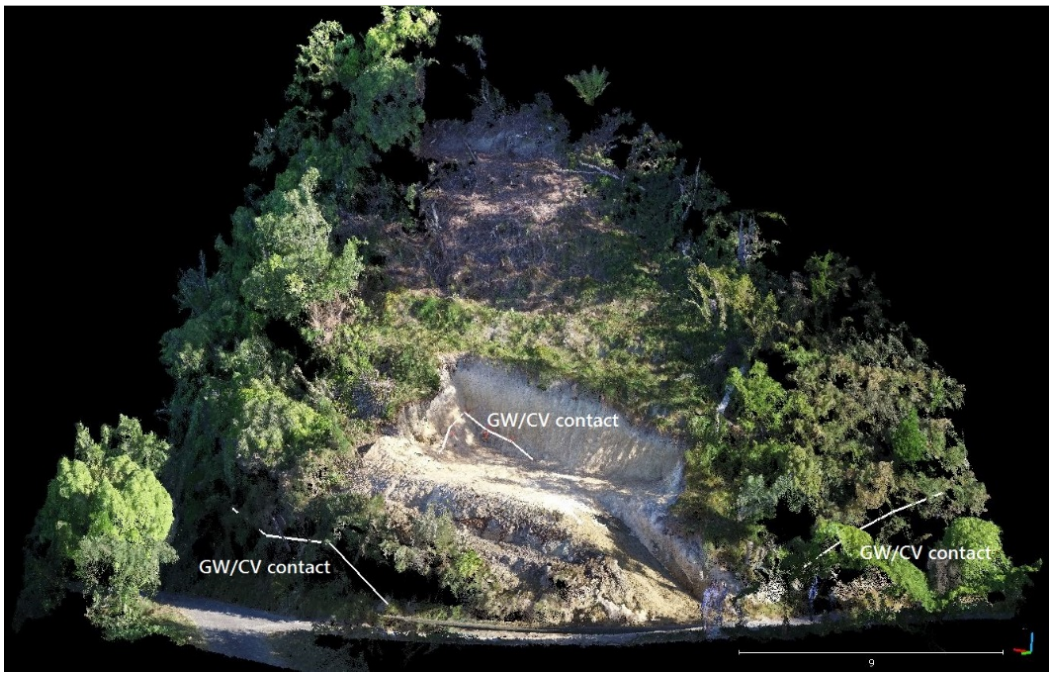


Figure 2. The resultant 22,609,500 point, 3D point cloud showing the excavated bench.

The model is highly accurate internally, however, there can be errors of up to 5m when matching the model to real-world coordinates and elevations. It is therefore often necessary to reposition the model using control points (points with known geometries and elevations).

Using the locations and elevations of the surveyed auger holes as control points, it was possible to align the two point clouds generated from the free and autonomous flight paths with each other, and also with the actual ground surface by picking common points in CloudCompare (CloudCompare, 2016), an open source point cloud manipulation software program.

The topography, as modified by our investigations, was modelled from the UAV derived point cloud giving a 'current' surface. It was necessary to clean the point cloud in CloudCompare by manually removing trees and other 'noise' not representing the ground surface from the model and interpolating a surface from the lowest points contained within 0.5m cells. This gave an accurate topographical surface.

After comparing the 'original' topographic model to the 'current' topographical model generated from the UAV data it was seen that there were inaccuracies to the east in the original model due to lack of survey information in that area. A number of points with x, y and z were picked from the 'current' surface and were added to the original topographic model thus forcing it to reflect the actual topography. It was also noticed that the site had been terraced at some time in the past. Lack of detail in the traditional survey meant that this was not obvious from the 'original' topographic model.

The owners supplied their proposed excavation plans. These were used to set bench levels and dimensions into the 'original' topography by selecting the points of the original topographical model that were within the proposed bench areas and setting their elevations to those of the proposed benches. Batters were calculated by triangulation between these benches. This gave us a 'proposed' final excavation surface.

The area of exposed rock was segmented out of the point cloud using CloudCompare for fracture analysis. CloudCompare generated a stereonet from the point cloud giving us mean joint direction and mean joint angle (Figure 3).

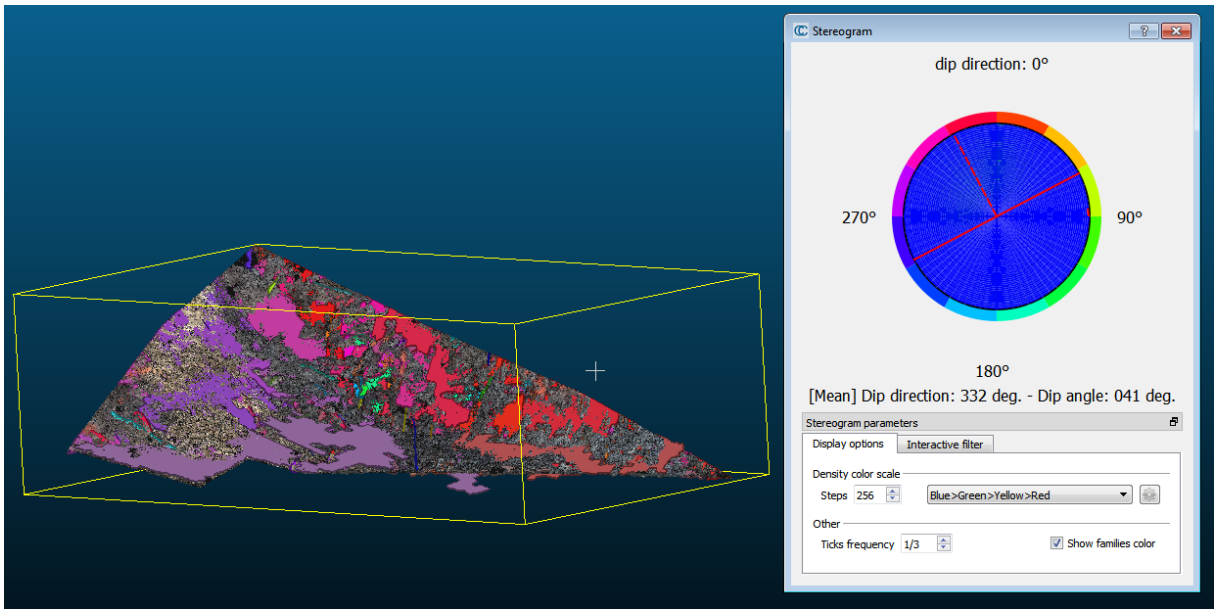


Figure 3. CloudCompare fracture orientation and stereonet

The stereonet results compared well with those compiled from field measurements ([Mean] Dip direction: 316 deg. – Dip angle: 041.5 deg.) Although these measurements correlated well, due to the highly fractured nature of the rock it was decided that there were no clear trends to the fracturing and this will not be used in the stability analysis.

The slope is considered to be 'dry'. There was no indication of groundwater seepage at the various cut slopes nearby, and groundwater was not encountered in our investigation holes, no further analysis was conducted to account for seasonal water flows.

Mohr Coulomb shear strength parameters for the two lithologies were summarised from a literature review of relevant references in the Wellington Region (Table 1).

Table 1. Material strengths

Author	Material	Cohesion (kPa)	Angle of friction (degrees)
Davidge (2007)	Colluvium	6	31
	Weathered GW	40	35
Christie et al. (2015)	CW Greywacke	10-15	35-36
Glue et al. (2015)	CW Greywacke	9-13	31.6-35.1
Kong et al. (2005)	Greywacke	30	26
Pender (1980)	HW Greywacke	39	33
Pender (1985)	HW Greywacke	50.4	33.08

On the completion of investigations and modelling we had; an accurate 'original' topographical surface, an accurate 'modified' topographical surface, an accurate 'proposed' excavation surface and an inferred greywacke/colluvium interface (Figures 4, 5). We also had highly detailed aerial imagery, a segmented point cloud representing freshly cut greywacke and some guidelines for material strengths. We now had the information required to model the slope.

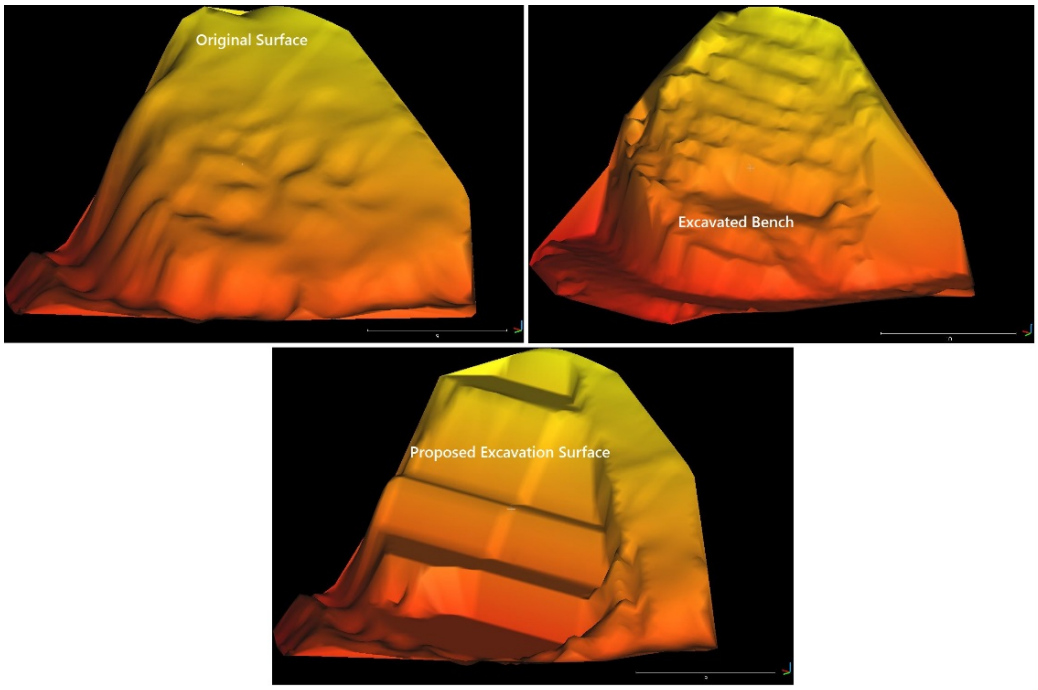
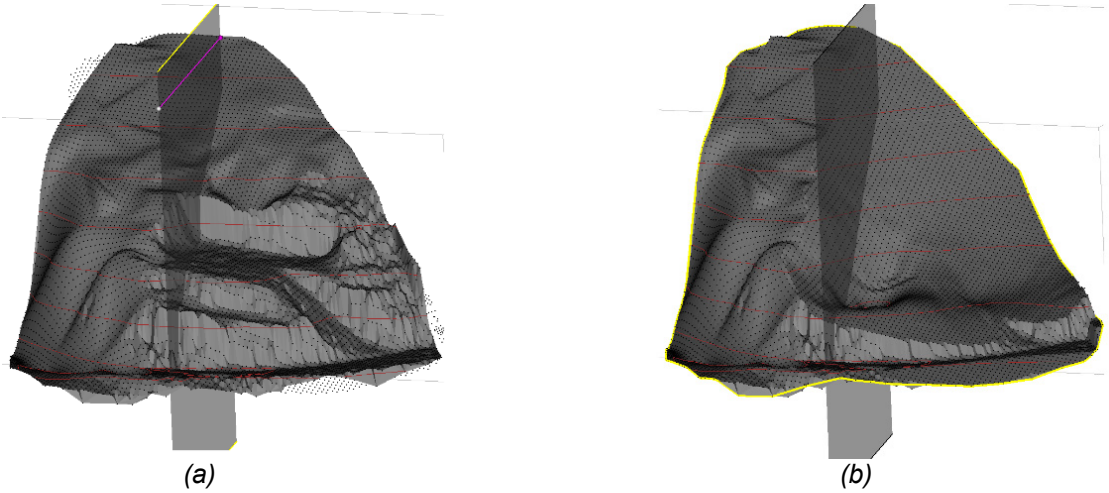


Figure 4. 'Original', 'current' (showing the bench excavated for investigation) and 'proposed' ground surfaces

4 SLOPE ANALYSIS

TSLOPE (TAGAsoft, 2016) a 2D and 3D limit equilibrium slope stability package was used to analyse slope stability. Initially a back calculation was performed to verify the strengths provided by the literature review. The natural slope has been stable for a long period. Following the excavation undertaken as part of the site investigations, the current and unsupported slope has remained stable over a 9 month period.

A stability analysis was performed using the colluvium strengths recommended by Davidge (2007). Figure 5 shows the current slope and the colluvium/greywacke interface located beneath the current surface. Figure 6 shows the slope in cross-section.



(a) *(b)*

Figure 5. (a) Current slope; and (b) GW / CV interface, showing cross-section line

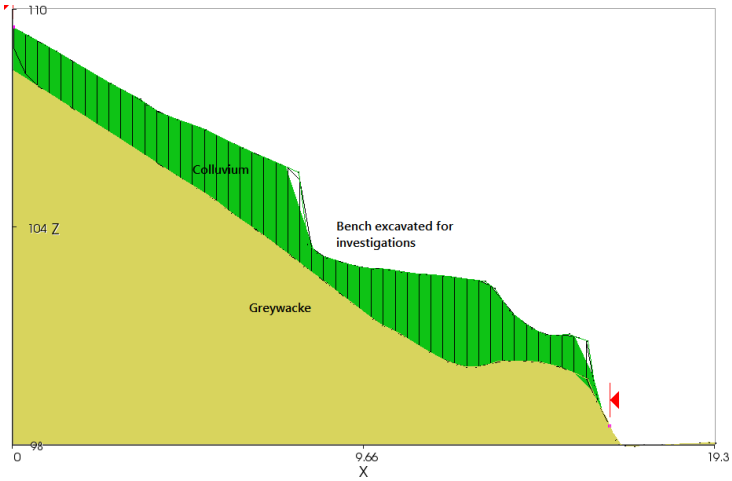


Figure 6. Cross-section showing slope failure controlled by greywacke/colluvium contact

A back calculation was performed using the 'current' slope geometry. The strengths from the back calculation (Figure 7) show that Davidge's (2007) parameters may be non-conservative and therefore inappropriate to use for a forward analysis of the excavated slope. A more appropriate strength to use in forward analyses may be picked from the red line on Figure 7 indicating a factor of safety of 1.0.

Further analyses will be able to inform design of the slope stabilisation system by incorporating the loads that need to be applied. These have yet to be completed.

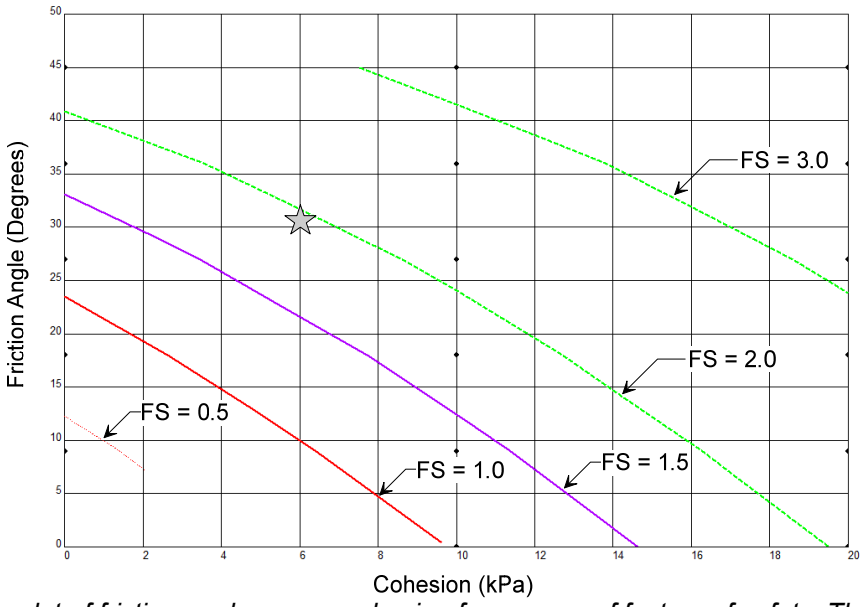


Figure 7. Cross plot of friction angle versus cohesion for a range of factors of safety. The star indicates Davidge (2007) parameters.

5 CONCLUSIONS

Using a UAV to survey a site can provide detailed and valuable information which can supplement or even replace more traditional methods. This method of surveying is fast, highly detailed and relatively inexpensive. Having a highly detailed point cloud/3D model and a high resolution orthomosaic is very helpful for site visualisation.

For the site described, using a model gained from a UAV flight during the process of site investigations allowed us to better predict the material strengths of the lithologies as this reflected a cut slope scenario with batters of a steeper angle than the original slope. This enabled more informed design parameters for slope retention.

When it is unsafe or impractical to access rock faces geological features may be mapped directly from the point cloud, allowing mapping where it may otherwise have been prohibitively dangerous or expensive. In this example, analysis of dip direction and orientation of fractures performed in CloudCompare gave us some indication of rock jointing patterns and the interface between greywacke and colluvium could be traced.

Being able to work in 3D in TSLOPE, and having a highly detailed topographical surface, made our modelling more accurate. This was particularly relevant in this situation as the greywacke/colluvium interface had a concave dish shape that was dipping out of the slope.

Although the models provided through photogrammetry are very accurate internally, depending on the accuracy called for, or the need to work in a known coordinate system, they may need to be aligned with the use of ground control points.

There are many benefits to UAV surveying and photogrammetry however the best results are obtained given favourable conditions. These include stable weather, few shadows and clear ground. Vegetation can be filtered out of the point cloud to allow for ground surface modelling but this will not be possible for an area under a dense canopy.

The work flow we have developed within this paper will become an important part of future projects. UAV's and photogrammetry have increased the ease with which site investigations may be carried out but the information gained from these methods must still be interpreted and supplemented using sound geological practice.

6 ACKNOWLEDGMENTS

I would like to acknowledge the help of Dr Ian Brown from IRBA and Mr Peter Wood from TAGA Engineering Software Ltd. I would like to thank Daniel Girardeau-Montaut and collaborators from CloudCompare, and John Kawolczyk and Anja Martel; owners of the property herein.

REFERENCES

ARANZ Geo (2016). www.leapfrog3d.com

Christie, E. B., Van Rooyen, O., Meiring, C. and Symmans, B. (2015). "Ground anchor testing in Wellington soils and weathered greywacke"

CloudCompare (2016). www.cloudcompare.org

Davidge, R. J. (2007). "Geotechnical investigation, proposed development potential, 67 Upland Road, Kelburn, Wellington", ABUILD Consulting Engineers Ltd., unpublished report

Glue, S. B., Torvelainen E. P., Christie, E. L., Meiring, C. and Symmans, B. S. (2015). "Straight shaft and bell shaped tension piles in Wellington greywacke"

Kong, V. and Pender, M. J., (2005) "Earthquake induced slope displacements and the shear strength of closely jointed rock masses", *Proc of the SECED Young Engineers Conference*, 21-22 March 2005, University of Bath

MINEsoft (2016). www.techbase.com

Pender, M. J. (1980). "Friction and cohesion parameters for highly and completely weathered Wellington greywacke", *Proceedings of Third Australia-New Zealand conference on geomechanics*, May 12-16, Wellington, New Zealand

Pender, M. J. (1985). "Stability of slopes in closely jointed rocks", *IPENZ Conference*, Wellington, New Zealand

Pix4d (2016). www.pix4d.com

TSLOPE (2016). www.tagasoft.com

11YGPC AUTHOR INDEX

Author Name	*Page No.*
A	
Anderson, D. R.	129
Anwar, S.	29
Awad, A. S.	95
B	
Bell, D.	1
Boam, E.	249
Bowen, H. J.	147
Brabhaharan, P.	249
Brown, M. K. H.	319
Burrows, N. P.	15
Byrne, N. J. C.	109
C	
Cantwell, A.	305
Cappellaro, C.	203
Carter, A. T.	275
Chan, G.	183
Cherfane, S.	63
Cubrinovski, M.	203
Cuniowski, T. G.	115
Curley, B. A.	153
D	
Dennison, D. L.	83
E	
Engel, J. M.	141
Everiss, R. J.	35
F	
Fairhall, J. B.	177
Farry, K.	103
Fityus, S.	191
Frampton, M.	237
G	
Gainsford, D.	223
Graafhuis, R. B.	171
H	
Harris, S. J.	293
H *(Cont.)*	
Howard, T.	305
Hunter, A. J.	299
J	
Jacobs, E. E.	83
Jaksa, M. B.	41
Jaukovic, I. C.	299
Johnston, J.	191
K	
Kelly, J.	153
King, D.	287
Kristinof, R.E.	135, 275
L	
Lees, J. J.	159
Leeves, J.	231
Li, N.	269
Lim, J. K.	215
M	
McEwan, H. L.	171
McPherson I.	123
Magagula, M. P.	281
Mangos, C. C.	89
Maynard, E. G.	75
Meehan, D.	165
Mills, D. P.	69
Mills, P. R.	243
Moniz, S.	63
Moon, V. G.	243
Morton, D. J.	69
Mostyn, G.	9
O	
Och, D. J.	109
P	
Palmer, S. J.	263
Pereira, A.	123
Piper, W. M.	129

Author Name	*Page No.*
P *(Cont.)*	
Pletz, Z. J.	197
Podnar, A.	21
R	
Rama, B. H.	263
Ranasinghe, R. A. T. M.	41
Reed, R. J.	275
Rees, S. D.	57
Ridl, R.	1
Ruxton, N.	49
S	
Salt, G.	223
Searle, J.	95
Semmens, S.	29
Shen, B.	9
Simms, B.	153
Sundar, R.	237
T	
Tanuwidjaja, R. C.	209
Teoh M. L.	9
Torvelainen, S. M.	257
V	
Villeneuve, M.	1
W	
Wallace, A. D.	147
Wardle, G. R.	281
Y	
Yan, M. M.	311

Neeson, F.C., Lacey, D., Buxton. D. and Storie, L. (eds.), *Proceedings of 11th ANZ Young Geotechnical Professionals Conference (11YGPC)*, 25th – 28th October, Queenstown, New Zealand

ISBN 978-0-473-37653-6

ISBN 978-0-473-37653-6

